REPORT DOCUMENTATION PAGE

Form Approved
OMB No. 0704-0188

Public reporting burden for this collection of information is estimated to average 1 hour per response, including the time for reviewing instructions, searching existing data sources, gathering and maintaining the data needed, and completing and reviewing the collection of information. Send comments regarding this burden estimate or any other aspect of this collection of information, including suggestions for reducing this burden to Washington Headquarters Services, Directorate for Information Operations and Reports, 1215 Jefferson Davis Highway, Suite 1204, Arlington, VA 22202-4302, and to the Office of Management and Budget, Paperwork Reduction Project (0704-0188), Washington, DC 20503

1. AGENCY USE ONLY (Leave Blank)	2. REPORT DATE: Feb 11,2000	3. REPORT TYPE AND DATES COVERED: Final, 1-March 1995 - 1 June, 1999.

4. TITLE AND SUBTITLE

Combustion Mechanisms of Heterogeneous Solid Propellants

5. FUNDING NUMBERS

Grant N00014-95-0559

6. AUTHOR(S)

E. W. Price, S. R. Chakravarthy, R. K. Sigman, R. Jeenu, J. M. Freeman, and J. M. Seitzman

7. PERFORMING ORGANIZATION NAME(S) AND ADDRESS(ES)

School of Aerospace Engineering
Georgia Institute of Technology
Atlanta, GA 30332-0150

8. PERFORMING ORGANIZATION REPORT NUMBER

Deliverable No. 3

9. SPONSORING/MONITORING AGENCY NAME(S) AND ADDRESS(ES)

Office of Naval Research
Arlington, VA 22217-5660

10. SPONSORING/MONITORING AGENCY REPORT NUMBER

11. SUPPLEMENTARY NOTES COR:

12a. DISTRIBUTION/AVAILABILITY STATEMENT

Approved for public release; distribution unlimited

12b. DISTRIBUTION CODE

13. ABSTRACT (Maximum 200 words)

The bulk of the research on this contract was concerned with the mechanisms that cause "plateau" burning of ammonium perchlorate/hydrocarbon (AP/HC) propellants. The long range goal is to identify the steps in the combustion process that dominate overall burning, and in particular to understand which of these steps in the combustion process lead to plateau burning.

Burning alone, matrixes (mixture of binder, fine AP, and catalysts) almost always burn slower than the bimodal propellant at all pressures. The improved burning with a catalyst is probably due to both increased surface layer heat release and to catalytic break down of the large fuel vapor molecules which cause the flame to stand closer to the surface. Deflagration rate of the large AP particles is always lower than the propellant rate, and contributes little to overall rate, except in close proximity to the matrix where a hot stoichiometric diffusion flame occurs and (apparently) supports the marginal matrix burning, accounting for the higher propellant rate.

Observations of local intermittency of burning seem to contribute to the low burning rate associated with plateaus and spontaneous quenches.

14. SUBJECT TERMS

Solid Propellant Combustion

15. NUMBER OF PAGES

289

16. PRICE CODE

17. SECURITY CLASSIFICATION OF REPORT	18. SECURITY CLASSIFICATION OF THIS PAGE	19. SECURITY CLASSIFICATION OF ABSTRACT	20. LIMITATION OF ABSTRACT
Unclassified	Unclassified	Unclassified	Unclassified

NSN 7540-01-280-5500

Standard Form 298 (Rev 2-89)
Prescribed by ANSI Std 239-18 298-102

FINAL REPORT

COMBUSTION MECHANISMS OF HETEROGENEOUS SOLID PROPELLANTS

By

E. W. Price, S. R. Chakravarthy, R. K. Sigman, R. Jeenu, J. M. Freeman, and J. M. Seitzman

Prepared for

OFFICE OF NAVAL RESEARCH
ARLINGTON, VA 22217

Under

Contract N00014-95-1-0559

February, 2000

GEORGIA INSTITUTE OF TECHNOLOGY
A UNIT OF THE UNIVERSITY SYSTEM OF GEORGIA
SCHOOL OF AEROSPACE ENGINEERING
ATLANTA, GEORGIA 30332

Reproduced From
Best Available Copy

20000217 032

INTRODUCTION

This report summarizes research done under ONR Grant # N00014-95-0559, which covered the time from 01 March 1995 to 01 June 1999. This contract continued research on mechanisms controlling combustion of solid propellants, started at Georgia Tech in 1968. The final report on the most recent previous ONR report is noted in Ref. 1. Because most of the research under the present contract has already been published, the bulk of this report consists of those publications (Appendices A–R). The text of the report assembles the highlights of the findings.

At the beginning of this contract some of the studies of new ingredients (central to the preceding contract) were continued (primarily involving ammonium dinitrimide, ADN)(Ref. 2,3; App. A,B). However, the bulk of the research on this contract was concerned with the mechanisms that cause "plateau" burning of ammonium perchlorate/hydrocarbon (AP/HC) propellants (Fig. 1). This topic was of current interest because the low dependence of burning rate on pressure permits design for higher motor performance or enhanced safety, and Thiokol Corporation had recently found formulations that yielded plateau and "biplateau" burning (Fig. 1) and high solids loadings (87.5% AP). Such burning rate behavior is not explained by conventional burning rate models. It was felt that the 25 years of research on combustion mechanisms (and combustion lab facilities) provided by the Georgia Tech program was a good starting point for study of mechanisms of plateau burning.

GOAL OF RESEARCH

The long-range practical goal of this program is to predict the steady and non-steady burning characteristics of propellants on the basis of formulation and facilitate optimization of formulations for different applications. The immediate goal is to identify the steps in the combustion process that dominate overall burning, understand how they interact with each other and how these processes change with formulation variables, pressure and flow environment. In the present contract the goal was primarily to understand what aspects of the combustion process lead to plateau burning.

APPROACH

The initial step in the present studies is to assess the response of individual ingredients of the propellant to controlled external heating ("thermal analysis") using TGA, DTA, DSC and hot stage microscope (App. C). Such tests provide estimates of melting and decomposition temperatures of ingredients and of the energetics of decomposition. For those ingredients that will self-deflagrate, the deflagration rate and flame behavior are determined vs. pressure using photographic methods. Quenched samples are examined microscopically. These deflagration studies are an important part of the ingredient studies because they involve the high pressure, heating rates and temperatures present in the combustion zone, which cannot be simulated in thermal analysis tests.

In the progression to combustion studies of propellants, recourse is often taken to the intermediate step of "sandwich burning". This is a well-studied technique (35 years by present investigators; Ref. 4) in which the "propellant" samples consist of laminates of binder or matrix between two oxidizer sheets. The samples are burned edgewise (Ref. 2,3,5,6; App. A,B,D,E) and permit study of the all-up combustion process in a two-dimensional form (which is easier to observe and model than a propellant with particulate oxidizer). Fig. 2, (from Ref. 7; App. F) shows an example of burning rate characteristics of sandwiches (from the preceding contract) that is particularly interesting because it shows a domain of test variables (encircled) in which plateau and mesa burning occur, with a binder that had not been considered to be conducive to such behavior.

Most of the studies during the present contract have been with particulate AP propellants. It had been found (Ref. 7; App. F) that bimodal AP size distribution was conducive (necessary?) to obtain plateau burning with high solids formulations, and particularly with certain binders and additives. There was evidence that bimodal AP distributions led to burning surfaces with "matrix" sites and coarse AP sites (Fig. 3, from Ref. 8; App. G)) with conspicuously different burning characteristics. Plateau burning appeared to depend on the contrasting characteristics of the two kinds of sites and of their interaction. The approach was to study the combustion of a) matrixes burning alone (Ref. 6-10, App. E-I), b) AP burning alone(Ref. 11; App. J), and c) burning of "all-up" propellants (Ref. 2,3,7,8,10,12-17; App. A,B,F,G,H,I,K-P). Combustion photography, interrupted burning and thermal analysis tests were made on ingredient mixes made in-house and on the Thiokol propellants provided on the ongoing ONR contracted Multi-University Research Initiative (MURI). In these studies it was known in advance that occurrence of plateaus was critically dependent on special combinations of values of several propellant variables, but that knowledge was fragmentary and poorly understood.

Part of the approach in this study was to develop a strategy for studying a phenomenon that depended on so many variables that it was impractical to test the full matrix of variables. Plateau burning was shown to depend upon:

a) AP particle size (coarse and fine)
b) Mass ratio of coarse to fine AP
c) Mass fraction of AP and binder (87.5-80% solids was chosen for propellants.[1]
d) Choice of type of binder (PBAN, HTPB/IPDI, and HTPB/DDI were chosen.[2]
e) Additives (DOA plastcizer and transition metal oxides were chosen).

The choice of combinations of variables actually studied was guided by past experimental results and various postulates regarding mechanisms for plateau burning. Thermal analysis, combustion photography, and microscopic study of quenched surfaces were carried out on ingredients, fine AP/binder matrixes and bimodal propellants. The resulting experimental evidence, in combination with past evidence and theory about propellant combustion mechanisms, was expected to either reveal "plateau-producing" mechanisms, or at least provide information that would test plausability of current and future postulated mechanisms.

[1] For practical reasons.
[2] Ditto

BACKGROUND AND SCOPE

This report concerns a class of "anomalous" burning behavior of AP composite propellants that includes low and negative dependence of burning rate on pressure over an appreciable range of pressure (Fig. 1). This kind of behavior was discussed at length in Ref. 7,8 (App. F,G), and the present report encompasses those results and more recent findings that test speculations, correct errors, extend the results, answer some questions, and pose some new mechanistic arguments. Much of the pertinent new experimental work was reported in Ref. 7-12 (App. F-K) – Unpublished work is presented here in App. C.

For background, it is noted here that anomalous burning was originally observed (Ref. 10, 18-21) in combustion of propellants with monomodal AP size distributions (which are necessarily quite fuel rich because of limitations in packing density of the AP). Such behavior is also observed (Ref. 22) with some AP propellants consisting of relatively coarse and relatively fine AP (e.g., 70% 400 μm and 30% 4μm). Such propellants can be viewed as suspensions of coarse AP in a matrix of fine AP and binder, with volume proportions of 46% and 54% (Fig. 3). These two "entities" have very different burning behavior, and the "anomalous" burning behavior reflects the individual behavior of each and a measure of coupling behavior between the two. In particular, burning of the coarse AP particles is much like the self deflagration of AP (Fig. 4), while the matrix burning tends to be marginal when burning on its own, quite often exhibiting plateau burning, locally intermittent burning, and spontaneous quenches in the mid pressure range. It is observed in both propellant testing and edge burning of "sandwiches" of matrix between laminae (Ref. 8,23; App. G) that the propellants (and sandwiches) always burn faster than either the AP or matrix alone, indicating that some measure of positive coupling always exists. In extreme cases, a propellant or sandwich will burn with a matrix that won't burn on its own at all (or sometimes with a plateau); and the AP sustains deflagration below its normal self deflagration limit when some matrix (or fuel) is around. Further, the anomalous deflagration of AP starting at about 2000 psi (Fig. 4) "goes away" in the presence of a matrix or fuel. Coupling appears to be by heat supply from the hot flame between the matrix vapors and the AP vapors from the coarse AP particles (or lamina). As one might expect, the details are pressure dependent, as the flame is nearly premixed (planar) at low pressure, but of increasingly complex structure as pressure increases. In order to understand plateau burning, it appears to be necessary to understand the pressure dependence of matrix burning, of AP burning, and of their coupling. This difficult problem is further complicated by the extreme dependence of the propellant surface geometry on pressure (Fig. 5). It is further complicated by the sensitivity of plateau behavior to particle size of the fine AP, ratio of coarse-to-fine AP, type of binder, and presence of minor additives.

It is worthy of note that if a study of effect of formulation variables were undertaken, a set of 5 choices for each of the four "sensitive" variables noted above, and for coarse AP particle sizes would yield $5^5 = 3125$ combinations for propellant formulations, which would have to be tested at 10 pressures (31,250 burning rate tests). The collected studies to date fall far short of that and do not reflect coordinated sets of variables. Because of this, generalizations about results and responsible mechanisms are

of uncertain relevance outside the specific formulation domains tested. This reservation applies to the interpretations in Ref. 10, App. I; and all others.

In the present studies, the combustion characteristics of matrixes were studied with PBAN/ECA, HTPB/IPDI, and HTPB/DDI binders; with 4 particle sizes of fine AP; with matrix AP/binder ratios from 50/50 to 73/27 (with nominal values of coarse AP/fine AP of 2/1 mass ratio for 88% AP formulations). The effect of DOA (10 to 20 % of binder) was tested as well as four transition metal oxides in different concentrations. Test methods included determination of strand burning rate, and flame behavior from combustion photography; burn-no burn tests; rapid depressurization quench tests for microscopic study of burning surfaces; and hot stage microscope (HSM) and other thermal analysis tests (special HSM tests on a wider range of binders). Full testing of even this modest range of variables and tests (call it 3 binders, 6 additives, 4 fine AP particle sizes, 3 coarse AP particle sizes, 5 ratios of AP/binder, and 5 kinds of tests, at a few pressures (say 5 average) calls for 6750 tests. Actual tests were chosen on the basis of practical choices, past findings and involving ideas regarding what processes were controlling pressure dependence of the burning rate. This paper is organized according to issues of burning rate-controlling mechanisms, and the collected experimental results are assembled here in ways to test these issues. Details are presented in the Appendices A-R.

ROLE OF THE COARSE AP

Consideration of Figure 5 leads to the impression that the coarse AP particles are burning more or less like self deflagration. There is no evidence of the intrusion of binder melt along the peripheries, and the particles lag behind the matrix when the propellant rate is high compared to the AP self deflagration rate (Fig. 5b where the propellant rate was four times the AP self-deflagration rate). However, there is decisive evidence for a role of the coarse particles in coupled burning with the matrix. An example is illustrated in Fig. 5a, where the overall premixed flame supports burning of the matrix and the coarse AP (at a pressure that is lower than the AP self deflagration limit). When protruding coarse AP particles (as in Fig. 5b) are removed from the surface (e.g., Fig. 6), it is evident that the outer periphery is burning down with the faster matrix. One might conclude that this simply illustrates that the matrix flame is enhancing the AP deflagration there. It will be argued later that in fact the vapors from the peripheral AP and the vapors from the fuel-rich matrix lead to a hot near-surface stoichiometric flamelet that locally enhances the rate of both AP and matrix. The existence of such flamelets is generally recognized to be pressure dependent. At lower pressures, the decreased gas phase reaction rates cause the leading edge flames (LEFs) of the diffusion flames to stand further out from the surface, leading in the limit to an overall premixed flame as reflected in the flat burning surface at 200 psi (Fig. 5a). Stated more generally, the coarse AP particles are a source of oxidizer vapors for hot (stoichiometric) gas flames, which cause the propellant burning rate to be higher than either the matrix rate or AP rate alone. Only in one special condition was the coarse AP particle potentially a leading front in the burning surface (Fig. 7) in a situation at 200 psi where the matrix would not burn on its own and the premixed flame-assisted coarse AP burned out ahead of the matrix (at a pressure below the AP self-deflagration limit).

BINDERS

From a combustion viewpoint, the role of the binder is to supply fuel for the oxidizer/fuel (O/F) reactions. With the smallest AP particle sizes that are used in the matrix, there is a potential for a portion of the O/F reactions to occur in the surface layer. Because the matrixes are very fuel rich, oxidizer vapors from the large AP particles may react above the surface with fuel vapors, and with the fuel-rich products of the matrix flame. Thus there are at least three locations in the combustion zone where exothermic O/F reactions can be important (surface layer, matrix flame and LEFs), and dependent on the kinetics of binder pyrolysis and O/F reaction kinetics. The role of each class of reaction sites depends on its own pressure dependence, as well as the coupling among them.

There also exists the potential for accumulation of binder melt in the surface layer of the matrix, which has been said to interfere with matrix burning. The details of binder "melting" and decomposition have been studied for decades, but remain uncertain because of difficulties of measurement under "combustion-zone-like" conditions (pressure, temperature, and heating rate). The exact mechanism by which binder melt interferes with burning is not yet clear (see Ref. 7, App. F). In this study, thermal response of binders was examined extensively with a hot stage microscope (Appendix C) and by inference from the appearance of melt on the surfaces of quenched propellant surfaces (Ref. 15-17, App. N,O,P). A small number of TGA and DTA tests were also run (App. C).

BINDER MELT FLOW

Most binders degrade to a melt-like condition during heat up in the combustion zone. For those binders that decompose at temperatures comparable to or higher than the AP decomposition, there is a possibility that concentrations of melt will occur and obstruct heat flow to the AP. This is referred to here as a "possibility" because it is difficult to observe directly during burning. However, the concept of pressure-dependent "melt-suppression" of burning has become widely invoked in theories of plateau burning, with the dependence on type of binder being attributed to difference in melt properties of the binders. This subject was discussed in Ref. 7-9/App. F-H, and it was noted above that recent studies of quenched surfaces have indicated that melt intrusion on the coarse AP particle surface does not occur (bimodal AP propellants with PBAN and HTPB binders).

Earlier studies (Ref. 24,25/App. Q) using hot stage microscope observation of thermal response of ingredients showed that many binders melt and decompose at much lower temperatures than PBAN and HTPB, and also indicated that HTPB cured by DDI melted at a much lower temperature than IPDI-cured HTPB (which melted at a lower temperature than PBAN/ECA binder). All three completed decomposition by the time a temperature of 510 °C was reached. After extensive additional testing, it is now concluded that for those three binders (Appendix C):

a) "Melting" proceeds in stages that involve progressive decomposition

b) There are qualitative effects of: 1) the use of plasticizer DOA; 2) curing procedure (6 day cure compared to 1 day cure with catalyst); and 3) sample heating rate

(2°C/sec vs. 6 °C/sec)

c) In the hot stage, the sample is heated on the underside and often seems to melt there before the whole sample melts down (even with thin (200 μm) samples). Quite often the first visible evidence of a melt is when bubbling starts there. By the time the sample becomes a puddle, active vaporization is in progress.

d) All three of the binders noted above exhibited the same behavior*, with minimal difference as to temperature. Notable melting and bubbling started at about 455°C and ended with sample disappearance by about 490°C. The final stage was a spreading, clear non-bubbling film that disappeared. An exception was when 20% DOA was added to the binder; in that case the samples showed a gloss and slump followed by partial puddling and bubbling, in the temperature range 200-300°C, followed by a dormant period until the usual 455-490°C behavior.

A separate test on decomposition behavior was made by TGA tests in 1 atm. nitrogen (Fig. 8). The results are only slightly different for the three binders, with weight loss for PBAN/ECA starting earlier and proceeding more gradually. Consistent with the HSM test results, decomposition rate peaked at around 460-470 °C and was complete for all three binders by 490-500 °C. When 20% DOA was included, an early decomposition started at about 210-240 °C and a 20% weight loss was reached by 360 °C.

In retrospect it seems clear that the ideas of comparing binders by a melt and decomposition temperature is naïve, except for comparison of widely different binders (Table C-1a of Appendix C). It also seems reasonable in the context of the thermal wave in a burning surface to view the binder surface layer as consisting of staged behavior. As the material heats up, the composition of the layer progresses to more degraded (but more thermally stable) intermediate products nearer the surface, and with bubbling activity starting beneath the surface from more volatile species, possibly creating a surface foam. Even before considering how such a binder degradation layer might contribute to plateau burning, one might reasonably ask how it depends on pressure. The dimensions of the thermal wave are burning-rate dependent, meaning that the "melt layer' thickness is greater at low burning rate, constant on "plateaus, and increasing in the negative slope region of mesas, with the surface temperature having the opposite trends (low at low rates, increasing where the rate is increasing, and decreasing in the negative slope regions). However, there is a second, monotonic effect of pressure due to pressure dependence of desorption rate, which is lower at higher pressure. About all that can be said, even qualitatively, about melt layer thickness is that it is comparable to the finest AP diameters (e.g., 2μm) and probably thicker when the burning rate is low.

Some direct information about binder melts can be obtained from microscopic examination of the surfaces of samples quenched from burnng at high pressure (using the rapid depressurization method of quenching). Some 200 such tests were run on propellants with plateau burning characteristics. Sample surface features of the matrix areas are shown in Fig. 9. The sample in Fig. 9a is for a propellant with 2 μm matrix AP particles, while Fig. 9b is for 10 μm matrix AP particles. A binder melt film covers 50-70 % of the surface. Openings occur over AP particles which appear to be AP decomposing and clearing away binder melt overlays or intrusions. In the case of four plateau propellants with 2 μm AP, the ratio of open area to melt film area were qualitatively alike

* 200μm thick samples heated at initial 2°C/sec decreasing to 0.4C/sec at 470°C.

over the whole pressure range, and insensitive to HTPB curing agent or % fine AP in the matrix. This seems like a negative result as far as a role for melt as a factor in plateau and mesa burning, since these propellants had strong and different plateau characteristics. However, the results may signify that the melt effects occur in a manner not yet revealed. Specifically, the melt may tend to be drawn by surface tension into the holes left by fine AP burn-out. This would be dependent on AP particle size and melt viscosity. The effect of such melt behavior, or its pressure dependence, are at present matters of speculation.

One further observation concerning quenched surfaces comes from samples that quench spontaneously. It is observed that the matrix surfaces are completely covered with binder melt. This suggests what was referred to in Ref. 7 as "surface layer disproportionation (SLD) failure", i.e., the collective response of ingredients fails to establish a surface condition where the ratio of oxidizer and binder vapor outflow matches that in the propellant. In these examples the binder melt accumulates until it drowns the AP. The results suggest that this may occur rather suddenly during near-normal burning.

In summary, it is concluded that:

a) Binder melting should be viewed as a multiple step process in the surface layer in which the more stable initial intermediate decomposition products will concentrate on the surface, and the more volatile intermediates will vent from below (details depending on thermal wave thickness, viscosity and surface tension).

b) The difference in melt-like behavior between PBAN/ECA, HTPB/IPDI, and HTPB/DDI are not conspicuous, although addition of DOA produces a temporary "softening" and bubbling at around 200-300°C. All three binders transitioned to bubbling puddles at around 455°C and ended decomposition at around 490°C (HSM tests).

c) Binder melt does not encroach on the coarse AP particle burning surfaces; matrix surfaces were around 60% covered by binder (quench tests), the degree of coverage being qualitatively the same with all three binders at all pressures. This suggests that the well established binder dependence of plateau burning, if melt flow dependent, is due to melt fill into depressions left by burnout of fine AP particles, a subject that is difficult to observe but needs study. See Ref. 15-17;App. N-P.

Matrix Burning

In this investigation, tests were run on independent burning of matrix samples (Ref. 8-10,12; App. G-I,K). It was found that the typical matrixes with 70% fine AP and 30% binder would not burn in the intermediate pressure range around 800 - 1200 psi. The dependence of this no-burn domain is shown in Fig. 10 for three binders, with large effects of AP particle size and type of binder. The no-burn domain was larger for lower AP/binder ratios (Fig. 11). Burning rates were depressed and burning was locally intermittent near the no-burn boundaries. These results have suggested melt interference with matrix burning, with fine AP particles being more susceptible than larger ones, and with degree of binder melt interference increasing in going from PBAN/ECA to HTPB/IPDI to HTPB/DDI. While this interpretation seems plausible, it is not quite clear how melt interferes (see above), and the binder thermal response tests (HSM and TGA) and quench tests described above and in App. C did not offer decisive support for a binder melt-flow mechanism. In this regard it should be noted that binder concentration

disproportionation, SLD), and it is not clear that burning must stop when the AP becomes melt-covered. As indicated in Fig. 9, the AP decomposes below the melt surface. However, it should be noted that the matrix surface shown in that figure was from a burning bimodal propellant; the same matrix burning alone might not burn (see 2μm AP matrixes in Fig. 10). It may be more appropriate to look upon failure of a matrix to support burning as a failure to achieve SLD, with due consideration of not only preferential concentration of one ingredient but also how the decomposition of the other ingredient is affected, what is happening to the heat sources, and finally, why the process does not converge on a steady efflux of oxidizer and binder species in the proportions present in the matrix. In some cases (e.g., low AP/binder ratio) it may seem to be simply a classical fuel-rich flammability limit, but if this pertained for the mixes in Fig. 10 and 11, one would have to explain why there is a particle size dependence.

It is appropriate to extend the above SLD arguments to the regions just outside the no-burn domain, where burning is seen to be locally intermittent. It seems likely that SLD failure occurs locally, but heat from adjoining non-quenched sites reconstitutes the quenched site, allowing burning to be handed over among sites with reduced net burning rate. In a bimodal propellant, the conditions for such behavior would depend on the pressure-dependent support provided by the near-surface part of the matrix-coarse AP flame.

FLAME COUPLING

One of the earliest findings about burning of bimodal propellants (reported by Miller, et. al. Ref. 22) was the singular dependence of the r vs p function on the mass ratio of the coarse AP to the fine AP (Fig. 12). This effect appears to be related to the ability of the matrix to dominate rate at low (35%) coarse AP content, and affect the rate in a near plateau-like way at 45% coarse AP; suggesting that the role of the matrix has become less, and "strangely" pressure dependent. The overall results suggest that spacing of the coarse AP particles is important to this effect. However, interpretation is complicated by the fact that the AP/binder ratio in the matrix decreases with increasing coarse AP. The overall trend of results involves what are now known to be two variables that are each important to plateau burning. They cannot be varied independently in propellant mixes[3], so it is not possible to distinguish between effects of coarse AP proximity and matrix AP/binder ratio. However, considerable insight into this subject has been gained from studies of edge burning of sandwiches of matrix lamina between AP laminae. In such tests the spacing between AP lamina and the AP/binder ratios in the matrix can be varied independently. The pertinent results of an intensive study are summarized in Reference 4,23. For the present topic one can summarize by the following (for matrix lamina consisting of 10 μm AP and PBAN binder in ratio 7/3):

a) Sandwich rates are always higher than either the AP rate or the matrix rate, and dependent on matrix thickness and AP/binder ratio of the matrix.

b) A maximum rate at each pressure ocurs for a lamina thickness of about 250 μm, comparable to the average width of matrix pockets in plateau burning bimodal propellants.

[3] Assuming a target overall AP/binder ratio is specified

c) Sandwiches exhibit plateau burning under these particular conditions (e.g. Fig. 2).

d) From interpretation of sandwich burning results, it has been concluded that the matrix flame and the leading edge of the coarse AP-matrix flame are strongly coupled under these conditions (near maxima, Fig. 2).

In short, plateau burning involves not only the pressure dependence of the matrix burning and the coarse AP-matrix diffusion flame, but also the pressure dependence of their interaction under suitable ingredient spacing conditions in the matix.

CATALYSTS

It is generally observed that addition of burning rate catalysts to AP composite propellants eliminates plateau burning. This seems to be consistent with the idea that plateau behavior is due to marginal burning of the matrix. This is illustrated by Fig. 13 for a matrix that burns on its own only at very low pressure. Addition of 0.05% Fe_2O_3 (0.5–1.0 μm) doubled the burning rate and extended the high pressure deflagration limit (HPDL) to over 500 psi. Use of 0.2% Fe_2O_3 increased the burning rate further and gave burning over the whole pressure range tested. In this same formulation, a comparison is made (Fig. 14) between effectiveness of Fe_2O_3 and TiO_2. The trend is the same as with Fe_2O_3, but the TiO_2 was much less effective. In Fig. 15, a comparison is made of several transition metal oxides (TMOs) in a matrix that burns over the whole tested pressure range without catalyst. In these tests the matrix AP size was 10 μm and the catalysts were 0.5–1.0 μm particle size. In this last series all the TMOs behaved like catalysts, but with Fe_2O_3 being the most effective and TiO_2 being the least effective. This trend was born out in DTA tests (Fig. 16) in which samples of matrixes were heated at 10 °C/min up to ignition. The rate of differential temperature rise was highest and time to ignition shortest with 2% Fe_2O_3 catalyst, with strong effect still at 0.05% Fe_2O_3, and only mild effect for 2% TiO_2 (compared to 0% catalyst). This suggests that very low concentrations of Fe_2O_3 would have the same effect as 2% TiO_2 in matrix burning. High concentrations of Fe_2O_3 generally eliminate plateau effects, but it will be shown that very low concentrations do not.

There has been some debate about whether TiO_2 is really a catalyst at all, and if so what reactions are catalyzed. This was examined by running isothermal TGAs at 300 °C on binders, AP and propellant samples, with and without TiO_2. In these tests (Fig. 17), little or no catalysis of decomposition was indicated for HTPB-DDI binder or AP alone, but TiO_2 markedly enhanced the decomposition rate of the propellant. This result suggests that TiO_2 catalyzes reaction between the oxidizer and binder. The DTA results indicate exothermic reactions, presumeably between oxidizer vapors and the binder (surface or vapors). TMOs are known to catalyze the decomposition of $HClO_4$ (exothermic)), and the decomposition products are powerful oxidizers that can react exothermally with the binder, thereby increasing the rate of mass loss of the catalyzed propellant as indicated in Fig. 17.

In the past it has been observed (e.g., Ref. 23,26-28) that TMOs concentrate on the burning surface, and Fe_2O_3 concentrations were observed (Ref. 23-28) even when the iron was introduced in the propellant as liquid ferrocene or via butacene (a binder prepolymer containing Fe atoms). It was concluded that concentration of the catalyst at

the burning surface was essential for effective burning rate enhancement. SEMs of quenched surfaces of the TiO_2-catalyzed propellants used in the present studies, taken at higher magnification often show extensive concentration of TiO_2 on the burning surface, both as clusters on the matrix surface, and structures in the center of the coarse AP surfaces. If concentration is indeed important for the catalysis process, then the dependence of degree of concentration on pressure may be important to plateau burning. To date this issue has not been studied. In this regard, in the case of Fig. 5, the TiO_2 structures on the coarse AP apparently do not modify the particle burning, since the quenched surfaces of a matching formulation with no TiO_2 show the same coarse AP surface configurations. This suggests that one should look to pressure dependence of catalyst concentration in the matrix areas.

If plateau burning of bimodal propellants is related to the marginality of the matrix burning, the present results indicate that the matrix marginality is diminished by catalyts, possibly explaining the general perception that catalysts eliminate plateau burning in the propellant. However, the results indicate that the matrix burning can be "tailored" by using very low concentrations of catalyst, the amount being dependent on the particular catalyst. However, an unresolved dilemma is posed by the fact that conditions for such matrix behavior as no-burn domains have not yet been correlated with particular features of the bimodal propellant plateaus. This is illustrated in Fig. 18, which compares burning data for two matrixes (one uncatalyzed and one with 2% TiO_2) and for the corresponding bimodal propellants. The catalyst establishes relatively normal burning of the matrix except for high pressure dependence of rate starting at 1000 psi, a property manifested also by the uncatalyzed and catalyzed propellant. The catalyzed propellant had a much enhanced rate at all pressures, with a plateau in the 600–1000 psi interval, not exhibited by the catalyzed matrix (but with a no-burn domain of the uncatalyzed matrix). Figure 19 shows the effect of TiO_2 in a bimodal AP propellant with HTPB/DDI/DOA binder with two different concentrations of 0.5 μm TiO_2 (2% and 4%). The rates are independent of % TiO_2, but the mix with 2% TiO_2 would not sustain burning above 700 psi, while the mix with 4% TiO_2 exhibited an increase in $\partial r/\partial p$ at the same pressure. Tests on the matrix burning alone yielded rates similar to the bimodal propellant, but they would not sustain burning above 215 psi (where a change in $\partial r/\partial p$ occurs with the bimodal propellant).

Similar formulations to those in Fig. 19 were made with 0.5 μm Fe_2O_3 catalyst. The rates of the 0.2% and 0.1% mixes are shown in Fig. 20, along with the result for 4% TiO_2. The most notable feature of this comparison is that 0.1% Fe_2O_3 gives a higher rate than 4% TiO_2, but the samples would not sustain burning above 1200 psi. In a further effort to find out what the catalysts are doing, a comparison was made of the matrix rate, propellant rate and a matrix consisting of the coarse AP, binder and catalyst. Figure 21 shows the results for 0.2% Fe_2O_3 and for 4% TiO_2 (these percentages refer to concentrations in the matrix). The most notable features of the results are: a) the propellant and fine AP matrix rates are almost the same with Fe_2O_3; b) the coarse AP binder matrix burned erratically above 700 psi; c) the coarse AP/binder matrix with 4% TiO_2 burned on the whole pressure range tested; d) where it sustained burning, the coarse AP matrix with Fe_2O_3 burned at a considerably higher rate than the matrix with TiO_2.

While the results to date with catalysts seem to be "telling us something", the research was suspended prematurely (the apparent fate of all other studies that involve

TiO_2 burned on the whole pressure range tested; d) where it sustained burning, the coarse AP matrix with Fe_2O_3 burned at a considerably higher rate than the matrix with TiO_2.

While the results to date with catalysts seem to be "telling us something", the research was suspended prematurely (the apparent fate of all other studies that involve too many variables and operative mechanisms). However some valuable insights have emerged. Even this superficial coverage shows that all catalysts are not alike, and that enhancement of rate and elimination of erratic burning don't follow the same rules. Further, the "rule" that bimodal propellants burn faster than their matrixes alone is broken with Fe_2O_3 catalyst (at least 0.2% catalyst, Fig. 21a). Unfortunately, these findings may depend on the particular set of formulation variables chosen. However, some generalizations about catalysts from this and previous studies merit review in the future, especially with regard to pressure dependence.

Catalysts act in several ways:

a) at low pressure they can indirectly catalyze the premixed flame by breaking down heavy fuel molecules into more reactive vapors, causing the flame to stand closer to the surface (Ref. 26-27/App. R);

b) if the matrix AP particles are small enough (high surface area and short diffusion distances), the catalyst can cause $HClO_4$ decomposition and reaction within the porous surface layer (all pressures, depending on degree of catalyst concentration on the surface, but particularly at low pressure because of more time for such reactions)(Ref. 23,27/App. R);

c) at higher pressures where the leading edges of the AP/matrix diffusion flames become important, the catalytic breakdown of fuel molecules acts locally around the oxidizer perimeter by allowing the leading edge flame to stabilize closer to the surface (Ref. 26,28);

d)effectiveness of a catalyst depends on its "ability" to concentrate on the burning surface(Ref. 5,7,8,23,27/App. D,F,G,R); and

e) to the extent that "melt suppression" of burning rate is a factor in plateau burning, too much catalysis may defeat it.

SUMMARY

This paper consists of only a part of a larger study, some of which is reported also in Ref. 2,3,5-17,25,27/App. B,C,D-R; previously unpublished results are present in App. C. The goal here was to highlight some findings and mechanistic interpretations that seem to be essential to understanding how bimodal AP propellants burn. To understand "plateau" burning, it would be necessary to establish the role of each mechanism, how it changes with pressure, and how the interactions between them change with pressure. The present findings do not constitute a theory of plateau burning, but do provide valuable insights for further research. Particularly for the binders used here, some of those insights involved are listed below (bimodal AP propellants).

Surface Layer

The surface layer of the matrix areas is the site of binder melt effects on burning and the melt effects appear to act by (binder-dependent) filling of depressions left by

particle size, and almost surely on concentration of catalyst in the layer. The exothermic reactions in the layer necessarily involve decomposition of $HClO_4$ and reactions of the vapor products with binder melt and/or binder vapors in a porous surface layer.

Matrix burning

Fine AP/binder matrixes require heat supply from their own fuel rich gas phase flame, which appears to be a premixed one for small AP particles (under 20 μm). In the matrix oxidizer/binder ratios typical of plateau propellants, their burning is marginal without catalysts. Fe_2O_3 is much more effective than TiO_2. Burning alone, matrixes almost always burn slower than the bimodal propellant at all pressures. The improved burning with catalyst is probably due to both increased surface layer heat release and to catalytic break down of the large fuel vapor molecules (which are more reactive in the gas matrix flame, causing the flame to stand closer to the surface).

Coarse AP Particles

Deflagration rate of these particles is always lower than the propellant rate (except at low pressure where the whole flame is premixed), and contributes little to overall rate, except in close proximity to the matrix. There, along the outer periphery, a hot stoichiometric diffusion flame occurs with its leading edge close to the coarse AP/matrix contact lines. This LEF apparently supports the marginal matrix burning, accounting for the higher propellant rate. Earlier sandwich burning studies indicate that the burning rate is a maximum for matrix area dimensions typical of plateau propellants, and sandwiches exhibit plateau burning under these conditions (Fig. 2). These observations relate to the critical aspects of mass fraction and particle size of the coarse AP in the propellant, which control the lateral dimensions of the matrix areas. As noted in sandwich burning tests, the hot LEFs also respond to catalytic fuel "cracking".

Surface Layer Disproportionation (SLD)

This concept has to do with adjustments in the surface layer that are necessary in order for the average flux of species from the surface to match the composition of the propellant. If the combined physical and chemical processes do not lead to successful disproportionation, steady burning cannot occur, i.e., some ingredient will concentrate without limit until burning stops. Several significant examples of SLD were evident and/or suggested in the present study. The most obvious was the protrusion of coarse AP particles illustrated in Fig. 5b. Another is the concentration of nonvolatile catalysts on the surface. Another is the tendency for binder melt to occupy a disproportionate portion of the matrix surface. One more has to do with the fact that binders break down into liquid intermediates with different thermal stabilities, a situation that would be expected to lead to more stable intermediates at the surface with less stable intermediates decomposing and bubbling up from below (foam?). Observations of local intermittency of burning seen to contribute to the low burning rate associated with plateaus and spontaneous quenches.

to more stable intermediates at the surface with less stable intermediates decomposing and bubbling up from below (foam?). Observations of local intermittency of burning seen to contribute to the low burning rate associated with plateaus and spontaneous quenches.

ACKNOWLEDGEMENTS

This work was performed under contract N00014-95-1-0559 with the Office of Naval Research; Drs. Judah Goldwasser and Richard S. Miller were the technical monitors.

REFERENCES

1. Price, E. W., Sigman, R. K., Chakravarthy, S. R., Chaing, H-J, Beiter, C. A., and Prasad, K., "Mechanism of Combustion of Heterogeneous Solid Propellants," Final Report, Office of Naval Research Contract N00014-89-J-1293, Sept 1998.
2. Price, E. W., Chakravarthy, S. R., Freeman, J. M., and Sigman, R. K., "Combustion of Solid Propellants and Sandwiches with Ammonium Dinitrimide," *Proceedings of the 34th JANNAF Combustion Subcommittee Meeting*, West Palm Beach, FL, Oct. 1997, CPIA Publication 662, Vol. II, pp. 415-425 (Attached as Appendix A).
3. Price, E. W., Chakravarthy, S. R., Freeman, J. M., and Sigman, R. K., "Combustion of Propellants with Ammonium Dinitrimide," *AIAA Paper 98-3387,* 34th AIAA/ASME/SAE/ASEE Joint Propulsion Conference and Exhibit, Cleveland, OH, July 13-15, 1998 (Attached as Appendix B).
4. Price, E. W., "Review of Sandwich Burning," *Proceedings of the 30th JANNAF Combustion Subcommittee Meeting,* Monterey, CA, November, 1993 .
5. Price, E. W., "Effect of Multidimensional Flamelets in Composite Propellant Combustion," *AIAA Journal of Propulsion and Power,* Vol. 11, No. 4, pp. 717-728 (Attached as Appendix D).
6. Chakravarthy, S. R., Price, E. W., and Sigman, R. K., "Binder Melt Flow Effects in the Combustion of AP – HC Composite Solid Propellants", *AIAA Paper 95-2710*, 31st AIAA/ASME/SAE/ASEE Joint Propulsion Conference and Exhibit, San Diego, CA, July 10-12, 1995 (Attached as Appendix E).
7. Price, E. W., Chakravarthy, S. R., Sigman, R. K., and Freeman, J. M., "Pressure Dependence of Burning Rate of Ammonium Perchlorate-Hydrocarbon Binder Solid Propellants," *AIAA Paper 97-3106*, 33rd AIAA/ASME/SAE/ASEE Joint Propulsion Conference and Exhibit, Seattle, WA, July 6-9, 1997 (Attached as Appendix F).
8. Price, E. W., Freeman, J. M., Jeenu, R., Chakravarthy, S. R., Sigman, R. K., and Seitzman, J. M., "Plateau Burning of Ammonium Perchlorate Propellants," *AIAA Paper 99-2364*, 35th AIAA/ASME/SAE/ASEE Joint Propulsion Conference and Exhibit, Los Angeles, CA, June 20-24, 1999 (Attached as Appendix G).
9. Freeman, J. M., Price, E. W., Chakravarthy, S. R., and Sigman, R. K., "Burning Characteristics of Monomodal Ammonium Perchlorate/Hydrocarbon Binder Propellants," *Proceedings of the 34th JANNAF Combustion Subcommittee Meeting*, CPIA Pub. 662, West Palm Beach, FL, October 27-30, 1997 (Attached as Appendix H).
10. Freeman, J. M., Price, E. W., Chakravarthy, S. R., and Sigman, R. K., "Contribution of Monomodal AP/HC Propellants to Bimodal Plateau-Burning Propellants," *AIAA*

Paper 98-3388, 34th AIAA/ASME/SAE/ASEE Joint Propellant Conference and Exhibit, Cleveland, OH, July 13-15, 1998 (Attached as Appendix I).

11. Price, E. W., Chakravarthy, S. R., Sigman, R. K., and Freeman, J. M., "Anomalous Combustion Behavior of Ammonium Perchlorate at Elevated Pressures," *Proceedings of the 33rd JANNAF Combustion Subcommittee Meeting*, Monterey, CA, Nov. 1996 (Attached as Appendix J).
12. Freeman, J. M., Jeenu, R., Price, E. W., and Sigman, R. K., "Effect of Matrix Variables on Bimodal Propellant Combustion," *Proceedings of the 35th JANNAF Combustion Subcommittee Meeting*, Tucson, AZ, Dec. 1998 (Attached as Appendix K).
13. Price, E. W., Chakravarthy, S. R., Sambamurthi, J. K., and Sigman, R. K., "Leading Edge Flame Detachment; Effect of Burning Rate on Ammonium Perchlorate Propellants," *Proceedings of the 30th JANNAF Combustion Subcommittee Meeting*, Monterey, CA, Dec. 1993 (Attached as Appendix L).
14. Price, E. W., Chakravarthy, S. R. Sambamurthi, J. K., and Sigman, R. K., "The Details of Ammonium Perchlorate Propellants: Leading Edge Flame Detachment," *Combustion Science and Technology,* Vol. 138, 1998, pp. 63-83 (Attached as Appendix M).
15. Price, E. W., Chakravarthy, S. R., Freeman, J. M., and Sigman, R. K., "Surface Features of AP Composite Propellants," *Proceedings of the 34th JANNAF Combustion Subcommittee Meeting*, West Palm Beach, FL, October 27-30, 1997 CPIA Pub. 662, Vol. IV, pp. 45-71 (Attached as Appendix N).
16. Price, E. W., Jeenu, R., Freeman, J. M., and Sigman, R. K., "Burning Surface Features of Four Bimodal AP Plateau Propellants (as inferred from dp/dt quench samples for four pressures)," presentation at ONR/MURI workshop, Reno, NV, Jan. 1998 (Attached as Appendix O).
17. Price, E. W., Jeenu, R., Freeman, J. M., and Sigman, R. K., "Quenched Surface Studies of Plateau Propellants," *Proceedings of the 35th JANNAF Combustion Meeting,* Tucson, AZ, Dec. 1998 (Attached as Appendix P).
18. Bastress, E. K., "Modification of the Burning Rates of Ammonium Perchlorate Solid Propellants," Ph. D. Thesis, Princeton University, Princeton, NJ, January, 1961.
19. Steinz, J. A., Stang, P. L., and Summerfield, M., "Effects of Oxidizer Particle Size on Composite Solid Propellant Burning: Normal Burning, Plateau Burning, and Intermediate Pressure Extinction," Aerospace and Mechanical Sciences Rept No. 810, Guggenheim Laboratories for the Aerospace Propulsion Sciences, Princeton University, Princeton, NJ, Oct. 1967.
20. Steinz, J. A., Stang, P. L., and Summerfield, M., "The Burning Mechanism of Ammonium Perchlorate-Based Solid Propellant Rockets," AIAA Paper # 68-658, *4th Propulsion Joint Specialists Conference,* June 10-14, 1968.
21. Steinz, J. A., Stang, P. L., and Summerfield, M., "The Burning Mechanism of Ammonium Perchlorate-Base Composite Solid Propellants," Aerospace and Mechanical Sciences Rept. No. 830, Guggenheim Laboratories for the Aerospace Propulsion Sciences, Princeton University, Princeton, NJ, Feb. 1969.
22. Miller, R. R., "Anomalous Ballistic Behavior of Reduced Smoke Propellants with wide AP Distributions," *Proceedings of the 15th JANNAF Combustion Meeting,* CPIA Pub. 297, Vol. II, Feb. 1979, pp. 265-269.

24. Price, E. W., Sigman, R. K., Chakravarthy, S. R., and Paulsen, P. D., "Hot Stage Microscope Studies of Decomposition of Propellant Ingredients," *Proceedings of the 30th JANNAF Combustion Meeting,* Monterey, CA, Nov. 1993, CPIA Pub. 606, Vol. II, pp. 289-296.
25. Price, E. W., Chakravarthy, S. R., Zachary, E. K., and Sigman, R. K., "Ingredient Response and Interaction during Heating in a Hot State Microscope," *Proceedings of the 31st JANNAF Combustion Subcommittee Meeting,* San Jose, CA, Oct. 1994 (Attached as Appendix K).
26. Price, E. W. and Sambamurthi, J. K., "Mechanism of Burning Rate Enhancement by Ferric Oxide," *Proceedings of the 21st JANNAF Combustion Subcommittee Meeting,* CPIA Pub. 412, Vol. I, 1985.
27. Chakravarthy, S. R., Price, E. W., and Sigman, R. K., "Mechanism of Burning Rate Enhancement of Composite Solid Propellants by Ferric Oxide," *AIAA Journal of Propulsion and Power,* Vol. 13, No. 4, July-Aug 1997, pp. 471-480 (Attached as Appendix R).
28. Markou, C. P., "Effect of Different Binders and Additives on Sandwich Burning," Ph. D. Thesis, School of Aerospace Engineering, Georgia Tech, Atlanta, GA, May, 1988.
29. Horton, M. D. and Price, E. W., "Deflagration of Pressed Ammonium Perchlorate," *ARS Journal,* Vol. 32, No. 11, Nov. 1962.
30. Boggs, T. L., "Deflagration Rate, Surface Structure, and Subsurface Profile of Self-Deflagrating Single Crystals of Ammonium Perchlorate," *AIAA Journal,* Vol. 8, No. 4, May, 1970, pp. 867-873.
31. Lengelle, G., Duterque, J., Trubert, J. F., "Solid Propellant Combustion," *AIAA Journal of Propulsion and Power,*(to be published).

Figures

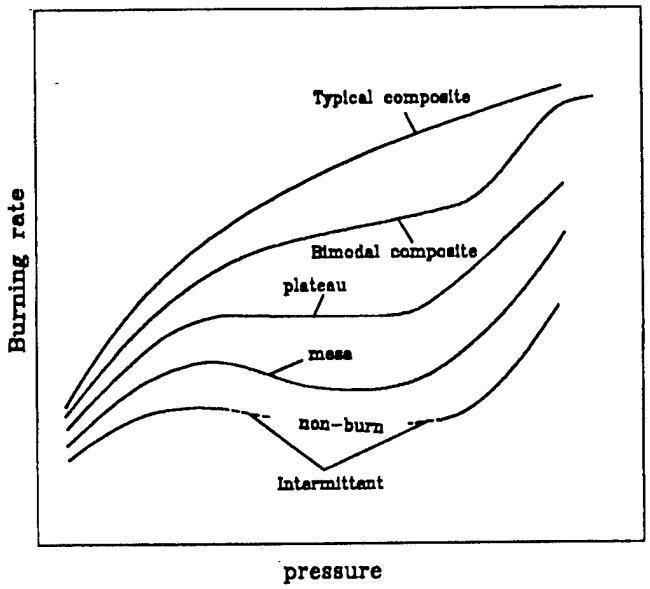

Fig. 1 Pressure dependence on burning rates of propellants.

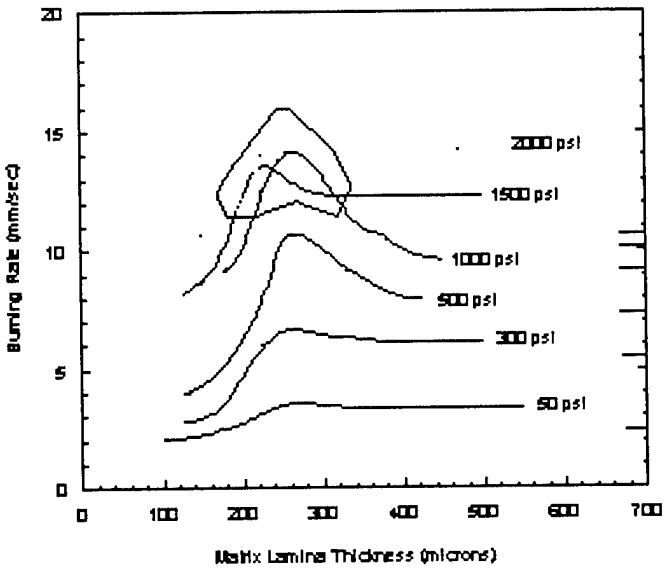

Fig. 2. Burning rates of edge-burned sandwiches of matrix between two AP lamina. The matrix was 70% 10 μm AP, 30% PBAN/ECA. The abcissa is lamina thickness. The AP rates are marked on the left ordinate scale, and the matrix rates.

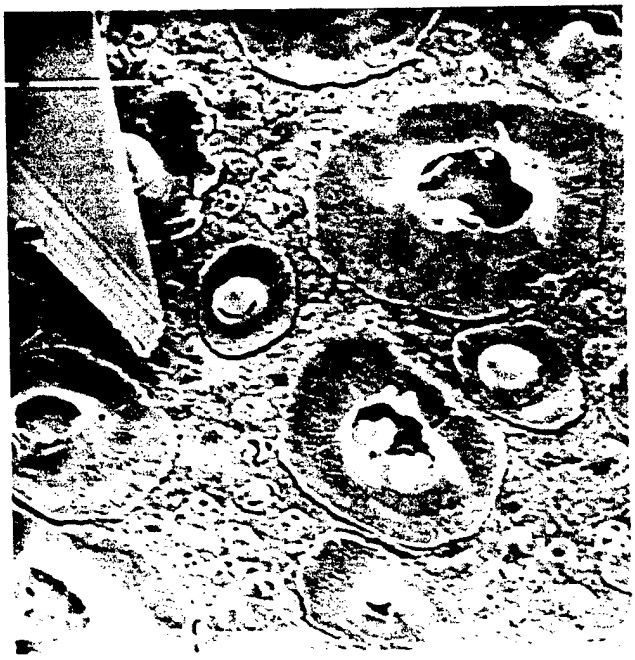

Fig. 3. A quenched burning surface that illustrates the disposition of coarse AP and matrix arears for a plateau-burning bimodal AP propellants (200μm coarse AP, 2m fine AP)(the sharp object is a knife blade).

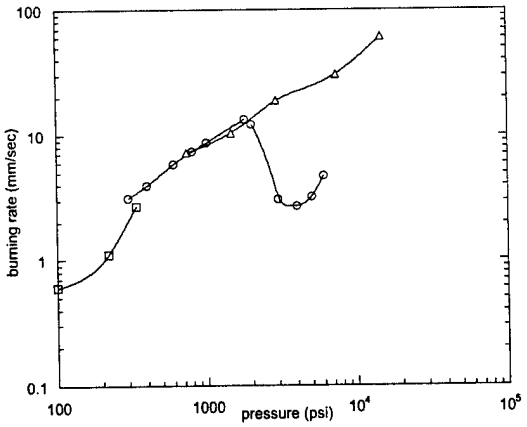

Fig. 4. AP "self" deflagration rate; □ refers to large AP discs with peripheral inhibitor (Ref. 29); O refers to single crystals burning in an N_2 atmosphere (Ref.30); Δ refers to inhibited strands (Ref. 31).

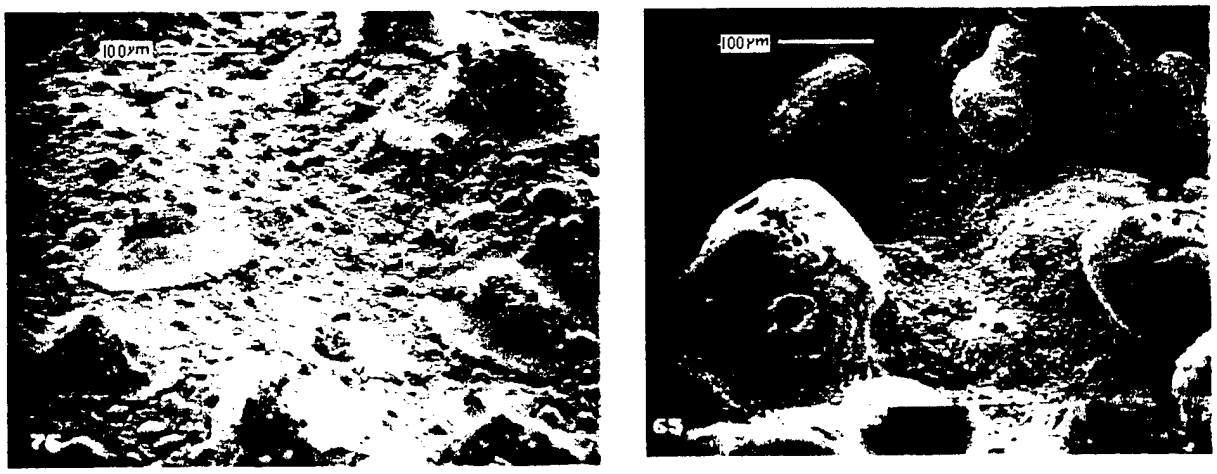

(a) (b)

Fig. 5. Quenched surfaces of a bimodal AP mesa-burning propellant (HTPB/DDI/DOA binder) at a) 200 psi and b) 1800 psi. (from App. G.)

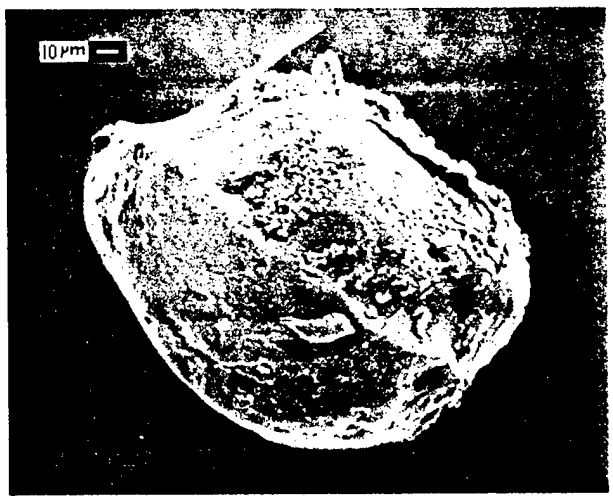

Fig. 6. A partially burned AP particle removed from the quenched surface of a sample corresponding to Fig. 5b (lower left section below the burning surface). (from App. G)

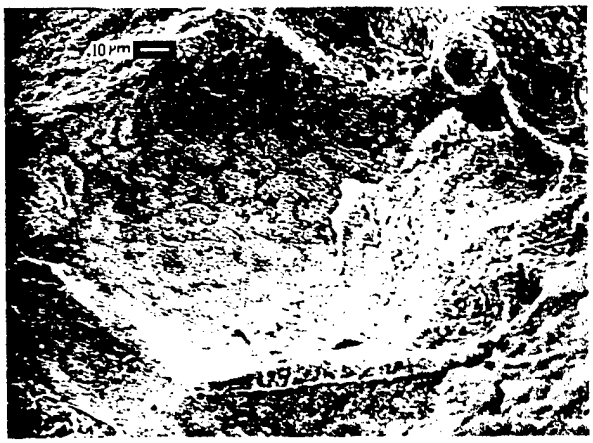

Fig. 7. Quenched surface of a slow burning bimodal plateau propellant under rather rare conditions where the AP rate exceeds the propellant rate. The picture shows a large recess where a 200 µm particle is in the last stages of burnout. (From App. G)

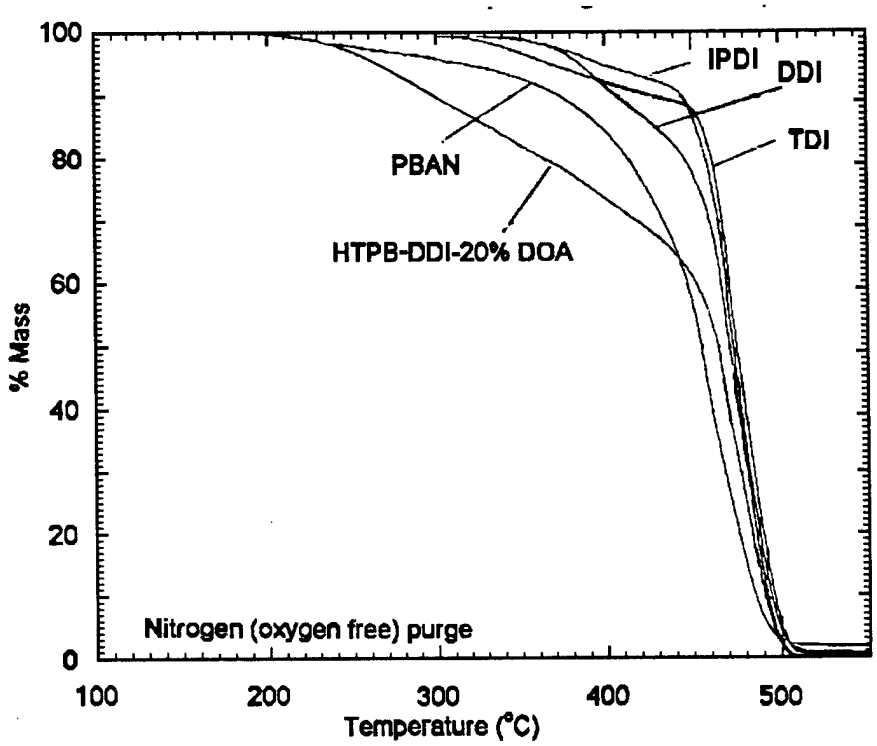

Fig. 8. Results of thermogravimetric analysis (TGA at a heating rate of 20°C/min). IPDI, DDI, and TDI refer to the curing agent used. (From App. C)

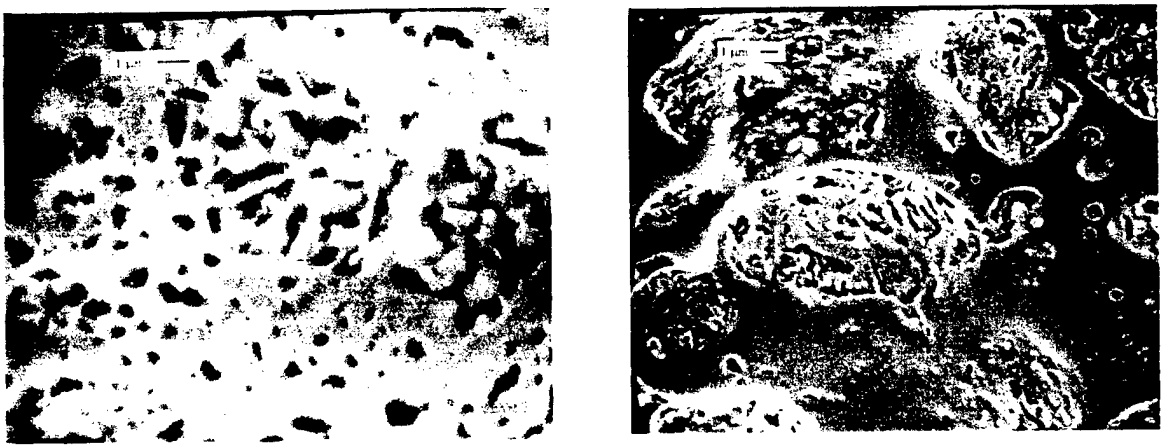

(a) (b)

Fig. 9. Matrix features of the quenched surfaces of two bimodal propellants that differed primarily in size of the fine AP particles (note differences in scale). HTPB/DDI/DOA binder, 200 μm AP, and a) 2μm matrix AP, b) 10 μm matrix AP.

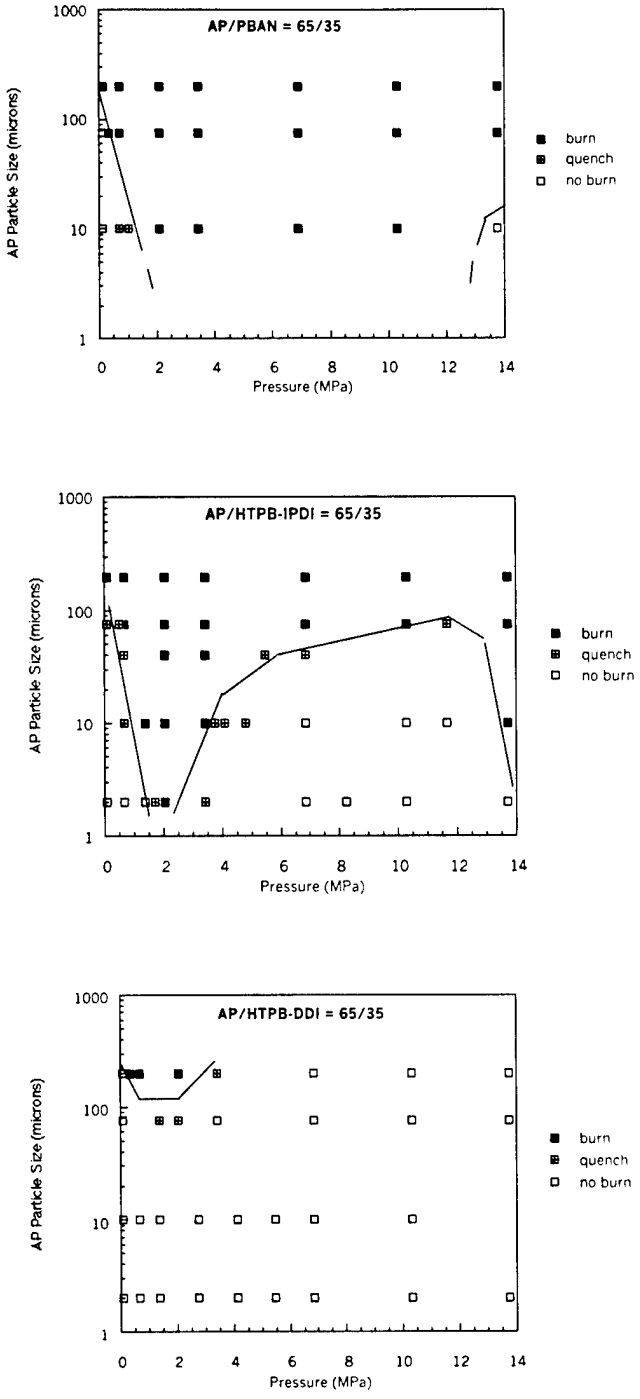

Fig. 10. No-burn domains for matrixes of 65% AP/35% binder for three binders showing sensitivity to types of binder. a) PBAN/ECA, b) HTPB/IPDI, c) HTPB/DDI. Burning will not sustain in areas below the indicated boundaries. PBAN matrix burned under nearly all conditions tested. HTPB/IPDI matrixes failed to burn under most conditions. See App. F for details.

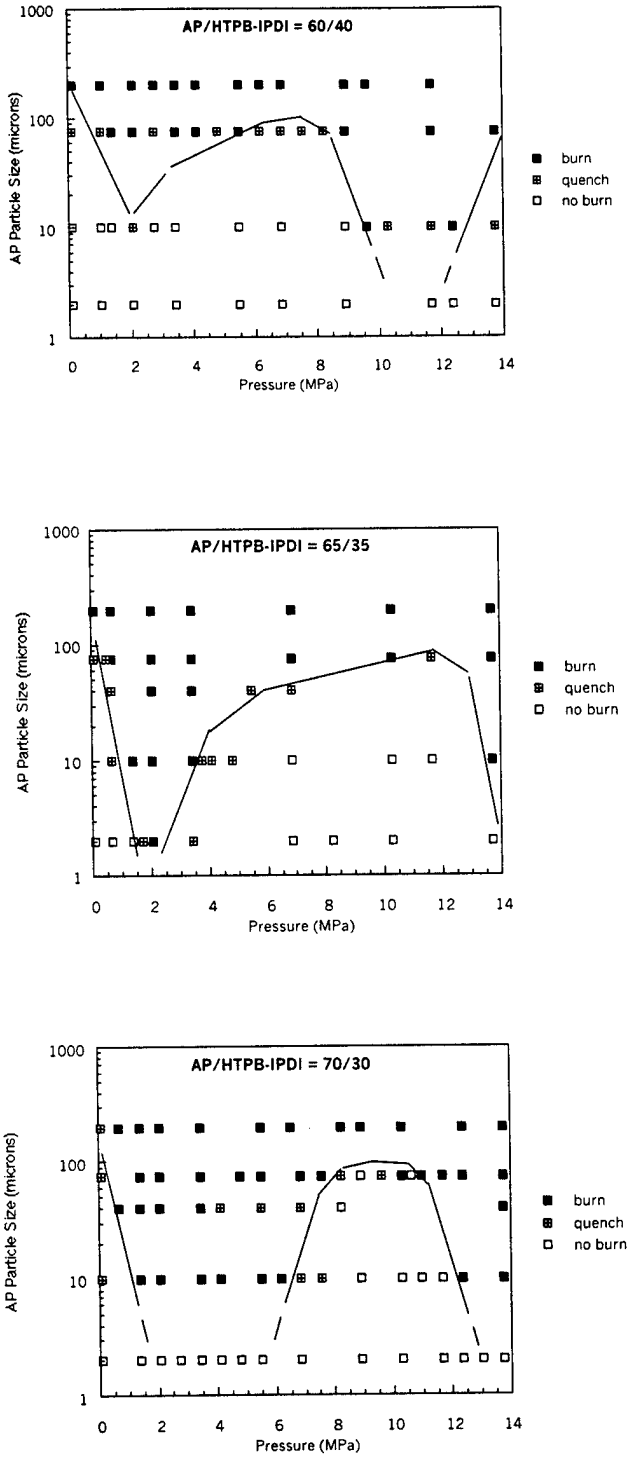

Fig. 11. No burn domains for matrixes with HTPB/IPDI binder and different ratios of AP and binder: a) 64/40, b) 65/35, c)70/30. See App. G for details.

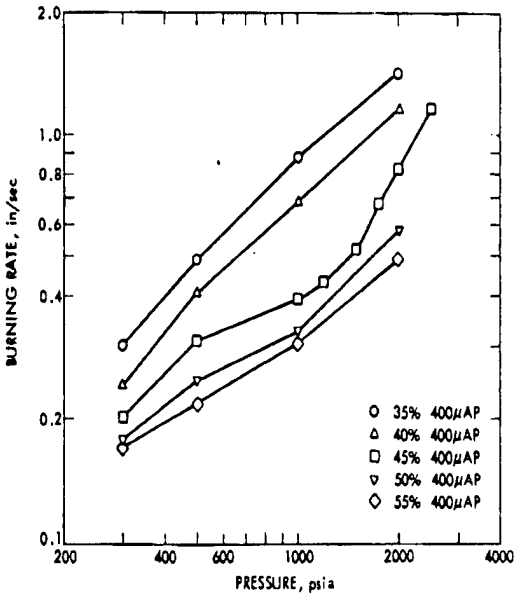

Fig. 12. Dependence of burning rate vs pressure for a bimodal propellant on fine AP to coarse AP. HTPB/IPDI binder 400 μm coarse AP, μm fine AP, approx. 88% AP. See Ref. 22 for details.

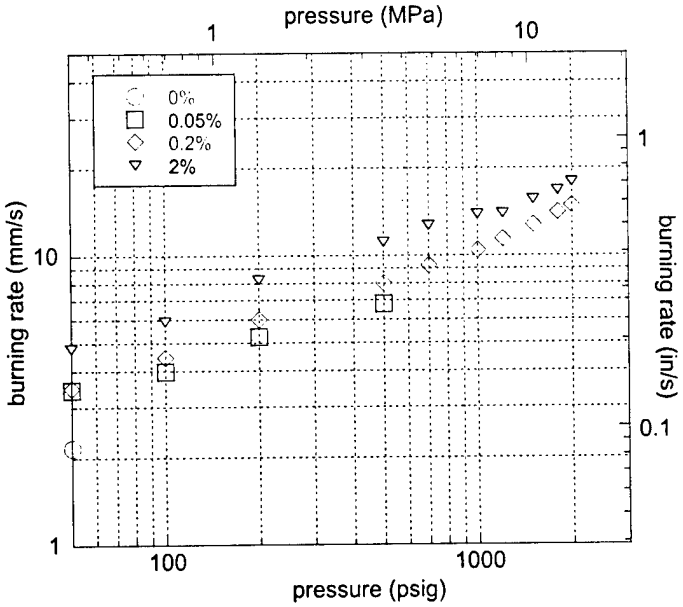

Fig. 13. Effect of Fe_2O_3 catalyst on the burning rate of a 73% 10μm AP/23% HTPB/DDI matrix (the uncatalysed matrix burned only in the 50 psi test). See App. K for details.

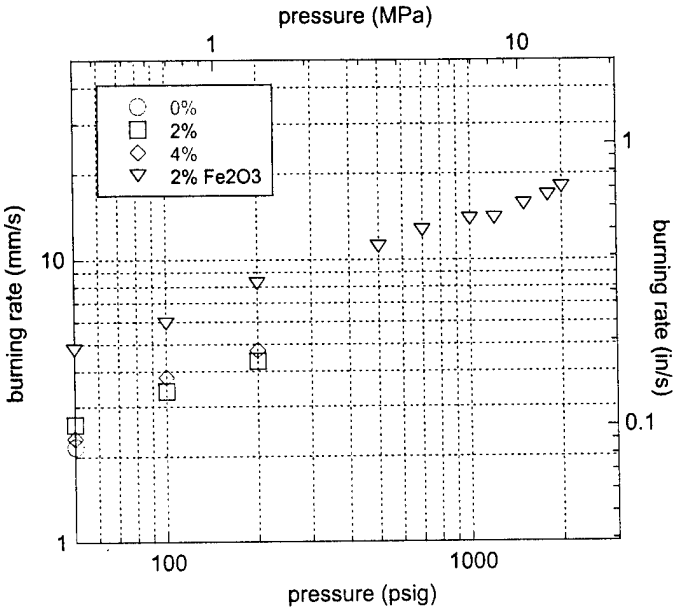

Fig. 14. Effect of TiO_2 catalyst (same matrix as Fig. 13). One curve for 2% Fe_2O_3 is included for comparison. See App. K for details.

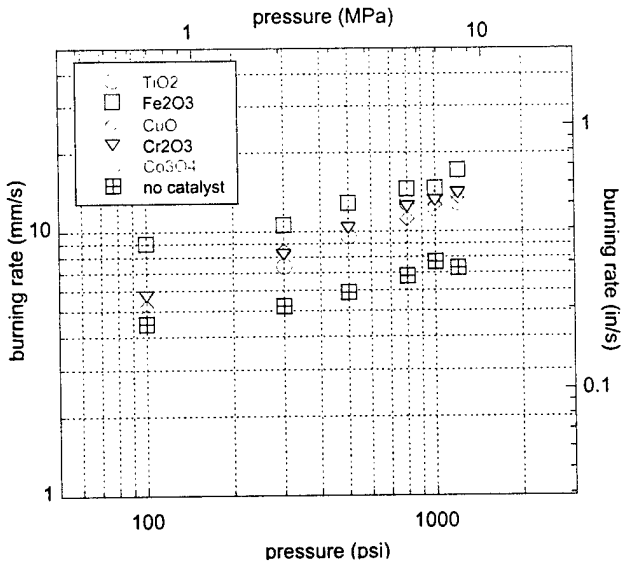

Fig. 15. Effect of several transition metal oxides on the burning rate of a 70% 10 μm AP/30% PBAN-ECA matrix (4% catalyst, nominally 1μm particle size) See App. K for details.

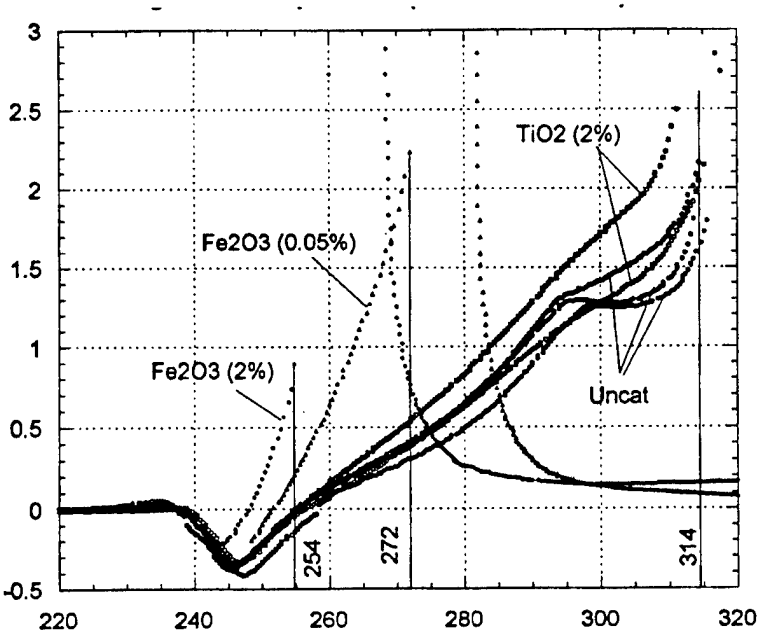

Fig. 16. Comparison of matrix endotherms and ignition in DTA test for different catalysts. Matrixes were 73% 10 μm AP/ 27% HTPB-DDI-DOA binder (catalyst added)(See App. G for details.).

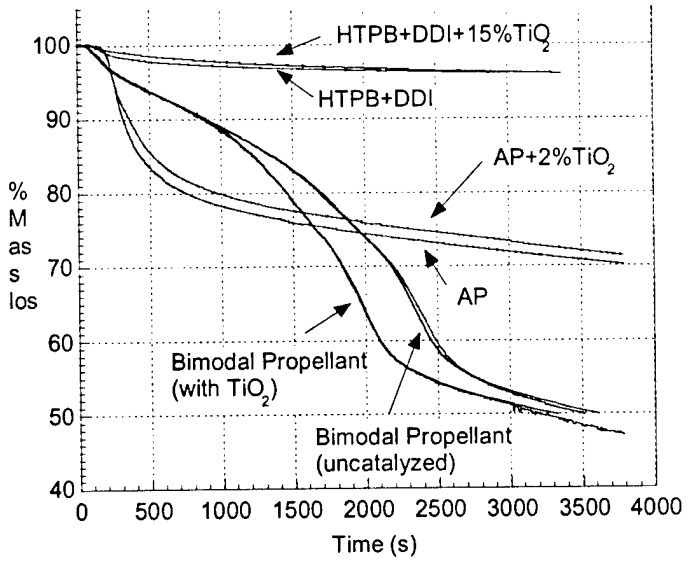

Fig. 17. Comparison of the effect of TiO_2 additive (0.5 μm) in binder, oxidizer and propellant. Sample %mass loss vs time for isothermal decomposition at 300°C. The propellant samples used bimodal AP 62/38 coarse to fine, 200 μm and 2 μm AP; 12% HTPB/DDI/DOA(.69/.17/.14) (See App. G for details.).

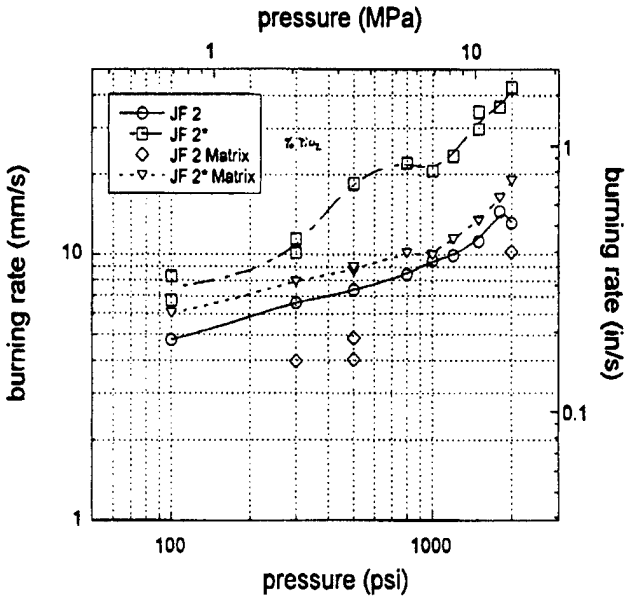

Fig. 18. Effect of TiO_2 (0.02 μm) on the burning of a bimodal propellant and the corresponding matrix. Propellant was 58.3% 200 μm AP, 29.2% 10 μm AP, 12% HTPD/IPDI binder, TiO_2 added (4% in matrix). ◊, uncatalyzed matrix (some samples self-extinguished); ∇, catalyzed matrix; O, uncatalyzed propellant; □ catalyzed propellant.

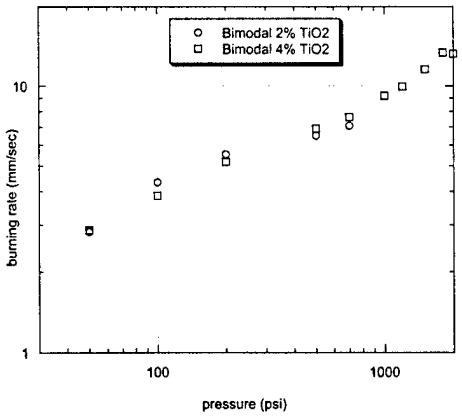

Fig. 19. Effect of catalyst concentration on burning of a bimodal propellant: 55.5% 200 μm AP, 32.4% 10 μm AP, 12% binder (HTPB/DDI/DOA 69/14/17), TiO_2 added. The 2% mix did bot sustain burning above 700 psi..

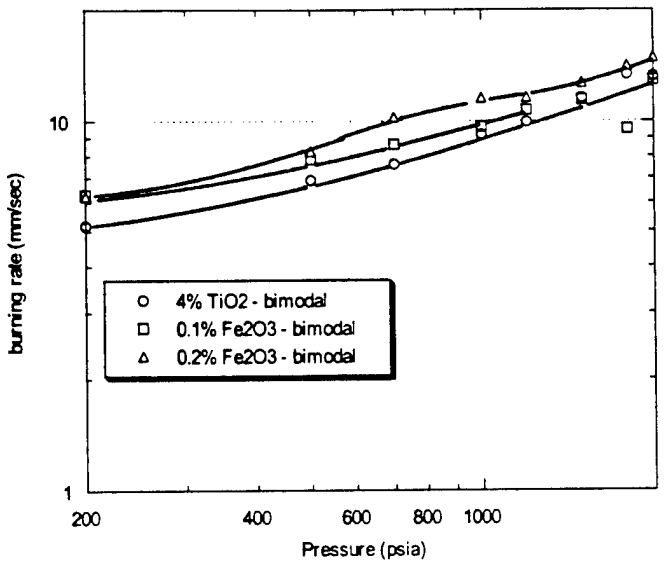

Fig. 20. Comparison of the catalysis of Fe_2O_3 and TiO_2. The basic formulations are the same as in Fig. 19.

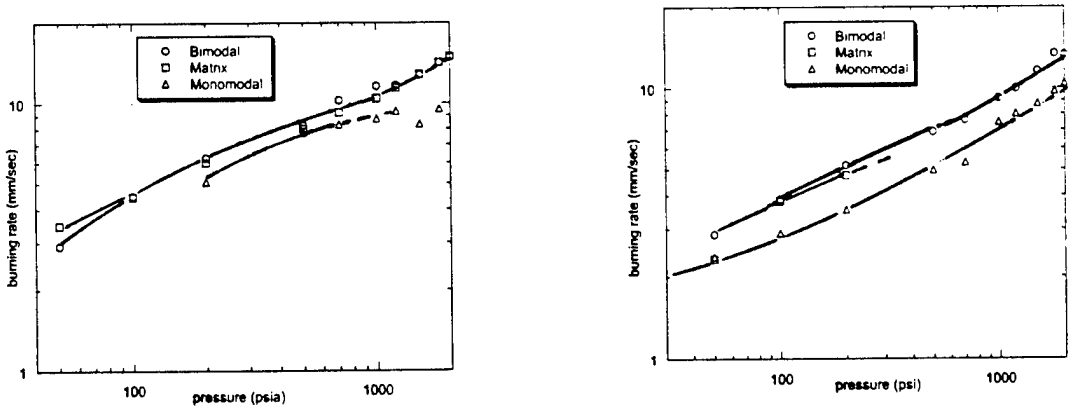

Fig. 21. Comparison of a bimodal propellant rate, matrix rate, and rate of a matrix consisting of the coarse AP and binder in the same ratio as the fine AP matrix, each with 0.2% Fe_2O_3 in (a) and 4% TiO_2 in (b). Basic formulations the same as in Fig. 19. Broken lines designate irregular burning.

APPENDIX A

Price, E. W., Chakravarthy, S. R., Freeman, J. M., and Sigman, R. K.

"Combustion of Solid Propellants and Sandwiches with Ammonium Dinitrimide"

Proceedings of the 34TH JANNAF Combustion Subcommittee Meeting

West Palm Beach, FL, Oct. 1997

CPIA Publication 662, Vol. II, pp. 415-425

COMBUSTION OF SOLID PROPELLANTS AND SANDWICHES WITH AMMONIUM DINITRAMIDE

E. W. Price, S.R. Chakravarthy, J.M. Freeman, and R.K. Sigman
Georgia Institute of Technology, Atlanta, Georgia 30332-0150

Abstract

This paper reports a series of experiments involving ammonium dinitramide (ADN), a new energetic oxidizer of potential use in composite solid propellants. The experiments include (a) self-deflagration of pressed pellets of ADN; (b) combustion of sandwiches with ADN laminae on both sides of a binder lamina that is either "pure" or filled with particulate oxidizer and other additives; and, (c) combustion of propellants with a bimodal oxidizer size distribution, wherein, combustion of coarse ADN and fine AP (ammonium perchlorate) and vice versa were used besides all-ADN formulations.

The results indicate the possibility of a major role for condensed phase heat release in the control of the self-deflagration of ADN, resulting in very high rates compared to that of AP self-deflagration. The sandwich burning rates are always slightly above the ADN self-deflagration rate, but follow the same trend as pressure is varied. This indicates a role for the oxidizer/fuel (O/F) flame present in the sandwiches, which seems to assist the self-deflagration of the ADN laminae. Results with oxidizer filled sandwiches show that O/F flame-assisted self-deflagration of ADN lamina always controls the sandwich burning rate regardless of the contents of the binder lamina (ADN or AP particles, with or without very fine ferric oxide catalyst or aluminum). A family of bimodal propellants reflect the sandwich results by showing higher rates for formulations with coarse ADN and any fine oxidizer (ADN or AP) than those with coarse AP and fine ADN or AP.

Introduction and Test Plan

This is an abbreviated report of experiments on deflagration of ADN alone, and in combinations involving dry pressed ADN-aluminum mixes, sandwiches and propellants. The ingredients were:

a) ADN from three different suppliers; 30μm prilled ADN from Dr. Alfred Stern at the Nave Surface Weapons Center, 350μm prilled from Dr. John Guimont at the Chemical Systems division of united Technologies and crystalline powder from Dr. John Wardle at Thiokol,
b) aluminum included H-30 and ALEX,*

This research was sponsored under ONR contract No. N00014-95-0559, technical monitor Dr. Richard S. Miller.

Approved for public release; distribution is unlimited.

c) AP (commercial grade, no TCP) from WECCO (ground and sieved to size), and
d) PBAN binder, 64.14% PBAN prepolymer, 20.86% ECA, and 15.00% DOA.

Tests were run on:

a) hard-pressed ADN laminae,
b) hard pressed mixes of ADN with 10% H-30 and with 10% ALEX aluminum (and comparison tests with AP),
c) sandwiches with ADN laminae and central laminae of PBAN, matrix of ADN and PBAN, and of AP and PBAN,
d) sandwiches with AP laminae and central matrix laminae of ADN and PBAN and of AP and PBAN,
e) sandwiches with ADN and with AP laminae with 7/3 AP/PBAN laminae containing 1% Pyrocat, and
f) bimodal PBAN propellants with 87.5% solids, two coarse to fine ratios, with AP and/or ADN (Table I).

In some cases tests were run at only one pressure (item b and a series in item c at 500 psi. with a PBAN binder lamina, rate versus lamina thickness). Other tests were mostly run over a pressure range of 100-1500 psi.

Results of the tests are shown in Figs 1-7. Summarizing comments on results and significance are made in the following figure by figure commentaries

Figure-by-Figure

Fig. 1: In this pressure range the rate is high compared to AP, and the pressure dependence of rate is low. The rates are dependent on ADN material used. There is appreciable scatter, so that the detailed trends with pressure may not be meaningful.

Fig. 2: The burning rate at 200 psi. of AP/PBAN sandwiches was slightly increased when 10% ALEX was added to the binder lamina; 10%, H-30 reduced the rate moderately. The burning rate of dry pressed ADN was substantially increased by addition of either ALEX or H-30. The combustion photography showed good ignition of ALEX, non-ignition of H-30. In corresponding tests with AP, addition of either aluminum resulted in non-burns at 300 psi. The interpretation is that:

a) fine aluminum does not agglomerate, while H-30 does and fails to ignite;
b) the enhancement in rate is apparently related to enhanced thermal conductivity or possibly to aluminum reaction at the surface, with the H-30 reaction limiting ignition by formation of sintered accumulates that resist ignition;
c) corresponding AP/Al samples would not ignite at this pressure, presumably because the surface layer exotherm of ADN is absent with AP;

d) when aluminum was added to the PBAN lamina with ADN outer laminae, the burning rate was unaffected by addition of either aluminum. The ALEX burned more rigorously, while H-30 burned as agglomerates, an outcome suggesting that the O/F flame is hot enough to ignite the aluminum, but the radiative heat release to the surface is not enough to affect rate in an ADN-binder system.

Fig. 3: The rate of ADN/PBAN sandwiches is higher than the ADN rate (whole pressure range). This indicates that the ADN/fuel flame occurs near enough to the ADN surface to enhance its rate.

Fig. 4: The rate of ADN/PBAN sandwiches was determined at 500 psi. for different PBAN lamina thicknesses up to 85μm. The enhancement in rate by the O/F flame is evident here as in Fig. 3. While there is a good deal of scatter (typical of ADN), the trend with binder lamina thickness is the same as for AP sandwiches, a trend that has been explained in the past (Ref. 1) to be due to leading edge O/F flamelet behavior.

Fig. 5 concerns burning rates of sandwiches with oxidizer/binder matrixes between oxidizer laminae. In Fig. 5a (ADN lamina with PBAN/ADN laminae) it is seen that the rate are rather insensitive to the presence of the ADN in the matrix lamina. The matrix burning alone (5/5 and 7/3 O/F ratios) burned at quite low rates suggesting that the sandwich rate is controlled by the ADN lamina flame and its interaction with the fuel present. In Fig. 5b, AP was used in the matrix: again the sandwich rates were higher than the ADN rate, and comparable to rates with PBAN/ADN matrix laminae, further emphasizing the mechanism that the sandwich rate is controlled by the ADN flame and its reaction with the fuel flow. In Fig. 5c and d, the arrangement of ingredients is the same as 5a and 5b. except the ADN laminae are replaced by AP laminae. Because of the lower rate of AP laminae (compared to ADN), the burning characteristics of the matrix laminae play a meaningful role. The relatively high rates of the ADN/PBAN 7/3 matrix dominates the sandwich rate and carries it almost to the pure ADN rate at 1500 psi. However, the 5/5 matrix has a low rate by itself and still gives a high sandwich rate, suggesting that the interlamina O/F flame interacts strongly with the matrix. The same can be said of Fig. 5d with AP/PBAN matrixes, but the matrix rates are lower, suggesting that the matrix flame is less important to the sandwich rate.

Fig. 6 shows the effect of pyrocat catalyst in the binder on rate of oxidizer/PBAN sandwiches. It seems to have no effect in sandwiches with ADN lamina. It has a major effect on rate of sandwiches with AP laminae giving AP sandwich rates comparable with pressed ADN rates. It has been argued that the mechanism of catalyst involves "cracking" of the larger fuel molecules into more reactive fuel species and a correspondingly closer approach of the O/F flame to the surface. That effect either doesn't happen with ADN laminae, or if it does it has minimal effect on the lamina O/F flame.

Fig. 7 shows the burning rate versus pressure relation for the bimodal AP propellant described above and in Table 1, involving combinations of AP and ADN oxidizers. In general all the mixes exhibit burning rate plateaus or mesas in the 700-1500 psi. range except the all-ADN mix #2 (coarse to fine (C/F) = 86/14). The lowest rate results with mix #6, an all-AP (C/F =86/14), and

was accompanied by a strong mesa (maximum at 800, minimum at 1300 psi). A similar curve at moderately higher rate resulted with mix #5, all-AP (C/F = 67/33). When the coarse AP in mix #5 was replaced by coarse ADN (mix #3) the rate was roughly doubled and the mesa became a plateau. When the fine AP in mix #5 was replaced by fine ADN (mix #4), the rate increase was less than with coarse AP replacement, and a small mesa results. The two all-ADN mixes (1 and 2 C/F = 67/33 and 86/14) gave the highest rates and pressure exponents (mix. #1 shows a plateau in the 300-500 psi. range which depends one data point at 500 psi. which is so far out of trends that it is "suspicious"). Summarizing, replacement of AP by ADN in either particle size increases rate, but preserves a plateau. The all-ADN mixes have about the same rate as pure ADN at 300 psi., but with very high pressure dependence (at 1000 psi. the propellant rate is about 2.4 times the ADN rate and 5 times the AP propellant rate (the pressure sensitivity is too high for motor application)) The ADN propellant has a **much greater pressure sensitivity** than ADN alone, whereas AP propellant has a lower sensitivity than AP alone. The combination of ADN and AP give intermediate rates and pressure sensitivities. The AP formulations exhibited plateau burning, a property that was present but less pronounced in the mixed systems

Discussion

Some of the highlights of the interpretation in the text are summarized below:

a) The deflagration rates of the dry pressed samples were apparently different for the three materials from different sources.
b) There was appreciable scatter in the data.
c) The ADN rate was not strongly dependent on pressure
d) Sandwiches of ADN with thin binder laminae consistently burned faster than ADN alone, indicating that gas phase O/F flamelets contribute to the rate.
e) Addition of oxidizer (AP or ADN) or Fe_2O_3 catalyst did not affect the ADN lamina sandwich rate much, suggesting that the presence of the fuel for the lamina O/F flamelets is the important factor. This conclusion is reinforced by the fact that the oxidizer-binder matrix materials involved had sharply different rates when burning alone.
f) Parallel tests with AP lamina sandwiches yielded appreciable dependence of rate on matrix variables, indicating a more important contribution of matrix combustion. In fact the 7/3 ADN/PBAN matrix had the same rate as the AP sandwich with thin matrix, considerably higher rate than the AP/PBAN sandwiches.
g) With bimodal oxidizer propellants, the burning rate increased and become more pressure dependent as AP was replaced by ADN, with replacement of the coarse AP by coarse ADN having a higher effect than replacement of fine AP by fine ADN (note these generalizations are based on formulations with coarse-to-fine mass ratios of 7/3 and 5/5 with 350μm coarse and 30μm fine).
h) The pressure dependence of all-ADN formulations had a prohibitively high dependence of rate on pressure (in sharp contrast to the measured ADN rate at 300 psi. the ADN rate and propellant rates are about the same, but at 1000 psi. the propellant rate is 2.4 times the ADN rate. It seems likely that the heat absorption by the binder in the condensed phase retards the

exothermic condensed phase ADN reaction, while the pressure-dependence of the gas phase oxidizer/fuel flame contributes more importantly at higher pressure.

i) Tests with aluminum powders that are added to ADN laminae (tests at 300 psi.) show that the ultra fine ALEX aluminum ignites in the ADN flame and enhances the rate, probably by increasing thermal conductivity of the solid and oxidation in the melt. H-30 aluminum enhanced the rate but did not ignite, with rate increase presumably being due to the same mechanisms as with ALEX. The aluminum flame with ALEX apparently did not enhance rate, since the rate is about the same as that with non-igniting H-30. Tests with aluminum in AP laminae would not ignite at 300 psi.

Table I. Propellant Compositions

Designation	Binder (PBAN) %	Coarse Oxidizer Type and %	Fine Oxidizer Type and %	Fine Oxidizer/ Binder Ratio	Coarse/Fine Oxidizer Ratio	Fine Oxidizer/ Binder Ratio
Mix #1	12.50	ADN - 58.33	ADN - 29.17	7/3	66.66/33.34	7/3
Mix #2	12.50	ADN - 75.00	ADN - 12.50	5/5	85.71/14.29	5/5
Mix #3	12.50	ADN - 58.33	AP - 29.17	7/3	66.66/33.34	7/3
Mix #4	12.50	AP - 58.33	ADN - 29.17	7/3	66.66/33.34	7/3
Mix #5	12.50	AP - 58.33	AP - 29.17	7/3	66.66/33.34	7/3
Mix #6	12.50	AP - 75.00	AP - 12.50	5/5	85.71/14.29	5/5

Figures

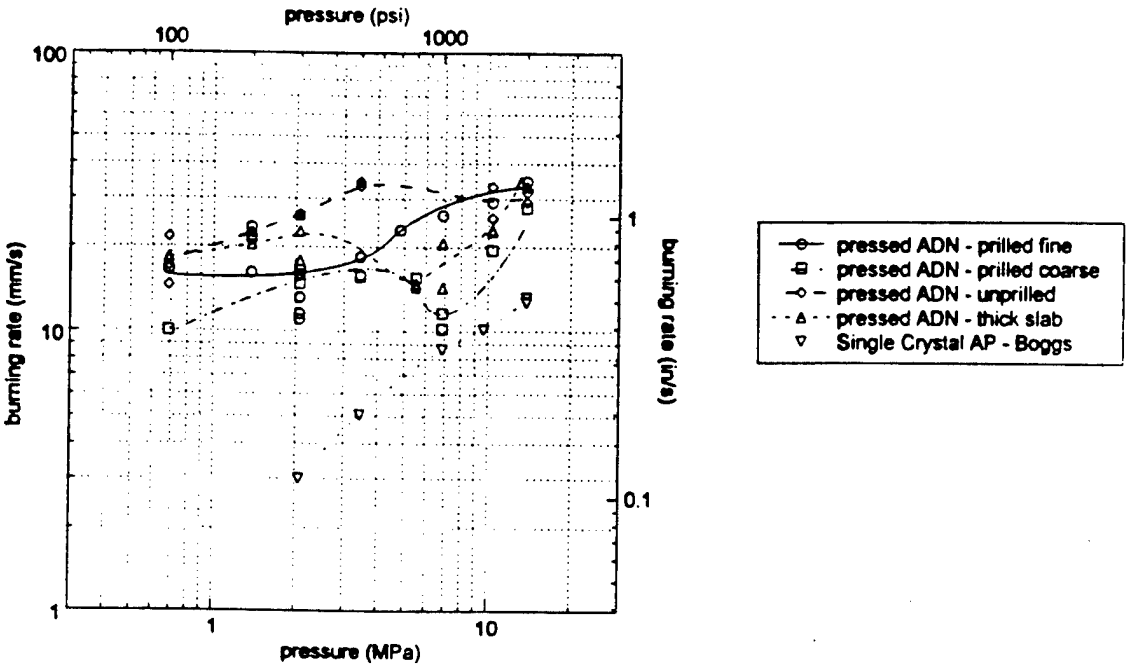

Fig. 1 Self-deflagration rate as a function of pressure for various pressed pellets of ADN. The AP self-deflagration rates are shown for comparison.

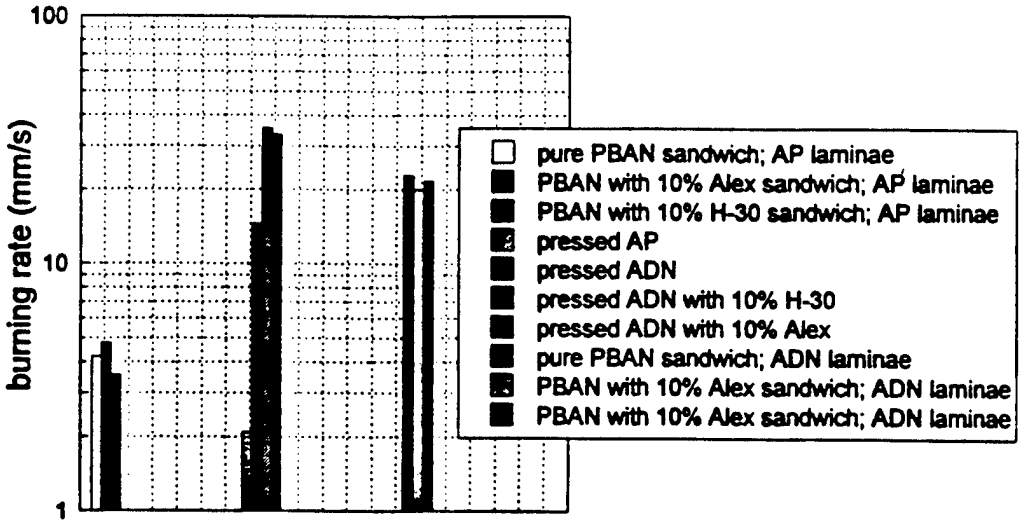

Fig. 2 Burning rates of dry-pressed mixtures of ADN and 10% aluminum (two types) at 300 psi (2.07 MPa). The rates for corresponding mixtures with AP are shown for comparison.

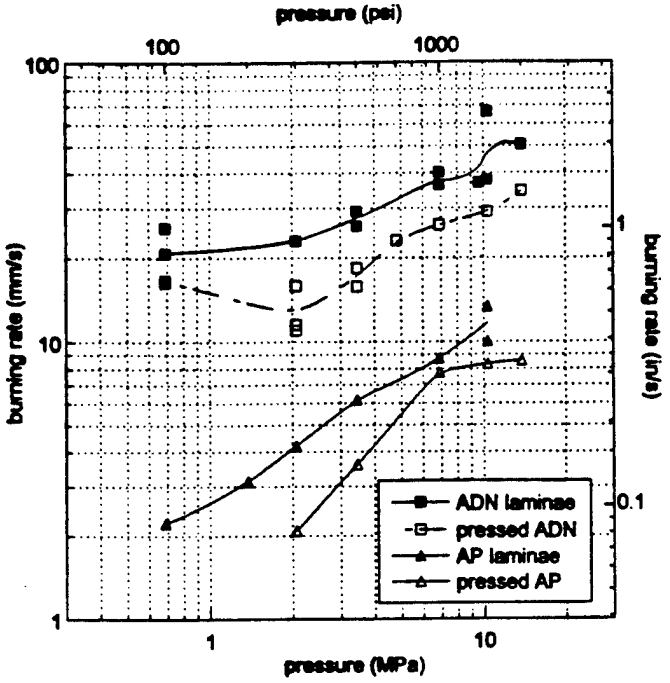

Fig. 3 Pressure dependence of burning rate of sandwiches with ADN laminae and PBAN lamina of thickness ~ 75 μm. Burning rates of corresponding sandwiches, and self-deflagration rates of pressed ADN and AP are shown for comparison.

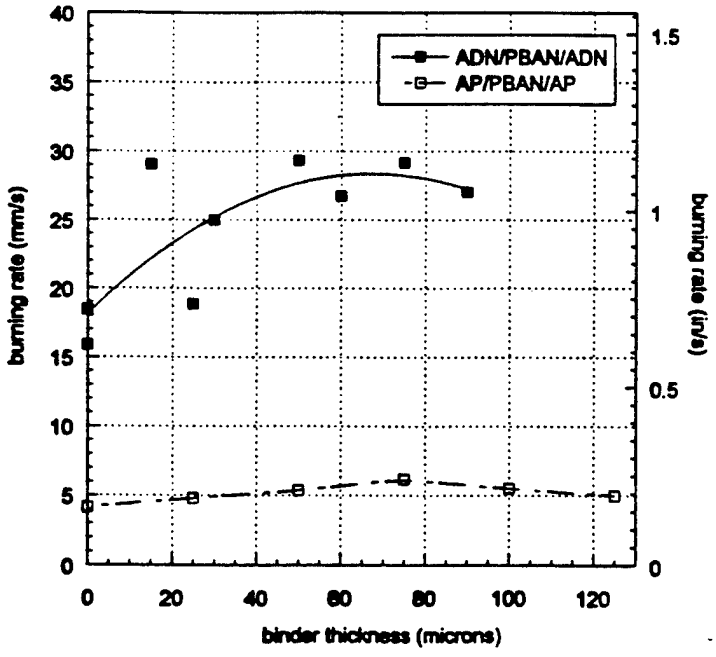

Fig. 4 Dependence of burning rate on binder lamina thickness for ADN sandwiches at 500 psi (3.45 MPa). The corresponding curve for AP sandwiches is shown for comparison.

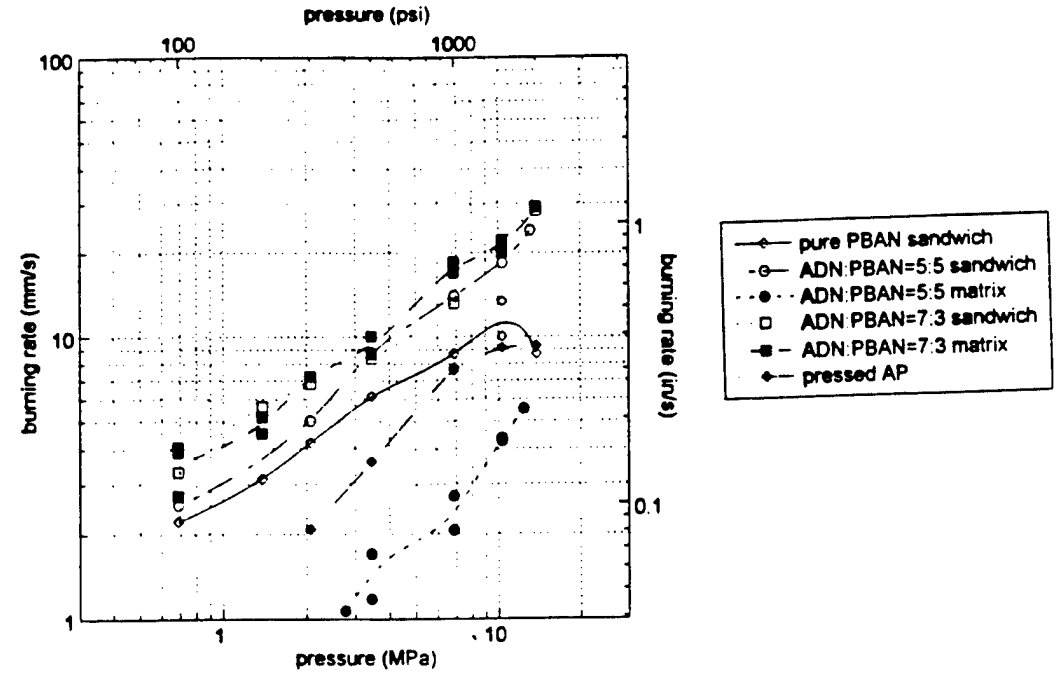

(c)

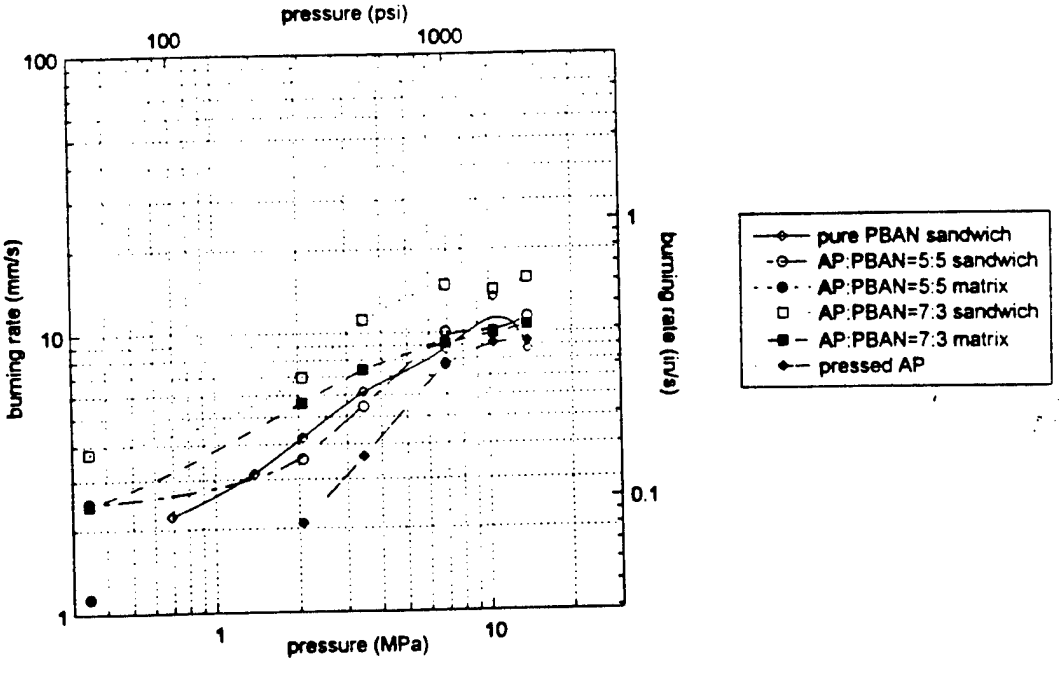

(d)

Fig. 5 Pressure dependence of burning rate of sandwiches with different oxidizer laminae and different types and contents of particulate oxidizer in the matrix lamina: (a) ADN laminae, ADN particles; (b) ADN laminae, AP particles; (c) AP laminae, ADN particles, and (d) AP laminae, AP particles.

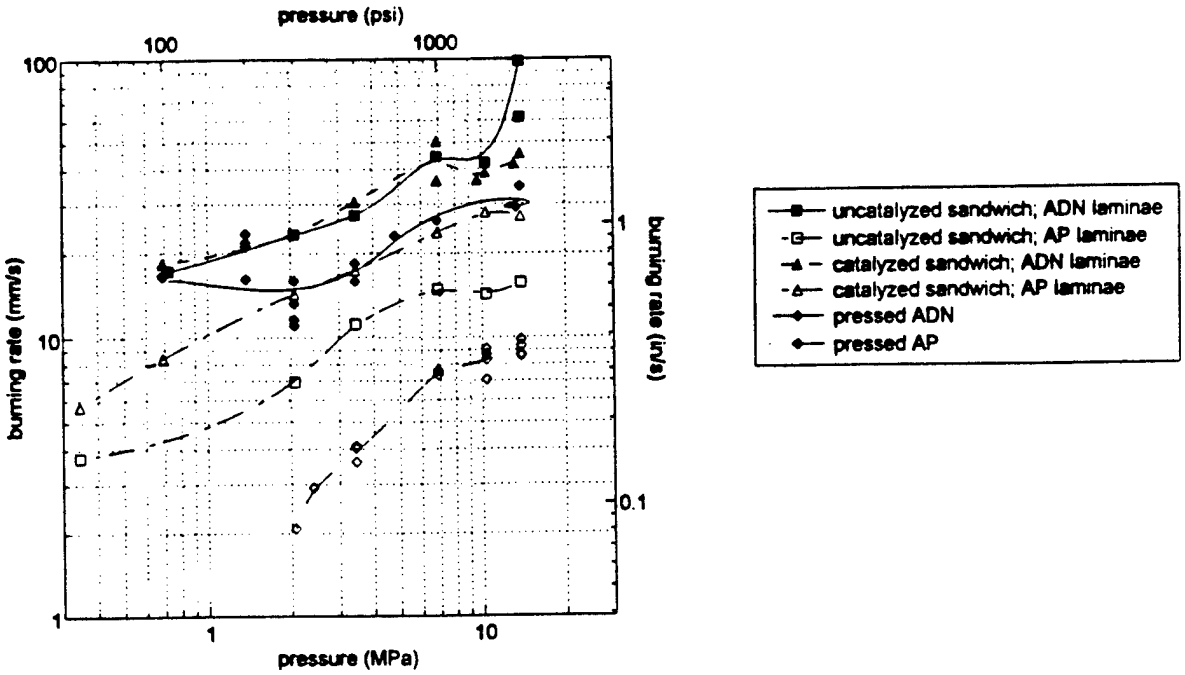

Fig. 6 Effect of catalyst (1% Pyrocat) on ADN and AP lamina sandwiches with fine AP/PBAN = 7/3 matrix lamina in the middle.

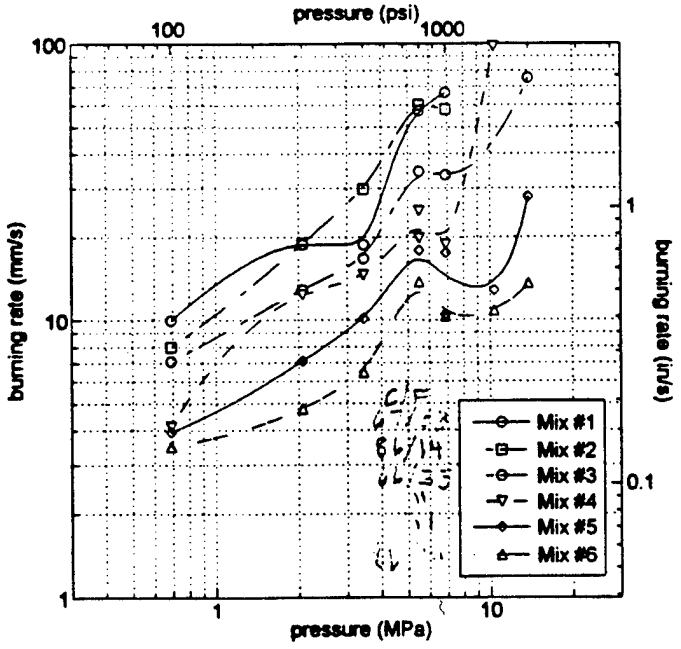

Fig. 7 Burning rate versus pressure for a family of bimodal propellants.

APPENDIX B

Price, E. W., Chakravarthy, S. R., Freeman, J. M., and Sigman, R. K.

"Combustion of Propellants with Ammonium Dinitrimide"

AIAA Paper 98-3387

34th AIAA/ASME/SAE/ASEE Joint Propulsion Conference and Exhibit

Cleveland, OH, July 13-15, 1998

AIAA 98-3387

COMBUSTION OF PROPELLANTS WITH AMMONIUM DINITRAMIDE

E. W. Price, S. R. Chakravarthy, J. M. Freeman,
and R. K. Sigman

Georgia Institute of Technology,
School of Aerospace Engineering,
Atlanta, Georgia

34th AIAA/ASME/SAE/ASEE
Joint Propulsion Conference & Exhibit
July 13-15, 1998 / Cleveland, OH

For permission to copy or republish, contact the American Institute of Aeronautics and Astronautics
1801 Alexander Bell Drive, Suite 500, Reston, VA 20191

COMBUSTION OF PROPELLANTS WITH AMMONIUM DINITRAMIDE

E. W. Price *, S. R. Chakravarthy †, J. M. Freeman ‡, and R. K. Sigman §
Georgia Institute of Technology, School of Aerospace Engineering, Atlanta, Georgia 30332-0150 USA

ABSTRACT

This paper reports a series of experiments involving ammonium dinitramide (ADN), a new energetic oxidizer of potential use in composite solid propellants. The experiments include (a) self-deflagration of pressed pellets of ADN; (b) combustion of sandwiches with ADN laminae on both sides of a binder lamina that is either "pure" or filled with particulate oxidizer and other additives; and, (c) combustion of propellants with a bimodal oxidizer size distribution, wherein, combustion of coarse ADN and fine AP (ammonium perchlorate) and vice versa were used, in addition to all-ADN and all-AP formulations.

The results indicate the possibility of a major role for condensed phase heat release in the control of the self-deflagration of ADN, resulting in very high rates compared to that of AP self-deflagration. The sandwich burning rates are always appreciably above the ADN self-deflagration rate, but follow the same trend as pressure is varied. This indicates a role for the oxidizer/fuel (O/F) flame present in the sandwiches, which seems to assist the self-deflagration of the ADN laminae. Results with oxidizer filled sandwiches show that O/F flame-assisted self-deflagration of ADN lamina always controls the sandwich burning rate regardless of the contents of the binder lamina (ADN or AP particles, with or without very fine ferric oxide catalyst or aluminum). The all-AP formulations exhibited plateau burning and addition of Fe_2O_3 yielded burning rates as high as pure ADN laminae. A family of bimodal propellants reflect the sandwich results by showing higher rates for formulations with coarse ADN and any fine oxidizer (ADN or AP) than those with coarse AP and fine ADN or AP. Pressure sensitivity of the burning rates was high!

INTRODUCTION AND TEST PLAN

This is an abbreviated report of experiments on deflagration of ADN alone, and in combinations involving dry pressed ADN-aluminum mixes, sandwiches, and propellants. The ingredients were:

a) ADN from three different suppliers: 30μm high-purity ADN from Dr. Alfred Stern at the Naval Surface Weapons Center, 350μm prilled ADN from Dr. John Guimont at the Chemical Systems Division of United Technologies, and crystalline powder from Dr. John Wardle at Thiokol
b) aluminum (Al) particles: H-30 (30 μm) and ALEX (submicron)
c) AP (low-alkali, no TCP) from Kerr-McGee (ground and sieved to size)
d) PBAN binder: 64.14% PBAN prepolymer, 20.86% ECA, and 15.00% DOA
e) Ultra-fine Fe_2O_3 (Pyrocat)

Tests were run on:

a) hard-pressed ADN laminae
b) hard pressed mixes of ADN with 10% H-30 or with 10% ALEX aluminum (and comparison tests with pressed AP/aluminum)
c) sandwiches with ADN (high purity) laminae and central laminae of PBAN, matrix of 30μm ADN and PBAN, or of 10μm AP and PBAN (see Ref. 1 for description of the sandwich method)
d) sandwiches with AP laminae and central matrix laminae of 30μm ADN and PBAN and of 10μm AP and PBAN
e) sandwiches with ADN or AP laminae with 7/3 = AP/PBAN central laminae containing 1% Pyrocat
f) bimodal PBAN propellants with 87.5% solids, two coarse to fine ratios, with AP and/or ADN (Table I)

In some cases tests were run at only one pressure (e.g. item b and one series in item c at 500 psi with a

---

* Regents' Professor Emeritus, Fellow AIAA
† Post-Doctoral Fellow (now at ITT Madras)
‡ Graduate Research Assistant, Student Member AIAA
§ Senior Research Engineer

Copyright © 1998 by J. M. Freeman, E. W. Price, R. K. Sigman, and S. R. Chakravarthy. Published by the American Institute of Aeronautics and Astronautics, Inc. with permission.

Table I. Propellant Compositions

Designation	Binder (PBAN) %	Coarse Oxidizer Type and %	Fine Oxidizer Type and %	Fine Oxidizer/ Binder Ratio	Coarse/Fine Oxidizer Ratio
Mix #1	12.50	ADN (30μm) – 58.33	ADN (300μm) - 29.17	7/3	66.66/33.34
Mix #2	12.50	ADN (30μm) – 75.00	ADN (300μm) - 12.50	5/5	85.71/14.29
Mix #3	12.50	ADN (30μm) – 58.33	AP (300μm) - 29.17	7/3	66.66/33.34
Mix #4	12.50	AP (10μm) - 58.33	ADN (300μm) - 29.17	7/3	66.66/33.34
Mix #5	12.50	AP (10μm) - 58.33	AP (300μm) - 29.17	7/3	66.66/33.34
Mix #6	12.50	AP (10μm) - 75.00	AP (300μm) - 12.50	5/5	85.71/14.29

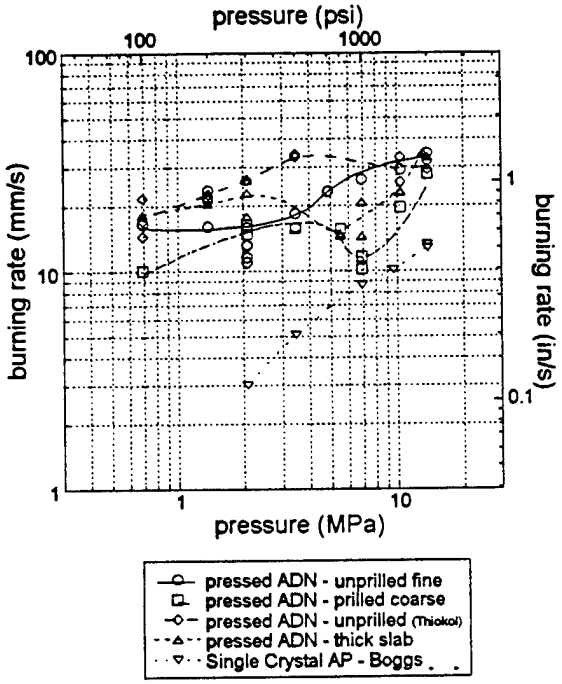

Figure 1. Self-deflagration rate as a function of pressure for various pressed pellets of ADN. The AP self-deflagration rate is shown for comparison

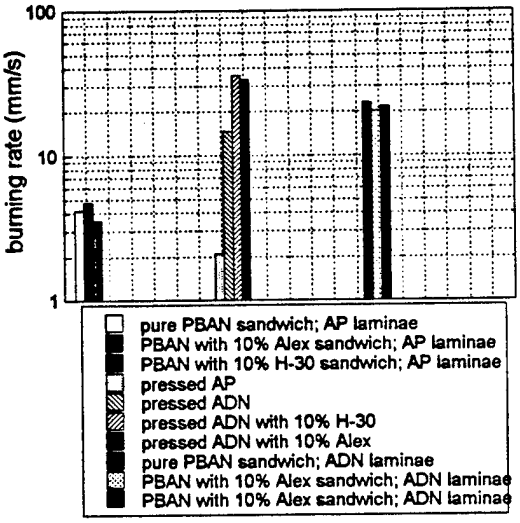

Figure 2. Burning rates of dry-pressed mixtures and sandwiches of ADN and 10% aluminum (two types) at 300 psi (2.07 MPa). The rates for corresponding mixtures with AP are shown for comparison.

PBAN binder lamina, rate versus lamina thickness). Other tests were mostly run over a pressure range of 100-1500 psi.

Results of the tests are shown in Figs 1-7. Summarizing comments on results and their significance are made in the following figure-by-figure commentaries.

RESULTS (FIGURE-BY-FIGURE)

Fig. 1: In this pressure range the rate of ADN is high compared to AP, and the pressure dependence of the rate is low. The rates are dependent on the ADN material used. There is appreciable scatter, so that the detailed trends with pressure may not be meaningful.

Fig. 2: The burning rate at 300 psi of AP/PBAN sandwiches was slightly increased when 10% ALEX was added to the binder lamina; 10%, H-30 reduced the rate moderately. The burning rate of dry pressed ADN was substantially increased by the addition of either ALEX or H-30. The combustion photography showed good ignition of ALEX, non-ignition of H-30. In corresponding tests with AP, addition of either aluminum resulted in non-burns at 300 psi. The interpretation is that:

a) fine aluminum does not agglomerate, while H-30 does and fails to ignite;

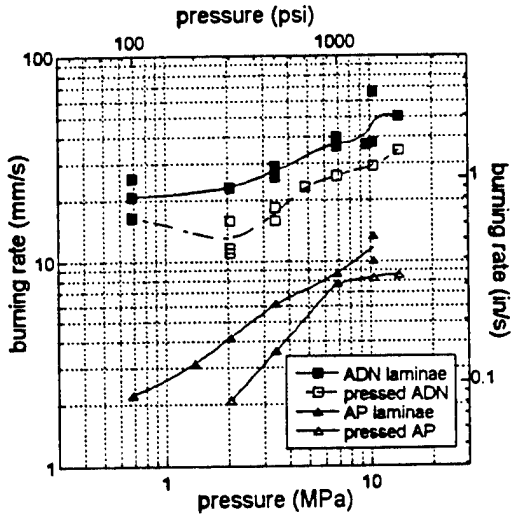

Figure 3. Pressure dependence of burning rate of sandwiches with ADN laminae and PBAN lamina of thickness ~ 75 μm. Burning rates of corresponding AP sandwiches, and self-deflagration rates of both pressed ADN and AP are shown for comparison.

b) the enhancement in rate is apparently related to enhanced thermal conductivity or possibly to aluminum reaction at the surface, with the H-30 reaction limiting ignition by formation of sintered accumulates that resist ignition;

c) corresponding AP/Al samples would not ignite at this pressure, presumably because the surface layer exotherm of ADN is absent with AP;

d) when aluminum was added to the PBAN lamina with ADN outer laminae (sandwiches), the burning rate was unaffected by addition of either aluminum. The ALEX burned more rigorously, while H-30 burned as agglomerates, an outcome suggesting that the O/F flame is hot enough to ignite the aluminum, but the radiative heat release to the surface is not enough to affect rate in an ADN-binder system.

Fig. 3: The rate of ADN/PBAN sandwiches is higher than the ADN rate (whole pressure range). This indicates that the ADN/fuel flame occurs near enough to the ADN surface to enhance its rate.

Fig. 4: The rate of ADN/PBAN sandwiches was determined at 500 psi for different PBAN lamina thicknesses up to 85μm. The enhancement in rate by the O/F flame is evident here as in Fig. 3. While there is a good deal of scatter (typical of ADN), the trend with binder lamina thickness is the

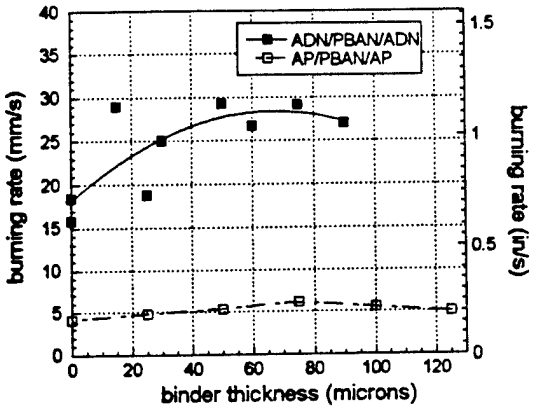

Figure 4. Dependence of burning rate on binder lamina thickness for ADN sandwiches at 500 psi (3.45 MPa). The corresponding curve for AP sandwiches is shown for comparison.

same as for AP sandwiches, a trend that has been explained in the past (Ref. 1) to be due to leading edge O/F flamelet behavior.

Fig. 5: This series of figures concerns the burning rates of sandwiches with oxidizer/binder matrices between oxidizer laminae. In Fig. 5a (ADN laminae with PBAN/ADN lamina) it is seen that the rates are rather insensitive to the presence of the ADN in the matrix lamina. The matrix burning alone (5/5 and 7/3 O/F ratios) burned at quite low rates suggesting that the sandwich rate is controlled by the ADN lamina flame and its interaction with the fuel that is present. In Fig. 5b, AP was used in the matrix: again the sandwich rates were higher than the ADN rate, and comparable to rates with PBAN/ADN matrix laminae, further supporting the interpretation that the sandwich rate is controlled by the ADN flame and its reaction with the fuel flow. In Figs. 5c and 5d, the arrangement of ingredients is the same as 5a and 5b except the ADN laminae are replaced by AP laminae. Because of the lower rate of AP laminae (compared to ADN), the burning characteristics of the matrix laminae play a meaningful role. The relatively high rates of the ADN/PBAN 7/3 matrix dominate the sandwich rate and carry it almost to the pure ADN rate at 1500 psi. However, the 5/5 matrix has a low rate by itself and still gives a high sandwich rate, suggesting that the interlamina O/F flame interacts strongly with the matrix. The same can be said of Fig. 5d with AP/PBAN matrices, but the matrix rates are lower, suggesting that the matrix flame is less important to the sandwich rate.

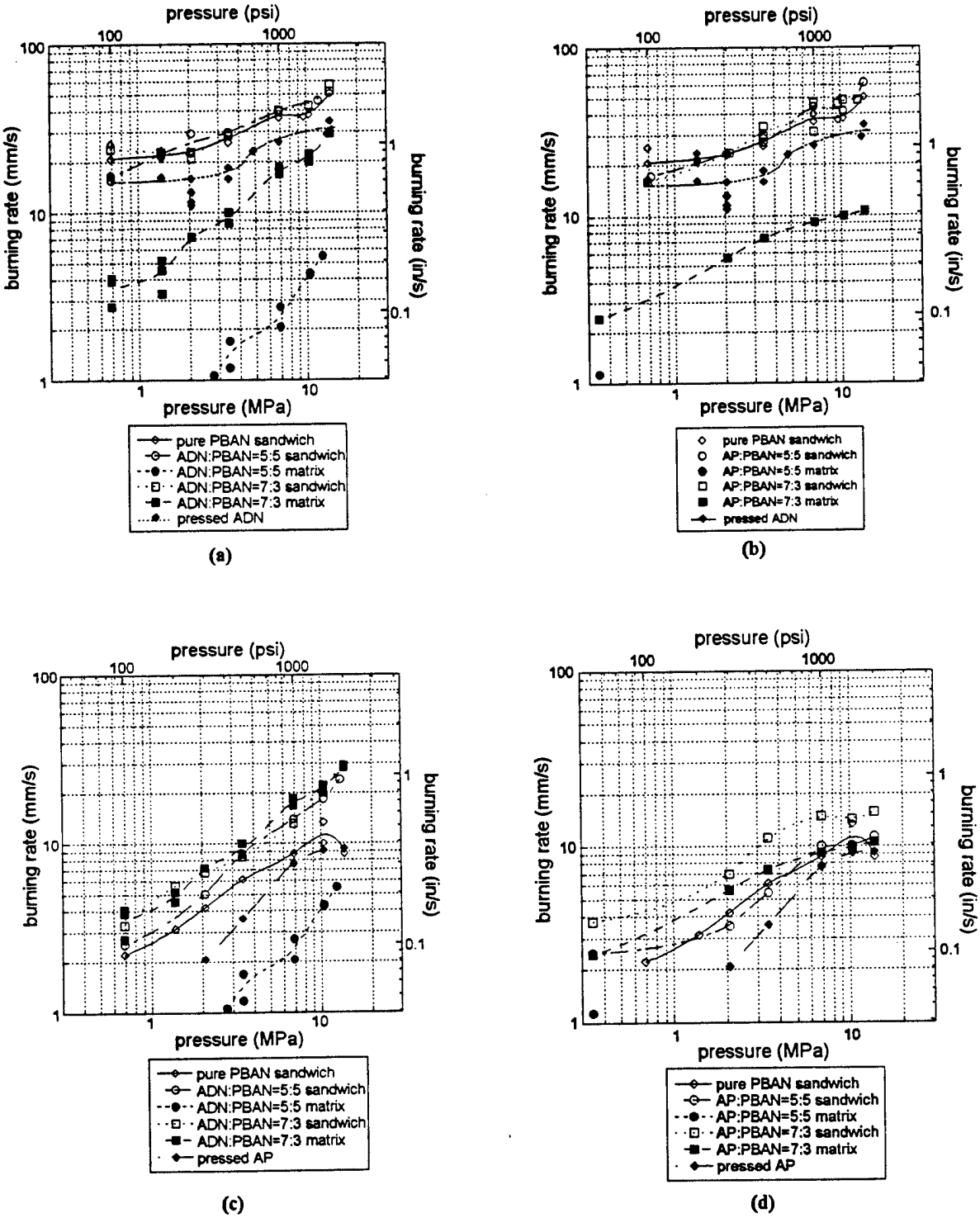

Figure 5. Pressure dependence of burning rate of sandwiches with different oxidizer laminae and different types and contents of particulate oxidizer in the matrix lamina: (a) ADN laminae, ADN particles; (b) ADN laminae, AP particles; (c) AP laminae, ADN particles; (d) AP laminae, AP particles.

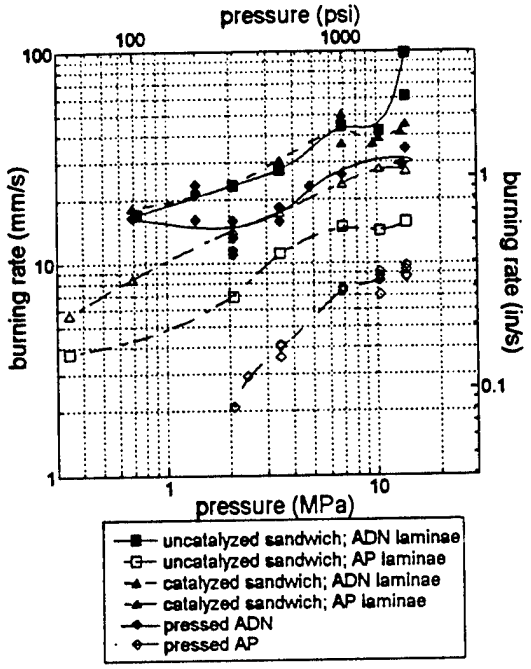

Figure 6. Effect of catalyst (1% Pyrocat) on ADN and AP lamina sandwiches with fine AP/PBAN = 7/3 matrix lamina in the middle.

Fig. 6: The effect of Pyrocat (Fe_2O_3) catalyst in the binder on rate of oxidizer/PBAN sandwiches is shown. It seems to have no effect in sandwiches with ADN lamina. It has a major effect on rate of sandwiches with AP laminae giving AP sandwich rates comparable with pressed ADN rates. It has been argued (Ref. 2) that the mechanism of catalysis involves "cracking" of the larger fuel molecules into more reactive fuel species and a correspondingly closer approach of the O/F flame to the surface. That effect either does not happen with ADN laminae, or if it does, it has minimal effect on the lamina O/F flame.

Fig. 7: This figure shows the burning rate versus pressure relation for the bimodal AP propellants described above in Table 1, involving combinations of AP and ADN oxidizers. In general all the mixes exhibit burning rate plateaus or mesas in the 700-1500 psi range except the all-ADN mix #2 (coarse to fine (C/F) = 86/14). The lowest rate resulted with mix #6, an all-AP (C/F =86/14), and was accompanied by a strong mesa (maximum at 800, minimum at 1300 psi). A similar curve at moderately higher rate resulted with mix #5, all-AP (C/F = 67/33). When the coarse AP in mix #5 was replaced by coarse ADN (mix #3) the rate was roughly doubled and the mesa became a plateau. When the fine AP in mix #5 was replaced by fine

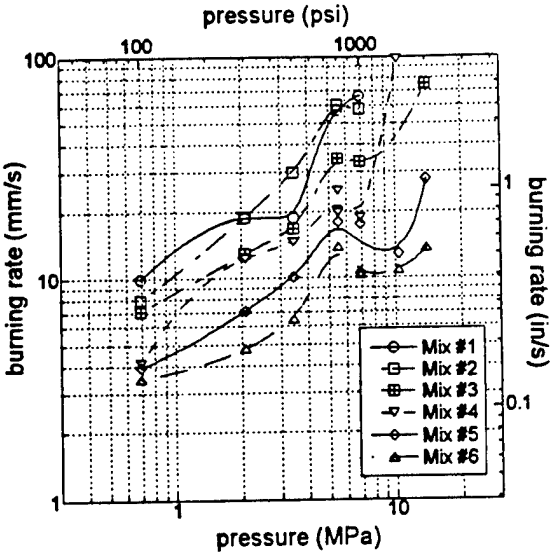

Figure 7. Burning rate versus pressure for a family of bimodal propellants.

ADN (mix #4), the rate increase was less than with coarse AP replacement, and a small mesa results. The two all-ADN mixes (1 and 2 C/F = 67/33 and 86/14) gave the highest rates and pressure exponents (mix. #1 shows a plateau in the 300-500 psi range which depends on one data point at 500 psi which is so far out of trends that it is "suspicious"). Summarizing, in an all-AP formulation, replacement of AP by ADN in either particle size increases rate, but preserves a plateau. The all-ADN mixes have about the same rate as pure ADN at 300 psi, but with very high pressure dependence (at 1000 psi the propellant rate is about 2.4 times the ADN rate and 5 times the AP propellant rate (the pressure sensitivity is too high for motor application)) The ADN propellant has a **much greater pressure sensitivity** than ADN alone, whereas AP propellant has a lower sensitivity than AP alone. The combination of ADN and AP give intermediate rates and pressure sensitivities. The AP formulations exhibited plateau burning, a property that was present but less pronounced in the mixed systems.

DISCUSSION

Some of the highlights of the interpretation in the text are summarized below:

a) The deflagration rates of the dry pressed samples were apparently different for the three materials from different sources.

b) There was appreciable scatter in the data, although the scatter seemed to be less when the 30μm high purity material was used.

c) The ADN rate was not strongly dependent on pressure in this pressure range.

d) Sandwiches of ADN with thin binder laminae consistently burned faster than ADN alone, indicating that gas phase O/F flamelets contribute to the rate.

e) Addition of oxidizer (AP or ADN) or Fe_2O_3 catalyst did not affect the ADN lamina sandwich rate much, suggesting that the presence of the fuel for the lamina O/F flamelets is the important factor. This conclusion is reinforced by the fact that the different oxidizer-binder matrix materials used had sharply different rates when burning alone.

f) Parallel tests with AP lamina sandwiches yielded appreciable dependence of rate on matrix variables, indicating a more important contribution of matrix combustion. In fact the 7/3 ADN/PBAN matrix alone had the same rate as the AP sandwich with that matrix, considerably higher rate than the AP/PBAN sandwiches.

g) With bimodal oxidizer propellants, the burning rate increased and became more pressure dependent as AP was replaced by ADN, with replacement of the coarse AP by coarse ADN having a higher effect than replacement of fine AP by fine ADN (note these generalizations are based on formulations with fine oxidizer-to-binder mass ratios of 7/3 and 5/5 with 350μm coarse and either 10 or 30μm fine).

h) The pressure dependence of all-ADN formulations had a prohibitively high dependence of rate on pressure (in sharp contrast to the measured ADN rate). At 300 psi the ADN rate and propellant rates are about the same, but at 1000 psi the propellant rate is 2.4 times the ADN rate. It seems likely that the heat absorption by the binder in the condensed phase retards the exothermic condensed phase ADN reaction, while the pressure-dependence of the gas phase oxidizer/fuel flame contributes more importantly at higher pressure.

i) Tests with aluminum powders that are added to ADN laminae (tests at 300 psi) show that the ultra fine ALEX aluminum ignites in the ADN flame and enhances the rate, probably by increasing thermal conductivity of the solid and by oxidation in the melt. H-30 aluminum enhanced the rate but did not ignite, with rate increase presumably being due to the same mechanisms as with ALEX. The aluminum flame with ALEX apparently did not enhance rate, since the rate is about the same as that with non-igniting H-30. Tests with aluminum in AP laminae would not ignite at 300 psi.

REFERENCES

1. Price, E. W., "Effect of Multidimensional Flamelets in Composite Propellant Combustion," *Journal of Propulsion and Power*, Vol. 11, No. 4, pp. 717-728.

2. Price, E. W., and Sambamurthi, J. K., "Mechanism of Burning Rate Enhancement by Ferric Oxide," *Proceedings of the 21st JANNAF Combustion Meeting*, CPIA Pub. 412, Vol. I, 1984

APPENDIX C

Thermal Analysis

(unpublished)

Thermal Analysis

In order to estimate the role of decomposition of each ingredient in combustion of propellants, the decomposition of each ingredient can be studied separately in controlled heating experiments. In such experiments, a small sample is subjected to controlled heat-up and observations are made of melting and decomposition in a hot-stage microscope (HSM), of weight loss (TGA), and the heat release (DTA or DSC). In the present study the HSM was used for most of the tests, using a heating rate of 2°C per second, and a video camera to record the sample response. TGA and DTA tests were run primarily on butadiene binders and their ingredients, and a large portion of the HSM tests were made on those materials as well, because of a widely held belief that differences in melt behavior of PBAN-ECA, HTPB-IPDI and HTPB-DDI binders were responsible for observed large differences in propellant burning rate.

Hot stage microscope tests

Table C-1 summarizes the principal results of the HSM tests, including both oxidizers and binders. The differences in melt behavior and in decomposition temperature of these ingredients are conspicuous, so much so as to raise questions about how combustion of mixtures would proceed. As an example, HNIW and ADN decompose at temperatures below the melting temperatures of polybutadiene binders. In a propellant combustion wave, this would lead to mechanical degradation of the surface layer, that is not encompassed in conventional combustion models.

In the HSM studies of the three polybutadiene binders, the expected differences in melting and decomposition behavior were not manifested. Because of prevailing theories that such differences did exist, and were responsible for the differences in propellant burning rate with these binders, these binders were examined in much greater detail. These studies are described in the following, where it is noted that with these binders, melting is a protracted process that can't be characterized by a single temperature. In addition, bubbling starts in the test sample before melting is complete and continues over a temperature range of 40–50°C. The extended studies were aimed at characterizing this complex behavior, determining differences among the three binders, and examining test variables that caused non reproducibility in testing.

Typical Sample Behavior (Polybutadiene Binders)

In a hot stage test of an unplasticized sample of HTPB binder, not much change is seen in the sample until a hot stage temperature of 455°C or so is reached. The first sign of "melting" is a small flow from the bottom edges of the sample, giving a rounding of sample edge irregularities (as seen in profile). The top of the sample does not lose its irregularities for some time. By 457°C, bubbling can be seen at the bottom of the sample, with vapors usually escaping out at the bottom edges (with concurrent spreading of the melt periphery). Eventually the whole sample becomes a bubbling melt. In the final stage, starting around 463-468°C, the bubbling stops, and a clear thin puddle remains that usually spreads by 50% (area) before drying up by 490°C. In the final stage (490-500°C)

some dark flecks sometimes appear, then change to whitish spots. When DOA is present in the sample, the sample becomes "glossy" at around 200-300°C, without otherwise losing its overall shape. The glossy appearance goes away by 320°C. Sometimes slump, flow and limited bubbling occurs in the range 250-350°C with a dormant period from 350-450°C. This anomalous behavior is discussed later (Incidental Test Variables).

Choosing Descriptors for Binder Behavior (polybutadiene binder tests)

In the hot stage experiment, the test sample rests on a heated sapphire plate. The temperature read-out is the temperature of the plate, and presumably of the bottom of the test sample. There is a slight flushing flow of unheated argon in the sample chamber, present to assure a nonreactive atmosphere and to keep the top viewing window clear. From the test results it appears that some cooling of the top of the sample occurs, delaying total melt-down and bubbling of the samples (some of this delay is no doubt due to finite heat transfer in the bottom-heated samples). Since the optical viewing is from the top, a visual description tends to reflect the behavior of the top of the sample, simply because the bottom of the sample is obscured (except as can be seen through the sample by back-lighting). A new set of descriptors is adopted here for binder tests, that is used in Table C-1a, and is indicative of those signs of melting and decomposition of the bottoms of the samples that can be seen in the HSM videos, as follows.

1. "Early response" consisting of various signs of melting seen in occasional tests (including all those with DOA plasticized samples) in the 200-350°C range, followed by no further response in the 330-450°C range (ER).
2. "Inactive" temperature range after early response (I).
3. "Bottom Edge Leaking", in which the edge profile extends outward moderately and smoothes the periphery (the bottom side is apparently melted but there is little force to make it flow) (BEL).
4. "Onset of bubbling", visible through the sample by transmitted back-lighting, in which the liquid state at the bottom is revealed by response to onset of gassification. The bubbles generally do not emerge via the top surface, apparently because the top is still too viscous. The gas appears to escape laterally at the bottom edges, accompanied by further outward flow of the melt at the bottom edges. (OOB)
5. "Vigorous bubbling". At this "point" the sample looks like a puddle, except for traces of the original top surface, that later fade. (VB)
6. "End of bubbling". At this point the sample is completely melted, roughly 75% "gone". Vaporization presumeably now continues at the top of a very shallow puddle. The puddle has stopped spreading. (EOB)
7. "Final phase". Shortly before complete disappearance, the puddle loses its color and spreads about 50%, suggestive of lower viscosity. Then the puddle dries up with no visible evidence of periphery remaining. (FP).

Incidental Test Variables (polybutadiene binder tests)

In conducting HSM tests, there were some parameters that were kept nominally constant, but later varied to determine how sensitive the results were to these parameters. Nominal conditions were:

1. Heating rate of the HSM: 2°C/sec. Later also at 6°C/sec.
2. Curing conditions of samples: cure at 40°C for 4 days (HTPB) or 7 days (PBAN). Some later HTPB tests used cure catalyst, and 1 day cure. Some tests were run on samples with 75 and 125% of normal curing agent.
3. Thickness of samples: Nominally 0.4–0.5 mm. Some later tests were done on samples of 0.2 mm thickness. The data on polybutadiene binders in Table C-1a are for 0.2 mm thick samples.

It was found that going from 2 to 6°C/sec heating rate had the effect of shifting most behavior to higher temperatures (roughly 20°C higher). However in these tests the prevalence and degree of the early response behavior in the 200-330°C range was often increased at higher heating rate. In this regard it should be noted that the heating rate was not well-controlled over the duration of the HSM tests, and usually decreased with increasing temperature. It is estimated that 2°C/sec tests dropped off to 1°C/sec in most tests. The tests on the thin samples of polybutadiene binders used for Table C-1a were somewhat different in that the heating rate had dropped off to 0.4°C/sec (and not continued through "final " phase). Earlier tests on thicker samples showed a longer stage of activity (to 20-25°C higher final temperature). Regarding effect of curing, it was observed that the samples with cure catalyst and 1 day cure melted down and bubbled very early (starting at 250°C). It was noted that before testing, these samples had a "sticky" quality. When the remaining samples were tested several months later they did not exhibit the early response, suggesting that the samples in the earlier tests were not fully cured, but cured during storage. The tests on sticky samples with 75% of normal curing agent (DDI) showed softening and a small bubble in the 250–400°C range and normal melt, bubble behavior starting at 457°C. Normal and 125% curative samples showed little activity until 455-460°C. It seems clear that incomplete curing is conducive to early response to heating. Regarding thickness of the samples, the main effect was better visibility of the early manifestations of melting and bubbling. In general, thick samples survived to higher temperatures, up to 510°C in some tests.

The data for polybutadiene binders in Table C-1a were obtained with 0.2 mm thick samples, and a 2°C per second heating rate that dropped off after 150°C and was about 0.4°C per second by 470°C. This drop-off was not intended. The result of the 10°C/sec tests suggest that the active melting-decomposition on these "2°C/sec tests" would have been extended to somewhat higher temperatures if the heating rate had been constant at 2°C per sec.

Summary of HSM Test Results

In general, the HSM tests provided clear distinction of melting and decomposition temperatures among the many ingredients tested, even though the kinetic nature of the events precludes their complete characterization by single temperatures. The effort to show distinction among the three polybutadiene binders became rather exhaustive, because it forced a search for small differences among materials that melted and decomposed progressively and concurrently, materials that were not conspicuously different. By the standards applied to selection of melting and decomposition of the other materials (Table C-1), these three binders would all show the same melting and

decomposition temperatures. The known difference in propellant burning rate with these binders motivated more detailed testing and comparison using the HSM. Even a more detailed consideration of sample response failed to show a difference among the three binders, although the study did show that sample behavior was strongly dependent on degree of sample cure, on presence of plasticizer (DOA) in the binder, and on sample heating rate during the test. The results seem to contradict current theories that the differences in propellant burning rate are due to differences in melt behavior of PBAN-ECA, HTPB-IPDI, and HTPB-DDI binders. They also suggest that the break down of binders is progressive in the surface layer of burning propellants, with concentration of more stable species at the surface and percolation of more volatile species to the surface (especially when DOA or some other easily decomposed additive is included in the binder).

TGA and DSC Testing

Thermogravimetric analysis tests were run on polybutadiene binder ingredients; "binders"; binders with transition metal oxides; ammonium perchlorate; and certain propellants. Differential thermal analysis tests were run on several of the same materials. Because most of the results have not been reported previously, they are presented here in (Fig. C-1 to C-8). Figure C-1 compares TGAs of PBAN and HTPB (R-45) prepolymers and cured binders (no plasticizer). Figure C-2 compares the cured binders alone, but with HTPB cured by three different isocyanates. Figure C-3 compares the TGAs of DDI and IPDI-cured HTPB with and without DOA plasticizer (20%), and Fig. C-4 shows the effect of %DOA. These results show that the HTPB prepolymer and cured polymers start to vaporize at 300°C, with increasing rate as temperature rises, and at high rate at 450-490°C (essentially complete at 500°C). The cured HTPB binders lag behind the prepolymers, more so with IPDI cureative than DDI. DTA tests show (Fig. C-5a,b) an exotherm around 400°C (greater with IPDI than DDI; note the difference in scale in C-5a and C-5b) which is probably due to cyclization (Ref. C-1), a reaction between vapor products and undecomposed binder. The end of the exotherm coincides with the onset of rapid decomposition at 440-450°C. It is reasonable to assume that cyclization produces a more stable product, probably explaining the difference among the cured binders and prepolymer (note the difference in scale in Fig. C-2). As noted in Ref. C-1, the cyclization reactions are less important in a combustion wave because of outward convection of the vapor reactants and limited time for reaction. Thus the decomposition in the combustion wave may be similar to that of the prepolymer, but "stretched" to higher temperature because of the rapidity of heating. However, cyclization probably does affect the results of hot stage microscope tests which are carried out at low heating rate. The contribution to sample behavior, if any, is unknown.

Returning to Fig. C-1, it is seen that decomposition-vaporization starts and continues at lower temperatures with PBAN than HTPB. At about 350°C the "vaporization" rate of the cured binder starts to exceed that of the prepolymer, suggesting loss of some of the curing agent (No DTA tests were run on PBAN, so the possible role of different cyclization is not tested.) The rapid decomposition phase of PBAN proceeds at about 25°C lower temperature than HTPB, but the decomposition ends at about the same temperature. These features are shown more clearly in Fig. C-2, in which the

prepolymer curves are omitted, and an additional curve is included for TDI-cured HTPB. The differences in the HTPB with different curatives occur primarily in the temperature range 350-450°C in which hot-stage microscope tests show relatively little thermal response, prior to vigorous melting and bubbling in the 450-500°C range (recall this 350-450°C range is also the range for cyclization reactions (Fig. C-5), which may differ with different curatives).

Figure C-3 shows the TGA results for pure DOA plasticizer, and for DDI and IPDI-cured HTPB binder with 20% DOA, and corresponding curves for unplasticized HTPB binders. The plasticizer decomposes at relatively low temperature (250-330°C), very rapidly above 280°C. The same process and rates seem to proceed in the plasticized binders, which then resume their normal rates after the DOA is gone. A similar but smaller effect was obtained with 10% DOA. The hot-stage microscope tests showed evidence of "wetness" of propellant samples in the 250-330°C range, evidence that temporarily disappeared above 350°C. This raises a curious question about what happens in the heat-up layer of a binder in a propellant combustion zone, where it appears that the DOA would decompose beneath the binder surface, disrupting the solid and foaming the liquid layer. This could be a pressue-dependent effect, important to plateau burning (DOA enhances plateaus). Unfortunately, meaningful real time observation of such behavior on the surface of a burning propellant would need to be on a dimensional scale too small to resolve by present methods.

At one point in the collective study, the role of catalysts on matrix and propellant burning became important. TGA and DTA tests were run with the goal of narrowing down the field of postulates regarding catalytic mechanisms and relative effectiveness of different catalysts (Fe_2O_3 and TiO_2 were chosen). Figure C-6 shows results of isothermal TGAs (300°C) for pure binder with and without TiO_2, AP with and without TiO_2, and propellants with and without TiO_2. The additive did not affect the decomposition-vaporization rate of either the binder or AP alone, but enhanced the gassification rate of the propellant. This result suggests that the catalysis involves reactions between oxidizer and binder. Since transition metal oxides are known to catalyze decomposition of $HClO_4$ (one of the two primary vapor decomposition products of AP), it seems likely that this is the first step in the catalyzed response of the propellant. However, $HClO_4$ is already a vapor, and the mechanism for the enhanced weight loss in the propellant must involve enhancement of binder decomposition by the $HClO_4$ and its decomposition products. The time required for diffusion of $HClO_4$ to the catalyst and binder surfaces to enable such reactions is made possible in this experiment by the long decomposition time and small AP particle size (2μm).

At higher temperatures, the postulated (exothermic) reactions make self-heating of the sample important, and very likely leads to enhanced self-heating when catalysts are present. This is illustrated in Fig. C-7 by DTA curves for matrix propellants (no coarse AP) with-and-without catalysts. In this progressive heating environment, self-heating causes the sample temperature to run-away (i.e., it ignites). The presence of catalysts causes the run-away of the sample temperature to start and proceed more rapidly and at lower control temperatures. The effect is only modest with 2% TiO_2 in the matrix with greater effect with 0.05% Fe_2O_3 and still greater effect with 2% Fe_2O_3. The range of temperatures in which the temperature run-aways occurred is the same range in which the first exotherm in the DTA of pure AP occurs (solid curve in Fig. C-8), a range in which

the decomposition rate is governed by the dissociative sublimation reaction (leading to NH_3 and $HClO_4$ products)(Ref. C-2). Since this reaction is endothermic, it must be assumed that $HClO_4$ decomposes within the DTA sample to start the exothermic reactions. In the TGA tests with matrix propellants mentioned above, the weight loss is higher with TiO_2 than without TiO_2 because TiO_2 catalyzes the $HClO_4$ decomposition, resulting in oxidative species that are very reactive with the binder, the reactions that lead to thermal run-away in the DTA test and enhanced weight loss in the isothermal TGA tests.

Summary

The hot stage microscope tests provided a tabulation of the visible aspects of sample melting and decomposition, and Table C-1 shows a conspicuous difference among the materials that were tested. The expected difference among the polybutadiene binders was not found. This later result precipitated more detailed testing of the polybutadiene binders involving variants in sample preparation and test methodology, that were found to affect test results. The results in Table C-1 are for well-cured samples, tested at 2°C/sec heating rate. Because these three binders exhibited progressive melting and concurrent decomposition over a 50°C temperature range in such tests, a more detailed description of the process was developed (as reflected in extra columns in Table C-1). No notable differences were evident among the polybutadiene binders, even for this more stringent comparison. The TGA and DTA tests were consistent with the HSM results. Specific findings include:

1. The crystal phase changes and melting of oxidizers can be clearly seen, and differ widely among the various oxidizers tested.
2. Decomposition of oxidizer melts occurs over a small temperature range that is widely different for different oxidizers.
3. The difference between melt temperature and decomposition temperature ranged from zero (HNIW) to about 125°C (AN). No melt was resolved for HNIW or AP: HNIW decomposition was abrupt while AP decomposition was progressive.
4. Melting of binders differed in temperature between 70°C (PEG) and 455°C (polybutadiene), with the melting and decomposition process becoming less distinct for the "high temperature" binders.
5. The butadiene binders that were tested didn't show distinguishable differences in melting-decomposition behavior when sample preparation and heating rate were the same.
6. Inclusion of DOA in the polybutadiene binder samples resulted in "glossing" of the sample surface in the temperature range 200 to 400°C. The TGA indicates that the DOA decomposes in that range.
7. TGA and DTA tests on polybutadiene binders, AP and propellants with either TiO_2 or Fe_2O_3 catalysts indicate that the catalysts act by speeding up $HClO_4$ decomposition, which leads to enhanced oxidative attack on binder. In propellant formulations with very fine AP, the associated surface layer heat release is probably a major factor in burning rate. Fe_2O_3 is apparently 20 times more effective than TiO_2 (0.5 μm particle size).

References

C-1. Chen, J. K. and Brill, T. B., "Chemistry and Kinetics of Hydroxy-Terminated Polybutadiene (HTPB) and Diisocyanate-HTPB Polymers during Slow Decomposition and Combustion-like Conditions," *Combustion and Flame,* Vol. 87, 1991, pp. 217-232.

C-2. Kraeutle, K. J., Atwood, A. I., and Curran, P. O., "Partial Decomposition of TCP-coated Orthorhombic Ammonium Perchlorate at Atmospheric Pressure: Analysis of Weight Loss Measurement," *Proceedings of the 36th JANNAF Combustion Subcommittee Meeting*, Cocoa Beach, FL, Nov. 1999.

Table C-1a
Comparison of Ingredient Thermal Response Temperatures*
BINDERS

Sample	Early Response	Bottom edge leaking	Onset of bubbling	Puddle	Vigorous Bubbling	End of Bubbling	Final phase	See text for explanation of terms
PBAN binder ECA cure **		458	457	461	465	468		
HTPB binder IPDI cure **		454	456	462	464	464		temp rise stopped at 465
HTPB binder DDI cure **		455	456	460	460	463		
NMMO binder N-100 cure		85-100	195	140	260-320	355		melt becomes viscous at 340 remains at 360 with no activity
GAP binder IPDI cure			160		220		266	Inflates into big bubbles, collapse at 246, abrupt decomp at 266 C
BAMO/THF		205-220	269	258	250-270	280		Very viscous at 280°C, a gummy residue remains
Polysulfide LP-3		262	280	269	305	322	335	

*Heating in 1 atm argon, initial heating rate 2°C per sec, decreasing to 1.-0.4°C by 470°C
** Samples were 0.2 mm thick

Table C-1a
Comparison of Ingredient Thermal Response Temperatures*
BINDERS (II)

Sample	Early Response	Bottom edge leaking	Onset of bubbling	Puddle	Vigorous Bubbling	End of Bubbling	Final phase	See text for explanation of terms
HTPB-DDI 10% DOA**	335-390	458	458	462	456-466	467		Early response absent in some tests, no response until ~ 458
HTPB-DDI 20%DOA**	207-240	300	455	450	468	470	475	In some tests, no response until 456°C
HTPB-DDI 30% DOA**	200-300	460	463	463	465	467		In some tests, no response until 460°C
HTPB-DDI reduced 25%**		457	457	462	466	470		Second test showed "Early Response" in 250-350°C range
HTPB-DDI Increased 25%**		460	450	461	463	471		
HTPB-DDI +15% TiO_2**		353	459	464	464-470	474	482	viscous melt
HTPB-DDI +15%Fe_2O_3**		461	462	465		473	484	

*Heating in 1 atm argon, initial heating rate 2°C per sec, decreasing to 1.-0.4°C by 470°C
** Samples were 0.2 mm thick

Table C-1a
Comparison of Ingredient Thermal Response Temperatures*
BINDERS (III)

Sample	Early Response	Bottom edge leaking	Onset of bubbling	Puddle	Vigorous Bubbling	End of Bubbling	Final phase	See text for explanation of terms
PEG (pure)				72	370-440	440		low viscosity
PBAN Prepolymer					410-490		~500	Based on TGA tests
HTPB (R45) Prepolymer					420-490		~500	Based on TGA tests
ECA					250-450		~470	Based on TGA tests
IPDI					220-370		~400	Based on TGA tests

*Heating in 1 atm argon, initial heating rate 2°C per sec, decreasing to 1.-0.4°C by 470°C

Table C-1a
Comparison of Ingredient Thermal Response Temperatures*
BINDERS (IV)

Sample	Early Response	Bottom edge leaking	Onset of bubbling	Puddle	Vigorous Bubbling	End of Bubbling	Final phase	See text for explanation of terms
DDI					270-330		~400	Based on TGA tests
DOA					270-310		~330	Based on TGA tests

*Heating in 1 atm argon, initial heating rate 2°C per sec, decreasing to 1.-0.4°C by 470°C

Table C-1b
Comparison of Ingredient Thermal Response Temperatures
OXIDIZERS

Sample	Melting Temp,	Boiling-Decomp,	Vaporization without Bubbling	Comments
AP	580*		340-460	
AN	170-186	274-390	333	
HMX	260-294**	292-310	310-320	
ADN	90-100	170-255		slight dry residue at 2 259°C
HNIW			272	abrupt melt-Decomposition at 272°C
KP			400	(handbook data)

*Melt temperature based on deflagration tests. At HSM heating rates , the sample is gone by 460°C

**The sample exhibits a melt-recrystalization-remelt in this range. Subsequent behavior similar to AN.

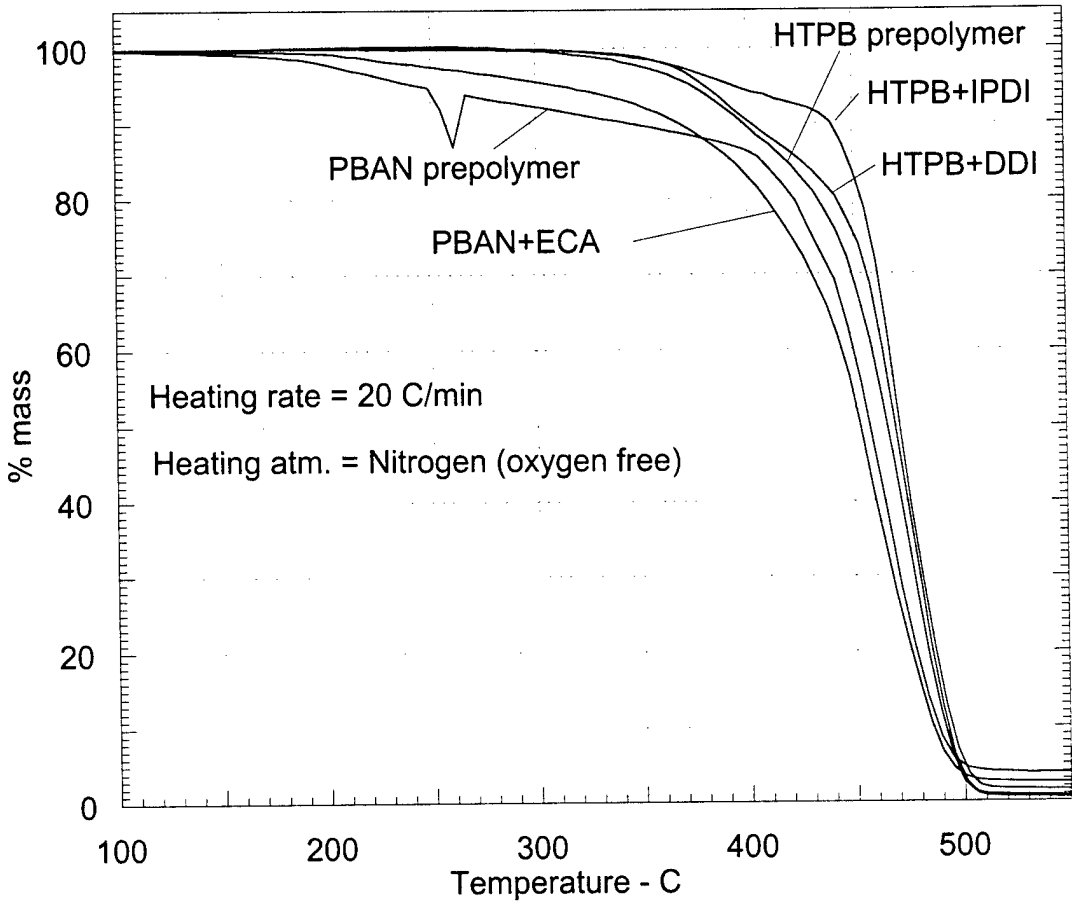

Fig. C-1. Thermogravimetric analysis of polybutadiene binders and prepolymers.

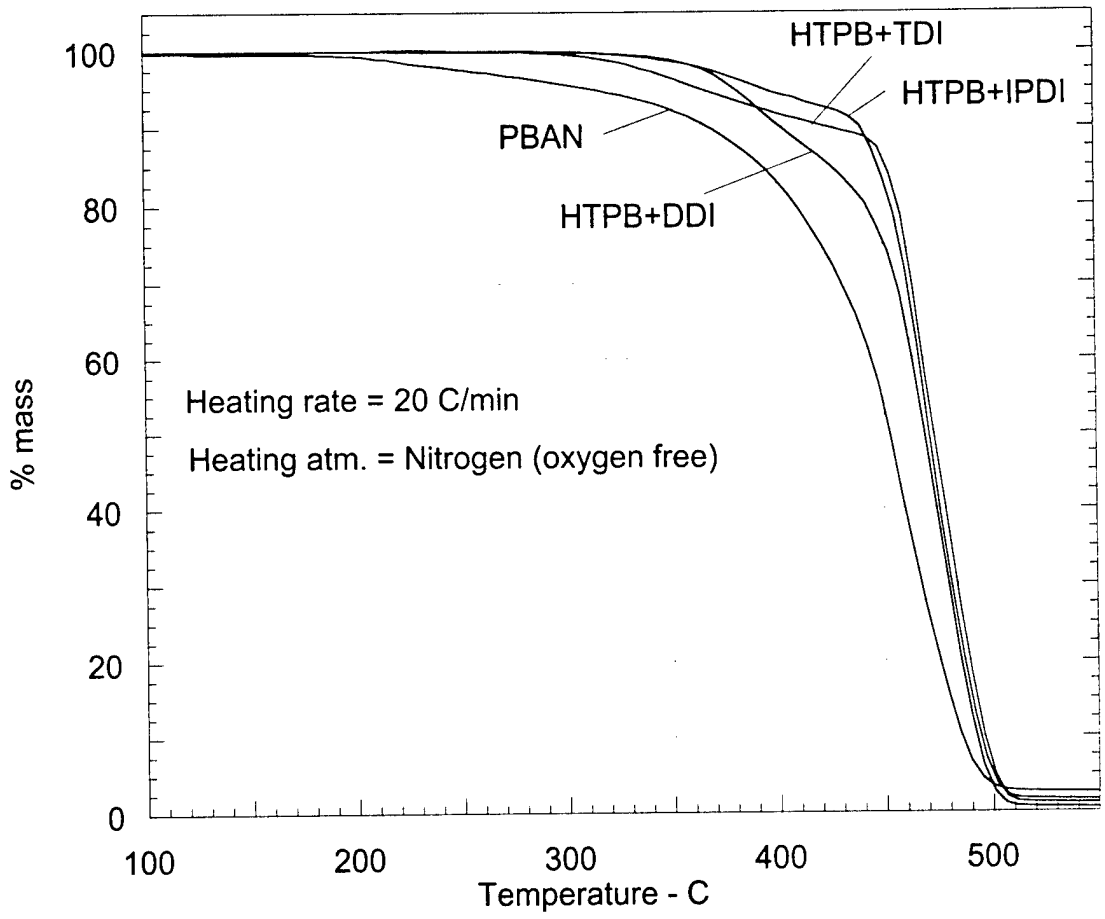

Fig. C-2. Termogravimetric analysis of cured binders

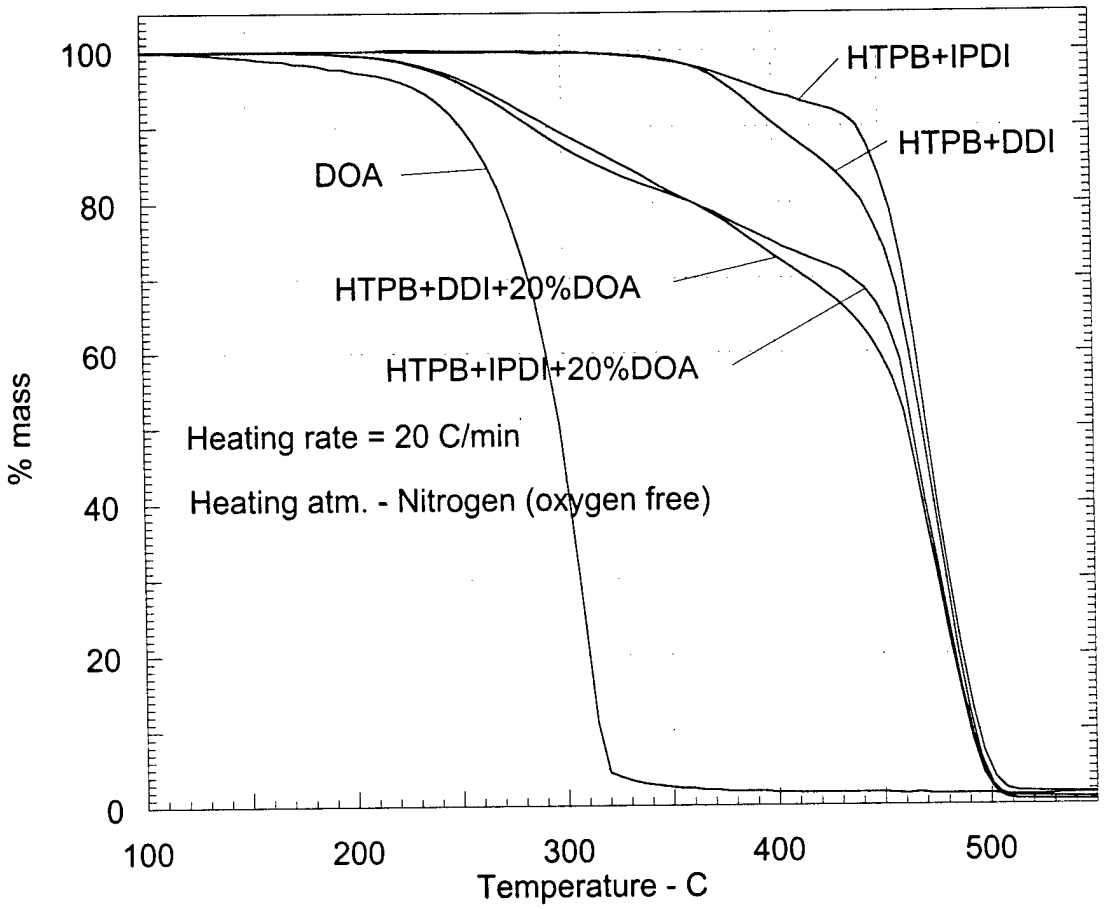

Fig. C-3. Effect of DOA plasticizer on TGA.

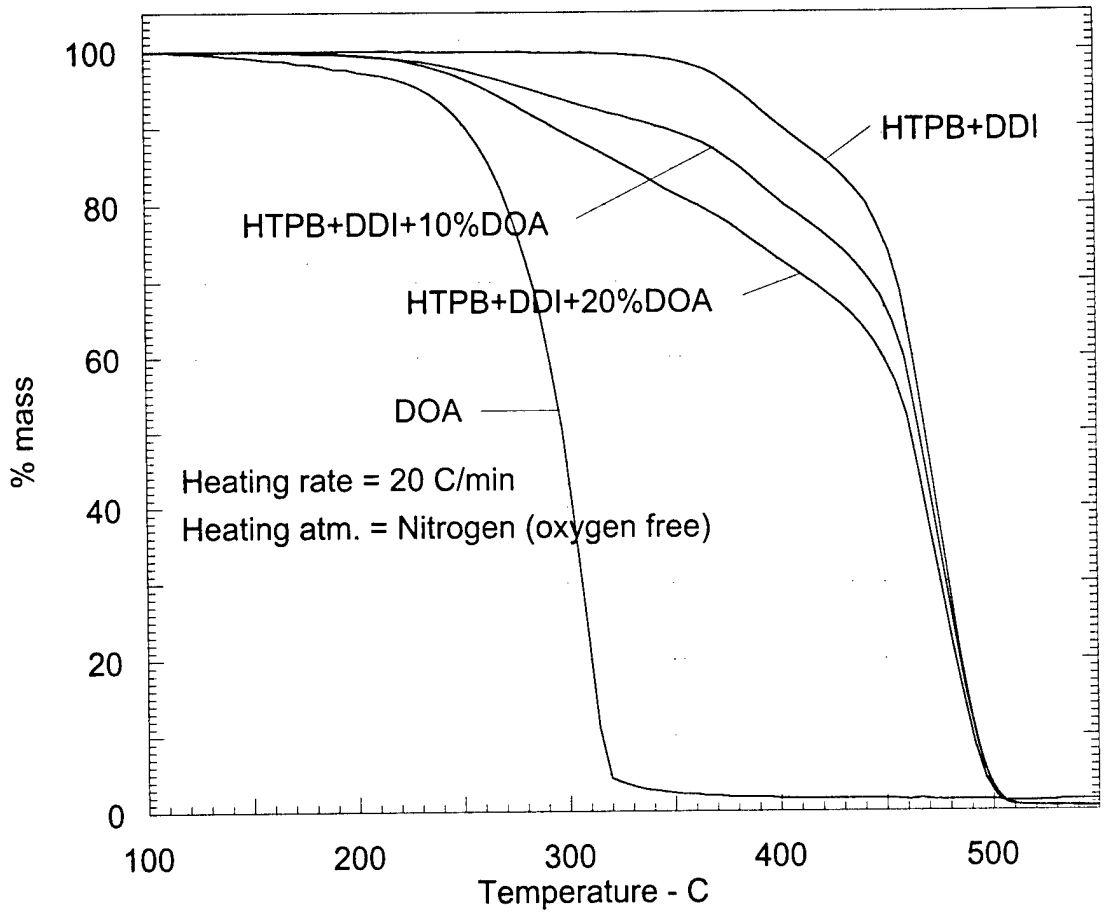

Fig. C-4. Effect of DOA in thermal decomposition of binder (TGA)

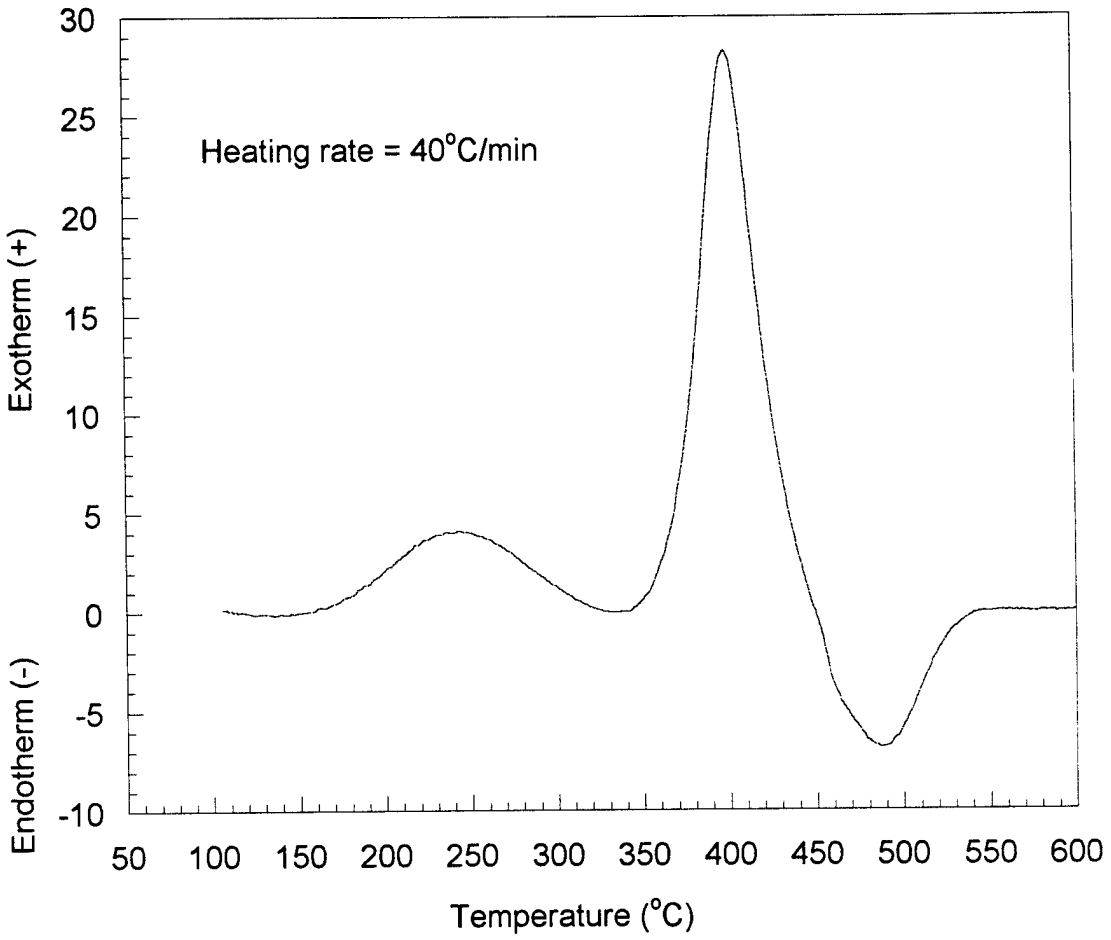

Fig. C-5a. Differential thermal analysis of HTPB binder cured with IPDI

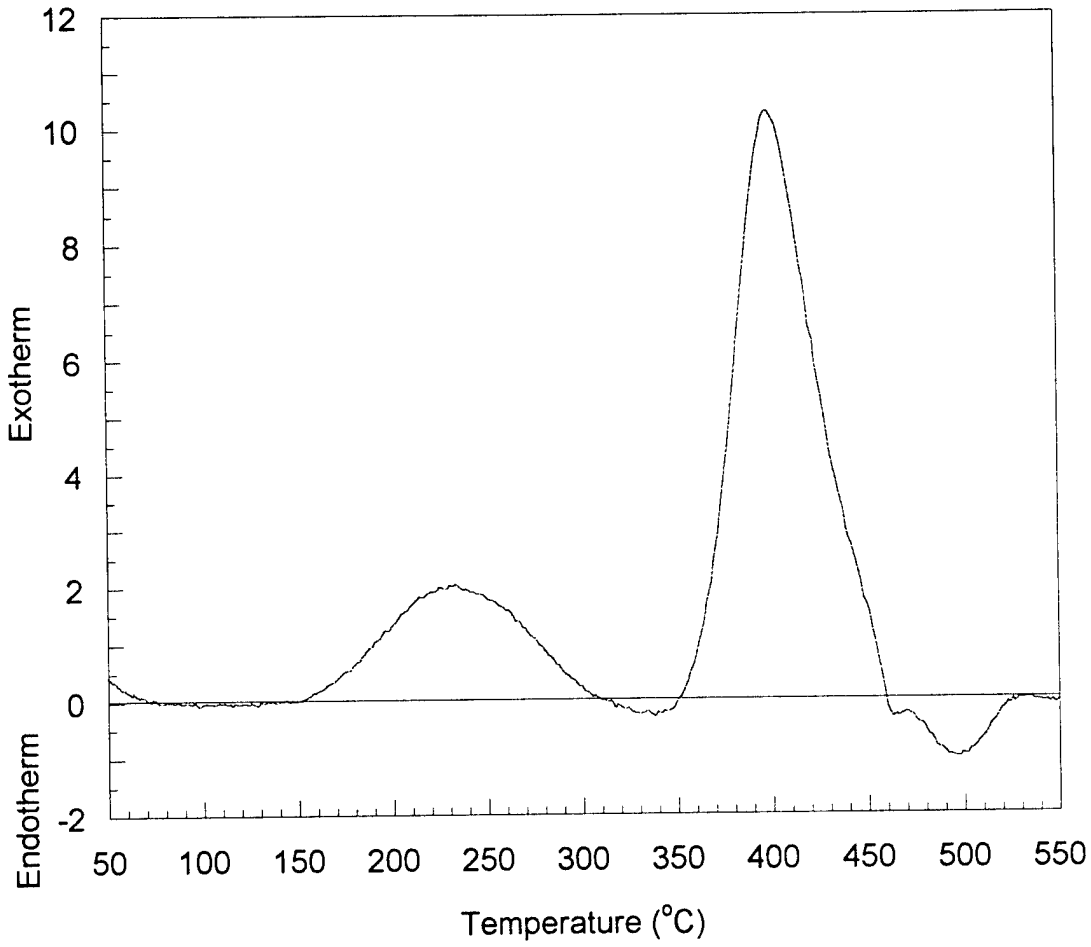

Fig. C-5b. Differential thermal analysis of HTPB binder cured with DDI

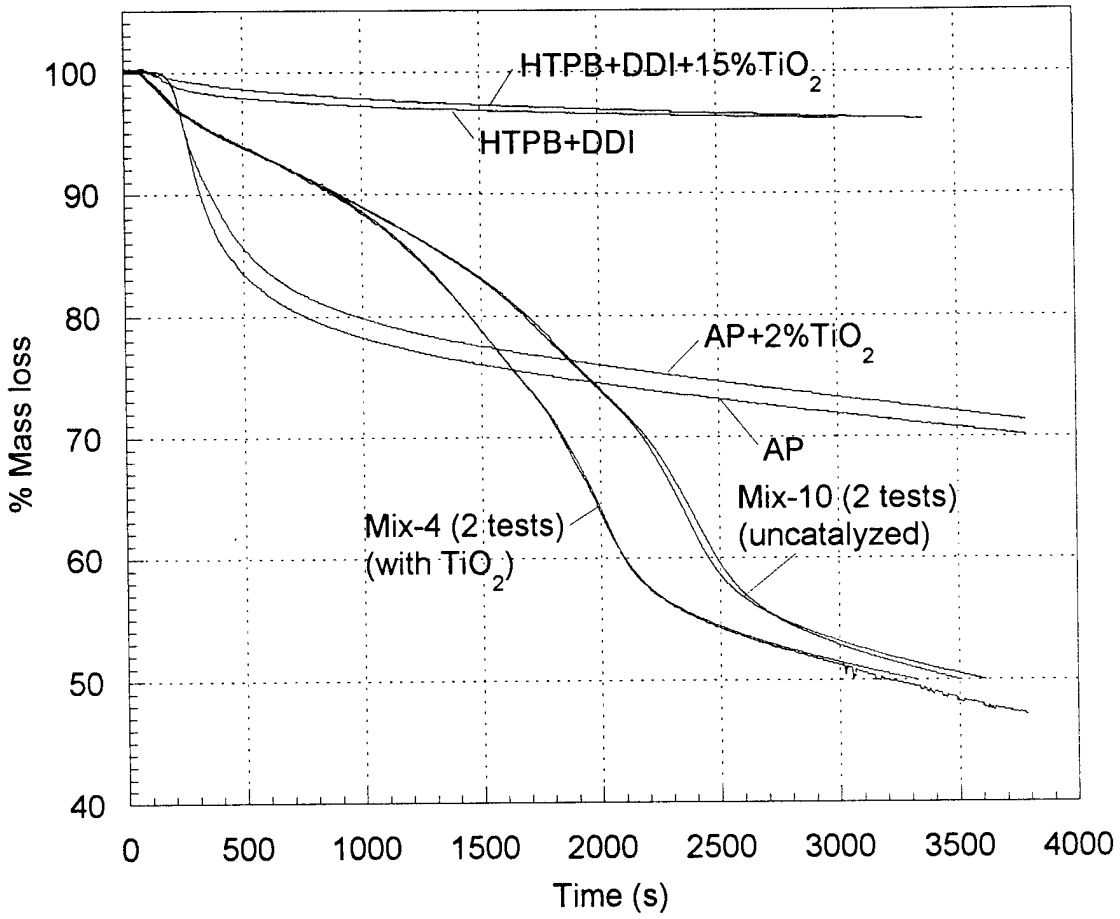

Fig. C-6. Effect of TiO2 on thermal decomposition of AP binder, and propellant. Isothermal decomposition at 300C.

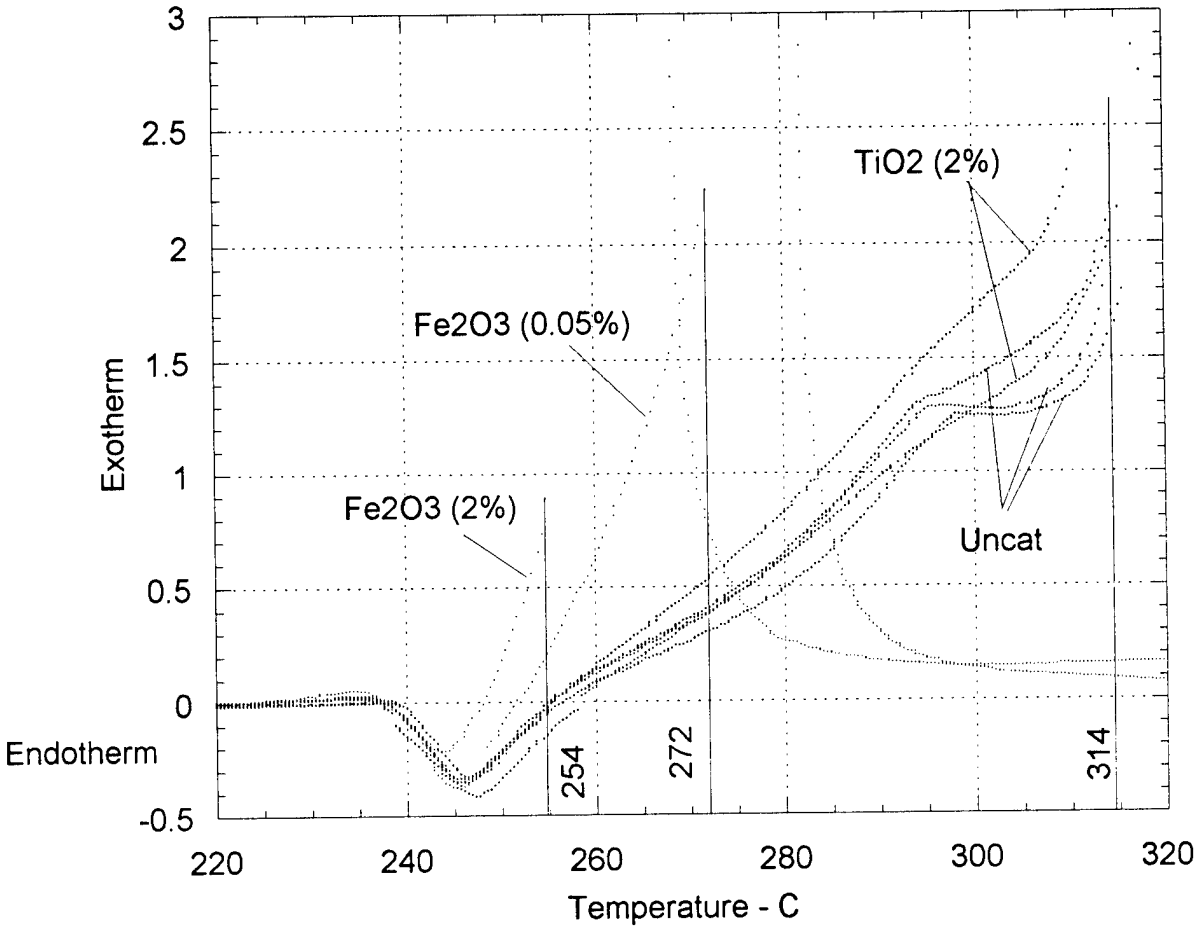

Fig. C-7. Comparison of matrix endotherms and ignition in DTA test for different catalysts. Matrixes were 73% 10 micron AP/27%HTPB-DDI-DOA binder (catalyst added).

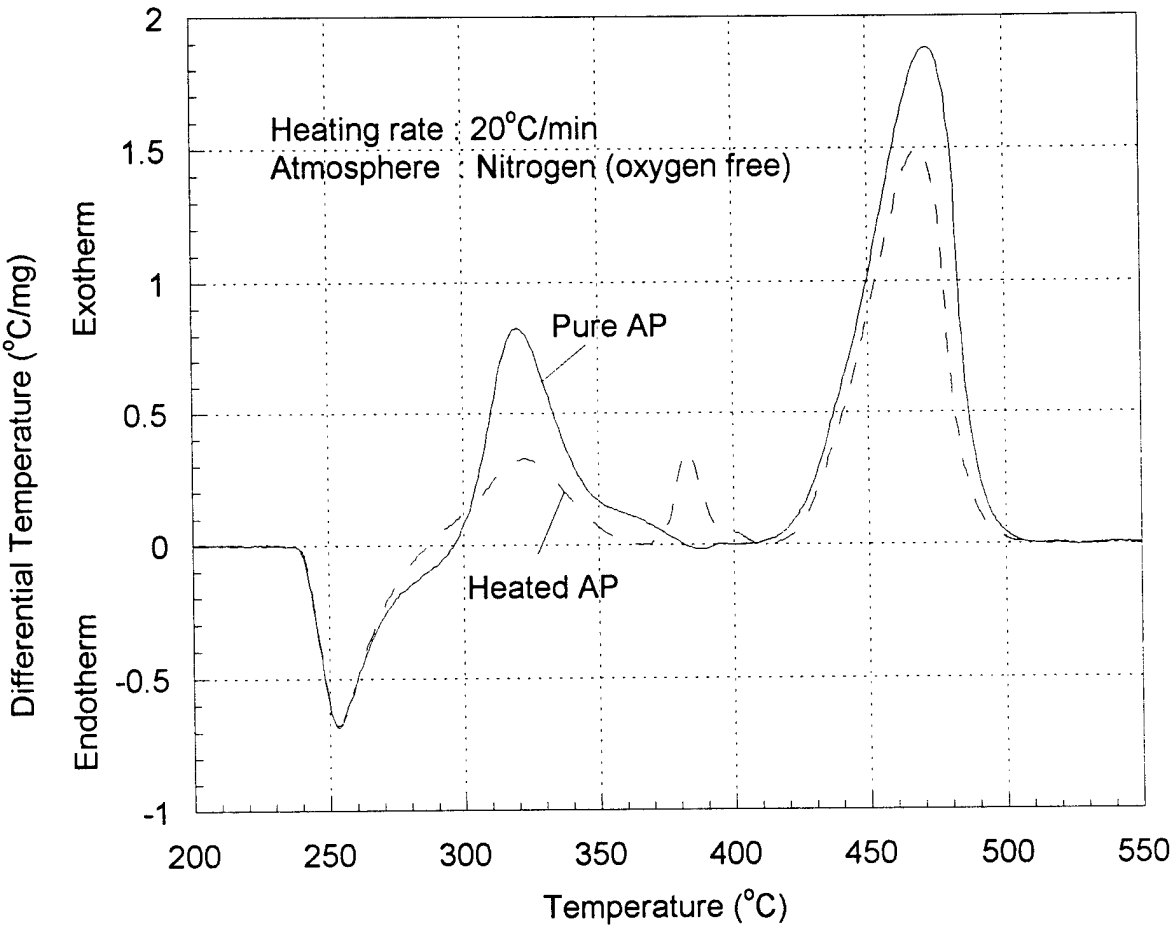

Fig. C-8. Differential thermal analysis of pure AP (dashed curve is for a sample previously heated at 250C).

APPENDIX D

Price, E. W.

"Effect of Multidimensional Flamelets in Composite Propellant Combustion"

AIAA Journal of Propulsion and Power,

Vol. 11, No. 4, pp. 717-728

Effect of Multidimensional Flamelets in Composite Propellant Combustion

E. W. Price

Reprinted from

Journal of Propulsion and Power

Volume 11, Number 4, Pages 717–728

AIAA

A publication of the
American Institute of Aeronautics and Astronautics, Inc.
370 L'Enfant Promenade, SW
Washington, DC 20024-2518

JOURNAL OF PROPULSION AND POWER
Vol. 11, No. 4, July–August 1995

Effect of Multidimensional Flamelets in Composite Propellant Combustion

Edward W. Price*
Georgia Institute of Technology, Atlanta, Georgia 30332-0150

This article reviews the results of a series of studies involving two-dimensional models of combustion of solid propellants. The results presented are selected to illustrate the role of the kinetically limited leading-edge portion of the oxidizer/fuel "diffusion" flamelets in controlling burning rate and aluminum agglomeration. Included are results from "sandwich burning," gas burner, numerical modeling of the two-dimensional flame, and tests on propellants to validate the applicability to propellants.

Introduction

THE mechanistic features of combustion of composite solid propellants differ conspicuously according to the kind of ingredients, scale of heterogeneity, and pressure. All propellants burn by decomposition, combustion, heat release, and heat return to the burning solid to sustain decomposition. Most analytical models are based on this "one-dimensional" view of burning. In this view of burning, the progress of chemical reactions is distributed in one dimension. It is recognized that heat release may occur at several locations, e.g., condensed-phase, surface, and gas-phase reactions. Problems arise in analytical modeling when the scale of heterogeneity of the propellant (e.g., particle size of oxidizer) is large enough for significant lateral temperature gradients in the microstructure, and for long enough mixing times of decomposition products (in surface liquid layers and gas phase) to limit reaction rates. The modeling problems are greatly aggravated when the melting and decomposition temperatures of the ingredients are markedly different. This is clarified by examples in Table 1. Another factor important to this article is the exothermicity of the oxidizer/fuel (O/F) flame (comparisons in Table 1). This article is concerned with propellant systems in which the oxidizer and binder decompose at comparable temperatures and in which the gas phase oxidizer/binder flame is strongly exothermic. These features are typical of combustion of most ammonium perchlorate/hydrocarbon (AP/HC) binder propellants. For such propellants a major part of the heat release can occur in an array of hot microflamelets standing in the mixing O/F flows ("mixing fans") formed above the oxidizer/binder contact lines on the burning surface. This is illustrated in idealized form in Fig. 1, using a two-dimensional microstructure for simplicity.

Modeling of AP/HC binder propellants[1,2] has sought to accommodate the deviations from one dimensionality in a variety of approximations involving the determination of some kind of average heat release and standoff distance of the AP flame and parts of the O/F flame. The averaging process is necessitated by the presence of a range of particle sizes, but usually ends up with some form of one dimensionalization that decouples the individual flamelets from the surface sites that feed the flamelet reactions. Considering the complexity of a rigorous model for a chaotic propellant structure, it is easy to understand why such approximations are used in models, and why the combustion details are often studied in simpler two-dimensional experiments as pictured in Fig. 1. The goal of this article is to look at the local details and nature of the O/F flamelets and see how they couple to the burning surface. The discussion will rely extensively on the experiments and analyses of two-dimensional models of propellants.

Before embarking on a discussion of O/F flamelets, it is appropriate for the sake of perspective to consider further the conditions under which such flamelets are present and are important. Under some conditions, such as those for which diffusion rates are high compared to O/F reaction rates, the O/F flame is premixed and approximately one dimensional (e.g., very fine AP or low pressure, or both). At very low pressure (i.e., low for rocket motor applications), all gas-phase reactions become so slow that little if any heat is returned to the burning surface and burning may be sustained by reactions in the condensed phase that are usually relatively unimportant at motor pressures (1000 psi). In heterogeneous propellants such low-pressure (subatmospheric) burning ordinarily occurs only if fine AP and/or catalysts are used in the propellant to enhance O/F reactions. The following observations are for typical AP/HC binder propellants in the pressure range 100–2000 psi:

1) The O/F reaction occurs in three-dimensional flamelets anchored in the mixing "fans" of oxidizer and fuel vapors that are in turn anchored at the contact lines of oxidizer and fuel on the surface.[3]

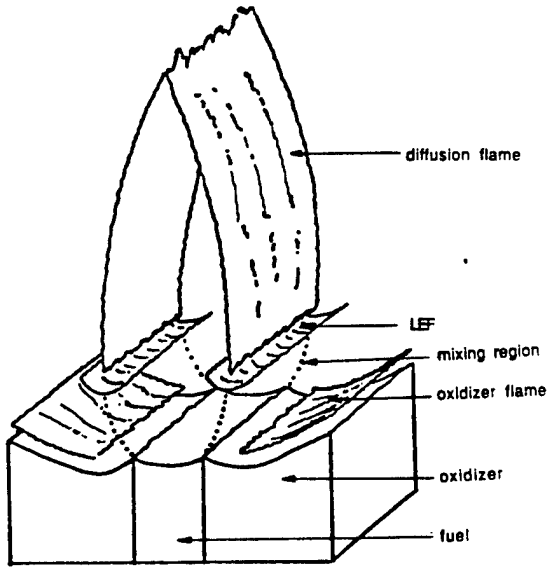

Fig. 1 Combustion zone structure for an AP/HC binders/AP sandwich.

Received Sept. 10, 1994; revision received Nov. 30, 1994; accepted for publication Dec. 2, 1994. Copyright © 1995 by E. W. Price. Published by the American Institute of Aeronautics and Astronautics, Inc., with permission.

*Regents' Professor Emeritus, School of Aerospace Engineering. Fellow AIAA.

Table 1 Approximate comparison of ingredient thermal response and energetics of oxidizer/fuel flames

Ingredient	Melting temperature, °C	Vaporization (decomposition) temperature, °C	Energetics of decomposition	Energetics of O/F flame
PBAN binder	480	500	Endothermic	—
HTPB binder (DDI-cured)	260	500	Endothermic	—
NMMO binder	85	200	Mildly endothermic	—
AP oxidizer	~580[a]	Rapidly above 400	Exothermic	—
AN oxidizer	145	245	Endothermic	—
KP oxidizer	—	400	Endothermic	—
HMX oxidizer	255	290	Exothermic	—
ADN oxidizer	90	165	Exothermic	—
CL-20 oxidizer	—	270	Exothermic	—
Aluminum	673	2493	Very endothermic	—
AP/PBAN	—	—	—	Very exothermic
AN/PBAN	—	—	—	Exothermic
HMX/PBAN	—	—	—	Nearly neutral
ADN/PBAN	—	—	—	Very exothermic

[a]Decomposes before melting except at heating rates $>10^5$°C/s.

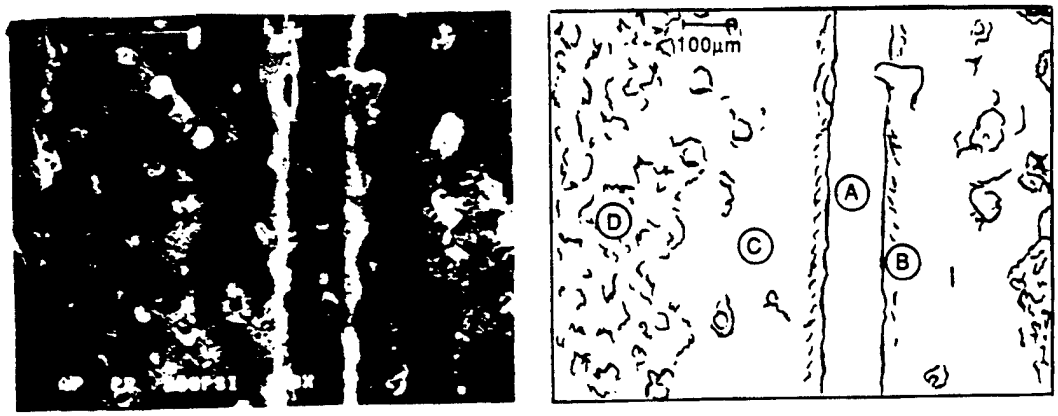

Fig 2 Details of an AP/PBAN/AP sandwich quenched by rapid depressurization from 500 psi (3.46 MPa): Ⓐ surface of the binder lamina, Ⓑ AP protruding along the laminas contact plane, Ⓒ location in a band of smooth surface (AP), concave upward. The leading edge of the burning front is located here, and Ⓓ frothy inclined surface typical of AP self-deflagration.

2) These flamelets are the principal site of heat release, coupled locally to the surface structure via the mixing fans.[3]

3) The part of each flamelet that is closest to the surface is most favorably located for returning heat to the surface, and is particularly intense because it consumes the accumulation of mixed O/F vapors prepared upstream of the "ignition point."

4) While the overall nature of the flamelet array is controlled by the rate of diffusion in the mixing fans, the location of the critical leading edge of each flamelet is also dependent on chemical kinetic rates in the mixing fans.

Modern combustion models for AP/HC binder propellants all incorporate these features (except the latter part of item 2) in one form or another.[4,5] The purpose of this article is to present and discuss studies aimed at determining the nature and role of the O/F flamelets more fully. These studies include edge burning of oxidizer-binder sandwiches, a gas burner study aimed at clarifying the nature of the leading-edge portion of the O/F flame, a numerical simulation of this leading-edge flame (LEF), and investigations aimed at determining the role of LEFs in ignition of aluminum. These studies used two-dimensional simulation of propellants to facilitate the observation, modeling, and interpretation of results. In this regard it should be understood that the critical features of the combustion zone occur on a dimensional scale of less than 100 μm (at motor pressures), below the spatial resolution of direct real-time experimental measurement. As a result, conclusions concerning experimental results are based on a variety of experimental data such as burning rate vs pressure and lamina thickness, observations of surfaces of quenched samples, and dependence of surface profiles on test variables. The gas burner studies were conducted at atmospheric pressure to facilitate detailed measurements.

Results from Combustion of AP/HC Binder Sandwiches

Studies of edge burning of laminates made up of alternate layers of oxidizer and fuel have been conducted by several investigators over the last 30 years; most of these studies are described in Ref. 5. For those studies that simulate propellant combustion, the features of the combustion zone are similar to those in the sketch in Fig. 1. The AP laminas are thick enough so that most of the edge surface of each self-deflagrates independently of the O/F flame, with an inclination that is determined by the relative burning rate of the sandwich and the AP (Fig. 1). The sketch shows the AP self-deflagration flame [which probably includes exothermic reactions in a surface froth (Fig. 2)]. The curvature of the AP surface profile closer to the lamina contact plane is an indication of heat flux from the O/F flame, with the point of maximum regression being the site of maximum net heat flux, and the rate-determining point (maximum heat in, minus heat loss by lateral heat flow). There is usually a region immediately adjacent to the binder lamina where the AP regression is retarded due to lateral heat loss to the (endothermic) binder lamina.[3] As can be seen in Fig. 2, the surface quality of the AP is different in the region that is heated by the O/F flame.

On theoretical grounds, one can argue that the stoichiometric surface in the mixing fan above each contact plane extends out over the AP surface because the oxidizer is relatively dilute compared to the binder. It can also be argued that the LEF will be centered on the stoichiometric surface, while the curvature of the AP surface profiles indicate that the LEF is close to the surface (e.g., 50 μm or so). As shown in Fig. 1, there is one LEF for each contact plane. Because the overall stoichiometry of the sandwiches discussed here are usually oxidizer-rich (i.e., thin binder laminae), the trailing diffusion flamelets "close" over the binder as in the sketch (Fig. 1). However, under propellant-like conditions, the sandwich binder lamina is usually very thin, the sandwich LEFs are close together, and the diffusion flame "tent" is very short. The LEFs are so close together that they may be coupled, consuming most of the fuel, leaving little for the diffusion limited parts of the flame tent (Fig. 3). The effect of this trend is evident in the dependence of sandwich burning rate on thickness of the binder lamina (Fig. 4). For binder thicknesses greater than 125 μm, the rate is relatively independent of thickness, indicating that burning is proceeding as two uncoupled burning fronts (with protruding binder in-between). A maximum burning rate occurs for thickness in the 50–75-μm range, a result that is explained[3] as optimum for LEF sharing of the fuel supply while minimizing heat "loss" through lateral heat flow to excess fuel that flows out between the LEFs without local exothermic reaction. For thinner fuel laminas the burning rate is lower because of insufficient fuel for the LEFs, so that the burning rate tends towards the AP self-deflagration rate as the thickness of the binder lamina approaches zero. These observations, described in more detail in Ref. 3, give an idea of the role of LEFs in sandwich burning, of the relevant dimensional scales, and of how they depend on pressure and lamina thickness. The relation to burning of

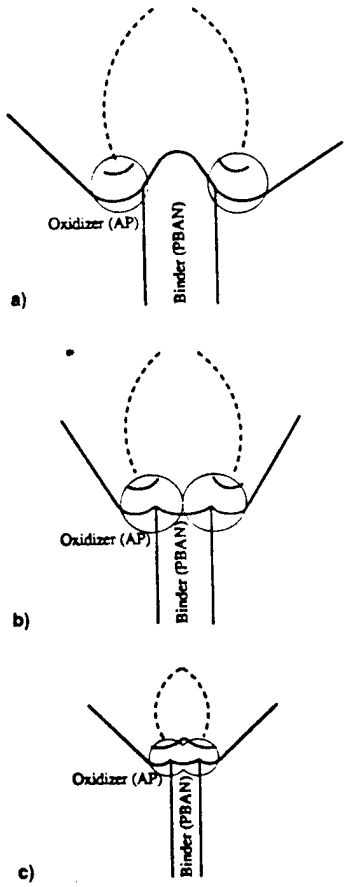

Fig. 3 Dependence of flame complex on thickness of binder lamina. Circles around LEFs indicate their domain of influence: a) thick binder lamina, b) 70–100 μm, and c) ~50 μm.

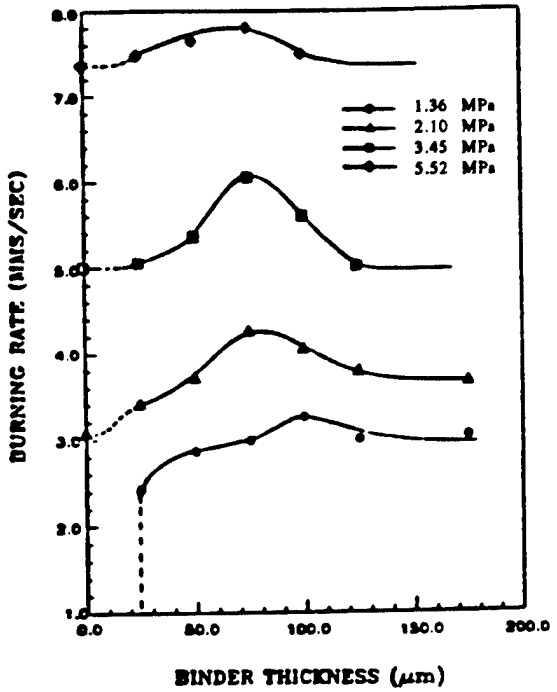

Fig. 4 Dependence of sandwich burning rate on thickness of the binder lamina.

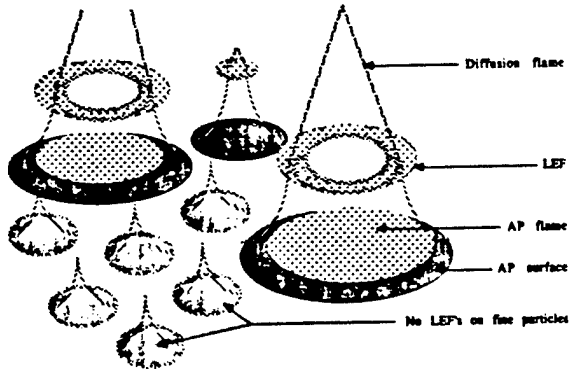

Fig. 5 Sketch of flame complex for a propellant with particulate AP.

a fuel-rich system with propellant-like microstructure is not too difficult to visualize (Fig. 5), except for the details of particle burnout, etc. The results are consistent with modern computational models in which it is found that LEFs are the primary source of heat to drive the combustion wave at intermediate pressures, with AP self-deflagration becoming more important above 1000 psi. There is direct evidence that condensed-phase or surface O/F interactions are not important in the >300-psi range in burning of AP/HC binder/AP sandwiches.[3]

As noted in Ref. 5, the results of sandwich burning studies by different investigators do not all agree. The disagreement appears to be due to the differences in binder and the failure to examine the effect of thickness of binder laminas (and widespread use of large thicknesses).

The results presented here are for polybutadiene acrylonitrile acrylic acid (PBAN) binder laminas of low thickness compared to most other sandwich-burning studies (for relevance to propellants). Tests with other binders showed some differences (example in Fig. 6) that appear to be related to tendency of some binders to form a melt layer that flows onto the AP surface. This is uneven and nonsteady along the edge of the laminas, causing a loss of two dimensionality of the combustion, including sometimes faster burning down one

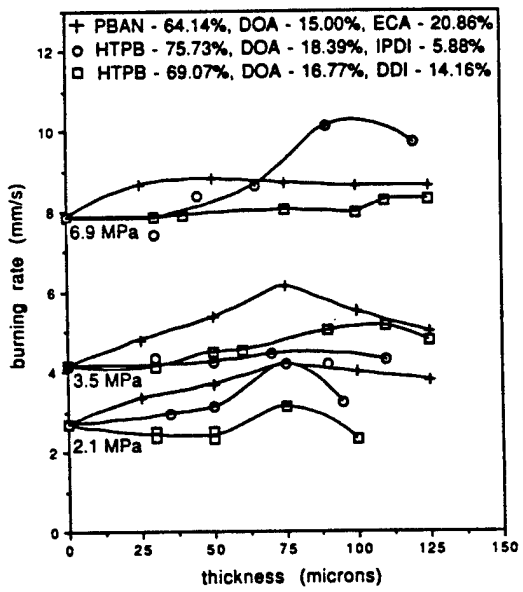

Fig. 6 Comparison of sandwich burning rates for different binders: burning rate vs binder lamina thickness.

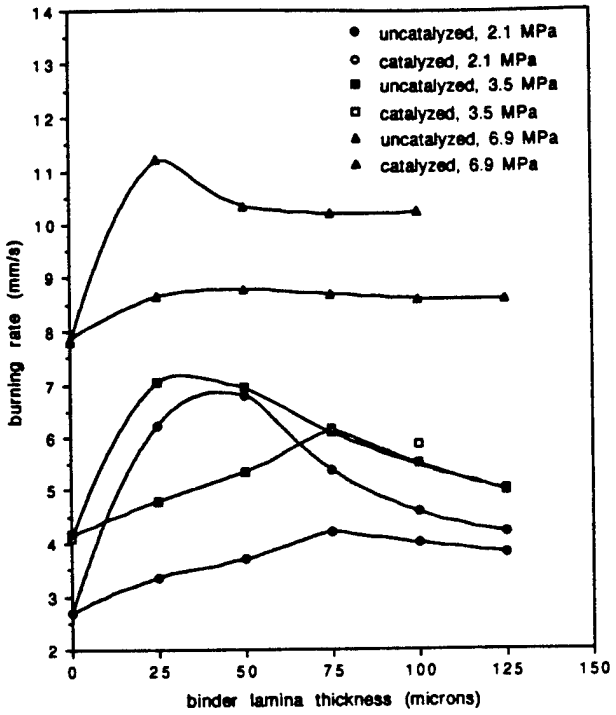

Fig. 7 Effect of Fe_2O_3 catalyst (10%, 2 μm, in the binder lamina) on the burning rate of AP/PBAN/AP sandwiches (from Ref. 6).

interface than the other. The test results are simpler and easier to interpret when melt flow effects are minimized as with PBAN binder, but more attention to melt flow effects is needed because widely used binders such as dimeryl diisocyanate (DDI)-cured hydroxyl-terminated polybutadiene (HTPB) are prone to melt effects, evident even in sandwich burning rates (Fig. 6). It is not yet clear what O/F flamelet arrays result when binder melts encroach on the oxidizer surface, and it seems unlikely that all past sandwich burning studies (or propellant burning studies) can be reconciled without learning more about how the melt flow proceeds, and about the corresponding effects on surface pyrolysis and flamelet arrays. Melt flow is minimal with the PBAN binder used in most of the studies reported here.

Effect of Burning Rate Catalysts in AP/HC Binder/AP Sandwiches

A number of investigators have added catalysts to the AP laminas, binder lamina, or contact planes, with various proposed catalytic mechanisms.[5] In the present studies, catalysts were added to the binder lamina, in order to simulate propellants.[6,7] An example of test results is shown in Fig. 7. In interpreting the results the following was noted:

1) There is only limited exposure of the catalyst to the AP decomposition region or to the AP-binder interface (because the catalyst particles are in the binder), suggesting that rate enhancement involves the binder decomposition or the LEF, or both.[7]

2) Simple catalysis of decomposition of the binder would not in itself affect burning rate much because the effect would primarily be to cause the binder surface to be recessed a little more.[8]

3) The presence of particulate catalyst in the mixing fan and LEFs would not have much catalytic effect because of limited collision rate with catalyst.

4) The effective catalysts were observed to concentrate on the binder surface, where preliminary binder-decomposition fragments have high collision probabilities in passing through the "catalyst bed"; even the Catocene catalyst produced iron oxide concentration on the binder surface.

5) The catalysts are known to be effective in "cracking" heavy hydrocarbons.

6) Flames with heavy hydrocarbons are known to form only where the hydrocarbons have pyrolyzed to more reactive light species.

From these observations it was concluded[6,7] that in these tests the catalyst acted by supplying more reactive fuel fragments to the LEFs, allowing the LEFs to locate closer to the surface with correspondingly higher heat flux to the surface. This interpretation is supported by the fact that the burning rate and surface profiles showed dependence on thickness of the binder lamina and on pressure similar to that observed with uncatalyzed sandwiches. Thus, the catalysts effectively catalyze the LEF, but actually act at the binder surface by decomposing the heavy binder-vapor fragments. In this regard, it is emphasized that the response of the LEF is responsible for the burning rate increase. It will be seen in a later section that the catalyst may act in a different way when higher contact area of AP, binder, and catalyst exists.

Conditions for Presence of LEFs, and LEF Coupling

An investigation was made[9-12] of the burning of sandwiches in which the "binder" lamina was a matrix of PBAN binder and fine AP (10 or 33.5 μm) with AP contents of 50 and 70%. With such fine AP particles, the AP and fuel vapors can diffuse together before appreciable O/F reaction, giving a premixed flame if the mixture (e.g., 70% AP) is not too fuel rich to burn. At high pressure with 33.5-μm particles, there was evidence in quenched samples that LEFs and AP self-deflagration occurred on individual particles, (no such evidence for 10-μm particles, or for 33.5-μm particles at 300 psi). For 50/50 matrices this was evident only adjoining the lamina contact planes, indicating coupled behavior between lamina LEFs (LLEFs) and particle LEFs (PLEFs). The burning rates of the sandwiches with AP-filled binder laminae are shown in Fig. 8 (PBAN binder).

In interpreting the results in Fig. 8, it should be noted that the matrix mixtures are fuel-rich, even at a 70/30 ratio. The 50/50 mixture would not burn on its own, and quenched sandwiches showed matrix surfaces that were dominated by solidified binder melt (except as noted above). If one looks at the matrix as a "diluted fuel lamina" and repeats the argument about location of the interlamina mixing fan, stoichiometric surface and LLEF, one would expect them to be shifted closer to the "extended" plane of the lamina contact surface (Fig. 9), reflecting the effect of a less concentrated fuel. One effect

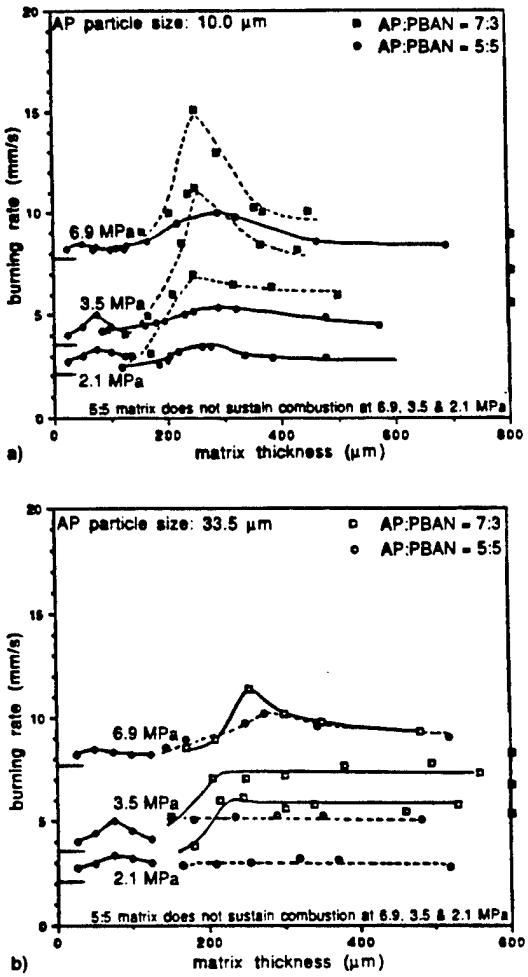

Fig. 8 Dependence of sandwich burning rate on thickness of the binder lamina from binder laminas consisting of a matrix of PBAN and particles (from Ref. 9): a) 10- and b) 33.5-μm AP. AP burning rates are indicated on the left, and matrix burning rates are indicated on the right ordinate lines. Pure binder sandwich burning rate curves are shown in the thickness range 25–125 μm.

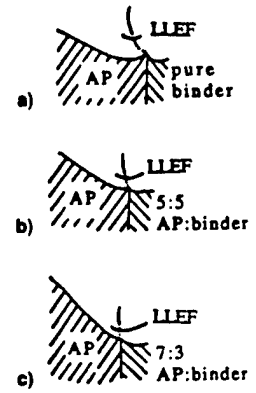

Fig. 9 Shift in LLEFs when the binder is "diluted" with AP a) narrow LLEF, over AP lamina. Heat flow from AP lamina to binder lamina, AP regression retarded at laminas contact plane; b) wider LLEF, stoichiometric point closer to surface and shifted toward laminas contact plane. Less lateral heat flow in solid, less retardation of AP at contact plane. More conservative LLEF, closer to surface, correspondingly higher rate; and c) wider LLEF, stoichiometric point over outer edge of AP lamina. LLEF extends well over matrix lamina, probably minimal lateral heat flow in solid.

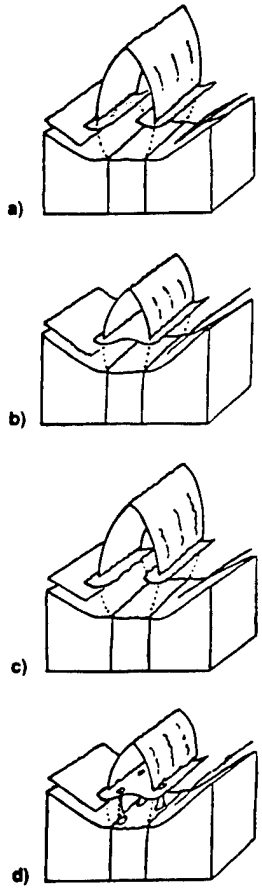

Fig. 10 Flame complex for sandwiches with AP-filled binder laminae (300-μm matrix lamina, 500 psi, 3.45 MPa): a) 50/50 AP/PBAN matrix, 10-μm AP; b) 70/30 AP/PBAN matrix, 10-μm AP; c) 50/50 AP/PBAN matrix, 33.5-μm AP; and d) 70/30 AP/PBAN matrix, 33.5-μm AP. Refer to Fig. 1 for an explanation of general features.

of this, evident in the quenched surfaces and combustion photography, is a reduction (and sometimes elimination) of the protrusion of AP adjoining the contact plane. The LLEF is located more favorably to heat this region than in the pure binder case, and also more favorably to reduce lateral heat loss to the fuel lamina by supplying more LEF heat directly to the fuel lamina.

The premixed AP vapors in the "diluted" matrix outflow are, of course, more than a diluent. On the fuel-rich side of the LLEF they are a combustible mixture, that extends the fuel rich side of the LLEF out over the matrix. This increases the total heat release in the LLEF, enabling the flame to stand closer to the surface and give a higher burning rate than resulted with pure binder laminas (Fig. 3), and higher than the matrix burning alone (indicated at the right in Fig. 8). The thickness of matrix lamina for maximum burning rate is around 250 μm, as compared with 50–75 μm for pure binder lamina. This is consistent with the interpretation described for pure binder laminas if one allows for 1) the greater extent of the fuel-rich side of the LEFs that leads to attainment of LLEF coupling at greater thickness of the matrix laminas and 2) the fuel supply becomes deficient with decreasing lamina thickness at greater matrix thickness because the fuel is dilute.

The nature of the O/F flame complex for matrix sandwiches is sketched in Fig. 10, based on theoretical reasoning and experimental results. For a 70/30 mixture with 10-μm AP, the LLEFs act as flameholders for a premixed "canopy" flame over the matrix lamina (Figs. 10b and 10d). For a 50/50 matrix the canopy is open (thick laminas) because the matrix does not support a flame alone (Figs. 10a and 10c). However, the fuel-rich side of the LLEF extends further than with pure binder, as noted earlier, because a flammable mixture is present. The burning rate of the samples with 70/30 matrices is higher than with 50/50 matrices at all matrix thicknesses except the lowest, suggesting that the size and location of the LLEFs (Fig. 10) are 1) closer to the surface and 2) more favorably

located laterally to heat the matrix surface and minimize lateral heat loss in the condensed phase into the matrix lamina. The quenched samples indicate that the sandwich burning rate is determined by LLEF-assisted regression of the AP lamina, as noted earlier for pure binder laminae.

The effect of particle size of the AP in the matrix gives important clues to the details of the O/F flamelets, as follows:

1) Effect of particle size (i.e., 10 and 33.5 μm) is small for 50/50 matrix ratio, and for 70/30 ratio at 300 psi. This suggests that under these conditions the matrix outflow is essentially premixed at the LLEF standoff height and premixed canopy flames (Figs. 10a and 10c) result.

2) Burning rates are higher with 10-μm AP than with 33.5-μm AP in the 70/30 matrix at 500 and 1000 psi, suggesting that mixing is not complete for the 33.5-μm AP (thereby limiting the contribution of the fuel-rich side of the LLEF to the rate).

3) A relatively strong maximum occurs in the rate vs lamina thickness curves (70/30 matrix at 500 and 1000 psi), especially for 10-μm AP. This indicates that the matrix flame does not

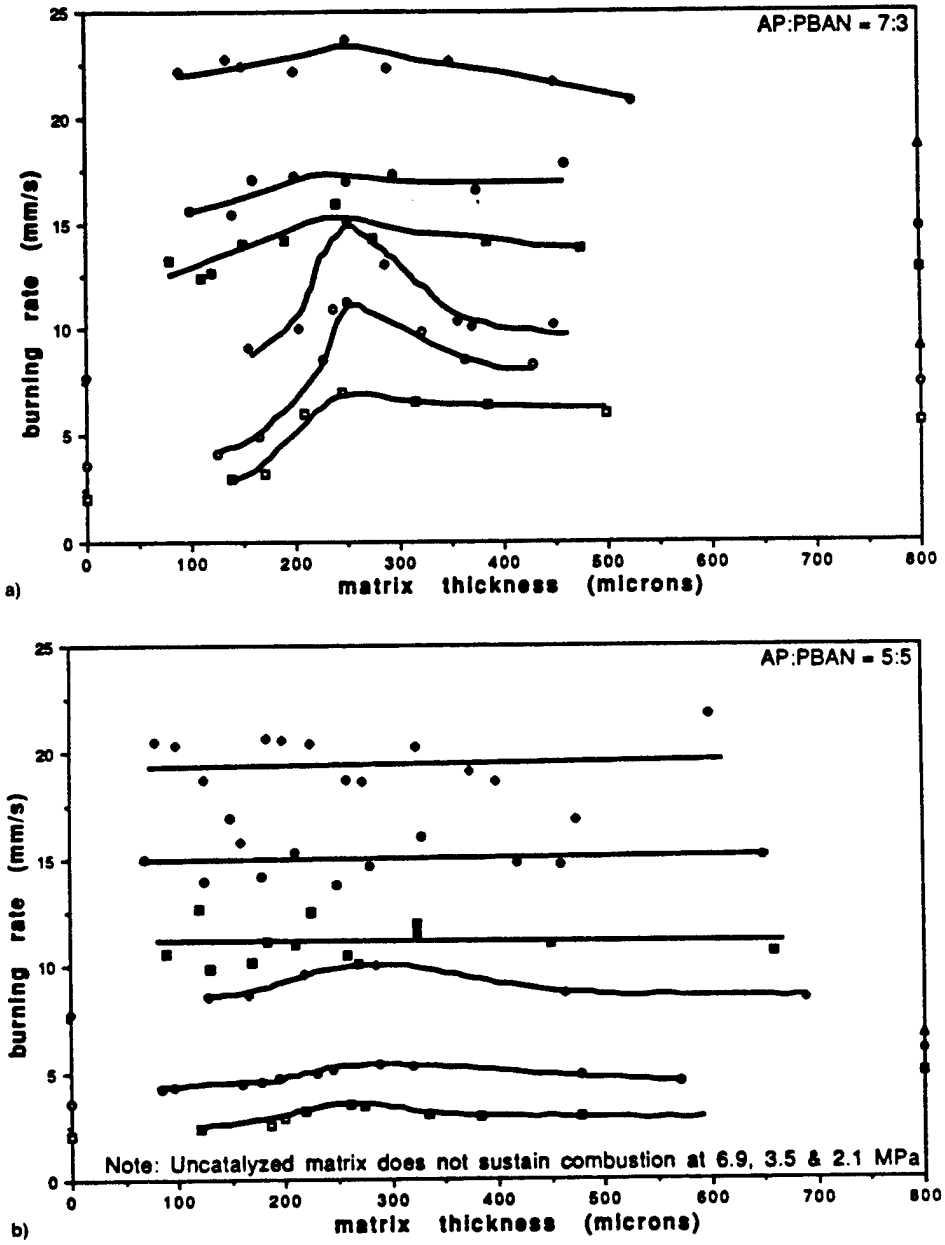

Fig. 11 Dependence of sandwich burning rate on thickness of the binder lamina for binder laminas consisting of a matrix of PBAN binder, fine AP (10 μm and 1% "Pyrocat" Fe_2O_3 catalyst: AP:PBAN = a) 7:3 and b) 5:5 (from Ref. 13).

control the rate, but rather enhances it via augmentation of the LLEFs. Extra matrix (i.e., thick lamina) apparently acts to drain heat (and possibly oxidizer species) from the rate controlling region of the sandwich.

4) The weaker maximum of the rate curves in 3 with 33.5-μm AP presumably reflects the weaker contribution of the fuel-rich side of the LLEFs due to incomplete mixing of the matrix outflow.

5) The quenched 70/30 samples that were burned at 500 and 1000 psi showed evidence that the 33.5-μm particles adjoining the AP laminae were burning individually (i.e., with PLEFs and AP self-deflagration). This may have been a factor in the burning rate, but it is notable that the same behavior was not evident with 10-μm AP, which gave higher burning rate.

Taken collectively, the results indicate that, for the conditions tested, the LLEFs dominate the burning rate, and that AP in the binder lamina enhances the LLEF effect by shifting the LEFF position and extending the fuel-rich side (and, hence, increasing LLEF heat release). Fine AP is more effective because more complete mixing has occurred at the LLEF height. The optimum lamina thickness for rate enhancement is around 250 μm for the conditions tested. Under the conditions tested the individual particles of AP either did not establish their own flamelets, or when they did (33.5 μm, 70/30, 500, and 1000 psi) no major effect on burning rate was evident. This suggests that in a typical bimodal propellant, the fine AP/binder matrix does not control the burning rate directly, but rather enhances the burning rate of the coarse AP particles. As the fine particle size and pressure increase, the fine particles burn more independently and enhance the coarse particle burning less (transition somewhere in the 500–1000-psi range for 33.5-μm AP in a 70/30 matrix, above 1000 psi in a 50/50 matrix).

Combination of Fine AP and Fine Fe_2O_3 in the Binder Lamina

An extension of the "filled" binder lamina studies was initiated by adding Fe_2O_3 to the matrix. Initially 10% of the 2-μm Fe_2O_3 used in the catalyzed binder lamina studies (described above and in Refs. 7 and 8) was attempted, using 10-μm AP and PBAN binder. Samples with 70/30 AP/PBAN ratio could not be processed, and samples with 50/50 ratio gave very erratic burning rates. A change was made to 1% of "Pyrocat" Fe_2O_3 (described by the manufacturer as 0.003-μm particles). Satisfactory results were obtained (Fig. 11, Ref. 13) with a major increase in the burning rate over similar samples without catalyst (Fig. 8). Addition of the catalyst increased the burning rate of the 70/30 matrix by about 100% at all three pressures, and caused the burning of the 50/50 matrix to be self-sustaining (matrix rates shown at the right in Fig. 11). The burning rates of the sandwiches with 50/50 matrix were about double the rate of the matrix alone and insensitive to lamina thickness. The rates of the sandwiches with 70/30 matrix were somewhat higher than the corresponding matrix, only mildly dependent on lamina thickness. The features of quenched samples are not yet completely available, but limited results show only a narrow portion of the AP laminas with the smooth surface quality, a narrow ledge that is no longer clearly "horizontal" (i.e., compared to the vertical laminas contact plane). As a preliminary conclusion, it appears that the LLEF plays a less important role in the burning rate in the catalyzed matrix sandwiches (some role is indicated by the fact that the sandwiches burn faster than the matrix alone). Many authors have argued that Fe_2O_3 acts by catalysis of reactions at the oxidizer/binder contact surfaces, an argument that is supported most strongly by burning tests of propellants at pressures near 1 atm. The evidence described in a preceding section for catalyzed binder laminas supported a contrary argument, but the situation is very different in the AP-filled binder laminas, because the amount of AP-binder contact area is enormously increased, and the very fine Fe_2O_3 has far greater surface area, more uniformly available in the solid. Thus, it seems plausible to assume that catalyzed contact-surface reactions contribute significantly or predominantly to the heat flow that determines burning rate in the catalyzed matrix sandwiches (the reactions may involve gas phase in microscopic interface crevises at contact surfaces). If LLEF heating were the primary factor in rate, one would expect a greater dependence of rate on lamina thickness than is evident in Fig. 11. It is possible that catalytic cracking of binder vapors also contributes to burning rate enhancement by bringing the LLEFs and the premixed matrix flame closer to the matrix surface in the manner argued earlier for the LLEFs in the case of sandwiches with catalyzed binder. Further study is needed.

Role of LLEFs in Behavior of Aluminum in the Combustion Zone

When powdered aluminum is used in AP propellants, the aluminum is observed to concentrate on the burning surface and depart as large agglomerates, a condition that can pose problems with combustion efficiency, slag formation, and prediction of combustor stability. A critical factor in agglomerate formation is the inflammation of the accumulating aluminum, which leads abruptly to the formation of a burning droplet that is too hot to remain on the burning surface. Several studies[14,15] suggested that inflammation of accumulating aluminum did not occur until exposed to the high temperatures of the O/F flamelets. This issue was examined by the introduction of aluminum powder in the binder laminae of AP/PBAN/AP sandwiches (binder laminae around 70 μm thick, pressure 500–1000 psi). Combustion photography and quenched samples showed sintered accumulations of aluminum, with inflammation always starting at locations nearest to the contact planes. Aluminum leaving the surface near the center of the binder lamina did not ignite near the surface (no oxidizer vapors). Sandwiches were then tested in which the aluminum was mixed with the AP before dry pressing (i.e., the AP laminae contained the aluminum). During burning, the AP surface became covered with a layer of sintered aluminum. This accumulation ignited only at the edge adjoining the contact plane where LLEF heating was present. Once ignited locally, the inflammation spread rapidly along the contact plane, and more slowly outward over the covered AP surface, forming one or more large burning agglomerates. Tests were

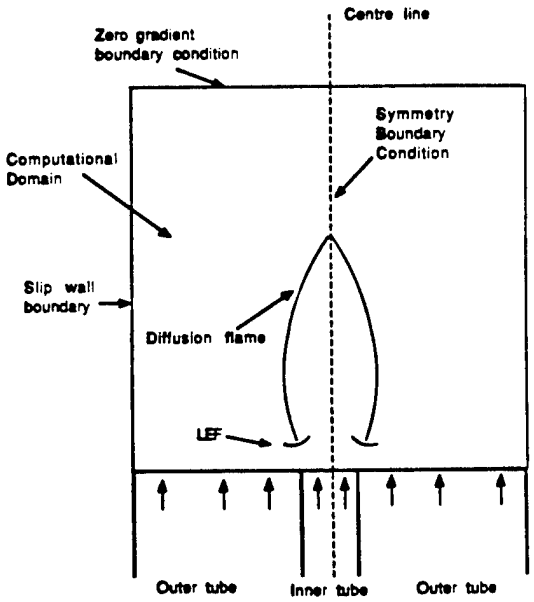

Fig. 12 Arrangement for a two-dimensional gas diffusion flame burner (numerical model and experiment).

also run on aluminized AP laminae alone (no binder lamina). The aluminum was observed to concentrate on the burning surface and leave the surface as large sintered accumulations with ignition and agglomeration being only occasional and apparently starting at sites where the sintered accumulations experienced break up. These results showed the critical role of the O/F flame in igniting surface aluminum accumulations, thereby limiting agglomerate size.

Theoretical-Numerical Analysis of Leading-Edge Flames

Because of the emergence of LEFs as a critical factor in edge-burning of AP sandwiches and propellants, it was decided to attack the problem of rigorous modeling of two-dimensional diffusion flames.[12,16,17] This effort was started because of the absence of direct observations of LEFs in propellant-sandwich combustion studies (because of inability to make such observations on microflamelets). In the modeling work the gases were assumed to emerge at the upstream boundary (Fig. 12) at specified velocity, density, and temperature (simulating a Wolfhard-type gas burner), and pressures near atmospheric were assumed (simulating a companion experimental study). Nonsteady laminar Navier–Stokes flow was assumed. Inlet gases were assumed to be $CH_4 + N_2$ in the center flow, and $O_2 + N_2$ in the outer flow. The chemistry was represented by a set of 48 elementary reactions involving 18 species. Temperature-dependent transport properties were used for each chemical specie. Details and computational methods are described in Ref. 16. Some notable results about LEFs are discussed here.

Figure 13 shows plots of distribution of species concentration, heat release rate (per unit volume), pressure, and flow direction (streamlines). Figure 13a shows the concentration of CHO, which is a short-lived intermediate product present only in the flame. There are locally high concentrations at the LEF sites. Figure 13b shows very high heat release rates at the same sites (high rates compared to the diffusion limited part of the flame further downstream), indicative of abrupt

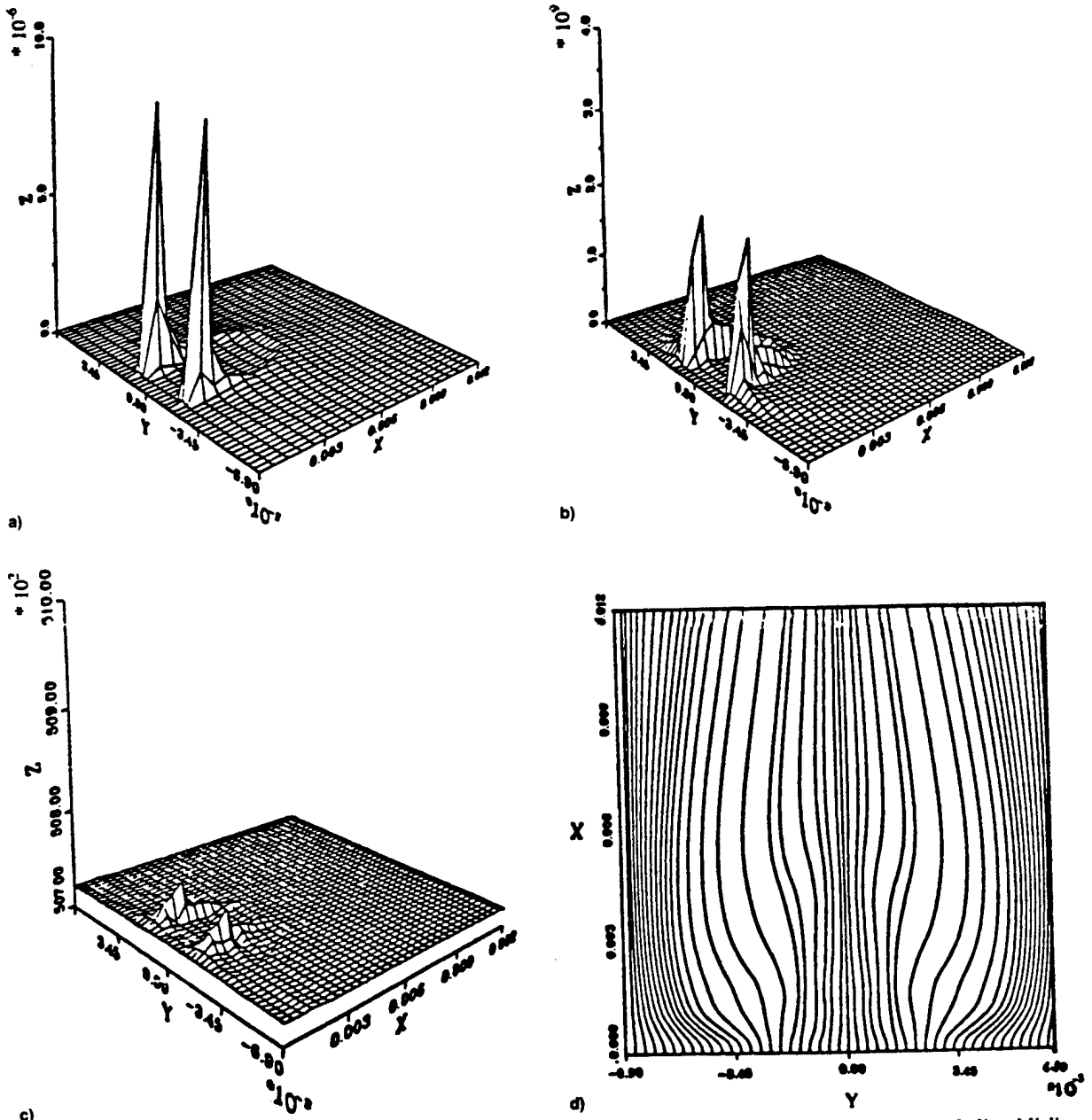

Fig. 13 Computed features of two-dimensional methane-air diffusion flame (N_2 diluted), burner configuration as in Fig. 12; X and Y dimensions are in meters; flow enters at lower left: a), b) and c), and at the bottom in d): a) CHO concentration (mass fraction); b) volumetric heat release rate (J/m^3 s); c) pressure [N/m^2]; and d) streamlines (Ref. 16).

consumption of the reactants that have mixed upstream of this site. Figure 13c shows that this concentrated reaction and the associated volume increase produce local pressure increases at the LEF sites, and Fig. 13d shows that this produces a divergence of the approach flow, as a result of which the vertical component of the velocity of the approach flow to the LEFs is reduced (i.e., does not increase as much as in a one-dimensional flame). These results support the idea of an intense leading-edge flame, an extended, less intense diffusion limited "tent" flame (Fig. 1). These computed LEFs show little lateral extent, contrary to those suggested in earlier sketches and discussion here. This "narrowness" is a feature of LEFs produced by combinations of pure fuel and oxidizer flows (i.e., diluted only by relatively inert gas). In a following section on LEFs in gas burner flames, crescent LEFs resulted when some fuel was included in the oxidizer inflow and some oxidizer in the fuel inflow. In the sandwich burning tests, the products of AP pyrolysis are a mixture of fuel and oxidizer species (e.g., NH_3 and $HClO_4$); and most of the binders, and especially the AP/binder matrix laminae, have oxidizer species in the laminae outflow. Thus, the propellant LEFs probably have appreciable lateral extent as suggested earlier in the discussion of the effect of addition of AP to the binder lamina.

Fig. 14 Double exposure images of one of the two diffusion flames in the gas burner, viewed edge-on. The bright central plume is the flame viewed by self-luminosity. The surrounding lines correspond to isotherms, produced by monochromatic light interference fringes (M-Z interferometry) (Ref. 18).

LEFs in Gas Burner Flames

To further verify the presence and nature of LEFs, a gas burner study was made[12-18] using a rectangular atmospheric pressure burner with a fuel flow in the middle and oxidizer flows on the outside (analogous to sandwiches and to the numerical study). A methane-air combination was used, with N_2 and CO_2 used as diluents. Outflow velocities were matched, but varied together from 15–50 cm/s. The flames were viewed edge-on photographically, including viewing with a Mach–Zehnder interferometer that permitted determination of the temperature field (example in Fig. 14). Temperatures were also measured with a traversing thermocouple. In addition, the flames were viewed side-on for intensity of CH radiation, a good indicator of heat release rate. The results of this study are detailed in Ref. 18. Some highlights are summarized here.

1) An intense leading-edge region of the flame was indicated in the CH intensity and temperature measurements, and the flame standoff distance from the burner surface was measured from photographs.

2) These LEFs were of limited lateral extent, consistent with results of the computational studies.

3) When fuel was added to the oxidizer flow and oxidizer added to the fuel flow, a crescent LEF resulted (Fig. 15).

4) The approach flow was deemed to be laminar, because turbulence would smear out interference fringes, an effect that was not observed (Fig. 14).

5) The "effective flame speed" of the LEF was taken to be the flow velocity from the burner, and was compared with the flame speed of one-dimensional premixed methane-air flames of the same temperature (Fig. 16). This effective flame speed was as much as 2.5 times the premixed flame speed.

In general, the experimental results were consistent with the numerical modeling results, indicating an intense, local LEF in the mixing fan, followed by a trailing diffusion limited flame with much lower heat release rate. The high effective

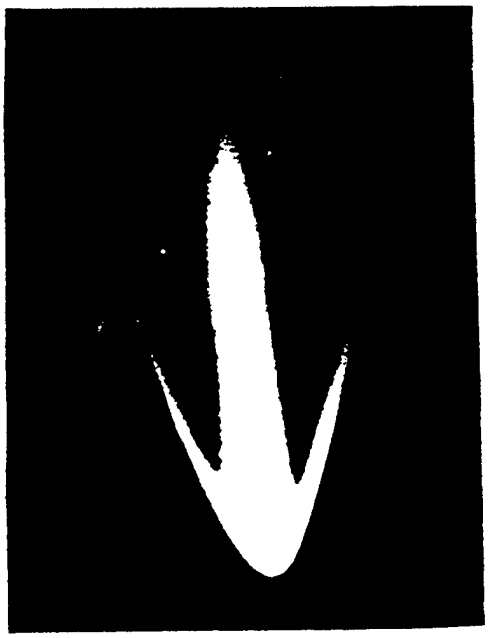

Fig. 15 Leading-edge flame in the gas burner when O and F inflows were enriched with F and O (mixtures well below flammability limits: methane-air with N_2 and CO_2 dilution, atmospheric pressure).

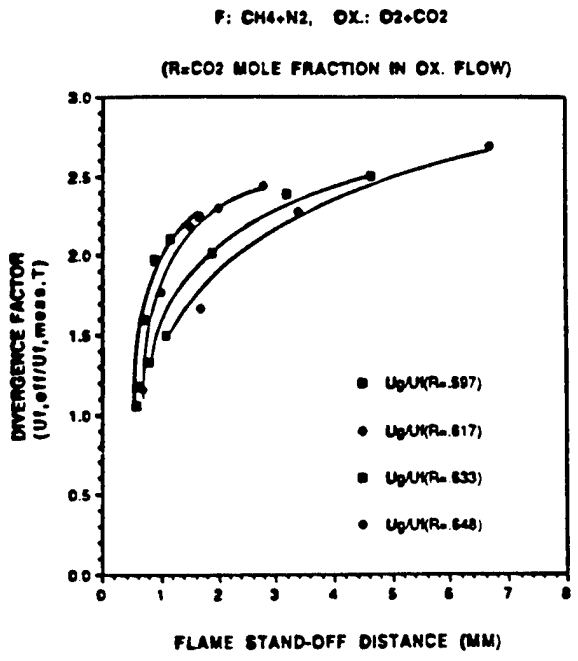

Fig. 16 Ratio of LEF speed to speed of methane-air flames of the same flame temperature (measured temperatures) (Ref. 18).

flame speed is presumably due to divergence and retardation of the approach flow to the LEF due to the pressure "island" (Fig. 13c) at the site of the LEF. The crescent flame (Fig. 15) supports the interpretation of sandwich burning tests in which the fuel flow was enriched by inclusion of oxidizer in the binder lamina. Similar LEF behavior (crescent LEF and high flame speed) has been reported[19,20] in stratified fuel-air mixtures in horizontal ducts. It may be worth re-emphasizing that this high effective flame speed is due to the high local heat release rate in the LEF, the resulting local pressure rise, and the resulting multidimensional convective flow in the neighborhood of the LEF. Not only is the upstream heat flow to the surface localized by the local nature of the heat source, but the location of the heat source is dependent on multidimensional aspects of both heat flow and gas flow.

Results with Propellants

The understanding of combustion of AP/HC binder sandwiches was applied in the present program to the granular AP propellant situation by two studies by Sambamurthi[21,22] and Beiter.[23,24] These investigations are summarized briefly here to demonstrate the role of the leading-edge flame in propellant burning.

In view of the critical role of the LEF in precipitating the ignition and agglomeration of aluminum accumulations on the burning surface, it was proposed[21,22] that this mechanism could be demonstrated by making and testing an aluminized propellant with bimodal oxidizer-particle-size distribution. In such propellants the burning surface consists of irregular arrays of coarse AP particles (400-μm mass mean diameter was used), with intervening areas consisting of a fuel-rich mixture of binder, fine AP, and aluminum. At low pressures the fine AP particles will decompose without "attached" LEFs (analogous to the results of Lee noted earlier), and the accumulating aluminum on the surface will be ignited by the PLEFs on the coarse particles. The whole area of accumulation between coarse particles will then coalesce, to give large agglomerates. If test pressure is increased, a threshold will be reached where PLEFs will occur in the O/F mixing fans of the fine AP particles. This in turn will provide a large increase in number and proximity of sites for ignition of the accumulating aluminum, with a corresponding decrease in agglomerate size. This postulate was tested by Sambamurthi, who prepared bimodal propellants with four different fine AP particle sizes. According to the mechanistic argument, the threshold pressure for onset of PLEFs on the "fine" AP particles would be lower for fine particles of larger size, so the corresponding threshold for decreases in agglomerate size would be at lower pressures. Sambamurthi used combustion photography and agglomerate quench tests[22] to determine agglomerate size. Figure 17 shows the trend of agglomerate size (mass average mean diameter) with pressure for the four sizes of fine AP used (17.5, 49, 82.5, and 196 μm). The results show an abrupt decrease in agglomerate size at a threshold pressure, as predicted in the foregoing scenario. The threshold pressure decreases with increases in AP particle size, as predicted. Keeping in mind that this rather singular trend in agglomerate size was forecast in advance on the basis of sandwich burning-based results and mechanistic arguments about leading-edge flames and aluminum ignition, the results are a good validation of the mechanistic argument. The results provide a mechanistic basis for the empirical "pocket" model of agglomeration proposed originally by Crump[25] and Price et al.,[26] and provide a more complete basis for the heuristic bimodal pocket model proposed by Cohen.[27]

The propellant study by Beiter has to do with the dynamic response of the combustion zone to pressure oscillations. In particular, the study considered the possibility that a large part of the dynamic response might result from the LEF behavior when the conditions are close to the threshold noted in the last paragraph. When the small particle LEFs are on

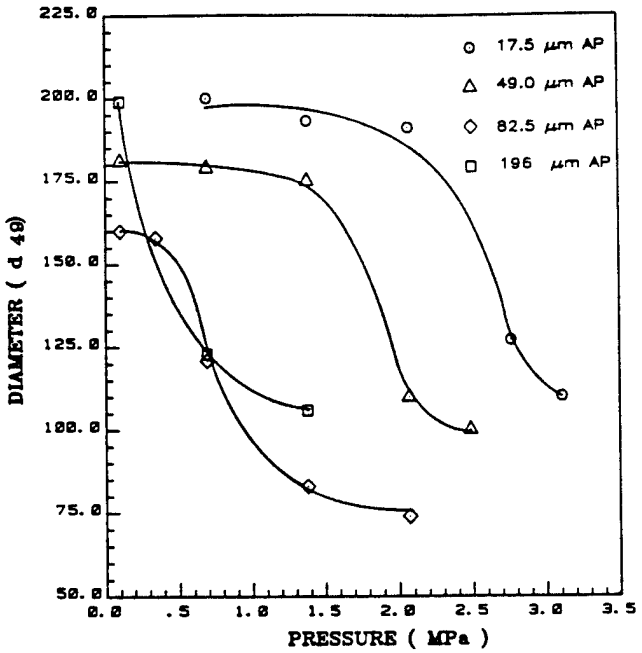

Fig. 17 Effect of pressure on mass average aluminum agglomerate size for propellants with coarse/fine AP in the ratio 8:2 (Ref. 22).

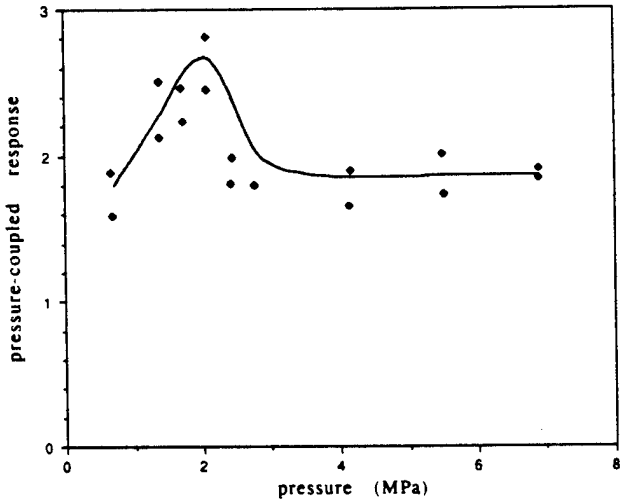

Fig. 18 Response function (vs pressure) for an AP/PBAN propellant with bimodal AP size distribution, obtained from pulsed T-burner tests at a frequency of 500 Hz (Ref. 24).

the brink of detachment, their stability is marginal, and they may oscillate between an attached PLEF condition and a more remote premixed canopy flame configuration. It was proposed that, if a bimodal propellant with very narrow size distribution of the fine AP were tested for pressure-coupled response function, a large portion of the fine AP particles would reach PLEF threshold conditions at the same pressure. Above that pressure, dynamic response would be typical of burning with the PLEF flame complex, and below it the response would be typical of coarse AP PLEFS with premixed canopy flames over the areas of fine AP-Al-binder matrix. In-between those two domains it seemed likely that a greatly increased response might occur due to the marginal stability of the fine particle LEFs. This postulate was tested by running a series of T-burner tests over the relevant pressure range.[23,24] Figure 18 shows the response function vs pressure for tests at 500 Hz with a propellant with 17.5-μm fine AP. While the data scatter in this type of test is rather appreciable, it seems clear that a peak in the response function curve occurred at 275 psi (1.91 MPa). Tests with the other sizes of fine AP were less decisive.

apparently due to scatter in T-burner data and difficulty in achieving uniform particle size of the fine AP. The design of the experiment requires that the fine AP particles all experience threshold conditions for PLEFs at the same pressure to produce a recognizable singularity in the collective dynamic response. In propellants with more conventional particle-size blends, the contribution of marginally stable LEFs is present to lesser degree over a wide pressure range, but is not distinguishable from other contributions to global dynamic response.

Summary

Studies of the edge-burning of laminates of oxidizer and binder layers ("sandwiches") have been conducted for some 30–35 years as a means to observe the combustion of heterogeneous solid propellants without the chaotic field of three-dimensional flamelets typical of AP propellants. The accumulating results of the sandwich burning tests led to increased attention to the leading-edge portion of the oxidizer/fuel diffusion flamelets. This portion of the flamelet (referred to variously as the "flame root," "phalanx flame," "primary flame," and "LEF") was not well-understood or modeled analytically, primarily because it is too small to observe experimentally, is not one dimensional, and cannot be modeled realistically without realistic description of species reaction and diffusion rates. However, it has been clear that this portion of the O/F flamelets is important to the propellant combustion because it is the part of the hot O/F diffusion flame that is closest to the propellant surface.

This article summarizes studies that clarify the nature of LEFs (gas burner and numerical modeling) and shows them to be local sites of high heat release rate, so high that they produce a local pressure peak and divergence in the approach flow, a result consistent with the interpretations of the sandwich-burning test results. This leads to close local coupling between the LEF and the surface regions close to the oxidizer contact lines (coupling via the O/F mixing fans). Tests on AP/PBAN/AP sandwiches with Fe_2O_3 burning rate catalyst in the binder lamina indicate that the catalyst acts by accelerating the breakdown of heavy binder product molecules to more reactive fragments, enabling the LEF to stand closer to the burning surface and thus increase burning rate.

Sandwich-burning tests on sandwich samples with AP-filled binder lamina matrix indicate that the AP in the matrix acted as a source of a reactive diluent in the fuel vapor, that caused a shift in position and size of the LLEF in a manner that enhanced burning rate. The results indicated that the sandwich burning rate was controlled by regression of the AP lamina under the influence of the LLEF. With the finer AP (10 μm), the mixing of the AP and binder vapors was apparently near complete before it reached the LLEF standoff distance (without appreciable exothermic reaction). With the coarser AP (33.5 μm), mixing was apparently less complete, resulting in less enhancement of the rate-controlling lamina LEF, and correspondingly less enhancement of burning rate. At higher pressure, PLEFs were apparently established on the individual particles (1000 psi, 70% 33.5-μm AP). However, the sandwich rate does not seem to have been enhanced by this condition, since the rate remained lower than for 10 μm AP, for which particle LEFs were not indicated. The collected results localize a boundary between two long recognized domains of burning of the matrix of fine oxidizer and binder. In one domain (fine AP, low AP content, low pressure) AP vapors mix and yield a premixed flame. In the other domain mixing is incomplete at lamina LEF height. At high enough pressure, PLEFs may be present in association with the larger exposed (fine) oxidizer particle surfaces. In all cases the sandwich burning rate is controlled by the lamina LEF-assisted regression of the AP laminas, indicating a complex coupling of the nature and pyrolysis of the matrix lamina with the lamina LEFs and the rate-controlling AP lamina regression.

Some preliminary results were presented of tests on sandwiches with both fine AP and fine Fe_2O_3 in the PBAN lamina. This combination resulted in very high burning rates. Details of the results indicate that the catalyst does more than break down heavy fuel molecules for easier reaction in the lamina LEF. There appears to be exothermic O/F reaction in the surface layer of the matrix. It seems likely that the high AP/binder surface contact area, in combination with very fine catalyst particle size, allows significant interfacial reactions at or very near the surface that are not manifested in results with simpler sandwiches.

Sandwich burning tests with aluminum powder in the PBAN lamina showed concentration of the aluminum on the binder surface, and showed that ignition-agglomeration of the aluminum initiated only in the region exposed to the hot LEF. Tests on single laminas of AP/aluminum mixture burned with aluminum concentration on the surface, but showed detachment from the surface with minimal ignition and agglomeration. These results indicate that LEFs provide the source of high temperature needed to break down the oxide coating on the sintered aluminum concentrations. In propellants this role of LEFs is the event that terminates accumulation and, hence, limits agglomerate size.

The tests on propellants were designed to test the importance of LEFs in two important aspects of propellant combustion: 1) aluminum agglomeration and 2) dynamic response to pressure oscillations. The propellants were designed to test the mechanistic arguments convincingly on the basis of qualitative trends in results, and results were consistent with the sandwich burning-derived mechanistic arguments.

At issue were possible effects of the transition (for propellants with bimodal AP) from a condition of attached PLEFs to a region where there are attached PLEFs on coarse particles only. The results indicated a strong transition in aluminum agglomerate size and a peak in response function associated with the flame transition. The 400/17.5-μm AP particle combination was used in both studies, with the indicated transition pressure being comparable (1.91 MPa for peak response function, 2.43 MPa for agglomerate size distribution). The moderate difference may be due to the large mass fraction of aluminum and to lower AP/binder ratio in the fine AP/binder matrix of the aluminized formulation.

It is important to note that the studies reported here were designed to study (and clarify) aspects of combustion that are not well-encompassed in current models of propellant combustion, aspects such as the following:

1) The nature and role of LEFs.

2) The localized coupling of each LEF with the specific site of the solid surface that is the source of the mixing O/F flow that feeds the LEF.

3) The nature of and conditions for interaction of adjoining LEFs, associated lateral heat flow (and species flow in the gas phase), and dependence of effect on LEF spacing (scale of heterogeneity).

4) The nature of the transition from LEF-controlled burning to premixed O/F flame-controlled burning.

5) The special contribution to pressure-coupled combustion response that is made by particle burning in the transition region noted in 4.

6) The critical role of PLEFs in limiting aluminum concentration (by initiating its burning) and the corresponding effect of AP particle size and pressure on agglomerate droplet size.

7) The consequences of combination of large and small particle sizes (AP laminas and matrix laminas), and the relation to difficulties in model correlation of burning rates of bimodal AP propellants with wide mode separation.

Acknowledgments

The author would like to thank several sponsors: principal sponsor, U.S. Office of Naval Research (R. S. Miller); U.S. Air Force Office of Scientific Research (L. Caveny), for sup-

port of aluminum combustion research; and for support of computational modeling of diffusion flames by the Thiokol Corporation (D. Flanigan). The contents of this report are drawn from research with several graduate students and the Ph.D. Dissertation of J. K. Sambamurthi, Christos Markou, S.-T. Lee, C. A. Beiter, H.-J. Chiang, and K. Prasad, and the current research of S. R. Chakravarthy. The author would like to thank R. K. Sigman for able support of all these studies as Combustion Lab Director.

References

[1]Beckstead, M. W., Derr, R. L., and Price, C. F., "A Model of Composite Solid Propellant Combustion Based on Multiple Flames," *AIAA Journal*, Vol. 8, No. 12, 1970, pp. 2200–2207.

[2]Glick, R. L., and Condon, J. A., "Statistical Analysis of Polydisperse Heterogeneous Propellant Combustion: Steady State," *Proceedings of the 13th JANNAF Combustion Meeting*, Vol. II, CPIA Publ. 281, 1976, pp. 313–345.

[3]Price, E. W., Sambamurthi, J. K., Sigman, R. K., and Panyam, R. R., "Combustion of Ammonium Perchlorate-Polymer Sandwiches," *Combustion and Flame*, Vol. 63, No. 1986, 1986, pp. 381–413.

[4]Cohen, N. S., "Review of Composite Propellant Burning Rate Models," *AIAA Journal*, Vol. 18, No. 3, 1980, pp. 277–293.

[5]Price, E. W., "Review of Sandwich Burning," *Proceedings of the 30th JANNAF Combustion Meeting*, Vol. 2, CPIA Publ. 606, 1993, pp. 259–279.

[6]Markou, C., "Effect of Different Binders and Additives on Sandwich Burning," Ph.D. Dissertation, Georgia Inst. of Technology, Atlanta, GA, 1988.

[7]Price, E. W., Sambamurthi, J. K., and Sigman, R. K., "Further Results on the Combustion Behavior of AP/Polymer Sandwiches with Additives," *Proceedings of the 22nd JANNAF Combustion Meeting*, Vol. I, CPIA, Publ. 432, Oct. 1985, pp. 41–54.

[8]Deur, J. M., and Price, E. W., "Steady State One-Dimensional Pyrolysis of Oxidizer-Binder Laminates," AIAA Paper 88-2938, June 1988.

[9]Lee, S.-T., "Multidimensional Effects in Composite Propellant Combustion," Ph.D. Dissertation, Georgia Inst. of Technology, Atlanta, GA, 1991.

[10]Lee, S.-T., Price, E. W., and Sigman, R. K., "Effect of Multidimensional Flamelets in Composite Propellant Combustion," *Journal of Propulsion and Power*, Vol. 10, No. 6, 1994, pp. 761–768.

[11]Price, E. W., et al., "Role of the Leading Edge of Diffusion Flames in Combustion of Solid Propellants," *Proceedings of the 27th JANNAF Combustion Meeting*, Vol. III, CPIA, Publ. 557, 1990, pp. 257–263.

[12]Price, E. W., Lee, S.-T., and Sigman, R. T., "Role of the Leading Edge of Diffusion Flames in Combustion of Solid-Propellants," *Proceedings of the 28th JANNAF Combustion Meeting*, Vol. 2, CPIA, Publ. 573, 1991, pp. 257–263.

[13]Chakravarthy, S. R., private communication, School of AE, Georgia Inst. of Technology, Atlanta, GA, Feb. 1994.

[14]Price, E. W., Sambamurthi, J. K., Sigman, R. K., and Sheshadri, T. S., "Conditions for Inflammation of Accumulated Aluminum in the Propellant Combustion Zone," *Proceedings of the 20th JANNAF Combustion Meeting*, Vol. 1, CPIA, Publ. 383, Oct. 1983, pp. 333–341.

[15]Price, E. W., "Combustion of Metalized Propellants," *Fundamentals of Solid-Propellant Combustion*, Vol. 90, Progress in Astronautics and Aeronautics, AIAA, New York, 1984, pp. 479–513.

[16]Prasad, K., "Numerical Simulation of Reactive Flows Through Two-Dimensional Burners," Ph.D. Dissertation, Georgia Inst. of Technology, Atlanta, GA, 1990.

[17]Prasad, K., and Price, E. W., "A Numerical Study of the Leading Edge of Laminar Diffusion Flames," *Combustion and Flame*, Vol. 90, No. 1992, 1992, pp. 155–173.

[18]Chiang, H.-J., "An Experimental Investigation of the Leading Edge of Diffusion Flames," Ph.D. Dissertation, Georgia Inst. of Technology, Atlanta, GA, 1990.

[19]Phillips, H., "Flame in a Buoyant Methane Layer," *Proceedings of the Tenth Symposium (International) on Combustion*, The Combustion Inst., Pittsburgh, PA, 1965, p. 1277.

[20]Feng, C. C., Lam, S. H., and Glassman, I., "Flame Propagation Through Layered Fuel-Air Mixtures," *Combustion Science and Technology*, Vol. 1, No. 1970, 1975, p. 59.

[21]Sambamurthi, J. K., and Price, E. W., "Aluminum Agglomeration in Solid Propellant Combustion," *AIAA Journal*, Vol. 22, No. 8, 1984, pp. 1132–1138.

[22]Sambamurthi, J. K., "Behavior of Aluminum on the Burning Surface of a Solid Propellant," Ph.D. Dissertation, Georgia Inst. of Technology, Atlanta, GA, 1983.

[23]Beiter, C. A., and Price, E. W., "The Role of Detachment of the Leading Edge of the Diffusion Flame in the Pressure-Coupled Response of Composite Propellants," *Journal of Propulsion and Power* (to be published).

[24]Beiter, C. A., "The Role of Combustion Zone Microstructure in the Pressure-Coupled Response of Composite Propellants," Ph.D. Dissertation, Georgia Inst. of Technology, Atlanta, GA, 1991.

[25]Crump, J. E., "Photographic Survey of Aluminum Combustion in Solid Propellants," *Proceedings of the Inter Agency Chemical Rocket Propulsion Group*, Vol. 1, CPIA Publ. 68, Jan. 1965, pp. 367–370.

[26]Price, E. W., Kraeutle, K. J., Prentice, J. L., Boggs, T. L., Crump, J. E., and Zurn, D. E., "Behavior of Aluminum in Solid Propellant Combustion," Naval Weapons Center TP 6120, China Lake, CA, March 1982.

[27]Cohen, N. S., "A Pocket Model of Aluminum Agglomeration in Composite Propellants," *AIAA Journal*, Vol. 21, No. 5, 1983, pp. 720–725.

APPENDIX E

Chakravarthy, S. R., Price, E. W., and Sigman, R. K.

"Binder Melt Flow Effects in the Combustion of AP – HC Composite Solid Propellants"

AIAA Paper 95-2710

31st AIAA/ASME/SAE/ASEE Joint Propulsion Conference and Exhibit

San Diego, CA, July 10-12, 1995

AIAA 95-2710
Binder Melt Flow Effects in the Combustion of AP - HC Composite Solid Propellants

S.R.Chakravarthy, E.W.Price and R.K.Sigman
Georgia Institute of Technology
Atlanta, GA

31st AIAA/ASME/SAE/ASEE
Joint Propulsion Conference and Exhibit
July 10-12, 1995/San Diego, CA

For permission to copy or republish, contact the American Institute of Aeronautics and Astronautics
370 L'Enfant Promenade, S.W., Washington, D.C. 20024

BINDER MELT FLOW EFFECTS IN THE COMBUSTION OF AP - HC COMPOSITE SOLID PROPELLANTS

S. R. Chakravarthy*, E. W. Price†, and R. K. Sigman‡
Georgia Institute of Technology, Atlanta, Georgia 30332 - 0150 USA

Abstract

The implications of binder melting and flowing on the burning surface of a heterogeneous propellant are examined phenomenologically, in the context of plateau burning behavior of certain AP composite propellants with special formulations. The effect of different diisocyanate curing agents on the melting characteristics of HTPB is observed. The effect of ambient pressure on the binder melt layer is explored by burning pure binder sandwiches. There is a qualitative indication of increased binder melt flow (a) at higher pressures, and (b) more with DDI cured HTPB than with IPDI cured HTPB.

A scenario for plateau burning is presented. Increased melt flow at higher pressures causes quenching of the fine AP - binder matrix regions in the propellant via increased coverage of the fine AP particles by molten binder. The absence of the matrix flame at higher pressures dictates a reduced interaction and concomitant heat feedback by the leading edges of the diffusion flames existing over adjacent coarse AP particles, resulting in a plateau. The necessity of special propellant formulations that exhibit plateau behavior is argued based on this mechanistic hypothesis.

Introduction

In conventional views of combustion of AP composite propellants, the binder is viewed as a source of fuel vapor species for the hot oxidizer/ fuel flamelets. A model of combustion typically assumes decomposition of the binder to a vapor according to some Arrhenius kinetic scheme[1]. A complete model presumably would have to describe the fuel vapor species formed, to be used as input to the O/F flame model. Only limited measurements of vapor species have been made (e.g., Ref. [2]). It has long been suspected that the fuel pyrolysis process is led by a melt-like state, and that the mobility of the melt can play a role in the microscopic details of the burning surface in ways that affect mean burning rate of the propellant. In particular, it has been suspected that melt flow over adjoining surface areas of oxidizer is responsible (in some formulations) for insensitivity ("plateau") or negative sensitivity ("mesa") of burning rate to ambient pressure, mid-pressure range extinction, and for "anomalies" in the low pressure deflagration limits[3]. Such combustion behavior has been associated with (i) binders that exhibit extensive melt[4], (ii) formulations that have relatively high binder content, (iii) formulations with very fine unimodal AP size[5], or (iv) high solids formulations with bimodal AP size distribution with wide separation of the fine and the coarse modes, and a 50% or larger portion of coarse AP[5-7]. Systematic studies of these effects are limited. However, it is recognized that the "anomalous" burning characteristics are advantageous in some motor applications, and that a potential exists for "tailoring" the burning behavior by exploiting binder melt behavior.

The strategy of this study is to examine (1) the melt characteristics of several binders using a hot stage optical microscope, (2) the behavior of melts during edge burning of sandwiches of various binders between AP laminae, (3) the burning behavior of "matrix" samples consisting of a fuel rich mixture of AP particles and various binders, and (4) the burning behavior of sandwiches consisting of such mixtures laminated between AP laminae. Of particular interest is the dependence of burning rate on pressure, and how it is affected by AP particle size and AP/binder mass ratio in the matrix. This is an extension of extensive earlier studies in which PBAN binder was used[8-10]. PBAN binder exhibits minimal melt flow effects, while the binders in the present study are chosen to exhibit a range of melt flow effects.

The strategy of using sandwich burning to help understand propellant burning has been explained in earlier reports. In the present problem, the propellant is unique in that the large oxidizer particles form an array in the propellant that amounts to roughly 40% of the volume, with the binder/ fine AP matrix filling the remaining volume. The space between coarse particles ranges from narrow membranes (where large particles are close to each other), to large patches filling the "voids" in the packing array of coarse particles. In sandwich burning tests, the sandwiches with thin pure binder laminae simulate the regions of the propellant surface with narrow binder membranes with little or no fine AP, while the sandwiches with fine AP filled matrix simulate regions of the propellant surface containing large patches of matrix in between the coarse particles.

---

* Graduate Research Assistant, Student Member AIAA
† Regents' Professor Emeritus, Fellow AIAA
‡ Senior Research Engineer
School of Aerospace Engineering

Copyright © by S. R. Chakravarthy, E. W. Price and R. K. Sigman. Published by the American Institute of Aeronautics and Astronautics Inc. with permission

Background

The earlier studies with PBAN binder[8-10] have led to qualitative understanding of the combustion zone structure of edge- burning sandwiches in the absence of significant melt flow effects. Because this provides a good framework for discussion of possible effects of melt flows, these earlier results are discussed in abbreviated form here.

It is instructive to consider the pure binder sandwich first. The leading edge of the O/F diffusion flame ("LEF") is anchored on the stoichiometric surface, close to the burning surface, and is a major source of near surface heat feedback for surface pyrolysis. This heat feedback is two dimensional in a sandwich (in general, three dimensional in a propellant), and a combined heat release from the pair of LEFs attached to the two lamina interface edges is reflected in a maximum burning rate for an optimum range of binder lamina thickness values (~50-75 μm) at a given pressure (Fig. 1). Below this optimum thickness range, the inadequacy in fuel supply becomes significant; and above the range, the multidimensional coupling of the LEFs is diminished.

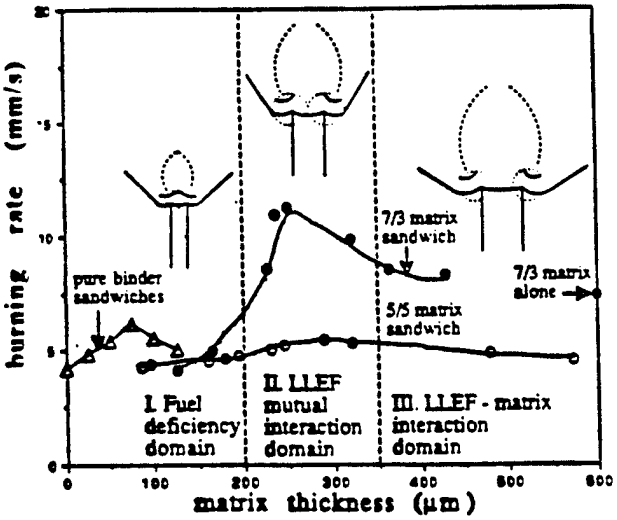

Fig. 1 Typical dependence of sandwich burning behavior on matrix lamina thickness for pure PBAN binder and AP/PBAN = 5/5 and 7/3 matrices. The burning rate of matrix alone is shown on the right ordinate. Circles in the flame structures indicate the zone of influence of the LLEFs.

The above feature is preserved in the case of matrix sandwiches, except that the burning rate peak occurs at a much thicker matrix lamina (~250-300 μm), due to the reduced concentration of the fuel in the presence of the AP particles (Fig. 1). If the matrix is adequately less fuel rich, such as AP/PBAN = 7/3 as opposed to 5/5, it may sustain a flame. This could be a premixed flame "canopying" the region between the LEFs attached to the lamina interface edges (designated as "lamina LEFs", or "LLEFs"), at low pressures and/ or for small particles, or an ensemble of tiny LEFs attached to the particles (designated as "particle LEFs", or "PLEFs"), at high pressure and/ or for large fine particles. It is seen from Fig. 1 that in the presence of the matrix flame, the interaction between the LLEFs is well augmented, reflected by a pronounced peak in the sandwich burning rate versus matrix lamina curve (comparing the 7/3 and 5/5 sandwich curves in Fig. 1). This effect is possibly due to the increased thermal conductivity of the gases in the region between the LLEFs in the presence of the matrix flame. The pronounced burning rate peak in the presence of the matrix flame is crucial to the mechanism for plateau burning behavior proposed in this paper.

Experimental

Experimental Techniques

Techniques employed in this study are virtually routine, and are not elaborated upon here. Three principal techniques were adopted: (i) combustion photography (video); (ii) examination of quenched samples in the SEM; and (iii) hot stage microscopy (HSM). Burning rate measurements were obtained from the video pictures[11]. The heating rate in the HSM experiments was approximately 3 °C/s. Samples were heated in ambient argon, at atmospheric pressure.

Ingredients

The binders used in this study are PBAN and HTPB. The latter was cured with a family of diisocyanate curatives, in proportions shown in Table 1. The last entry has DDI and IPDI in equal proportions based on number of gram equivalents of the -NCO functional group. DDI and IPDI were taken up for more extensive studies; through out this paper, HTPB cured by DDI and IPDI are designated as "HTPB-DDI" and "HTPB-IPDI" respectively. 0.01-0.05% dibutyl tin dilaurate (T-12) was added to the HTPB binders to accelerate curing. The physical behavior of these binders does not seem to be significantly altered by the addition of T-12, as observed on the hot stage.

Table 1. Binder Compositions

No.	Prepolymer		DOA	Curing Agent	
	Type	% wt.	% wt.	Type	% wt.
1.	PBAN	64.14	15.00	ECA	20.86
2.	HTPB	69.07	16.77	DDI	14.16
3.	HTPB	75.73	18.39	IPDI	5.88
4.	HTPB	80.00	15.00	TDI	5.00
5.	HTPB	89.40	-	MDI	10.60
6.	HTPB	72.17	17.53	DDI	7.60
				IPDI	2.70

Four different AP particle size distributions were employed in this study. The one designated as the "2 μm AP" was supplied by Dr. Carol Hinshaw of

Thiokol Corporation in the form of a mixture of that size AP and HTPB prepolymer in such a proportion that, with the plasticizer (DOA) and the different curing agents, the common maximum ratio obtainable was AP/binder = 65/35. For these reasons, "2 μm AP" could be used only with HTPB- based binders, and only up to the above mentioned ratio. The "10 μm AP" was supplied by Dr. Karl Kraeutle, formerly of the Naval Air Warfare Center, China Lake, CA. The "75 μm AP" and "200 μm AP" are the nominal designations for AP particles that remained between sieves of 90 and 75 μm, and, 250 and 200 μm mesh sizes, respectively. The fabrication of sandwiches is detailed elsewhere[12].

Results

1. Hot Stage Microscopic Studies

A comparison of binder behavior in the HSM is shown in Table 2 for PBAN and for HTPB with four different diisocyanate curing agents, and a combination of DDI and IPDI. The results are available in more detail as a video tape from the authors[13]. It was observed that PBAN samples retained their shape until just below the vaporization temperature. DDI cured HTPB melted into a low viscosity fluid at 260 °C, approximately 240 °C below the vaporization temperature. All the binders vaporized at around 500 °C, with the temperature range in melt state for the HTPB samples increasing according to curative in the order MDI, IPDI, TDI and DDI. The greater difference in the melting and vaporization temperatures imply a relatively thicker layer of binder melt in the pyrolysis wave of the burning propellant.

2. SEM Observations

(i) Pure binder sandwiches: Pure binder sandwiches with HTPB-DDI and HTPB-IPDI binders at a binder lamina thickness of about 70 μm were quenched by rapid depressurization at different pressures, and their surfaces were examined in the SEM. Some micrographs are displayed in Fig. 2. Figs. 2(a), (b) and (c) are for HTPB-DDI sandwiches quenched at 300, 500 and 1000 psi respectively. Fig. 2(d) is for HTPB-IPDI sandwich quenched at 500 psi.

From comparison of Figs. 2(a), (b) and (c), it can be seen that at low pressure the binder melt flow onto the AP surface appears to have been a relatively smooth process; as the pressure is increased, it seems more complicated -- the binder melt is in shreds and pieces at 1000 psi. In the case of HTPB-IPDI, the overall extent of binder melt flow is lesser than for HTPB-DDI at any given pressure (comparison of Figs. 2(b) and (d)), but the extent seems to mildly increase with pressure (pertinent figures not presented here for reasons of economy of space). However, the binder melt flow does not appear shredded in HTPB-IPDI sandwiches at higher pressures. The shredding of the HTPB-DDI melt layer is then obviously an artifact of the depressurization quench process; but it is also a fair indicator of the low viscosity and thickness of the melt layer at higher pressures.

(ii) 2 μm AP/HTPB-DDI = 65/35 matrix sandwiches: An interesting feature is observed for the combination of a highly melting binder (HTPB-DDI) and very fine particles (2 μm AP). Fig. 3 shows the surface of a sandwich with a ~250-275 μm thick lamina of 2 μm AP/HTPB-DDI = 65/35 matrix, quenched at 1000 psi. The matrix surface is seen to exhibit clumps of AP particles of size much larger than the original 2 μm nominal size. It is also seen that the left side lamina interface is at a lower level than the right side, indicating unsymmetric burning -- a problem witnessed in general with binder melt flow. As an aside, the above matrix does not sustain combustion by itself in the pressure range from atmospheric pressure up to 2000 psi; and the sandwich burning rate is controlled by the AP lamina rate for any matrix thickness at 1000 psi.

3. Pressure Deflagration Limit Tests

Noticing that the HTPB-DDI cured matrix in the sandwiches addressed in item 2(ii) above did not sustain combustion, a larger family of tests was performed to explore the pressure deflagration limits of AP/binder = 65/35 mixtures with the variables being (a) binder type - PBAN, HTPB-IPDI and HTPB-DDI (order of increasing melt flow ability), and (b) AP particle size - 2, 10, 75 and 200 μm. The mixture ratio was chosen at 65/35 in order to be compatible with that used in the 2 μm AP mixtures; also, no tests were done with AP(2 μm)/PBAN mixtures for the same reason, mentioned earlier.

Table 2. Hot Stage Microscopic Observations

No.	Binder	Melting Temperature [°C]	Decomposition Temperature [°C]	Remarks
1.	PBAN	480	500	melting and vaporization almost simultaneous
2.	HTPB-DDI	260	500	melts instantly; low viscosity
3.	HTPB-IPDI	330-370	500	melts slowly and mildly
4.	HTPB-TDI	300	500	melts instantly; viscosity > item 2
5.	HTPB-MDI	400	500	hardly melts; just loosens up.
6.	HTPB-DDI/IPDI	265-300, 400	500	melts slowly, and in stages.

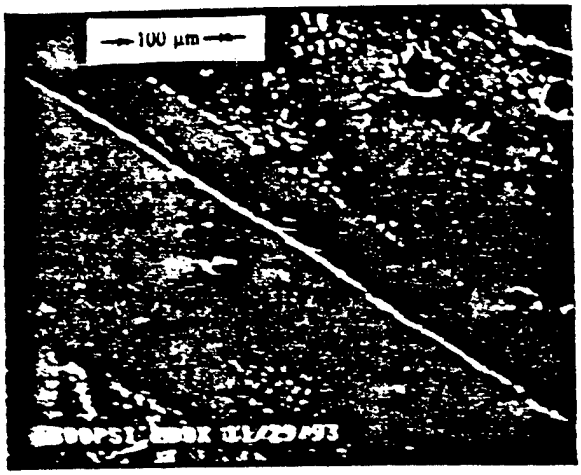

(a)

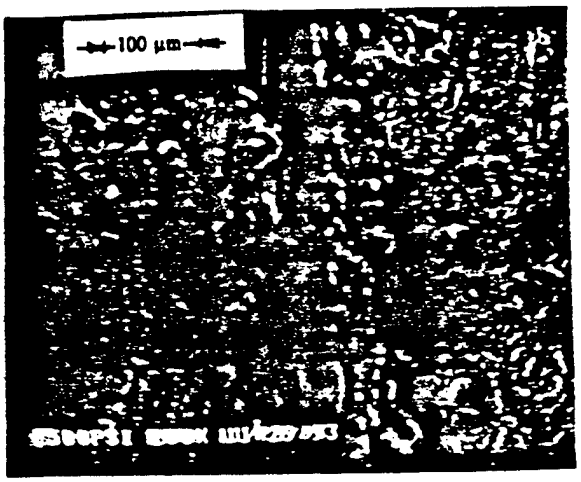

(b)

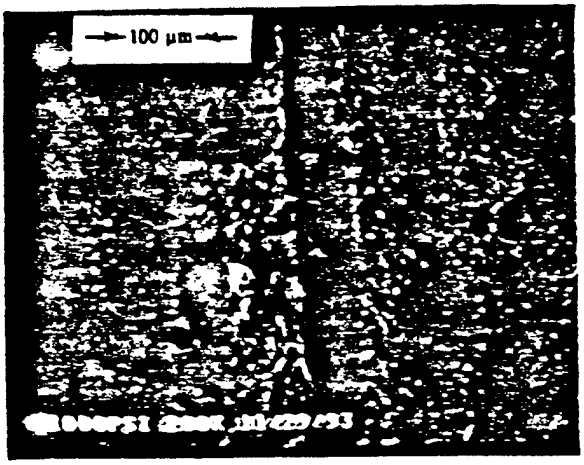

(c)

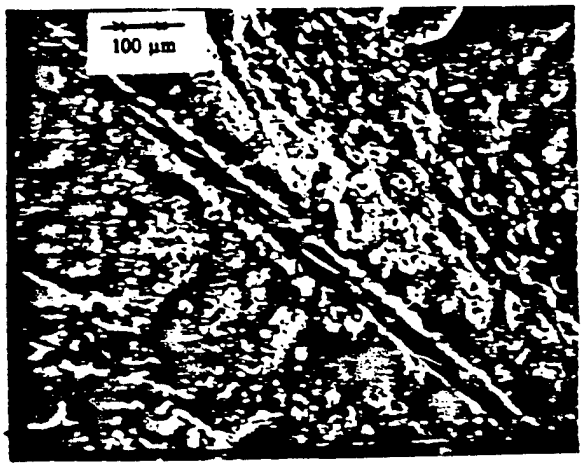

(d)

Fig. 2 SEM of quenched surfaces of pure HTPB sandwiches of binder lamina thickness ~70 µm, with different curing agents, and at different pressures. (a) DDI; 300 psi, (b) DDI; 500 psi, (c) DDI; 1000 psi, and (d) IPDI; 500 psi

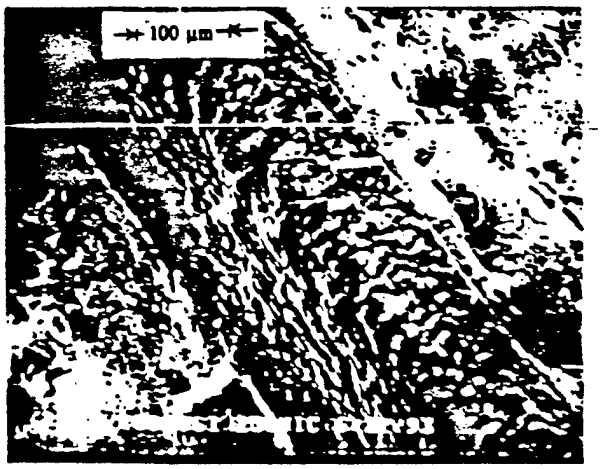

Fig. 3 SEM of a sandwich with 2 µm AP/HTPB-DDI = 65/35 matrix lamina (thickness ~ 250-275 µm) quenched at 1000 psi

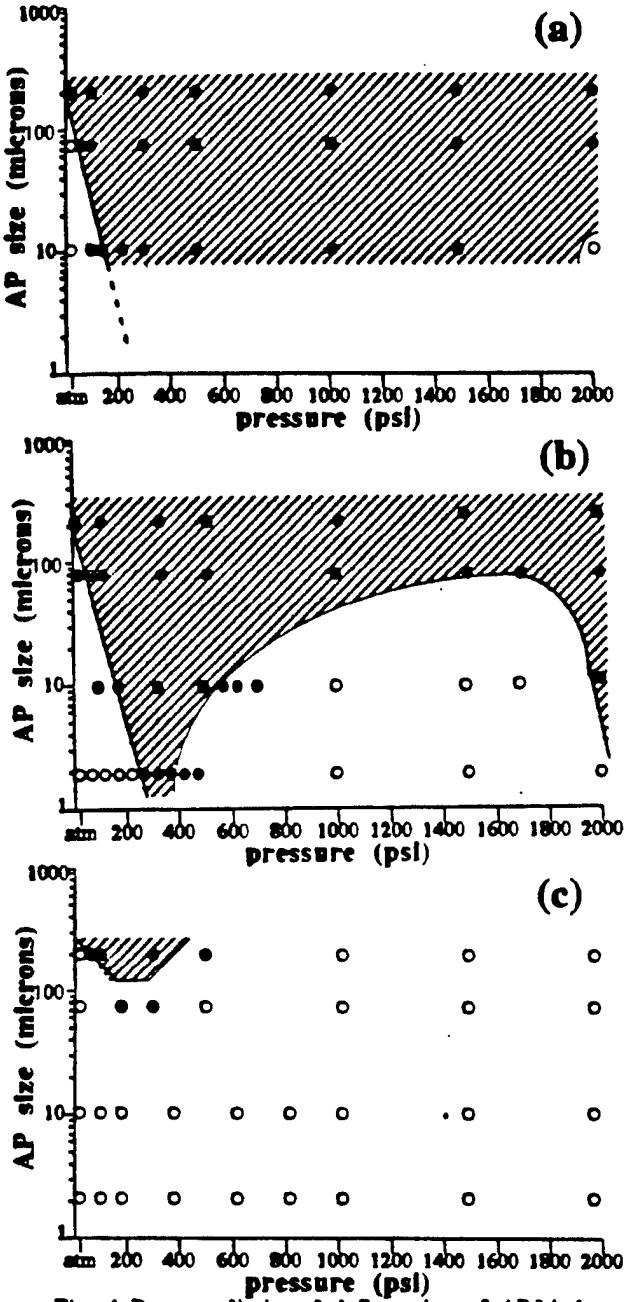

Fig. 4 Pressure limits of deflagration of AP/binder = 65/35 mixtures for AP sizes 2, 10, 75 and 200 μm; and binders: (a) PBAN, (b) HTPB-IPDI, and (c) HTPB-DDI. Circles indicate discrete test points: closed - burning, open - not burning, porous - quenches after ignition. Shaded areas indicate approximate zones of deflagration. Results for the 2 μm AP/PBAN mixture are not available.

It should be noted that, as propellants, these formulations are too fuel rich. However, the reason they were considered in the first place is because they (some of them) would be used in the matrix lamina of sandwiches, where the AP laminae provide for further oxidizer, analogous to the coarse AP particles in a propellant. In other words, the matrix mixtures are not atypical of regions of fine AP/binder in a propellant that uses a blend of coarse and fine AP.

The results are shown in Fig. 4 for matrix samples with three different binders with different melt characteristics. All three show non-deflagration regions at low pressure (< 100 psi, fairly high deflagration limits compared to commercial propellants, but typical of ones with fuel rich formulations). What is most notable about Fig. 4 (note particularly Fig. 4b) is a second domain of non-burning in the intermediate pressure range. In the case of the binder that exhibits the most melt flow (Fig. 4c), this fuel rich matrix would burn only with the coarsest AP, and only in a narrow pressure range around 200 psi. In the case of the binder that exhibits the least melt flow (Fig. 4a), there was no indication of this second domain of non-burning. Collectively, the results show intermediate pressure ranges when burning would not sustain, with a wider pressure range for finer AP, or greater binder melt.

4. Burning Rate Measurements

(i) Burning rate dependence on matrix lamina thickness for 10 μm AP/PBAN sandwiches: The theory for burning of matrix sandwiches outlined in the section on background was developed in Ref. 9 based on experimental data obtained at 300, 500 and 1000 psi. Since plateau burning is a phenomenon involving pressure dependence of rate, data at more pressure levels is necessary to form a consistent theory. Work in this direction is continuing, and results for an expanded pressure range from 50 to 1500 psi are presented in Fig. 5, for both the 7/3 and 5/5 matrix sandwiches.

While the general trends observed in Ref. 9 are preserved, new features are also observed. Firstly, the 5/5 matrix was observed previously to fail to sustain burning, a result now found to hold also at 1500 psi. However, burning is sustained at 50 psi. The burning rate curves for sandwiches at 50 psi are flatter than others. The peak-to-peak difference in the 7/3 and 5/5 sandwich curves increases between 50 and 500 psi, and levels off at higher pressures. There is no substantial burning rate increase between 1000 and 1500 psi, except for large lamina thickness values, particularly for the 7/3 matrix sandwiches. Notice that neither the AP nor the 7/3 matrix burning rates at 1500 psi themselves are much higher than at 1000 psi. This indicates a significant role for LLEF-matrix interaction at higher pressures.

(ii) Effect of binder melt flow in pure binder sandwiches: Sandwiches with pure HTPB-IDPI and HTPB-DDI were burned at 300, 500 and 1000 psi. The burning rate dependence on the binder lamina thickness for these sandwiches is shown in Fig. 6. The PBAN case is also presented for comparison[12]. The HTPB rates are in general lower than the PBAN rates. While

there is a consistency in the trends of PBAN curves (peaks at smaller thickness values with increase in pressure, a trend explained as due to better LEF coupling at higher pressure[8]), no such consistent trends are observed for the HTPB-based sandwiches. It may be remarked here that such a lack of consistency may make simple interpretation of results impossible, but does not render the results themselves irrelevant.

The video pictures showed unsymmetric burning behavior, more markedly for the HTPB-DDI sandwiches than for the HTPB-IPDI ones. Unsymmetric burning is characteristic of binder melt flow[14]. It was also observed in sandwiches with very thick binder laminae, where the binder tends to protrude well above the rest of the sandwich surface, and melt down the sides and flow over the adjacent AP laminae[15]. Departure from symmetry occurs in various ways. One side may begin to lead, and progress in an unstable manner; or, the other side may catch up, and overtake the first one, and so on, in an alternating fashion; or, the sandwich may regress steadily with an unsymmetric profile. These features do frustrate burning rate measurement efforts, and the relevance of such measurements is admittedly ambiguous, at best. It would do well to note that much research on sandwiches in the 1970s was done unknowingly using thick HTPB binder laminae, complicating the results with melt flow effects and limiting the relevance of interpretation of results with two dimensional modeling[15].

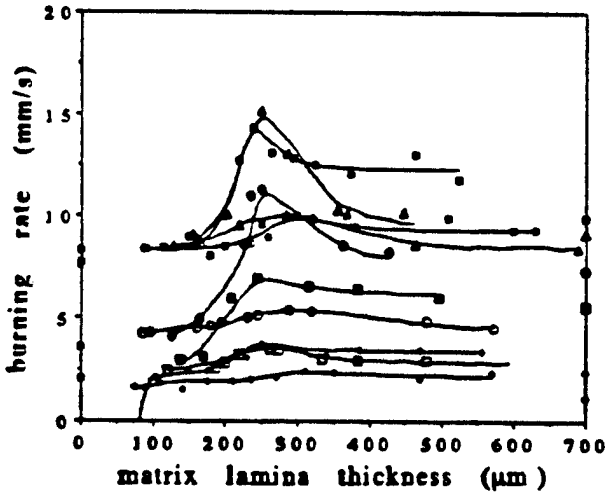

Fig. 5 Burning rate vs. matrix lamina thickness for AP(10 μm)/PBAN = 7/3 and 5/5 matrix sandwiches at different pressures. AP rates are indicated on the left ordinate (rate increases with pressure), and matrix rates on the right. AP does not burn at 50 psi, and the 5/5 matrix does not burn except at 50 psi. Data at 300, 500 and 1000 psi is taken from Ref. 9.

(iii) Burning rate - pressure dependence for matrix sandwiches: Sandwiches with AP/HTPB-IPDI = 65/35 matrix were burned at different pressures for three fine AP sizes - 2, 10 and 75 μm. The matrix lamina thickness was 250-275 μm corresponding to the maxima in the curves in Fig. 5. The burning rates of these sandwiches are shown in Fig. 8 along with those of the corresponding matrices burning alone.

Recall that the matrix in these sandwiches is the same as the one for Fig. 4b. That figure shows a very narrow pressure range 300-350 psi in which the 2 μm AP self-sustains combustion. On the other hand, one may observe in Fig. 7 that it does not burn even in this pressure range, indicating a lack of reproducibility of the deflagration limits. However, the corresponding sandwich burning rate curve registers a mesa just above this pressure range. The sandwich rate follows the AP self-deflagration rate from upwards of 500 psi. Similarly, the 10 μm AP matrix sandwich curve exhibits a plateau between 500 and 1500 psi, where the matrix does not burn. Above 1500 psi, the rate increases steeply corresponding to re-establishment of the matrix flame at 2000 psi. On the other hand, the 75 μm AP matrix stops burning in a brief pressure range around 1800 psi. The corresponding sandwich registers neither a plateau, nor a jump in the burning rate curve.

Discussion

Interpretation of the results of this study (like those of most such studies of combustion of heterogeneous propellants) depends primarily upon rationalization of accumulated observations of "global" combustion behavior, because real time observation of the microscopic processes (on the scale of the propellant heterogeneity) is not practical. This limitation is aggravated in the present situation by the presence of the melt flows that appear to obscure details that otherwise would be revealed in quenched samples. However, the earlier studies with PBAN binder (extended here to a wider pressure range) provide a reasonably complete picture of the details of the combustion zone structure in the absence of melt flows, so the task here is to diagnose the added effect of melt flows. This may be a disarmingly simple statement of the problem, because the combustion process in the absence of melt flows is physically and chemically complex and strongly dependent on pressure and microstructural details of the propellant, and the effect of melt flows can be correspondingly complex.

The present results do show that a) the different binders have conspicuously different melt characteristics, b) the propellants with most conspicuous melts exhibit the most conspicuous deviation in global combustion behavior from that of PBAN/AP systems, and c) the deviations are conspicuously dependent on pressure, fine AP size, and mass ratios of AP to binder and coarse AP to fine AP.

In trying to interpret the available results, it is helpful to note some key features of the AP - binder

combinations in the propellants (and sandwich analogues) that are under consideration.

1. The pure AP (e.g., crystals) does not self-deflagrate below about 270 psi. In large AP particles (and sandwich laminae), the AP remote (> 100 μm) from the O/F interfaces reflects the behavior of pure AP samples (i.e., the O/F flamelets are too far away to affect the "remote AP"). At low pressures, the burning around the outer edge of the large particles controls the decomposition of the large particles. This is a region that is vulnerable to the encroachment of melts.

2. The fine AP particles reaching the burning surface are located mainly in patches of the fine AP/ binder matrix, and these patches are relatively fuel rich, so much so that the matrix is typically near the threshold for burning without support from the coarse AP (Fig. 4). This threshold is dependent on fine AP particle size, binder content, pressure, and on the melt characteristics of the binder. Under these conditions, combustion of these matrix areas on the burning surface is strongly coupled to the peripheral O/F flamelets associated with the large oxidizer particles (or laminae). The results of Ref. 9 indicate that the oxidizer and fuel vapors from the matrix areas are premixed before they establish a flame, and the resulting premixed flamelets are in varying degree supported by the hotter leading edge flamelets around the periphery of the large oxidizer particles (and laminae). This coupled behavior of flamelets was clearly manifested in the burning rate trends of matrix- filled sandwiches, with the effect being dependent on the thickness of the matrix lamina (in a thickness range comparable to the width of matrix patches on the propellant surface).

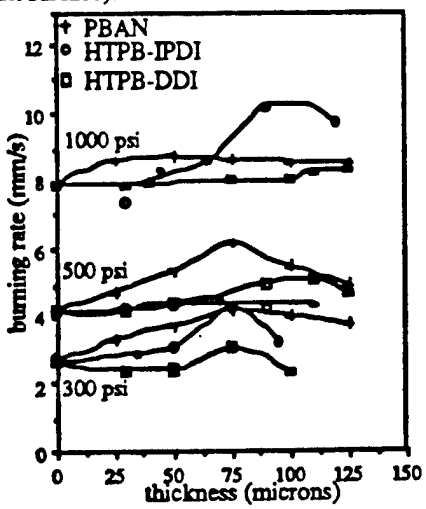

Fig. 6 Burning rate dependence on binder lamina thickness for sandwiches with pure binder laminae at different pressures.

The present experimental results establish the dependence of burning rate characteristics of matrix samples and sandwiches on melt characteristics of the binder, and show that the melt can flow out on the AP surfaces. The results do not reveal directly or in detail how the melt or the flooded AP behave, so one is left to speculate about how the melt modifies the flame complex present with the "lo-melt" binder like PBAN, and how that explains the singular aspects of combustion noted here and elsewhere for "hi-melt" binders.

It seems appropriate to consider two kinds of melt flow effects separately. Consider first the effect of melt flow onto the surface of large AP particles and laminae. It may be transitory, or may establish a steadily replenished melt coverage. It is not clear how the melt-covered part of the AP pyrolyzes. The observed asymmetry of the profiles of some pure binder sandwiches (item 4(ii) of the previous section) suggests that the melt can upset the symmetry of the flame complex, possibly in a steady fashion. The SEMs (Fig. 2) point out, however, that the melt flow necessarily causes a departure from two dimensionality. This would lead to a dispersal of the usually concentrated leading edge O/F flame. The shredded appearance of the quenched melt flows at higher pressures, besides being potentially an artifact of the depressurization process, may suggest that a) a hotter layer of the binder melt layer that is in contact with the AP is vaporizing through a cooler layer, and b) the AP is decomposing under the melt coverage (also suggesting that coverage might be intermittent). Whether steady or intermittent, the time averaged effect of the melt flow is to displace the LEFs away from their usual locations over the rate controlling sites above the outer periphery of the large AP particles (laminae), with a corresponding decrease in the burning rate (Fig. 6). The three dimensional dispersal of the LEFs would also cause a smearing out of the coupling between them in a time averaged sense, resulting in the absence of any conspicuous trends in the burning rate versus binder lamina thickness curves for the HTPB sandwiches, unlike as observed for PBAN sandwiches.

The effect of melt flow on the fine AP particles used in the matrix is quite different. These particles are in a very fuel rich environment, and the particles are small compared to the observed extent of melt flows onto large particles (laminae). Thus one might suspect that the fine particles arrive at the surface through a covering of binder melt. It was observed in Ref. 9 with PBAN binder that larger particles (33.5 μm) burned with their own LEFs at 1000 psi if the matrix was not too fuel rich, but under most conditions (finer AP, etc.) the surface of the matrix quenched appeared to be wetted with binder. In the present results with binders that yield more melt than PBAN, the above binder-melt flooded surface description seems justified, but it leaves the question, what happens to the AP particles? They cannot just accumulate in the pyrolyzing binder melt. They very likely concentrate and then sublime individually or in clumps, followed by vapor phase premixing and premixed O/F flames as

described for PBAN sandwiches. A thicker melt layer and finer AP particles would present a greater opportunity for such clumping (Fig. 3). With larger fine AP, the onset of individual particle burning (noted above for PBAN) would be strongly affected by increased melt flow (this was not examined in the present study except in the deflagration limit determinations, Figs. 4b and c).

Binder melt flow appears to be a pressure dependent phenomenon. In Figs. 2a, b and c, the binder melt appears to exist at equal or greater distances away from the lamina interface, at higher pressures. As pressure increases, the LEFs get closer to the surface, and closer to each other[8]. These factors support a lesser lateral extent of the melt flow at higher pressures. The contrary experimental observation could be (a) due to the higher burning rate at higher pressure, and/ or (b) possibly due to decreased binder melt viscosity at higher pressure. The former reason would hold if the mass rate of vaporization of the binder melt cannot match the rate at which the melt arrives at the surface at high pressures. The latter effect could be due to either a direct pressure dependence of the melt viscosity, or due to higher surface temperatures at higher pressures[3], or both. Increased coverage of the burning surface by binder melt flow at higher pressures is supported by the XPS measurements of Yin et al[4].

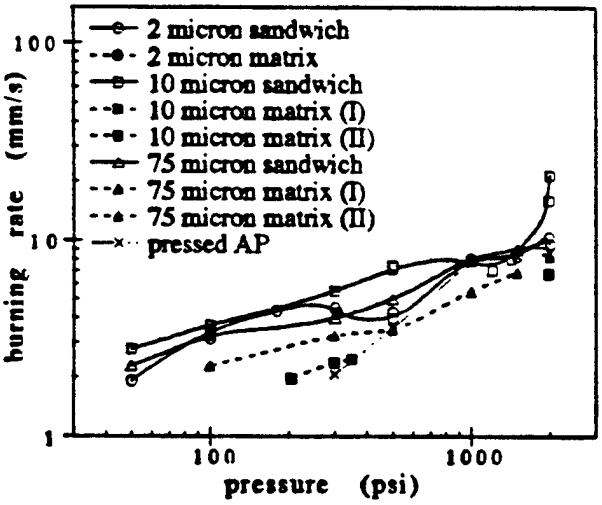

Fig. 7 Burning rate vs. pressure curves for AP/HTPB-IPDI=65/35 matrix sandwiches of lamina thickness ~250-275 μm. The 2 μm AP matrix does not sustain combustion in this pressure range.

The pressure effect on binder melt is also observed in Fig. 4. Matrix propellants with relatively "lo-melt" PBAN binder were observed to burn by themselves, while "intermediate-melt" HTPB-IPDI showed a region in the AP particle size - pressure domain where burning would not sustain. Matrix propellants with "hi-melt" HTPB-DDI would sustain burning only under very limited conditions. In Fig. 4b for HTPB-IPDI for instance, for a given AP size, the matrix stops burning above a certain pressure level (in the intermediate pressure range 500-1500 psi) which is higher for larger AP particles. When the matrix is burning alone (not assisted by LLEFs), the binder can cover areas and quench burning. If this occurs only locally on the surface, burning may be locally intermittent at each surface site, thereby reducing mean burning rate. Under more severe conditions (more binder melt, finer AP, higher intermediate pressure), the extinction can involve the whole surface at once.

The matrix burning may be piloted by the LEFs on the adjacent large particles in a bimodal propellant (the AP laminae in a sandwich). This would facilitate its burning in a larger pressure range than indicated by the deflagration limits in Fig. 4, where the matrix was tested alone. However, increase in pressure and the accompanying increase in binder melt would dictate a situation where the region above the matrix cannot hold an O/F premixed flame connecting the LEFs attached to the peripheries of adjacent large particles (laminae). The absence of this "canopy" premixed flame at higher pressures (in the intermediate range 500-1500 psi) (a) causes a reduced overall gas phase heat feedback to the surface, and (b) lowers the multidimensionally coupled heat release of the lamina LEFs, as noted in the background section. The latter point can be seen by comparing the AP/PBAN = 7/3 and 5/5 sandwich curves at different pressures in Fig. 5. (A matrix with a mixture fraction of AP/PBAN = 7/3 sustains burning at all pressures, whereas the one with 5/5 does not sustain burning at any of the pressure levels tested, except 50 psi.) Notice that the greatest difference in the peaks of these curves is for an "optimum" lamina thickness of approximately 250-275 μm.

When a matrix of appropriate mixture fraction, AP particle size, and melt characteristics exhibits extinction in the mid-pressure range, it effects a transition in the mode of propellant burning from a canopy flame assisted LLEF interaction ("7/3 mode") to one where such an assistance is absent ("5/5 mode"). Fig. 8 depicts such a hypothetical scenario where the transition from the AP/PBAN = 7/3 to the 5/5 sandwiches is shown for a matrix lamina thickness of 275 μm. Such a transition is seen to result in a burning rate trend that is of low or no sensitivity to pressure ("plateau") or sometimes a negative sensitivity ("mesa").

The above hypothesis is tested positive on sandwiches, as shown in Fig. 7. Although repeatability of matrix burning for the 2 μm AP case could not be achieved, it is anticipated that the matrix would be more disposed to burn when sandwiched between the AP

lamina because of reduced heat loss to the surroundings, and increased heat flux from the LLEFs, as mentioned earlier. Correspondingly, we notice a plateau or mesa (for finer AP) in the sandwich curves just outside the matrix deflagration domains. As the 10 μm AP matrix resumes burning at 2000 psi, the burning rate of the sandwich is seen to increase. Testing above 2000 psi would probably reveal the mechanism of "biplateau" burning behavior[7], where the burning rate levels off again after the jump.

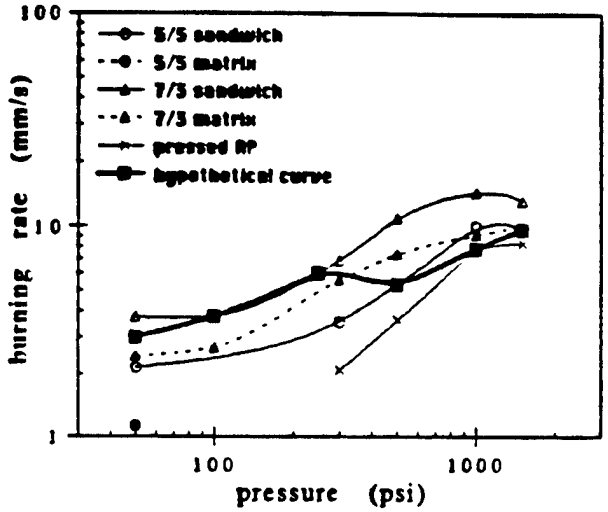

Fig. 8 A scenario for plateau burning behavior: transfer of control of sandwich burning from a burning matrix (7/3) to a non-burning matrix (5/5) situation, effected by binder melt flow over the fine AP particles in the matrix.

The need[3-7] for (a) a considerable amount of coarse particles to be present, and (b) a wide separation in the size distributions of the fine and coarse particles, now becomes evident. The LLEFs are the "anchors" of the complex flame front burning into the solid. They follow the coarse particle/ matrix interface contours. If the interaction between the LLEFs (or the lack of it) is crucial to a behavior, such as plateau burning in this case, its occurrence must be prevented from being smeared by the statistical nature of the propellant geometry. This is achieved by having a sufficient number of coarse particles in the propellant. Again, if the size distributions are broad, and closer together, the distinction between "fine" and "coarse" particles is blurred, and the effects of flame interactions discussed above will get statistically smeared.

The matrix needs to be designed so as to exhibit an intermediate pressure range extinction. With the fine AP/ binder ratio fixed accordingly, a higher loading of coarse particles in the propellant would mean placing them closer to each other. But the "average" distance between the coarse particles should be maintained roughly corresponding to the LLEF mutual interaction domain in Fig. 1. This dictates the size of the coarse particles; and the requirement of wide separation between the coarse and fine sizes, in turn, dictates the size of the fine particles.

We have thus far postponed consideration of the reason for different diisocyanate curing agents to cause HTPB to melt differently. This aspect is being addressed in a rather superficial manner here since it is not an area of expertise of the authors. It has been reported that the first step in the pyrolysis of the binder is the cleaving of the urethane linkages caused by the cross linking agent (curing agent)[2]. In DDI, the -NCO groups are symmetrically positioned, while in IPDI they are unsymmetrically positioned[16,17]. This may result in a wider temperature range for cleaving of urethane linkages with IPDI, and hence a less decisive "melt" process.

Conclusion

This work explores the role of binder melt flows in the combustion of AP composite propellants, with particular attention to those special formulations that exhibit a "plateau" burning behavior. A hypothetical mechanism for plateau burning is evolved that explains the need for such special formulations.

Binder melt flows assume significance depending upon the relative dimensions of the AP particles to the binder melt layer thickness at a given pressure. Accordingly, in a typical bimodal propellant, the effect of melt flow is different on large particles than in areas of the burning surface where a matrix mixture of fine particles and binder exists.

It is not clear what happens in detail when binder melt flows onto the surface of large AP particles. The net time averaged effect seems to be (a) to disperse the array of leading edge O/F flamelets (LEFs) that are usually concentrated at the rate controlling sites above the periphery of the large particles, and (b) displace adjoining LEFs apart in such a way as to lessen the coupling between them. These two effects result in a decreased heat feedback to the rate controlling sites on the surface, thus reducing the mean burning rate.

In the matrix areas, the existence of the fine AP particles in a pool of binder melt layer allows for concentration and sometimes, clumping of the particles, more for finer ones. Burning, if possible, must progress in an essentially local and intermittent fashion in such a situation.

The ability of the HTPB binder to melt substantially before vaporization can be tailored by the choice of an appropriate diisocyanate curing agent such as DDI or IPDI. It appears that the tendency of the binder to melt into a relatively low viscosity fluid increases with increase in pressure. This causes greater coverage of the adjacent fine AP particles in the surface layer of the matrix by the binder melt flow, at higher pressures. Depending on the fine AP particle size relative to the lateral extent of binder melt flow at a

given pressure, the matrix may not sustain combustion; thus, an upper deflagration limit for the matrix exists in the intermediate pressure range 500-1500 psi. Naturally, this limit increases with increasing fine size and decreasing binder melt (depending on the curative type).

The presence of an O/F premixed "canopy" flame over the fine AP/binder matrix is crucial to the multidimensional coupling of the leading edge flames existing over the periphery of the large particles sandwiching the matrix. Since the chances of the matrix burning decreases with increasing pressure, this augmented flame interaction would get weakened, resulting in a mean burning rate that does not increase with pressure as usual. Thus a "plateau" in the burning rate - pressure relation is registered. At high enough pressure, again depending on fine AP particle size (> 2000 psi for 10 μm particles, for example), the fine particles may begin to hold small O/F LEFs, which would result in a sharp increase in the burning rate.

An important parameter in the augmentation (or lack of) of the LEFs on adjacent large particles by the presence (or absence) of a canopy flame above the matrix between them, is the spacing between the large particles. Further, these features need to be distinctly preserved in spite of the statistical distribution of the particles. Such considerations require special formulations where there is a relatively high fraction of large particles, whose size is distinctly far removed from the size of the fine particles.

Acknowledgments

This work was performed under contract no. N00014-89-J-1293 for the US Office of Naval Research with Dr. Richard S. Miller as technical monitor. Useful suggestions and information on binder formulations were offered by Dr. Russell Reed, NAWC, China Lake, CA. Dr. Carol J. Hinshaw of Thiokol Corporation supplied several ingredients used in this study.

References

1. Cohen, N. S., Fleming, R. W., and Derr, R. L., "Role of Binders in Solid Propellant Combustion," AIAA Journal, Vol. 12, No. 2, February 1974, pp. 212-218.

2. Chen, J. K., and Brill, T. B. ,"Chemistry and Kinetics of Hydroxyl-terminated Polybutadiene (HTPB) and Diisocyanate-HTPB Polymers during Slow Decomposition and Combustion-like Conditions," Combustion and Flame, Vol. 87, 1991, pp. 217-232.

3. Cohen, N. S., and Hightower, J. O., "An Explanation for Anomalous Combustion Behavior in Composite Propellants," Proceedings of the 29th JANNAF Combustion Meeting, October 1992.

4. Yin, J., Li, B., Wang, K., and Chen, B., "Combustion Mechanism of a Negative Pressure Exponent Composite Solid Propellant," Journal of Propulsion and Power, Vol. 8, No. 1, January - February 1992, pp. 37-44.

5. Miller, R. R., "Anomalous Ballistic Behavior of Reduced Smoke Propellants with Wide AP Distributions," 15th JANNAF Combustion Meeting, September 1978, CPIA Pub. No. 281, Vol. II, February 1979, pp. 265-269.

6. Fong, C. W., and Smith, R. F., "The Relationship between Plateau Burning Behavior and Ammonium Perchlorate Particle Size in HTPB-AP Composite Propellants," Combustion and Flame, Vol. 67, 1987, pp. 235-247.

7. Hinshaw, C. J., and Mancini, V. E., "Biplateau Burning Propellant Containing Aluminum," TR-10137, Thiokol Corporation, Interim Report to ONR, contract no. N00014-92-C-0134, March 1993.

8. Price, E. W., Sambamurthi, J. K., Sigman, R. K., and Panyam, R. R., "Combustion of Ammonium Perchlorate - Polymer Sandwiches," Combustion and Flame, Vol. 63, 1986, pp. 381-413.

9. Lee, S. -T., Price, E. W., and Sigman, R. K., "Effect of Multidimensional Flamelets in Composite Propellant Combustion," Journal of Propulsion and Power, Vol. 10, No. 6, November - December 1994, pp. 761-768.

10. Price, E. W., "Effect of Multidimensional Flamelets in Composite Propellant Combustion," Journal of Propulsion and Power, accepted for publication, July - August 1995.

11. Chakravarthy, S. R., Price, E. W., and Sigman, R. K., "Mechanism of Burning Rate Enhancement of Composite Solid Propellants by Ferric Oxide," AIAA Paper 95-0601, 33rd Aerospace Sciences Meeting, Reno, NV, January 1995.

12. Lee, S.-T., "Multidimensional Effects in Composite Propellant Combustion," Ph.D. Thesis, Georgia Institute of Technology, Atlanta, GA, May 1991.

13. Price, E. W., Chakravarthy, S. R., Zachary, E. K., and Sigman, R. K., "Ingredient Response and Interaction during Heating on a Hot Stage Microscope," Proceedings of 31st JANNAF Combustion Meeting, San Jose, CA, October 1994.

14. Handley, J. C., "An Experimental Investigation of Catalysis in the Combustion of Composite Solid Propellants," Ph.D. thesis, Georgia Institute of Technology, Atlanta, GA, 1976.

15. Price, E. W., "Review of Sandwich Burning," Proceedings of the 30th JANNAF Combustion Meeting, CPIA Pub. No. 606, Vol. 2, 1993.

16. Chen, J. K., Cheng, S. S., and Chou, S. C., "DSC, TG and Infrared Spectroscopic Studies of HTPB and Butacene Propellant Polymers," AIAA Paper 94-3176, 30th AIAA/ASME/SAE/ASEE Joint Propulsion Conference, Indianapolis, IN, June 1994.

17. Reed, R., private communications, September - October 1994.

APPENDIX F

Price, E. W., Chakravarthy, S. R., Sigman, R. K., and Freeman, J. M.

"Pressure Dependence of Burning Rate of Ammonium Perchlorate-Hydrocarbon Binder Solid Propellants"

AIAA Paper 97-3106

33rd AIAA/ASME/SAE/ASEE Joint Propulsion Conference and Exhibit

Seattle, WA, July 6-9, 1997

AIAA 97-3106
Pressure Dependence of Burning Rate of Ammonium Perchlorate-Hydrocarbon Binder Solid Propellants

E. W. Price, S. R. Chakravarthy, R. K. Sigman, and J. M Freeman
Georgia Institute of Technology
Atlanta, GA

33rd AIAA/ASME/SAE/ASEEJoint Propulsion Conference & Exhibit
July 6 - 9, 1997 / Seattle, WA

For permission to copy or republish, contact the American Institute of Aeronautics and Astronautics
1801 Alexander Bell Drive, Suite 500, Reston, VA 22091

PRESSURE DEPENDENCE OF BURNING RATE OF AMMONIUM PERCHLORATE-HYDROCARBON BINDER SOLID PROPELLANTS

E. W. Price*, S. R. Chakravarthy†, R. K. Sigman‡, and J. M. Freeman§
Georgia Institute of Technology, School of Aerospace Engineering, Atlanta, Georgia 30332-0150 USA

Abstract

This report is concerned with the mechanisms that govern the pressure depedence of the burning rate of ammonium perchlorate-hydrocarbon binder solid propellants, with emphasis on propellants with bimodal ammonium perchlorate particle size distributions that tend to exhibit "plateau" and "mesa" burning. The microscopic details of the flame complex, the ingredient decomposition, and the burning surface configuration are considered as three dimensionally coupled, pressure dependent processes. New experimental results are presented concerning these processes and how they depend on pressure. No attempt is made to produce a complete model of plateau burning; however, useful guidance is provided toward that goal.

Introduction

In the 1960's, it was observed (e. g., Ref.1, 2) that ammonium perchlorate-hydrocarbon (AP/HC) binder propellants with monomodal oxidizer size distribution sometimes exhibited an "anomalous" dependence of burning rate on pressure in the mid- pressure range. In this pressure range the burning rate became independent of pressure ("plateau burning;" Figure 1). With some formulations of propellant, the burning rate actually decreased with increasing pressure, or even exhibited a mid-pressure range in which burning would not sustain. It was reported that this "anomalous" burning was accompanied by locally intermittent burning at changing sites on the burning surface. The anomalous behavior was observed to be sensitive to choice of AP particle size, binder, and oxidizer/binder ratio. These propellants were necessarily very binder-rich because of limits in packing density of particles with uniform particle size.

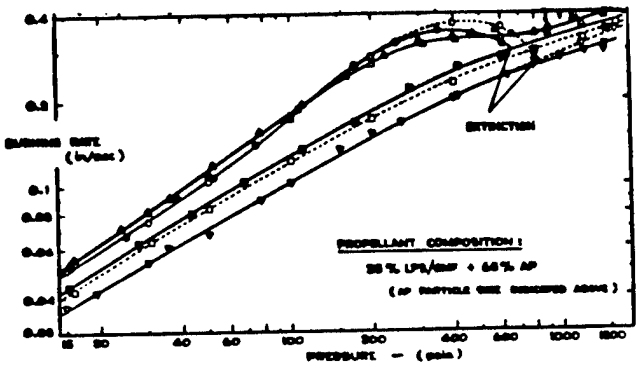

Figure 1– Burning rates of propellants with 65% AP and 35% binder. Monomodal AP of various particle sizes (Ref. 2)

Because such fuel-rich compositions of the propellant yielded unacceptably low specific impulse for propulsion applications, this anomalous behavior was not studied fully. More recently, similar behavior was observed with high solids formulations using bimodal oxidizer particle size distribution (Ref. 3, 4, 5). This behavior was observed for certain combinations of coarse and fine oxidizer size in which the two sizes were widely different and the size of the fine AP was small (≤ 20 μm). The behavior was present only for a limited range of the proportions of coarse and fine AP. This paper examines the details of combustion of such bimodal AP propellants.

Burning rate of bimodal propellants has been predicted by modern burning rate models (Ref. 6, 7) which sometimes yield relatively low sensitivity of burning rate to pressure over a similar range of propellant variables, but the models do not predict plateaus, mesas, or non-burning behavior. This issue was studied in Ref. 8, where a good

---

* Regents' Professor Emeritus, Fellow AIAA
† Post-Doctoral Fellow
‡ Senior Research Engineer
§ Graduate Research Assistant, Student Member AIAA

Copyright © by E. W. Price, S. R. Chakravarthy, R. K. Sigman, and J. M. Freeman. Published by the American Institute of Aeronautics and Astronautics with permission.

presentation of past experimental results was assembled. In that reference, it was concluded that some detailed aspects of the combustion that are critical to the anomalous burning were absent or inadequately represented in current models, and it was noted that further experimental study would be required in order to extend burning rate models to properly represent the "anomalous" burning behavior. The present paper describes several features of propellant combustion that may contribute separately or interactively to the anomalous burning phenomenon, features that are not clearly represented in current burning rate models. The present knowledge does not permit an all-up scenario for anomalous burning, but the processes may be useful in formulating relevant experimental studies and deciding what is needed for realistic modeling of the combustion.

Before presenting the concepts in this paper, it may be helpful to examine the general features of combustion of bimodal propellants, with the help of a simplified view of the combustion zone (Figure 2). The burning surface is made up of an array of coarse AP particles and surrounding connected areas consisting of a mixture (referred to here as the "matrix") of fine AP and binder. In the simplest view one might argue that the coarse AP particles and the matrix burn independently. However, this is not possible because the coarse particle burning involves fuel from the matrix "vapors"; further the matrix may be one that won't burn on its own. In addition, the two are thermally connected by lateral heat transfer in the condensed phase, and under some conditions by flow of binder melt onto the outer peripheries of the coarse AP surfaces.

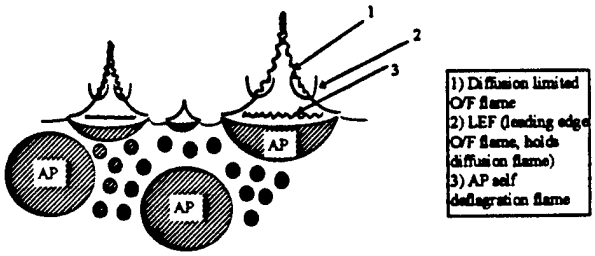

Figure 2–Simplified view of the combustion zone for a propellant with bimodal AP particle size distribution

The matrix probably burns with a premixed flame under most conditions, often burning interactively with the flames of the coarse AP near the contact surface with the coarse AP particles. The importance of interaction no doubt depends on how well the matrix will burn on its own and how far apart the coarse AP particles are. These effects have been studied previously in sandwich burning experiments (Ref. 9, 10). In the case of propellants, it should be noted that changes in ratio of coarse to fine AP are accompanied by concurrent changes in coarse particle spacing, and of the O/F ratio of the matrix.

The details of the combustion of the matrix material remain undetermined. The fine AP particles on the surface are usually observed to be covered by binder melt on quenched samples, and the details cannot be resolved during burning by available photographic methods.

The details of combustion that are responsible for "anomalous" burning occur at microscopic scales that are too small for direct observations during burning, and understanding requires an indirect strategy involving knowledge of:

a) melting, decomposition, and self deflagration of the individual ingredients of the propellant;

b) global burning behavior (e. g. burning rate vs. pressure and "macroscopic" flame photography) of propellants and special oxidizer-binder structures (e. g. sandwiches, designed to provide simpler observation and interpretation of burning behavior); and

c) basic flame theory.

Microscopic details can usually be accessed only by investigating the global effects of changing the microstructure and ingredients of the propellant (e. g. particle size) and sometimes by microscopic study of quenched samples. While these harsh experimental realities are not new to veteran researchers, it is important to face them collectively here because much of the discussion in this paper involves microscopic details of the combustion that have not been clarified unambiguously by earlier studies, and that can only be resolved by the collective strategy outlined above.

In this paper, the subject of pressure dependence of burning rate of bimodal AP/HC binder propellants is examined by considering the pressure dependence of several contributing processes to combustion

a) Melting and decomposition of individual ingredients (using primarily

results from hot stage microscopic tests)

b) Self-deflagration of AP
c) Microstructure of the burning surface based on difference in activation energies of decomposition of oxidizer and binder
d) Combustion of fuel rich AP/binder matrices typical of matrix areas in bimodal propellants
e) Interaction of coarse particle and matrix flamelets
f) Binder melt flows
g) Intermittent burning

The details and relative importance of processes a-g in the phenomenon of plateau burning are not sufficiently advanced to construct a realistic model for "anomalous" burning, but consideration of the pressure dependence and interaction of the processes seems essential to a realistic "all-up" model. Further, consideration of these processes seems essential to valid theories for propellant ignition and oscillatory combustion.

Ingredient Melting and Decomposition

There is voluminous literature on decomposition of ingredients, less on melting. This topic is addressed only superficially here, in order to compare the relative behavior of oxidizer (AP) and fuel (binder). It is observed in hot stage microscope tests (Ref. 11) that hydrocarbon binders exhibit fluid-like behavior at temperatures from 250-500° C, (Table 1) with the behavior of the binders differing strongly from each other both as to "melt temperature" and viscosity of the melt. For HTPB binders it is observed that melt characteristics differ conspicuously (Table 1) depending on the curative used (suggesting that melting involves breakdown of cross-link bonds). In hot stage microscope tests, the melt starts to bubble at a considerably higher temperature, and then becomes fully vaporized within a range of 10° C or so (heating rate of 3° C/sec). Binders also differ widely with respect to decomposition temperature, but the binders considered thus far in this study (PBAN, IPDI-cured HTPB and DDI-cured HTPB) all decompose at about the same temperature (500° C). Among those three binders, the difference between melting and decomposition temperatures ranges between 20 (PBAN) and 240° C (DDI cured HTPB). While the quantitative validity of the results from slow heating tests to combustion zone behavior are doubtful, the qualitative differences among the binders are large and appear to agree with observations of combustion tests.

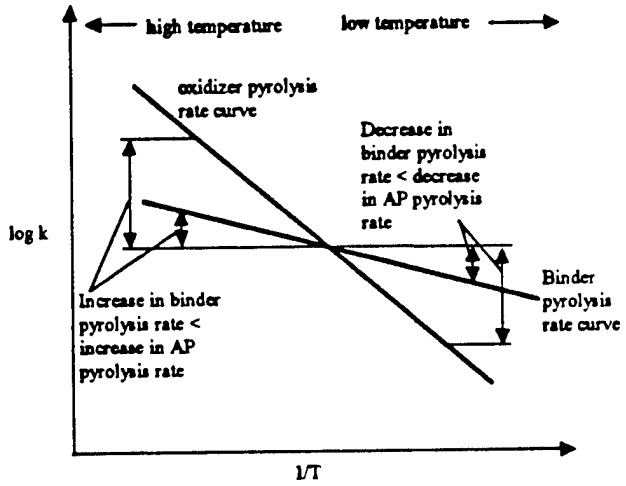

Figure 3–A sketch illustrating the relative dependence of pyrolysis rate of oxidizer and binder (vs. T)

More detailed studies of ingredient decomposition and linear pyrolysis of AP and binders indicate that the activation energy for AP is roughly 30 kcal/mole and the effective activation energies for most binders are in the range of 5-10 kcal/mole, illustrated schematically in Figure 3. In this figure, the pyrolysis rate curves are shown as crossing in the mid range of 1/T. This point seems to correspond to combustion at around 800 psi (5.55 MPa), based on the observation that quenched surfaces of propellants tend to be flat around that

Table 1. Hot Stage Microscope Observations

No.	Binder	Melting Temperature [°C]	Decomposition Temperature [°C]	Remarks
1.	PBAN	480	500	melting and vaporization almost simultaneous
2.	HTPB-DDI	260	500	melts instantly: low viscosity
3.	HTPB-IPDI	330-370	500	melts slowly and mildly
4.	AP	~580[a]	Rapidly above 400	

[a] Decomposes before melting except at heating rates > 10 °C/s.

pressure. These properties of the pyrolysis will be used later to explain the differences in structure of the surface layer and flame complexes for different pressures.

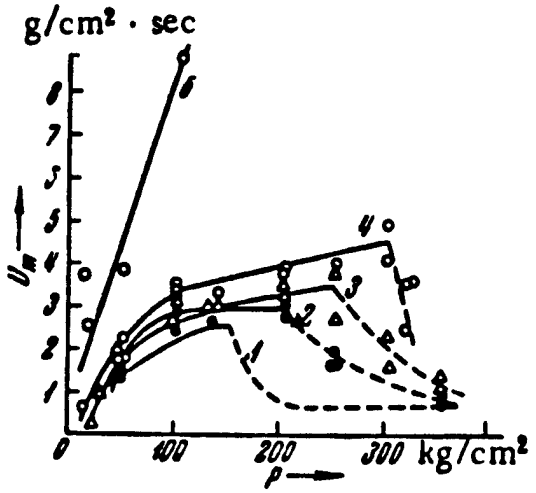

Figure 4–Dependence of the self-deflagration rate of ammonium perchlorate on pressure and temperature (Ref. 13)

AP Self-Deflagration

Ammonium perchlorate decomposes, and will self deflagrate at most motor pressures. A similar behavior is evident in large particles during propellant combustion, but is dependent on proximity to the binder (where heat loss to the binder limits the deflagration, while heat feedback from exothermic gas phase reaction with binder vapors can enhance the AP deflagration). Extensive studies of self-deflagration have been made of pure single and doped single crystals, and of dry-pressed samples made from granular AP. Samples of pure AP self-deflagrate at pressures above 280 psi (1.4 MPa), with dependence on sample temperature and environmental pressure as shown in Figure 4. The deflagration rate is dependent on pressure in a very complex, temperature dependent manner described in some detail by Hightower, Boggs and others Ref. 12, 13. The deflagration surface is characterized by certain nonuniformities that depend on pressure (Ref. 12, 14, 15, 16) and that are evident also on surface areas of large particles (Figure 5) during propellant combustion (at sites sufficiently distant, say 100 μm, from the particle periphery). In studies of propellant combustion and sandwich burning, it is observed that the burning rate is strongly dependent on the AP deflagration rate in the mid-pressure range (1000-1500 psi: 6.94-10.4 MPa) (Ref. 17, 18). It is not yet clear whether the strong mesa in the AP self deflagration rate in the 1500-4000 psi (10.4-27.8 MPa) range (or the causes of the mesa) is manifested in particle burning in propellants, but it may contribute (or be made to contribute) to corresponding plateau burning behavior in propellants.

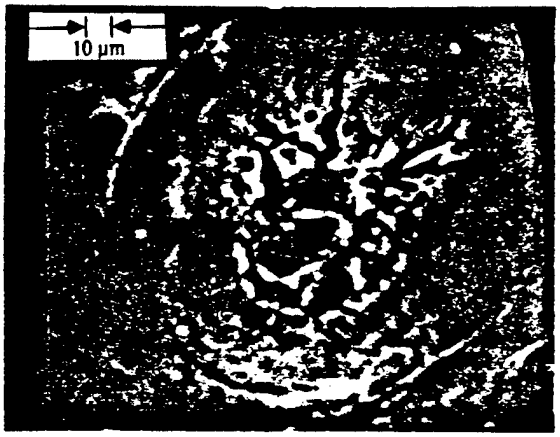

Figure 5–Surface of a coarse AP particle, showing features in the central area characteristic of AP self-deflagration (SEM of a dp/dt quenched propellant sample burned at 500 psi, 3.45 MPa)

Surface Disproportionation

It is widely recognized that large AP particles tend to protrude on the burning surfaces of the propellant at low pressures, and that the particle surfaces are recessed and concave at higher pressures. This behavior is generally attributed to non-self deflagration at low pressure, or to higher binder pyrolysis rate at low pressure and higher pyrolysis-deflagration rate of AP at higher pressure. Both views are overly simplistic, individually or together, in that the ingredients at the contact regions between oxidizer particles and adjoining binder are subject to thermal (and possibly chemical) interaction, with effects that are dramatically particle size dependent. These matters are only superficially addressed in analytical models; however, they are potentially very important factors in plateau burning, so a more direct look at factors controlling micro surface geometry is described below.

Consider first the 1-D burning of a column of a liquid consisting of two soluble ingredients that decompose independently with Arrhenius rate law of kinetics and widely different activation energies. Suppose that the liquids are oxidizer and fuel that burn (exothermally) with a one-dimensional premixed gas phase flame, and that the pyrolysis rates of the ingredients are equal at the surface

temperature present during burning at 800 psi (5.55 MPa). At lower pressure, the flame stands further from the surface, with correspondingly lower surface heat flux, surface temperature, and burning rate. Under these conditions, the fluid "F" (Fuel) with the lower activation energy will decompose more rapidly than the other fluid "O" (Oxidizer), leading to rising concentration of O and the ratio of O/F at the surface. Steady state burning cannot be reached until concentration profiles in the surface layer yield a ratio of O/F flux from the surface equal to $(O/F)_p$ of the "propellant" mixture in the column, and the concentration profile has to change with surface temperature (and hence burning rate) to satisfy the mass flux ratio $(O/F)_p$. By the same reasoning at high pressure, the ratio of O/F at the surface must be above $(O/F)_p$ for steady burning. In the present report this accommodation of the surface to maintain

$$\left(\dot{O}/\dot{F}\right)_s = \left([O]/[F]\right)_p$$

is called "disproportionation," a long word to convey the idea of a necessary change in proportions of O and F in the surface layer in order to have steady state burning (the transient process by which disproportionation proceeds is a real but neglected aspect of ignition and oscillatory combustion theory as well; see Ref. 19).

The conditions for the foregoing illustration were chosen to conform to a "homogeneous" AP/HC binder propellant as described earlier. If the AP particle size is very small, the particles will be in thermal equilibrium with adjoining binder, and near the burning surface (at low pressure), the fine AP is in suspension in a binder melt layer. Because the binder pyrolyzes more easily than the oxidizer (at the lower temperatures corresponding to low pressure burning), the binder will be depleted at the surface, and an elevated concentration of AP particles will occur. In effect, the surface layer disproportionates after ignition of a fresh cut surface until the AP receives enough heat flux to maintain the $(O/F)_p$ efflux ratio. This is a stable configuration because the heat flux to the binder has gone down to the point where further depletion stops (the dynamics of the disproportionation are affected by the concurrent transient change in O/F efflux and corresponding change in gas phase flame, potentially important to ignition processes and oscillatory burning). The state of the concentrating AP particles is a matter of speculation, since it consists of decomposing particles and underlying cooler particles. The concentration is limited by packing density, and some particles may leave the surface during decomposition.

At elevated pressure, it is the binder that concentrates on the surface. Being a connected structure, the binder would tend to protrude as a filigree, but most binders would be molten at these temperatures, so that surface tension causes it to flow into films or droplets, controlled by unevaluated properties such as viscosity and surface wetting with AP. The encroachment over AP particles increases the binder surface exposed to heat flux, while reducing heat flux to the AP, compensating for its relatively higher intrinsic decomposition rate of the AP at these higher surface temperatures, to permit surface effluxes in the $(O/F)_p$ proportion.

The foregoing argument is plausible for combustion of the fuel-rich fine AP/binder matrices in bimodal AP plateau propellants, discussed later. For larger AP particles, the disproportionation concept still applies, but the burning surfaces and flame become three dimensionally complex, and the disproportionation process will then be viewed simply as the requirement for oxidizer/binder vapor efflux equal to $(O/F)_p$ in a system with ingredients that have different melting temperatures and decomposition kinetics. Among the important, well known disproportionation-like things that happen with large AP particles are the protrusion on the burning surface at low pressures, the recessed condition at high pressure and binder melt flow over the outer periphery of the oxidizer particle surface at medium to high pressure.

Combustion of Fuel-Rich AP/HC Binder Matrices

Background

For bimodal AP/binder propellants the ratio of coarse to fine AP is typically 60/40 (mass ratio), in a formulation that is 87.5% AP, 12.5% binder. The density of the oxidizer is typically 2 times that of the binder, so the O/F volume ratio is 43/57. In combustion modeling it is customary to assign a portion of the binder to burn with coarse AP particles and a portion to burn with the fine AP. In bimodal propellants, the binder vapors mix with vapors from the fine AP particles so quickly that the coarse AP particles have to burn with the premixed vapors from the adjoining fine AP matrix. Then interactive burning occurs between the coarse AP and the matrix, and depends on the degree of

isolation of the coarse AP (which is high if the size is large and/or mass fraction low). Under these "isolated" conditions, the matrix may burn relatively independently of the coarse particles, and under some conditions may contribute strongly to the propellant burning rate and its dependence on pressure. As noted in the introduction, matrix burning often exhibits plateau burning, mesa burning, and extinction in the mid-pressure range. In the present study, these aspects of burning of fine AP/HC binder matrices were studied experimentally.

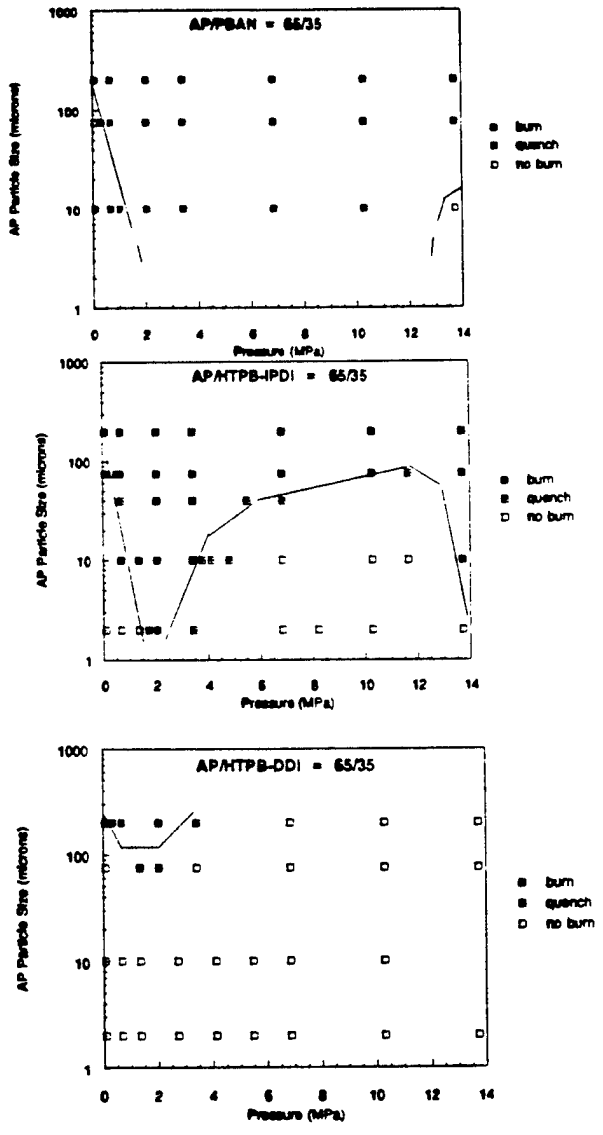

Figure 6– Burn-no-burn boundaries for AP/binder matrix with O/F ratio 65 to 35 (three binders; see Table 2)

Burn-No-Burn Domains

Initially, a study was made (Ref. 20) of the conditions under which matrices would burn on their own. The variables of interest were O/F ratio, type of binder, AP particle size, and pressure. A typical set of test results is shown in Figure 6, which shows burn and no-burn conditions in a particle size vs. pressure diagram (solid data points correspond to conditions for which samples burned to completion, while open points correspond to tests in which samples would not sustain burning. These tests were with 65 % AP/35% binder matrix, samples with 3 x 3 mm burning surfaces. The figure shows the burn-no-burn boundaries using three different binders. Note that these are three binders that have comparable energetics and temperature for decomposition, but differing melt characteristics (Table 1). Figure 7 shows the effect of AP/binder ratio burn-no-burn boundaries for one binder. The results show that no-burn conditions occur in the mid-pressure range (as well as the usual low pressure deflagration limit), and that fine particle size, low O/F ratio, and "high degree of binder melt" are all conducive to the no-burn state. Specifically, the effect of binder type is conspicuous in Figure 6, ranging from absence of a mid-pressure range no-burn domain with PBAN binder, to a well-defined no-burn domain with IPDI cured HTPB, to essentially no-burn under the whole pressure range with DDI cured HTPB. Low O/F ratio expands the no-burn domain.

Table 2. Binder Composition

No.	Prepolymer		DOA	Curing Agent	
	Type	% wt.	% wt.	Type	% wt.
1.	PBAN	64.14	15.00	ECA	20.86
2.	HTPB	69.07	16.77	DDI	14.16
3.	HTPB	75.73	18.39	IPDI	5.88

Burning Rates

A limited amount of burning rate data was obtained, which confirms past observations (Ref. 1, 2, 21) that burning rates are low near the no-burn domains. This is illustrated by Figure 8, which shows burning rates for three different particle sizes of Figure 6 (same O/F ratio, IPDI cured HTPB). With 10 μm particle size, there is a wide pressure range of no-burn condition, with conspicuously low values for burning rates below the no-burn domain.

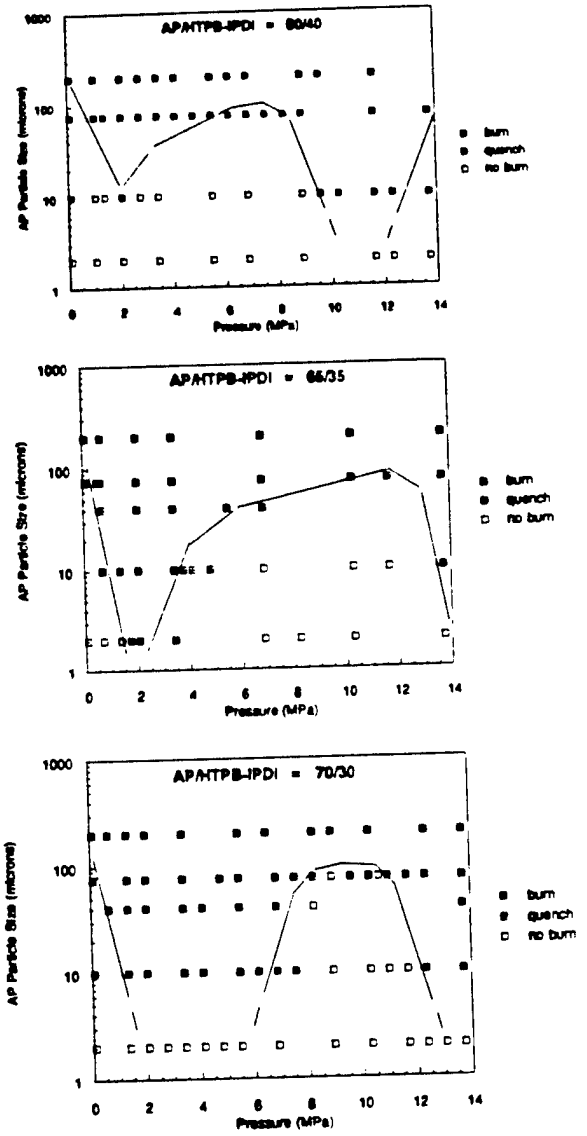

Figure 7– Burn-no-burn boundaries for AP/binder matrix for IPDI/HTPB binder (three O/F ratios)

With 75 μm particle size, the no-burn domain is much narrower, across which a sharp drop in the burning rate occurs. With 200 μm AP (which does not have a no-burn domain), a mild mesa is observed in the pressure range of no-burn for matrices with the finer AP. For comparison, a burning rate curve for 60/40 75 μm AP/PBAN is also shown in the figure. While this O/F ratio with PBAN did not show any no-burn domain, the burning rate shows a strong mesa in the pressure range of 2.5 to 7.5 MPa. This result is for a relatively low melt binder and formulation that did not exhibit a no-burn domain, suggesting that the "anomalous" behavior is not entirely dependent on binder melt effects; however, this mesa may be related to a no-burn domain at a slightly lower O/F ratio. It also is worthy to note that the burning rates of the PBAN formulations are higher than the corresponding IPDI/HTPB formulations under all conditions tested to date. As with earlier investigations, the full matrix of relevant formulation variables (particle size, O/F ratio, and binder type) has not been tested. Further tests are planned. The present tests have been with contemporary binders, which are notably different from those used in the systematic study by the Princeton team in the 1960s (Ref. 1, 2, 22). It would be worthwhile to bridge the gap to more fully evaluate the effect of binder variables.

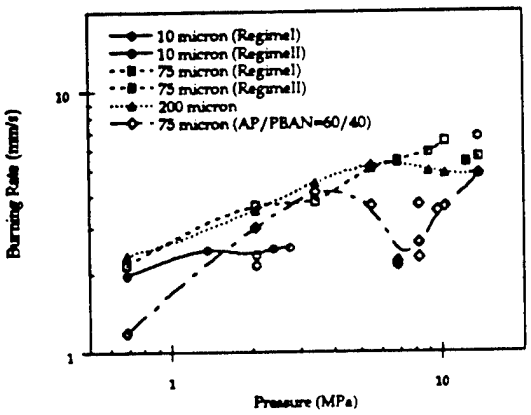

Figure 8–Burning rate vs. pressure for different oxidizer particle sizes of AP/IPDI cured HTPB matrices with O/F ratio 65/35

Quenched Sample Tests and Flame Photography

Some evidence of detailed processes in the combustion zone can be inferred by microscopic studies of the quenched surfaces of samples, usually obtained by rapid depressurization quench. While the tests were by no means comprehensive, some generalizations seem warranted.

1. For small particle sizes (e. g. < 20 μm), the AP particle surfaces appear wetted with binder melt. (This is thought to be due to the rapid depressurization quench process.) Surface irregularities corresponding to AP particle size are evident, especially with a lo-melt binder, high O/F ratio, and larger particles. At the highest O/F ratios, the surface appears to be dry.
2. Areas of "glossy" surface, suggestive of

complete melt coverage of AP are evident with low O/F ratio, PBAN binder, as well as with hi-melt binders. Surrounding ridges are present, and with irregular surfaces without obvious AP exposure. This appearance is most notable under conditions close to the no-burn domain.

3. When coarse AP particles are used, they are discernible and recessed relative to the surface (at high pressure (e. g., > 7 MPa)). This configuration continues to the higher pressures tested, but the entire surface develops a veiled character (unexplained) that obscures detail (pervasive melt?).
4. As observed by earlier investigators, large AP particles (> 70 μm) protrude above the mean surface at low pressure (e. g., < 2.3 MPa). The degree of protrusion was more evident with lo-melt binder, larger AP particle size, and high O/F ratio. This behavior (protruding AP) was more conspicuous in the early work of Bastress (Ref. 1) and others who generally used binders that decomposed at low temperatures relative to the oxidizer.
5. In general, surface irregularity becomes larger in both degree and scale near no-burn domains. The irregularities are of larger extent than the AP particle size, and appear to correlate with locally intermittent burning reported by Bastress (Ref. 1) and others (associated with proximity to the no-burn domain).

The foregoing pressure-dependent features of the burning surface are related to disproportionation behavior in that coarser AP tends to protrude at low pressure and be recessed above 7 MPa or so. Over the whole pressure range, binder melt tends to obscure fine AP, with two exceptions: a) at high O/F ratio and low pressure, fine AP appears to concentrate at the surface (as predicted by disproportionation arguments), and b) individual AP particle surfaces appear with PBAN binder with O/F ratio > 7/3 and particle size > 30 μm above 3.5 MPa. The collected results suggest that samples burned with premixed flames under most of the conditions tested (except largest AP, high O/F, lo-melt binders, high pressure). Given the pervasiveness of binder melt, it is not clear how decomposition of the fine AP proceeds. Such conditions are consistently correlated with lower burning rate, and presumably reflect either large O/F flame standoff, reduced O/F flame temperatures, and/or area-wise intermittent burning (near no-burn domain).

Relative to effect on burning rate of a bimodal propellant, the plateau burning and/or no-burn behavior of matrix formulations seems to be responsible for the plateau burning of bimodal propellants in the mid-pressure range; however, this effect depends on a major contribution to, or control of the propellant burning rate by the matrix, perhaps accompanied by a suppression of burning of the coarse particles in the bimodal AP blend. Further, desired plateau effects may be mitigated by interactive burning between matrix and the coarse AP (due to high coarse content or "low coarse" size, conditions that give high "proximity"). These considerations have been quantified by systematic testing of bimodal propellants, but cannot be generalized because of the wide range of relevant important variables such as type of binder, O/F ratio of the propellant, ratio of coarse to fine AP, relative size of coarse and fine AP, and presence of additives (aluminum, burning rate catalysts and suppressants, combustor stability agents, flash suppressants). With this in mind further advances in understanding of the matrix combustion processes seems warranted.

Interactive Burning of Coarse AP and AP-binder Matrices

Background

Having noted that AP and matrices can both exhibit plateau and mesa burning on their own, an obvious question is, when they are burning together, are their individual plateaus reflected in the propellant burning rate? Also, is a plateau ever manifested under conditions where neither the AP nor matrix individually shows a plateau? The answers to these crucial questions depend on how the AP and matrix combustion interact. It has been suggested that the burning of bimodal AP propellants may be dominated either by rapid deflagration of coarse AP particles (Ref. 23) or by the contiguous matrix (Ref. 24). While such a picture of combustion behavior is convenient, and may pertain under special conditions, the conditions under which plateau burning has been observed will be seen to be quite different. A realistic model will no doubt require detailed consideration of the interaction of the AP and matrix combustion, including:

1. The local effect of the leading edge of the O/F diffusion flame ("LEF," see Figure 2) on deflagration of coarse particles, and how it is

changed by changes in matrix variables.

2. Implicit in 1), the effect of matrix variables on the coarse particle LEF, and in turn the reciprocal effect of LEF changes on matrix pyrolysis (the coarse particle and matrix O/F flames are coupled).
3. As an extension of 2), the manner in which coarse particle LEF's support burning of matrices under conditions where the matrices won't burn on their own.
4. Lateral heat flow between coarse particles and the adjoining matrix in the condensed phase.
5. Lateral thermal and species diffusion in the mixing fan.
6. Relative pyrolysis rate of AP (coarse particles) and matrix, and the surface accommodation (disproportionation, including the possibility that no accommodation will occur and burning may fail, i. e., local quench).
7. The behavior of accumulating surface melt and its contribution to disproportionation (including effect on LEF's).
8. The scale of lateral effects, and the relation to coarse AP radii, matrix thickness, thermal wave and melt layer thicknesses, and pressure.

Most of these interactive effects are absent or only superficially represented in propellant combustion models, but are probably all important to plateau burning. Probably the best source of this information is results from sandwich burning experiments, in which the AP laminae takes the place of coarse AP particles, and the intricate boundaries of the matrix are replaced by planar contact surfaces with the AP laminae. This more simple system was studied in some detail for PBAN binder using combustion photography and quench burning methods (Ref. 10). These studies were recently extended to a larger pressure range (Ref. 25.) and to samples with IPDI cured HTPB.

Results Based on Sandwich Burning Tests

Figure 9 shows the dependence of sandwich burning rate on matrix lamina thickness for several pressures for PBAN binder and a) 70/30 ratio of 10 μm AP to binder in the matrix and b) 50/50 ratio of 10 μm AP to binder. Figure 10 shows the corresponding (but incomplete) data for the same conditions but IPDI cured HTPB binder; note that the 50/50 matrices do not burn on their own except at 50 psi (0.345 MPa), and the 70/30 HTPB matrix has a no-burn domain in the 7 to 12 MPa range

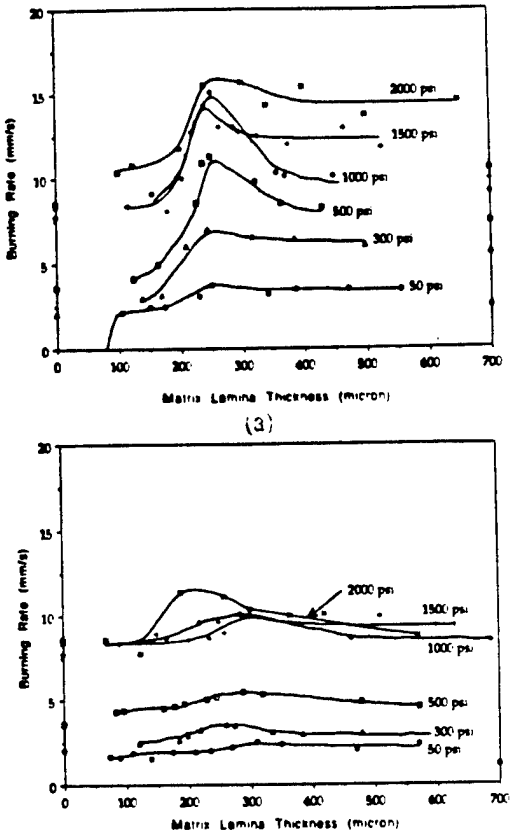

Figure 9–Burning rates of sandwiches of AP/PBAN matrix between AP laminae, shown vs. matrix lamina thickness for several pressures. AP particle size 10 μm a) O/F ratio 7/3 b) O/F ratio 5/5. AP rates shown at the left, pure matrix rate shown at the right

(Figure 7). Rather than repeat all the interpretations of these results (see Ref. 9, 10, and 25), listed below are some conclusions that pertain to interactive burning (PBAN lo-melt binder).

1. The lamina (or large particle) leading edge flame shares oxidizer vapors from the lamina and O/F vapors from the matrix. The location and "size" of the LEF depends on the matrix variables and pressure.
2. The LEF is centered over the AP (e. g., 25 μm in from the lamina contact plane), and enhances the AP deflagration. In sandwich burning, the rate is controlled by the LEF-enhanced AP deflagration.
3. Elaborating on 1), the presence of oxidizer in the matrix vapor causes the LEF to be shifted towards the edge of the AP lamina, increases the fuel rich side of the LEF to extend out further in the matrix vapor flow and produce greater heat release. This allows the LEF to stabilize closer

to the surface, increasing surface heat flux and AP regression rate. This is favored by high O/F ratios in the matrix.

4. The maximum in the rate versus matrix lamina thickness curve is indicative of interaction of adjoining LEF's. The thickness of the matrix lamina for maximum rate is around 250 μm; since the LEF's are strongly interactive at this thickness, the matrix burning is strongly coupled with, and enhances the LEF's.
5. Above 350 μm matrix thickness, the LEF interaction diminishes, and independent burning characteristics of the matrix begin to show up (usually as a protrusion of the center of the lamina). The matrix enhancement of the LEF's is decreased when the matrix O/F ratio is decreased, and a corresponding decrease in sandwich burning rate and increase in protrusion of the center of the matrix lamina results.
6. Lateral heat flow proceeds from the oxidizer to the matrix in the condensed phase. The regression rate of the AP surface nearest to the matrix lamina is correspondingly reduced, resulting in AP protrusion. This protrusion is apparently enhanced by local failure of the AP flame, an interpretation that is supported by an otherwise atypical smoothness of the surface suggestive of dissociative sublimation. These effects are all diminished by high matrix O/F ratios, consistent with the shift of the LEF and rate controlling site in the AP towards the lamina contact plane. With a 7/3 matrix, the LEF is centered very close to the contact plane.
7. Sandwiches always burn faster than AP alone, and faster than the matrix alone. Matrices that burn on their own usually burn faster than the AP alone. However the difference between the sandwich rate and AP rate usually is less when pressure is above 1000 psi (6.89 MPa).
8. When the matrix particles are > 20 μm, the matrix flame may not be premixed at high pressure (e. g., 1000 psi, 6.89 MPa). Thirty three and a half micron particles adjoining the AP laminae show evidence in quenched samples (Ref. 9) of particle-attached burning above 500 psi (3.47 MPa).
9. Matrix surfaces are generally slightly recessed relative to the "protruding" region of AP at the contact plane, except as noted in 5.
10. There is a boundary among the variables of particle size, matrix O/F ratio, and pressure below which the surface of fine AP particles appears (quenched samples) to be coated with a thin film of binder melt. It is possible that the binder foams up out of the substructure during quench. Quenched sandwich tests at pressures above 1000 psi (6.89 MPa) are not available, but tests on bimodal propellants at pressures above 1500 psi (10.5 MPa) exhibit an absence of typical structural detail that is apparently due to pervasive melt flow.
11. Referring to Figure 9a, in the lamina thickness range 150 to 300 μm, plateau and mesa burning occur in the 1000 psi (6.89 MPa) to 1500 psi (10.5 MPa) pressure range. These are conditions under which strong interactive burning of adjoining LEF's (and premixed matrix flame) are present, and with a binder that is regarded as "lo-melt," with a matrix that burns by itself. These conditions are presumably pertinent to the effect of coarse particle spacing in bimodal propellants.
12. Referring to the results with a 50/50 matrix in Figure 9b, plateau and mesa burning is indicated over the whole range of matrix lamina thickness from 100 μm up in the pressure range 1000-1500 psi (6.89-10.5 MPa). This is a matrix that does not burn on its own.

The foregoing 12 observations are all pertinent to coarse AP/fine AP + PBAN propellants. Most notable are results indicating that plateaus can occur with a lo-melt binder and self-burning matrix, and that they occur in a domain of interactive LEF's. The results with a 50/50 matrix suggest that excess melt (even with PBAN) near the interface plane hampers burning (quench sample tests at these higher pressures are not yet available to clarify details).

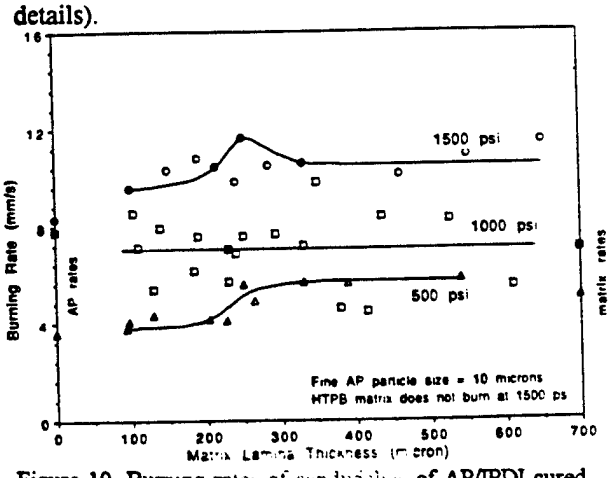

Figure 10--Burning rates of sandwiches of AP/IPDI cured HTPB vs. matrix lamina thickness for several pressures. AP particle size 10 μm, O/F ratio 7/3

Returning to Figure 10, sandwich burning with an IPDI cured HTPB matrix (70/30 O/F ratio) yielded:

a) lower rates than with PBAN
b) less reproducible burning rates (serious scatter, especially in the 1000 psi (6.89 MPa) tests which correspond to the matrix no-burn boundary, Figure 7)
c) no obvious plateau burning in the pressure range 500-1500 psi (3.45-10.5 MPa), but it is difficult to judge due to limited data and large scatter
d) dependence of rate on lamina thickness was minimal (except in the thin lamina limit)
e) sandwich rate at 1000 psi (6.89 MPa) appears to be somewhat less than AP rate and comparable to matrix rate
f) the matrix would not burn at 1500 psi (10.5 MPa)

Lacking more complete results, much inference from these results would be reckless. However, it is notable that the matrix is in a no-burn domain at 1500 psi (10.5 MPa) and near a no-burn domain at 1000 psi (6.89 MPa) (see Figure 7). The lower burning rate compared to PBAN matrix sandwiches is consistent with propellant results, and it is reasonable to believe that binder melt flow is responsible for the observed differences from PBAN results. A similar contrasting behavior was reported earlier for sandwiches with pure binder laminae (Ref. 25 and 26).

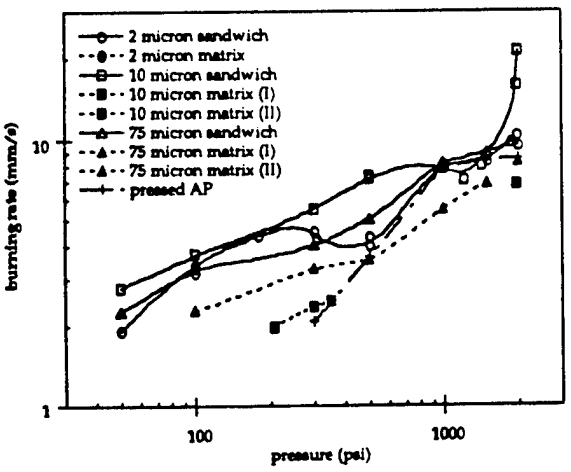

Figure 11–Effect of AP particle size on burning rate vs. pressure for sandwiches with 250 μm matrix lamina of 65% AP and 35% IPDI cured HTPB binder

Subsequent to the tests described in Figure 10, an abbreviated set of matrix sandwich burning tests was run under conditions chosen specifically to look for plateau burning, using 3 different sizes of AP with IPDI cured HTPB binder in a matrix with 65 to 35 O/F ratio. The results (Figure 11) show mesa burning with the samples with 2 μm AP, plateau burning with samples with 10 μm AP, and a low slope region with 75 μm AP in pressure ranges corresponding to no-burn domains of the matrices (Figure 6b). It is important to note that the three sandwiches had a matrix lamina thickness of ~250-275 μm (based on Figure 9) corresponding to strong interaction between the LEF's, and the premixed matrix flame (where present).

Interaction Distances in Typical Bimodal Propellants

It is important to compare the interaction distances that were observed in sandwich burning tests with the interparticle spacing of the coarse AP in typical bimodal propellants. For this purpose some calculations were made for hexagonal arrays of spheres (coarse particles) assuming the space in between consisted of AP/binder matrix. In such an array, the distance between particles is

$$2t = 2\left\{\left[\frac{\gamma\left(\alpha\rho_M + (1-\alpha)\rho_{Ox}\right)}{\alpha\rho_M}\right]^{1/3} - 1\right\}d$$

where

$$\rho_M = \frac{1-\alpha}{\frac{\tau-\alpha}{\rho_{Ox}} + \frac{1-\tau}{\rho_b}}$$

and where

γ = solid fraction of the packing structure (for hexagonal structure $\gamma = 0.6981$)
α = mass fraction of coarse particles in the propellant
ρ_{Ox} = density of oxidizer = 1.95 g/cc for AP
ρ_M = density of fine AP/binder matrix
d = coarse oxidizer particle diameter
τ = total oxidizer mass fraction (coarse & fine) in the propellant
ρ_b = density of binder ≈ 0.903 g/cc for PB binder

Assuming a fixed AP/binder mass ratio in the propellant, Figure 12 shows the spacing between AP

particles as a function of fine AP content in the propellant. The upper coordinate scales show the corresponding ratio of coarse AP to fine AP, and of fine AP to binder in the matrix.

Allowing for the fact that the particle spacing is the least dimension in the matrix microstructure, matrix distances in typical formulations are apparently less than 150 μm for typical plateau burning propellants with 400 μm coarse AP. Thus it would appear that, based on results with PBAN matrix sandwiches, the matrix areas on the burning surface of the bimodal propellant mostly burn interactively with the coarse particles.

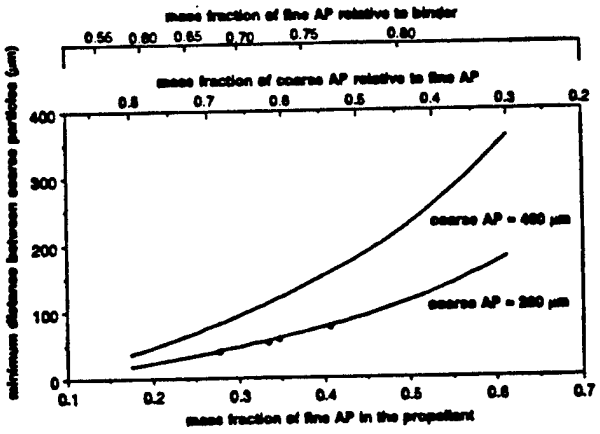

Figure 12–Spacing between coarse AP particles vs. percent fine AP particles for an idealized bimodal propellant. Total AP 87.5%, binder 12.5%. Solid dots in the graph correspond to actual propellants that exhibit plateau burning (Ref. 3)

Intermittent Burning

It was noted earlier that conditions near matrix no-burn boundaries had been observed to exhibit "abnormally" low burning rate and uneven surface regression, and uneven and fluctuating gas phase flames. This behavior was an integral part of "anomalous" burning (the name "anomalous" was subsequently used by Summerfield to designate behavior that did not conform to the granular diffusion flame theory, Ref. 2) associated with no-burn boundaries , and plateau and mesa pressure dependence observed by Bastress (Ref. 1). Evidently intermittent burning will reduce the net heat flux to the surface and hence reduce average burning rate, and extreme cases lead to self-quenching. Bastress (Ref. 1) suggested that local areas of burning surface may become depleted of AP sites (because AP particles gasify faster than the binder at the pressures involved (around 1200 psi, 8.3 MPa). Burning would have to be sustained by neighboring areas until new AP particles were exposed in the quenched area. If this did not happen soon enough, the adjoining areas would go dormant also, and burning would "fail." This may be the birth of the concept of failure of disproportionation to achieve vapor efflux O/F ratio matching the propellant O/F ratio. It also brings out the idea that disproportionation failure may lead to a new mode of burning in which local failure is followed by "rejuvenation" of the surface with the help of still burning adjoining sites that are "out of phase" in a failure-rejuvenation-reignition-burn to quench cycle. If this is the primary basis for plateau-mesa burning in practical systems, then it deserves intensive study, not only for design of plateau burning systems, but also to learn how such systems behave during ignition, under cross flow conditions, and during oscillatory combustor instability. Of course, it is also desirable to ascertain the effect of the coarse AP particles, which may maintain burning when the matrix is in a disproportionation failure domain.

The Bastress mechanistic argument noted above did not receive much notice for two reasons. One was lack of requisite observations of details of the process (not unique to Bastress). Another was growing favor for a melt-flow interpretation for interference with burning. While this argument was not (and still has not been) supported by detailed mechanistic and experimental studies, thirty years of burning rate studies have made it clear that propellants with "hi-melt" binders are more prone to plateau burning. However, there are notable instances in which plateau burning occurred with "lo-melt" binders, starting perhaps with polysulfide binder matrices in Bastress' work, and including the plateau burning sandwiches described in the present work (with PBAN binder).

Perhaps the most classic case of plateau-mesa burning without binder melt contribution is that of self deflagration of pure single crystal ammonium perchlorate alluded to earlier in this paper and in Ref. 12, 13, 15, 16. In the mesa region (above 2000 psi, 13.88 MPa), the burning is clearly locally intermittent with associated uneven surface

regression. In fact, it appears that steady planar surface regression of AP does not occur at any pressure (Ref. 16).

It is premature to attribute all plateau and mesa burning in composite AP propellants to intermittent burning behavior, because there is a paucity of observational data to date. However, there is a clear link, and it is an easy way to understand the "anomalous" low burning rates. The underlying details of the nonsteady burning may be described conceptually as "disproportionation failure," but that does not go very far towards describing the details.

Binder Melt Flow

Flow or accumulation of binder melts over AP particles apparently has a significant effect on burning rate with some binders. In the present study (Figure 6 and Figure 7), hi-melt DDI cured HTPB (Table 1) matrix formulations burned under almost no conditions, IPDI cured HTPB (medium melt) matrices burned over a substantial range of conditions but had conspicuous no-burn domains, and PBAN (lo-melt) matrices did not have a no-burn domain. In general, high solids propellants with DDI cured HTPB binders have lower burning rates than those with IPDI cured HTPB or PBAN binders at all pressures, and plateau burning is more common with hi-melt binders. The real issue is why? And if it is due to melt incursion over AP surfaces, how does that come about, what are the microphysics of the process, and what causes the unique pressure dependence?

At low pressure the thermal wave is thick, and the melt layer correspondingly thick (but strongly dependent on choice of binder). As pressure and burning rate go up and thermal wave thickness goes down, the melt layer thickness tends to go down. However, the melt layer thickness becomes of the same order as the matrix particle size, and at high enough pressure it tends to become a protruding filigree due to disproportionation. Rather than protrude, it melts with a potential to flow onto adjoining recessed large AP surfaces. Cohen suggests that such melt flow becomes more likely at these higher surface temperatures because of lower melt viscosity (Ref. 8). The same thing presumably will not occur at low pressure in the thick binder melt layer because the binder pyrolyzes ahead of the AP. Thus the situation becomes conducive to binder melt flow at higher pressures (e. g., around 1200 psi; 8.21 MPa) as just described. There is visible evidence in combustion photography of excess melts at these pressures, and quenched samples show coverage of matrix surfaces and encroachment of melt over peripheries of large particles (400 μm) and sandwich AP laminae. This accomplishes the disproportionation requirement by exposing larger areas of binder (and smaller AP areas) to incoming heat flux. This is a regime where AP self deflagration can make a major contribution to burning rate, but this process is also impeded by the binder incursion, resulting in lower burning rate, plateaus and mesas.

While the foregoing argument seems to provide a plausible scenario for plateau burning in the pressure range noted, it cannot be reduced to a theory without far more systematic observations of melt flows (vs. binders, pressures, O/F ratio, etc.) and without addressing the following issues:

a) The wetting behavior of hot binder melts on hot AP surfaces.
b) Identification of forces that drive melts over the AP surface.
c) Life cycle of a pyrolyzing melt incursion over an already pyrolyzing AP surface.
d) Behavior of the covered AP surface.
e) Response of LEF position to binder incursion, resulting net LEF heat release, and modified distribution of LEF energy to the AP and binder.

According to disproportionation arguments (for the three primary binders of this paper, that all decompose at somewhere near the same temperature) at low vapor pressure, vaporization of the binder precedes that of the oxidizer, so that the surface layer should be a concentration of fine AP particles, while depleted of binder. At high pressure, the surface should be dominated by binder melt. This was found (with quenched samples) to be the case with PBAN binder in 75/25 mixtures of 10-20 μm AP/PBAN. With lower AP fractions, the binder seemed to give a thin film over the fine AP at all pressures (Figure 13). At this point (with limited data), it is suggested that

a) Conditions are closer to disproportionation failure
b) The persistence of melt coverage is an artifact of the quench event, i. e., a melt foam may be formed on the surface during depressurization, that settles over the entire surface.

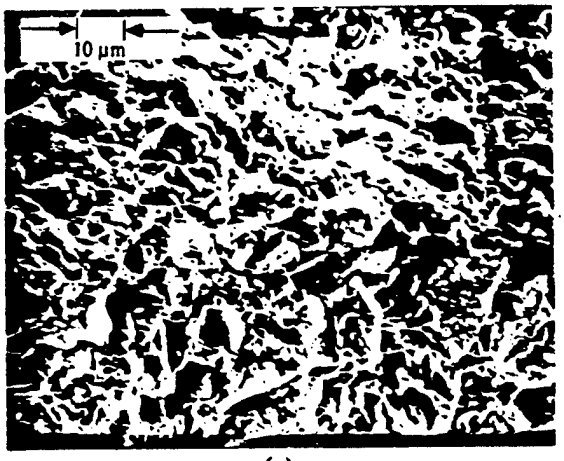

(a)

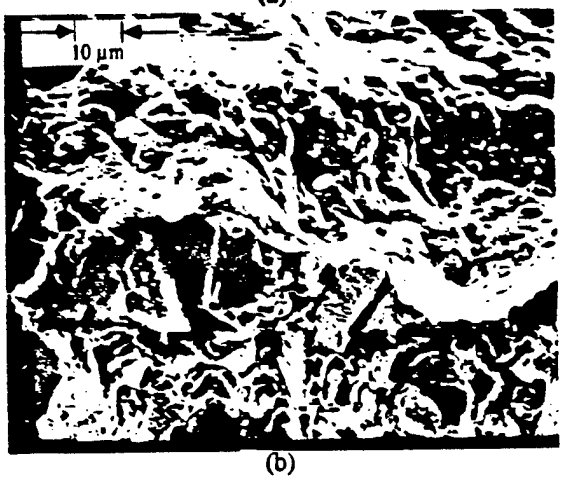

(b)

Figure 13—Quenched matrices that have been cleared to show subsurface features (bottom), and surface features (top) Matrix was 75% 10-20 μm AP, 25% PBAN binder a) 300 psi (2.07 MPa) b) 1200 psi (8.28 MPa).

Conclusions

This paper examines several detailed aspects of the combustion of AP composite propellants that may contribute collectively to the phenomenon of plateau burning. The "examination" involves revisiting old issues, introducing new ones, and presenting some new experimental results. Attention is directed at aspects of the combustion process that are either neglected or treated only superficially in conventional propellant burning rate models. The picture that emerges is that of three dimensionally complex interactive condensed and gas phase processes proceeding on a microscopic scale much smaller than the coarse (400 μm) AP particles, more comparable to the finest AP used (< 10 μm).

It is noted that the surface processes (and oxidizer and binder surfaces) must proceed in such a way that the space-time averages of efflux of oxidizer and binder species conform to the O/F ratio of the propellant (in order to have macroscopically steady state burning). As the flame complex and heat flux field change with pressure, the surface details must change correspondingly to satisfy the required O/F flux. When the heat flux tends to pyrolyze "too much" oxidizer, the oxidizer must recede relative to the binder until a new surface configuration yields the correct O/F ratio. This reconfiguration of the surface is referred to as "disproportionation" because it involves a spontaneous reapportionment of the ratio of exposed oxidizer and binder surface area, (i. e., compared to the ratio for a cut surface). If the normal thermal response of the ingredients does not provide this disproportionation, the burning must fail locally, a condition giving rise to ignition failures, locally intermittent burning, or complete cessation of burning. Plateaus in burning rate curves seem to be associated with formulations and pressures that border on domains of variables where disproportionation failure occurs.

The idea of disproportionation and failure to achieve it is convenient in explaining macroscopic combustion behavior, but is also a beguiling disguise for an exquisitely complex interplay of propellant microstructure, three dimensional heat transfer, ingredient melt and decomposition behavior, and 3-dimensional micro flame behavior, and the interaction of these conditions and processes. Disproportionation is a consequence of this array of coupled processes, about which all too little is known, and the burning rate is determined by the pressure dependent array of conditions that satisfies the disproportionation requirement.

Experimental results indicate that plateau burning occurs in AP self-deflagration (at high pressure); in combustion of fuel rich matrices of fine AP and binders (which also have no-burn domains in the mid-pressure range); and in burning of bimodal AP propellants that are composed partly of fine AP/binder matrices. Experiments with sandwich burning have shown plateau burning, and comparison of the results with the microstructure of plateau burning propellants suggest that plateau burning occurs under conditions where burning of the coarse particles and matrix burning are coupled, a circumstance that will greatly complicate analytical

modeling.

Collected results suggest that accumulation and flow of binder melt is an effective route to disproportionation failure and a frequent cause of plateau burning. However, there are instances of plateau burning where no melt flow is present.

It should be noted that the present report focuses on a limited set of arguments and studies on propellants with AP oxidizer and three binders with similar decomposition temperatures (but different melt characteristics) The details of behavior may be quite different with other ingredients, and the set of arguments regarding pressure dependence of burning rate would be correspondingly different. There is no reason for optimism that plateau burning is possible at all, for many ingredient systems.

Finally, it should be evident that the present paper does not present a formula for how to formulate plateau burning propellants. As noted by Cohen (Ref. 8), there is a great deal of experimental data needed before a realistic plateau burning model can be constructed. While the present paper provides some new data and assembles some earlier data and interprets it in the context of the present topic, there is a profound need for systematic testing. Improvements in experimental methods will be required to better establish the state of the burning surface with spatial resolution on the one micrometer scale.

Acknowledgments

This research was sponsored by the U. S. Office of Naval Research under contract N00014-95-3-0559. Thanks is due to Dr. R. S. Miller, contract technical monitor; and also due to Beth Zachary for support in preparation of the manuscript.

References

1 Bastress, E. K.., "Modification of the Burning of the Burning Rates of Ammonium Perchlorate Solid Propellants by Particle Size," Ph. D. Thesis, Princeton University, Princeton, New Jersey, January 1961.

2 Steinz, J. A., Stang, P. L., and Summerfield, M., "The Burning Mechanism of Ammonium Perchlorate-Based Composite Solid Propellants," Aerospace and Mechanical Sciences Report No. 830, Guggenheim Laboratories for the Aerospace Propulsion Sciences, Department of Aerospace and Mechanical Sciences, Princeton University, Princeton, N. J., February 1969.

See Also:
Steinz, J. A., Stang, P. L., and Summerfield, M., "The Burning Mechanism of Ammonium Perchlorate-Based Composite Solid Propellants," AIAA Paper 68-658, 4th Propulsion Joint Specialist Conference, June 10-14, 1968.

3 Hinshaw, C. J. and Minicini, V. E., "Biplateau Burning of Propellants Containing Aluminum, TR-10137, Thiokol Corporation, Interim Report to ONR, contract No. N00014-92-C-0134, March 1993.

4 Klager, K. and Zimmerman, G. A., " Steady Burning Rate and Affecting Factors: Experimental Results," Chapter 3 in De Luca, L, Price, E. W., and Summerfield, M. (Eds.), "Nonsteady Burning and Combustion Stability of Solid Propellants," Vol. 143, Progress in Astronautics and Aeronautics, AIAA, Washington, D. C., 1992.

5 Fong, C. W. and Smith, R. F., "The Relationship Between Plateau Burning Behavior and Ammonium Perchlorate Particle Size in HTPB-AP Composite Propellants," *Combustion and Flame*, Vol. 67, 1987, pp. 235-247.

6 Beckstead, M. W., "A Model for Solid Propellant Combustion," *Proceedings of the 14th JANNAF Combustion Meeting*, CPIA Publication 292, Vol. I, Dec. 1977, pp. 281-306.

7 Cohen, N. S. and Strand, L. D., " An Improved Model for the Combustion of AP Composite Propellants," *AIAA Journal*, Vol. 12, No. 20, December 1982, pp. 1739-1746.

8 Cohen, N. S. and Hightower, J. O., "An Explanation for Anomalous Combustion Behavior in Composite Propellants," *Proceedings of the 29th JANNAF Combustion Meeting*, October 1992.

9 Lee, S.-T., "Multidimensional Effects in Composite Propellant Combustion," Ph. D. Thesis, Georgia Institute of Technology, Atlanta, Georgia, May 1991.

10 Lee, S.-T., Price, E. W., and Sigman, R. K., "Effect of Multidimensional Flamelets in Composite Propellant Combustion," *Journal of Propulsion and Power*, Vol. 10, No. 6, Nov.-Dec. 1994, pp. 761-768.

11 Price, E. W., Chakravarthy, S. R., Zachary, E. K., and Sigman, R. K., "Ingredient Response and Interaction during Heating in a Hot Stage Microscope," *Proceedings of the 31st JANNAF Combustion Meeting*, CPIA Pub. 620, October 1994.

12 Boggs, T. L., "Deflagration Rate, Surface Structure, and Subsurface Profile of Self-Deflagrating Single Crystals of Ammonium Perchlorate," *AIAA Journal*, Vol. 8, No. 5, May 1970, pp. 867-873.

13 Glaskova, A. P., "Anomalies in the Burning of Ammonium Perchlorate and Ammonium Nitrate," *Fizika Goreniya I Vzryva*, Vol. 4, pp. 314-332.

14 Hightower, J. D., and Price, E. w., "Experimental Studies Relating to the Combustion Mechanism of Composite Propellants," *Astronautics Acta*, Vol. 14, No. 1, 1968, pp. 11-21.

15 Boggs, T. L., Prentice, J. L., Kraeutle, K. J., and Crump, J. E., "The Role of the Scanning Electron Microscope in the Study of Solid Propellants," *Proceeding of the Second Annual Scanning Electron Microscope Symposium*, Chicago, Illinois, April 1969.

16 Price, E. W., Chakravarthy, S. R., Sigman, R. K., and Freeman, J. M., "Anomalous Combustion Behavior of Ammonium Perchlorate at Elevated Pressures," *Proceedings of the 33rd JANNAF Combustion Meeting*, October 1996.

17 Price, E. W., Sambamurthi, J. K., Sigman, R. K., and Panyam, R. R., "Combustion of Ammonium Perchlorate-Polymer Sandwiches," *Combustion and Flame*, Vol. 63, 1986, pp. 381-413.

18 Beckstead, M. W., "Solid Propellant Combustion Mechanisms and Flame Structure," Pure and Applied Chemistry, Vol. 65, No. 2, 1993, pp. 297-307.

19 Deur, J. M., "A Surface coupled Flamelet Approach to Dynamic Response in Heterogeneous Propellant Combustion," Ph. D. Thesis, Georgia Institute of Technology, Atlanta, Georgia, 1988.

20 Chakravarthy, S. R., Price, E. W., and Sigman, R. K., "Binder Melt Flow Effects in the Combustion of AP-HC composite Solid Propellants," AIAA Paper 95-2710, 31st AIAA/ASME/SAE/ASEE Joint Propulsion Conference and Exhibit, June 10-12, 1995.

21 Lengelle, G., Brulard, J., and Moutet, H., "Combustion Mechanisms of Composite Solid Propellants," *Proceedings of the Sixteenth Symposium (International) on Combustion*, The Combustion Institute, Pittsburgh, PA, 1976, pp. 1257-1269.

22 Steinz, J. A., Stang, P. L., and Summerfield, M., "Effects of Oxidizer Particle Size on Composite Solid Propellant Burning: Normal Burning, Plateau Burning and Intermediate Pressure Extinction," Proceedings of the 4th ICRPG Combustion Conference, CPIA Pub. 162, Vol. I, Dec. 1967, pp. 499-512.

23 Miller, R. R., "Effects of Particle Size on Reduced Smoke Propellant Ballistics," AIAA Paper 82-1096, AIAA/SAE/ASME 18th Joint Propulsion Conference and Exhibit, June 21-23, 1982.

24 Foster, R. L., and Miller, R. R., "The Influence of the Fine AP/Binder Matrix on Composite Propellant Ballistic Properties," *Proceedings of the 17th JANNAF Combustion Meeting*, CPIA Pub. 329, Vol. III, September 1980, pp. 91-104.

25 Chakravarthy, S. R., "The Role of Surface Layer Processes in Solid Propellant Combustion," Ph. D. Thesis, Georgia Institute of Technology, Atlanta, Georgia, 1995.

26 Price, E. W., "Effect of Multidimensional Flamelets in Composite Propellant Combustion," *Journal of Propulsion and Power*, Vol. 11, No. 4, pp. 717-728.

APPENDIX G

Price, E. W., Freeman, J. M., Jeenu, R., Chakravarthy, S. R., Sigman, R. K., and Seitzman, J. M.

"Plateau Burning of Ammonium Perchlorate Propellants"

AIAA Paper 99-2364

35th AIAA/ASME/SAE/ASEE Joint Propulsion Conference and Exhibit

Los Angeles, CA, June 20-24, 1999

AIAA 99-2364

Plateau Burning of Ammonium Perchlorate Propellants

E. W. Price, J. M. Freeman, R. Jeenu, S. R. Chakravarthy, R. K. Sigman, and J. M. Seitzman

School of Aerospace Engineering
Georgia Institute of Technology
Atlanta, GA 30332-0150

35th AIAA/ASME/SAE/ASEE Joint Propulsion Conference and Exhibit
20–24 June 1999
Los Angeles, California

For permission to copy or to republish, contact the American Institute of Aeronautics and Astronautics, 1801 Alexander Bell Drive, Suite 500, Reston, VA, 20191-4344.

Plateau Burning of Ammonium Perchlorate Propellants

E. W. Price, J. M. Freeman, R. Jeenu, S. R. Chakravarthy, R. K. Sigman, and J. M. Seitzman
School of Aerospace Engineering, Georgia Institute of Technology, Atlanta, GA 30332-0150

Abstract

This is a partial summary of several reports by the above authors. An effort is made to identify and discuss the interplay of several mechanisms that cause plateau burning.

Introduction

This paper concerns a class of "anomalous" burning behavior of AP composite propellants that includes low and negative dependence of burning rate on pressure over an appreciable range of pressure (Fig. 1).

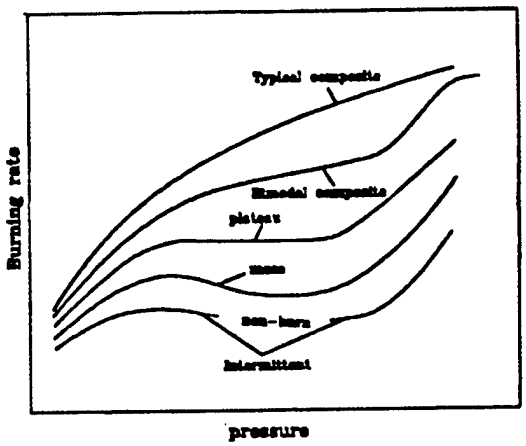

Fig. 1 Pressure dependence on burning rates of propellants.

This kind of behavior was discussed at length in Ref. 1, and the present paper discusses new findings since that time, that test speculations, correct errors, extend the results, answer some questions, and pose some new mechanistic arguments. Much of the pertinent new experimental work was reported in Ref. 2 to 4.

For background, it is noted here that anomalous burning was originally observed(Ref. 5-8) of combustion of propellants with monomodal AP size distributions (which are necessarily quite fuel rich because of limitations in packing density of the AP). Such behavior is also observed with some AP propellants consisting of relatively coarse and relatively fine AP (e.g., 70% 400 μm and 30% 4μm). Such propellants can be viewed as suspensions of coarse AP in a matrix of fine AP and binder, with volume proportions of 46% and 54% (Fig. 2). These two "entities" have very

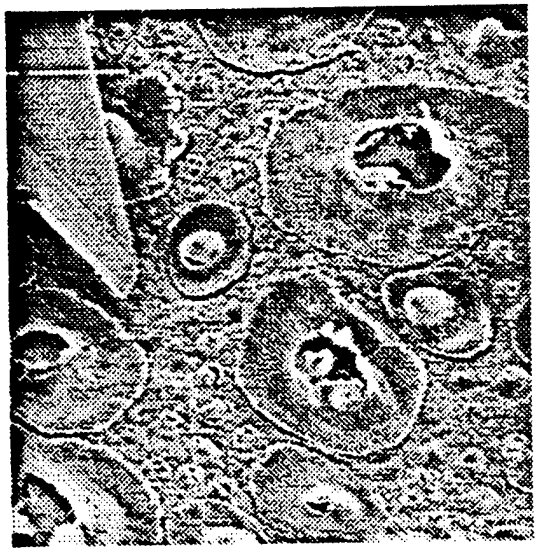

Fig. 2 A quenched burning surface that illustrates the disposition of coarse AP and matrix arears for a plateau-burning bimodal AP propellants (200μm coarse AP, 2μm fine AP)(the sharp object is a knife blade).

different burning behavior, and the "anomalous" burning behavior reflects the individual behavior of each and a measure of coupling behavior between the two. In particular, burning of the coarse AP particles is much like the self deflagration of AP (Fig. 3), while the matrix burning tends to be marginal when burning on its own, quite often exhibiting plateau burning, locally intermittent burning, and spontaneous quenches in the mid pressure range. It is observed in both propellant testing and edge burning of "sandwiches" of matrix between AP

Copyright © 1999 by E. W. Price, J.M.Freeman, R.Jeenu, S.R.Chakravarthy, R.K.Sigman, and J.M.Seitzman. Published by the American Institute of Aeronautics and Astronautics, Inc. with permission.

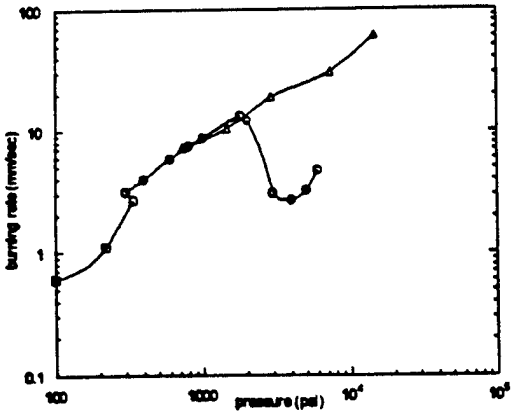

Fig. 3. AP "self" deflagration rate; □ refers to large AP discs with peripheral inhibitor (Ref. 11); O refers to single crystals burning in an N_2 atmosphere (Ref.12); Δ refers to inhibited strands (Ref. 13).

laminae (Ref. 9, 10) that the propellants (and sandwiches) always burn faster than either the AP or matrix alone, indicating that some measure of positive coupling always exists. In extreme cases, a propellant or sandwich will burn with a matrix that won't burn on its own at all (or sometimes with a plateau); and the AP sustains deflagration below its normal self deflagration limit when some matrix (or fuel) is around. Further, the anomalous deflagration of AP starting at about 2000 psi (Fig. 3) "goes away" in the presence of a matrix or fuel. Coupling appears to be by heat supply from the hot flame between the matrix vapors and the AP vapors from the coarse AP particles (or lamina). As one might expect, the details are pressure dependent, as the flame is nearly premixed (planar) at low pressure, but of increasingly complex structure as pressure increases. In order to understand plateau burning, it appears to be necessary to understand the pressure dependence of matrix burning, of AP burning, and of their coupling. This difficult problem is further complicated by the extreme dependence of the propellant surface geometry on pressure (Fig. 4). It is further complicated by the sensitivity of plateau behavior to particle size of the fine AP, ratio of coarse-to-fine AP, type of binder, and presence of minor additives.

It is worthy of note that if a study of effect of formulation variables were undertaken, a set of 5 choices for each of the four "sensitive" variables noted above, and for coarse AP particle sizes would yield $5^5 = 3125$ combinations for propellant formulations, which would have to be

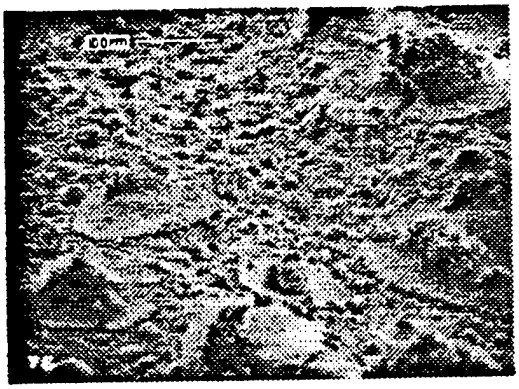

(a)

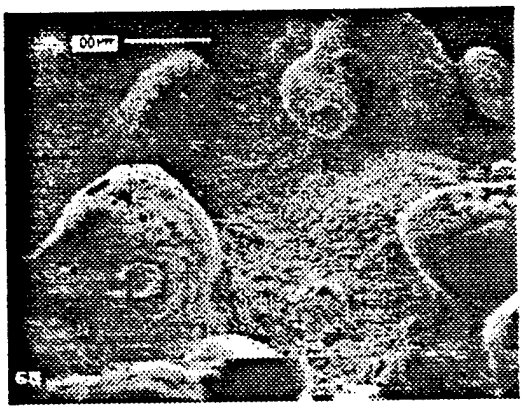

(b)

Fig. 4. Quenched surfaces of a bimodal AP mesa-burning propellant (HTPB/DDI/DOA binder) at a) 200 psi and b) 1800 psi.

tested at 10 pressures (31,250 burning rate tests). The collected studies to date fall far short of that and do not reflect coordinated sets of variables. Because of this, generalizations about results and responsible mechanisms are of uncertain relevance outside the specific formulation domains tested. This reservation applies to the interpretations in Ref. 1 and all others.

In the present studies, the combustion characteristics of matrixes were studied with PBAN/ECA, HTPB/IPDI, and HTPB/DDI binders; with 4 particle sizes of fine AP; with AP/binder ratios from 50/50 to 73/27 (with nominal values of coarse AP/fine AP of 2/1 mass ratio for 88% AP formulations). The effect of DOA (10 to 20 % of binder) was tested as well as four transition metal oxides in different concentrations. Test methods included determination of strand burning rate, and flame behavior from combustion photography; burn-no burn tests; rapid depressurization quench tests

for microscopic study of burning surfaces; and hot stage microscope (HSM) and other thermal analysis tests (special HSM tests on a wider range of binders). Full testing of even this modest range of variables and tests (call it 3 binders, 6 additives, 4 fine AP particle sizes, 3 coarse AP particle sizes, 5 ratios of AP/binder, and 5 kinds of tests, at a few pressures (say 5 average) calls for 6750 tests. Actual tests were chosen on the basis of practical choices, past findings and involving ideas regarding what processes were controlling pressure dependence of the burning rate. This paper is organized according to issues of burning rate-controlling mechanisms, and the collected experimental results are assembled here in ways to test these issues.

Role of the Coarse AP

Consideration of Figure 4 leads to the impression that the coarse AP particles are burning more or less like self deflagration. There is no evidence of the intrusion of binder melt along the peripheries, and the particles lag behind the matrix when the propellant rate is high compared to the AP self deflagration rate (Fig. 4b where the propellant rate was four times the AP self-deflagration rate). However, there is decisive evidence for a role of the coarse particles in coupled burning with the matrix. An example is illustrated in Fig. 4a, where the overall premixed flame supports burning of the matrix and the coarse AP (at a pressure that is lower than the AP self deflagration limit). When protruding coarse AP particles (as in Fig. 4b) are removed from the surface (e.g., Fig. 5), it is evident that the outer periphery is burning down with the faster matrix. One might conclude that this simply illustrates that the matrix flame is enhancing the AP deflagration there. It will be argued later that in fact the vapors from the peripheral AP and the vapors from the fuel-rich matrix lead to a hot near-surface stoichiometric flamelet that locally enhances the rate of both AP and matrix. The existence of such flamelets is generally recognized to be pressure dependent. At lower pressures, the decreased gas phase reaction rates cause the leading edge flames (LEFs) of the diffusion flames to move further out from the surface, leading in the limit to an overall premixed flame as reflected in the flat burning surface at 200 psi (Fig. 4a). Stated more generally, the coarse AP particles are a source of oxidizer vapors for hot gas flames, which cause the propellant burning rate to be higher than either the matrix rate or AP rate alone. Only in one special condition was the coarse AP particle potentially a leading front in the burning surface (Fig. 6) in a situation at 200 psi where the matrix would not burn on its own and the premixed flame-assisted coarse AP burned out ahead of the matrix.

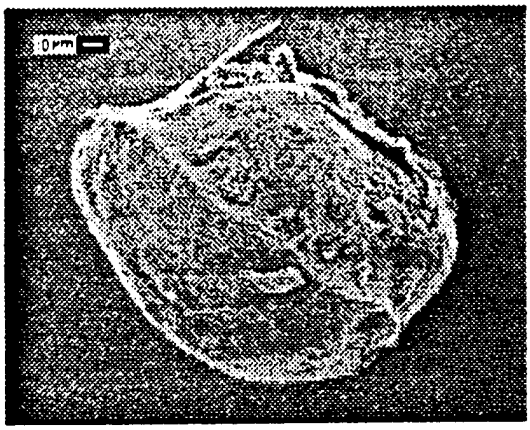

Fig. 5. A partially burned AP particle removed from the quenched surface of a sample corresponding to Fig. 4b (lower left section below the burning surface).

Fig. 6. Quenched surface of a slow burning bimodal plateau propellant under rather rare conditions where the AP rate exceeds the propellant rate. The picture shows a large recess where a 200 μm particle is in the last stages of burnout.

Binders

The role of the binder is to supply fuel for the oxidizer/fuel (O/F) reactions. With the smallest AP particle sizes that are used in the

matrix, there is a potential for a portion of the O/F reactions to occur in the surface. Because the matrixes are very fuel rich, oxidizer vapors from the large AP particles may react with fuel vapors, and with the fuel-rich products of the matrix flame. Thus there are at least three locations in the combustion zone where exothermic O/F reactions are important(surface layer, matrix flame and LEFs), and dependent on the kinetics of binder pyrolysis and O/F reaction kinetics. The role of each class of reaction sites depends on its own pressure dependence.

There also exists the potential for accumulation of binder melt in the surface layer of the matrix, which has been said to interfere with matrix burning. The details of binder "melting" and decomposition have been studied for decades, but remain uncertain because of difficulties of measurement under "combustion-zone-like" conditions (pressure, temperature, and heating rate). The exact mechanism by which binder melt interferes with burning is not yet clear. In this study, thermal response of binders was examined extensively with a hot stage microscope and by inference from the appearance of melt on the surfaces of quenched propellant surfaces. A small number of TGA and DTA tests were also run.

Binder Melt Flow

Most binders degrade to a melt-like condition during heat up in the combustion zone. For those binders that decompose at temperatures comparable to or higher than the AP decomposition, there is a possibility that concentrations of melt will occur and obstruct heat flow to the AP. This is referred to here as a "possibility" because it is difficult to observe directly during burning. However, the concept of pressure-dependent "melt-suppression" of burning has become widely invoked in theories of plateau burning, with the dependence on type of binder being attributed to difference in melt properties of the binders. This subject was discussed in Ref. 1 and 15, and it was noted above that recent studies of quenched surfaces have indicated that melt intrusion on the coarse AP particle surface does not occur (bimodal AP propellants with PBAN and HTPB binders).

Earlier studies (Ref. 15) using hot stage microscope observation of thermal response of ingredients showed that many binders melt and decompose at much lower temperatures than PBAN and HTPB, and also indicated that HTPB cured by DDI melted at a much lower temperature than IPDI-cured HTPB (which melted at a lower temperature than PBAN/ECA binder). All three completed decomposition by the time a temperature of 510 °C was reached. After extensive additional testing, it is now concluded that:

a) "Melting" proceeds in stages that involve progressive decomposition

b) There are quantitative effects of: 1) the use of plasticizer DOA; 2) differences depending on curing procedure (6 day cure compared to 1 day cure with catalyst); and 3) differences due to sample heating rate (1°C/sec vs. 5 °C/sec)

c) In the hot stage, the sample is heated on the underside and often seems to melt there before the whole sample melts down (even with 200 μm thick samples). Quite often the first visible evidence of a melt is when bubbling starts there. By the time the sample becomes a puddle, active vaporization is in progress.

d) All three of the binders noted above exhibited the same behavior, with minimal difference as to temperature. Notable melting and bubbling started at about 450°C ended with sample disappearance by about 510°C. The final stage was a spreading, clear non-bubbling film that disappeared. An exception was when DOA was added; in that case the samples showed a gloss and slump followed by partial puddling and bubbling, in the temperature range 300 – 380°C, followed by a dormant period until the usual 450 – 510°C behavior.

A separate test on decomposition behavior was made by TGA tests in 1 atm. nitrogen (Fig. 7). The results are only slightly different for the three binders, with weight loss for PBAN/ECA starting earlier and proceeding more gradually. Consistent with the HSM test results, decomposition rate peaked at around 450-460 °C and was complete for all three binders by 500-510 °C. When 20% DOA was included, an early decomposition started at about 210-240 °C and a 20% weight loss was reached by 360 °C.

In retrospect it seems clear that the ideas of comparing binders by a melt and decomposition temperature is naïve except for comparison of widely different binders. It also

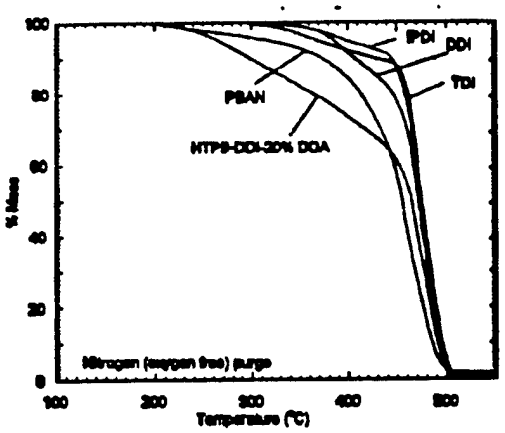

Fig. 7. Results of thermogravimetric analysis (TGA at a heating rate of 20°C/min). IPDI, DDI, and TDI refer to the curing agent used.

seems reasonable in the context of the thermal wave in a burning surface to view the binder surface layer as consisting of staged behavior. As the material heats up, the composition of the layer progresses to more degraded (but more thermally stable) intermediate products nearer the surface, and with bubbling activity starting beneath the surface from more volatile species, possibly creating a surface foam. Even before considering how such a binder degradation layer might contribute to plateau burning, one might reasonably ask how it depends on pressure. The dimensions of the thermal wave are burning-rate dependent, meaning that the "melt layer' thickness is greater at low burning rate, constant on "plateaus, and increasing in the negative slope region of mesas, with the surface temperature having the opposite trends (low at low rates, increasing where the rate is increasing, and decreasing in the negative slope regions). However, there is a second monotonic effect of pressure due to pressure dependence of desorption rates, which is lower at higher pressure. About all that can be said, even quantitatively, about melt layer thickness is that it is comparable to the finest AP diameters (e.g., 2μm) and probably thicker when the burning rate is low.

Some direct information about binder melts can be obtained from microscopic examination of the surfaces of samples quenched from burnng at high pressure (using the rapid depressurization method of quenching). Some 200 such tests were run on propellants with plateau burning characteristics. Sample surface features of the matrix areas are shown in Fig. 8. The sample in Fig. 8a is for a propellant with 2

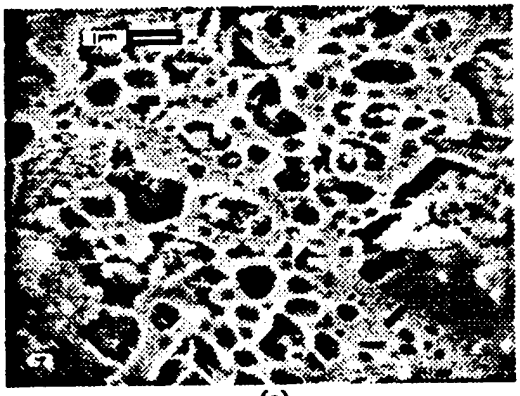

(a)

(b)

Fig. 8. Matrix features of the quenched surfaces of two bimodal propellants that differed primarily in size of the fine AP particles (note differences in scale). HTPB/DDI/DOA binder, 200 μm AP, and a) 2μm matrix AP, b) 10 μm matrix AP.

μm matrix AP particles, while Fig. 8b is for 10 μm matrix AP particles. A binder melt film covers 50-70 % of the surface. Openings occur over AP particles which appear to be decomposing and clearing away binder melt overlays or intrusions. In the case of four plateau propellants with 2 μm AP, the ratio of open area to melt film area were quantitatively alike over the whole pressure range, and insensitive to HTPB curing agent or % fine AP in the matrix. This seems like a negative result as far as a role for melt as a factor in plateau and mesa burning, since these propellants had strong and different plateau characteristics. However, the results may signify that the melt effects occur in a manner not yet revealed. Specifically, the melt may tend to be drawn by surface tension into the holes left

by AP burn-out. This would be dependent on AP particle size and melt viscosity. The effect of such melt behavior, or its pressure dependence, are at present matters of speculation.

One further observation concerning quenched surfaces comes from samples that are quenched spontaneously. It is observed that the matrix surfaces are completely covered with binder melt. This suggests what was referred to in Ref. 1 as surface layer disproportionation (SLD) failure, i.e., the collective response of ingredients fails to establish a surface condition where the ratio of oxidizer and vapor outflow matches that in the propellant. In these examples the binder melt accumulates until it drowns the AP.

In summary, it is concluded that:

a) Binder melting should be viewed as a multiple step process in the surface layer in which the more stable initial intermediate decomposition products will concentrate on the surface, and the more volatile intermediates will vent from below (details depending on thermal wave thickness, viscosity and surface tension).

b) The difference in melt-like behavior between PBAN/ECA, HTPB/IPDI, and HTPB/DDI are not conspicuous, although addition of DOA produces a temporary "softening" and bubbling at around 220-360°C . All three binders transitioned to bubbling puddles at around 450°C and ended decomposition at around 500°C (HSM tests).

c) Binder melt does not encroach on the coarse AP particle burning surfaces; matrix surfaces were around 60% covered by binder (quench tests), the degree of coverage being qualitatively the same with all three binders at all pressures. This suggests that the well established binder dependence of plateau burning, if melt flow dependent, is due to melt fill into depressions left by burnout of fine AP particles, a subject that is difficult to observe but needs study.

Matrix Burning

In this investigation, tests were run on independent burning of matrix samples (Ref. 2, 3, 13). It was found that the typical matrixes with 70% fine AP and 30% binder would not burn in the intermediate pressure range around 800 – 1200 psi. The dependence of this no-burn domain is shown in Fig. 9 for three binders, with

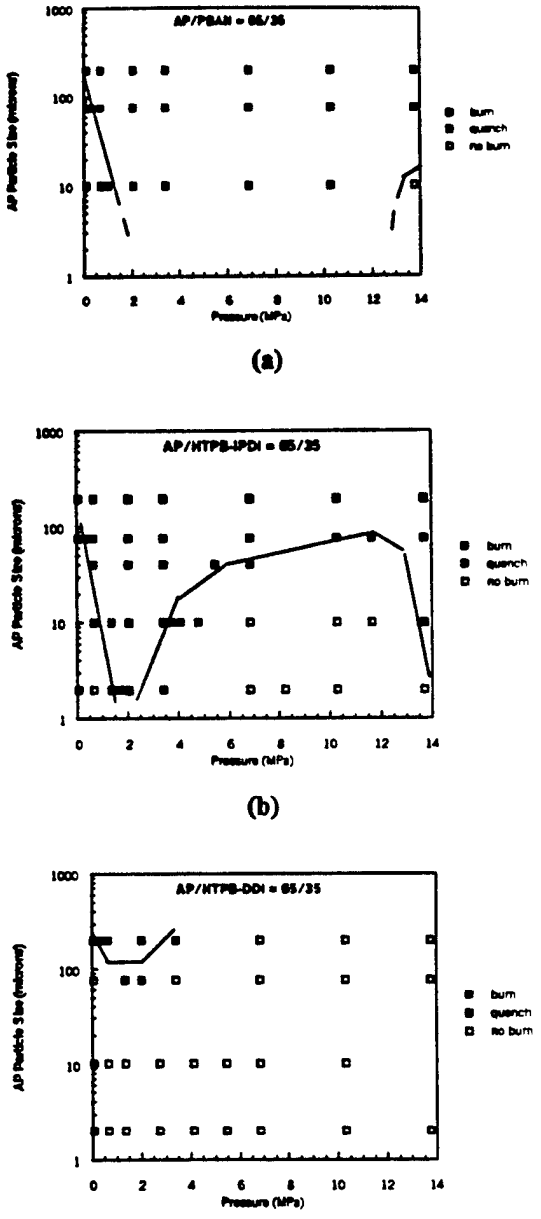

Fig. 9. No-burn domains for matrixes of 65% AP/35% binder for three binders showing sensitivity to types of binder. a) PBAN/ECA, b) HTPB/IPDI, c) HTPB/DDI. Burning will not sustain in areas below the indicated boundaries. PBAN matrix burned under nearly all conditions tested. HTPB/IPDI matrixes failed to burn under most conditions. See Ref. 16 for details.

large effects of AP particle size and type of binder. The no-burn domain was larger for lower AP/binder ratios (Fig. 10). Burning rates were

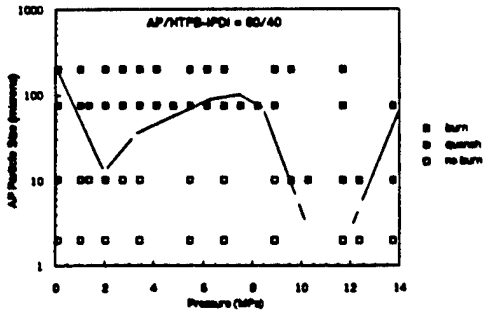

(a)

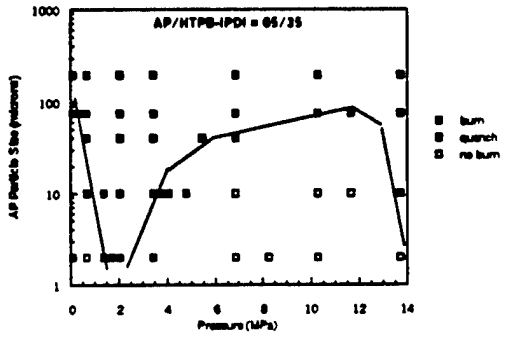

(b)

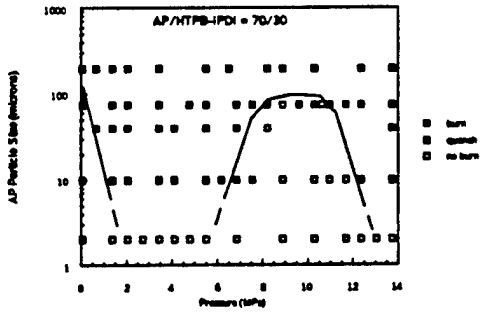

(c)

Fig. 10. No burn domains for matrixes with HTPB/IPDI binder and different ratios of AP and binder: a) 64/40, b) 65/35, c)70/30. See Ref. 3 for details.

depressed and burning was locally intermittent near the no-burn boundaries. These results have suggested melt interference with matrix burning, with fine AP particles being more susceptible than larger ones, and with degree of binder melt interference increasing in going from PBAN/ECA to HTPB/IPDI to HTPB/DDI. While this interpretation seems plausible, it is not quite clear how melt interferes (see above), and the binder thermal response tests (HSM and TGA) and quench tests described above did not offer decisive support for a binder melt-flow mechanism. In this regard it should be noted that binder concentration on the surface is due to the preferential decomposition of AP (surface layer disproportionation, SLD), and it is not clear that burning must stop when the AP becomes melt-covered. As indicated in Fig. 4, the AP decomposes below the melt surface. However, it should be noted that that the matrix surface shown in that figure was from a burning bimodal propellant; the same matrix burning alone might not burn (see 2μm AP matrixes in Fig. 9). It may be more appropriate to look upon failure of a matrix to support burning as a failure to achieve SLD, with due consideration of not only preferential concentration of one ingredient but also how the decomposition of the other ingredient is affected, what is happening to the heat sources, and finally, why the process does not converge on a steady efflux of oxidizer and binder species in the proportions present in the matrix. In some cases (e.g., low AP/binder ratio) it may seem to be simply a classical fuel-rich flammability limit, but if this pertained for the mixes in Fig. 17 and 18, one would have to explain why there is a particle size dependence.

It is appropriate to extend the above SLD arguments to the regions just outside the no-burn domain, where burning is seen to be locally intermittent. It seems likely that SLD failure occurs locally, but heat from adjoining non-quenched sites reconstitutes the quenched site, allowing burning to be handed over among sites with reduced net burning rate. In a bimodal propellant, the conditions for such behavior would depend on the pressure-dependent support provided by the near-surface part of the matrix-coarse AP flame.

Flame Coupling

One of the earliest findings about burning of bimodal propellants (reported by Miller, et. al. Ref. 17) was the singular dependence of the r vs p function on the mass ratio of the coarse AP to the fine AP (Fig. 11). This effect appears to be related to the ability of the matrix to dominate rate at low (35%) coarse AP content, and affect the rate in a near plateau-like way at 45% coarse AP; suggesting that the role of the matrix has become less, and

"strangely" pressure dependent. The overall results suggest that spacing of the coarse AP particles is important to this effect. However, interpretation is complicated by the fact that the AP/binder ratio

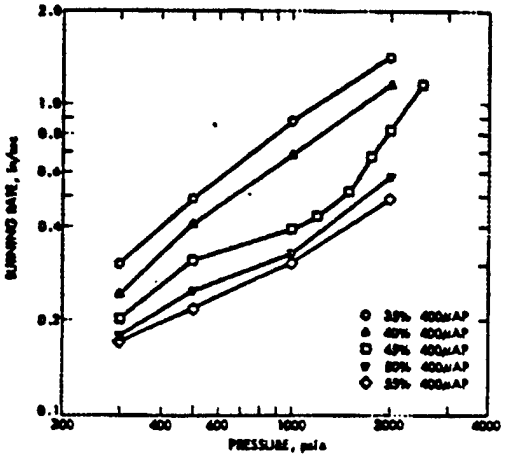

Fig. 11. Dependence of burning rate vs pressure for a bimodal propellant on fine AP to coarse AP. HTPB/IPDI binder 400 μm coarse AP, μm fine AP, approx. 88% AP. See Ref. 17 for details.

in the matrix decreases with increasing coarse AP. The overall trend of results involves what are now known to be two variables that are each important to plateau burning. They cannot be varied independently in propellant mixes[1], so it is not possible to distinguish between effects of coarse AP proximity and matrix AP/binder ratio. However, considerable insight on this subject has been gained from studies of edge burning of sandwiches of matrix lamina between AP laminae. In such tests the spacing between AP lamina and the AP/binder ratios in the matrix can be varied independently. The pertinent results of an intensive study are summarized in Reference 1. For the present topic one can summarize by the following (for matrix lamina consisting of 10 μm AP and PBAN binder in ratio 7/3):

1. Sandwich rates are always higher than either the AP rate or the matrix rate, and dependent on matrix thickness and AP/binder ratio of the matrix.
2. A maximum rate at each pressure ocurs for a lamina thickness of about 250 μm, comparable to the average width of matrix pockets in plateau burning bimodal propellants.
3. Sandwiches exhibit plateau burning under these particular conditions.
4. From interpretation of sandwich burning results, it has been concluded that the matrix flame and the leading edge of the coarse AP-matrix flame are strongly coupled under these conditions (near maxima, Fig. 12).

In short, plateau burning involves not only the pressure dependence of the matrix burning and the coarse AP-matrix diffusion flame, but also the pressure dependence of their interaction under suitable ingredient spacing conditions in the matix.

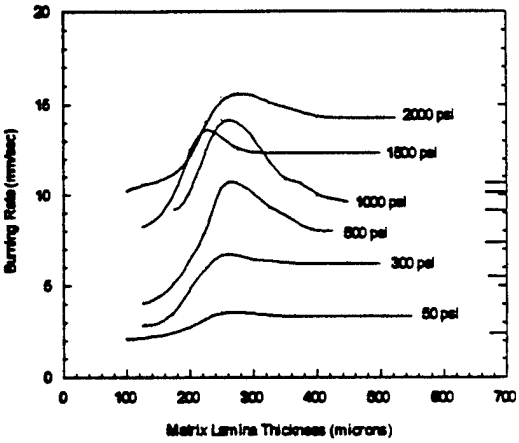

Fig. 12. Burning rates of edge-burned sandwiches of matrix between two AP lamina. The matrix was 70% 10 μm AP, 30% PBAN/ECA. The abcissa is lamina thickness. The AP rates are marked on the left ordinate scale, and the matrix rates.

Catalysts

It is generally observed that addition of burning rate catalysts to AP composite propellants eliminates plateau burning. This seems to be consistent with the idea that plateau behavior is due to marginal burning of the matrix. This is illustrated by Fig. 13 for a matrix that burns on its own only at very low pressure. Addition of 0.05% Fe_2O_3 (0.5 – 1.0 μm) doubled the burning rate and extended the high pressure deflagration limit (HPDL) to over 500 psi. Use of 0.2% Fe_2O_3 increased the burning rate further and gave burning over the whole pressure range tested. In this same formulation, a comparison is made (Fig. 14) between effectiveness of Fe_2O_3

[1] Assuming a target overall AP/binder ratio is specified

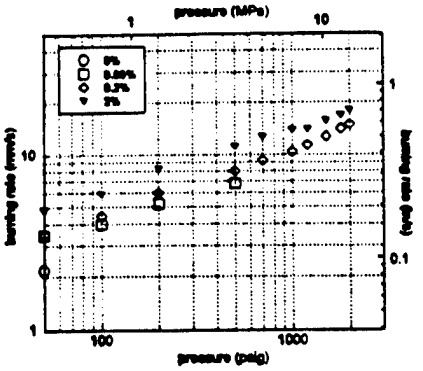

Fig. 13. Effect of Fe_2O_3 catalyst on the burning rate of a 73% 10μm AP/23% HTPB/DDI matrix (the uncatalysed matrix burned only in the 50 psi test). See Ref. 3 for details.

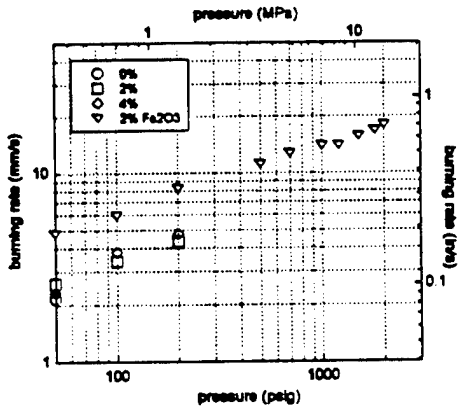

Fig. 14. Effect of TiO_2 catalyst (same matrix as Fig. 13). One curve for 2% Fe_2O_3 is included for comparison. See Ref. 3 for details.

and TiO_2. The trend is the same as with Fe_2O_3, but the TiO_2 was much less effective. In Fig. 15, a comparison is made of several transition metal oxides (TMOs) in a matrix that burns over the whole tested pressure range without catalyst. In these tests the matrix AP size was 10 μm and the catalysts were 0.5 – 1.0 μm particle size. In this last series all the TMOs behaved like catalysts, but with Fe_2O_3 being the most effective and TiO_2 being the least effective. This trend was born out in DTA tests (Fig. 16) in which samples of matrixes were heated at 10 °C/min up to ignition. The rate of differential temperature rise was highest and time to ignition shortest with 2% matrixes were heated at 10 °C/min up to ignition.

The rate of differential temperature rise was highest and time to ignition shortest with 2%

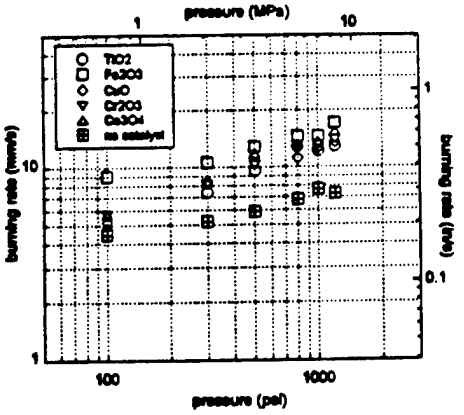

Fig. 15. Effect of several transition metal oxides on the burning rate of a 70% 10 μm AP/30% PBAN-ECA matrix (4% catalyst, nominally 1μm particle size) See Ref. 3 for details.

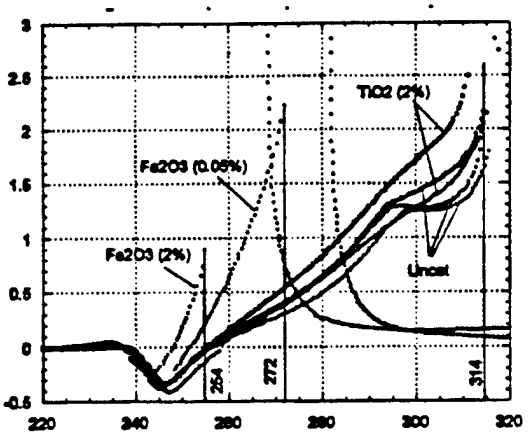

Fig. 16. Comparison of matrix endotherms and ignition in DTA test for different catalysts. Matrixes were 73% 10 μm AP/ 27% HTPB-DDI-DOA binder (catalyst added).

Fe_2O_3 catalyst, with strong effect still at 0.05% Fe_2O_3, and only mild effect for 2% TiO_2 (compared to 0% catalyst). This suggests that very low concentrations of Fe_2O_3 would have the same effect as 2% TiO_2 in matrix burning. High concentrations of Fe_2O_3 generally eliminate plateau effects, but it will be shown that very low concentrations do not.

There has been some debate about whether TiO_2 is really a catalyst at all, and if so what reactions are catalyzed. This was examined

by running isothermal TGAs at 300 °C on binders, AP and propellant samples, with and without TiO_2. In these tests (Fig. 17), no

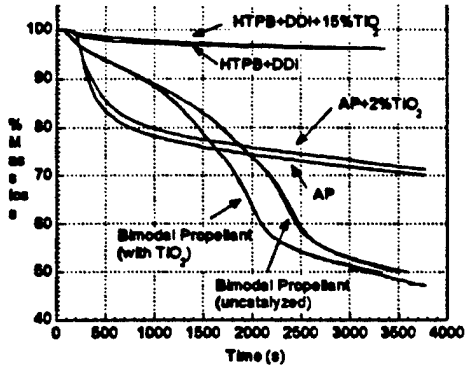

Fig. 17. Comparison of the effect of TiO_2 additive (0.5 μm) in binder, oxidizer and propellant. Sample %mass loss vs time for isothermal decomposition at 300°C. The propellant samples used bimodal AP 62/38 coarse to fine, 200 μm and 2 μm AP; 12% HTPB/DDI/DOA(.69/.17/.14).

catalysis of decomposition was indicated for HTPB-DDI binder or AP alone, but TiO_2 markedly enhanced the decomposition rate of the propellant. This result suggests that TiO_2 catalyzes reaction between the oxidizer and binder. The DTA results indicate exothermic reactions, presumeably between oxidizer vapors and the binder (surface or vapors). TMOs are known to catalyze the decomposition of $HClO_4$ (exothermic)), and the decomposition products are powerful oxidizers that can react exothermally with the binder, thereby increasing the rate of mass loss of the catalyzed propellant as indicated in Fig. 17.

In the past it has been observed (e.g., Ref. 18,19,20) that TMOs concentrate on the burning surface, and Fe_2O_3 concentrations were observed (Ref. 20) even when the iron was introduced in the propellant as liquid ferrocene or via butacene (a binder prepolymer containing Fe atoms). It was concluded that concentration of the catalyst at the burning surface was essential for effective burning rate enhancement. SEMs at higher magnification often show extensive concentration of TiO_2 on the burning surface, both as clusters on the matrix surface, and structures in the center of the coarse AP surfaces. If concentration is indeed important for the catalysis process, then the dependence of degree of concentration on pressure may be important to plateau burning. To date this issue has not been studied. In this regard, in the case of Fig. 4, the TiO_2 structures on the coarse AP apparently do not modify the particle burning, since the quenched surfaces of a matching formulation with no TiO_2 show the same coarse AP surface configurations. This suggests that one should look to pressure dependence of catalyst concentration in the matrix areas.

If plateau burning of bimodal propellants is related to the marginality of the matrix burning, the present results indicate that the matrix marginality is diminished by catalyts, possibly explaining the general perception that catalysts eliminate plateau burning in the propellant. However, the results indicate that the matrix burning can be "tailored" by using very low concentrations of catalyst, the amount being dependent on the particular catalyst. However, an unresolved dilemma posed by the fact that conditions for such matrix behavior as no-burn domains have not yet been correlated with particular features of the bimodal propellant plateaus. This is illustrated in Fig. 18, which compares burning data for two matrixes (one uncatalyzed and one with 2% TiO_2) and for the corresponding bimodal propellants. The catalyst establishes relatively normal burning of the matrix except for high pressure dependence of rate starting at 1000 psi, a property manifested also by the uncatalyzed and catalyzed propellant. The catalyzed propellant had a much enhanced rate at all pressures, with a plateau in the 600 – 1000 psi interval, not exhibited by the catalyzed matrix (but with a no-burn domain of the uncatalyzed matrix). Figure 19 shows the effect of TiO_2 in a bimodal AP propellant with HTPB/DDI/DOA binder with two different concentrations of 0.5 μm TiO_2 (2% and 4%). The rates are independent of % TiO_2, but the mix with 2% TiO_2 would not sustain burning above 700 psi, while the mix with 4% TiO_2 exhibited a sharp increase in $\partial r/\partial p$ at the same pressure. Tests on the matrix burning alone yielded rates similar (but slightly lower) to the bimodal propellant, but would not sustain burning above 215 psi (where a change in $\partial r/\partial p$ occurs with the propellant).

Similar formulations to those in Fig. 19 were made with Fe_2O_3 catalyst. And the rates of the 0.2% and 0.1% mixes are shown in Fig. 20, along with the result for 4% TiO_2. The most noteable feature of this comparison is that 0.1% Fe_2O_3 gives a higher rate than 4% TiO_2, but the samples would not sustain burning above 1200 psi.

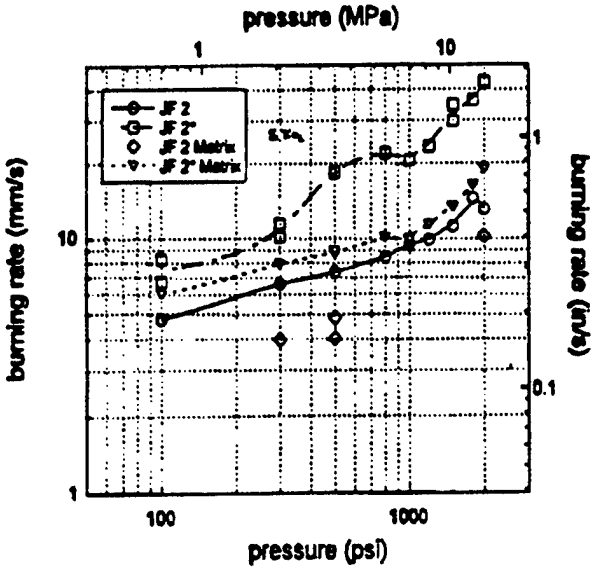

Fig. 18. Comparison of the effect of 2% of 0.02 μm TiO_2 on the burning of a matrix and of an 87.5% solids bimodal propellant having the same matrix formulation. Propellant was the same matrix with enough 200 μm AP added to give a coarse-to-fine ratio of 2/1. The data symbols designate: ◊, uncatalyzed matrix; ∇, catalyzed matrix; O, uncatalyzed propellant; □, catalyzed propellant.

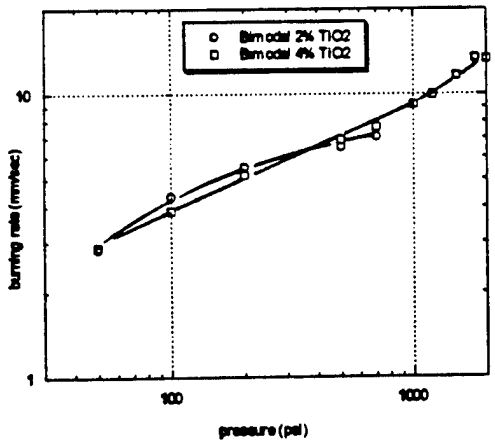

Fig. 19. Effect of catalyst concentration on burning of a bimodal propellant with HTPB-DDI-DOA.

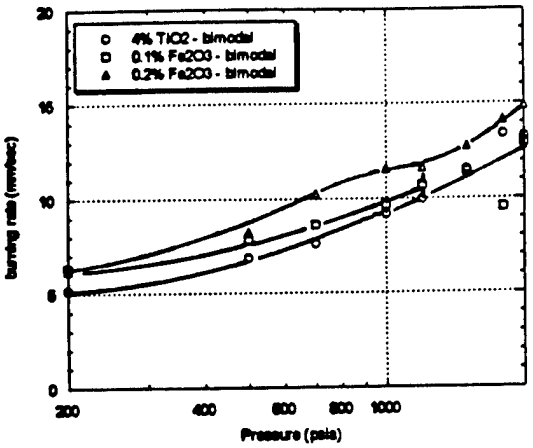

Fig. 20. Comparison of the catalysis of Fe2O3 and TiO2. The basic formulations are the same as in Fig. 19.

In an effort to find out what the catalysts are doing, a comparison was made of the matrix rate, propellant rate and a matrix consisting of the coarse AP, binder and catalyst. Figure 21 shows the results for 0.2% Fe_2O_3 and for 4% TiO_2 (these percentages refer to concentrations in the matrix). The most notable features of the results are: a) the propellant and fine AP matrix rates are almost the same with Fe_2O_3; b) the coarse AP binder matrix burned erratically above 700 psi; c) the coarse AP/binder matrix with 4% TiO_2 burned on the whole pressure range tested; d) where it sustained burning, the coarse AP matrix with Fe_2O_3 burned at a considerably higher rate than the matrix with TiO_2.

While the results to date with catalysts seem to be "telling us something", the research was suspended prematurely (the apparent fate of all other studies that involve too many variables and operative mechanisms.). However some valuable insights have emerged. Even this superficial coverage shows that all catalysts are not alike, and that enhancement of rate and elimination of erratic burning don't follow the same rules. Further, the "rule" that bimodal propellants burn faster than their matrixes alone is broken with Fe2O3 catalyst (at least 0.2%

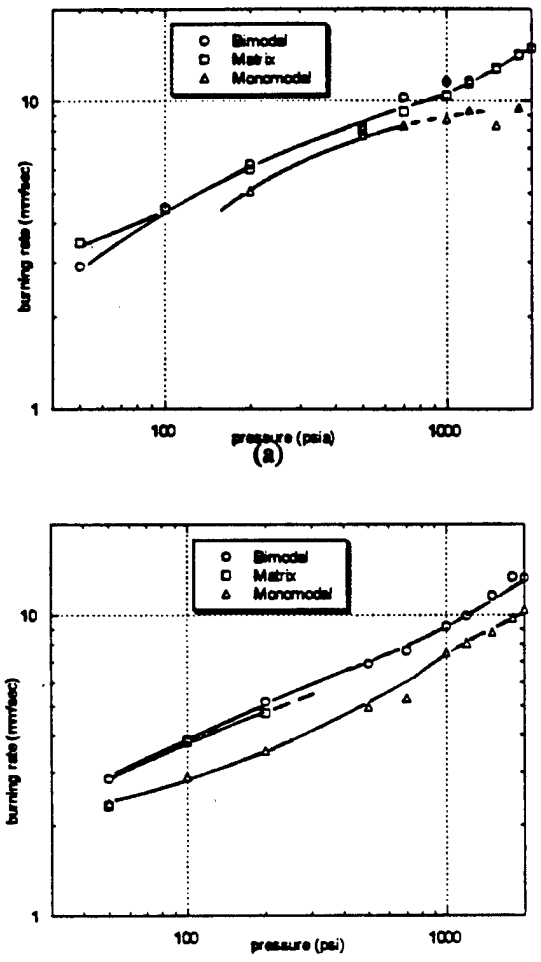

Fig. 21. Comparison of a bimodal propellant rate, matrix rate, and rate of a matrix consisting of the coarse AP and binder in the same ratio as the fine AP matrix, each with 0.2% Fe2O3 in (a) and 4% TiO2 in (b). Basic formulations the same as in Fig. 19. Broken lines designate irregular burning.

catalyst). Unfortunately, these findings may depend on the particular set of formulation variables chosen. However, some generalizations about catalysts from this and previous studies merit review in the furure, especially with regard to pressure dependence.

Catalysts act in several ways:

a) at low pressure they can indirectly catalyze the premixed flame by breaking down heavy fuel molecules into more reactive vapors, causing the flame to stand closer to the surface (Ref. 18,19);

b) if the matrix AP particles are small enough (high surface area and short diffusion distances), the catalyst can cause $HClO_4$ decomposition and reaction within the porous surface layer (all pressures, depending on degree of catalyst concentration on the surface, but particularly at low pressure because of more time for such reactions);

c) at higher pressures where the leading edge of the AP/matrix diffusion flames become important, the catalytic breakdown of fuel molecules acts locally around the oxidizer perimeter by allowing the leading edge flame to stabilize closer to the surface;

d) effectiveness of a catalyst depends on its "ability" to concentrate on the burning surface; and

e) to the extent that "melt suppression" of burning rate is a factor in plateau burning, too much catalysis may defeat it.

Summary

This paper consists of only a part of a larger study, some of which is reported also in Ref. 1-4, 15, and 16.The goal here was to highlight some findings and mechanistic interpretations that seem to be essential to understanding how bimodal AP propellants burn. To understand "plateau" burning, it would be necessary to establish the role of each mechanism, how it changes with presure, and how the interactions between them change with pressure. The present findings do not constitute a theory of plateau burning, but do provide valuable insights for further research. Particularly for the binders used here, some of those insights involved are listed below.

Surface Layer

The surface layer of the matrix areas is the site of binder melt effects on burning and the melt effects appear to act by (binder-dependent) filling of depressions left by burn-out of fine AP particles. These fine AP particles decompose under the melt film (particle size dependent). There appear to be reactions in this heterogeneous layer tht involve heat release (especially with very fine AP), and such reactions are strongly enhanced by presence of catalysts. The catalytic effects in this layer depend on catalyst particle size, and almost surely on concentration of catalyst in the layer. The exothermic reactions in the layer necessarily involve decomposition of $HClO_4$ and reactions

of the vapor products with binder melt and/or binder vapors in a porous surface layer.

Matrix burning

Fine AP/binder matrixes require heat supply from their own fuel rich gas phase flame, which appears to be a premixed one for small AP particles (under 20 μm). In the oxidizer/binder ratios typical of plateau propellants, their burning is marginal without catalysts. Fe_2O_3 is much more effective than TiO_2. Burning alone, matrixes almost always burn slower than the bimodal propellant at all pressures. The improved burning with catalyst is probably due to both increased surface layer heat release and to catalytic break down of the large fuel vapor molecules (which are more reactive in the gas matrix flame, causing the flame to stand closer to the surface).

Coarse AP Particles

Deflagration rate of these particles is always lower than the propellant rate (except at low pressure where the whole flame is premixed), and contributes little to overall rate, except in close proximity to the matrix. There, along the outer periphery, a hot stoichiometric diffusion flame occurs with its leading edge close to the coarse AP/matrix contact lines. This LEF apparently supports the marginal matrix burning, accounting for the higher propellant rate. Earlier sandwich burning studies indicate that the burning rate is a maximum for matrix area dimensions typical of plateau propellants, and sandwiches exhibit plateau burning under these conditions. These observations relate to the critical aspects of mass fraction and particle size of the coarse AP in the propellant, which control the lateral dimensions of the matrix areas. As noted sandwich burning tests, the hot LEF also respond to catalytic fuel "cracking".

Surface Layer Disproportionation

This concept has to do with adjustments in the surface layer that are mecessary in order for the average flux of species from the surface to match the composition of the propellant. If the combined physical and chemical processes do not lead to successful disproportionation, steady burning cannot occur. Several significant examples of SLD were evident and or suggested in the present study. The most obvious was the protrusion of coarse AP particles illustrated in Fig. 4b. Another is the concentration of nonvolatile catalysts on the surface. Another is the tendency for binder melt to occupy a disproprtionate portion of the matrix. One more has to do with the fact that binders break down into liquid intermediates with different thermal stabilities, a situation that would be expected to lead to more stable intermediates at the surface with less stable intermediates decomposing and bubbling up from below (foam?).

Acknowledgements

This work was performed under contracts N00014-95-1-0559 with the Office of Naval Research; Drs. Judah Goldwasser and Richard S. Miller were the technical monitors.

References

1. Price, E. W., Chakravarthy, S. R., and Sigman, R. K., "Pressure Dependence of Burning Rate of Ammonium Perchlorate-Hydrocarbon Binder Solid Propellants," AIAA Paper # 97-3106, 33rd AIAA/ASME/SAE/ASEE Joint Propulsion Conference and Exhibit, July 6-9, 1997.
2. Freeman, J. M., Price, E. W., Chakravarthy, S. R., and Sigman, R. K., "Burning Characteristics of Monomodal Ammonium Perchlorate/Hydrocarbon Binder Propellants," *Proceedings of the 34th JANNAF Combustion Subcommittee Meeting*, CPIA Pub. 662, West Palm Beach, FL, October 27-30, 1997.
3. Freeman, J. M., Price, E. W., Chakravarthy, S. R., and Sigman, R. K., "Contribution of Monomodal AP/HC Propellants to Bimodal Plateau-Burning Propellants, AIAA Paper # 98-3388, 34th AIAA/ASME/SAE/ASEE Joint Propulsion Conference and Exhibit, July 13-15, 1998.
4. Freeman, J. M., Price, E. W., and Sigman, R. K., "Effect of Matrix Variables on Bimodal Propellant Combustion," Proceedings of the *35th JANNAF Combustion Subcommittee Meeting*, Tucson, AZ, Dec. 1998.
5. Bastress, E. K., "Modification of the Burning rates of Ammonium Perchlorate Solid Propellants by Particle Size," Ph. D. Thesis, Princeton University, Princeton, NJ, January 1961.
6. Steinz, J. A., Stang, P. L., and Summerfield, M., "Effects of Oxidizer Particle Size on Composite Solid Propellant Burning: Normal Burning, Plateau Burning, and

Intermediate Pressure Extinction," Aerospace and Mechanical Sciences Rept No. 810, Guggenheim Laboratories for the Aerospace Propulsion Sciences, Princeton University, Princeton, NJ, Oct. 1967.

7. Steinz, J. A., Stang, P. L., and Summerfield, M., "The burning Mechanism of Ammonium Perchlorate-Based Composite Solid Propellants," AIAA Paper # 68-658, 4th Propulsion Joint Specialists Conference, June 10-14, 1968.
8. Steinz, J. A., Stang, P. L., and Summerfield, M., The Burning Mechanism of Ammonium Perchlorate-Based Composite Solid Propellants," Aerospace and Mechanical Sciences Rept No. 830, Guggenheim Laboratories for the Aerospace Propulsion Sciences, Princeton University, Princeton, NJ, Feb., 1969.
9. Price, E. W., "Effect of Multidimensional Flamelets in Composite Propellant Combustion," *Journal of Propulsion and Power*, Vol. 11, No. 4, pp. 717-728.
10. Chakravarthy, S. R. , "The Role of Surface Layer Processes in Solid Propellant Combustion," Ph. D. Thesis, Georgia Institute of Technology, Atlanta, GA 1995
11. Horton, M. D. and Price, E. W., "Deflagration of Pressed Ammonium Perchlorate", *ARS Journal*, Vol. 32, No. 11, Nov. 1962.
12. Boggs, T. L., "Deflagration Rate, Surface Stucture, and Subsurface Profile of Self-Deflagrating Single Crystals of Ammonium Perchlorate," *AIAA Journal*, Vol. 8, No. 4., May 1970, pp. 867-873.
13. Lengelle, G. Duterque, J, Trubert, J. F., "Solid Propellant Combuastion," *AIAA Journal of Propulsion and Power*, (to be published).
14. Freeman, J. M., Price, E. W., Chakravarthy, S. R., and Sigman, R. K., "Contribution of Monomodal AP/HC Propellants to Bimodal Plateau-Burning Propellants, AIAA Paper # 98-3388, 34th AIAA/ASME/SAE/ASEE Joint Propulsion Conference and Exhibit, July 13-15, 1998.
15. Price, E. W., Chakravarthy, S. R., Zachary, E. K., and Sigman, R. K., "Ingredient Response and Interaction during Heating in a Hot Stage Microscope," *Proceedings of the 31st JANNAF Combustion Subcommittee Meeting*, San Jose, CA, Oct. 1994.
16. Chakravarthy, S. R., Price, E. W., and Sigman, R. K., "Binder Melt Flow Effects in the Combustion of AP-HC Propellants," AIAA/ASME/SAE/ASEE Joint Propulsion Conference and Exhibit, June 10-12, 1995.
17. Miller, R. R., "Anomalous Ballistic Behavior of Reduced Smoke Propellants with wide A P Distributions," *Proceedings of the 15th JANNAF Combustion Meeting*, Vol. II, CPIA Pub. 297, Feb. 1979, pp. 265-269.
18. Price, E. W., Sambamurthi, J. K., and Sigman, R. K., "Further Results on the Combustion of AP/Polymer Sandwiches with Additives," *Proceedings of the 22nd JANNAF Combustion Meeting*, CPIA Pub. 432, Vol. 1, 1985.
19. Markou, C. P., "Effect of Different Binders and Additives on Sandwich Burning," Ph. D. Thesis, School of Aerospace Engineering, Georgia Institute of Technology, Atlanta, GA, May 1988.
20. Chakravarthy, S. R., Price, E. W., and Sigman, R. K., "Mechanism of Burning Rate Enhancement of Composite Solid Propellants by Ferric Oxide," *AIAA Journal of Propulsion and Power*, Vo. 13, No. 4, July-Aug. 1997, pp. 471-480.

APPENDIX H

Freeman, J. M., Price, E. W., Chakravarthy, S. R., and Sigman, R. K.

"Burning Characteristics of Monomodal Ammonium Perchlorate/Hydrocarbon Binder Propellants"

Proceedings of the 34th JANNAF Combustion Subcommittee Meeting

CPIA Pub. 662

West Palm Beach, FL, October 27-30, 1997

BURNING CHARACTERISTICS OF MONOMODAL AMMONIUM PERCHLORATE/HYDROCARBON BINDER PROPELLANTS

J. M. Freeman, E. W. Price, S. R. Chakravarthy, and R. K. Sigman
Georgia Institute of Technology,
School of Aerospace Engineering
Atlanta, GA 30332-0150

ABSTRACT

Early research studies of the effect of ammonium perchlorate particle size on propellant burning rate were done with propellants of uniform particle size. It was observed that such (necessarily fuel rich) propellants often exhibited plateau, mesa, or extinguished burning in the mid-pressure range. It was later observed that high solids propellants with bimodal AP size distribution exhibited similar burning behavior. Such propellants typically have substantial areas of the burning surface that have a close similarity to the "anomalous burning" of the monomodal fuel rich propellants. The goal of this paper is to present additional data on "anomalous burning" of monomodal propellants to further the interpretation of the mechanisms responsible for such "anomalous burning." Such information is needed for modeling the burning of bimodal propellants and rational design of high solids plateau burning in propellants. The results include determination of the no-burn conditions (particle size, oxidizer-to-fuel ratio, type of binder, and pressure). For selected conditions, the dependence of burning rate on pressure is shown (selected combinations of AP size, oxidizer-to-fuel ratio and binder that are near the no-burn domain). Combustion photography tests are used to examine intermittent flamelet behavior.

INTRODUCTION

Many early research studies of combustion of ammonium perchlorate (AP) composite propellants sought to determine the effect of AP particle size by testing formulations with fairly uniform particle size (narrow unimodal size distribution). Due to packing limitations, such formulations contained about 75% AP. Results with such fuel rich formulations have not been particularly useful in understanding combustion of high-solids loadings (86-89% AP) which typically have a blend of different particle sizes. However, they exhibited some unique combustion behavior that is potentially important to some modern propellants that exhibit "plateau" burning, i.e. very low or negative sensitivity of burning rate on pressure. Such burning behavior is exhibited by some formulations with blends of very fine AP and relatively coarse AP (bimodal AP size distribution). In such formulations the burning surface consists of areas of fine AP/binder matrix and areas consisting of individual coarse AP particles. The matrix areas approximate the physical characteristics of the unimodal propellants, and the novel characteristics of those unimodal propellants are very likely a factor in plateau burning behavior of bimodal propellants. This possibility motivated the present return to the study of unimodal propellants.

Earlier studies (e. g. Ref 1) had shown that some fuel-rich "matrices" exhibited:

a) plateau burning
b) spontaneous extinction in the same mid-pressure range as the plateaus
c) locally intermittent burning without complete extinction

While this novel behavior was not fully characterized (e.g. as a function of oxidizer particle size, ratio of AP/binder, and type of binder), it became clear that the "anomalous" burning (a-c above) was strongly dependent on those propellant variables. The present study started out by examining the domain of variables in which the matrix would, and would not, sustain burning. Figure 1a illustrates a burn-no-burn map showing the dependence on AP particle size and pressure for polybutadiene acrylonitrile acrylic acid (PBAN) binder and an oxidizer-to-fuel ratio (O/F) of 65/35. It was anticipated that formulations near the burn-no-burn boundary would exhibit plateau- or mesa-burning, and the present paper examines the validity of that postulate and seeks to clarify the microscopic details of the

---

Distribution Statement - Approved for public release, distribution unlimited.
* This work was performed under grant no. N00014-95-1-0559 from the Office of Naval Research, with Dr. Richard S. Miller as the Technical Monitor.

combustion responsible for this behavior. It was soon realized that the plateau behavior of the burning rate (r(p)) was strongly sensitive to all three parameters: AP particle size, binder type, and O/F ratio. A reasonably complete study would call for burning rate measurements at eight to ten pressures on formulation including a minimum of five different particle sizes, four different binders, and four different O/F ratios (ten tests on each of 5x4x4=80 propellants), in addition to other testing to clarify the controlling combustion mechanisms. The present paper describes some results, including strategy to focus the study on the range of formulation variables most critical to occurrence of plateau behavior.

EXPERIMENTAL

TESTING STRATEGY

Due to the scope of this study, a planned strategy was necessary to focus on potentially important variable combinations. Four independent variables (particle size, binder, O/F ratio, and pressure) were identified, resulting in a fifth dependent variable (burning rate). In the initial work done for this study (Ref 2), the conventional use of pressure as the primary variable was chosen. A second variable, AP particle size, was chosen to produce maps of the burn-no-burn domain. These maps only designated the burning domain for one binder at one particular O/F ratio, therefore several maps would be produced by only small variations in the third or fourth variable (binder and O/F ratio, respectively). Initially one such map was made for three binders (PBAN, IPDI-cured HTPB, and DDI-cured HTPB)* each with the same O/F ratio (65/35), as in Fig 1. No burning rate data was taken at that time.

The current study chose to vary a fourth variable (O/F) above and below the initial value for each binder. Since the PBAN matrix burned over almost the entire domain, the O/F ratio was lowered to 60/40. In contrast, the HTPB-DDI matrix, which had a nearly complete no-burn domain, was increased to a 70/30 O/F ratio. The O/F ratio for the HTPB-IPDI matrix was varied both above and below the 65/35 baseline mix to observe the effect on the burn-no-burn domain. It was expected that the no-burn domain would slowly evolve with changing O/F ratio to eventually have a complete burn domain at high oxidizer loading, or a complete no-burn domain at very fuel-rich, low oxidizer loading, as seen in Fig 2.

For fine particle sizes with mid-pressure no burn domains, it was expected that the burning rates would drop when approaching the no-burn boundary, as was seen in earlier studies of monomodal propellants that had extinction points (Ref. 3). Particle sizes that bordered the edge of the no-burn domain were thought to exhibit a degree of plateau burning. It was postulated that the plateaus and extinction ranges would be well suited to three-dimensional figures, such as Fig. 3. One such surface could be generated for each map, showing the evolution of the plateau behavior and hopefully giving some insight and predictability to such behavior.

EXPERIMENTAL TECHNIQUE

Combustion photography (video) was used as the primary technique in this study. The method used was routine and the window bomb design was similar to that used by Boggs (Ref. 4), operable in the atmospheric to 2000 psi pressure range. Burning rates were obtained from video pictures as described in detail elsewhere (Ref. 5). The binders used in this study were HTPB and PBAN, with the former being cured by two different agents. Table 1 presents the composition used in the preparation of each binder.

The AP used in this study fell into five different size distributions: 2 μm, 10 μm, 40 μm, 75 μm, and 200 μm. The "2 μm AP" comes from an AP and prepolymer mixture supplied by Dr. Carol Campbell of the Thiokol Corp. Dr. Karl Kraeutle, formerly from the Naval Air Warfare Center, provided the "10 μm AP". The "40 μm, 75 μm, and 200 μm AP" are designation for sieved particles falling between 37-45 μm, 75-90 μm, and 200-250 μm, respectively. The typical sample size was 3mm x 3mm x 10mm, which were cut from 5 gram batches. These batches were hand-mixed and cured in a vacuum oven (equipped with rotating sample holders to prevent particle settling) for 24 hours at a temperature of 40° C.

---

* PBAN - polybutadiene acrylonitrile acrylic acid
HTPB = hydroxyl-terminated polybutadiene
IPDI = isophorone diisocyanate
DDI = dimeryl diisocyanate

RESULTS AND DISCUSSION

In the initial work for this study, it became clear that the binder type had a significant effect on the burn-no-burn domain. PBAN, the binder with the least degree of melt layer on the surface, showed no significant no-burn domain. HTPB-DDI, with the highest degree of melt, had a no-burn region over nearly the entire pressure range. A mid-pressure no-burn domain was exhibited by HTPB-IPDI, whose melt characteristics fall between the other two binders. These melt effects are evident with finer AP particle sizes where a larger no-burn domain was observed. Binder melt flow is more likely to inhibit the burning of the finer particles which may be burning as premixed flames, as opposed to the larger particles which have distinct diffusion flames over them, along with their own monopropellant flame. It is interesting to note that the video photography reveals a large amount of char that rolls up along the sample edges, presumably similar to that reported by other researchers (Ref. 6). This seems to be dependent on the AP particle size, the matrices with larger particle sizes (75 μm and 200 μm) have considerable amounts of this char/melt accumulation. The finer particle sizes generally have little or no char on the edges. All these formulation are high in binder content compared to typical propellants, but the large particle mixes would have larger spacing between particles, which would be consistent with more melt accumulation.

As the O/F ratio is changed, the burn-no-burn domain does evolve somewhat as expected, as seen in Fig. 4 which presents the HTPB-IPDI case. These domains close in on the mid-pressure no-burn region as well as showing wider ranges of burning regions for fine particles at low pressures. The no-burn domain of the 2 μm particle size matrices is almost universal in this study, but this may be due to the AP being ultra-fine. Sizes in the 5 μm range may not exhibit this behavior and such studies should be undertaken. It was thought that the PBAN mix at a 60/40 O/F ratio may somewhat resemble the HTPB-IPDI mix at 65/35, which had a mid-pressure extinction region and reappearance of burn domain at high pressure for the finer particle sizes. Unfortunately the no-burn region engulfed most of the pressure domain for the finer particle sizes, as seen in Fig. 5. There was a low pressure region where the samples burned anomalously had typically quenched themselves before burning of the sample was complete. This area falls within the region that burning was predicted from the initial test series, presenting the idea that the PBAN matrixes may be more sensitive to changes in O/F ratio. The HTPB-DDI matrixes at an O/F ratio of 70/30 had only a minimal burn domain as they did for the 65/35 ratio.

The burning rates were expected to be the most revealing clue to the nature of plateau burning. However the intermittent and anomalous behavior of these low AP content propellants made measurements difficult. The data exhibited significant scatter, particularly near the no-burn domain, where the samples showed the most obvious effects of anomalous burning. In most cases, regression of the sample surface was erratic, with some areas burning ahead, then stopping as the flame complex goes out or moves to another area, thereby letting other areas of the sample catch up to, and many times pass the area that burned ahead. As of yet, the time and dimensional scales of the intermittent processes had not been determined, but can be said to be of the order of hundreds of microns and tenths of seconds. The burning rates of the HTPB-IPDI formulations are presented in Fig. 6. In general the matrices with more coarse AP had the tendency to show behavior similar to plateaus and mesa burning. The slopes are low as would be expected with such low AP content propellants. Inadequate data was available for the mixes with finer AP sizes, which correspond to the matrix between coarse particles in bimodal propellants, for any assessments to be made about their behavior. Likewise, insufficient data impeded the efforts to obtain 3-D surfaces like that shown in Fig. 3. The results were indicative of the trend presented in Fig. 3, particularly in the plateau behavior of the large particle sizes.

CONCLUSION

As of yet, no models have been developed to explain the mechanisms that lead to plateau burning behavior. In understanding the complex mechanisms in a bimodal propellant, it is necessary to study individual components of the formulation and their effect on the propellant's behavior. The burning characteristics of the surrounding matrix inevitably affect the behavior of the coarse particles in a bimodal propellant. The study of monomodal matrixes may hold the key to understanding the mechanisms that produce plateau and mesa burning characteristics. The present study has attempted to explore these ideas with encouraging results. Though there is inadequate data to yield any theories or models for quantifying plateau burning behavior, the results do indicate a strong dependence on particle size and binder. Continued work with a diverse range of binders and additional particle sizes is hoped to give keen insight into the mechanisms of plateau burning. Microscopy of quenched surfaces of the matrices should also provide helpful, and is planned for future work.

REFERENCES

1. Steinz, J. A., Stang, P. L., and Summerfield, M., "The Burning Mechanism of Ammonium Perchlorate-Based Composite Solid Propellants," Aerospace and Mechanical Sciences Report No. 830, Guggenheim Laboratories for the Aerospace Propulsion Sciences, Department of Aerospace and Mechanical Sciences, Princeton University, Princeton, N. J., February 1969.

2. Chakravarthy, S. R., "The Role of Surface Layer Processes in Solid Propellant Combustion," Ph. D. Thesis, Georgia Institute of Technology, Atlanta, Georgia, 1995.

3. Bastress, E. K., "Modification of the Burning rates of Ammonium Perchlorate Solid Propellants by Particle Size," Ph. D. Thesis, Princeton University, Princeton, New Jersey, January 1961.

4. Boggs, T. L., "Deflagration Rate, Surface Structure, and Subsurface Profile of Self-Deflagrating Single Crystals of Ammonium Perchlorate," *AIAA Journal*, Vol. 8, No. 5, May 1970, pp. 867-873.

5. Chakravarthy, S. R., Price, E. W., and Sigman, R. K., "Mechanism of Burning Rate Enhancement of Composite Solid Propellants by Ferric Oxide," AIAA Paper 95-0601, 33rd Aerospace Sciences Meeting, Reno, NV, January 1995.

6. Cohen, N. S., Fleming, R. W., and Derr, R. L., "Role of Binders in Solid Propellant Combustion," *AIAA Journal*, Vol. 12, No. 2, February 1974, pp. 212-218.

TABLES

Table 1. Binder Compostion by Percent Weight

Binder	Prepolymer		DOA†	Curing Agent		
	PBAN	HTPB		ECA‡	IPDI	DDI
PBAN	64.14	–	15.00	20.86	–	–
HTPB-IPDI	–	75.73	18.39	–	5.88*	–
HTPB-DDI	–	69.07	16.77	–	–	14.16*

*Approximately 0.01% dibutyl tin dilaurate (T-12) added to HTPB binders to accelerate curing
† DOA = dioctyl adipate
‡ ECA = epoxy curing agent

FIGURES

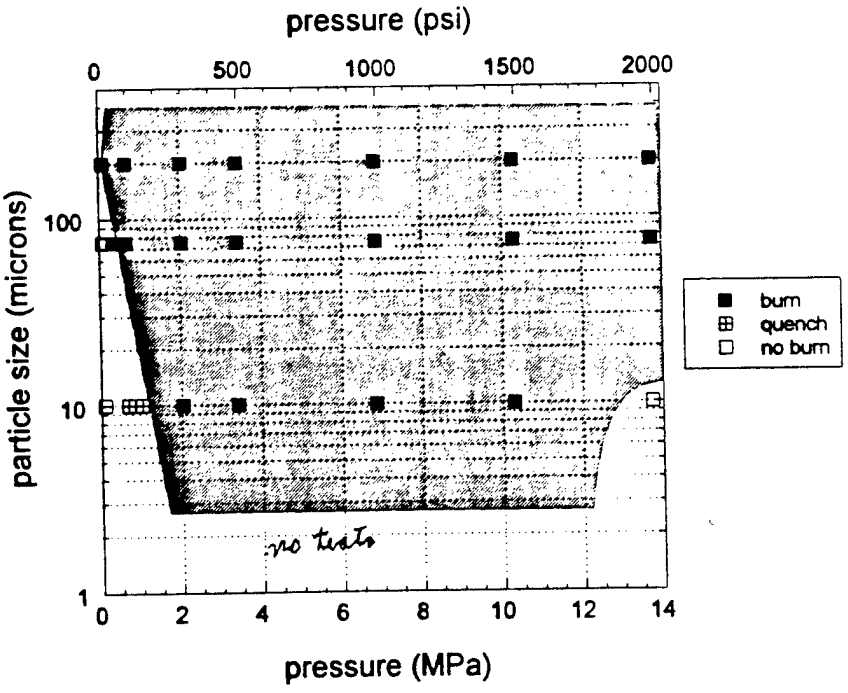

(a)

Figure 1. Burn-no-burn domain for AP/binder=65/35 as a function of particle size across a range of pressure, where the binder is (a) PBAN, (b) HTPB-IPDI, and (c) HTPB-DDI.

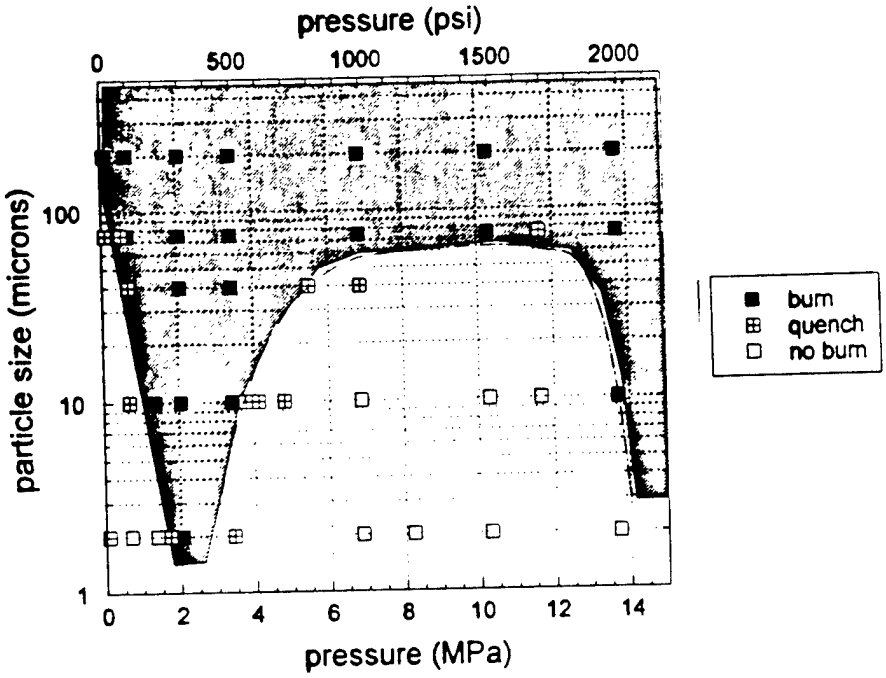

(b)

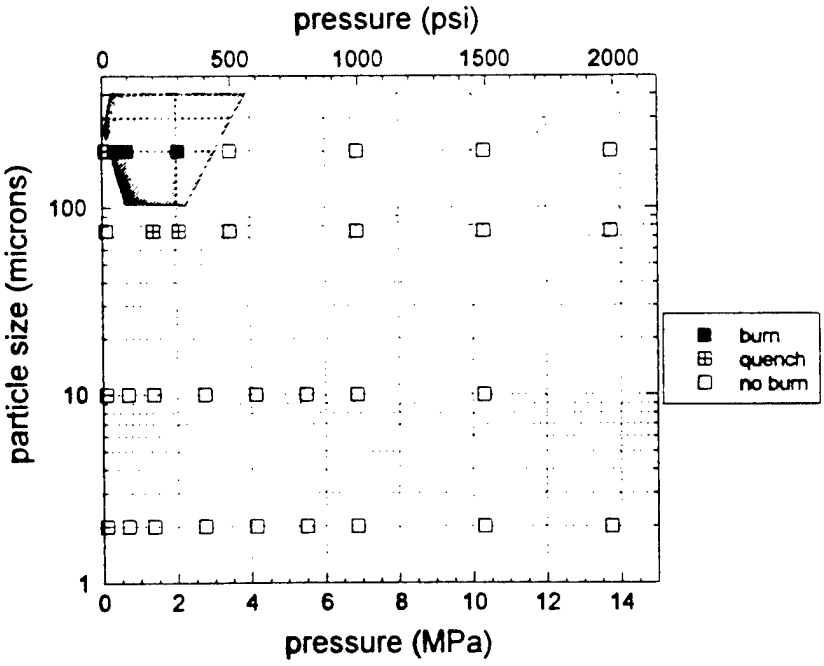

(c)

Figure 1. Burn-no-burn domain for AP/binder=65/35 as a function of particle size across a range of pressure, where the binder is (a) PBAN, (b) HTPB-IPDI, and (c) HTPB-DDI.

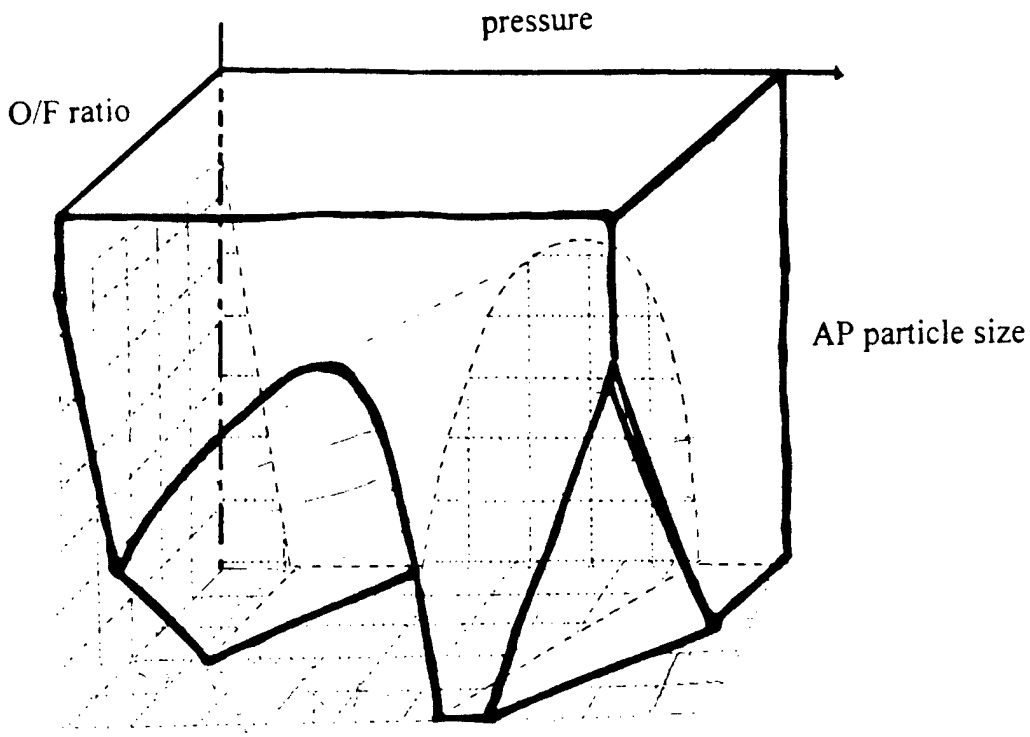

Figure 2. Evolution of burn-no-burn domain as a function of O/F ratio.

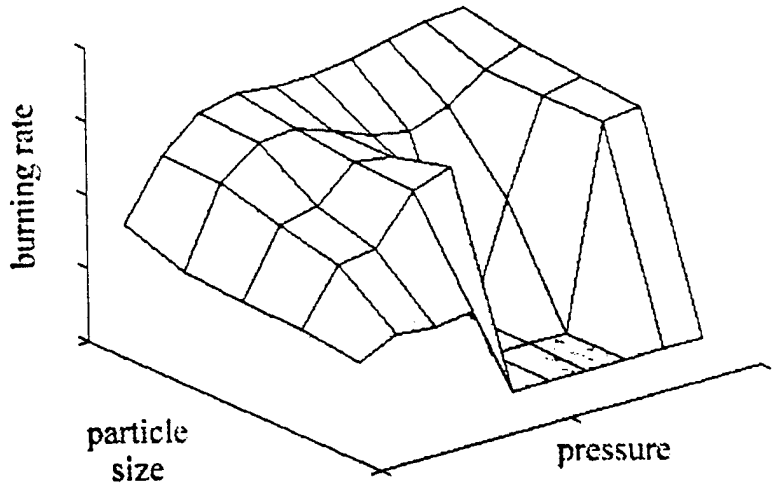

Figure 3. 3-D surface of burning rate as a function of pressure and oxidizer particle size.

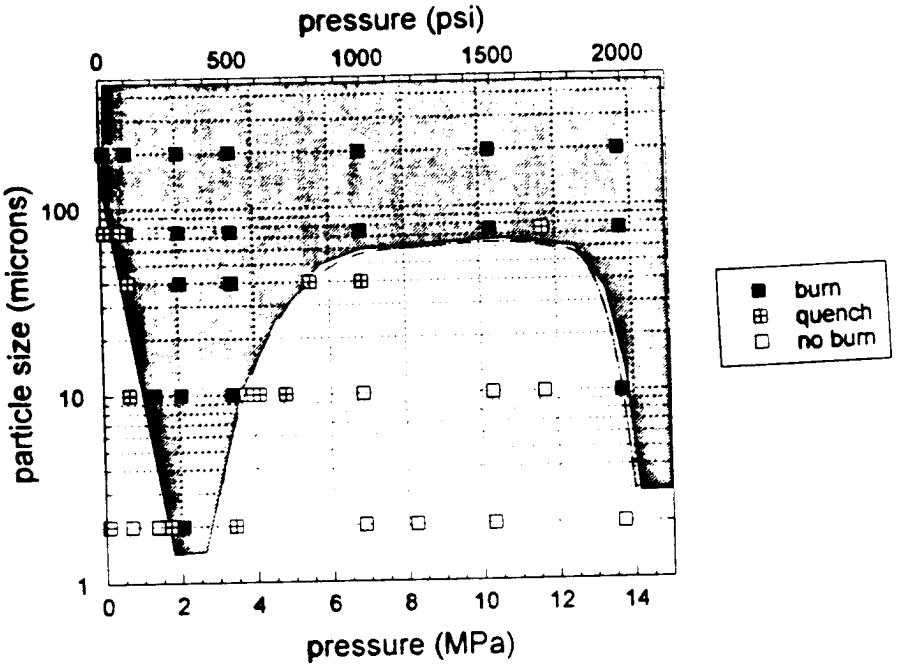

(c)

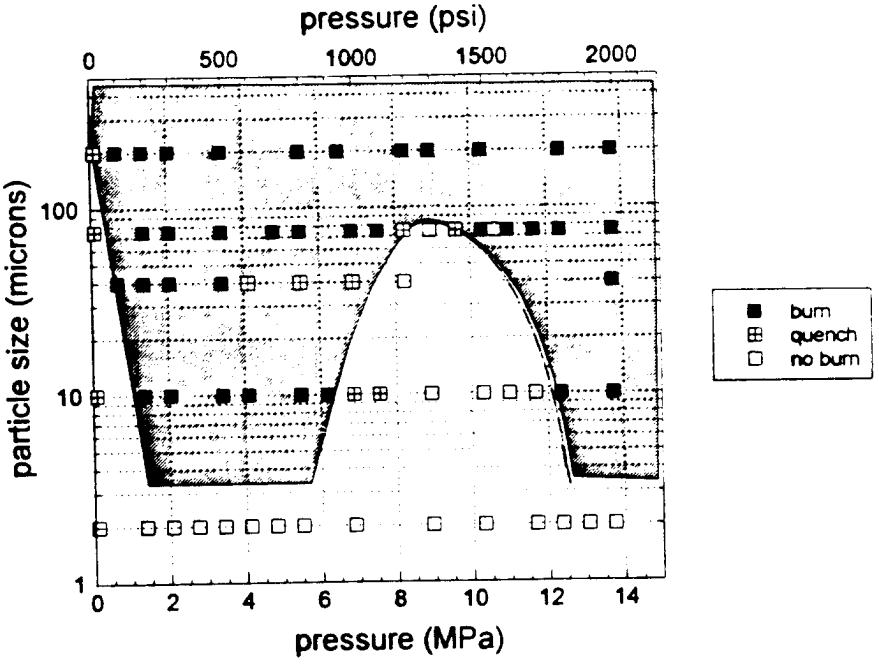

(d)

Figure 4. Burn-no-burn domain as a function of particle size across a range of pressure for AP/ HTPB-IPDI= (a) 60/40, (b) 62.5/37.5, (c) 65/35, and (d) 70/30.

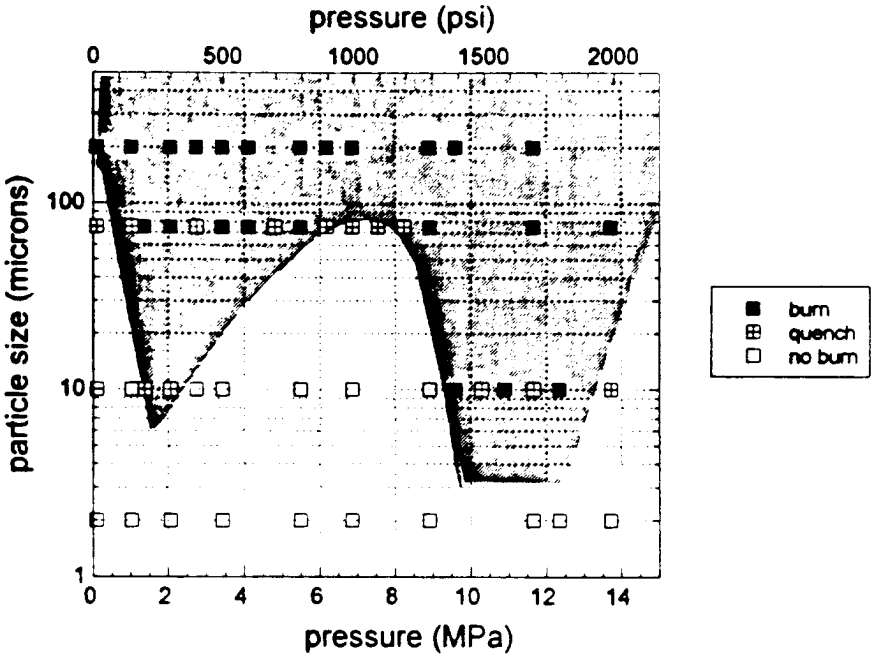

(a)

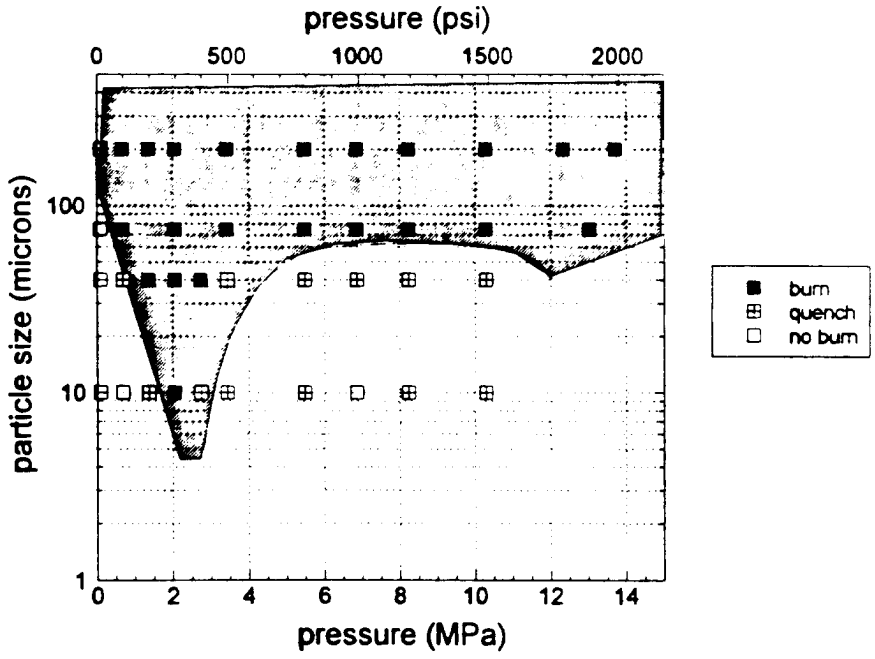

(b)

Figure 4. Burn-no-burn domain as a function of particle size across a range of pressure for AP/ HTPB-IPDI= (a) 60/40, (b) 62.5/37.5, (c) 65/35, and (d) 70/30.

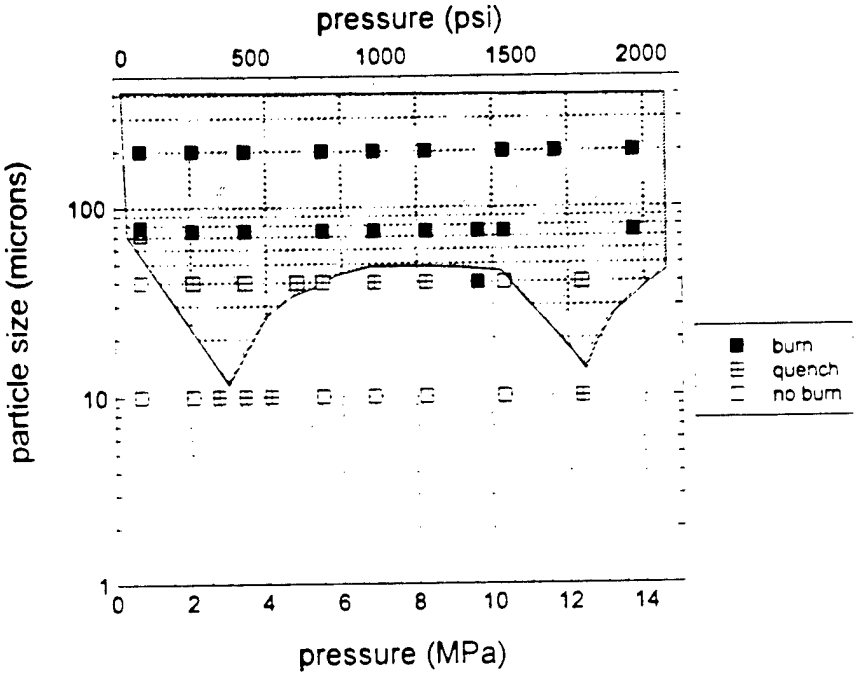

(a)

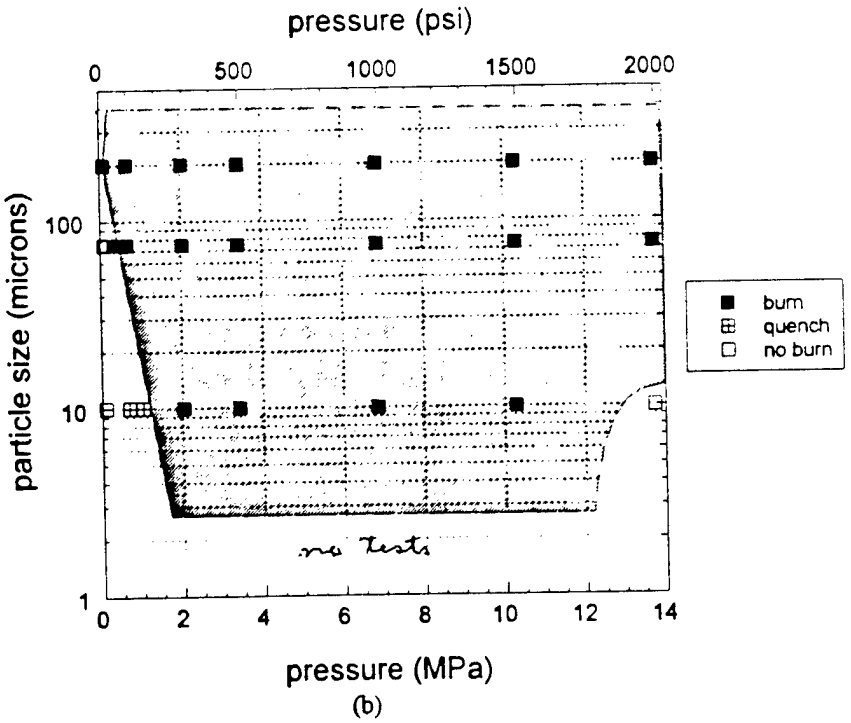

(b)

Figure 5. Burn-no-burn domain as a function of particle size across a range of pressure for AP/ PBAN = (a) 60/40 and (b) 65/35.

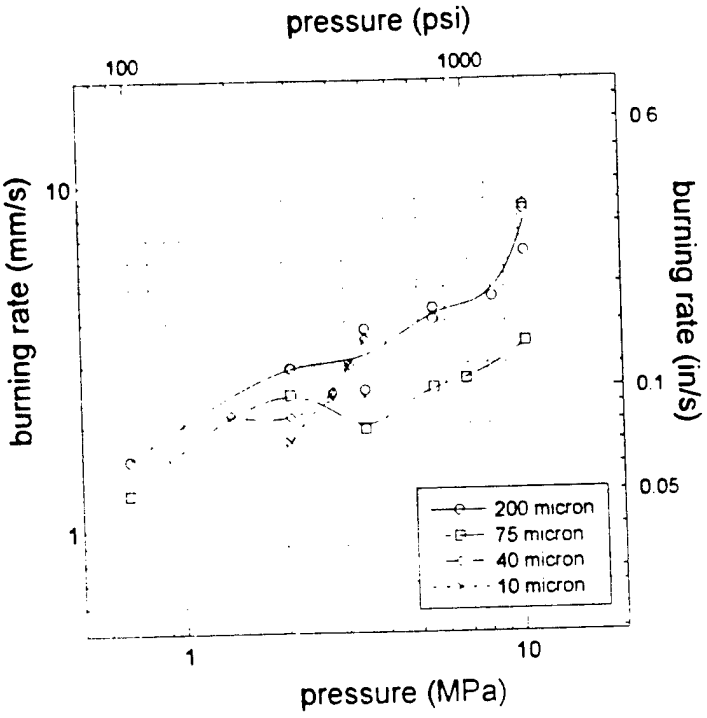

(a)

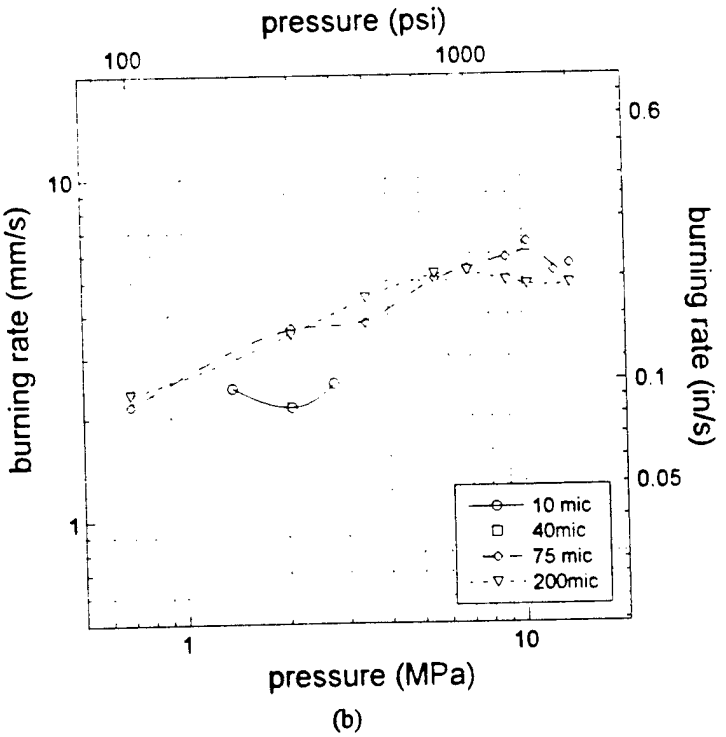

(b)

Figure 6. Burning rates for AP/HTPB-IPDI matricies with O/F ratios of (a) 62.5/37.5, (b) 65/35, and (c) 70/30.

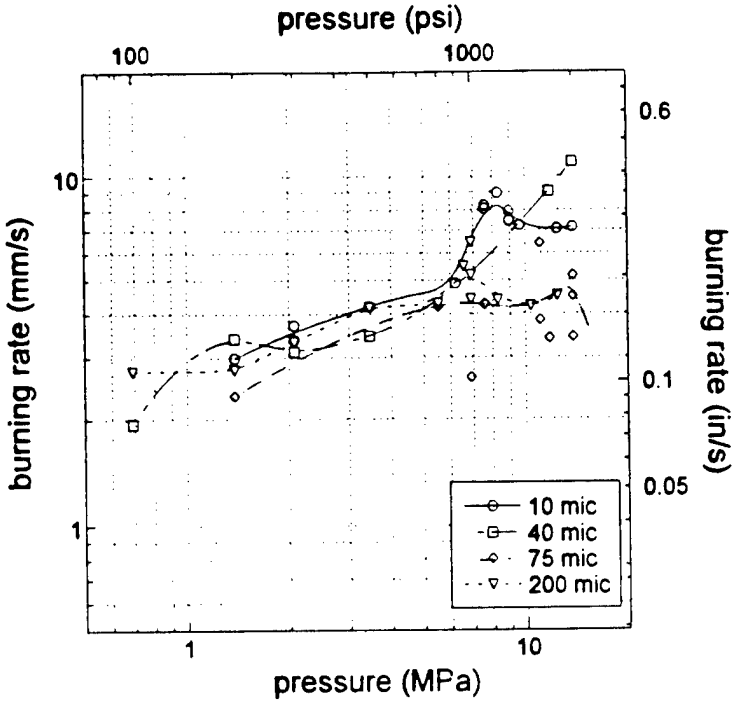

Figure 6. Burning rates for AP/HTPB-IPDI matricies with O/F ratios of (a) 62.5/37.5, (b) 65/35, and (c) 70/30.

Appendix I

Freeman, J. M., Price, E. W., Chakravarthy, S. R., and Sigman, R. K.

"Contribution of Monomodal AP/HC Propellants to Bimodal Plateau-Burning Propellants"

AIAA Paper 98-3388

34th AIAA/ASME/SAE/ASEE Joint Propellant Conference and Exhibit

Cleveland, OH, July 13-15, 1998.

AIAA 98-3388

CONTRIBUTION OF MONOMODAL AP/HC PROPELLANTS TO BIMODAL PLATEAU-BURNING PROPELLANTS

J. M. Freeman, E. W. Price, S. R. Chakravarthy,
and R. K. Sigman

Georgia Institute of Technology,
School of Aerospace Engineering,
Atlanta, Georgia

34th AIAA/ASME/SAE/ASEE
Joint Propulsion Conference & Exhibit
July 13-15, 1998 / Cleveland, OH

For permission to copy or republish, contact the American Institute of Aeronautics and Astronautics
1801 Alexander Bell Drive, Suite 500, Reston, VA 20191

CONTRIBUTION OF MONOMODAL AP/HC PROPELLANTS TO BIMODAL PLATEAU-BURNING PROPELLANTS

J. M. Freeman *, E. W. Price †, S. R. Chakravarthy ‡, and R. K. Sigman §
Georgia Institute of Technology, School of Aerospace Engineering, Atlanta, Georgia 30332-0150 USA

ABSTRACT

The goal of this paper is to present additional data on "anomalous burning" of monomodal propellants, and their effect on bimodal propellants. Such information is needed for modeling the burning of bimodal propellants and rational design of high-solids, plateau-burning propellants. The results include the determination of the no-burn conditions for these very fuel-rich monomodal pocket propellants (or matrices) based on particle size, oxidizer-to-fuel ratio, type of binder, and pressure. For several conditions, the dependence of burning rate on pressure is shown (selected combinations of AP size, oxidizer-to-fuel ratio and binder that are near the no-burn domain). A family of bimodal propellants derived from these matrices is then tested. The burning rates and quenched surface features of these propellants are presented for comparison to the corresponding matrices.

INTRODUCTION

Many early research studies of combustion of ammonium perchlorate (AP) composite propellants sought to determine the effect of AP particle size by testing formulations with fairly narrow unimodal size distribution[1-2]. Due to packing limitations, such formulations contained about 75% AP. Results with such fuel rich formulations have not been particularly useful in understanding combustion of high-solids loadings (86-89% AP) which typically have a blend of different particle sizes. However, they exhibited some unique combustion behavior that is potentially important to some modern propellants that exhibit "plateau" burning, i.e. very low or negative sensitivity of burning rate on pressure, demonstrated in Figure 1. Such burning behavior is exhibited by some formulations with blends of very fine AP and relatively coarse AP (bimodal AP size distribution). In such formulations the burning surface consists of areas of fine AP/binder matrix and areas consisting of individual coarse AP particles. The matrix areas approximate the physical characteristics of the unimodal propellants, and the novel characteristics of those unimodal propellants are very likely a factor in plateau burning behavior of bimodal propellants. This possibility motivated the present return to the study of unimodal propellants.

Earlier studies had shown that some fuel-rich "matrices" exhibited:

a) plateau burning
b) spontaneous extinction in the same mid-pressure range as the plateaus
c) locally intermittent burning without complete extinction

While this novel behavior was not fully characterized (e.g. as a function of oxidizer particle

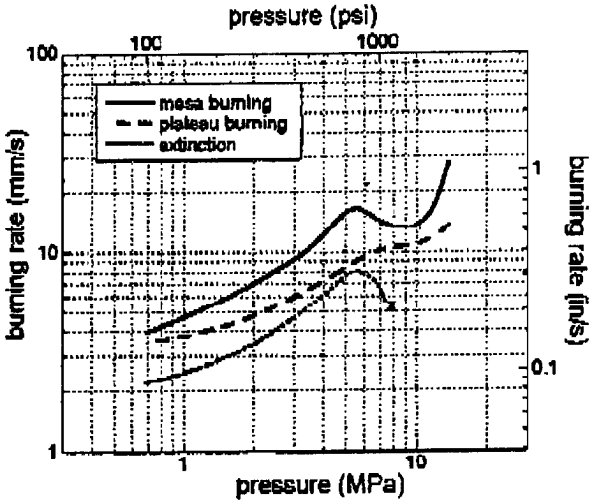

Figure 1. Examples of plateau burning and extinction.

---

* Graduate Research Assistant, Student Member AIAA
† Regents' Professor Emeritus, Fellow AIAA
‡ Post-Doctoral Fellow (now at IIT Madras, India)
§ Senior Research Engineer

Copyright © 1998 by J. M. Freeman, E. W. Price, R. K. Sigman, and S. R. Chakravarthy. Published by the American Institute of Aeronautics and Astronautics, Inc. with permission.

size, oxidizer-to-fuel ratio (O/F)*, and type of binder), it became clear that the "anomalous" burning (a-c above) was strongly dependent on those propellant variables.

In the following years, several researchers found that the burning rate's behavior with varying pressure was strongly sensitive to several parameters, including: AP particle size, binder type and formulation, and O/F ratio[3-9]. Foster and Miller[4] found that, in bimodal formulations with a wide oxidizer distribution (i.e. very fine and very coarse particles) and high fine-AP loading, the matrix had a dominant effect in controlling the burning rate. In the range where their monopropellant extinguished, the companion bimodal propellant experienced a rate suppression. Schimdt and Poynter[8] noted the large effect of type and amount of plasticizer used in the binder. Unfortunately, none of the studies used comparable formulations; generally the binders had dissimilar compositions or the total-solids loadings were different, factors that have been seen to greatly effect the plateau behavior.

A reasonably complete study on the matrices alone would call for burning rate measurements at eight to ten pressures on formulation including a minimum of five different particle sizes, four different binders, and four different O/F ratios (ten tests on each of 5x4x4=80 possible matrices → 800 unrepeated test runs), in addition to other testing to clarify the controlling combustion mechanisms. Likewise, an even larger number would arise form the testing of the bimodal propellants where other variables come in to play: ratio of coarse-to-fine AP, total solids, and the addition of ballistic modifiers. Such an investigation would be a considerably large endeavor.

The present paper describes some results, including strategy to focus the study on the range of formulation variables most critical to occurrence of plateau behavior. Combustion photography and quenched-surface examination are implemented to enhance interpretations gained from the burning rate results.

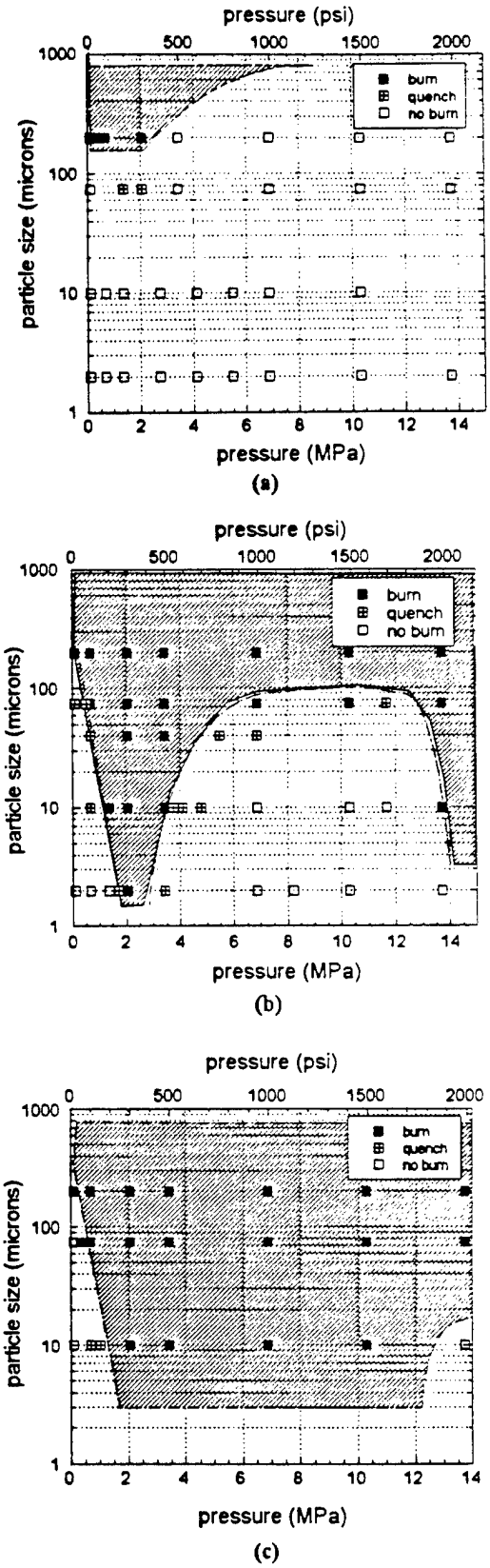

Figure 2. Effect of binder on burn domain for constant AP/binder = 65/35; a) HTPB-DDI, b) HTPB-IPDI, c) PBAN.

* here O/F is used to designate AP/binder ratio, and not the ratio oxygen/hydrocarbon as is more typical of combustion research because AP is a monopropellant (containing both fuel and oxidizer in the classical sense)

EXPERIMENTAL

Experimental Technique

The present study started out by examining the domain of variables in which the matrix would, and would not, sustain burning. Figure 2 illustrates a typical burn/no-burn map showing the dependence of AP particle size and pressure It was anticipated that formulations near the no-burn boundary would have plateau- or mesa-burning rates, and the present paper examines the validity of that postulate and seeks to clarify the microscopic details of the combustion responsible for this behavior.

Combustion photography (video) was used as the primary technique in this study. The method used was routine and the window bomb design was similar to that used by Boggs[10], operable in the pressure range of atmospheric to 2000 psi. Burning rates were obtained from video pictures as described in detail elsewhere[11,12]. The binders used in this study were polybutadiene acrylonitrile acrylic acid (PBAN) and hydroxyl-terminated polybutadiene (HTPB), with the latter being cured by two different agents: isophorone diisocyanate (IPDI) and dimeryl diisocyanate (DDI). Table 1 presents the composition used in the preparation of each binder.

The AP used in this studywas of high purity and fell into five different size distributions, designated as: 2-μm, 10-μm, 40-μm, 75-μm, and 200-μm. The "2-μm AP" comes from an AP and prepolymer mixture supplied by Dr. Carol Campbell of the Thiokol Corp. Dr. Karl Kraeutle, formerly from the Naval Air Warfare Center, provided the "10-μm AP" which has a particle size range of 10-20 μm. The "40-μm, 75-μm, and 200-μm AP" are designations for sieved particles falling between 37-45 μm, 75-90 μm, and 200-250 μm, respectively.

The typical propellant sample size was 3mm *x* 3mm *x* 10mm, which were cut from 5 gram batches. These batches were hand-mixed and cured in a vacuum oven (equipped with rotating sample holders to prevent particle settling) for several days at a temperature of 40° C.

Additionally, scanning electron micrography (SEM) was used to view the micro-details of the burned surface after rapid depressurization interrupted the combustion. Details on this technique are also provide in depth in Ref. 11.

Testing Strategy

Monomodal Matrices

Very fuel-rich, low AP content, monomodal propellants were mixed to simulate the "pocket propellant", or matrix, surrounding the coarse AP particles. In this phase of the study, the effect of both AP content and oxidizer particle size on the burning domain of these matrices was investigated.

Due to the potential scope of this study, a planned strategy was necessary to focus on potentially important variable combinations. Four independent variables (particle size, binder, O/F ratio, and pressure) were identified, resulting in a fifth dependent variable (burning rate). In the initial work which lead to this study[11], the conventional use of pressure as the primary variable was chosen. A second variable, AP particle size, was chosen to produce "maps" of the no-burn domain. These maps only designated the burning domain of one binder at one particular O/F ratio, therefore several maps would be produce by only small variations in the third or fourth variable (binder and O/F ratio, respectively). Initially one such map was made for three binders (PBAN, IPDI-cured HTPB, and DDI-cured HTPB) each with the same O/F ratio (65/35), as seen Fig 2. No burning rate data was taken at that time.

The current study choose to vary a fourth variable (O/F) above and below the initial value for each binder. Since the PBAN matrix burned over almost the entire domain, the O/F ratio was lowered to 60/40. In contrast, the HTPB-DDI matrix, which had a nearly complete no-burn domain, was increased to a 70/30 O/F ratio. The O/F ratio for the HTPB-IPDI matrix was varied both above and below the 65/35 baseline mix to observe the effect on the no-burn domain. It was expected that the no-burn domain would slowly evolve with changing O/F ratio to eventually have a complete burn domain at high oxidizer loading, or a complete no-burn domain at very fuel-rich, low oxidizer loading, as seen in Fig 3.

Table 1. Binder Composition by Percent Weight

Binder	Prepolymer		DOA†	Curing Agent		
	PBAN	HTPB		ECA‡	IPDI	DDI
PBAN	64.14	–	15.00	20.86	–	–
HTPB-IPDI	–	75.73	18.39	–	5.88*	–
HTPB-DDI	–	69.07	16.77	–	–	14.16*

*Approximately 0.01% dibutyl tin dilaurate (T-12) added to HTPB binders to accelerate curing

† DOA = dioctyl adipate

‡ ECA = epoxy curing agent

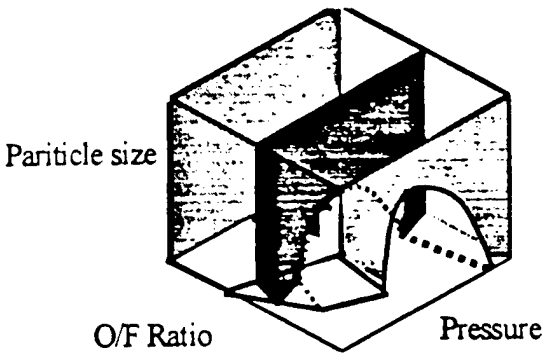

Figure 3. 3-D surface of burn-no-burn maps, as a function of pressure, oxidizer particle size, and O/F ratio.

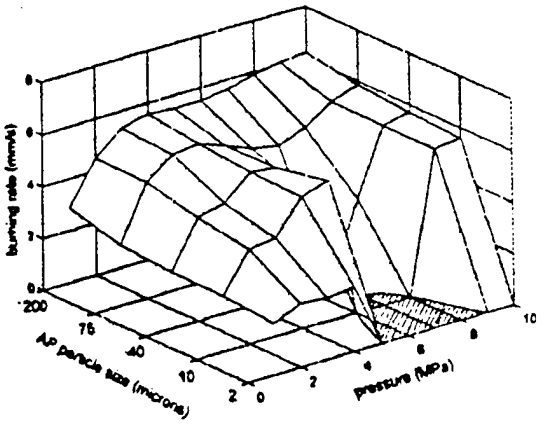

Figure 4. 3-D surface of burning rate as a function of pressure and oxidizer particle size.

For fine particle sizes with mid-pressure no burn domains, it was expected that the burning rates would drop when approaching the no-burn boundary, as was seen in earlier studies of monomodal propellants that had extinction points[13]. Particle sizes, that bordered the edge of the no-burn domain where thought to exhibit a degree of plateau burning. It was postulated that the plateaus and extinction ranges would be well suited to three-dimensional figures, such as Fig. 4. One such surface could be generated for each map, showing the evolution of the plateau behavior and hopefully giving some insight and predictability to such behavior.

JF Propellant Series

This series of propellants was based off an in-house formulation known as ADN Mix #5. This name however is a misnomer, as the propellant is an all-AP blend[14]. To avoid this confusion from here on out, we shall refer to the mix as "SC 1" (after S.R. Chakravarthy). It is a bimodal AP(10-μm & 300-μm)/PBAN propellant, 87.5% solids, matrix O/F = 7/3, coarse AP-to-fine AP ratio = 2/1.

This family of propellants has a bimodal AP composition with an 87.5%-by-mass solids loading.

Table 2. Propellant Formulations (by % mass)

	Standard	With 2% TiO_2
% binder	12.5	12.5
% fine AP	29.17	29.17
% coarse AP	58.33	56.33
% TiO_2	0	2
f_{AP}/b	7/3 (= 2.33)	7/3 (= 2.33)
c/f	2.00	1.93

The fine AP-to-binder ratio is constantly maintained at 7/3 in all the formulations. Both the coarse AP and fine AP sizes are varied to investigate their effect. Additionally, titanium dioxide (TiO_2) is added (at the expense of coarse AP) to several mixtures to investigate its effect as a ballistic modifier[15]. The mass distributions for these propellants are given in Table 2.

A quick guide to the "JF-propellant" designation system (after J.M. Freeman) is given below (see Table 3):

JF 1 = PBAN binder, 10-μm & 200-μm AP

Table 3. Propellant family in this study.

Mix	Binder	Fine AP size	Coarse AP Size	TiO_2 Size
JF1	PBAN	10 μm	200 μm	–
JF1*	PBAN	10 μm	200 μm	0.02
SC1	PBAN	10 μm	300 μm	–
JF1a	PBAN	10 μm	400 μm	–
JF1b	PBAN	2 μm	200 μm	–
JF1b*	PBAN	2 μm	200 μm	0.02
JF1b#	PBAN	2 μm	200 μm	0.5
JF1 Matrix	PBAN	10 μm	–	–
JF1* Matrix	PBAN	10 μm	–	0.02
JF1b Matrix	PBAN	2 μm	–	–
JF1b* Matrix	PBAN	2 μm	–	0.02
JF1b# Matrix	PBAN	2 μm	–	0.5
JF2	HTPB-IPDI	10 μm	200 μm	–
JF2*	HTPB-IPDI	10 μm	200 μm	0.02
JF2a	HTPB-IPDI	10 μm	400 μm	–
JF2b	HTPB-IPDI	2 μm	200 μm	–
JF2b*	HTPB-IPDI	2 μm	200 μm	0.02
JF2b#	HTPB-IPDI	2 μm	200 μm	0.5
JF2 Matrix	HTPB-IPDI	10 μm	–	–
JF2* Matrix	HTPB-IPDI	10 μm	–	0.02
JF2b Matrix	HTPB-IPDI	2 μm	–	–
JF2b* Matrix	HTPB-IPDI	2 μm	–	0.02
JF2b# Matrix	HTPB-IPDI	2 μm	–	0.5

JF 2 = HTPB-IPDI binder, 10-μm & 200-μm AP
__* = propellant contains 2% fine TiO_2 (0.02 μm)
__# = propellant contains 2% coarse TiO_2 (0.5 μm)
__a = coarse AP size is 400 μm
__b = fine AP size is 2 μm

i.e. JF 2b* = HTPB-IPDI propellant with 2-μm & 200-μm AP, 2% fine TiO_2
JF 1a = PBAN propellant with 2-μm & 400-μm AP, no TiO_2

At this time it should be noted that the "b" 2-μm mixes contain a percentage of 10-μm AP to bring the fine AP/binder (matrix O/F) loading up to 7/3 (2-μm AP was unavailable in powdered form due to shipping hazards, however an AP/polymer mix was available though the AP content was not high enough for the desired formulation). Thus the 29.17% of 2-μm AP that was desired to be in the propellant is replaced by 27.63% of 2-μm & 1.54% of 10-μm for the HTPB-IPDI mixes, while the PBAN mixes have 18.92% 2-μm and 10.25% 10-μm. [In terms of the fine AP alone, 5.3% and 35.1% is 10-μm AP, respectively.]

The JF 1 formulation will be referred to as the "baseline" mix, and the JF 2 propellant will be called the "HTPB-baseline."

RESULTS AND DISCUSSION

Monomodal Matrices

No-Burn Domains

In work prior to this study[11], it became clear that the binder type had a significant effect on the no-burn domain, as in Fig. 2. PBAN, the binder which is thought to have the least degree of melt layer on the surface[16], showed no significant no-burn domain. HTPB-DDI, with the highest degree of melt, had a no-burn region over nearly the entire pressure range. A mid-pressure no-burn domain was exhibited by HTPB-IPDI, whose melt characteristics fall between the those of the other two binders. These melt effects are evident with finer AP particle sizes where a larger no-burn domain was observed. It is hypothesized that binder melt flow is more likely to inhibit the burning of the finer particles which may be totally immersed in the melt layer and burning as premixed flames. The larger particles have distinct diffusion flames over them, along with their own monopropellant AP flame, and are not "drowned" by the melt. It is interesting to note that the video photography reveals a large amount of char that rolls up along the sample edges, presumably similar to that reported by other researchers[17]. This seems to be dependent on the AP particle size, the matrices with larger particle sizes (75-μm and 200-μm) having considerably more amounts of this char/melt accumulation than the finer particle sizes which generally have little or no char on the sample edges. All these formulations are high in binder content compared to usable propellants, but the large particle mixes would have a larger spacing between particles, which would be consistent with more melt accumulation.

As the O/F ratio is changed, the no-burn domain does evolve somewhat as expected, as seen in Fig. 5, which presents the HTPB-IPDI case. These domains close in on the mid-pressure no-burn region as well as showing wider ranges of burning regions for fine particles at low pressures. The no-burn domain of the 2-μm particle-size matrices over the entire pressure range is almost universal in this study, but this may be due to the AP being ultra-fine. Sizes in the 5-μm range may not exhibit this behavior and such studies should be undertaken. It was thought that the PBAN mix at a 60/40 O/F ratio may somewhat resemble the HTPB-IPDI mix at 65/35, which had a mid-pressure extinction region and reappearance of burn domain at high pressure for the finer particle sizes. Unfortunately the no-burn region engulfed most of the pressure domain for the finer particle sizes, as seen in Fig. 6. There was a low pressure region where the samples burned anomalously and typically quenched themselves before burning of the sample was complete. This area falls within the region that burning was predicted from the initial test series, presenting the idea that the PBAN matrices may be more sensitive to changes in O/F ratio. The HTPB-DDI matrices at an O/F ratio of 70/30 had only a minimal burn domain as they did for the 65/35 ratio.

Burning Rates

The burning rates were expected to be the most revealing clue into the nature of plateau burning. However the intermittent and anomalous behavior of these low-AP-content propellants made measurements difficult. The data exhibited significant scatter, particularly near the no-burn domain, where the samples showed the most obvious effects of anomalous burning. In most cases, regression of the sample surface was erratic, with some areas burning ahead, then stopping as the flame complex goes out or moves to another area, thereby letting other areas of the sample catch up to, and many times pass, the area that burned ahead.

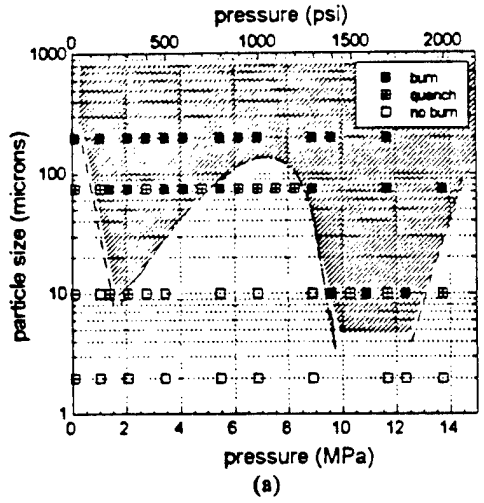

(a)

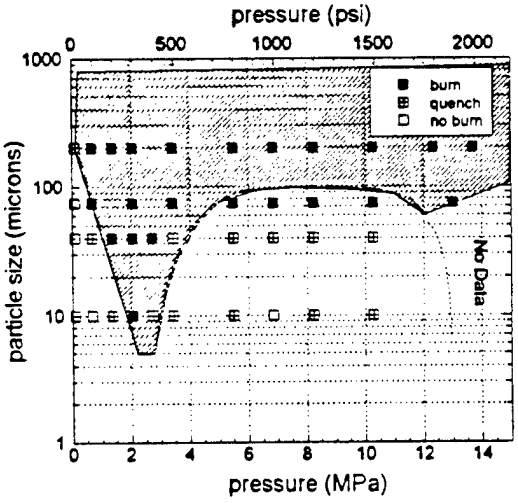

(b)

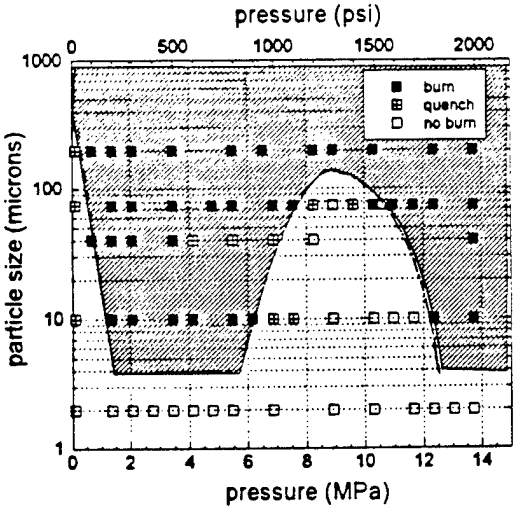

(c)

Figure 5. Effect of varying O/F ratio on burn domain; AP/HTPB-IPDI = a) 60/40, b) 62.5/37.5, c) 70/30.

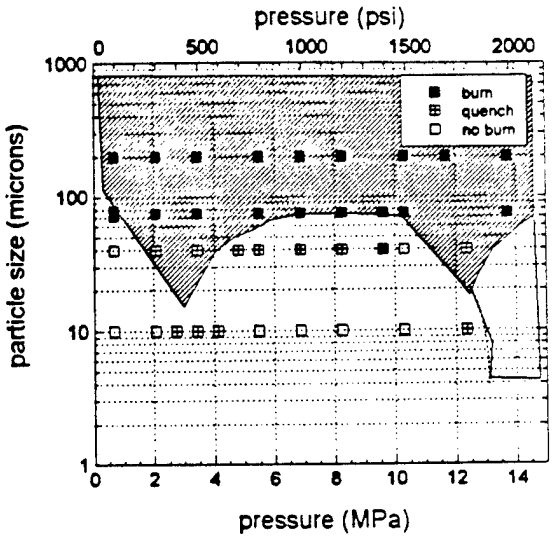

Figure 6. Effect of lowering AP content to 60% for PBAN monomodal matrix.

As of yet, the time and dimensional scales of the intermittent processes had not been determined, but can be said to be of the order of hundreds of microns and tenths of seconds. The burning rates of the AP/PBAN = 60/40 matrices from Fig. 6 are presented in Fig. 7.

In general the matrices with larger AP particles had the tendency to show behavior similar to plateaus and mesa burning. The slopes are low as would be expected with such low-AP-content formulations. Figures 8-10 present the burning rates for AP/HTPB-IPDI = 62.5/37.5, 65/35, and 70/30 mixtures, respectively; again the curves have a low

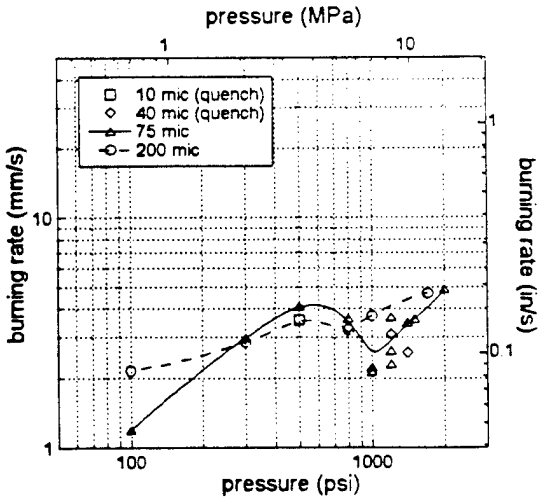

Figure 7. Burning rate for AP/PBAN = 60/40 matrix, showing plateau and mesa effects.

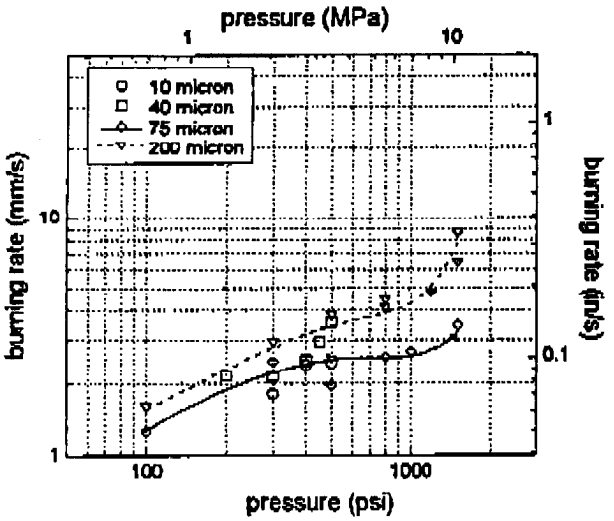

Figure 8. Burning rate for several AP particles sizes for AP/HTPB-IPDI = 62.5/37.5 matrices.

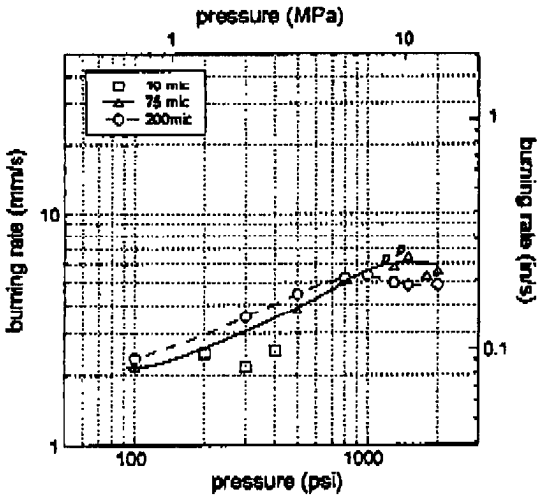

Figure 9. Burning rate for several AP particle sizes for AP/HTPB-IPDI = 65/35 matrices.

exponent and plateau-like behavior.

Because of the data scatter in the intermittent burning domain, inadequate data was available for the mixes with the finer AP size (10-μm, which corresponds to the matrix between coarse particles in bimodal propellants) for any assessments to be made about their behavior. Likewise, insufficient data impeded the efforts to obtain 3-D surfaces like that shown in Fig. 3. The results were indicative of the trend for the mean rate to be depressed during

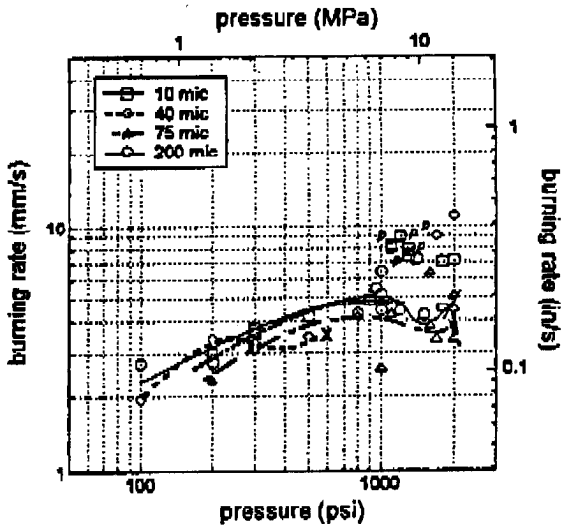

Figure 10. Burning rates for several AP particle sizes at AP/HTPB-IPDI = 70/30. Note extinction of 10 μm and 40 μm curves.

intermittent burning, particularly in the plateau behavior of the large particle sizes.

Effect of TiO_2

The addition TiO_2 seems to have a profound effect on the combustion of the formulations. In order to mimic the addition of 2% modifier in the propellants (and still maintaining the matrix O/F = 70/30), 4.58% TiO_2 of two differing sizes (0.5-μm and 0.02-μm) was added to the 70/30 HTPB-IPDI and PBAN matrices containing 2-μm and 10-μm AP. When implementing the fine TiO_2 (0.02-μm), not only were the no-burn domains eliminated, but the burning rates were dramatically increased, as shown in Figure 11 for the 10-μm AP matrices.

The coarse TiO_2 was only added to 2-μm matrices. Without TiO_2, these matrices were very reluctant to burn, burning to completion at only one or two pressures. For the 2-μm AP/PBAN mix, the fine TiO_2 had the same effect as in the 10-μm case, the curves being nearly identical (the HTPB-IPDI counterpart did not cure to sufficient strength to be worked with). But the coarse TiO_2 had a different result. In the PBAN matrix, there was a no-burn region at mid-pressure (1000-1500 psi). At this same pressure range, the HTPB-IPDI matrix had a dramatic rise in rate producing a mesa, as demonstrated in Figure 12.

Thought to be inert, the oxide was reportedly only supposed to inhibit melt flows by raising the

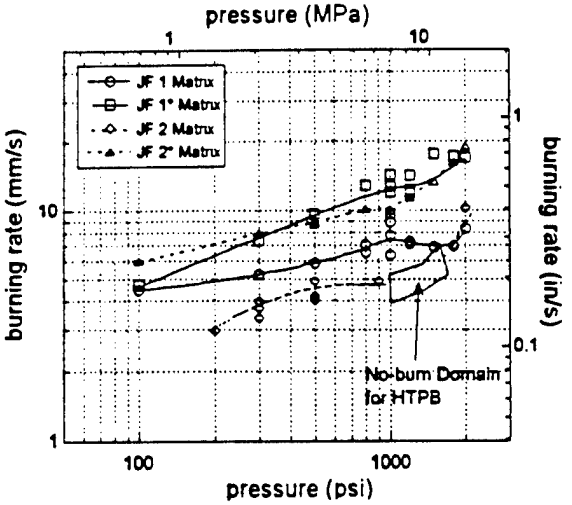

Figure 11. Increase in burning rates of 70/30 matrices with 10-μm AP by adding fine TiO_2 (0.02 μm). * denotes formulations with fine TiO_2.

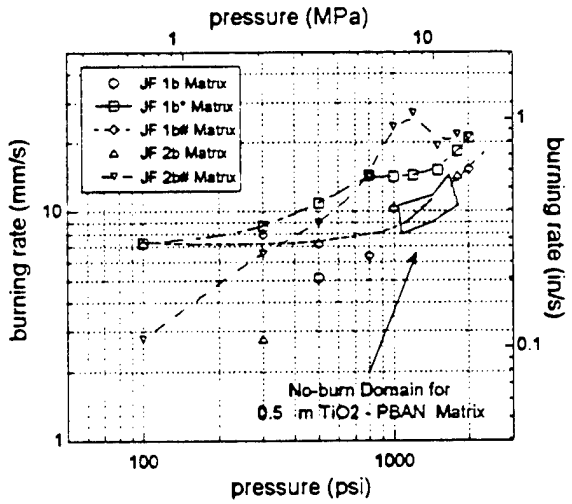

Figure 12. Effect of TiO_2 on 2-μm matrices. * denotes fine TiO_2, # denotes coarse TiO_2.

viscosity of the binder[15]. While this may be true from the macroscopic point of view, on the microscopic scale of the fine AP particles, the coarser TiO_2 size is on the order of fine AP size (particularly the 2-μm AP) and would be of little help in keeping the melt layer from "drowning" these particles. Additionally, the TiO_2 is not present in a sufficient density in the matrix to keep the binder melt away from all the fine particles. If TiO_2's only effect is melt-flow suppression, why would the low-melt PBAN matrix experience a no-burn domain?

Figure 13. Effect of TiO_2 on flame structure (AP/PBAN = 70/30 matrix at 1500 psi).

Unfortunately, the mechanism by which TiO_2 modifies the burning rate is, as of yet, undetermined. Pressed pellets of AP and 10% TiO_2 showed no appreciable deviation from the normal AP rate (tested only at 2000 psi). Similarly, thermogravimetric analyses (TGA's, courtesy of Dr. R. Jeenu) of pressed AP&TiO_2 and mixtures of TiO_2 & binder were no different from pure AP or pure binder, respectively. However, TGA's of propellants did show an increased rate of mass loss when TiO_2 was present.

It may be possible that the oxide has some sort of catalytic effect. Video pictures showed that the TiO_2 matrices burned more intensely than the unmodified formulations over the entire pressure range (100-2000 psi). Figure 13 shows that the formulation with TiO_2 (on the right) burns with a relatively flat surface and without intermittency, whereas the unmodified matrix (on the left) shows a very distorted surface and intermittent flame. Additionally the flamelets are taller and presumably hotter, lending to the higher burning rate. It could be that TiO_2 has some effect in the gas phase reactions, or a catalytic effect on decomposition at the surface.

SEM analysis of quenched surfaces reveal the oxide accumulating on the surface, as shown by comparing Figures 14-15. At modest magnification (roughly 500 times), the 10 μm AP particles are clearly visible (Fig. 14), however the matrix with TiO_2 is "littered with debris" (Fig. 15). The HTPB-IPDI matrices look similar, both without TiO_2 as in Figure 16, and with (not shown). When 2-μm AP is

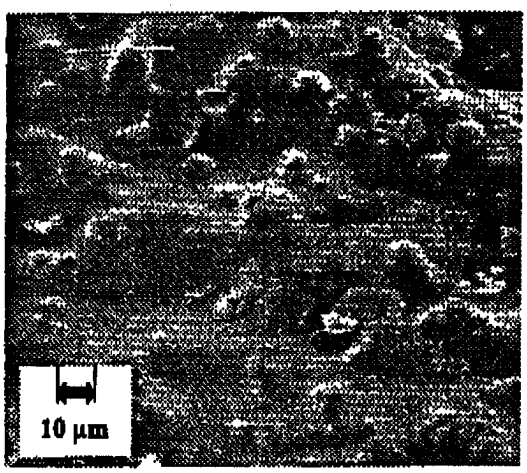

Figure 14. AP(10-μm)/PBAN = 70/30 quenched by rapid depressurization at 1000 psi.

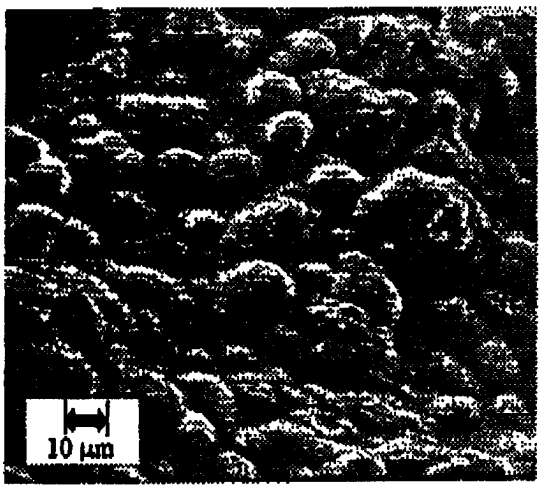

Figure 16. AP/HTPB-IPDI = 70/30 matrix using 10-μm AP quenched by rapid depressurization at 1000 psi.

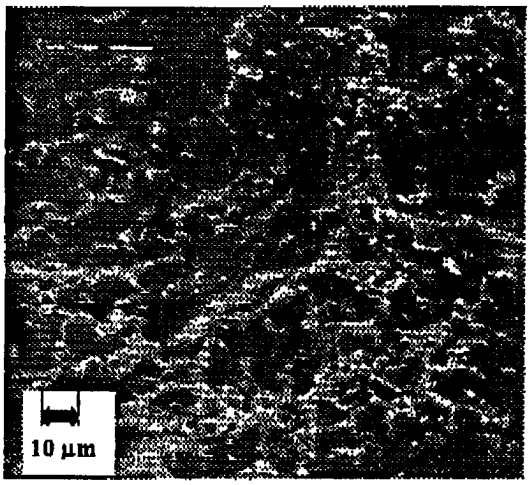

Figure 15. AP(10-μm)/PBAN = 70/30 matrix with fine TiO_2 addition, quenched by rapid depressurization at 1000 psi.

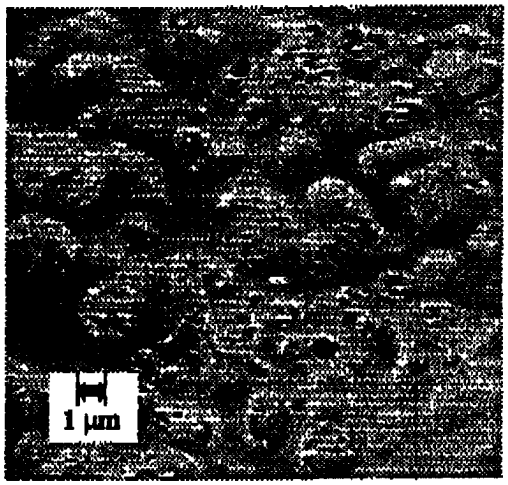

Figure 17. AP/PBAN =70/30 matrix with 2-μm AP quenched at 1000 psi.

substituted for the 10-μm AP in the PBAN matrix (and viewed at higher magnification), the surface structure resembles the 10-μm formulation. The fine AP is visible as small protrusions on the surface and "blowholes" can be seen suggestive of decomposition (Figure 17). For the 2-μm case, the HTPB-IPDI matrix does differ from that of the PBAN matrix (Figure 18). Here the AP is not protruding and larger blowholes are seen, indicative of a thicker melt layer and the fine AP decomposing beneath the surface to a greater extent than the PBAN matrix*.

With these formulations, the addition of TiO_2 seems to only clutter the surface with accumulation as before (Figure 19). This surface accumulation would support an argument for surface-reaction mechanisms being aided by the presence of TiO_2.

Bimodal propellants

Burning Rate Curves

Figure 20 demonstrates the burning rate characteristics for the baseline propellant and the "b"

* [Note: This high-magnification, blowhole structure was seen in samples that spontaneously quenched in the no-burn region and cannot reasonably be argued as an artifact of the rapid depressurization quenching technique.]

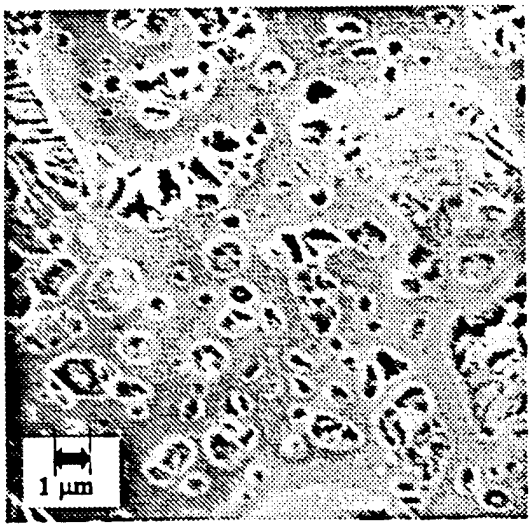

Figure 18. AP/HTPB-IPDI = 70/30 matrix with 2-μm AP quenched at 1000 psi.

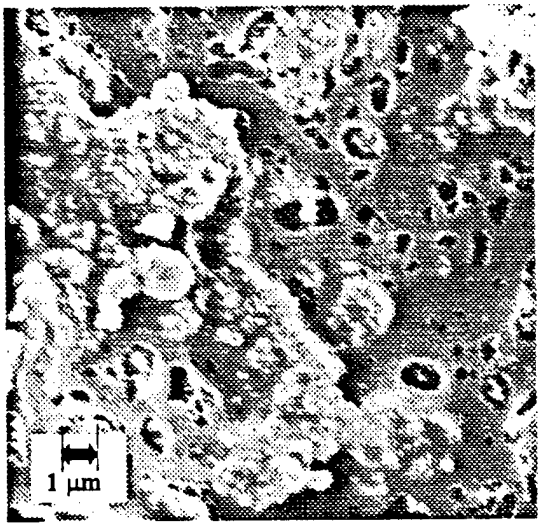

Figure 19. AP/HTPB-IPDI = 70/30 matrix with 2-μm AP and coarse TiO_2 quenched at 1000 psi

variations (those using 2-μm fine AP). Very little difference is noted between the rates of the two binders, nor does the fine particle size appear to have an effect. It is worthwhile to note that the 2-μm AP/PBAN propellant (JF1b) experienced a region of partial burns or "self-quenching" above 800 psi.

Figure 21 shows the effect of changing the coarse AP size. The 400-μm "a" mixes have nearly the same rates as their respective baseline counterparts in the low pressure regime below 100 psi. Above 1000 psi, the rates drop, particularly for the HTPB case, in the region where the matrix

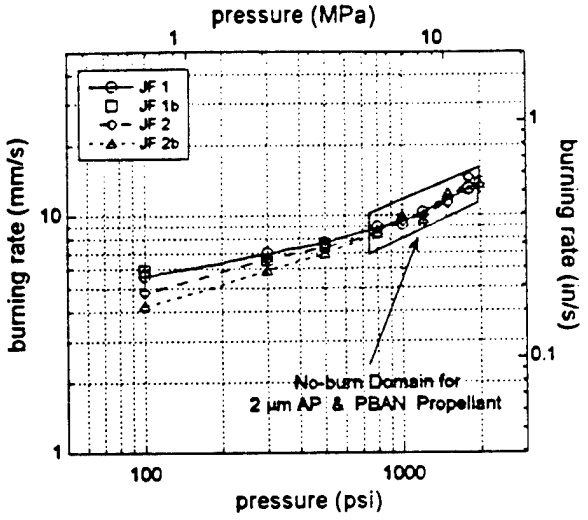

Figure 20. Burning rates for "JF-baseline" propellants and their 2-μm fine AP propellants.

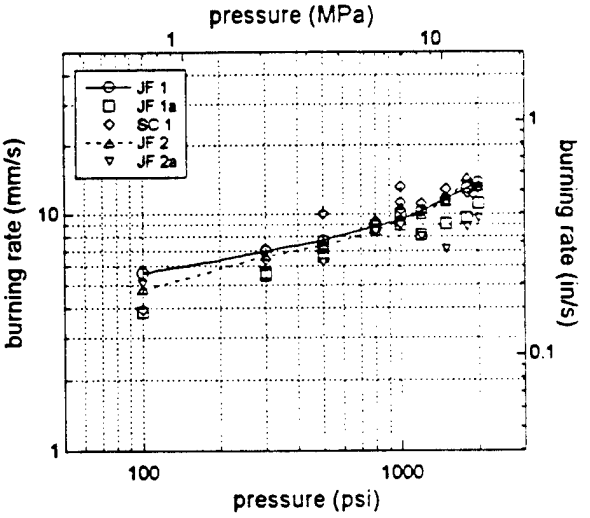

Figure 21. Effect of increasing coarse AP size of bimodal propellants.

shows a no-burn domain. This leads to the achievement of more pronounced mesas or plateaus. The addition of coarse AP to the matrices to gain the high-solids loading of a propellant appears to have a limited effect, bringing matrices which are reluctant to burn up to a common rate.

The addition of TiO_2 raises the burning rate in all cases and eliminates the no-burn region experienced by the 2-μm AP/PBAN propellant (JF1b), as seen in Figure 22. In the PBAN mixes, JF1* and JF1b*, the change in fine AP particle size again seems to have no effect. Similarly, there is little difference between the HTPB mixes varying the fine oxidizer size, JF2* and JF2b*, though these

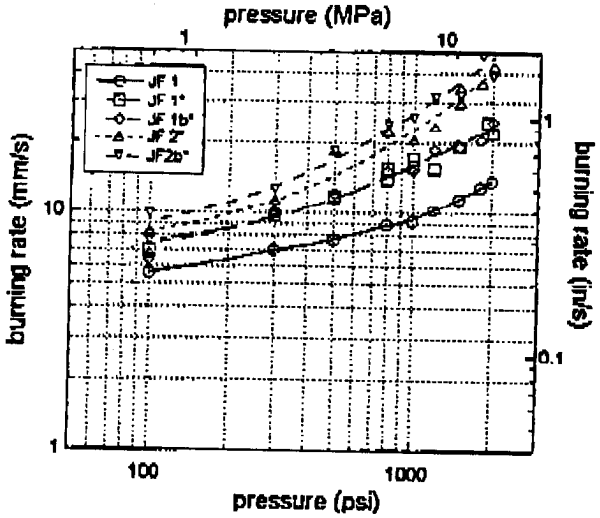

Figure 22. Effect of addition of 2% fine TiO_2 as ballistic modifier (with baseline comparison curve).

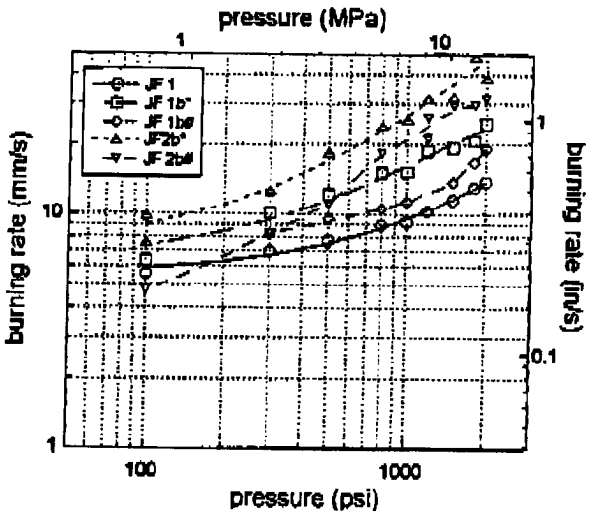

Figure 23. Effect of adding 2% coarse TiO_2 to the bimodal propellants.

rates are significantly higher than the rates of the unmodified PBAN propellant. The burning rates of these propellants with TiO_2 seem to be dominated by the matrix rates, the coarse AP only adding a small incremental increase. This behavior is similar to that reported by Foster and Miller[4]. Interestingly, the coarse TiO_2 does not have they same effect, shown in Figure 23.

As was the case in the matrix results, the coarse TiO_2 does not increase the burning rates to the same extent as did the fine TiO_2. The PBAN propellant's rate (JF1b#) is barely affected, but the corresponding matrix had a large no-burn domain. The HTPB propellant with coarse TiO_2 (JF2b#) had a rate which started at low pressure near the baseline propellant's rate and headed toward the rate of HTPB propellant with fine TiO_2, a trend also shown by its companion matrix result. Apparently, when the matrices burn at a high rate alone, the addition of coarse AP to achieve propellant loadings results in only a marginal increase from the matrix rate. But, as with the unmodified propellants, when the matrix is reluctant to burn (as was the coarse TiO_2-PBAN matrix, JF1b# matrix, Fig. 12) the coarse AP addition serves to extend burning across the entire pressure range, but not at a high rate.

One possible explanation of this lends itself to Cohen's argument of melt-impediment, and the degree of "melt" of the two binders. PBAN is generally considered a "less melty" binder than HTPB-IPDI. It so happens that when these binders are melt-impeded, the have similar burning rates. When TiO_2 is added to "remove" the problem of melt impediment, it increases the burning rate proportional to the amount of melt that can be removed, (i.e. the binder's hidden potential comes out). HTPB, having a greater degree of "melt", has more potential, if all the melt can be removed. The coarser TiO_2 does not appear to be able to "gel" the melt as well in the lower pressure range.

Another possibility is catalysis of reactions at the surface. The finer TiO_2 will have a greater surface area in the propellant than the coarse when included in the same mass percentage. Thus, in the thin surface melt layer where condensed phase reactions are possible, more of the propellant matrix will be exposed to the TiO_2 when a finer particle size is used or if the fine particles accumulate on the surface to a higher degree, which would result in a higher burning rate.

Quenched surface micrography tends to support the latter of these two arguments. The fine TiO_2 also accumulates in flake-like clusters on the surface, supplying an even greater surface area to accelerate the possible decomposition mechanism. The coarser TiO_2 tends to clump together, but does not accumulate in the surface-blanketing manner of the fine TiO_2. But neither particle size shows a large effect at removing the melt or stopping it from impeding the fine AP's decomposition.

Quenched Samples

At this time, a near complete set of quenched samples is only available at one pressure: 1000 psi

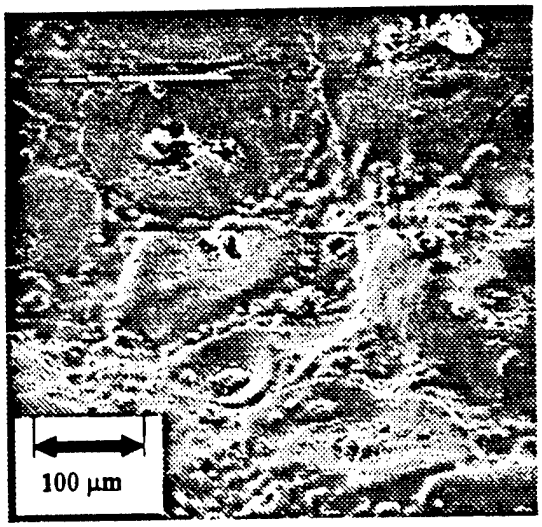

Figure 24. Baseline PBAN propellant quenched by rapid depressurization at 1000 psi.

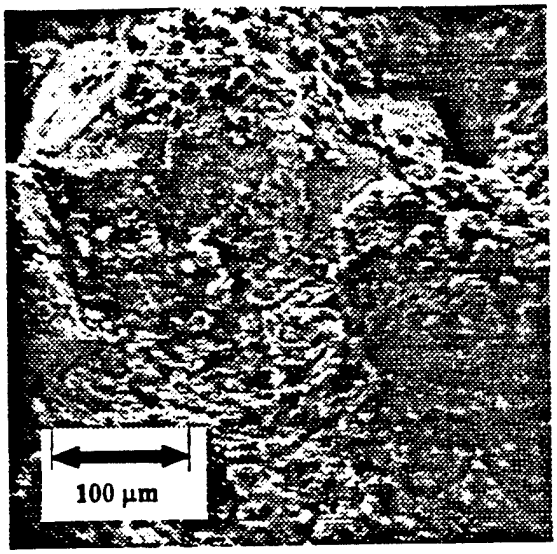

Figure 25. Bimodal PBAN propellant with 10-μm fine AP and fine TiO_2, quenched at 1000 psi by rapid depressurization.

(6.9 MPa). Quenches over a range of pressures (300-1800 psi) are available for several of the formulations, and comparable mixes are expected to have similar behavior, based on the direct comparisons that can be made at this point.

The unmodified formulations (those without TiO_2) have features characteristic of composite AP propellants, seen in Figure 24. Both the coarse AP and the fine AP particles can be seen at low magnification, particularly at low pressures where the AP self- deflagration rate is slow, thus allowing for the binder to decompose ahead of the AP. The coarse AP particles have "puff balls" and "smooth bands" that have been observed by previous investigators[18]. While there does not seem to be appreciable binder melt/melt flow on the coarse AP, the fine AP seems to be "glossed over." This is surprising, in that PBAN was suspected to be the less "melty" binder, based on previous work[16]. Though upon comparison of results by other researchers, this result does seem to coincide with former results[12].

The addition of larger coarse-AP particles has no noticeable effect on the surface features.

When 2-μm particles are substituted for the 10-μm, the low magnification pictures appear to be "dryer," but this is an optical illusion due to the matrix surface being more obstructed by an increased number of fine AP particles (same total mass, smaller diameter → more particles). Closer inspection also shows tiny blow-holes around/covering the AP particles, suggestive of subsurface decomposition (as in the matrix micrographs earlier, Figs. 17-18). Since 2-μm particles are nearly completely submerged in the thermal wave, they may begin decomposing while a large percentage of their volume is still covered by binder, possibly decomposing from all sides, radially inward, instead of top-down, as might be more characteristic of coarser AP.

When the substitution of HTPB is made, the large scale seems similar to the PBAN case. But at high magnification, with the 2-μm formulation, the surface seems more nearly level. This may be an indication that the AP particles are submerged in a deeper melt layer.

The most notable effect comes with the inclusion of TiO_2 particles to the matrix (Figure 25). At low magnification the surface appears to be a littered sea of debris. The coarse AP protrudes in large mounds, which are topped with what appears to be matrix material. The matrix itself looks like a "bowl of cornflakes" as was seen earlier in Fig. 15. With the notable increase in burning rate seen by the matrix, it may be that it is burning ahead and leaving a field of coarse AP behind to either catch-up or leave the surface unignited.

The combination of TiO_2 and 2-μm AP gives similar results to previous cases. On the large scale, the surface looks similar to the previous TiO_2 propellant, a chaotic sea of debris. While at the smaller scales, the 2-μm particles are evident, with their characteristic blow-holes. Here as well the

TiO_2 appears to cluster into large, flake-like structures.

The size of the TiO_2 also seems to have an effect on the propellants surface topology. When the TiO_2 size is increased from 0.02 μm to 0.5 μm the flaking behavior is eliminated. The coarser particles do seem to clump together, but the number density in the propellant and apparent surface coverage is reduced.

CONCLUSION

As of yet, no models have been developed to convincingly explain the mechanisms that lead to plateau burning behavior or the rate increase by TiO_2 addition. In understanding the complex mechanisms in a bimodal propellant, it is necessary to study individual components of the formulation and their effect on the propellant's behavior. The burning characteristics of the surrounding matrix appears to dominantly affect the behavior of the bimodal propellant when TiO_2 is used. The study of monomodal matrices may hold the key to understanding the mechanisms that produce plateau and mesa burning characteristics. The present study has attempted to explore these ideas, with encouraging results. Continued work with a diverse range of binders and additional particle sizes is hoped to give keen insight into the mechanisms of plateau burning.

REFERENCES

1. Steinz, J. A., Stang, P. L., and Summerfield, M., "Effects of Oxidizer Particle Size on Composite Solid Propellant Burning: Normal Burning, Plateau Burning, and Intermediate Pressure Extinction," Aerospace and Mechanical Sciences Report No. 810, Guggenheim Laboratories for the Aerospace Propulsion Sciences, Department of Aerospace and Mechanical Sciences, Princeton University, Princeton, N. J., October 1967.

2. Steinz, J. A., Stang, P. L., and Summerfield, M., "The Burning Mechanism of Ammonium Perchlorate-Based Composite Solid Propellants," Aerospace and Mechanical Sciences Report No. 830, Guggenheim Laboratories for the Aerospace Propulsion Sciences, Department of Aerospace and Mechanical Sciences, Princeton University, Princeton, N. J., February 1969.

3. Miller, R. R., "Effects of Particle Size on Reduced Smoke Propellant Ballistics," AIAA Paper 82-1096, AIAA/SAE/ASME 18th Joint Propulsion Conference and Exhibit, June 21-23, 1982.

4. Foster, R. L., and Miller, R. R., "The Influence of the Fine AP/Binder Matrix on Composite Propellant Ballistic Properties," *Proceedings of the 17th JANNAF Combustion Meeting*, CPIA Pub. 329, Vol. III, September 1980, pp. 91-104.

5. Foster,R. L., Condon, J. A., and Miller, R. R., "Low Exponent Technology," AFRPL-TR-81-95, Hercules Inc., Allegany Ballistics Laboratory, Feb. 1982.

6. Miller, R. R., Stacer, H. L., and Goshgarian, B., "Effects of Curative Type on the Ballistics of Reduced Smoke HTPB Propellants," *Proceedings of the 19th JANNAF Combustion Meeting*, CPIA Pub. 366, Vol. II, September 1982.

7. Miller, R. R., "Anomalous Ballistic Behavior of Reduced Smoke Propellants with Wide AP Distributions," *Proceedings of the 15th JANNAF Combustion Meeting*, CPIA Pub. 297, Vol. II, February 1979.

8. Schmidt, W., and Poynter, R., "Zirconium/ Aluminum Combustion," AFRPL-TR-80-8, Aerojet Solid Propulsion Company, Mar. 1980.

9. Fong, C. W. and Smith, R. F., "The Relationship Between Plateau Burning Behavior and Ammonium Perchlorate Particle Size in HTPB-AP Composite Propellants," *Combustion and Flame*, Vol. 67, 1987, pp. 235-247.

10. Boggs, T. L., "Deflagration Rate, Surface Structure, and Subsurface Profile of Self-Deflagrating Single Crystals of Ammonium Perchlorate," *AIAA Journal*, Vol. 8, No. 5, May 1970, pp. 867-873.

11. Chakravarthy, S. R., "The Role of Surface Layer Processes in Solid Propellant Combustion," Ph. D. Thesis, Georgia Institute of Technology, Atlanta, Georgia, 1995.

12. Lee, S.-T., "Mulitdimensional Effects in Composite Propellant Combustion," Ph. D. Thesis, Georgia Institute of Technology, Atlanta, Georgia, May 1991.

13. Bastress, E. K., "Modification of the Burning rates of Ammonium Perchlorate Solid Propellants by Particle Size," Ph. D. Thesis,

Princeton University, Princeton, New Jersey, January 1961.

14. Price, E. W., Chakravarthy, S. R., Freeman, J.M., and Sigman, R. K., "Combustion of Propellants with Ammonium Dinitramide Oxidizer," AIAA Paper 98-3387, 34th AIAA/ASME/SAE/ASEE Joint Propulsion Conference, Cleveland OH, July 12-15, 1998.

15. Hinshaw, C. J. and Cohen, N. S., "Achievement of Plateau Ballistics in AP/HTPB Propellants," *Proceedings of the 32nd JANNAF Combustion Meeting*, September 1995.

16. Price, E. W., Chakravarthy, S. R., Zachary, E. K., and Sigman, R. K., "Ingredient Response and Interaction during Heating in a Hot Stage Microscope," *Proceedings of the 31st JANNAF Combustion Meeting*, CPIA Pub. 620, October 1994.

17. Cohen, N. S., Fleming, R. W., and Derr, R. L., "Role of Binders in Solid Propellant Combustion," *AIAA Journal*, Vol. 12, No. 2, February 1974, pp. 212-218.

18. Hightower, J. D., and Price, E. W., "Experimental Studies Relating to the Combustion Mechanism of Composite Propellants," *Astronautics Acta*, Vol. 14, No. 1, 1968, pp. 11-21.

APPENDIX J

Price, E. W., Chakravarthy, S. R., Sigman, R. K., and Freeman, J. M.

"Anomalous Combustion Behavior of Ammonium Perchlorate at Elevated Pressures"

Proceedings of the 33rd JANNAF Combustion Subcommittee Meeting

JANNAF 1996

ANOMALOUS COMBUSTION BEHAVIOR OF AMMONIUM PERCHLORATE AT ELEVATED PRESSURES*

E. W. Price, S. R. Chakravarthy, R. K. Sigman, and J. M. Freeman
Georgia Institute of Technology, Atlanta, Georgia 30332-0150

Abstract

The rate of self-deflagration of ammonium perchlorate (AP) decreases sharply with increase in pressure between 2000-4000 psi, depending on sample initial temperature and purity. This is associated with sporadic burning and formation of "needles" in regions of accelerated regression on the surface of self-deflagrating AP in that pressure regime. This paper reviews literature relating to this "anomalous" burning behavior in the light of fresh experimental results. Scanning Electron Microscope (SEM) observations of both single crystals and pressed pellets of AP deflagrating at different pressures in the 400-2300 psi range were made in order to obtain an integrated scenario that leads to such a phenomenon at high pressures. It is seen that needle formation could potentially be an artifact of the process adopted to quench burning of samples at pressures below 2000 psi, contrary to previous results. This, in turn, signifies the role of multidimensional heat transfer processes taking place at the burning surface that may cause formation of needles. Additional tests aimed at studying the relevance of the anomalous behavior in commercial grade AP used in propellant processing are also reported.

Introduction

Ammonium perchlorate (AP) is the principal ingredient used in almost all composite solid rocket propellants today. A unique feature of AP among propellant ingredients is its ability to deflagrate on its own at pressures above about 280 psi (initial temperature ~25 °C). The total heat release that occurs in the deflagration wave of AP is not great compared to the overall heat release in composite propellant combustion; however, it is observed that many propellants, particularly ones with coarse AP particles, exhibit burning rates with "pressure exponents", $(\partial r / \partial p)_T / (r / p)$, that approach the pressure exponent of AP self-deflagration rate at high pressures (>1000 psi). The surface features of large parts of the central portions of coarse AP particles in propellants have also been observed to be identical to those of self-deflagrating pure AP at these pressures. These observations have led the propellant community to believe in a dominating role for AP deflagration in the combustion of composite propellants at high pressures [1].

Recent interest in high pressure "plateau" and "biplateau" propellants has led to active research on mechanisms responsible for such behavior. One plausible mechanism is based on the influence of self-deflagration characteristics of the coarse AP particles present in such propellants at high pressures. Interestingly, deflagration of pure AP normally experiences a major mesa, i.e., negative $(\partial r / \partial p)_T / (r / p)$, just above 2000 psi (Fig. 1 [2]), and it seems likely that this would lead to a plateau in the propellant burning rate in that pressure range. Even as the validity of such a reasoning is yet to be tested, the mesa burning of AP in itself is a result of an extraordinarily complex deflagration process that merits attention in its own right. What appears under typical conditions of intermediate pressures (300-2000 psi) as a steady regression of a nominally flat surface of an AP sample at the macroscopic scale is, in reality, controlled at the microscopic level

* This work was performed under ONR grant N00014-95-J-0559 with Dr. R. S. Miller as technical monitor. Ms. Laurie Finnegan of Western Electrochemical Company (WECCO) supplied some AP used in this study.
Approved for public release; distribution unlimited.

in a thin reaction layer consisting of a reactive liquid froth [3] and gas phase involving over a thousand reaction steps [4]. The complexity is compounded further in the high pressure (2000-4000 psi) region by transition from steady regression to intermittent burning, sporadic and transitory existence of the gas phase flame on the burning surface, presence of conspicuously (at the macroscopic level) large areas of non-uniform regression, and formation of sporadic but large pockets of "needle-like" structures (visible at the microscopic level), all believed to be strongly associated with the mesa in the pressure dependence of the deflagration rate. These features are well known for a long time, but not widely recognized, and still not well understood. Perhaps for this reason, the behavior itself has come to be termed "anomalous".

Studies relating to AP combustion are reported in hundreds of papers. Many of them, however, are based on thermal decomposition tests involving low heating rate tests at very low pressures unlike in a typical deflagration situation. Most of the numerous studies on deflagration of AP are confined to intermediate pressure ranges that exclude the singular mesa burning behavior exhibited at high pressures. Further, some studies that do cover the high pressure range seem to have unintentionally employed AP samples of uncertain purity resulting in failure to register the anomalous burning behavior. In general, most papers do not indicate information about purity besides other specifications pertinent to test samples, which raises serious doubts about validity of even the results corresponding to intermediate pressures [5]. There are a few reports [2, 6-10] that do focus closely on the anomalous high pressure deflagration behavior of AP. Available results are mainly in the form of deflagration rates, high speed motion pictures taken during deflagration, and microscopic features of surfaces and surface profiles of quenched samples, mostly as a function of pressure, purity, and/or initial temperature. Some of these investigations employ samples cut from pure single crystals of AP [2], or from ones that were isomorphously doped with calculated small amounts of relevant impurities [6]. Some papers also demonstrate an equivalence in deflagration features between pure single crystals and hard pressed pellets of polycrystalline powder of AP [2,6,7], while others concern themselves only with pressed AP of high purity [8-10].

As noted earlier, the anomalous high pressure behavior of AP deflagration is strongly dependent on the purity of AP. Also, the needle-like structures mentioned earlier were observed to be approximately 200 μm deep. On the other hand, production grade AP that is commercially available to propellant manufacturers most often contains impurities differing widely in kind and content. Certainly, propellants contain in the form of polycrystalline particles of finite size usually of the order of or less than 200 μm; implying that needle formation may be impeded in coarse particles during propellant combustion. However, the processes that govern needle formation might still be present which might in turn influence the burning characteristics of the propellant. Production grade AP particles are also routinely coated with tricalcium phosphate (TCP), an anti-caking agent, in order to prevent the powder from clumping. These issues raise questions about the applicability of observations on long slabs of pure single crystal AP to finite size impure polycrystalline particles in a propellant (surrounded by binder that may act as a heat sink). This paper is intended to review past observations regarding the anomalous combustion of AP in the light of these concerns.

In reviewing the available results, outstanding gaps have been found to exist in the test pressure ranges and choice of quench methods adopted by different investigators, gaps that are so crucial to the phenomenon that is central to this work. Moreover, the results of one research team have been corroborated by the other in the open literature [6, 8], overlooking disparity in test conditions and methods. The present work furnishes fresh results that are aimed at cleaning up some of the inferences obtained from such past studies. Since many tests performed were specific to the context of gaps in past studies, presentation of new results are intimately interwoven with review of past results in the remaining part of this paper.

Experimental

Ingredients and Samples

Both single crystals and pressed pellets of AP were used in this study. The single crystals are from the same batch as that used by Boggs et al. [2, 6, 7] nearly 25-30 years ago. The test samples were of dimensions 10 x 5x 2 mm approximately. The crystals were preserved in a desiccator. Several different AP lots were used to press pellets. The "baseline" lot may be referred to as the "old Kerr McGee AP". This lot was received at this laboratory from the manufacturer in 1979. It is a low alkali variety, and is of ultra high purity (99.7% pure). Information from the Kerr McGee data sheet about the composition of this type of AP is provided in Table I. The "new Kerr McGee AP" was procured in 1991. Accurate information about the purity/composition of this lot is not available. Additionally, recent supplies of "Wecco AP without TCP" and "Wecco AP with TCP" were also tested. Information on Wecco AP is provided in Table II. The Wecco AP may be considered "production grade", available to propellant manufacturers in recent times. All these lots were of a nominal particle size of 200 μm. The Kerr McGee lots were ground for 8 minutes in a Vibrating Sample Mill to reduce the particle size to a nominal value of 30 μm (wide cut distribution) before using them to press pellets. A few pellets were pressed with the Kerr McGee lots as received (200 μm), but it was not possible to consistently obtain samples with reasonable integrity; this was so even after drying the lots in vacuum for several hours. The available quantities of Wecco AP lots were too small to be used in the vibrating mill, so pellets of Wecco AP were pressed with the lots as received (200 μm) only; there were no problems of integrity with these samples even without vacuum drying the ingredient AP powder. Pressing was done by holding a mold assembly containing approximately 1.6 gm of AP in a hydraulic press at ~32000 psi for 2 hours. These compaction specifications are quite higher than those prescribed by Boggs et al. [5]. The resulting pellets were of 1" diameter and approximately 2 mm thickness. The ingredient AP lots and pressed pellets were always stored at 120 °F. The pressed pellets were cut into approximately 10 x 5 x 2 mm slabs to be used as samples in combustion tests. A few propellants were mixed in the mass ratio AP/PBAN = 75/25 using "ultra high purity" Kerr McGee AP of sizes 200, 400 and 600 μm, and the Wecco AP without TCP (as received, 200 μm) mentioned above. These Kerr McGee AP lots are of unknown vintage, and accurate information on their purity is also not available. The PBAN binder is a mixture of liquids in the ratio PBAN:DOA:ECA = 64.14:15:20.86 by mass.

Experimental Methods

Testing was mainly in the form of quenching samples and examining their surface features in the SEM. Two different kinds of quenching methods were adopted -- rapid depressurization (or "dp/dt") quenching and thermal quenching. The rapid depressurization quench technique has been described in detail elsewhere [11]. The thermal quenching technique is similar to that adopted by Boggs [2]. It consists primarily of two blocks of copper in a vice-like arrangement, and the sample is clamped between them and placed in a pressure vessel. The copper blocks are 13 mm wide, 4.75 mm deep and 3.5 mm thick. Upon ignition, the sample regresses up to the point where it meets with the copper plates, and stops burning subsequently due to excessive heat drain to copper plates. Besides the quench tests, limited number of tests were also performed in order to obtain deflagration rates. The details of these experiments are also available in Ref. 11. Details about the SEM can also be found in the same reference. The highest pressure level at which the quench bomb has been successfully operated is 2300 psi, where as the deflagration rates were obtained by using a "window bomb" which is safely operable up to 2000 psi only. It will be seen later that this disparity poses a limitation to the present study.

Results and Discussion

The characteristics of anomalous deflagration of AP at high pressures have been described in great detail in several papers [2, 6-8]. The subject is revisited with fresh observations in order to (a) evolve a scenario that attempts to integrate the anomalous behavior with "regular" burning at lower pressures, (b) to set the stage to highlight some of the discrepancies in previous results that have been caused by the choice of test methods, and discuss its implications, (c) to set the stage for evaluation of samples of different purity and vintage, (d) discuss the relevance of the anomalous behavior in propellant combustion.

Characteristics of AP Deflagration

In this section, the characteristics of AP deflagration are described based on SEM observations of both pressed old Kerr McGee AP and single crystals by rapid depressurization in the pressure range 400-2300 psi.

At the outset, it seems appropriate to look at the unburned surfaces of pressed and single crystal AP samples. These surfaces indicate conditions that exist for the deflagration wave to pass through. Figs. 2 and 3 show the features. It can be immediately seen that there is a striking difference between the unburned surfaces of single crystal and pressed AP. The pressed AP surface seems to be a mosaic of porous blocks compacted against each other, without many voids in between them. The surface in any one of the blocks is, microscopically, made of an intricate web of holes and groves < 0.5 μm, in the fashion of tendrils, which makes the surface appear porous. It should be mentioned here that this surface pattern is identical to that on the surfaces of unburned AP particles at a similar magnification. The single crystal unburned surface, on the other hand, is relatively smooth, sparsely populated with tiny cuts and pores, about 0.1 μm wide and of varying lengths and shapes, observable at very high magnification (5000X).

It is remarkable, then, that there are negligible differences between the surface features of deflagrating pressed and single crystal AP, as seen in samples quenched by rapid depressurization. This may be due to the fact that the reaction layer of deflagrating AP consists of a liquid froth [3] which could smear particulars regarding the pre-combustion geometry. Since the surface features of pressed AP and single crystals differ little at a given pressure, description of the two may be handled together. In describing the surface features, it seems convenient to identify some basic "elements" in the surface features of all quenched samples regardless of pressure. The effect of pressure may then be seen as changes in and rearrangement of these elements. The porous surface of unburned pressed AP (and not that of single crystals) may be termed the "original surface". Beside this, there are "ridges", "valleys", "froth", "pores", "puff balls", and "cracks".

"Ridges" are protruding regions on the surface. The quality of their surfaces is identical to that of the protruded "smooth band" region of the AP laminae immediately adjacent to the binder lamina in sandwiches [12], Fig. 4. While dealing with sandwiches, it was argued with the aid of comparison between samples with binder, gold, mica and no lamina between AP laminae that the protruding smooth band region in the AP was caused by lateral heat flow to the adjacent lamina if the latter was made of a good thermal conductor. It was thought that AP experienced dissociative sublimation instead of regular deflagration under conditions of heat loss, resulting in a protruded region of smooth surface quality. The smooth quality of the ridges in the self-deflagration of AP may also be seen as indicative of local heat loss, in an otherwise overall adiabatic situation. Earlier work on single crystals, which enabled cleaving perpendicular to the burning surface, has shown thicker phase transition layers at the ridges, indicating a relatively shallower temperature rise, and in turn, slower burning. The sharpness of the ridges may then be considered as a parameter that indicates the extent of lateral heat flux, and the shape of the ridges may provide the direction of such flux.

"Valleys" are areas of greatest regression on the burning surface. Regions of "froth" and "pores" usually coexist, with the pores surrounding the froth. They are always found in valleys. These regions are representative of intense bubbling activity during deflagration. This aspect has been recognized well by earlier workers [2, 6]. Assuming that the flame exists primarily in these regions, the relative areas of these to the ridges may serve to estimate flame standoff based on multidimensional heat flow considerations.

"Puff balls" are more or less particulate structures sporadically strewn on the surface, their population density depending on pressure. Their size varies appreciably, usually averaging around 10 μm, not depending on pressure. It may be noted that such sizes are greater than the reaction layer thickness at high intermediate pressures (~1000 psi). It appears that they may grow and accumulate from the froth on the surface. Some of them have holes indicating possible bubbling through them, Fig. 5. "Bursting" of puff balls has been reportedly observed in high speed motion pictures [2]. The quality of the surface inside the holes resembles the "original surface". Past studies of chemical analyses of these structures, obtained by brushing them off the quenched sample surface, have shown them to be made of AP. The smallest sizes of the puff balls correspond to the size of the froth regions, but it is not clear what governs the maximum size of these structures. It is also not clear if they were made of different chemical species involved in some reversible reactions during burning, and resulted in AP formation during or after quenching. In any case, such relatively huge structures on the burning surface could act as deadweights and soak up heat, if they were not exothermic sites themselves. It is not clear how ridges and valleys are formed during deflagration, starting from a relatively plane surface. It is likely that planar deflagration (in a truly one dimensional manner) is inherently unstable, especially given very small inevitable imperfections on the initial surface. It is then likely that formation of puff balls is a mechanism that "guides" the choice of certain regions as ridges and certain others as valleys as the deflagration wave proceeds into an originally homogeneous material. Recall that the motion pictures revealed a rather static relative arrangement of ridges and valleys for appreciably long periods of time during deflagration [2].

"Cracks" seem to have been caused by transition from cubic phase to orthorhombic during deflagration, and back to cubic after quenching. Cracks do not seem to develop on the ridges.

Pressure Dependence of Surface Features: At 400 psi, the chief features of the burning surface (Fig. 6) are: (a) ridges that are not very sharp, but prolonged over large distances (>100 μm); (b) a large number of puff balls, many with blow holes; and (c) relatively fewer number of sites with froth and pores. Puff balls can be found over ridges as well as valleys.

At 1000 psi (Fig. 7), the length scales of the ridges is shortened, and the pattern of alternating ridges and valleys is more regular than at low pressures; they form a rather orderly array of flowery patterns, with the froth and pores occupying the central regions. Puff balls are fewer in number than at lower pressures, and are almost always located in valleys. Few of them have open holes in them. This suggests that bubbling may still be taking place even after substantial puff ball formation at a froth site at low pressures; whereas, time scales are so short at high pressures (i.e., at 1000 psi) that bubbling may cease at froth sites with a considerable growth of puff balls.

Samples quenched at 1500 psi and 2000 psi did not look very different from each other, but quite different from the 1000 psi samples, which in turn differed appreciably from the 400 psi case, as noted above. This is qualitatively in accordance with the nature of the deflagration rate-pressure curve for AP (Fig. 1), and its demarcation into different regimes by Boggs [2]. The steep increase in burning rate with pressure between 300 and 1000 psi indicates the effect of a gas phase flame that exists closer to the surface at higher pressure. This is manifested in the decrease in the characteristic length scales of the surface features (such as length and width of the ridges) in this pressure regime. As pressure increases further, the gas phase flame gets progressively closer to the surface so much so that it gets localized in areas (steeper valleys) between ridges.

The high pressure samples are marked by sharp wavy ridges, absence of puff balls, froth and pores, and conspicuous cracks in the valley areas (Fig. 8). Boggs [2] indicates transition to such a picture at 1000 psi for the same single crystals (as used in this study) tested more than 25 years ago, i.e., puff balls, froth and pores are not found at 1000 psi; this will be addressed later. According to the present study, above 1500 psi, the froth and pores are replaced by what appears to be dry parched areas, suggesting a very thin non-bubbly liquid layer, if ever present. This picture is fairly consistent with the scenario of major participation of an exothermic reactive liquid froth as well as a gas phase flame in controlling the deflagration rate of AP [13]; the decrease in the pressure exponent may be due to decreasing contribution of exothermicity from a thinning reactive froth at higher pressures, and the concomitant limitations imposed on the gas phase flame (short reaction distances and collision probabilities [14]). Holes of the size of the order of a few microns appear in the valleys in a sporadic (non-systematic) fashion, particularly at 2000 psi. It is not clear if these holes enlarge rapidly above 2000 psi into large areas of enhanced regression followed by development of needle-like structures.

However, no needles are observed up to 2000 psi in the present work, in sharp contrast to data of Boggs et al. that show needles on samples quenched at as low as 1500 psi [2, 6, 7]. This is not very well in accordance with the sharp decline in deflagration rate the onset of which does not occur below 2000 psi (Fig. 1). Strong correlation between appearance of needles and mesa burning behavior is not a necessary condition in explaining the phenomenon, but it is slightly hard to reconcile non-uniform burning seen in high speed motion pictures that occurs above 2000 psi with appearance of needles at lower pressures observed by quenching samples. The emphasis here is to suspect the means of quenching samples adopted in the past studies. This discrepancy shall be addressed in the next section.

Continuing the description of surface features as a function of pressure, it can be seen in Fig. 9 that the overall surface at 2300 psi is very different from that at 2000 psi. The pressure level of 2300 psi lies well within the regime corresponding to the mesa burning behavior. It is marked by large scale non-uniform regression, and different qualities on different parts of the surface. There are some areas that show regular patterns of ridges and valleys similar to features of "regular" deflagration at lower pressures (1500-2000 psi). There are other areas where large pits are found surrounded by regions the appear damp as if some liquid has been absorbed by the solid underneath to saturated proportions. Inside these pits are a disorderly array of needle-like structures that have been referred to in the last paragraph. The non-uniform surface conforms well not only with a drop in the mean burning rate as in Fig. 1, but also with the transitory existence of the gas phase flame in the pressure range 2000-4000 psi noticed in the high speed motion pictures [2].

Rapid Depressurization Versus Thermal Quenching

The foregoing description of features of AP deflagration surface as a function of pressure was based on samples quenched by rapid depressurization. It was pointed out that earlier studies on single crystals by Boggs et al. [2, 6] reported, in particular, appearance of needles at pressures as low as 1500 psi; whereas, needles were observed in the present study only at 2300 psi. Reports by Boggs et al. were based on thermal quenching of samples, particularly at higher pressures. This led to a series of thermal quenching tests on single crystals as part of the present work. Figs. 10, 11 and 12 show surface features of single crystal samples thermally quenched at 2000, 1000 and 400 psi respectively. It can be observed that beside the 2000 psi sample, the 1000 psi one too exhibits areas with needles; although Fig. 12 is so chosen as not to unduly exaggerate the point, a small patch of the surface at 400 psi was indeed found to have a cluster of needles! More disturbing than just the needle formation issue is the observation of a totally different set of overall surface features at each pressure obtained by thermal quenching than with rapid depressurization. The thermally quenched samples do not exhibit conspicuous froth and pores, and puff balls at the lower pressures. Parts of the surfaces that have wavy ridges at 1000 psi (Fig. 11) do appear somewhat similar to that shown by Boggs et al. [2, 6], but other parts that are dissimilar and with needles cannot be ignored. These features clearly lead one to be more inclined to believe the rapid depressurization results presented earlier in this paper, which are more closely

in conformance with pressure dependence trends in the burning rate data and combustion photography observations.

The papers by Boggs et al. [2, 6] are careful to compare (a) single crystal AP versus pressed AP, and (b) thermally quenched samples versus rapid depressurization (dp/dt) quenched samples. Equivalence between single crystals and pressed samples has been established in the present work for old Kerr McGee AP not only via dp/dt, but also by thermal quenching, as shown in Fig. 13; pressed AP thermally quenched at 2000 psi shows needles and other surface features similar to those in Fig. 10. Boggs et al. [2, 6] base their claim for equivalence of the two quench methods on comparative tests performed up to 1200 psi, and on earlier work by Hightower and Price [3] that adopted dp/dt up to 800 psi; the equivalence was "extrapolated" to higher pressures. They also compare observations obtained by Varney [8] at 1200 and 4800 psi quenched by dp/dt, with the test at the latter pressure level showing needles on the surface of pressed AP. However, hard evidence for equivalence between the two methods was lacking in the pressure range 1200-4800 psi, the regime that includes the anomalous burning behavior of AP, and this fact was overlooked in the past studies.

The surface features of thermally quenched samples in the present study show a greater departure from the dp/dt quenched samples than those shown by Boggs et al. [2, 6]. It is likely that the magnitude of heat drain relative to the sample size was more in the thermal quenching tests in the present work than in the previous studies.

The Role of Multidimensional Lateral Heat Transfer in Anomalous AP Deflagration

The results of thermal quenching in the present studies, albeit being possibly dramatic, point to role of heat transfer processes that may be responsible for needle formation. The thermal quench tests provide enormous heat sinks by way of the copper plates, which seems to aid non-uniform burning and formation of needles even at low pressures.

As mentioned earlier, the sharpness of the ridges and their orientation serve as indicators of the magnitude and direction of heat fluxes lateral to the direction of burning. As such, we notice stronger heat flow from the reaction sites (presumed to coincide with froth/pores areas) at higher pressure. It may be that there is a threshold level of local heat drain that triggers non-uniform burning and needle formation. This heat drain was supplied by the copper plates in the thermal quench tests, resulting in such features even at low pressures.

In the thermal quench results, it is clear that needles were formed primarily in areas that experienced greater regression than the average surface. These areas were mostly in the center of the sample, and clearly, they burned even after the areas closer to the copper plates had been quenched. Longer the quenching process, taller were the needles. This has been indicated in earlier works as well [2]. Further, combustion photography in those works indicated that transitory local pockets of flame could be found in regions that regressed ahead of the rest of the surface. The needle formation then seems to be the terminal phase of flame propagation in a locally low lying area surrounded by areas of retarded regression that serve as an enormous heat drain. Growth of needles may occur simultaneously as the flame moves away from the surface, and eventually goes elsewhere, still sustaining the overall deflagration wave, but resulting in a reduced mean burning rate in the process. As the area with needles suffers from lack of a flame, it has to protrude, and the stack of needles may then collapse and pile up in a crisscrossing manner, as has been found in some thermally quenched samples. Note that once they collapse, they may either be consumed (by sublimation) or be ejected from the surface; in any case, they may be ripped apart by the rapid depressurization process in a dp/dt quench test.

The above scenario is at best speculative. It is not clear what limits the growth of needles before the flame moves over to another position. Glaskova and Bobolev [10] have suggested that water produced during the reaction may condense on the surface because the surface temperature of deflagrating AP may fall below the boiling point of water at these pressures; the condensed water may then inhibit burning. While this may indeed be taking place, it does not contradict the heat transfer scenario suggested by the thermal quenching tests of the present study.

Deflagration of Commercial Grade AP

Fig. 14 shows deflagration rates of many samples. It can be seen that the old Kerr McGee AP burning rates are quite lower than the single crystal AP burning rates reproduced from Fig. 1 (Boggs' data [2]). On the other hand, burning rates of the Wecco AP without TCP and the new Kerr McGee AP compare very well with Boggs' single crystal data; the Wecco data better than the new Kerr McGee data. In general, production grade AP lots of recent times seem to have negligible impurity effects when compared to older times. This is supported by comparison of tests with production grade AP by Boggs et al. [5] and Atwood et al. [15] performed a couple decades apart. AP from different manufacturers not only shows different deflagration rates/characteristics as seen here, but also leads to different burning rates and pressure-coupled combustion responses of propellants using them [16]. Pressed pellets of the Wecco AP with TCP did not burn at any pressure in the range 300-2000 psi; Refs. 5 and 15 show AP with TCP to burn at limited pressure levels with substantially lower burning rates than the corresponding rates for AP without TCP. In reality, these tests may have little relevance to combustion of commercial propellants using AP particles coated with TCP, since the TCP coating exists only along the periphery of particle burning surfaces which may hardly affect the deflagration wave in the central region of the particle surfaces.

The surface features of the new Kerr McGee AP and the Wecco AP without TCP quenched at 1000 and 2300 psi by dp/dt are shown in Figs. 15 and 16. The Wecco AP samples exhibit some voids that may have been present during pressing, since these samples were pressed from a lot that had a nominal particle size of 200 μm. The Wecco AP sample at 1000 psi also exhibits a rather orderly array of large pits on the surface with white specks sprinkled in them; the reason for this feature is unknown. Apart from these peculiarities, the figures show features similar to 1000 and 2000 psi of the single crystal/old Kerr McGee AP features (also dp/dt quenched) shown in Fig. 7 and 8 respectively. In particular, the surface regression at 2300 psi seems to be macroscopically uniform, and the needles are conspicuously absent. Unfortunately, deflagration rate data are not available at 2300 psi to see if the mesa does not occur in that pressure range for these samples. This is a limitation in this study. The surface at 1000 psi also shows lesser number of puff balls than with single crystals and old Kerr McGee AP.

Effects of Purity and Aging

The Wecco AP data sheet shows an overall impurity level greater than that of the old Kerr McGee AP (comparing Tables I and II). However, the Wecco AP contains an extremely low level of potassium (which has the potential of altering the deflagration characteristics of AP substantially [6]). It is not clear if the significantly lower burning rates of the old Kerr McGee AP are due to an impurity effect or aging. The disparity between the single crystal burning rates at high pressures obtained this study and those by Boggs [2] nearly 30 years ago shows an aging effect and probably not an impurity effect. The equivalence of surface features between the single crystals and the old Kerr McGee AP quenched now indicates a possible aging effect on the old Kerr McGee AP also. It is not clear if disparity in formation of puff balls observed in single crystal and old Kerr McGee AP samples quenched now, as opposed to lack of puff balls (at 1000 psi) in single crystals seen in Refs. 2 and 6 and in new Kerr McGee and Wecco AP lots obtained recently, is related to either aging of old samples, impurities in new/production grade samples, or different choices of quench methods in the present and past studies.

Effect of Particle Size

Comparison of deflagration rates of pellets pressed with new Kerr McGee AP as received (nominally 200 μm) and ground for 8 minutes (nominally 30 μm) shows that particle size of the initial AP powder hardly influences the deflagration characteristics, if the pellets are pressed hard enough for a long enough duration, a result that supports the earlier conclusion by Boggs et al. [5].

Surface Features of Coarse AP Particles in Propellants at 2300 PSI

Fig. 17 shows surfaces of four propellants quenched by rapid depressurization at 2300 psi. Three of the propellants were made with Kerr McGee AP of size 200, 400 and 600 μm, and the fourth one with the Wecco AP without TCP. All propellants have an AP content of 75%; the binder was chosen to be PBAN to minimize melt flow effects. The purpose of this series of tests was to examine if anomalous burning behavior of AP, i.e., needle formation, non-uniform burning, etc., are present in finite sized particles in propellants. The needles in single crystals were reported to be around 200 μm deep. It was not clear if the thermal wave would "sense" the finiteness of a particle of size 200 μm in a propellant, and impede needle formation ahead of time. Unfortunately, the features shown in Fig. 17 do not answer such questions. Far from it, the propellant surface seems to be filled with binder melt flow to such a great extent that it is hard to clearly identify the edges of the AP particles. AP particles at this pressure are found recessed. The few AP particles that could be identified beyond doubt do not exhibit the usual symptoms of anomalous burning at the same length scales as with single crystals. Moreover, the surface features do not resemble normal burning of AP at any pressure either. This may be due to the way binder melt flow alters AP deflagration when it encroaches upon the peripheries of AP particles, and the heat drain that the binder causes to these particles. In view of such uncertainties, distinction between features of Kerr McGee "ultra high purity" AP (Fig. 17a) and Wecco AP particles (Fig. 17d) cannot be clearly delineated. Perhaps, with bimodal propellants with high AP loading and very fine AP, the melt flow effects may be felt predominantly by the fine AP, and not the coarse AP. The screening tests represented by Fig. 17 should be not be considered to establish that anomalous AP deflagration behavior is not relevant to propellant combustion.

Conclusion

The surface features of AP obtained as a function of pressure affirm the existing theory of steady state deflagration at pressures up to 2000 psi. Rapid depressurization quenching performed in this study and companion tests using thermal quenching have revealed that the presence of needles at pressures as low as 1500 psi reported in earlier studies may be an artifact of the thermal quenching process. This sheds light on the dependence of the needle formation process on the presence of heat sinks on the burning surface; and points to the role of possible multidimensional lateral heat flow occurring locally on the burning surface in formation of needles, even under overall adiabatic conditions.

Deflagration of commercial grade AP manufactured in recent times does not seem to exhibit any anomalous behavior. Suspicions about aging effects on single crystals as well as AP powder have been raised by disparities in deflagration rates obtained in tests performed now and nearly 30 years ago. Particulate AP in the size range 200-600 μm present in propellants do not exhibit anomalous surface features at high pressures, but their deflagration seems to be severely affected by the presence of excessive binder melt flows encroaching on their peripheries.

References

1. Beckstead, M. W., Derr, R. L., and Price, C. F., "A Model of Composite Solid-Propellant Combustion Based on Multiple Flames," AIAA Journal, Vol. 8, No. 12, December 1970, pp. 2200-2207.

2. Boggs, T. L., "Deflagration Rate, Surface Structure, and Subsurface Profile of Self-Deflagrating Single Crystals of Ammonium Perchlorate," AIAA Journal, Vol. 8, No. 5, 1970, pp. 867-873.

3. Hightower, J. D., and Price, E. W., "Combustion of Ammonium Perchlorate," Proceedings of the Eleventh Symposium (International) on Combustion, The Combustion Institute, 1967, pp. 463-472.

4. Brill, T. B., Brush, P. J., and Patil, D. G., "Thermal Decomposition of Energetic Materials 60. Major Reaction Stages of a Simulated Burning Surface of NH_4ClO_4," Combustion and Flame, Vol. 94, 1993, pp. 70-76.

5. Boggs, T. L., Zurn, D. E., and Netzer, D. W., "Ammonium Perchlorate Combustion: Effects of Sample Preparation; Ingredient Type; and Pressure, Temperature and Acceleration Environments," Combustion Science and Technology, Vol. 7, 1973, pp. 177-183.

6. Boggs, T. L., Price, E. W., and Zurn, D. E., "The Deflagration of Pure and Isomorphously Doped Ammonium Perchlorate," Proceedings of the Thirteenth Symposium (International) on Combustion, The Combustion Institute, 1971, pp. 995-1008.

7. Boggs, T. L., and Kraeutle, K. J., "Role of the Scanning Electron Microscope in the Study of Solid Rocket Propellant Combustion, I. Ammonium Perchlorate Decomposition and Deflagration," Combustion Science and Technology, Vol. 1, 1969, pp. 75-93.

8. Varney, A. M., "An Experimental Investigation of the Burning Mechanism of Ammonium Perchlorate Composite Solid Propellants," Ph.D. Thesis, Georgia Institute of Technology, May 1970.

9. Glaskova, A. P., "Anomalies in the Burning of Ammonium Perchlorate and Ammonium Nitrate," Fizika Goreniya i Vzryva, Vol. 4, No. 3, pp. 314-32, 1968.

10. Glaskova, A. P., and Bobolev, V. K., "Influence of the Initial Temperature on the Combustion of Ammonium Perchlorate," Doklady Akademii Nauk SSSR, Vol. 185, No. 2, March 1969, pp. 346-348.

11. Chakravarthy, S. R., "The Role of Surface Layer Processes in Solid Propellant Combustion," Ph.D. Thesis, Georgia Institute of Technology, Atlanta, GA, 1996.

12. Price, E. W., Sambamurthi, J. K., Sigman, R. K., and Panyam R. R., "Combustion of Ammonium Perchlorate-Polymer Sandwiches," Combustion and Flame, Vol. 63, 1986, pp. 381-413.

13. Guirao, C., and Williams, F. A., "A Model for Ammonium Perchlorate Deflagration between 20 and 100 atm," AIAA Journal, Vol. 9, No. 7, July 1971, pp. 1345-1356.

14. Wenograd, J., and Shinnar, R., "Combustion of Ammonium Perchlorate -- Some Negative Conclusions," AIAA Journal, Vol. 6, No. 5, May 1968, pp. 964-966.

15. Atwood, A. I., Price, C. F., Boggs, T. L., Curran, P. O., and Zwierzchowski, N. G., "Ignition and Combustion Properties of Ammonium Perchlorate," Proceedings of the 27th JANNAF Combustion Meeting, CPIA, October 1990.

16. Altman, D., Price, E. W., Culick, F. E. C., Summerfield, M., Faget, M. A., and Thibodaux, G., "Report of Special Investigating Committee on Space Shuttle Solid Rocket Motor Pressure Perturbations," prepared for the National Aeronautics and Space Administration, January 1994.

Table I. Kerr McGee Data Sheet for old AP lot

Constituents	Weight %
Assay as NH_4ClO_4	99.7
Sodium as Na	0.0025
Potassium as K	0.0025
Bromate as NH_4BrO_3	0.001
Chlorate as NH_4ClO_3	0.002
Chloride as NH_4Cl	0.002
Sulfate as $(NH_4)_2SO_4$	trace
Iron as Fe_2O_3	–
Non-alkali metals	0.003
Sulfated ash as $NaClO_4$	0.06
Tricalcium phosphate (TCP)	–
Water insoluble	0.003
Acid insoluble	–
Moisture - surface	0.005
- total	0.05
pH saturated solution	4.5

Table II. Wecco Data Sheet

Constituents	Weight %	
	Without TCP	With TCP
Assay	98.9	98.7
Bromates as NH_4BrO_3	0.000	0.000
Total H_2O	0.03	0.04
External H_2O	0.00	0.01
Internal H_2O	0.03	0.03
Chloride as NH_4Cl	0.03	0.03
Chlorate as NH_4ClO_3	0.00	0.00
Phosphate as TCP	0.00	0.17
Sulfated ash	0.1	0.3
Acid insoluble	0.00	0.00
Iron (Fe_2O_3)	0.000	0.000
Potassium	0.0042	0.0041
pH of water solution	5.2	6.2

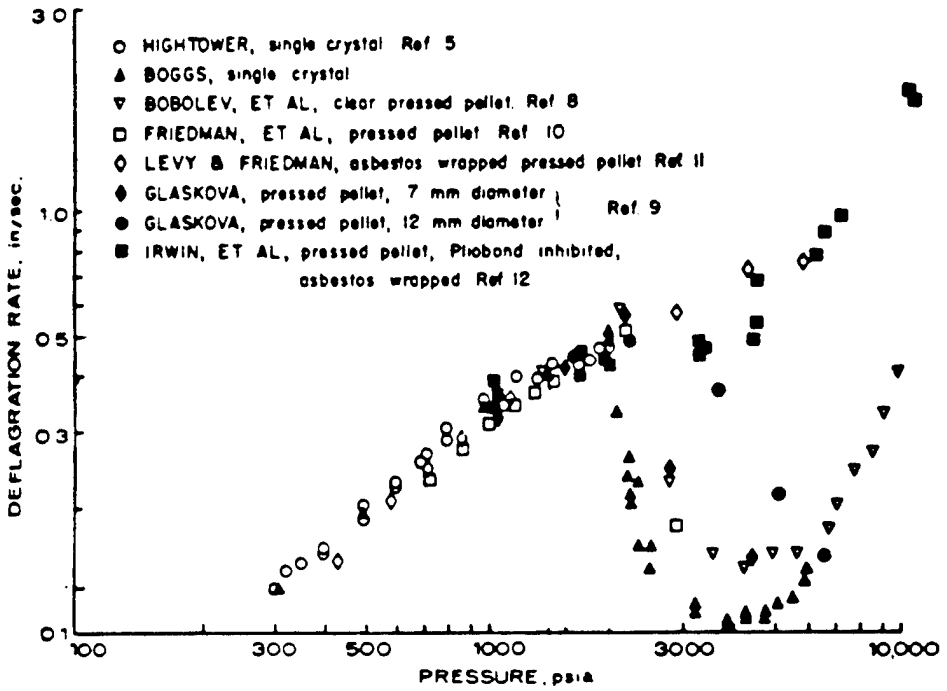

Fig. 1 Deflagration rate of ammonium perchlorate (taken from Ref. 2)

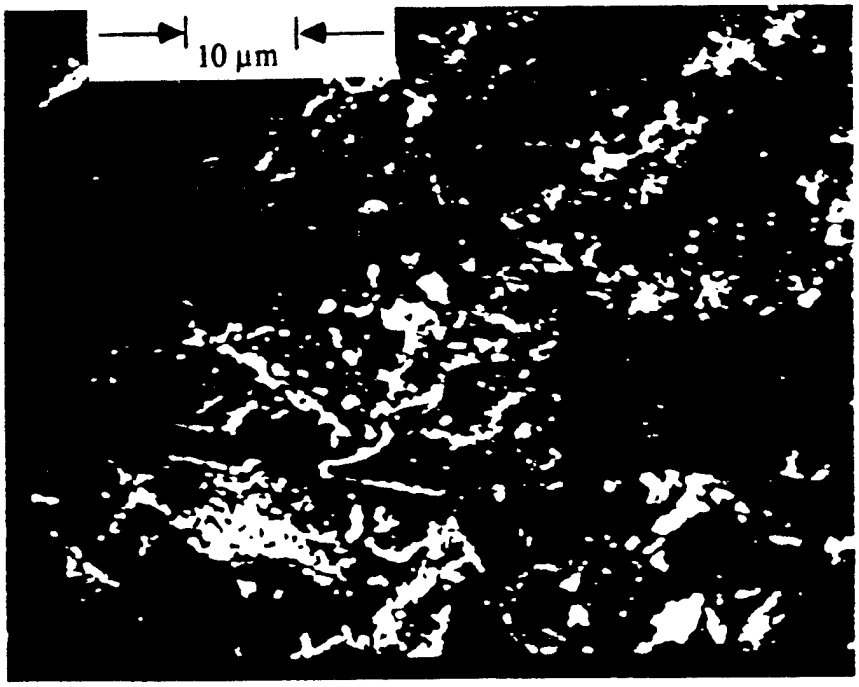

Fig. 2 Microscopic features of an unburned surface of a pressed pellet of "old Kerr McGee AP"

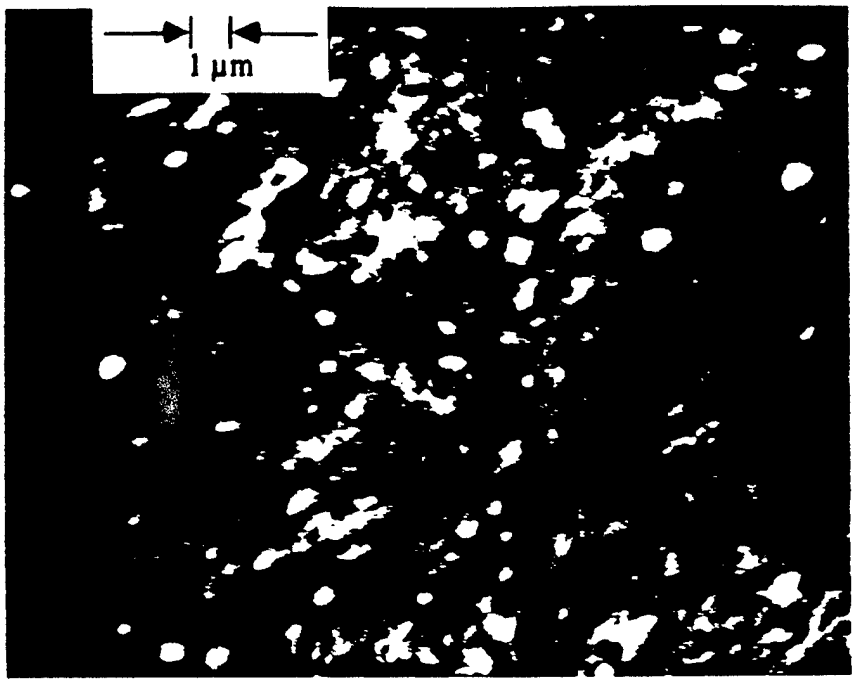

Fig. 3 Microscopic features of an unburned surface of pure single crystal AP

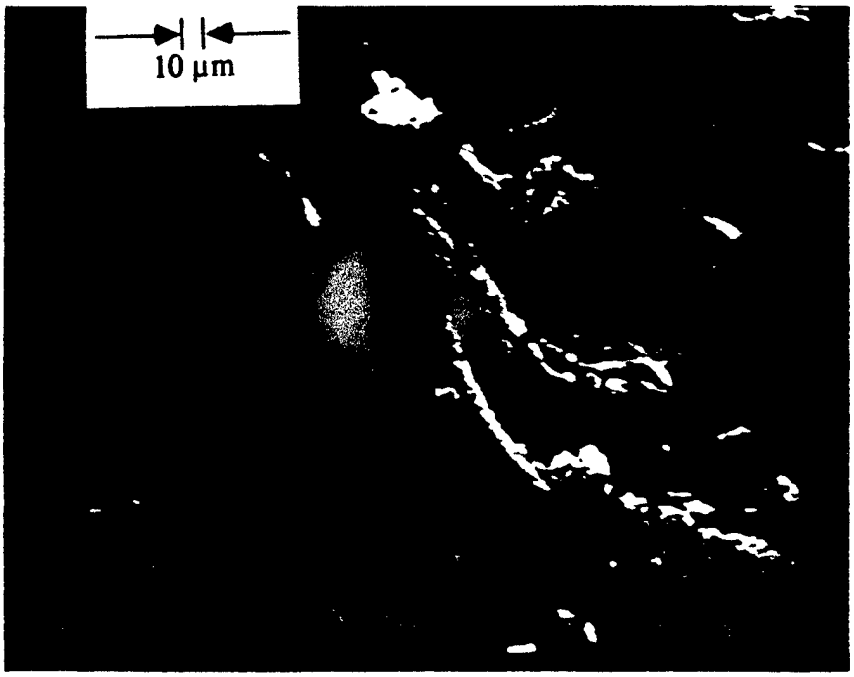

Fig. 4 An example of "ridges" on the surface of self-deflagrating AP

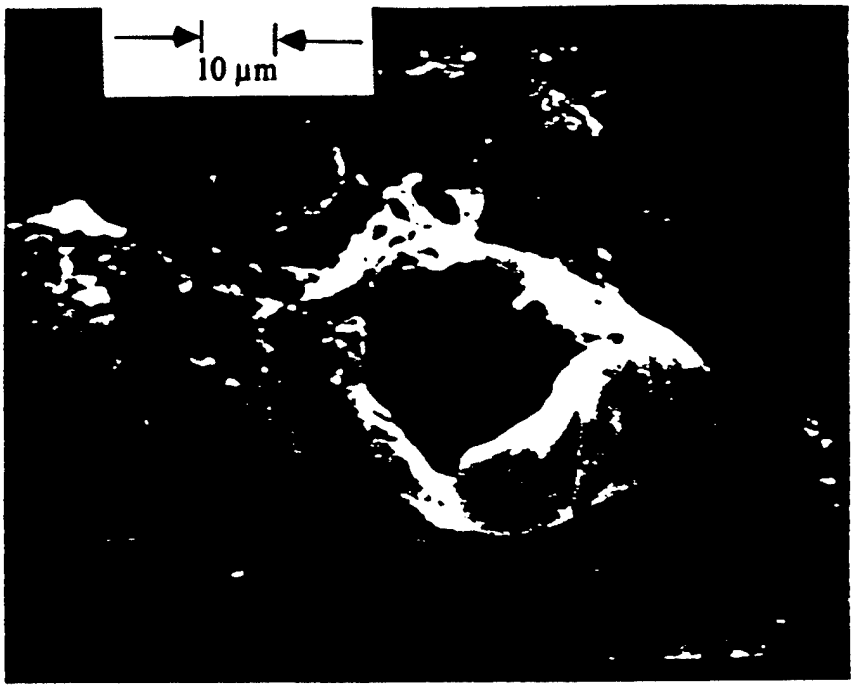

Fig. 5 An example of "puff balls" on the surface of self-deflagrating AP

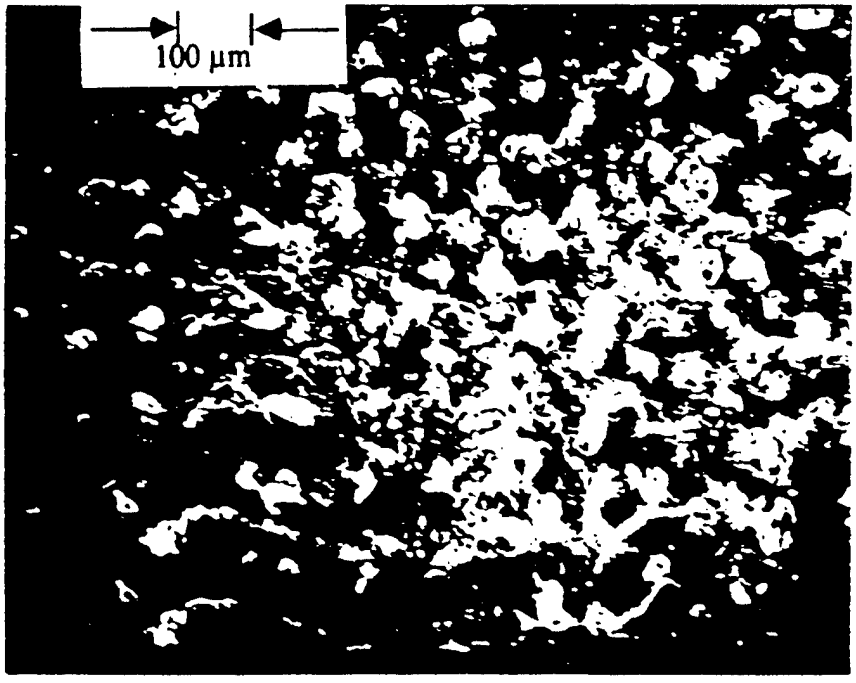

Fig. 6 Surface features of single crystal AP quenched by rapid depressurization at 400 psi

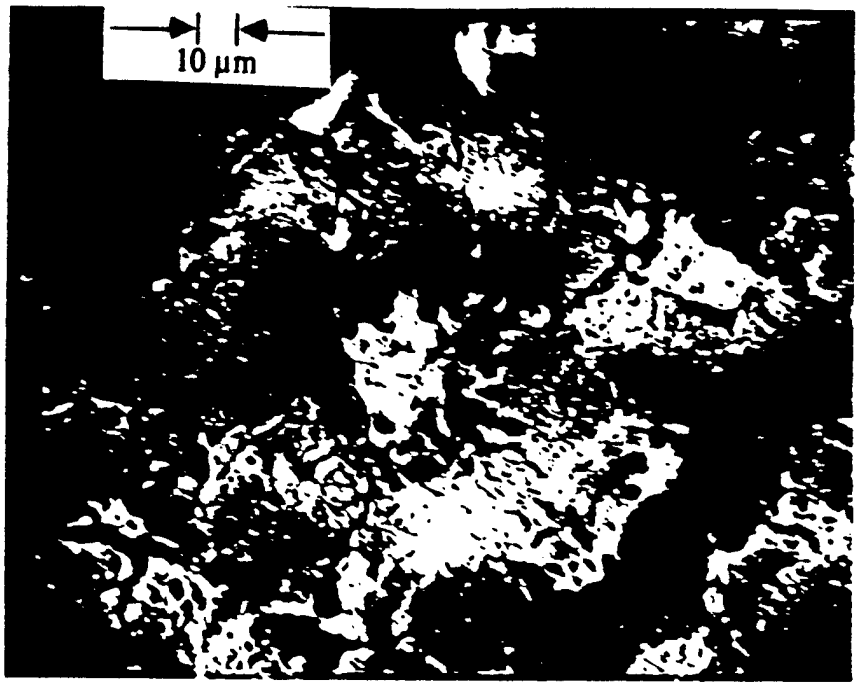

Fig. 7 Surface features of pressed AP quenched by rapid depressurization at 1000 psi

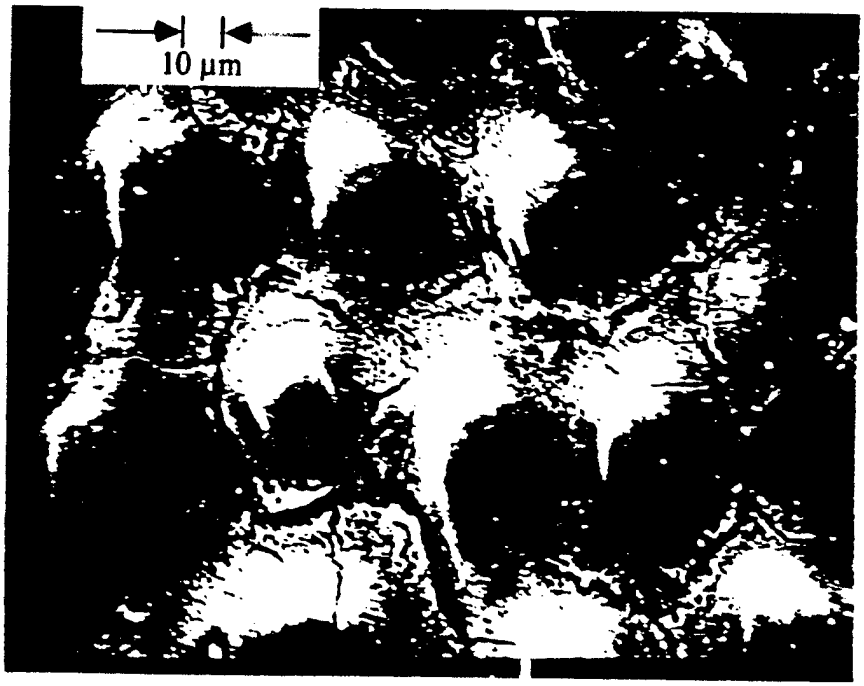

Fig. 8 Surface features of single crystal AP quenched by rapid depressurization at 2000 psi

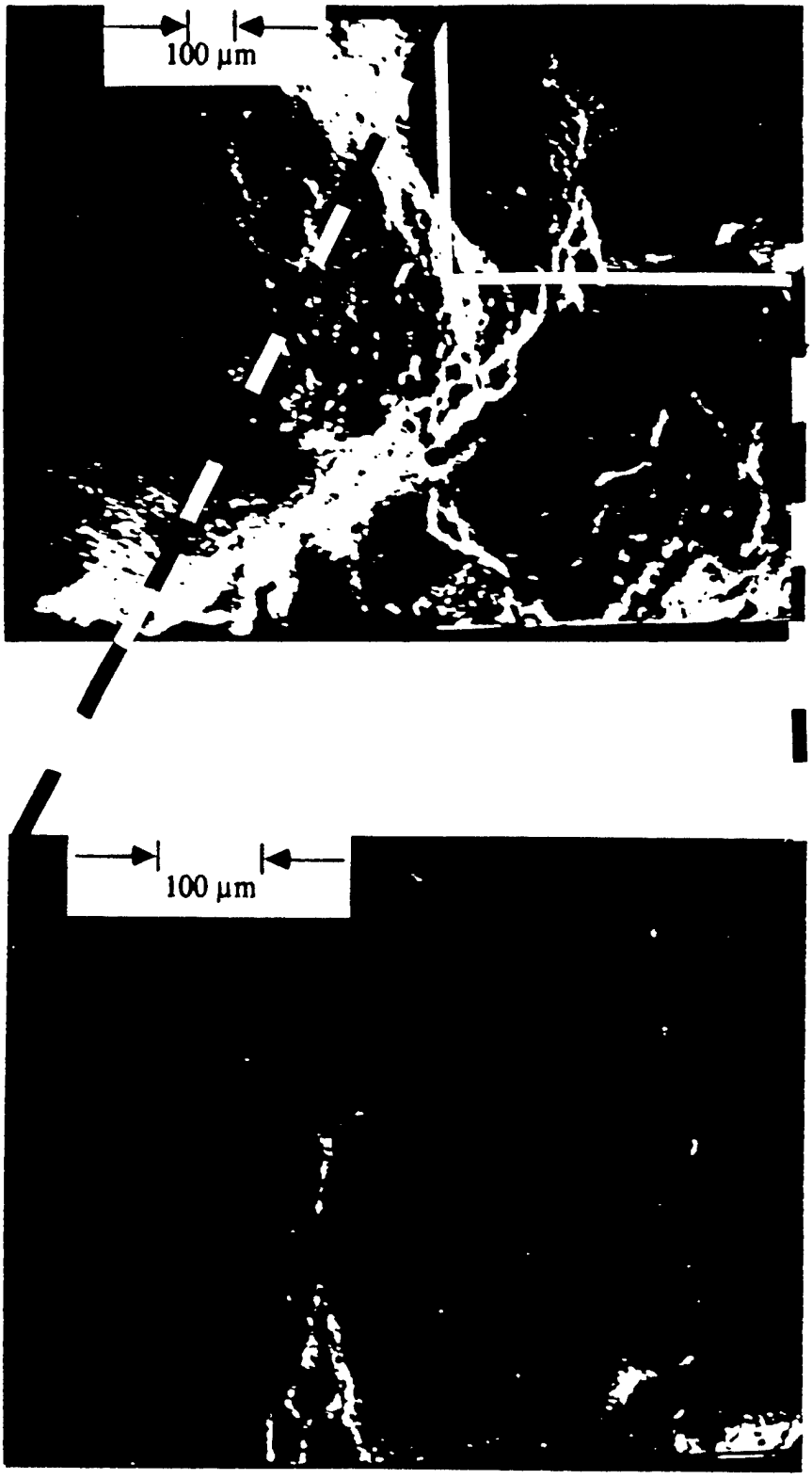

Fig. 9 Surface features of pressed AP quenched by rapid depressurization at 2300 psi

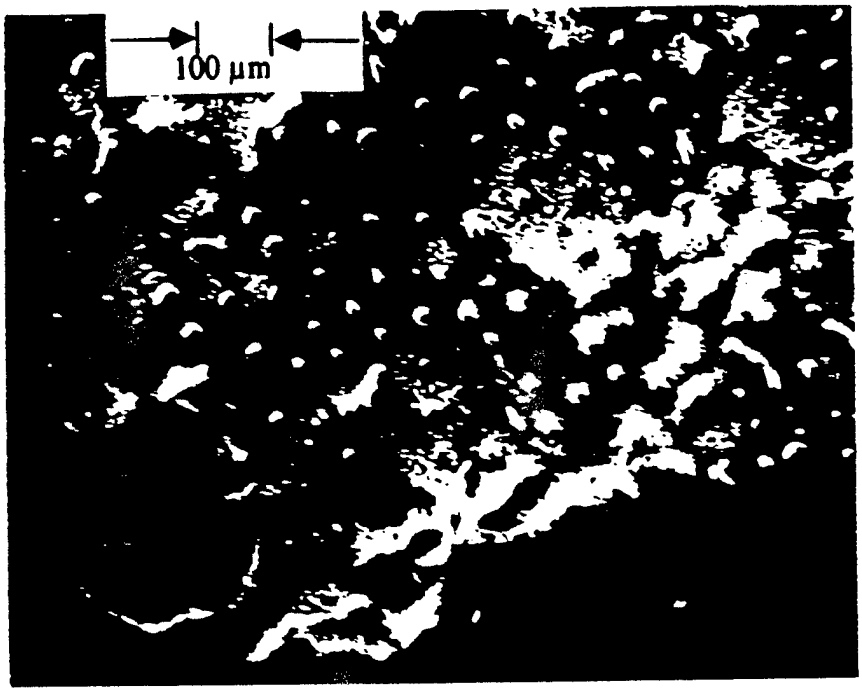

Fig. 10 Surface features of single crystal AP quenched thermally at 2000 psi

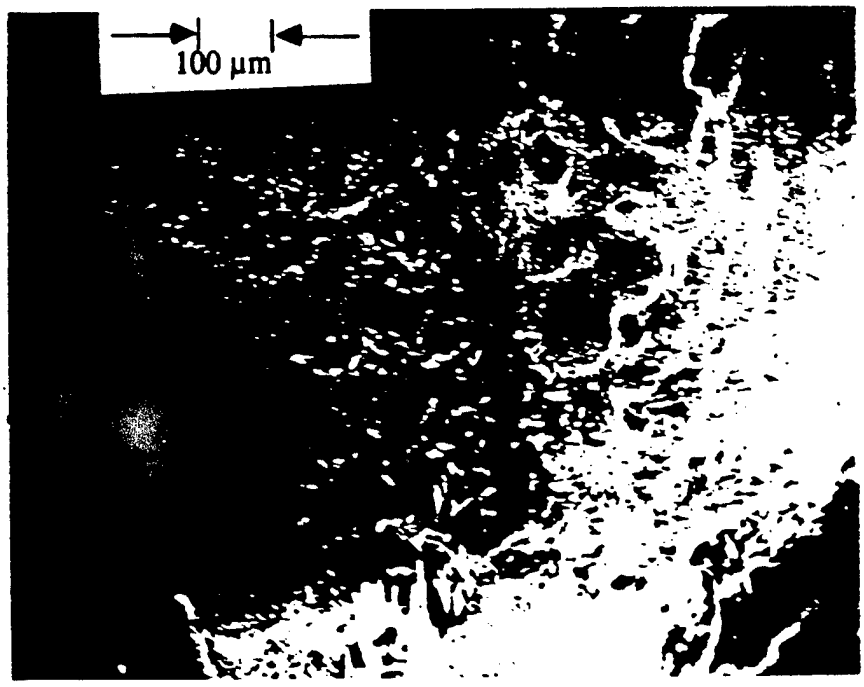

Fig. 11 Surface features of single crystal AP quenched thermally at 1000 psi

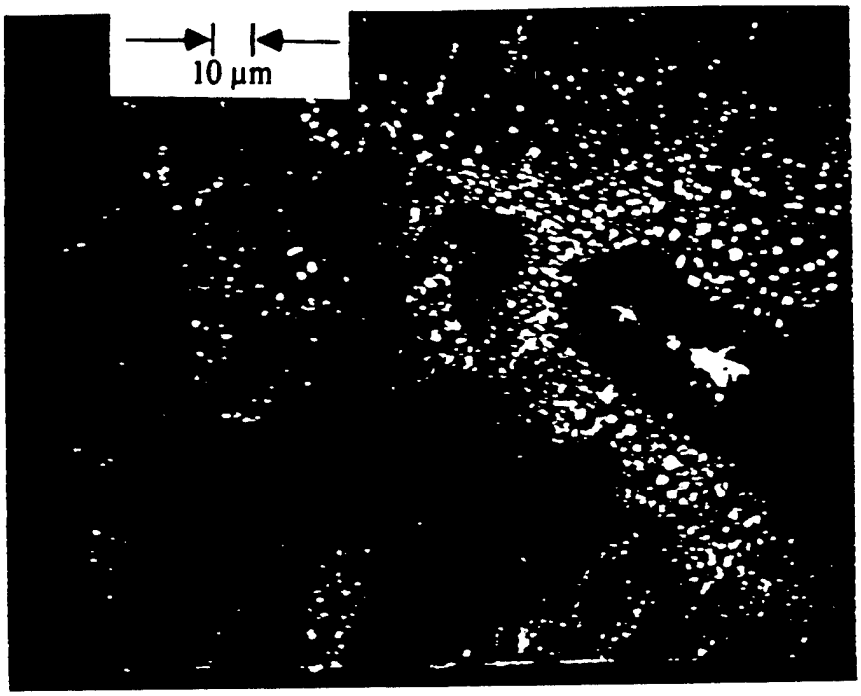

Fig. 12 Surface features of single crystal AP quenched thermally at 400 psi

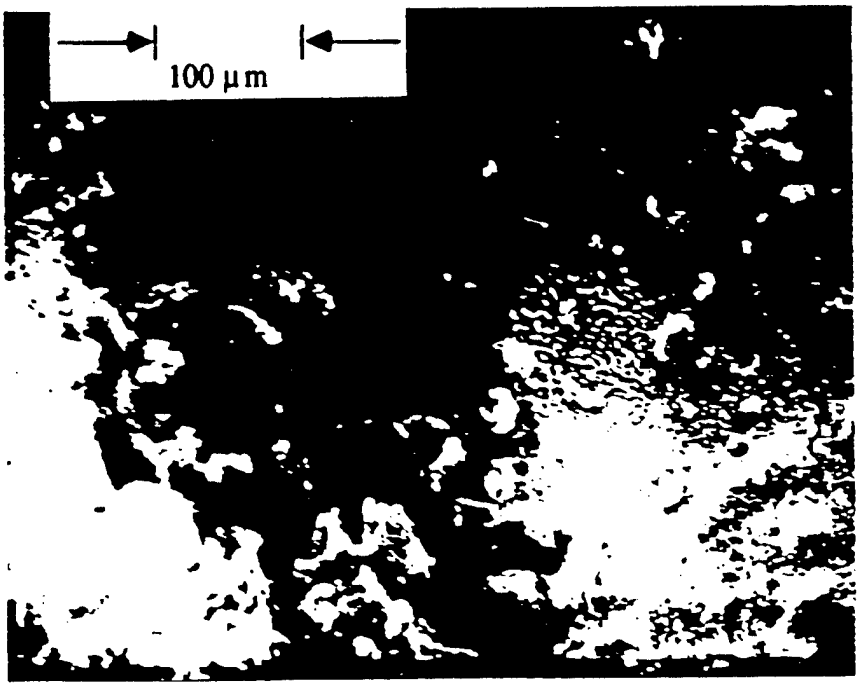

Fig. 13 Surface features of pressed AP quenched thermally at 2000 psi

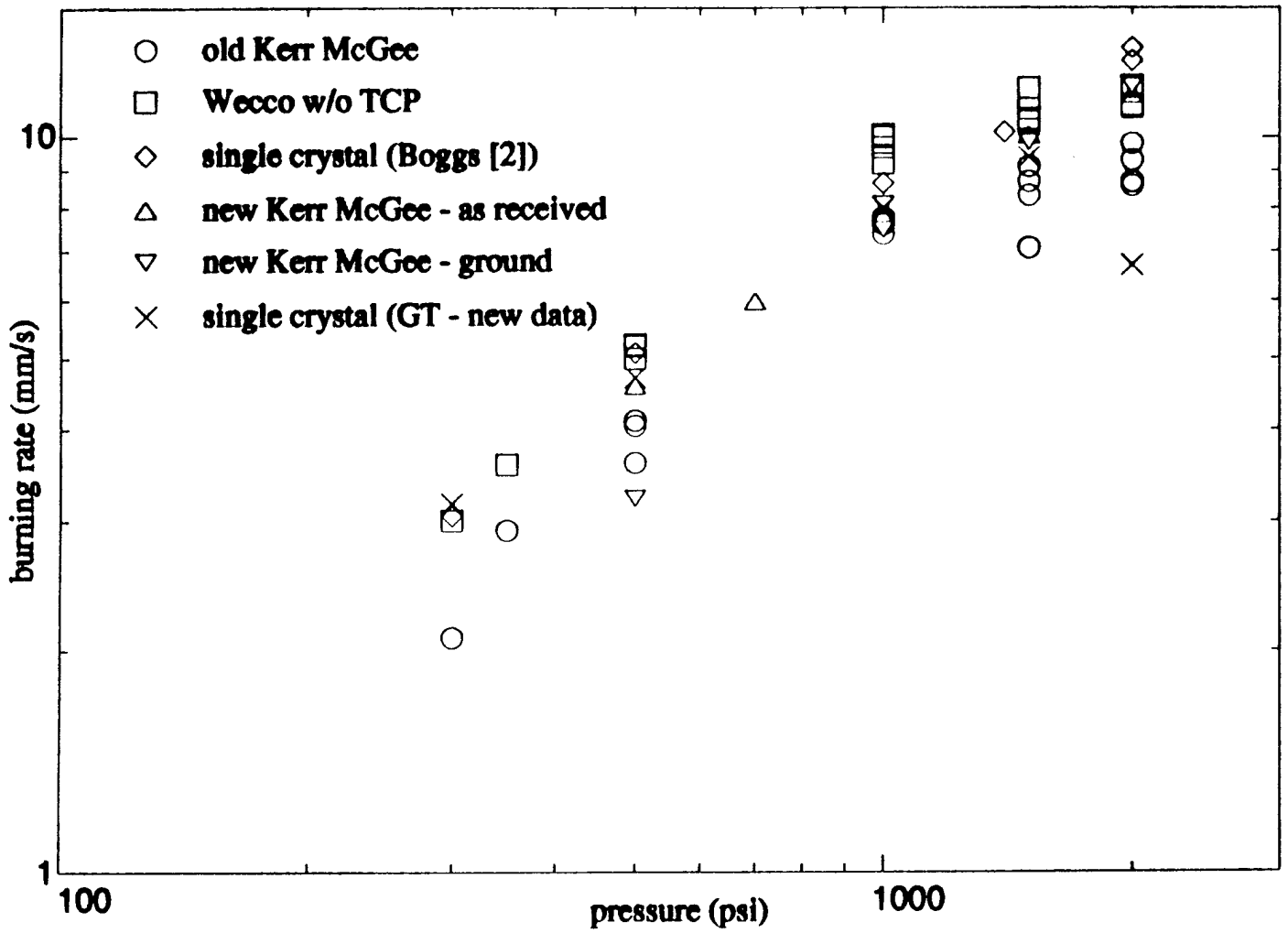

Fig. 14 Deflagration rates of various samples of AP tested in the present study

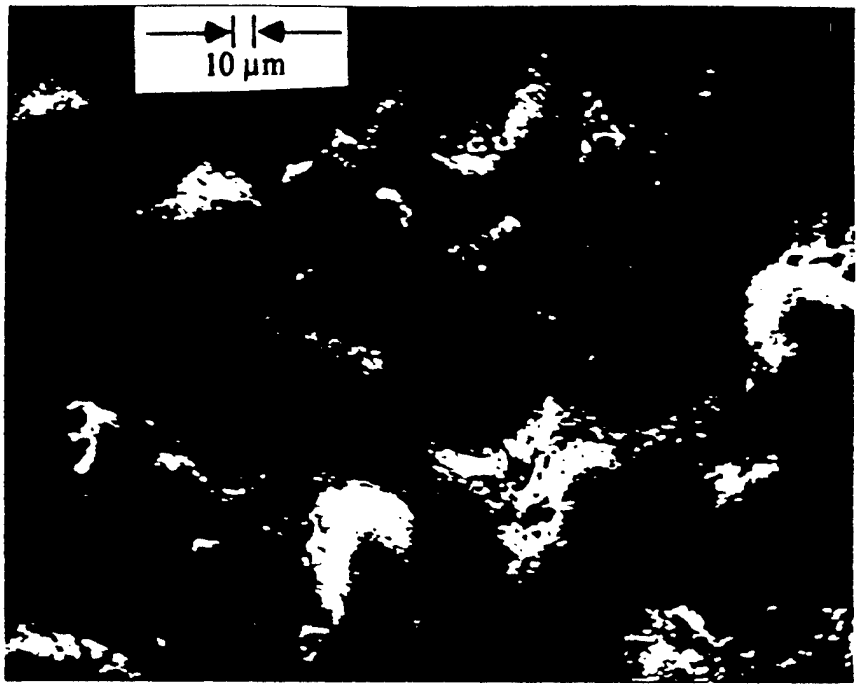

(a)

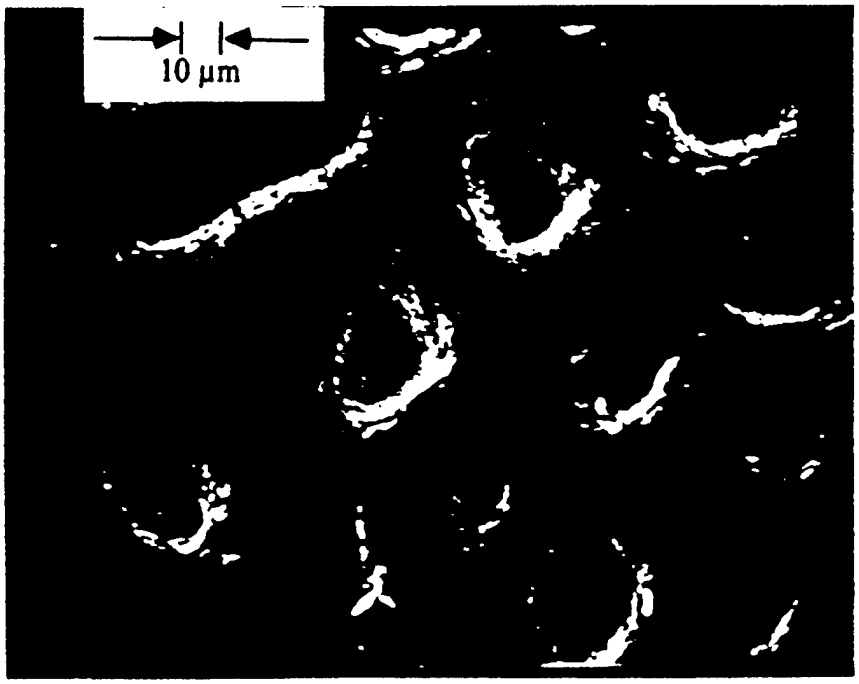

(b)

Fig. 15 Surface features of pressed pellets of ground new Kerr McGee AP quenched by rapid depressurization at (a) 1000 psi, (b) 2300 psi

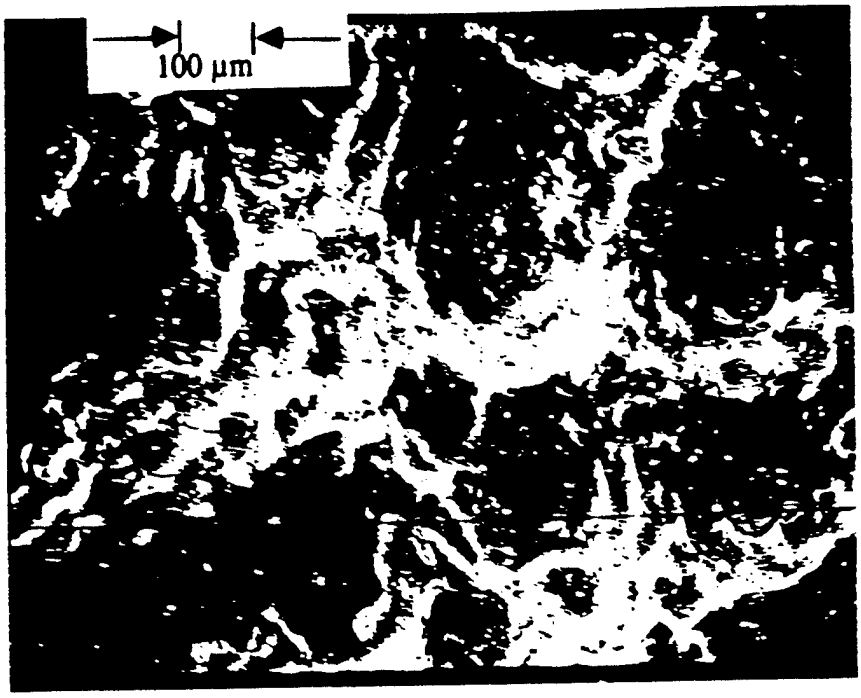

(a)

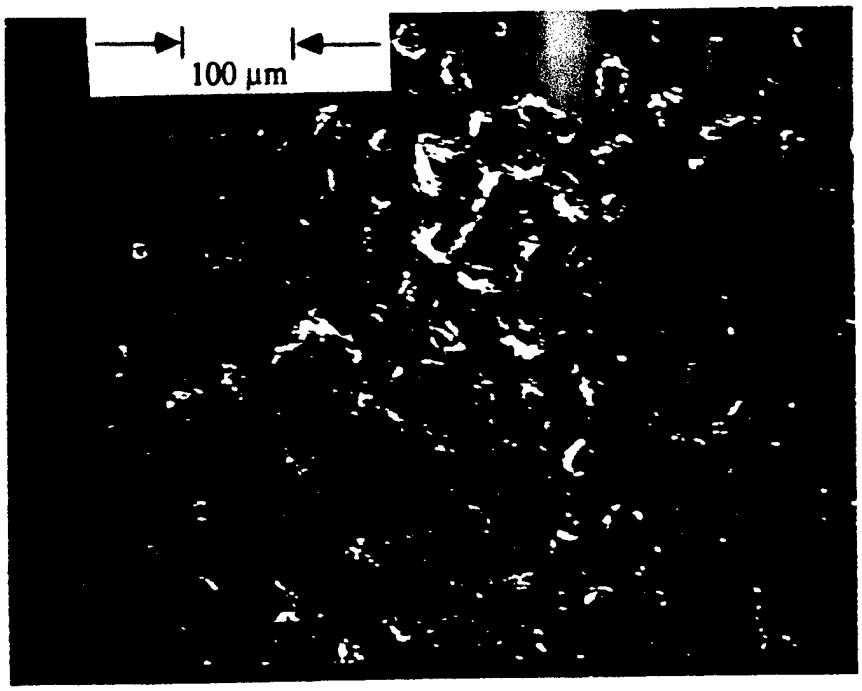

(b)

Fig. 16 Surface features of pressed pellets of Wecco AP without TCP quenched by rapid depressurization at (a) 1000 psi, (b) 2300 psi

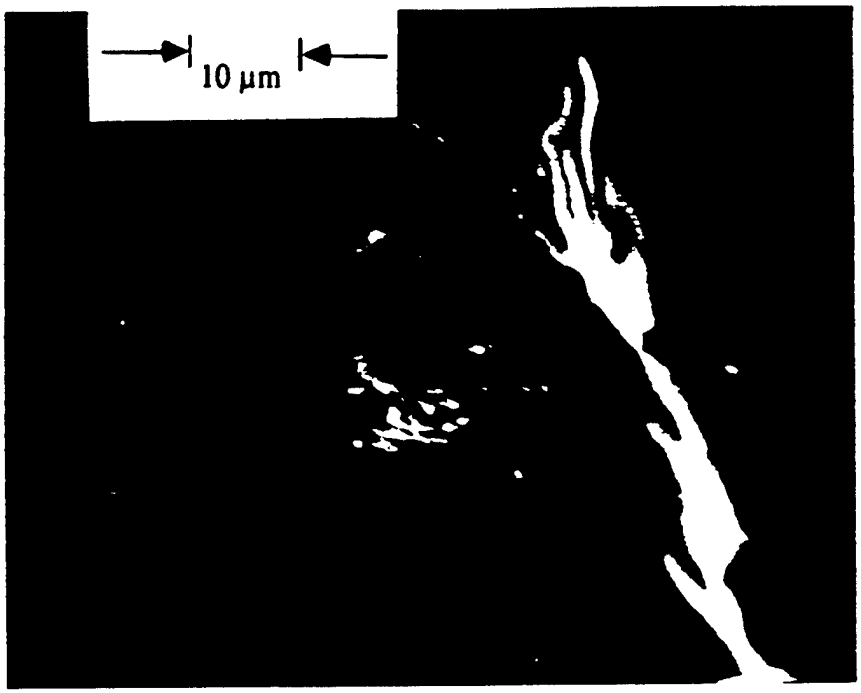

(a)

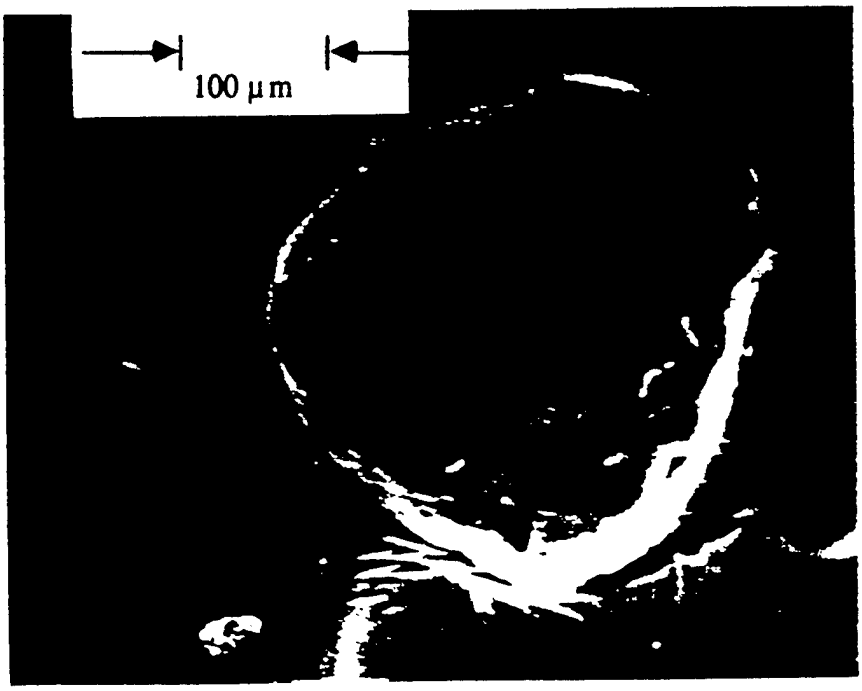

(b)

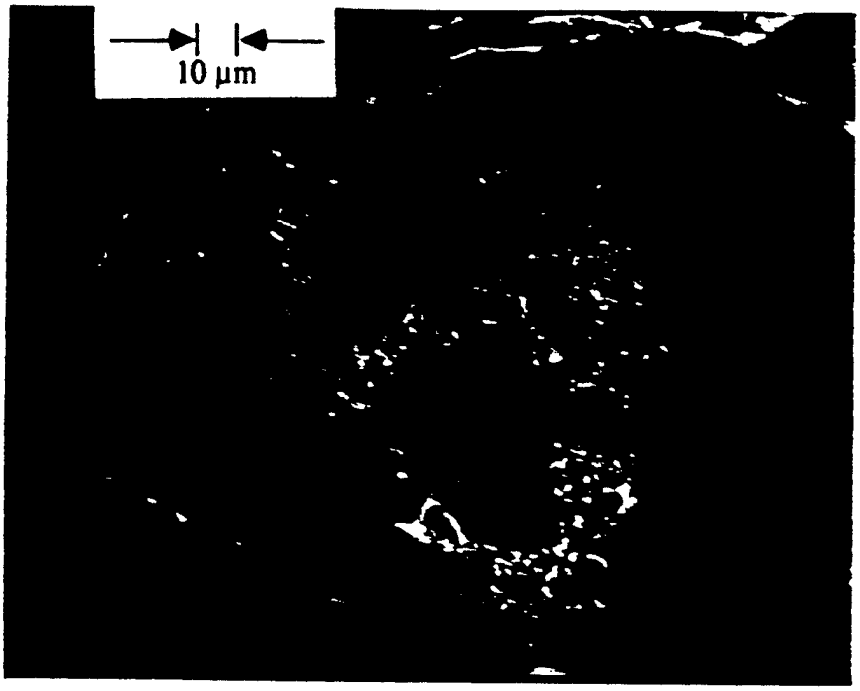

(c)

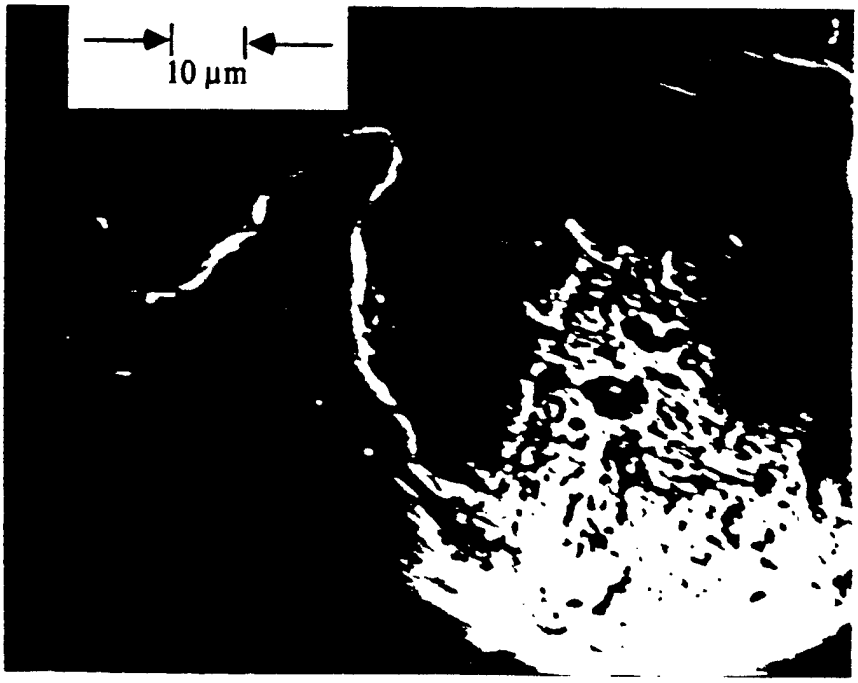

(d)

Fig. 17 Surface features of propellants quenched by rapid depressurization at 2300 psi; propellants contain 25% PBAN binder and different kinds of monomodal AP distributions: (a) 200 μm; (b) 400 μm; (c) 600 μm; (d) Wecco w/o TCP (200 μm). The first three are Kerr McGee AP.

APPENDIX K

Freeman, J. M., Jeenu, R., Price, E. W., and Sigman, R. K.

"Effect of Matrix Variables on Bimodal Propellant Combustion"

Proceedings of the 35th JANNAF Combustion Subcommittee Meeting

Tucson, AZ, Dec. 1998

EFFECT OF MATRIX VARIABLES ON BIMODAL PROPELLANT COMBUSTION

J. M. Freeman, R. Jeenu, E. W. Price, and R. K. Sigman
Georgia Institute of Technology,
School of Aerospace Engineering
Atlanta, GA 30332-0150

ABSTRACT

The goal of this paper is to present additional data on "anomalous burning" of monomodal propellants to further the interpretation of the mechanisms responsible for such "anomalous burning." Such information is needed for modeling the burning of bimodal propellants and rational design of high solids plateau burning in propellants.

Many studies have been conducted on fuel-rich "matrices" consisting of fine oxidizer particles and binder, These matrices, also known as "pocket propellants" because they simulate the pocket areas between coarse oxidizer particles in a bimodal propellant, were seen to exhibite:

a) plateau burning
b) spontaneous extinction in the same mid-pressure range as the plateaus, and
c) locally intermittent burning without complete extinction.

While this novel behavior was not fully characterized (e.g. as a function of oxidizer particle size, ratio of AP/binder, and type of binder), it became clear that the "anomalous" burning (a-c above) was strongly dependent on those propellant variables.

In this study, various formulations were tested to note the effect of changing: AP/binder ratio, AP particles size, binder/ binder curative, and addition of catalysts/ballistic modifiers. With the addition of very coarse AP, bimodal propellants were then formulated from these matrices to determine whether the trends seen in the monomodal matrices would show up in the propellants. From those analyses the dependence of propellants characteristics on the matrix formulation is then discussed.

A standard window bomb setup with video photography was used to obtain the burn-no-burn domains, burning rates, and macroscopic details of the "anomalous" burning behavior.

INTRODUCTION

Historically, a wide variety of solid rocket propellants have been formulated and tested. Of particular interest to this study are "wide-distribution", bimodal ammonium perchlorate-composite propellants. These propellants consist of very coarse and very fine ammonium perchlorate (AP) crystals (with a large difference in average diameters, say 5-200 times), held together in a polybutadiene binder, which may also contain other additives for stability or enhanced performance. Such propellants have been seen to show intriguing burning-rate behavior as a function of pressure, yielding plateaus in the burning rate versus pressure curves.

Previous studies(Ref. 1) on the "matrix" of fine AP and binder that exists between the coarse particles has shown "anomalous" behavior that could not be explained by the simplistic models of the time. Such "anomalous" behavior included intermittent burning and spontaneous quenching of the burning matrix at certain pressures. Very fuel-rich matrices have been seen to burn at high and low pressures, but not in an intermediate range (500-1500 psi) (Ref. 2). This same mid-pressure region is typically where the plateaus occur in bimodal propellants. The present study is aimed at understanding the link between the effect of changing the composition of the matrix and the plateau behavior.

Several variables can be adjusted in the formulation of a propellant matrix. In general, matrices contain only a binder and fine particles of an oxidizer; thus one can change the type of oxidizer, the type of binder (and in

---

Distribution Statement - Approved for public release, distribution unlimited.

* This work was performed under grant no. N00014-95-1-0559 from the Office of Naval Research, with Dr. Judah Goldwasser as the Technical Monitor.

which can have varying sizes and types. Each new formulation would need to be tested over a wide range of pressures as well, leading to a enormous test set should all the possibilities be explored. Therefore, this study takes two baseline formulations and makes various small changes in one variable at a time in order to more fully understand it's effect in the burning characteristics. Then a set of several bimodal propellants are tested to see how these changes affect the behavior of more realistic propellants.

EXPERIMENTAL

TESTING STRATEGY

Previous studies defined a multi-dimensional space of at least five independent variables (oxidizer particle size, type of binder, type of oxidizer, oxidizer-to-fuel ratio, and additive) as potential variables that could affect the burning rate of a very fuel-rich matrix as a function of pressure (Refs. 2 & 3). In these studies, the AP particle size and O/F ratio where seen to have a significant effect on the pressure domain in which the matrix would burn. The choice of binder also played an important role in defining the burn domain.

For this study, a baseline matrix oxidizer-to-fuel ratio, or fine AP-to-binder ratio (f_{AP}/b) as it will be called in the study, was set at 70% 10-μm AP and 30% binder, by mass. Based on the earlier results, a polybutadiene acrylonitrile acrylic acid (PBAN) matrix should burn across the entire testable pressure range, the isophorone diisocyanate (IPDI) cured hydroxyl-terminated polybutadiene (HTPB) would be expected to have a mid-pressure (800-1500 psig) no-burn region, and the dimeryl diisocyanate (DDI) cured HTPB wasn't expected to burn except at low pressures (below 300 psig). Due to the limited burn domain of the HTPB-DDI, its baseline matrix f_{AP}/b was raised to 73/27. From these baselines, systematic changes were made to investigate the effects of one variable at a time.

Using these matrices, a family of bimodal propellants was developed by adding 200-μm AP until a total AP loading of 87.5%-by-mass was obtained. Both the coarse AP and fine AP sizes are varied to investigate their effect. The mass distributions for the baseline matrix and propellant are given in Tables 1.

EXPERIMENTAL TECHNIQUE

Combustion photography (video) was used as the primary technique in this study. The method used was routine and the window bomb design was similar to that used by Hightower and Price (Ref. 4), operable in the atmospheric to 2000 psi pressure range. Formulations are typically tested at nine pressures: 100, 300, 500, 800, 1000, 1200, 1500, 1800, and 2000 psig. Burning rates were obtained from video pictures as described in detail elsewhere (Ref. 5). The binders used in this study were HTPB and PBAN, with the former being cured by two different agents, DDI and IPDI. Table 2 presents the composition used in the preparation of each binder.

The AP used in this study comes from several different sources. The "2 μm AP" comes from AP and prepolymer mixtures supplied by Dr. Carol Campbell of the Thiokol Corp. Dr. Karl Kraeutle, formerly with the Naval Air Warfare Center, provided the "10 μm AP". All other particle sizes come from a high-purity Kerr-McGee lot which is sieved to obtain a narrow distribution around a median (i.e. "200 μm" falls between 180-212 μm). The typical propellant test samples were 4 mm x 3 mm x 10 mm, and were cut from 10 gram batches. These batches were hand-mixed and cured at a temperature of 50° C for 2 or 7 days, depending on the binder.

RESULTS AND DISCUSSION

EFFECT OF BINDER/CURATIVE

The binder has one of the largest effects on the burning rate and flammability of the matrix. Figures 1-3 show the effect of binder and curative on the burning rates of matrices and bimodal propellants. At the baseline composition of f_{AP}/b=70/30, the PBAN matrix burns across the entire pressure range. The IPDI-cured HTPB matrices have a large no-burn domain between 800-1800. When DDI is used to cure the HTPB, the matrix will not burn above 50 psig. Polysulfide (PS) results from the work of Bastress (Ref. 6) can also be compared since his study used the same mixture ratio and a similar AP particle size. The burning rate of the PS matrix is the highest of the four, as seen in Figure 1. This trend in burning rates (PS>PBAN>HTPB-IPDI>HTPB-DDI) is directly opposite the

trend of the degree to which the binders melt before decomposition. DDI-cured HTPB is regarded to have the highest degree of "binder melt" and PS has the least, but what effect melt plays on the burning surface has yet to be definitively determined.

In bimodal propellants with 200 μm coarse AP particles, the effect of binder is not noticeable between the PBAN and HTPB-IPDI propellants, with a 70/30 matrix, as in Figure 2. A DDI-cured HTPB propellant with a 73/27 was tested and compared to similar IPDI-cured and PBAN propellants. Again there was little difference between the PBAN and HTPB-IPDI propellants, though the PBAN had a consistently higher burning rate. The HTPB-DDI propellant's rate was similar to the others, however, the propellant did not burn above 500 psi, shown in Figure 3.

EFFECT OF AP PARTICLE SIZE

Effect in Matrix

As reported previously, the size of the AP in the matrix has a large effect on the no-burn domain. Smaller particles are less apt to burn, but generally the matrix with finer particles will burn at a faster rate at pressures where it does burn. Figure 4 shows the particle size effect in HTPB-IPDI binder matrix at O/F of 70/30. The 2-μm AP matrix burns only around 300 psig. The 10-μm matrix has a large no-burn domain from 800-1800 psig. There is a small no-burn domain for the 75-μm matrix, while the 200-μm mix has a plateau (or mesa) above 1000 psi, where the others do not burn.

Effect of Coarse AP Size in Bimodal Propellants

The baseline PBAN propellant was modified by using either 300 μm or 400 μm coarse AP, in place of the standard 200 μm. Figure 5 illustrates that increasing the coarse AP size promotes plateau burning. The larger particles tended to give burning rates that dropped off above 1000 psi giving a plateau until 1500 psi, where they rose again.

The plateau effect occurs at a lower pressure in 88% solids HTPB-DDI propellants with matrix f_{AP}/b=73/27, as seen in Figure 6. The standard 200 μm formulation has a decrease in the slope of the burning rate between 200 and 800 psi. Increasing the coarse particle size decreases the exponent of the curve in this region, resulting in a plateau. Conversely, decreasing the coarse size tends to yield a smooth, straight curve with little or no plateau.

Effect of Fine AP Size in Bimodal Propellants

The size of the fine AP in the matrix of a bimodal propellant has little effect on the propellants burning rate, as seen in Figures 7 & 8. In Figure 7, the rates for several bimodal propellants with 70/30 f_{AP}/b matrices are nearly identical. Similar results were obtained for HTPB propellant with 73/27 matrices, as presented in Figure 8. Little or no effect is seen for the IPDI-cured propellants, as in 70/30 case. The DDI-cured propellant with 10-μm AP would not sustain combustion above 500 psig, but was at the same rates as the IPDI-cured where it did burn. The rates for 2-μm DDI-cured HTPB propellant were supplied by Thiokol and are used for comparison (our tests showed the burning to be intermittent in the pressure range above 700 psi).

EFFECT OF O/F RATIO

Effect on Matrix

The effect of the matrix O/F, or f_{AP}/b, has been reported earlier for matrices of interest to this study (Ref. 3&4). It was found that the flammability limits of the matrix steadily increased as the percentage of AP increased, reducing the no-burn domain. Figure 9 shows this effect for several monomodal mixes of 200-μm AP and HTPB-IPDI binder.

Effect of Matrix O/F in Bimodal Propellants

In general, slight changes in the matrix O/F ratio have little effect in the bimodal propellant, at least for the levels tested. Figure 10 shows the effect of increasing the matrix to 73/27 = f_{AP}/b in a PBAN bimodal propellant with 87.5% total solids. The same effect is seen when increasing the fine AP content in a DDI-cured HTPB

bimodal propellant with 88% solids, as seen in Figure 11. Starting at 73/27 and increasing to 76/24 has little to no effect as with the PBAN case. Further increase to 79/21 does show a substantial increase in burning rate, and high rates may likely occur in the other propellants when the matrix is very high in fine AP.

Effect of Total Solids Loading

At high solids loadings used for practical propellants, there was only a nominal effect of increasing the total solids from the baseline of 87.5% to 88%. Changing the baseline PBAN propellant to 88% total solids did not yield a significant change in the burning rate curve, as seen in Figure 12. Likewise, increasing the HTPB-IPDI baseline to 88% gave no appreciable difference. At these high loadings, a key factor in plateau behavior may be the interstitial spacing between coarse particles. Increasing the total solids by means of adding coarse AP will reduce the spacing slightly. This would tend to lead to faster burning of the matrix, as it will be in closer proximity to the hot leading edge part of the diffusion flame attached to coarse particles. However, this reduction in spacing is not as great as the changes affected from altering the size of the coarse particles, and the effect is not significant at these loadings.

EFFECT OF TRANSITION METAL OXIDES AS CATALYSTS

Effect of Various Metal Oxides

Many studies have investigated the use of transition metal oxides (TMOs) in increasing the burning rate of propellant. Kishore and Sunitha (Ref. 7) performed a comprehensive literature survey on the effect of TMOs in composite solid propellants. Fong and Hamshere (Ref. 8) found that Fe>Cr>Cu in catalytic ability in their tests involving pthalocyanines and CTPB. Kishore, Verneker, and Sunitha (Ref. 9) found Fe>Co in tests using TMOs and CTPB and polysulfide. Chakravarthy determined that the method by which iron was included in the propellant did not affect its ability to act as a long as the catalyst concentrated on the surface. By assuming other TMOs work by similar means and require a concentration on the surface, the results by differing methods of metal inclusion above may be expected to be somewhat universal for any binder and TMO.

To test this hypothesis, five TMOs were tested in an AP/PBAN=70/30 matrix. The catalysts were all present in the amount of 4.17% (equivalent to 2% in a bimodal propellant with 87.5% total solids). The catalysts used were: Fe_2O_3, Co_3O_4, CuO, Cr_2O_3, and TiO_2. The first four TMOs have been tested in various propellants but few results were available regarding the effect of TiO_2 or whether it had any catalytic effect.

As seen in Figure 13, Fe_2O_3 has the greatest effect, as would be expected from historical data. Likewise, the previous trends are confirmed for the other known catalysts: Fe>Co>Cr>Cu in catalytic ability. Iron oxide is consistently the most effective, especially at low pressure, the other four TMOs having similarly sloped curves, at nearly similar rates. TiO_2 has been seen to give increased burning rates and plateau behavior in some bimodal propellants, though the method was not attributed to catalysis. From these results, it would appear that TiO_2 acts in a manner similar to the other TMOs. Furthermore, copper, cobalt, and chromium may be as effective as titanium in producing plateau behavior, based on the similar rates of the matrices.

Effect of Initial Concentration

Varying amounts of catalyst were added to a AP/HTPB-DDI=73/27 matrix to determine the dependence on initial concentration, shown in Figure 14. The uncatalysed matrix did not burn at any pressure tested above 100 psig, and only very slowly at 50 psig. The addition of 0.05% ferric oxide by mass in the matrix increased the deflagration limit to 500 psig and doubled the rates of the uncatalysed matrix. Increasing the amount to 0.2% extended the burning domain to at least 2000 psig, with a further increase in the rate at a given pressure. At the 2% level, the rates were approximately four-and-a-half times higher than the uncatalysed matrix.

TiO_2 was not as effective as Fe_2O_3 was in the HTPB-DDI matrix, consistent with its being less effective in the PBAN mixes (Figure 15). In this case, the TiO_2 was not able to get rid of the no-burn region, even at the 4% level in the matrix. Neither mixes with 2% or 4% TiO_2 burned above 200 psig, though the increase in concentration did slightly increase the rate between mixes. Though it appears to be catalytic, TiO_2 does not have as profound an effect as Fe_2O_3 does. Earlier investigators determined Fe_2O_3 to have a catalytic effect on AP decomposition by itself.. TiO_2 does not appear to do this in an significant amount, based on Thermal-Gravimetric Analysis (TGA). TGA of AP alone, or binder alone, showed no effect of the TiO_2. When the propellant itself tested, with the binder and AP together, the TiO_2 did have an effect, as seen in Figure 16. It is theorized that the TiO_2 may work by "cracking" the heavy hydrocarbon vapors of the decomposing binder as well as decomposing the $HClO_4$ vapors

coming off the AP near the surface. Any such changes to the gaseous products would not yield an change in TGA studies that measure mass loss from the solid. It may also be that the TiO_2 creates species to be released from the solid or near the surface (such as $HClO_4$ decomposition products) which attack the binder and further increase the mass loss, as seen by the TGA results.

EFFECT OF ADN

Addition of ADN to Matrix

Two matrices were formulated with a blend of 10-μm AP and 30-μm ADN to yield a matrix composition of AP/ADN/binder = 46/24/30, consistent with oxidizer/binder = 70/30. . It was expected that use of a energetic oxidizer such as ADN would have increased the burning rate. The AP/ADN/PBAN matrix had a lower burn rate than the baseline AP/PBAN until approximately 1500 psig, where the baseline was in a plateau region, as seen in Figure 17. With ADN in the HTPB-IPDI matrix, the no-burn domain was eliminated, though the rates were not significantly higher in this case either.

Substitution of 10% AP for ADN in Bimodal Propellants

In a previous study (Ref. 10), ADN particles were used to replace either the fine AP, coarse AP, or both in a PBAN bimodal propellant with 10 μm and 300 μm AP and f_{AP}/b=70/30. In these bulk amounts, the ADN had a tremendous effect in raising the burning rate values with the unfortunate side-effect of giving a high exponent.

In the present study, bimodal propellants with 10% of their mass replaced with coarse(350 μm) or fine (30 μm)ADN in place of the coarse or fine AP, respectively, were formulated. Due to the limited availability of ADN, not enough pressures were tested for the curves to be well formed, but the results, given in Figures 18-20, are qualitative.

Figure 18 shows the effect substituting coarse ADN in a PBAN propellant, at the 10% level as well as replacing all the coarse AP. The substitution dramatically increases the burning rate at high pressures, nearly doubling the baseline. At low pressures, however, the rates are not increased a third as high, resulting in much steeper exponents for the ADN-modified curves. The effect of substituting fine ADN for fine AP is shown in Figure 19. In these propellants the rates are not effected as much, though they are significantly higher than the baseline. Replacement of 10% of the fine ADN increases the rate only one-and-a-half times at high pressures, and even less at lower pressures, similar to the trend with the coarse ADN. Replacing 10% of the propellant mass with ADN in place of AP gives a greater increase in burning rate when using HTPB-IPDI, as seen in Figure 20. Both the fine and coarse ADN show a steep climb in burning rate after 500 psig, before which the rates are close.

COUPLED EFFECT OF CHANGING MULTIPLE VARIABLES

Though varying one parameter at a time as in this study is useful for gaining general insight on specific variables, there is the problem of coupling between multiple variables. Figure 21 shows the effect of a small increase in f_{AP}/b in an HTPB-DDI bimodal propellant and a change in fine AP particle size. Between using 2-μm particles and 10-μm particles there is only a slight difference at f_{AP}/b = 73/27. For 10-μm fine particles, there is insignificant change between f_{AP}/b = 73/27 or 76/24. But at 76/24, the change from 10-mm fine AP particles to 2-mm particles is tremendous, around 800 psig, the burning rate curve breaks and makes a sharp rise to triple the burning rate at high pressures. An additional complication is that all four of these propellants have approximately 2% TiO_2 added to them. This three-variable coupling produces the high, unexpected rate in Figure 21.

CONCLUSION

Small adjustments to the matrix composition has been seen to greatly effect the no-burn domain of the matrix. However such changes made to a bimodal propellant are not as significant. Several different propellants have been formulated during this study, all having nominally the same burning rate. Some large deviations from the baseline propellant's burning rate due arise when multiple changes are made, especially when catalysts are added. The physical role of the catalysts is not yet fully understood and further work is needed before a controlling mechanism can be identified. Additionally, work should be undertaken to characterize the coupled effects of small

CONCLUSION

Small adjustments to the matrix composition has been seen to greatly effect the no-burn domain of the matrix. However such changes made to a bimodal propellant are not as significant. Several different propellants have been formulated during this study, all having nominally the same burning rate. Some large deviations from the baseline propellant's burning rate due arise when multiple changes are made, especially when catalysts are added. The physical role of the catalysts is not yet fully understood and further work is needed before a controlling mechanism can be identified. Additionally, work should be undertaken to characterize the coupled effects of small changes in several variables. In conclusion, this study has present a large volume of data to further the understanding of bimodal propellant combustion and the changes due to changes in composition.

REFERENCES

1. Steinz, J. A., Stang, P. L., and Summerfield, M., "The Burning Mechanism of Ammonium Perchlorate-Based Composite Solid Propellants," Aerospace and Mechanical Sciences Report No. 830, Guggenheim Laboratories for the Aerospace Propulsion Sciences, Department of Aerospace and Mechanical Sciences, Princeton University, Princeton, N. J., February 1969. .

2. Freeman, J.M., Price, E.W., Chakravarthy, S.R., and Sigman, R.K., "Burning Characteristics of Monomodal Ammonium Perchlorate/Hydrocarbon Binder Propellants," *Proceedings of the 34th JANNAF Combustion Subcommittee Meeting*, CPIA Pub. 662, West Palm Beach, FL, October 27-30, 1997.

3. Freeman, J.M., Price, E.W., Chakravarthy, S.R., and Sigman, R.K., "Contribution of Monomodal AP/HC Propellants to Bimodal Plateau-Burning Propellants," AIAA Paper 98-3388, 34th AIAA/ASME/SAE/ASEE Joint Propulsion Conference, Cleveland OH, July 13-15, 1998.

4. Chakravarthy, S. R., "The Role of Surface Layer Processes in Solid Propellant Combustion," Ph. D. Thesis, Georgia Institute of Technology, Atlanta, Georgia, 1995.

5. Hightower, J.D. and Price, E.W., "Combustion of Ammonium Perchlorate," *Eleventh Symposium (International) on Combustion*, The Combustion Institute, 1969.

6. Bastress, E. K., "Modification of the Burning rates of Ammonium Perchlorate Solid Propellants by Particle Size," Ph. D. Thesis, Princeton University, Princeton, New Jersey, January 1961.

7. Kishore, K. and Sunitha, M.R., "Effect of Transition Metal Oxides on Decomposition and Deflagration of Composite Solid Propellant Systems: A Survey," *AIAA Journal*, vol. 17, no. 10, 1979, pp. 1118-1125.

8. Fong, C.W., and Hamshere, B.L., "The Mechanism of Burning Rate Catalysis in Composite Propellants by Transition Metal Complexes," *Combustion and Flame*, vol. 65, 1986, pp. 71-78.

9. Kishore, K., Verneker, V.R., and Sunitha, M.R., "Action of Transition Metal Oxides on Composite Solid Propellants," *AIAA Journal*, vol. 18, no. 11, 1980, pp. 1404-1405.

10. Price, E. W., Chakravarthy, S. R., Freeman, J.M., and Sigman, R. K., "Combustion of Propellants with Ammonium Dinitramide Oxidizer," AIAA Paper 98-3387, 34th AIAA/ASME/SAE/ASEE Joint Propulsion Conference, Cleveland OH, July 12-15, 1998.

TABLES

Table 1. Baseline Formulations (by % mass)

	Matrix	Bimodal Propellant
% binder	30	12.5
% fine AP	70	29.17
% coarse AP	--	58.33
fine AP/binder	70/30	70/30
coarse AP/fine AP	--	66/33

Table 2. Binder Composition by Percent Mass

Binder	Prepolymer		DOA†	Curing Agent		
	PBAN	HTPB		ECA‡	IPDI	DDI
PBAN	64.14	--	15.00	20.86	--	--
HTPB-IPDI	--	75.73	18.39	--	5.88*	--
HTPB-DDI	--	69.07	16.77	--	--	14.16*

*Approximately 0.01% dibutyl tin dilaurate (T-12) added to HTPB binders to accelerate curing

† DOA = dioctyl adipate (plasticizer)

‡ ECA = epoxy curing agent

FIGURES

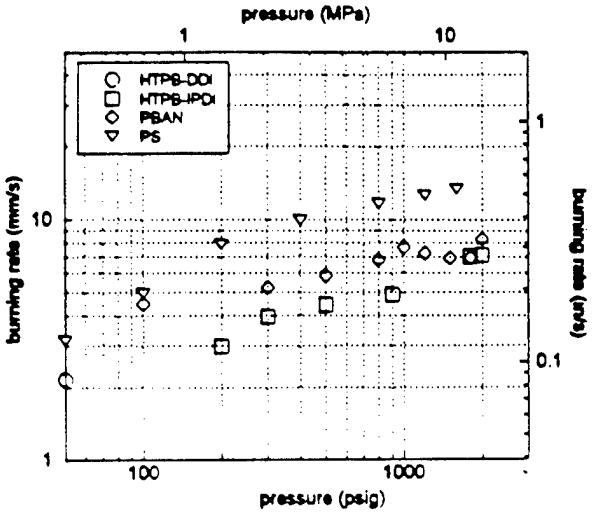

Figure 1. Effect of binder in AP(10μm)/binder = 70/30.

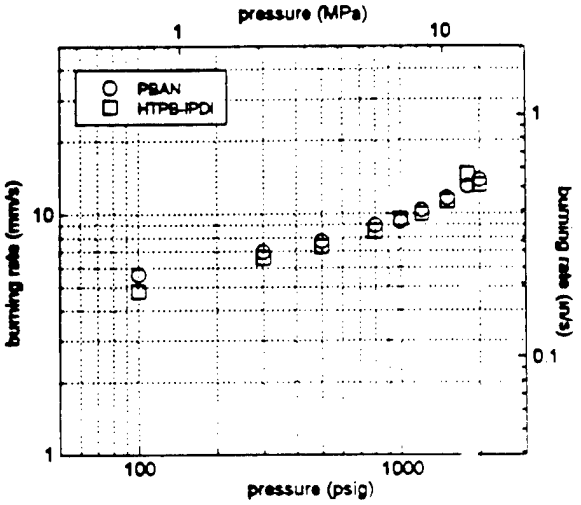

Figure 2. Effect of binder in bimodal propellants with 70/30 matrix, 87.5% total solids

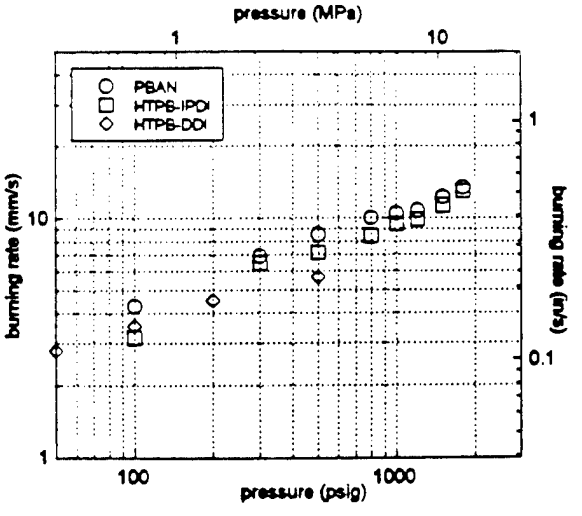

Figure 3. Effect of binder in bimodal propellants with 73/27 matrix, 88% total solids.

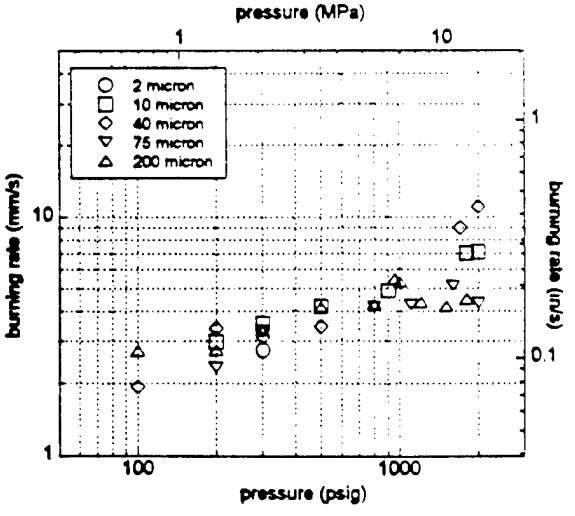

Figure 4. Effect of particle size in AP/HTPB-IPDI = 70/30 matrix.

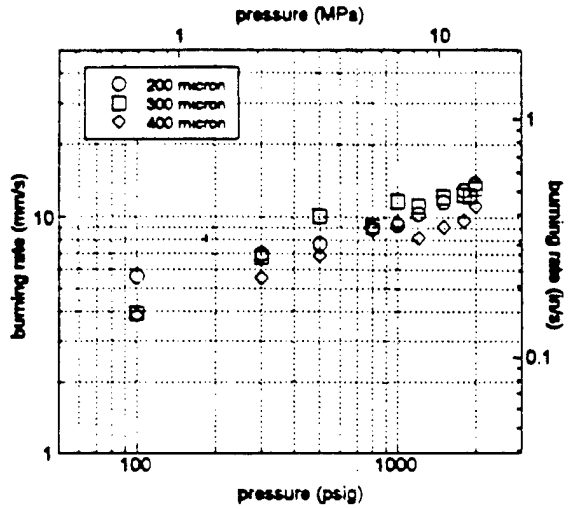

Figure 5. .Effect of coarse AP size in bimodal PBAN propellant, 70/30 matrix.

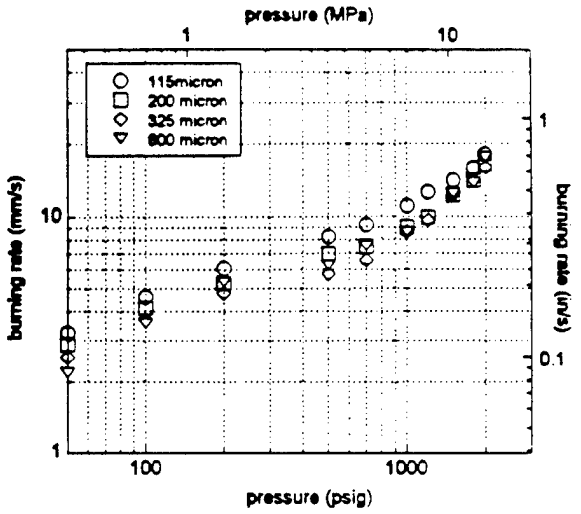

Figure 6. Effect of coarse AP in catalysed HTPB-DDI bimodal propellant, 73/27 matrix.

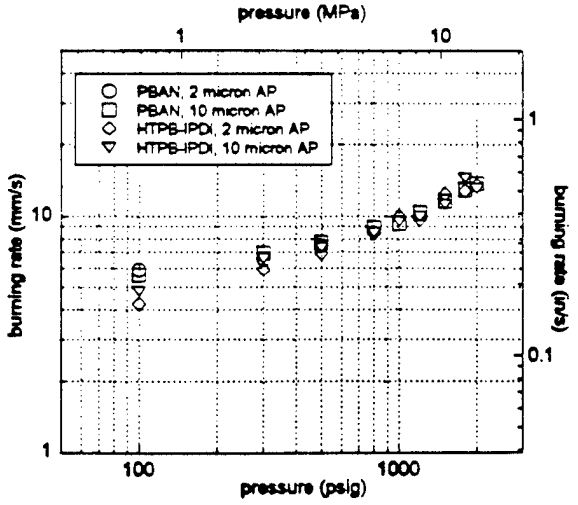

Figure 7. Effect of fine AP size in bimodal propellants, 70/30 matrix, 87.5% total solids.

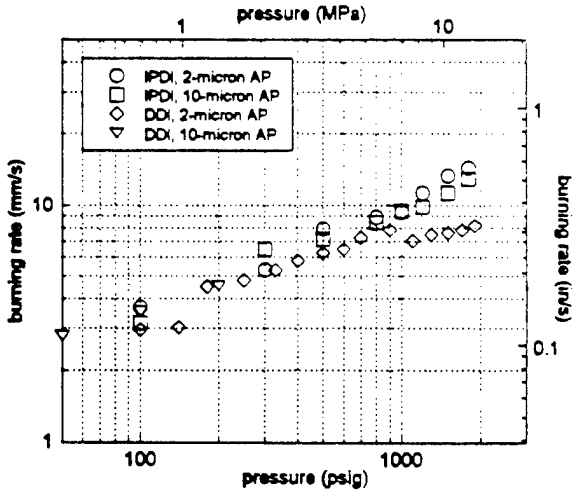

Figure 8. Effect of fine AP size in HTPB bimodal propellants, 73/27 matrix, 88% total solids.

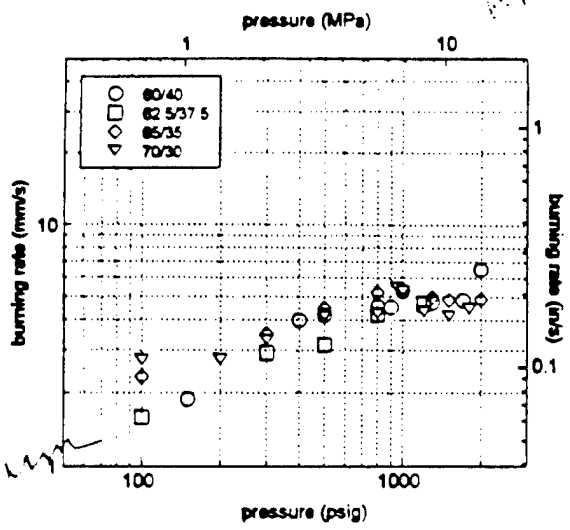

Figure 9. Effect of O/F ratio in HTPB-IPDI matrices (200-μm AP).

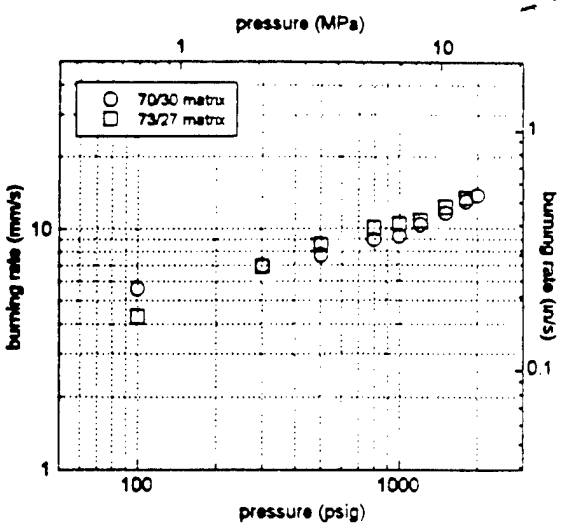

Figure 10. Effect of matrix O/F in PBAN bimodal propellant.

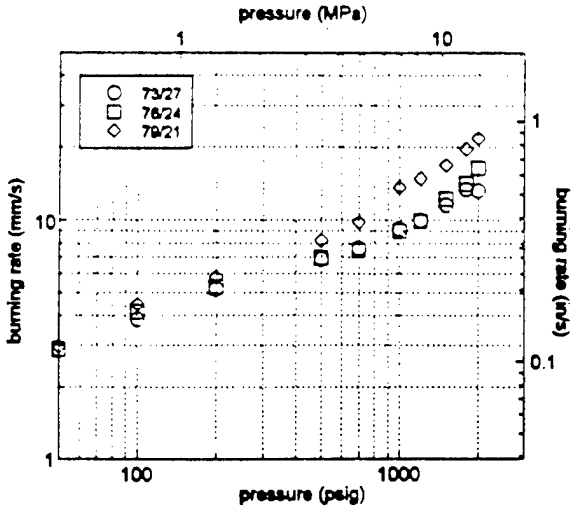

Figure 11. Effect of matrix O/F ratio in HTPB-DDI bimodal propellant, 88% total solids.

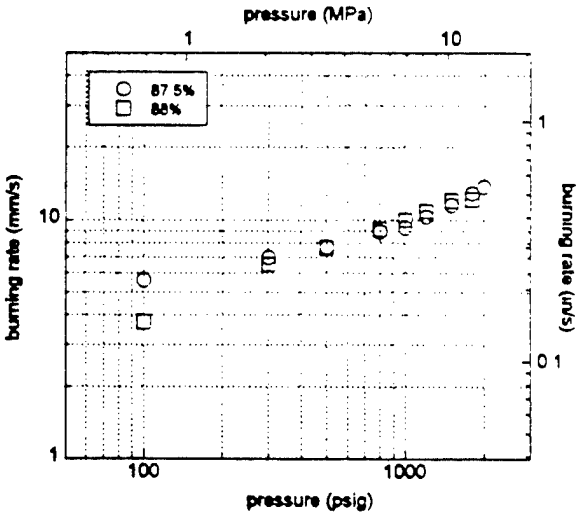

Figure 12. Effect of total solids loading in PBAN bimodal propellant, 70/30 matrix.

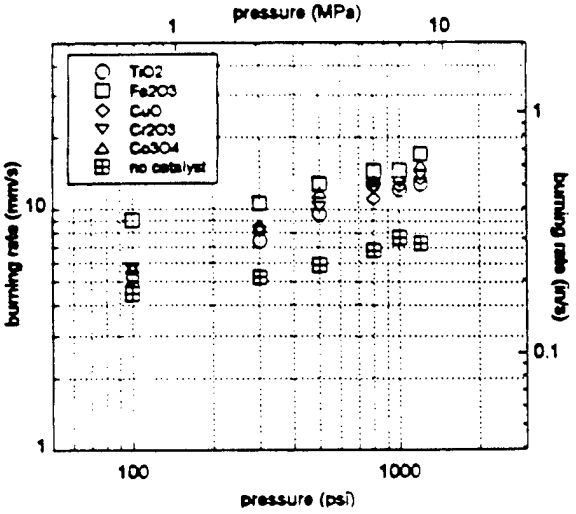

Figure 13. Effect of transition metal oxides in PBAN matrix.

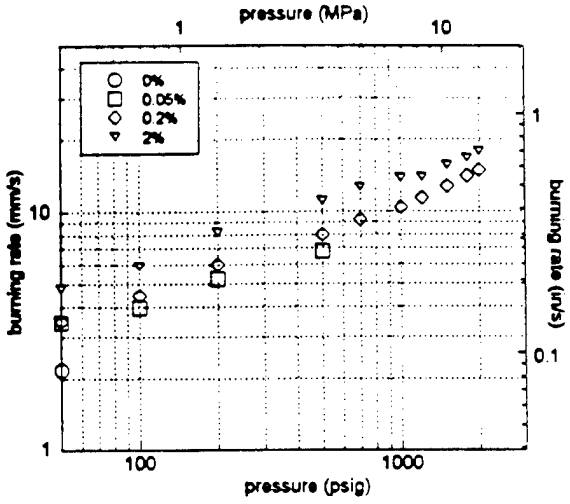

Figure 14. Effect of initial catalyst concentration in HTPB-DDI 73/27 matrix.

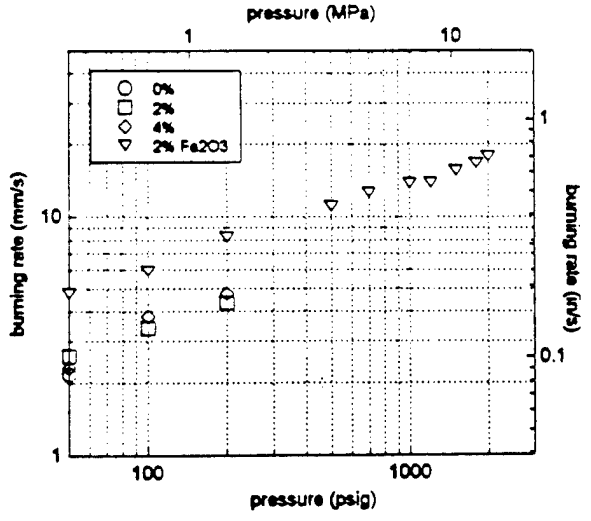

Figure 15. TiO_2 vs. Fe_2O_3 in catalytic ability in HTPB-DDI matrix = 73/27

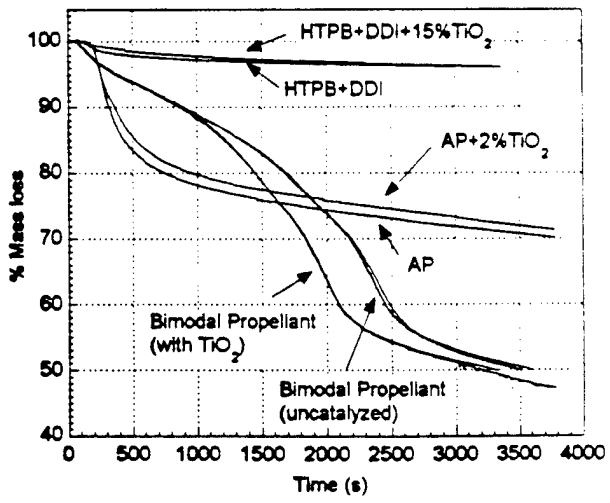

Figure 16. . Thermal decomposition (TGA) of propellants and ingredients with and without TiO_2 at 300 °C

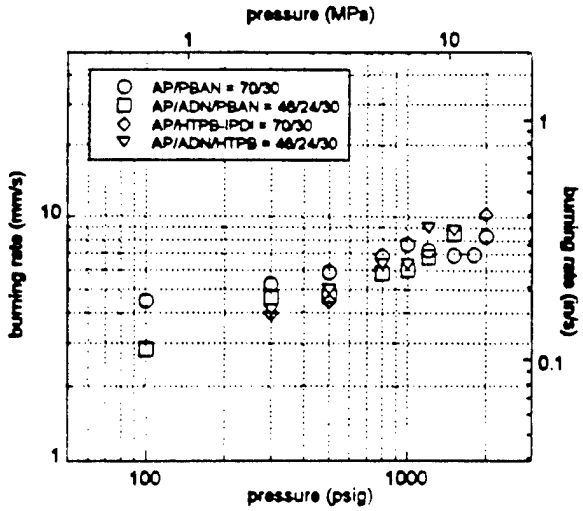

Figure 17. Effect partial ADN replacement of AP in matrix.

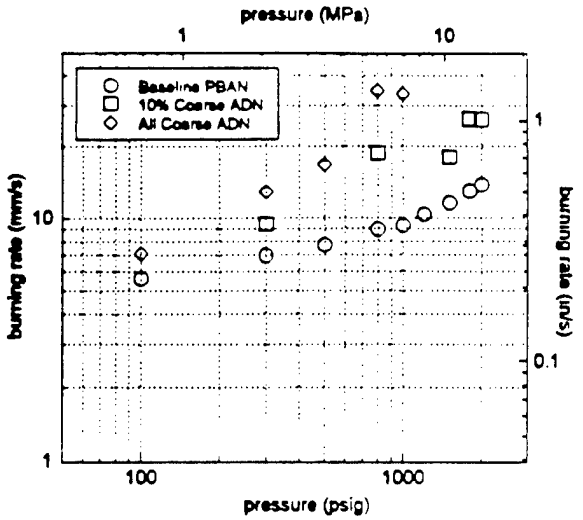

Figure 18. Effect of ADN substitution of coarse AP in PBAN bimodal propellant.

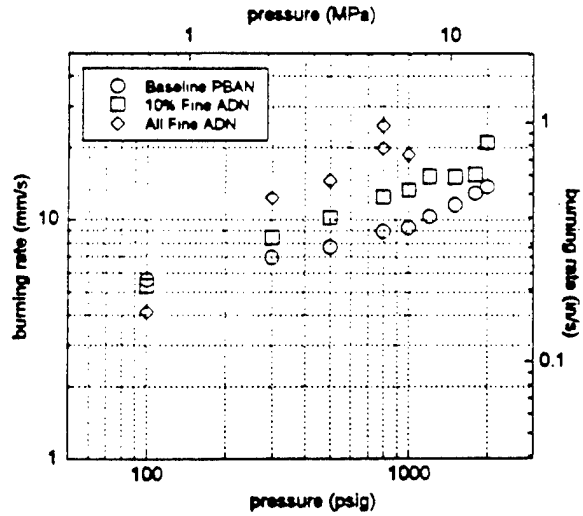

Figure 19. Effect of ADN substitution of fine AP in PBAN bimodal propellant.

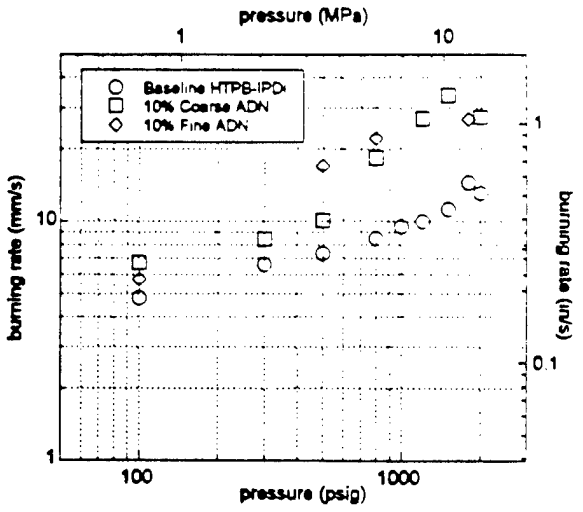

Figure 20. Effect of ADN substitution in HTPB-IPDI bimodal propellant.

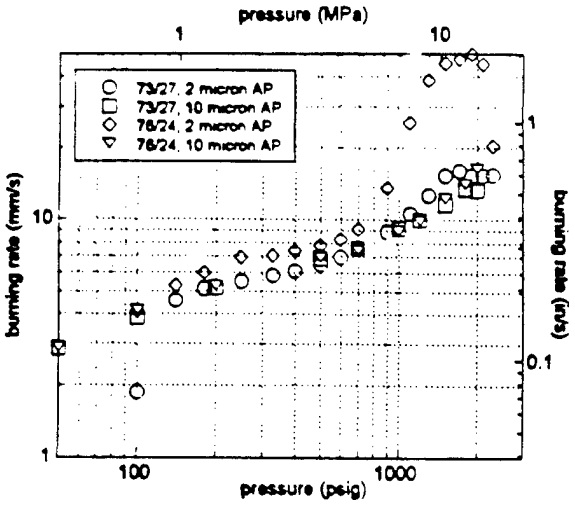

Figure 21. Coupled effect of change multiple variables.

APPENDIX L

Price, E. W., Chakravarthy, S. R., Sambamurthi, J. K., and Sigman, R. K.

"Leading Edge Flame Detachment; Effect of Burning Rate on Ammonium Perchlorate Propellants"

Proceedings of the 30th JANNAF Combustion Subcommittee Meeting

Monterey, CA, Dec. 1993

UNNAE'93

LEADING EDGE FLAME DETACHMENT; EFFECT ON BURNING RATE OF AMMONIUM PERCHLORATE PROPELLANTS

E. W. Price, S. R. Chakravarthy, J. K. Sambamurthi and R. K. Sigman

Abstract

Inner details of the transition from premixed to diffusion controlled burning are examined by considering the transition at the individual particle flamelet level. These considerations lead to prediction of observable singular burning rate behavior of bimodal AP formulations. Burning rate measurements verify the predictions, supporting the view that particle flamelets become detached and retreat to more remote premixed locations at definite (particles size dependent) pressures, revealed by the burning rate tests.

Introduction

It has been generally accepted since the late 1950's that ammonium perchlorate (AP) composite propellants burn with a premixed flame at low pressure, and by individual particle flamelets at high pressure (a concept postulated in the early stages of development of the Summerfield granular diffusion flame model). However no burning rate model has embodied the details of the transition between the premixed domain and the particle flamelet domain.

In the flamelet domain, each particle has an oxidizer/ fuel mixing fan extending outward from the particle periphery, governed by inter diffusion of oxidizer and fuel flows. In this mixing fan there is a surface corresponding to stoichiometric proportions of oxidizer and fuel. In classical diffusion flame theory this stoichiometric surface is the site of a flame sheet, a particle flamelet (Fig. 1). The location of the flamelet at the stoichiometric surface follows from the higher reaction rates at this location because of the higher temperature achieved under stoichiometric conditions. With a fuel rich AP propellant, the flamelet "tent" tends to be closed over the AP particle, and it is inclined over the particle because AP is a relatively dilute oxidizer, while the binder is a relatively concentrated fuel. However the conditions in the leading edge portion of the mixing fan are not suitable to support a flamelet (too "lossy"), so that the flamelet starts at a point typically 50μm from the surface where the supply of mixed reactants is large enough for a self sustaining leading edge flame (LEF) (Fig. 1). The actual location of these flamelets is dependent on pressure because a LEF is a miniature premixed flame, and its stable location becomes increasingly distant from the surface as pressure is decreased. At some pressure (particle size dependent), the LEF location is at the tip of the stoichiometric surface (and consuming most of the oxidizer). Any further outward displacement due to lower pressure puts the flamelet in a region of decreasing

This research was sponsored under ONR grant No.N00014-95-0559, technical monitor: Dr. Richard .S. Miller. J. K. Sambamurthi is currently employed at NASA Marshall Space Flight Center, and S.R. Chakravarthy is employed by the Indian Institute of Technology, Madras, India.

Approved for public release; distribution is unlimited.

O/F ratio (and hence decreasing flame temperature) with distance from the surface, a condition not conducive to a stable location for the flamelet. It is postulated that, upon detachment, the flame retreats to a location where a fully mixed flame stabilizes. The details of this transition are not known. Presumably if progressively higher pressure is then considered, the LEF will become attached again. It is not clear that the processes are simply reverses of each other, but it seems likely that major transitions occur over a narrow pressure range. This would correspond to a large difference in heat flux to the surface and difference in local surface regression rate, the differences between a large portion of the heat release in the form of near surface hot flamelets, and a fuel rich, more remote premixed flame.

The burning rate changes associated with transition into or out of the attached LEF domain are not discernible in most propellants because a large range of particles sizes is present, with correspondingly different LEF detachment pressures (Fig. 1). This becomes an inner detail of the overall transition between premixed and diffusion limited domains for the propellants.

If one had a propellant consisting of packed parallel rods of oxidizer, all of the same diameter, then there might be an abrupt change in burning rate at the transition point. Lacking that ideal research propellant, the present study (starting in 1984) used propellants utilizing bimodal oxidizer particle size with the size of the two modes widely separated and with the fine mode having fairly narrow size distribution. In such formulations the burning surface is made up of areas corresponding to individual large AP particles and areas consisting of a fuel-rich fine AP-binder "matrix". In the present investigation it was postulated that the matrix areas might have a sufficiently coordinated transition to show a distinctive burning rate change for the propellant over a narrow pressure interval.

To test the foregoing concept, a series of bimodal propellants was prepared with different particle sizes in the matrix component of the propellant, to see if there was a LEF transition pressure range indicated in the burning rate versus pressure curve. If so, the argument implies that the transition pressure would be lower for coarser particles in the matrix, that the transition would be stronger for a matrix with more fine AP (more matrix, higher O/F ratio in the matrix), and that use of a catalyst would increase rate every where but preserve the transition and shift it to lower pressure. These arguments were explored earlier by Sambamurthi (Ref. 1), and had an impact on design of later studies of aluminum agglomeration (Ref. 2) and of mechanism of dynamic response of the combustion zone to pressure oscillations (Ref. 3). The propellants used in Ref. 3 were "nominally" the same as in Ref. 1, but did not duplicate the burning rate results of Sambamurthi (even though the LEF detachment concept was reaffirmed in the principal outcomes of both Ref. 2 and Ref 3). In the present study, the experiments of Sambamurthi were repeated and tests run over a more complete pressure range. The present report summarize the combined investigations and reports the results.

Experimental

The propellant mixes listed in Table I were prepared (87.5% AP, 12.5% PBAN binder), with binder composition being 64.14% PBAN prepolymer, 15% DOA plastisizer, and 20.86% ECA. When additives were used, they were simply added to the above formulation (1%, 1μm particle size). Test were run on uncoated 3x5x10mm samples, burned in a nitrogen flushed window bomb with external illumination and video coverage for burning rate determination.

Results

The burning rate data are presented in Figs 2 and 3.

Discussion

The experimental results from the recent tests confirm earlier (published and unpublished) results of Sambamurthi (Ref. 1). They are also consistent with the anticipated trends described in the introduction (the negative results in Ref. 3 remain unexplained, but are apparently irrelevant). Specifically, the results:

1. Support the argument that LEF detachment occurs and that an accompanying change in flame stand off distance leads to strong decrease in heat flux to the surface.

2. Establish a pressure interval in which detachment occurs, and show how that interval changes with particle size (Fig. 2).

3. Show that (within the limits tested) a larger change in rate occurs when the ratio of coarse to fine AP is decreased (matrix area and matrix O/F ratio are increased).

4. Increase in rate occurs over the whole pressure range when Fe_2O_3 catalyst is added, and the transition is preserved and moved to lower pressure. This is consistent with the conclusion in Ref. 4 that Fe_2O_3 acts by breaking down heavy fuel molecules, giving more reactive fuel species to the flame.

5. The absence of any effect of Al_2O_3 additive suggests that the effect of Fe_2O_3 is not purely thermo-physical.

6. Indicate that matrixes with particle sizes smaller than the sizes used here will yield premixed flames below the transition pressures found here.

In addition there is room for some humility in view of

1. Continuing absence of any analytical model for the detachment-attachment process.

2. The complication of interaction of adjoining flamelets (competition for the same fuel flow, etc.)

3. Potential limitation of the quantitative results to propellants with AP oxidizer with hydrocarbon binders like PBAN that have minimal melt flows on the burning surface.

References

1. Price, E. W., Sambamurthi, J. K., Sigman, R. K., and Panyam, R. R., "Combustion of Ammonium Perchlorate-Polymer sandwiches," *Combustion and Flame*, 63, 1986, pp. 381-413.

2. Sambamurthi, J. K., and Price, E. W., "Aluminum Agglomeration in Solid Propellant Combustion," *AIAA Journal*, Vol. 22, No. 8., 1984, pp. 1132-1138.

3. Beiter, C. A., and Price, E. W., "The role of Detachment of Leading Edge of the Diffusion Flame in the Pressure-Coupled response of Composite Propellants," *Journal of Propulsion and Power* (in press).

4. Price, E. W., and Sambamurthi, J. K., "mechanism of Burning Rate Enhancement by Ferric Oxide," *Proceedings of 21st JANNAF Combustion Meeting*, 1984.

Table I Propellant compositions

Designation	Coarse AP %	Fine AP %	Binder %	Additive %	Coarse/Fine AP ratio
Mix 1	70.00	17.50 (17.5μm)	12.50	-	80/20
Mix 2 baseline	70.00	17.50 (49.0μm)	12.50	-	80/20
Mix 3	70.00	17.50 (82.5μm)	12.50	-	80/20
Mix 4	61.25	26.25 (49.0μm)	12.50	-	~~80/20~~ 70/30
Mix 5	69.20	17.30 (49.0μm)	12.50	1.00 (Fe_2O_3)	80/20
Mix 6	69.20	17.30 (49.0μm)	12.50	1.00 (Al_2O_3)	80/20

Figures

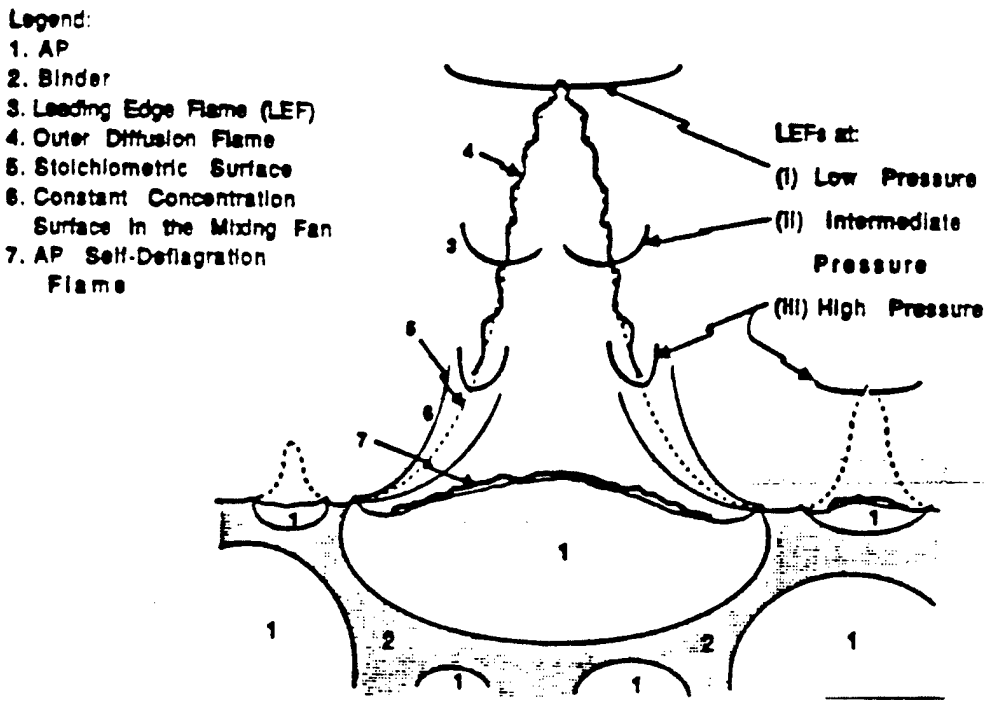

Figure 1. Sketch of flame structure.

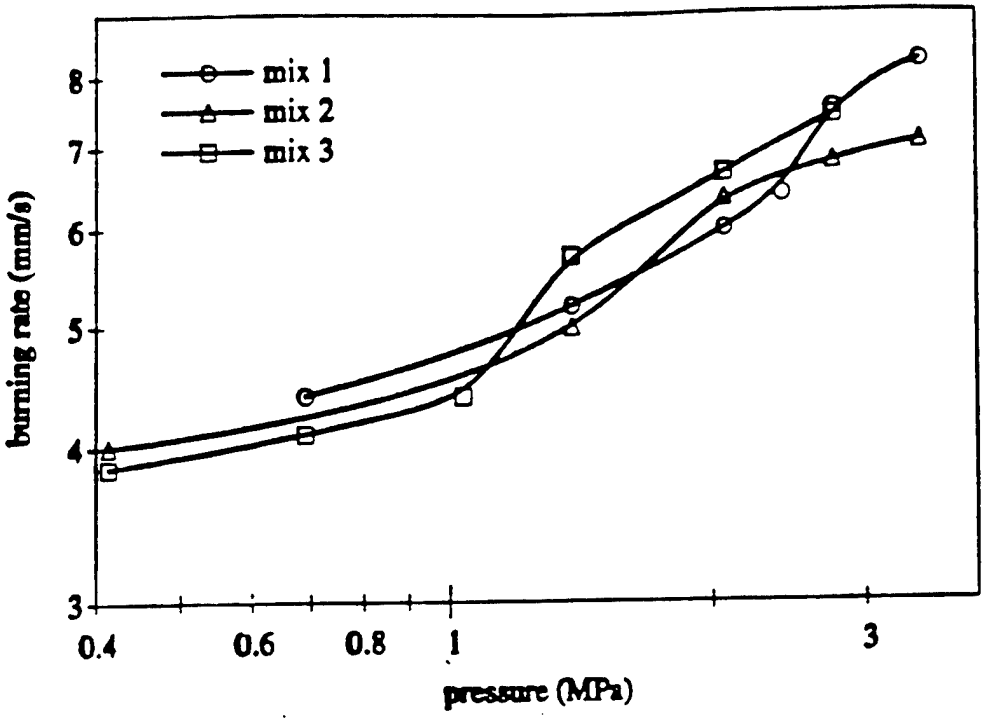

Figure 2. Burning rates of 3 bimodal propellants in the LEF transition range. All have C/F =80/20. Mix 1 has 400 and 17.5μm AP. Mix 2 has 400 and 49.5μm AP. Mix #3 has 400 and 82.5μm AP.

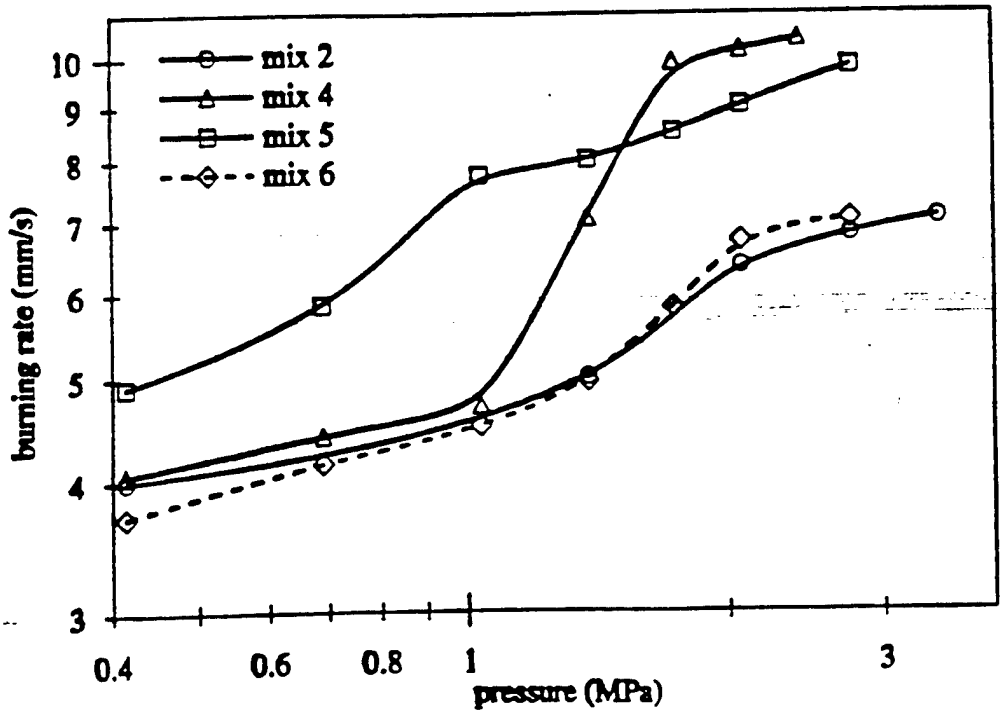

Figure 3. Burning rates of mixes 2, 4-6. All have 400 and 49μm AP. Mix #4 has 70/30 coarse-to-fine. Mix #5 has 1% Fe_2O_3. Mix #6 has 1% Al_2O_3.

APPENDIX M

Price, E. W., Chakravarthy, S. R. Sambamurthi, J. K., and Sigman, R. K.

"The Details of Ammonium Perchlorate Propellants: Leading Edge Flame Detachment"

Combustion Science and Technology

Vol. 138, 1998, pp. 63-83.

Reprints available directly from the publisher
Photocopying permitted by license only

© 1998 OPA (Overseas Publishers Association) N.V.
Published by license under
the Gordon and Breach Science
Publishers imprint
Printed in Malaysia

The Details of Combustion of Ammonium Perchlorate Propellants: Leading Edge Flame Detachment

E. W. PRICE[a], S. R. CHAKRAVARTHY[a,*], J. K. SAMBAMURTHI[b] and R. K. SIGMAN[a]

[a] *School of Aerospace Engineering, Georgia Institute of Technology, Atlanta, GA 30332-0150;*
[b] *M/S ED33, NASA Marshall Space Flight Center, Huntsville, AL 35812*

(Received 7 July 1997; In final form 29 June 1998)

The transition from particle flamelet burning to premixed flame burning of ammonium perchlorate (AP)/hydrocarbon (HC) binder propellants is identified with detachment of the oxidizer/fuel (O/F) flamelet from the stoichiometric tip of the diffusion field over the AP particle. The conditions (pressure, particle area, local stoichiometry) for detachment are revealed by singular regions of the burning rate *versus* pressure curves for selected bimodal propellants.

Keywords: Solid propellant combustion; laminar premixed-to-diffusion flamelet transition

INTRODUCTION

The combustion characteristics of ammonium perchlorate (AP) propellants are controlled by a flame complex involving the exothermic deflagration of AP particles and oxidizer/fuel (O/F) flamelets that evolve in the O/F mixing zones emerging from the AP-binder contact lines on the burning surface (Fig. 1). Under some conditions (fine AP, low pressure, and/or in presence of catalysts) combustion is also affected by intermediate exothermic reaction steps at the contact lines (gas phase, and/or heterogeneous reactions). The

*Corresponding author. Present address: Department of Aerospace Engineering, IIT Madras, Chennai 600 036, India.

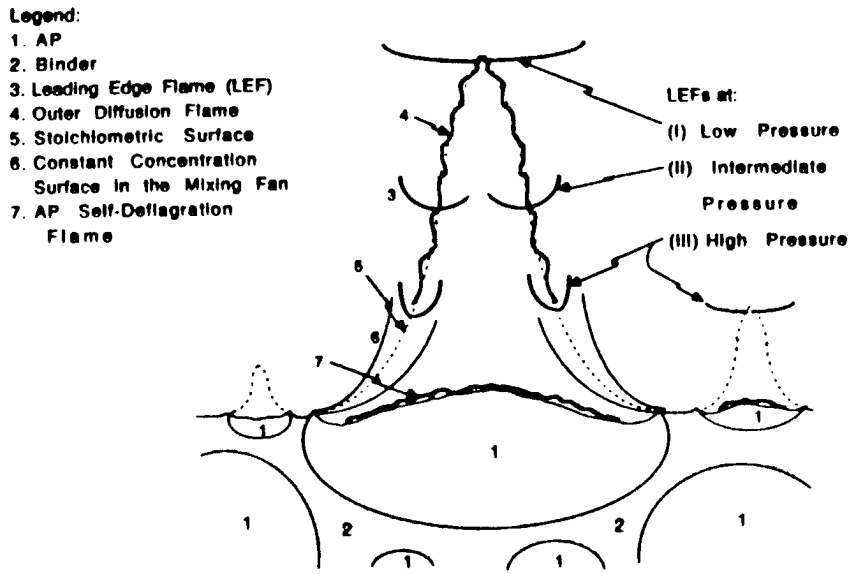

FIGURE 1 Leading edge flame (LEF) locations at three different pressures. The upper one is near detachment. The sketch is for a large particle; small particle at left, without LEF.

earliest combustion modelers (*e.g.*, Summerfield *et al.*, 1960) recognized that the gas phase O/F reactions could depend on a competition between O/F mixing rate and chemical reaction rates, with the mixing rates being strongly dependent on particle size and the reaction rates being strongly dependent on pressure. As a result, the combustion could be represented as a one-dimensional premixed flame at low pressure (or fine AP), while a more complex flame construct was required at the pressures more typical of rocket motor operation (*e.g.*, 3.5–14 MPa). In these constructs it became evident that the transition to pure diffusion control of the O/F gas phase flame was never fully achieved because there was always a region near the surface contact lines in the mixing fans in which the assumptions of diffusion limited flames are seriously violated. Specifically, there is a near-surface region in the mixing fan in which reaction rates are not effectively infinite (as assumed in diffusion limited theory) because temperatures are low, and mixing rates are very high (due to steep lateral O and F concentration gradients). As a result, modern combustion models, *e.g.*, derivatives of the BDP model (Beckstead *et al.*, 1970), divide the O/F flamelets into a "primary" portion in which kinetic considerations are important, and an outer diffusion limited flamelet. This division of the O/F flamelet is (a) an expediency to avoid a very difficult problem of complete modeling of the flamelet, and (b) a minimum requirement to get a propellant combustion model that is consistent with experimentally determined features of propellant combustion.

This paper is concerned with the features of the above mentioned leading edge portion of the O/F gas phase flamelet (referred to here as the "LEF") that determine the relative importance of the LEF and the outer diffusion flamelet, and in particular, a singular behavior that occurs as conditions change in the direction of a premixed O/F flame. This subject was discussed superficially by Price *et al.* (1986), and the present paper is aimed at further clarification in the context of "real" propellants, and verification by further propellant formulation and burning rate studies.

The singular behavior noted above is related to a concept referred to as "LEF detachment", which is explained below and in Figure 1. The figure shows the "complete" diffusion flame for an oxidizer particle burning in a fuel-rich environment. The LEF is shown at the two lateral locations that correspond to a cross sectional cut of the full 3-D particle flamelet; the LEFs are shown at three different heights corresponding to three different pressures. The lateral location of the cross sections of the LEF in each case is centered on the stoichiometric surface of the O/F mixing fan. The central point of this description (for the present purposes) is to point out that there is a low pressure limit for existence of a classical LEF-diffusion flame combination, below which the particle flamelet no longer can be associated with stoichiometric surfaces, and instead must stabilize in a region that is increasingly fuel rich (*vs.* distance from the surface). In some situations (to be discussed below) the mixture above the "stoichiometric tip" (Fig. 1) may be quite fuel rich. Under these conditions there may be no location for a stable flamelet immediately above the stoichiometric tip, in which case a discontinuity in flamelet standoff distance (*vs.* pressure) will occur, with a corresponding drop in local heat flux to the surface. Under extreme conditions there may be no stable location for the flamelet. In that case the fate of the reactant mixture will be determined by interaction with adjacent flamelets still present on larger particles. Lacking such interaction, burning will cease (Lee *et al.*, 1994).

In the following, the singularity in LEF condition beyond the stoichiometric tip is referred to here as LEF detachment. From the description it is evident that the detachment condition will be present at higher pressures when the AP surface is smaller (either smaller particles or later and earlier in burning of a particle). It will be shown later that for a given propellant

formulation there is a unique relation between AP diameter on the surface and pressure for LEF detachment. In this regard, the consequences of detachment would be clear if the propellant consisted of a fuel-rich parallel array of uniform sized AP end-burning rods. As pressure is decreased, detachment would occur on all AP surfaces at once, with transition to premixed flame or extinction (depending on O/F ratio and rod diameter). While details of this transition are poorly understood and not directly observable in the microscopic propellant combustion environment, it seems evident that the transition will reveal itself by changes is macroscopic aspects of combustion such as burning rate, at least for a uniform rod propellant. The burning rate would be much lower just below the transition pressure than just above, because of the higher standoff distance of the premixed O/F flame.

In a conventional propellant, the size of the AP surfaces on the burning surface covers a broad range. LEF attachments and detachments occur on individual particles according to the pressure, the time during burning of the particle, and the size of the particle. While such events contribute to the burning rate, they are only statistically related to pressure, so that the effect on burning rate has no tell tale singularities *vs.* pressure as proposed above for "rod" propellants. Such singularities might be revealed in the burning rate of propellants with monomodal AP size distribution, but studies on such propellants have been limited, and compromised collectively by diversity of ingredients, formulation and test conditions, and focus on other effects. The limited extent of testing has been due to the low solids loading possible with narrow particle size distribution. The resulting low O/F ratio is not generally suitable for propulsion applications. It was decided in the present study to look for LEF detachment effects in the burning rate of high solids propellants made by blending AP of two different particle sizes in which the "fine" size was sieved to yield a narrow size distribution and the coarse size was very much larger (*e.g.*, 30 and 400 μm). This would allow for LEF transition to be manifested in a relatively narrow pressure range for the fine particles, with a corresponding singular shift in burning rate over that pressure range. The present paper presents burning rates for several such bimodal propellants in which effects of the following variables were examined:

(a) particle size of fine AP,
(b) ratio of masses of coarse to fine AP (which in turn alters the O/F fine AP-binder ratio),
(c) addition of Fe_2O_3 catalyst, and of Al_2O_3 for comparison.

Also presented is an elementary analysis comparing the height of stoichiometric tips and standoff distance of premixed flames, as a qualitative determination of limits for LEF transition.

EXPERIMENTAL DETAILS

Ingredients and Propellants

The ingredients used in the propellants were AP and polybutadiene acrylonitrile acrylic acid (PBAN) binder. The AP was commercial grade high purity Kerr McGee low alkali variety (99.7% purity). The "coarse" fraction of the AP in the propellant was obtained by screening the available material to limit its size range between 355 – 425 μm. The coarse AP size was then designated as 400 μm. The fine AP was prepared by ball milling the as-received material in a TI-200 Vibrating Sample Mill (Heiko Co.) for 8 minutes, and sieving it for samples that passed one screen size and were retained in the next size, as follows:

"large" fine passed 90 mesh and was retained on 75 mesh;
"medium" fine passed 53 mesh and was retained on 45 mesh;
"small" fine passed 37.5 mesh.

These grades were designated by the midpoints of the mesh pairs as 82.5 μm, 49 μm, and 17.5 μm. No quantitative determinations of size distributions were made. The PBAN binder is a mixture of 64.14% PBAN prepolymer, 15% dioctyl adipate (DOA) plasticizer, and 20.86% epoxy curing agent (ECA). The ferric oxide and aluminum oxide used in two of the formulations were ~1 μm crystalline materials, obtained from Fisher Company in anhydrous form.

The propellants were mixed by stirring in the binder ingredients, followed by the additive (if any), fine AP and coarse AP, in that order. The mixes were typically 10 gm, and were placed in a vacuum oven at 40°C f rs, and periodically stirred by hand for 5 – 10 minutes (eve to remove bubbles and minimize separation of coarse and fi y were then placed in a regular oven to cure for 7 days at 48.

A family of six propellants were tested in this study (Tab. s consisted of 87.5% total solids, and 12.5% binder. Three n e with the three fine AP size grades. The mix with the mid P (49 μm) was designated as the baseline formulation for the re The fourth formulation had a different coarse/fine ratio for

TABLE I Propellant compositions

Designation	Coarse AP, %	Fine AP, %	Binder, %	Additive, %	Coarse/Fine, AP ratio
Mix 1	70.00	17.50 (17.5 μm)	12.50	-	80/20
Mix 2 (baseline)	70.00	17.50 (49 μm)	12.50	-	80/20
Mix 3	70.00	17.50 (82.5 μm)	12.50	-	80/20
Mix 4	61.25	26.25 (49 μm)	12.50	-	70/30
Mix 5	69.20	17.30 (49 μm)	12.50	1.00 (Fe_2O_3)	80/20
Mix 6	69.20	17.30 (49 μm)	12.50	1.00 (Al_2O_3)	80/20

the baseline. Two additional propellants were made, one with 1% of the AP blend replaced by Fe_2O_3 catalyst, and the other by Al_2O_3 (as a control for the Fe_2O_3 tests).

Burning Rate Measurements

Combustion photography was used to measure the burning rates of propellants. Samples were cut to dimensions of $10 \times 5 \times 3$ mm, and burned lengthwise in a pressurized window bomb flushed with nitrogen. Motion pictures or videos were obtained of the burning event. Flame front position in selected frames along a line parallel to the sample length were plotted as a function of time. A straight line was fitted to the data in the least square sense, with the correlation > 99.9%. The slope of the straight line of burning front position *vs.* time (adjusted for the magnification of the images) gave the burning rate. Approximately 50% of the tests were repeated at random, to test for reproducibility of the data within 5% error.

EXPERIMENTAL RESULTS

The first set of tests was aimed at examining the effect of fine particle size on the pressure range of LEF transition. Figure 2 shows burning rates of mixes 1 – 3 plotted against pressure. Each of the propellants registers a "step" in its burning rate in a narrow pressure range. The pressure level for this high slope region of the burning rate *vs.* pressure curve is higher for smaller fine AP particle size in the propellant.

The second test was to study the effect of an increase in the amount of fine AP present in the binder, at constant total AP content in the propellant (which implies less coarse AP and correspondingly larger spacing between

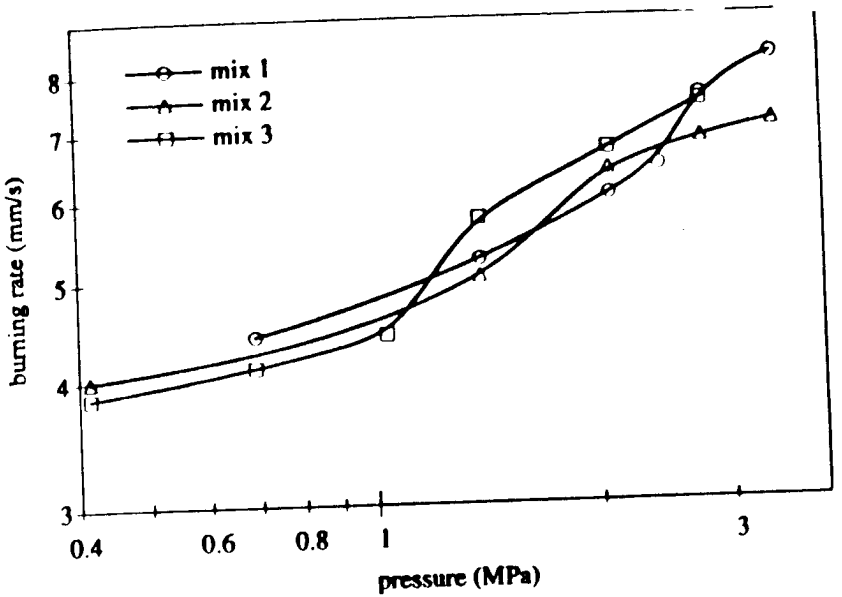

FIGURE 2 Burning rates of bimodal propellants with 70% 400 μm AP, 17.5% fine AP, and 12.5% PBAN binder, having different sizes of the fine AP: 17.5 μm (mix 1), 49 μm (mix 2), and 82.5 μm (mix 3).

the coarse particles). The burning rate curve for mix 4 is shown as part of Figure 3. The step in the burning rate curve for mix 4 is (a) larger and sharper, and (b) occurs at a lower pressure level than for mix 2. From a practical viewpoint, this mix (coarse/fine AP = 7/3) is more of interest because it is more amenable to mixing in commercial mixers than the other mixes with coarse/fine AP = 8/2.

The third set of tests was to examine the effect of a burning rate catalyst on LEF transition using a coarse/fine AP = 8/2, with 49 μm fine AP. The results, shown as part of Figure 3, indicate no major effect due to inclusion of aluminum oxide (the control mix). With the inclusion of ferric oxide (mix 5), there is a (a) moderate-to-substantial increase in burning rate in the entire pressure range tested, (b) shift in the burning rate step to lower pressure.

SIMPLIFIED ANALYSIS

Application of a full analytical-computational model of LEFs (*e.g.*, Prasad and Price, 1992) to the problem of detachment would be a formidable

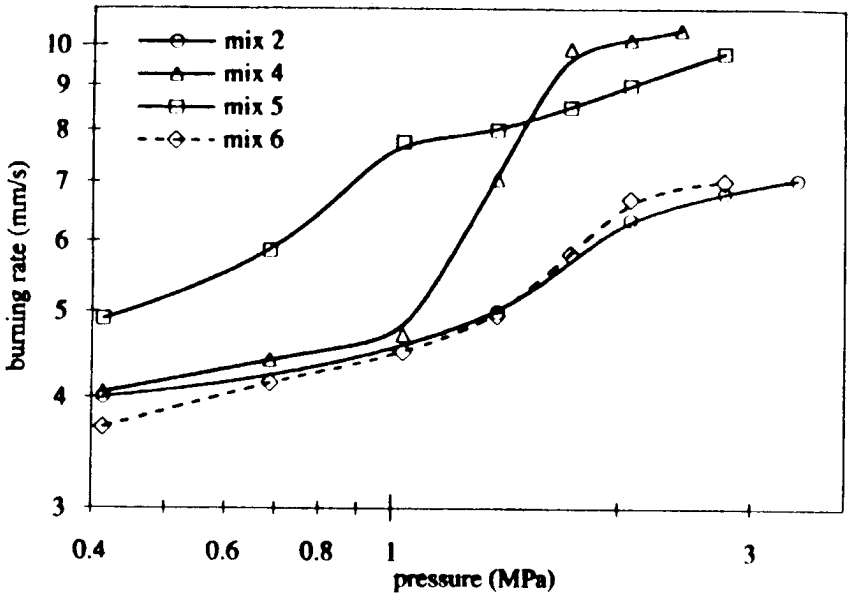

FIGURE 3 Effect of variation of fine AP/binder ratio and the inclusion of ferric oxide on the burning rate *vs.* pressure curves of bimodal propellants.

problem, even in the context of a simplified geometrical model. However, some limits on conditions for detachment can be estimated by (a) use of a Burke-Schumann model (Burke and Schumann, 1928) to calculate the dependence of stoichiometric tip height on the oxidizer particle size, and (b) use of a 1-D premixed flame model to calculate the dependence of flame standoff distance on pressure, both for a given oxidizer/fuel ratio.

A lower limit on the oxidizer particle size, d^*_{lower}, corresponding to LEF detachment can be obtained by considering the standoff distance of a stoichiometric premixed flame, δ_{stoic}, and calculating the particle size corresponding to a stoichiometric tip height equal to δ_{stoic}. In this approach, the premixed stoichiometric flame would indicate a *minimum* possible standoff distance for the LEF, which would normally have a larger standoff distance because it is nonadiabatic and stoichiometric only along the stoichiometric surface.

On the other hand, the LEF standoff would be less than that of a premixed flame produced by an O/F ratio (typically fuel-rich) equal to that of the overall propellant, because the LEF is locally stoichiometric. Calculation of the particle size corresponding to a stoichiometric tip height equal to the standoff distance ($\delta_{\text{fuel-rich}}$) of such a premixed flame will result in an upper limit for the particle size, d^*_{upper}, corresponding to LEF transition. This transition is, in fact, an *attachment* of LEFs on oxidizer particles which were burning in a (fuel-rich) premixed flame before the transition. It is easy to visualize LEF attachment in a situation of increasing pressure. Taken together, the two limits constitute bounds of a plausible hysterisis of LEF transition under conditions of quasisteady pressure fluctuations, explained in the "Discussion" section.

This section primarily involves writing out separate expressions for (a) the stoichiometric tip height in the mixing fan above an oxidizer particle surrounded by binder, and (b) the standoff distance of a one-dimensional premixed flame (of any stoichiometry) from the burning surface of a solid assumed to be homogeneous. The two expressions are matched for the condition on LEF transition, and the equality rearranged to obtain a range of d^* (upper or lower limit depending on the premixed flame stoichiometry) for LEF transition at a given pressure.

Approximate Analysis

First, we use approximate expressions for the stoichiometric tip height and the premixed flame standoff distance, in order to illustrate the pattern of the pressure-particle size relationship governing LEF transition. The height of a jet diffusion flame may be written as (Strahle, 1993)

$$h = ud^2/D \tag{1}$$

On the other hand, the premixed flame standoff distance for a one-dimensional solid is (Strahle, 1993; Liñán and Williams, 1993; Beckstead *et al.*, 1970)

$$\delta = \dot{m}/w \tag{2}$$

where, $\dot{m}$ is the propellant mass burning rate ($= \rho_P r$). Further, we use

$$u = \dot{m}/\rho_g \tag{3}$$

and,

$$w = A_f e^{-E_f/R_0 T_f} C^n_{A_1} C^{\prime}_{A_2} \tag{4}$$

where, the premixed flame is assumed to occur in a global reaction of the form

$$\nu_1 A_1 + \nu_2 A_2 \rightarrow \nu_3 A_3 + \nu_4 P \tag{5}$$

If the reaction rate is of the form $w = kp^n$, where $n (= \sigma + e)$ is the order of the reaction, then comparing (1) and (2) and using (3) and (4), we form the Damköhler second number:

$$\mathrm{Dm}_2 = \frac{h}{\delta} = \frac{kp^n d^2}{\rho_g D} \tag{6}$$

The pressure and temperature dependencies of the gas phase density and the diffusion coefficient can be written as

$$\rho_g = \frac{p}{(R_0/\bar{M})T_f}, \quad \text{and,} \quad D = \frac{D_{ref} T_f^{n_D}}{p} \tag{7}$$

(Beckstead *et al.*, 1970; Krishnan and Jeenu, 1992)

Determining the oxidizer particle size for a stoichiometric tip height that is comparable to a premixed flame standoff distance involves setting $Dm_2 = 1$; we get, after rearrangement,

$$d^* = \frac{\text{constant}}{p^{n/2}} \tag{8}$$

With hydrocarbon fuels, the order of a global reaction in the premixed flame $n \sim 2$ usually (Strahle, 1993). Equation 8 suggests that the pressure-particle size relationship governing LEF transition is hyperbolic in nature.

Rigorous Expressions

While the above analysis gives a simple expression for the particle size-pressure relationship for flame transition (Eq. (8)), more rigorous expressions for the stoichiometric tip height and the premixed flame standoff distance that are already available in literature can be employed. In this context, certain simplifying assumptions are made. In the diffusion flame analysis, the geometry is assumed to be two coaxial flows (oxidizer – inner, fuel – outer) bounded within a non-interacting coaxial tube. The inner tube diameter is the oxidizer particle size, which is to be determined for LEF transition at a given pressure. The outer tube diameter is adjusted to represent the overall stoichiometry of the propellant (see Eq. (12) below). As before, a global reaction is assumed for the premixed flame, as given by Eq. (5).

Following the analysis presented by Williams (1985), and retaining the symbols and definitions of variables in that analysis, the solution for the flame shape above a coaxial burner with oxidizer flow surrounded by fuel flow (under-ventilated case) can be shown to be

$$\gamma = 1 - (1+\nu)c^2 - 2(1+\nu)c \sum_{k=1}^{\infty} \frac{1}{\varphi_k} \frac{J_1(c\varphi_k)}{[J_0(\varphi_k)]^2} J_0(\xi\varphi_k) e^{(\mathrm{Pe}-a_k)\psi/2} \tag{9}$$

where, $a_k = \sqrt{\mathrm{Pe}^2 + 4\varphi_k^2}$, $\mathrm{Pe} = \rho_g u b C_p/\lambda_g$, and $\psi = z/b$.

The above expression includes streamwise diffusion effects, and is an axisymmetric counterpart of the two-dimensional expression reported by Chung and Law (1984). As treated by Williams (1985), we ignore all terms in the above series except the first (*i.e.*, for $k = 1$). Setting $\gamma = 0$ and $\xi = 0$ in Eq. (9), we can obtain an expression for the stoichiometric tip height, h. Setting $h = \delta$, where δ is the premixed flame height obtained in Eq. (11) below, the oxidizer particle size can obtained, after some rearrangement, as

$$d^* = \frac{4\lambda_g \varphi_1 c}{\rho_p r C_p \left\{ \left[1 + \frac{2\lambda_g}{\rho_p r C_p \delta} \ln\left(\frac{2(1+\nu)cJ_1(c\varphi_1)}{|1-(1+\nu)c^2||\varphi_1|J_0(\varphi_1)|^2} \right) \right]^2 - 1 \right\}^{1/2}} \tag{10}$$

In order to compute the premixed flame standoff distance, the propellant is treated in a homogeneous one-dimensional fashion, as mentioned earlier. This is quite valid if/when the mixture does indeed burn in a premixed flame. The one-dimensional steady-state (premixed) deflagration of a homogeneous solid was first treated by Denison and Baum (1961), and Williams (1973) evolved a formal solution to the problem using activation energy asymptotics. The premixed flame standoff distance is obtained as part of that solution as (in the notation used in the present paper)

$$\delta = \frac{\lambda_g}{\rho_p r C_p} \ln\left\{ \frac{C_p(T_f - T_s) + L + C_s(T_s - T_0)}{L + C_s(T_s - T_0)} \right\} \tag{11}$$

An expression for r is presented by Williams (1973) involving the kinetics of the premixed flame, but for the present purposes, we use the propellant burning rate data.

Numerical Calculations

In performing the numerical calculations, the following additional equations were used:

(i) For the diffusion flame analysis, the ratio of inner to outer tube diameters in the coaxial flow is calculated as

$$c = \frac{d}{2b} = \frac{1}{(1/2 + \sqrt{3}/\pi)\left\{\frac{2\sqrt{3}}{\pi}\left[1 + \left(\frac{(1-\beta)}{\beta}\frac{\rho_{ox}}{\rho_b}\right)\right]\right\}^{1/2}} \qquad (12)$$

(ii) The chemical reaction rate is expressed as in Eq. (4);

(iii) The pressure and/or temperature dependencies of the gas phase density and the diffusion coefficient are as given in Eq. (7), and the surface temperature is written as

$$T_s = \left(\frac{T_{s,\mathrm{ref}}}{p_{\mathrm{ref}}}\right)^{\pi_{T_s}} p \qquad \text{(Zanotti } et\ al.\text{, 1992)}$$

(iv) The latent heat of pyrolysis and the specific heat capacity of the homogeneous solid were written out in terms of the ingredient properties, as

$$L = \beta L_{ox} + (1-\beta)L_b \quad \text{and} \quad C_s = \beta C_{ox} + (1-\beta)C_b$$

The numerical values of all the parameters used in the calculations are shown in Table II. Parameters strongly dependent on the propellant mixture fraction were linearly extrapolated/interpolated based on the available values for two mixture fraction levels (Ermolin, 1993). Although several references are available that give numerical values of a number of parameters, Ermolin (1993) is the only recent source known to the authors that explicitly deals with kinetic parameters of a premixed flame involving AP and polybutadiene binder. Certain values given by him, particularly their trends with mixture ratio and/or pressure, are clearly debatable. However, the purpose of the present exercise is to obtain typical trends for the locus in the pressure-particle size domain governing upper and lower limits of LEF transition, and therefore, the values in that reference were used without any modification. Even so, values for kinetic parameters for a global reaction corresponding to stoichiometric mixture ratio of AP/binder (~90% by mass in the solid) were neither available, nor could be reasonably

TABLE II Numerical values of parameters

$A_1 \Rightarrow HClO_4$[a]	T_f = 2400, 2550, 2600 K at p = 0.08, 40 and 100 atm respectively, for β = 0.84[a]
$A_2 \Rightarrow C_4H_6$[a]	$T_{s,ref}$ = 950 K[b,d]
$A_3 \Rightarrow CO$[a]	n = 1.782[a]
A_f = 7.6 × 1010 (g/cm^3)$^{1-n}$·s for β = 0.77[a]	n_D = 1.75[d]
= 6.3 × 109 (g/cm^3)$^{1-n}$·s for β = 0.84[a]	n_{T_s} = 0.05[b]
C_b = 0.46 cal/g·K[b], C_{ox} = 0.2612 cal/g·K[b]	p_{ref} = 30 atm[b,d]
C_p = 0.435 cal/g·K[c]	ν = 1/9[d,e]
D_0 = 7.6 × 10-6 cm^2·atm/s·K n_D[d]	ν_1 = 1[a]
E_f = 14955 cal/mol for β = 0.77[a]	ν_2 = 1.267 for β = 0.77[a]
= 9349 cal/mol for β = 0.84[a]	= 1.15 for β = 0.84[a]
M_1 = 100.45797 g/mol	ν_3 = 2.47, 2.65, 3.13 at p = 0.59, 40 and 100 atm for β = 0.77[a]
M_2 = 54.08782 g/mol	= 1.22, 1.21, 1.7 at p = 0.08, 40 and 100 atm for β = 0.84[a]
M_3 = 28.01 g/mol	ν_4 = 4.035, 3.84, 3.29 at p = 0.59, 40 and 100 atm for β = 0.77[a]
M_4 = 24.7 g/mol for β = 0.77[a]	= 4.83, 4.83, 4.31 at p = 0.08, 40 and 100 atm for β = 0.84[a]
= 26.6 g/mol for β = 0.84[a]	ρ_b = 0.903 g/cm^3[c], ρ_{ox} = 1.95 g/cm^3[c,e]
Q_b = 33 cal/g[b], Q_{ox} = 480 cal/g[b]	$\sigma, \epsilon = n/2$[a]
β = 0.5833 (for mix 1, 2, 3)	
R_0 = 8.3143 J/mol·K	
T_0 = 300 K	
T_f = 2500, 2650, 2700 K at p = 0.08, 40 and 100 atm respectively, for β = 0.77[a]	

[a] Ermolin, 1993.
[b] Zanotti *et al.*, 1992.
[c] Price *et al.*, 1978.
[d] Krishnan and Jeenu, 1992.
[e] Beckstead *et al.*, 1970.

extrapolated based on existing values for fuel-rich mixtures. Therefore, the results of the present study do not include calculation of the lower limit of particle size for LEF detachment. In any case, by using the propellant burning rate data in Eq. (11), the premixed flame standoff distance cannot be obtained for different stoichiometries, and the calculations using the rigorous expressions are necessarily limited to the upper limit of particle size for LEF transition (attachment). Burning rates of mix 2 were used in the above calculations.

Figure 4 shows results of the numerical calculations for the upper limit of particle size for LEF transition (attachment) using both approximate (Eq. (8)) and rigorous (Eq. (10)) expressions. As anticipated earlier, the line corresponding to comparable stoichiometric tip height and fuel-rich premixed flame standoff in the particle size-pressure domain appears to be hyperbolic in nature. In spite of the drastic assumptions, the predicted numerical values of particle sizes at different pressures are comparable with the particle size and pressure ranges of steps in burning rates for mixes 1 – 3. (The mixture ratio of the fine AP/binder matrices in mixes 1 – 3 were used in the calculations, *i.e.*, β = 0.5833). The error bars in the experimental data correspond to the width of the step along the pressure axis and the mesh

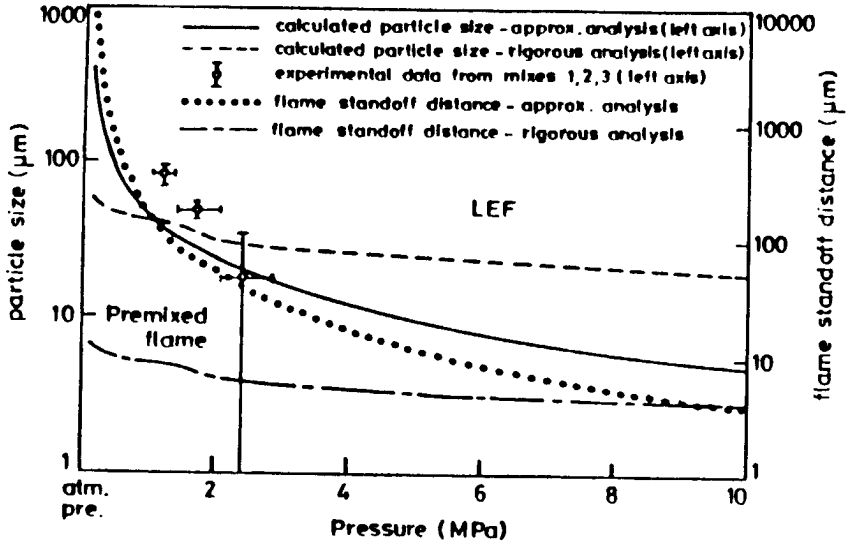

FIGURE 4 AP size as a function of pressure for transition from premixed flame to LEFs predicted from calculations, and comparison with experimental data.

sizes of the AP particles in the different mixes. The particle sizes for flame transition predicted with the rigorous expressions show a weaker trend with pressure than those with the approximate expressions. The step in the rigorous curve corresponds to the step in the burning rate *versus* pressure of the propellant.

The flame standoff distance ($h = \delta$) is also plotted as a function of pressure in Figure 4, on the right axis. The values are unrealistically low when the rigorous expression (Eq. (11)) is used, whereas the approximate expression (Eq. (2)) gives rise to a trend that falls steeply to unrealistically low values with increase in pressure. The prediction of low flame standoff distances is typical of analytical models concerning quasi-steady one-dimensional deflagration of homogeneous solids (De Luca, 1992). Recently, Brewster *et al.* (1997) have drawn attention to the fact that the formal solution for the premixed flame standoff distance obtained by Williams (1973) is in the limit of large activation energies which may not be applicable to premixed flames in solid propellants. They treat the example of HMX, but indeed, the Zeldovich number (as defined by Liñán and Williams, 1993) for AP-polybutadiene binder propellants is < 10 (calculated using data from Ermolin, 1993), a value not too high for the activation energy to be considered large. Brewster *et al.* (1997) have obtained an expression for the premixed flame standoff distance in the limit of "vanishingly small" activation energies, which gives slightly larger numerical values than Eq. (11) at elevated pressures as shown for HMX. Employing that expression may lead to a better correlation of the critical particle size for LEF transition, but it is not done here because (a) the present purpose is to merely formulate a simple mathematical approach to the idea of LEF transitions for which Eqs. (8) and (10) serve as an illustration, and (b) it is not clear how to incorporate Ermolin's (1993) data for two reactants into the form considered by Brewster *et al.* (1997) where the gas phase reaction involves one major species and a generic chain carrier species.

DISCUSSION

The idea of LEF transitions is implicit in all models that encompass (even superficially) both premixed flames (low pressure, fine particle size) and particle-attached flamelets (*e.g.*, the granular diffusion flame model (Summerfield *et al.*, 1960)). The present paper simply examines the microscopic details of transition at the level of individual AP particles.

1. Results of the Present Study

The experimental results support the idea of transition from premixed to LEF burning, in that:

(a) the burning rates of the propellants show an upward shift that occurs at pressures that are in the range where such transition is reasonable;
(b) the transition is delayed to higher pressure when fine particles are used (Fig. 2);
(c) the larger increase (Fig. 3) in the burning rate of mix 4 (coarse/fine AP = 7/3) than for mix 2 (coarse/fine AP = 8/2) is consistent with the larger dependence of the overall rate on the matrix flame;
(d) the transition is shifted to a lower pressure for mix 4 compared to mix 2 (Fig. 3), as can be expected with a greater fine AP content (mix 4). The matrix in mix 4 is less fuel-rich, which leads to a shorter premixed flame standoff distance. On the other hand, the stoichiometric tip height increases due to thinner binder layers with more fine AP, and higher mass burning rate. The two effects result in existence of LEFs at a lower pressure than in the case of a propellant with lesser fine AP content (mix 2).

A similar reasoning is applicable for the behavior of the catalyzed propellant (mix 5). The catalyst (ferric oxide) is observed to accumulate on the burning surface. It has been argued that the catalyst is well situated to enhance (a) the breakdown of heavy fuel molecules (Price and Sambamurthi, 1984; Markou, 1988), and (b) the exothermic decomposition of perchloric acid vapors from the AP particles along the AP/binder contact lines (Chakravarthy *et al.*, 1997). The combined effect is to furnish hotter and more reactive gases for reaction in the gas phase. This enables a lower standoff for the gas phase flame (causing an overall increase in the burning rate at all pressures), and hence a transition to LEFs at a lower pressure than without the catalyst (as in mix 6). The results with Al_2O_3 (mix 6) show no effect on burning rate (Fig. 3), indicating that the effect of Fe_2O_3 is chemical, and not physical.

The most important aspect of the theoretical predictions presented in this study (Fig. 4) is perhaps the "hyperbolic" nature of the curve corresponding to attachment of LEFs in the particle size-pressure domain, *i.e.*, as the particle size is decreased, it takes increasingly higher pressures for LEF attachment to occur. Even in the face of very limited experimental data and probably inadequate correlation of the theoretical predictions with the data, it must be remembered that in the hypothetical limit of zero particle size, the burning should logically proceed by a premixed flame. As observed in Figure 4, a wide range of large-to-medium sized particles burn with attached flames in most of the pressure range of interest in rocket motor applications. It is then easy to see how modern models of combustion of AP propellants such as the BDP model (Beckstead *et al.*, 1970) succeed without explicit representation of premixed burning for fine particles and/or low pressures. However, renewed interest in plateau burning of propellants has been made possible recently by the use of large amounts of very fine AP in the propellant formulation (Hinshaw and Mancini, 1993). There may be large areas of fine AP/binder matrix on the burning surface of such propellants that are burning in a premixed fashion even at high pressures. This could be one of the underlying reasons why the BDP type of models cannot successfully predict high-pressure plateau burning behavior of propellants with very fine particles (Cohen and Highsmith, 1992).

2. Further Considerations on the Details of Transition between Premixed Flames and LEFs

In looking at the process of attachment-detachment of LEFs, there are a number of important features that go beyond the description that has been made and validated above, features that are needed for realistic modeling. For example, it was argued above that the detachment represented a singular condition during progressive decrease in pressure, in which the O/F flame cannot stabilize at locations immediately above the stoichiometric tip because the concentration field moves to an increasingly fuel-rich condition above the tip.

The details of transition can be visualized further if one addresses *attachment* of the LEF instead of detachment. In a practical sense, this would occur in a dynamic system where pressure is rising or the AP surface area is increasing (*e.g.*, during the first half of burning of a particle). As the pressure increases (from a sufficiently low level for a given exposed AP size range), the premixed flame moves progressively closer to the surface. Presumably, the premixed flame would also develop convolutions over the mixing fans as pressure rises, representing regions of less fuel-rich O/F ratio. These local inward convolutions would progressively deepen until they arrive at the stoichiometric tip, at which point they become LEFs. The LEFs burn with a much higher (near stoichiometric) flame temperature, and under such conditions, they would immediately locate themselves at some more advanced location (nearer the surface) commensurate with the new higher local flame temperature.

This would imply a sort of hysterisis, in which LEFs would proceed to detachment progressively with decreasing pressure, followed by a jump to a premixed flame condition; when the pressure change is reversed, the premixed flame would progressively move in (through states it skipped during detachment) until it attaches, whereupon it jumps to a more advanced LEF site (through a progression of states that were stable during the approach to detachment). If the real process is anything like the above speculation, it would represent a dramatic cycle of flame oscillation during pressure fluctuation in a motor (Beiter and Price, 1998).

This issue needs to be addressed and clarified by a realistic model (even quasisteady), perhaps initially using an axisymmetric geometry, capable of representing the LEF and the multidimensional diffusion field, and incorporating the overall stoichiometry of the system.

3. Further LEF Detachment Issues

In this report it has been assumed that the particles on the burning surface have diffusion "fans" that lead to unambiguous stoichiometric tips (in the ideal case, cylindrical symmetry is assumed). In even the most ideal propellant (uniform parallel rods of oxidizer) the assumption of cylindrical

symmetry of mixing fans is violated, although perhaps not seriously enough to negate the concept of stoichiometric tips. In the matrix portion of the bimodal propellant, each particle surface adjoins other particle surfaces of somewhat different size. This poses at least three different issues pertinent to LEF attachment:

(a) To the extent that stoichiometric tips remain distinguishable, their heights will differ and the LEF detachment pressures will differ, to a degree inherent in the progressive changes during particle burning, and subject also to manipulation of particle size distribution.
(b) Adjoining particles disturb the symmetry of mixing fans, potentially to the point of complicating the qualitative nature of the mixing fans and identity of the stoichiometric tips (stoichiometric surfaces may even close over the binder at sites of thin binder layers between particles). These effects are enhanced by increase in O/F ratio.
(c) The LEFs of adjoining particles may be interactive, with small particle flamelets being stabilized by large particle LEFs. The results of the present experimental work indicate that these effects were small enough (in the fine particle matrix areas) to permit LEF detachment to be manifested in the burning rate-pressure curves.

The effects (a)–(c) are expected to become more important even in bimodal propellants if the proximity of coarse particles to fine ones is increased by increasing the proportion of coarse particles, decreasing the coarse particle size, or increasing the O/F ratio.

In more conventional propellants with wide particle size distribution, the transition from premixed burning to particle-attached burning with increasing pressure is a long-recognized phenomenon, which is generally not detailed in combustion models. From the issues noted above it is easy to understand why; it is a very complicated phenomenon both in mechanistic detail and statistical character. The present work is a starting point, which can be applied now for propellants with suitably crafted microstructure.

CONCLUSION

The details of transition between premixed flame burning and particle-attached burning can be examined by the concept of leading edge flame attachment, and effects are manifested by a transition in the burning rate in a narrow pressure range for bimodal AP propellants. Through this transition in the $r(p)$ function, the dependence of the transition on particle size and pressure was identified and the controlling mechanisms were clarified. The results permit some measure of tailoring of formulation to control burning rate, and provide basic information for understanding other aspects of propellant combustion that depend on whether premixed or particle attached O/F flames are present (Beiter and Price, 1998; Sambamurthi and Price, 1984).

Acknowledgements

This work was performed under contracts N00014-85-K-0803 and N00014-95-J-0559 with the US Office of Naval Research; Richard S. Miller was the technical monitor.

NOTATION

A_i, P	species in the premixed flame global reaction
A	pre-exponential factor
C	specific heat capacity
D	diffusion coefficient of reactant gases
E	activation energy
$J_0(\varphi)$, $J_1(\varphi)$	Bessel functions of the first kind of order 0 and 1, of argument φ
L	latent heat per unit mass of condensed phase pyrolysis
M	average molecular weight of products
Pe	Peclet number
r	propellant burning rate
T	temperature
X_i	mole fraction of species i
d	oxidizer size
h	diffusion flame/stoichiometric tip height
k	global kinetic reaction rate constant
n	order of global reaction in the premixed flame
p	ambient pressure
u	axial gas phase velocity
w	reaction rate of premixed flame

Greek Symbols

β	fine oxidizer/binder mixture fraction (by mass) in the propellant
δ	premixed flame standoff distance

ν	stoichiometric ratio
ν_l	stoichiometric coefficients in the premixed flame global reaction
ρ	density
λ	thermal conductivity
φ_k	k^{th} root of $J_1(\varphi) = 0$; $\varphi_1 = 3.83$

Subscripts

b	binder
f	flame
g	gas
ox	oxidizer
P	propellant
p	constant pressure
s	surface; solid
0	initial

Superscript

*	condition corresponding to LEF transition

References

Beckstead, M. W., Derr, R. L. and Price, C. F. (1970) A Model of Composite Solid-propellant Combustion Based on Multiple Flames, *AIAA J.*, 8(12), 2200 - 2207.

Beiter, C. A. and Price, E. W. (1998) The Role of Detachment of the Leading Edge of the Diffusion Flame in the Pressure-coupled Response of Composite Propellants, *Journal of Propulsion and Power*, 14(2), 160 - 165.

Brewster, M. Q., Ward, M. J. and Son, S. F. (1997) New Paradigm for Simplified Combustion Modeling of Energetic Solids: Branched Chain Gas Reaction. In: *33rd AIAA/ASME/SAE/ASEE Joint Propulsion Conference and Exhibit*, AIAA 97 - 3333.

Burke, S. P. and Schumann, T. E. W. (1928) Diffusion Flames, *Ind. and Engg. Chem.*, 20, 998 - 1004.

Chakravarthy, S. R., Price, E. W. and Sigman, R. K. (1997) Mechanism of Burning Rate Enhancement of Composite Solid Propellants by Ferric Oxide, *Journal of Propulsion and Power*, 13(4), 471 - 480.

Chung, S. H. and Law, C. K. (1984) Burke-Schumann Flame with Streamwise and Preferential Diffusion, *Combust. Sci. and Tech.*, 37, 21 - 46.

Cohen, N. S. and Highsmith, T. O. (1992) An Explanation for Anomalous Combustion Behavior in Composite Propellants. In: *29th JANNAF Combustion Meeting*, Chemical Propulsion Information Agency.

De Luca, L. (1992) Stability Theory by Flame Models. In: De Luca, L., Price, E. W. and Summerfield, M. (Eds.), *Nonsteady Burning and Combustion Stability of Solid Propellants*, Progress in Astronautics and Aeronautics, AIAA, Washington, DC, Vol. 143, Chap. 14, pp. 519 - 600.

Denison, M. R. and Baum, E. (1961) A simplified model of unstable burning in solid propellants, *ARS J.*, 31, 1112 - 1122.

Ermolin, N. E. (1993) Kinetic Parameters of Overall Gas-phase Reactions for Propellants Based on Ammonium Perchlorate and Polybutadiene Binder, *Fizika Goreniyai Vzryva*, 29, 97 - 104.

Hinshaw, C. J. and Mancini, V. E. (1993) Biplateau Propellant Containing Aluminum, Interim Report to ONR on contract no. N00014-92-C-0134, Thiokol Corporation, TR 10137.

Krishnan, S. and Jeenu, R. (1992) A Surface Reaction Model for Catalyzed Composite Propellants, *AIAA J.*, 30(11), 2788 - 2791.

Lee, S.-T., Price, E. W. and Sigman, R. K. (1994) Effect of Multidimensional Flamelets in Composite Propellant Combustion, *Journal of Propulsion and Power*, 10(6), 761 - 768.

Liñán, A. and Williams, F. A. (1993) Fundamental Aspects of Combustion, Oxford University Press, New York, p. 24.

Markou, C. P. (1988) Effect of Different Binders and Additives on Sandwich Burning, *Ph.D. Dissertation*, Georgia Institute of Technology, Atlanta, GA.

Prasad, K. and Price, E. W. (1992) A Numerical Study of the Leading Edge of Laminar Diffusion Flames, *Comb. Flame*, 90, 155 - 173.

Price, E. W., Samant, S. S., Sigman, R. K., Meyer, W. L., Powell, E. A., Handley, J. C. and Strahle, W. C. (1978) The Fire Environment of a Solid Propellant Burning in Air, Report for Air Force Weapons Laboratory on contract no. F29601-76-C-0119, Georgia Institute of Technology, Atlanta, GA.

Price, E. W. and Sambamurthi, J. K. (1984) Mechanism of Burning Rate Enhancement by Ferric Oxide, In *21st JANNAF Combustion Meeting*, Chemical Propulsion Information Agency, Pub. 412(1).

Price, E. W., Sambamurthi, J. K., Sigman, R. K. and Panyam, R. R. (1986) Combustion of Ammonium Perchlorate-polymer Sandwiches, *Comb. Flame*, 63, 381 - 413.

Sambamurthi, J. K. and Price, E. W. (1984) Aluminum Agglomeration in Solid Propellant Combustion, *AIAA J.*, 22(8), 1132 - 1138.

Summerfield, M., Sutherland, G. S., Webb, M. J., Taback, H. J. and Hall, K. P. (1960) Burning Mechanism of Ammonium Perchlorate Propellants, In: Summerfield, M. (Ed.) *Solid Propellant Rocket Research*, ARS Progress in Astronautics and Rocketry, Academic Press, New York, Vol. 1, Chap. 6, pp. 141 - 182.

Strahle, W. C. (1993) An Introduction to Combustion, Gordon and Breach Science Publishers, Amsterdam.

Williams, F. A. (1973) Quasi-steady Gas-phase Flame Theory in Unsteady Burning of a Homogeneous Solid Propellant, *AIAA J.*, 11, 1328 - 1330.

Williams, F. A. (1985) *Combustion Theory*, 2nd edition, Benjamin/Cummings Publishing Co., California.

Zanotti, C., Volpi, A., Bianchessi, M. and De Luca, L. (1992) Measuring Thermodynamic Properties of Burning Propellants, In: De Luca, L., Price, E. W. and Summerfield, M. (Eds.) *Nonsteady Burning and Combustion Stability of Solid Propellants*, Progress in Astronautics and Aeronautics, AIAA, Washington, DC, Vol. 143, Chap. 5, pp. 145 - 196.

APPENDIX N

Price, E. W., Chakravarthy, S. R., Freeman, J. M., and Sigman, R. K.

"Surface Features of AP Composite Propellants"

Proceedings of the 34th JANNAF Combustion Subcommittee Meeting

West Palm Beach, FL, October 27-30, 1997

CPIA Pub. 662, Vol. IV, pp. 45-71

JANNAF ... 1997

SURFACE FEATURES OF BIPLATEAU AP COMPOSITE PROPELLANTS

E. W. Price, S. R. Chakravarthy, J. M. Freeman, and R. K. Sigman
School of Aerospace Engineering
Georgia Institute of Technology
Atlanta, Georgia 30332-0150 U.S.A.

ABSTRACT

Quench tests and scanning electron microscopy were used to study the burned surfaces of five plateau burning propellants. The formulations of the propellants permitted observation of the effect of curing agent (DDI and IPDI), effect of TiO_2 additive, ratio of coarse-to-fine AP (bimodal AP), and addition of aluminum, over the pressure range 200-2300 psi. Surfaces were extremely complicated and pressure dependent. TiO_2 concentrated into large structures on the surface, particularly on coarse AP particles, obscuring details of the rest of the surface except at pressure extremes (all but one formulation w/o TiO_2). Binder melt was pervasive as a thin film over all surface structures over a formulation-dependent pressure rage mostly coincident with the burning rate mesa (it is speculated that this is the result of foaming of the binder-fine AP matrix during quench). The quenched surfaces are described (vs pressure and formulation), numerous micrograms are presented, and some implications of the results are discussed.

INTRODUCTION

The burning rate of solid propellants ordinarily increases with pressure, a dependence that will be referred to here as the $r(p)$ function. It is advantageous in rocket motor design to have a relatively low, or even negative sensitivity of burning rate to pressure, at least in the design range of operating pressure. Such burning rate behavior has been observed in AP/hydrocarbon binder propellants when the AP ingredient consists of bimodal particle size distribution with widely separated size modes (e.g., coarse AP 200-400 μm and fine AP 2-20 μm). With such propellants it has been possible (Ref. 1) to obtain $r(p)$ functions with plateaus at two different pressures. In some instances, the $r(p)$ functions even exhibit "mesas", i.e., pressure ranges in which the $r(p)$ function proceeds to an initially high value of $(\partial r / \partial p)_{|(r/p)}$, to a zero value, negative value, zero value, and positive value as pressure is increased. The controlling mechanisms for such behaviors are still uncertain (Ref. 2, 3), and are the objective of a cooperative investigation by several universities and laboratories (Ref. 4). For these studies, samples of several propellant formulations have been supplied by Thiokol Corporation to investigators who are participating in the cooperative study. The authors of this paper had noted earlier (Ref. 3) that bimodal propellants exhibit extraordinarily complex pressure-dependent burning surfaces that imply three dimensionally complex burning on a microscopic scale. Details of these processes can be resolved to some extent by microscopic study of quenched samples. The present paper reports observations made on Thiokol propellants no. 2, 4, 5, 8, and 10 quenched from pressures of 200-2300 psi and examined by scanning electron microscopy.

EXPERIMENTAL PROPELLANTS

The propellants used in this study are nominally 88% solids with 12% HTPB binder, with nominally 200 μm coarse AP and 2 μm fine AP, and 2% submicron TiO_2. The AP had nominally 0.15 % TCP anti-caking powder. The variables investigated here were comparisons:

This work was sponsored by the CalTech Multidisciplinary University Research Initiative under ONR grant no. N00014-95-1-1338, Program Manager Dr. Richard S. Miller.

Distribution authorized to U.S. Government agencies and their U.S. contractors; Critical Technology; 23 Oct 97 . Other requests for this document shall be referred to NAVAIRWARCENWPNDIV

a. DDI vs. IPDI curing agent for the HTPB (with TiO_2)
b. With and without TiO_2 (DDI cured binder)
c. With two different ratios of coarse to fine AP
d. Aluminized versus non-aluminized

Further details on formulation can be obtained from Table I and from Ref. 5.

QUENCH BURNING

Test samples were 3 x 5 x 10 mm, ignited on the end surface with a nichrome wire and a fine AP-toluene-based cement igniter paste. The test vessel was a nitrogen filled chamber with a multi-layer mylar burst diaphragm at one end (with a nichrome wire between layers). Burst was initiated by electrical heating of the nichrome wire. Depressurization rate is 10^4 to 10^5 psi/sec, depending on chamber pressure. At low pressure a few samples stopped burning before the diaphragm burst, or re-ignited from effect of hot surface residue.

The possibility that the quench event caused surface changes (e.g., removal of loose structures, induction of flow of binder melts, foaming due to expansion of subsurface vapors) has to be "respected" and/or evaluated during interpretation of quenched surfaces, and will be discussed in that context.

SCANNING ELECTRON MICROSCOPY

Quenched samples were sputter coated with gold and examined in an 151 Super 60 SEM. The structural detail of interest ranges from resolution of 2 μm AP particles to surface quality and shape of fine AP-binder matrix structures, to details and overall structure of coarse AP particles, to larger scale surface irregularities resulting (presumably) from locally intermittent burning, to evaluation of small and large clusters of TiO_2, and to identification of 95 μm aluminum particles. For the most part, these different structures can be recognized by their size, shape and locations. However it requires that micrograms be taken with several magnifications and surface sites. In addition, because of the three dimensional complexity of the surfaces, it is often desirable to view the structure from different angles (a time-consuming procedure, not yet done in this study).

RESULTS

SCOPE OF RESULTS

Quenched samples and SEMs were obtained for the formulations and conditions listed in Table I. One propellant (mix #4) was chosen as a reference, and the surface features are described in the following. The other propellants are then compared with the reference propellant as listed in Table I. The comparisons include comparison of burning rate graphs and surface features of quenched samples (verbal and some SEMs). In the interest of brevity in describing the surface features, a list of descriptive words evolved as a "shorthand" for distinctive or critical surface features, described in Table II. Figures 1a to 1f illustrate the features described in Table II and Figures 2a to 2d show the burning rate curves for the tested propellants paired with the curves for the reference propellant and for pure AP.

SURFACE FEATURES FOR REFERENCE PROPELLANT

Thiokol mix #4 was chosen as a reference because there were other mixes that differed from it by only one variable (Table I). Mix #4 was 88% solids, 12% DDI cured HTPB binder, AP coarse-to-fine ratio 62/38, no aluminum, 2% TiO_2. An exception was made for the aluminized propellant, which has IPDI cured HTPB binder and is compared with mix #5 (IPDI cured HTPB binder, no aluminum). The features of the mix #4 quenched surfaces will be shown in extra detail to provide a basis for verbal comparative description of the results from the other mixes tested.

At 200 psi, the surface is fairly level: the matrix areas are littered with particles of varied shape and size in the 5-25 μm size range, sitting in a surface that appears to have been wet: the coarse AP particles (Fig. 1a) standout clearly (sharp edges), with rather smooth surfaces that seem to be concave

except for raised central areas shaped like volcanoes with sizable irregular peaks consisting of sintered TiO_2.

At 500 psi, the surface is in sharp contrast to the one at 200 psi. The matrix surface looks dry and is rather planar (Fig 3a) with large depressions where the coarse AP has burned on ahead. The coarse AP seem to be partially obscured by over-hang of the matrix layer. The visible coarse AP surfaces have concentrations of sintered TiO_2, Fig. 3b. The AP surfaces surrounding the central TiO_2 are porous and recessed, and the AP surface further out looks partially porous.

At 1000 psi, the matrix areas are raised relative to the coarse AP, but convoluted to follow the coarse AP surfaces, not level, not as dry looking as at 500 psi, and showing protrusions and dimples typically 10 μm across. The coarse AP particles (Fig. 3c) are concave with raised central areas covered with TiO2 (areas typically 70-100 μm across).

At 1500 psi, the surface is a jumble (Fig. 3d). The matrix leads (is recessed). The surfaces of the coarse AP are very irregular, with sharply defined edges, large areas of sintered TiO_2 that are not always centrally concentrated. Areas that are dominated by TiO_2 (Fig. 3e) are variably porous. Classical smooth bands are largely absent on the coarse AP.

At 1800 psi, the entire surface is glossed over by a binder film (Fig. 3f). The general topography is similar to that at 1500 psi, but the only small scale structures that can be seen are a few bumps of nominally 5 μm over the whole surface. Large depressions may be recessed coarse AP surfaces.

At 2000 psi, the general topography is similar to that at 1800, but surface detail is more visible (less melt gloss). Some coarse AP surfaces are visible deeply recessed, and overburdened at the edges by matrix material that typically slopes upward away from the coarse particle (Fig. 3g). The coarse AP particles have major mountains in the central areas, sometimes elongated in the direction of AP surfaces. These protrusions often have more than one peak. Because they are slightly glossed with binder melt, their identity as sintered TiO_2 can only be inferred from observations at lower pressures. In areas of extensive melt gloss, the number density of the protrusions is too high to be coarse AP particles.

At 2300 psi, the surfaces are similar to those at 2000 psi. The coarse AP particles may be less recessed, everything seems a little less glossed (Fig. 3h).

EFFECT OF CURING AGENT (MIX #5, IPDI): COMPARE WITH MIX #4, DDI

At 200 psi, the surface (Mix #5) appears drier and there is more TiO_2 clutter on the matrix surface, which seems to lead. There is more major sintered TiO_2 in the central area of the coarse AP particle. (Fig. 1e: compare with Fig. 1a)

At 500 psi, the matrix clearly leads, the coarse AP particles are not concave upward (Fig. 1b: compare with Fig. 3a, b) but have smooth surfaces with large will-sintered TiO_2 on the raised central areas.

At 1000 psi, the matrix and coarse AP periphery lead(with mix #4, the matrix lagged), the AP surface is porous, but the overall surface appearance is dominated by "boulders" (typically 120μm) (Fig. 1g) that apparently evolve from the concentrations of TiO_2 that form on the central AP surfaces. (Fig. 1g: compare with Fig. 3c). No boulders with mix #4.

At 1300 psi, the "leading edge" is a bunch of holes with matrix-AP interfaces. The TiO_2 concentrations dominate the scene, with boulder-like protrusions some interconnected (Fig. 4a). Very dry look. Mix #4 did not have "boulders" (not tested at 1300 psi, but no boulders at 1500 psi).

At 1500 psi, the surface features look like those at 1300, but they (Fig. 4b) are glossed over by binder melt. (At this pressure mix #4 had dry-surface, no boulders; compare with Fig. 3d)

At 1800 psi, appearance is similar to 1500 psi, more melt gloss than mix #4. Interconnected boulders still visible, glossed.

At 2000 psi, the boulder formations are more interconnected, still melt glossed (Fig. 4c), but drier leading fronts are visible, deeply recessed. Matrix areas are wet, but show a variety of protrusions < 10 μm. At this pressure Mix #4 was similar, maybe a little less recessed dry area, some clearly defined coarse AP surfaces.

At 2200 psi the surface (Fig. 4d) is fairly dry, with large irregular TiO_2 structures, deeply-recessed leading front areas, larger than at 2000 psi. The coarse AP structures are hard to completely resolve because of TiO_2 boulder overburden. Much drier than Mix #4, TiO_2 structures much larger, but open leading front areas also larger.

The binder melt gloss occurred over a lower pressure range with IPDI cured binder (as did the mesa). The TiO_2 was processed differently; i. e. unlike the DDI case, the concentration of TiO_2 formed boulders in the mid-pressure range with the burning rate-controlling region recessed deeply. The melt gloss was evident at 1500 psi, whereas the DDI samples did not show gloss until 1800 psi. Note that the onset of melt gloss in both cases occurs at the pressure corresponding to the peak burning rate before the negative slope region of the r(p) function, and the return to positive slope corresponds to decline in melt flow effects. The elevation of the rate of the IPDI formulation over that of the DDI formulation (whole pressure range) seems to be related to an ability to maintain areas of interactive burning of matrix and coarse AP beneath the TiO_2 overburden.

EFFECT OF TiO_2 (MIX #10, NO TiO_2) COMPARE WITH MIX #4, 2 % TiO_2

At 200 psi matrix looks drier than with TiO_2. Coarse particles similar except only mild (less) protrusion in the middle with an appreciable area of puffy, porous material in the center (in place of the TiO2 accumulation with Mix #4). Edges of coarse particles are clearly defined (Fig. 5a).

At 500 psi surface is very crowded with coarse dome-shaped AP particles (surface with Mix #4 is dominated by dry looking matrix areas, with coarse AP burned ahead, with porous surfaces and TiO_2 in center of coarse particles). With no TiO_2, cooperative burning of coarse AP and matrix seems to lead the burning, with most matrix consumed there (i. e., its recessed) (Fig. 5b). Looking at several particles, it appears that they first become exposed with a porous surface that remains on a raised contour while the outer area burns faster . Late in particle burning the outer edge is dished up slightly. None of these details can be discerned with TiO_2 present. At this pressure Mix #10 and Mix #4 have about the same rate. Compare Fig. 5b and Fig. 3a, b.

At 1000 psi the coarse particles burn ahead of the matrix both with and without TiO_2; (Fig. 3c, 5c); the coarse particles appear to burn outward under the matrix (first half of burning ?) and burn out with surface concave upward near burnout. Matrix areas are covered with porous (reacting) clusters (up to 15 μm) with no TiO_2; matrix looks slightly wetter with TiO_2.

At 1800 psi the surface is glossed, fairly level, coarse AP peripheries generally identifiable with surfaces concave upward but with central puffs still identifiable (Fig. 5d). The matrix surfaces are raised, with dimpled wet look. The features with TiO_2 (Fig. 3f) are more heavily glossed, the surface chaotic (apparently due to protruding matrix, TiO_2 accumulations).

At 2300 psi the non TiO_2 sample is fairly dry, the TiO2 one still somewhat glossy. Surfaces are very irregular in both cases. (Fig. 5e; compare with Fig. 3b). Extensive areas of the coarse AP particles (Fig. 5f) have a convoluted porous quality suggestive of anomalous AP deflagration (Ref. 6).

In general, the similarities and differences from Mix #4 (TiO_2) were that for no TiO_2 (Mix #10):

a) There was less glossing of the surface (1800, 2300 psi).
b) There were no boulders.
c) Surfaces were less irregular (all pressures).
d) The surface at 2300 psi was unique to all the propellants tested at this pressure in that the coarse AP particles, while often clearly identifiable, were very irregular in surface shape and surface condition (as is the overall surface).

e) The burning rate is lower than any of the other mixes tested.
f) The porous surfaces and irregularity of the burning surface, along with the low burning rate at 2300 psi suggest that "anomalous deflagration" of the AP contributes to the low burning rate, as suggested in Ref. 6.

EFFECT OF COARSE-TO-FINE RATIO: MIX #4 VS. MIX #8 (C/F = 62/38 AND 55/45; FIG. 2C)

At 500 psi, coarse AP particle surfaces are clearly defined, concave upward except for raised TiO_2 covered protrusions in the middle. Matrix area is relatively large, slightly lower than coarse AP peripheries, and populated by smooth bumps (5-20 μm). Coarse AP particles seem to be unevenly distributed. Surface is dry looking, but matrix bumps may be glossed.

At 800 psi, the surface is a mountainous terrain with deep depressions about the size of coarse AP particles, protrusions of comparable size, and many "bumps" that are typical of TiO_2 accumulations. However, surface features are all glossed over by binder melt, and no details are resolved (Fig. 6b).

At 1000 psi, the surface is glossed over by melt. The surface irregularities are more numerous, apparently dominated by TiO_2 boulders. The appearance of gloss is on a rising part of the mesa (Fig. 6c; compare with Fig. 3c)

At 1800 psi, the surface is extremely irregular, on a scale too small to relate to coarse AP particles. The protrusions are presumably TiO_2 structures, more numerous and taller than at 1000 psi. The surface is glossed over so details cannot be resolved. It seems likely that depressions corresponding to coarse AP particles are there, with multiple TiO_2 boulders on each particle (Fig. 6d; compare with Fig. 3f).

At 2300 psi, the surface has irregularities on several scales: 1000 μm, 150 μm, and 10 μm. Large irregularities are indicative of locally intermittent burning. 150 μm irregularities are typical of coarse AP particles and/or TiO_2 concentrations (apparently coated with fine TiO_2). The nominal 10 μm irregularities are present on all surfaces, are presumably clusters of TiO2. No melt gloss is evident.

In general, the surface is more irregular with this C/F = 55/45 mix than with mix #4 (62/38). The melt gloss was heavier and started at exceptionally low pressure (800 psi, at the start of the rate rise towards the mesa). The number of TiO_2 boulders is higher than mix #4.

EFFECT OF ALUMINUM: MIX #2 VS. MIX 5 (15% AL VS. 0% AL)

At 200 psi, the surface is mildly uneven; coarse AP particles slightly elevated, concave with raised center which is topped by TiO_2 accumulation; no or rare Al particles; a slight melt gloss present.

At 500 psi, the surface is dry, mildly irregular; coarse AP particles clearly visible, similar to 200 psi: relatively large matrix area (Fig. 7a)

At 1000 psi, the surface is more irregular than at lower pressures; increased obscuration by TiO2 accumulations, substantial melt glossing; coarse AP particles recessed and concave, only a few resolvable. The corresponding unaluminized formulation (mix #5) showed no melt gloss until 1300 psi and showed a TiO_2 boulder field at 1000 psi. Relative coarse AP vs. matrix area not resolvable, Al particles possibly present, not distinguishable from protruding (glossed) TiO2 concentrations (50-150 μm range) (Fig. 7b).

At 2000 psi, similar to 1000 psi; very complex surface structures, glossed. Similar to mix #5 (Fig. 7c).

DISCUSSION

Study of quenched surfaces has in the past provided valuable clues to rate controlling processes in sandwich burning studies (Ref. 7, 8), although that success was elusive for many years because of the complicating effects of binder melt flow. The quench-burning method has not been used intensively with propellants, and it is perhaps too much to expect success in elucidating rate controlling mechanisms with the present propellants which have the extra complications of "hi-melt" binders, bimodal AP particle size

distribution, and TiO_2 additive. All of these formulation variables have been shown to have major (pressure dependent) effects on burning rate, caused by poorly understood mechanisms. Certainly the tests to date show burning surfaces of awesome complexity, which may or may not contain the desired clues to rate-controlling processes. While the examinations to date have revealed some major trends in surface features vs. pressure and formulation, the meaning of those trends (relative to rate controlling processes) is still a matter of speculation. Some of those trends are noted here in the following:

TiO_2 is resolvable mainly centrally located on coarse AP particles as a sintered structure protruding upward. It is reasonable to suppose that this layer is laid down on the coarse particle by the overlying matrix as it burns away. It is hypothesized that this crust remains as the AP particle burns outward and downward, but that new TiO_2 is carried away in the flow during burning to the full particle diameter, leaving the TiO_2 crust in the center. As the AP particle burns away in the latter half of burning, the TiO_2 crust apparently draws up into a "boulder," which then seems to linger to some extent, dominating the view of the surface (the boulders are attached to the surface; the nature of their interior has not been determined). These features are less conspicuous or absent except at pressures where the mesa (elevated region) in the rate curve is present, suggesting that boulders enhance the burning rate. In pictures that show sintered TiO_2 on the central areas of AP particles, the sites are usually raised, suggesting that TiO_2 does not enhance rate there. However, lingering boulders sit in the path of hot oxidizer-fuel flames, and may get hot enough to heat the surface by radiation, explaining the higher burning rate.

Surface melt gloss does not correlate as consistently with elevation of rate as does TiO_2, although it, like presence of boulders, is not conspicuous above or below the mesa. In some cases (mix #4, 5), the melt gloss occurs only at the top of, and high pressure side of the mesa, while in other cases (e. g., mix #8), the melt gloss is present during both the rising and falling part of the mesa. The gloss is apparently not caused by the TiO_2, because it is present at 1800 psi with the formulation that did not have TiO_2 (or much of a mesa). The gloss was conspicuous with mix #5 (IPDI) at 1800 psi, but less at other pressures (IPDI gives higher burning rates than DDI at all pressures, and is known to be less conducive to binder melt). Because of the poor correlation of the trends of melt gloss (over the mesa pressure range) with formulation, it is postulated that it is an artifact of the quench event, probably expansion and subsidence of a melt foam. This offers an explanation for the glossing of even the TiO_2 structures located up to 100 mm above the mean surface level. However, the presence of the gloss would then be indicative of a distinctive condition of the matrix surface prior to quench, a possible clue to how the matrix burns.

It was suggested earlier (Ref. 3) that the occurrence of a mesa in the r(p) function of the propellant might be in part related to the anomalous burning of AP starting at 2000 psi. In Fig. 2, it is evident that the negative slope regions of the propellants are not far from that for AP. It is also notable that, with the one formulation that gave an unobstructed view of the AP surface at 2300 psi (Mix #10, Fig. e, f), the AP surfaces exhibited porous areas reminiscent of the areas of needle structures found in AP self deflagration tests (Ref. 6, 9).

In samples below the "gloss" range where TiO_2 boulder arrays obstructed much of the active surface, there were often deeply recessed sites in which adjoining matrix and coarse AP surfaces were visible, suggesting that such sites were the principle sites of heat release. Presumably the presence of any one such site is always transitory (i. e., until the coarse AP particle is gone), so that burning may be locally intermittent.

It is notable that mix #8 (low coarse-to-fine ratio) exhibited melt gloss starting at relatively low pressure, in a region where rate was increasing with increasing pressure and that the rate proceeded to a maximum mesa rate that was higher than any of the other mixes tested. Melt glossing did not occur with other mixes until the beginning of the plateau or maximum of the mesa.

Up to this point only limited consideration has been given to two important (but complex) aspects of the surface. One (a) is the tendency for slow-burning components of the propellant to be predominant on the surface. Another (b) is the evidence of how surface structures progress with time during burning (notably, what does the population of coarse AP particles on the surface as revealed by the quenched sample tell about how the burning of individual particles progress with time?).

With respect to (a), the sintered TiO_2 structures are an extreme manifestation of concentration of the "slowest burning" ingredient. Is this phenomenon a manifestation of how TiO_2 manages to increase burning rate, or simply an obstacle to viewing? Further with respect to (a), the apparent covering of the burning surface with binder melt in the 1500-2200 psi range seems to be a manifestation of a parallel surface disproportionation process as proposed in Ref. 3, which may either neutralize the role of TiO_2 (with corresponding reduction of burning rate), or simply cause locally intermittent burning (with corresponding reduction in burning rate).

The obscuration of the active reaction sites on the surface impedes decisive interpretation of results of studies of the quench surfaces, but awakens a new "respect" for the complexity of the combustion process. The samples are being examined in greater detail, and efforts are being made to remove the TiO_2 concentrations to get a better look at the active combustion sites. A mix with no TiO_2 and IPDI and DDI cured binders will be sought in order to minimize TiO_2 and melt gloss obscurations of the surface.

REFERENCES

1. Cohen, H. S., and Hinshaw, C. J., "Achievement of Plateau Ballistics in Ammonium Perchlorate—HTPB Propellants," *31st JANNAF Combustion Meeting*, Oct. 1995.
   (See also Hinshaw, C. J., and Minicini, V. B., Biplateau Burning of Propellants Containing TR 10137, Thiokol corporation, Interior Report to ONR, contract No N00014-92-C-0134, March 1993.)
2. Cohen, N. S., and Hightower, J. O., "An Explanation for Anomalous Combustion Behavior in Composite Propellants," *Proceedings of the 29th JANNAF Combustion Meeting*, Oct. 1992.
3. Price, E. W., Chakravarthy, S. R., Sigman, R. K., and Freeman, J. M., "Pressure Dependence of Burning Rate of Ammonium Perchlorate-Hydrocarbon Binder Solid Propellants," AIAA Preprint 97-3106, 33rd AIAA/ASME/SAE/ASEE Joint Propulsion Conference & Exhibit, July 6-9, 1997, Seattle, WA.
4. "MURI Program: Novel New Ingredients to Stabilize Rocket Motors," Progress Review, CPIA Publication No. 658, May 1997.
5. Private communication from Dr. Carol Campbell, Mail Stop 243, Thiokol Corporation, Science and Engineering, P. O. Box 707, Brigham City, Utah, 84302-0707.
6. Chakravarthy, S. R., Price, E. W., Sigman, R. K., and Freeman, J. M., "On the Anomalous Deflagration Behavior of Ammonium Perchlorate at Elevated Pressures," 32nd JANNAF Combustion Meeting, Oct 1996.
7. Price, E. W., Sambamurthi, J. K., Sigman, R. K., and Panyam, R. R. "Combustion of Ammonium Perchorate-Polymer Sandwiches." *Combustion and Flame*, Vol. 63, No. 1986, 1986, pp. 381-413.
8. Price, E. W., "Effect of Multidimentional Flamelets in Composite Propellant Combustion," *Journal of Propulsion and Power*, Vol. 11, No. 4, pp. 717-728.
9. Boggs, T. L., "Deflagration Rate, surface Structure, and Subsurface Profile of Self-Deflagrating Single Crystals of Ammonium Perchlorate," *AIAA Journal*, Vol. 8, No. 5, May 1970, pp. 867-873.

Table I: Formulations And Test Conditions For Which Quench Results Were Obtained

			QUENCH PRESSURES, psi								
Figure #	Mix #	Deviation from Ref. Formulation*	200	500	800	1000	1300	1500	1800	2000	2300
a	4	Reference *	X	X		X		X	X	X	X
b	5	IPDI cured binders	X	X		X	X	X	X	X	X
c	10	Motions IPDI ?	X	X		X			X	X	X
d	8	C/F ratio 55/45		X	X	X		X	X		X
e	2	AP displaced by 15% Al	X	X		X				X	

* Ref. formulation 88% solids, DDI cured HTPB, 2% TiO_2, C/F = 62/38, 0% Al
Ref. formulation for mix #2 is mix #5 (both are IPDI cured)

Table II: Surface Features Shown in SEMs

a) Coarse AP particles, typically showing sharp outer periphery, smooth surface ("smooth band") adjoining outer periphery and inner area variously protruding, porous, or covered by TiO2 structures. (Fig. 1a)

b) Dry matrix surface, showing irregularities that are clusters of fine AP or TiO2, or other residue; such surfaces are either even with, raised, or recessed relative to coarse AP smooth band. (Fig. 1b)

c) Wet matrix surface has a gloss, all irregularities are smooth, sometimes dimpled (residual of blow holes?). (Fig. 1c)

d) Wet overall surface: all the surface has a glossy look. Larger objects (e.g. boulders and coarse AP) are visible but detailed surface features are obscured. (Fig. 1d)

e) Smooth bands on periphery of AP quenched surfaces usually transition to protruding central region (low pressure) or irregular porous region (hi pressure), often covered by TiO2. (Fig. 1a, e)

f) Sintered TiO2, typically on central surface of coarse AP. (Fig. 1e)

g) Boulders: the surface sometimes is dominated by boulder-shaped objects, typically 50-100 mm apparently evolved from the TiO2 accumulations on the coarse AP particles; mid-pressure range. At highest pressure there are often more than one per AP particle, sometimes partially merged. The active burning process is substantially obscured, beneath the boulder field. Under wet surface conditions, the boulder field is glossed too. (Fig. 1f)

h) Leading front: In the active combustion surface, sometimes the matrix areas are recessed between the coarse AP particles("matrix leads"); sometimes the matrix areas are raised relative to the most advanced part of the coarse AP surface("AP leads"), sometimes the adjoining areas are at the same level ("interactive burning"). (Fig. 1a, 1e, 3b, 3c, 3e, 3g) These features are sometimes unresolved when overlaid by boulders or binder melt

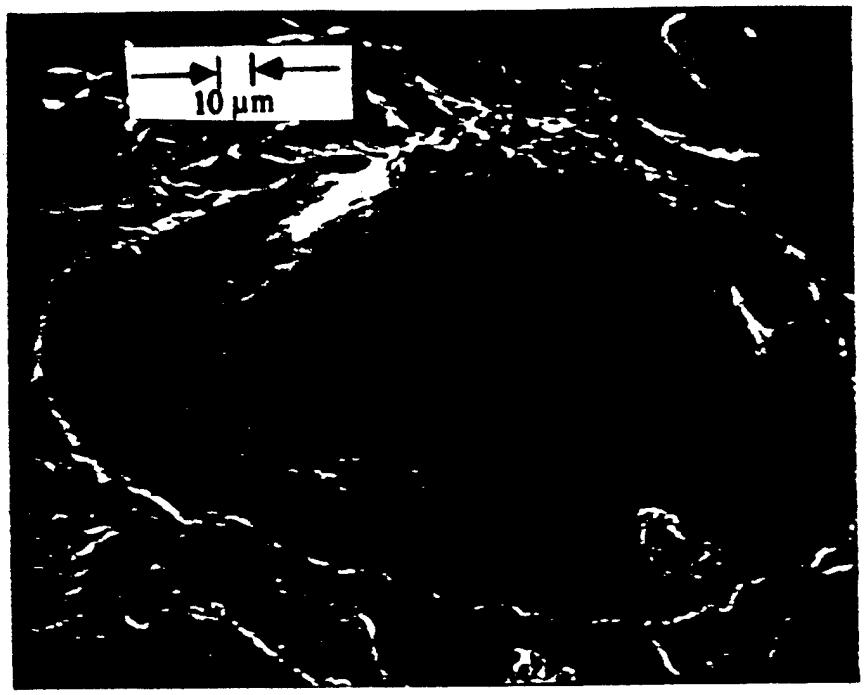

(a)

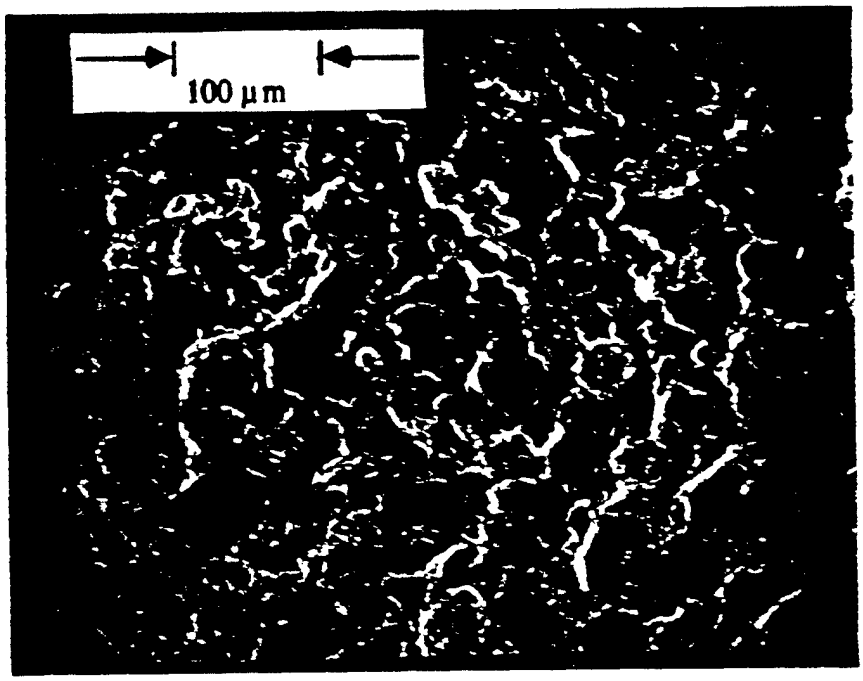

(b)

Figure 1—Illustrations of surface features used in written descriptions of quenched surfaces as listed in Table III:
(a) Features of coarse AP particle (Mix #4, 200 psi);
(b) Dry matrix (Mix #5, 500 psi)

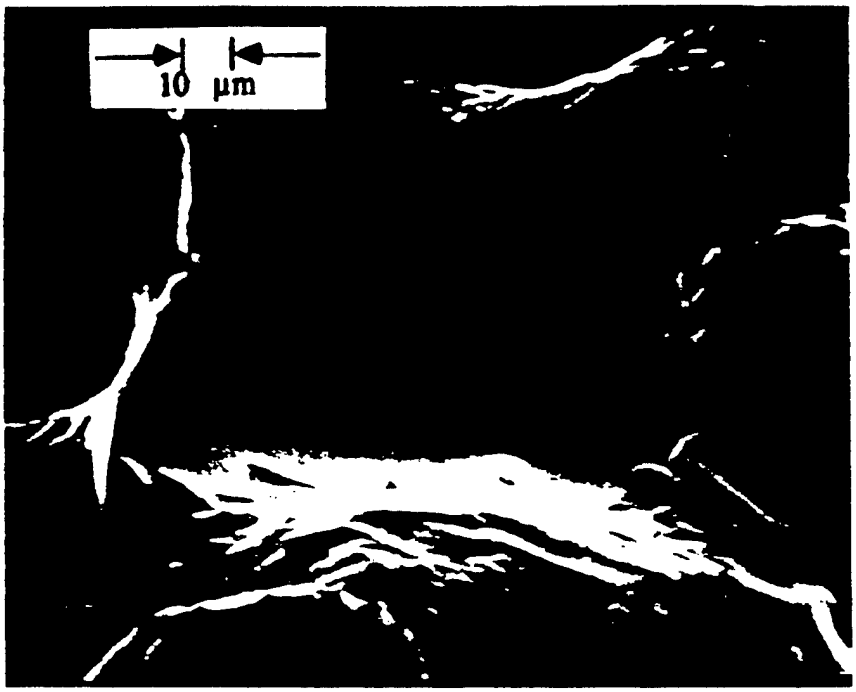

(c)

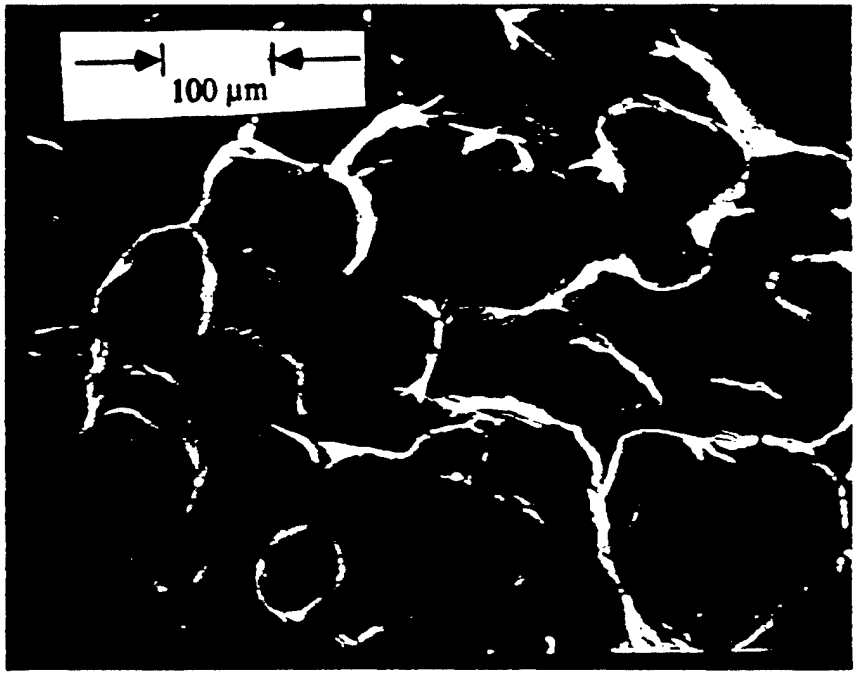

(d)

Figure 1–Illustrations of surface features used in written descriptions of quenched surfaces as listed in Table III:
(c) Wet matrix surface (Mix #5, 1800 psi)
(d) Wet overall surface (gloss) (mix #5, 1800 psi);

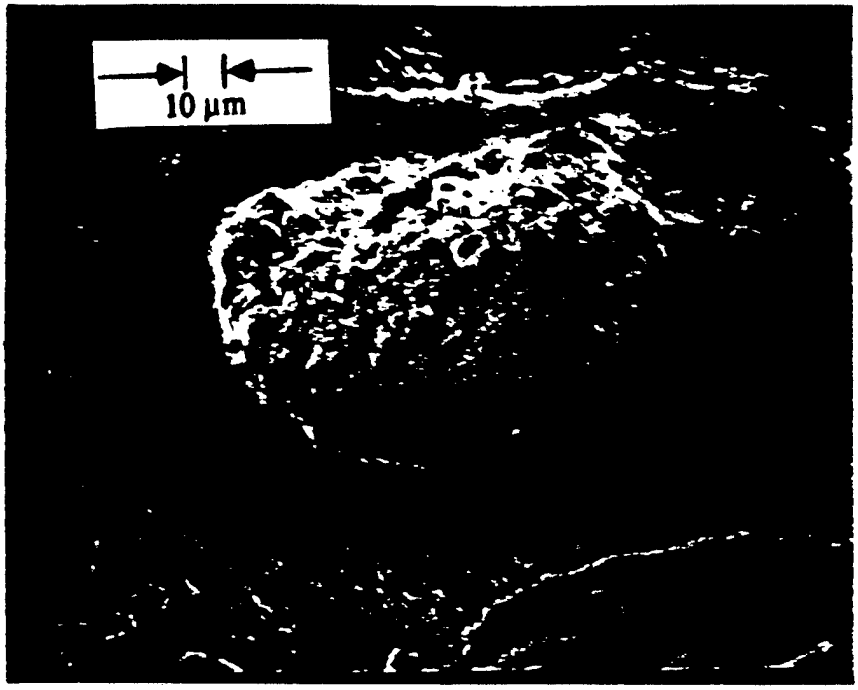

(e)

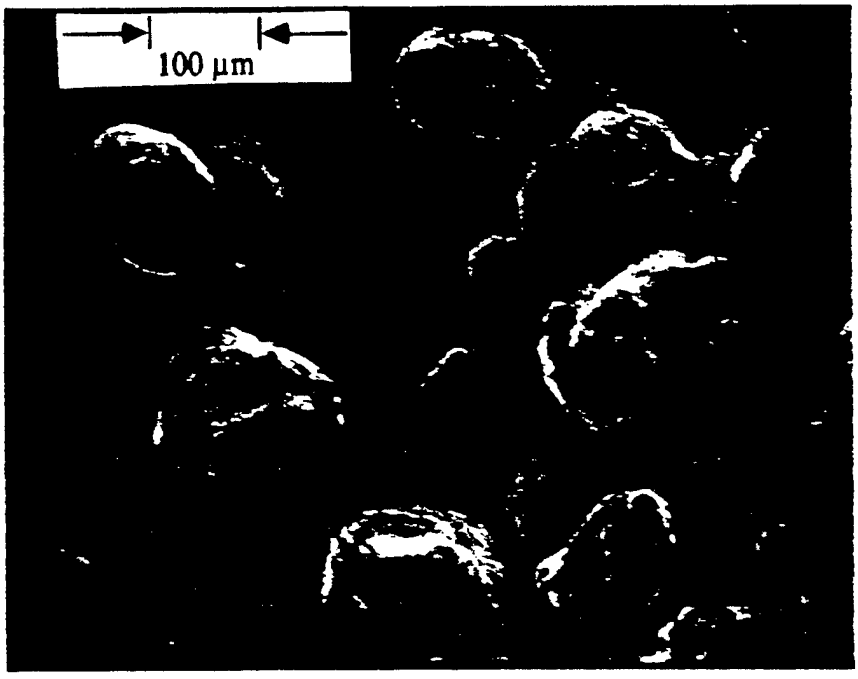

(f)

Figure 1--Illustrations of surface features used in written descriptions of quenched surfaces as listed in Table III:

(e) Smooth band on coarse AP: Sintered TiO_2 (Mix #5, 200 psi)

(f) Boulders (Mix #5, 1000 psi)

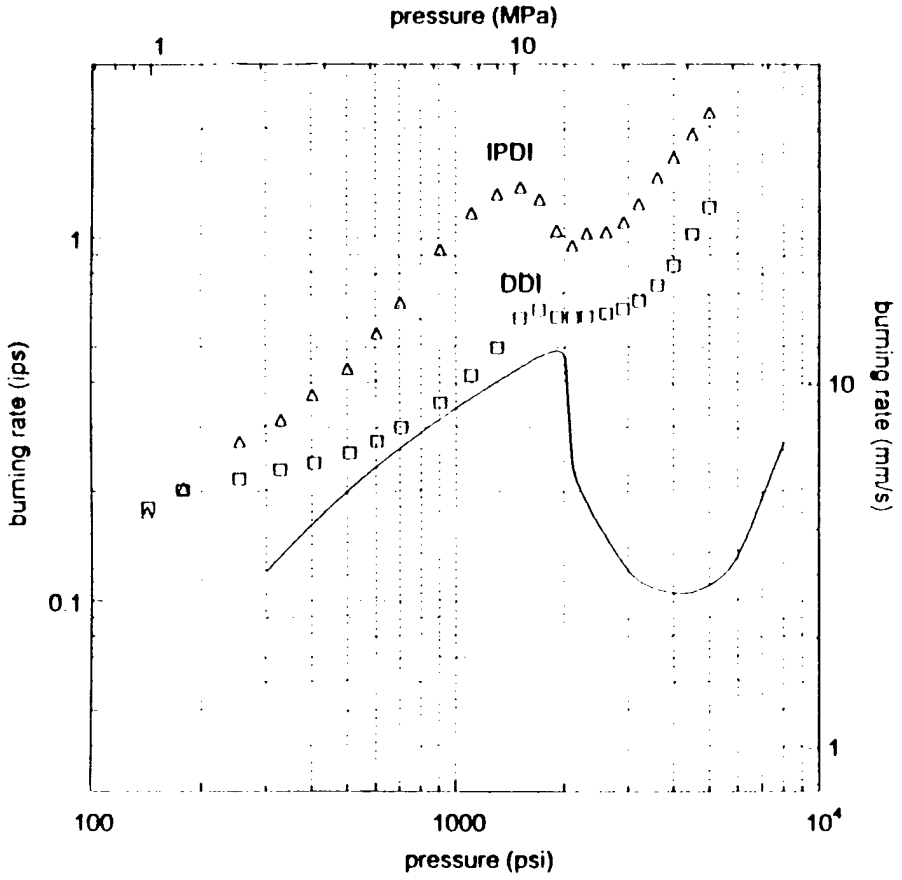

(a)

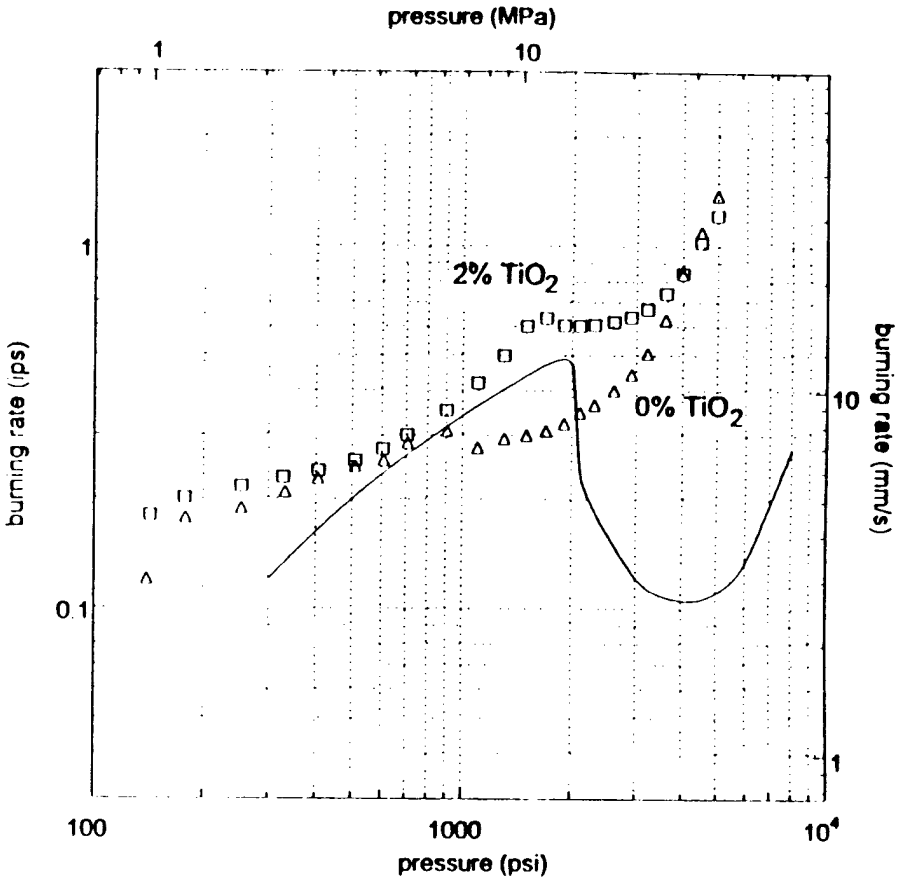

(b)

Figure 2--Burning rate curves for the propellants covered in this report, shown as comparison pairs with the rate for Mix #4. The r(p) for ammonium perchlorate also shown in all pair graphs.

(a) Effect of curing agent (DDI, IPDI)

(b) Effect of TiO_2

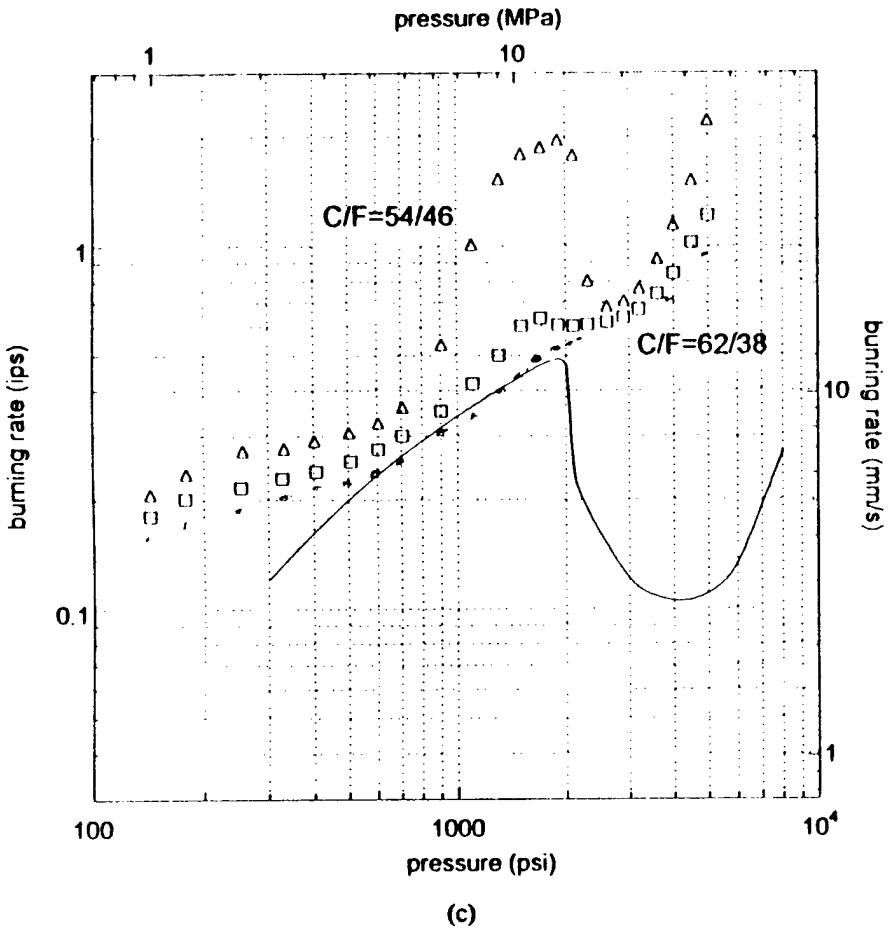

(c)

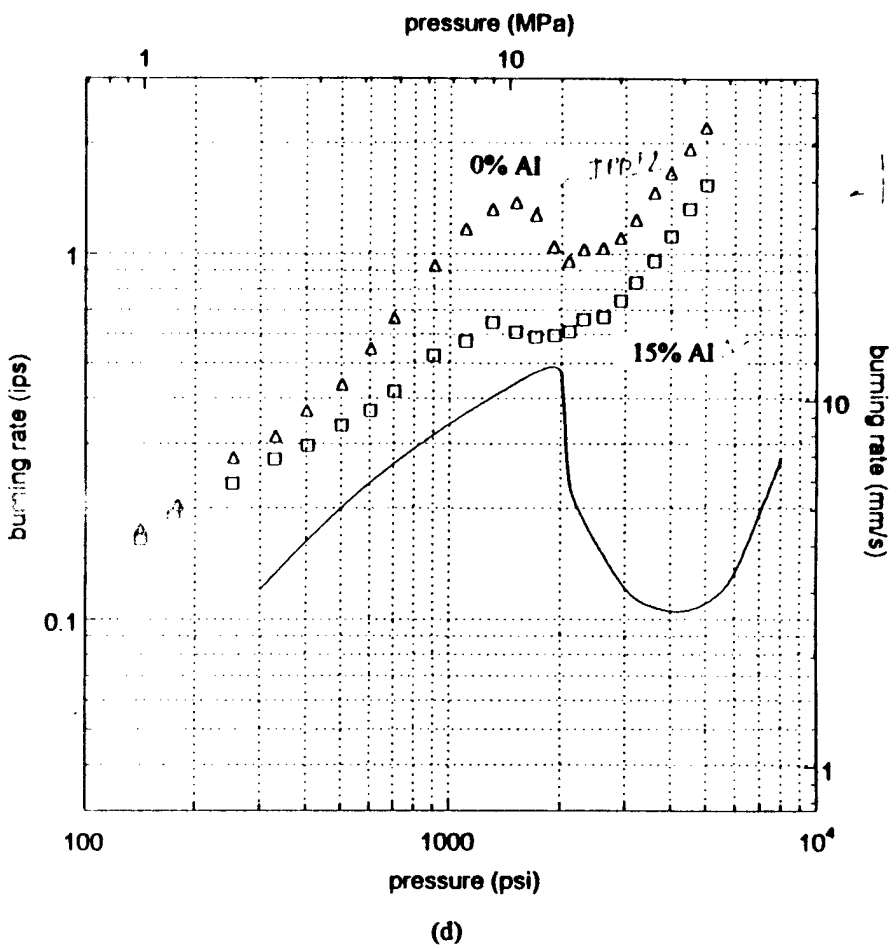

(d)

Figure 2--Burning rate curves for the propellants covered in this report, shown as comparison pairs with the rate for Mix #4. The r(p) for ammonium perchlorate also shown in all pair graphs.

(c) Effect of AP coarse-to-fine ratio

(d) Effect of adding aluminum at the expense of AP mix

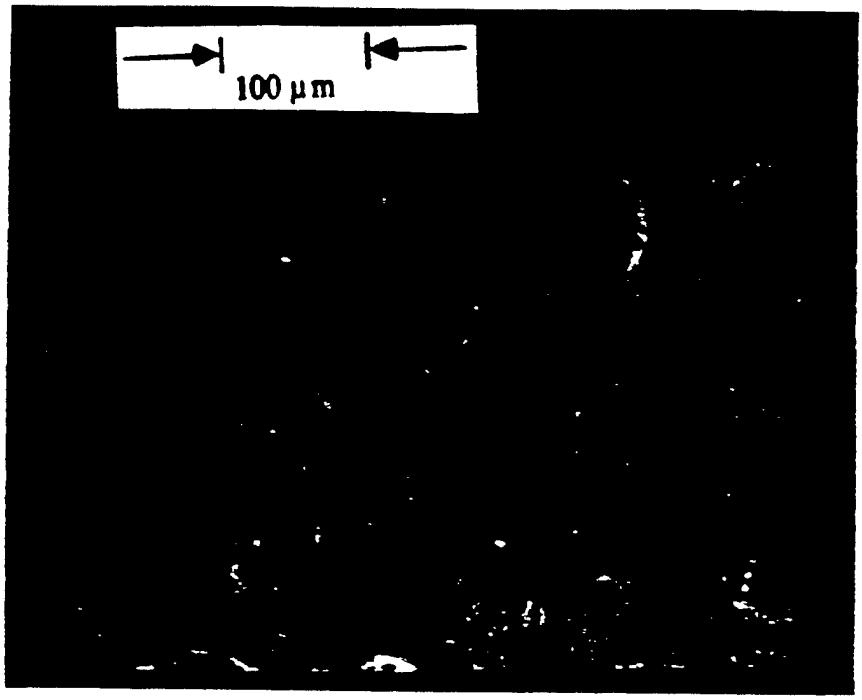

(a)

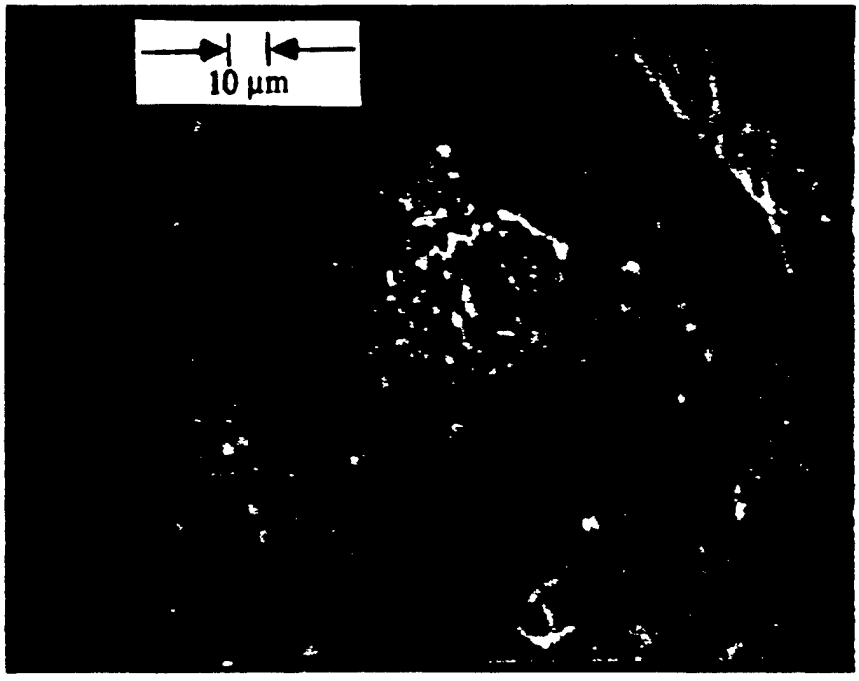

(b)

Figure 3–Surface features of Mix #4 (reference) propellant
(a) 500 psi
(b) 500 psi

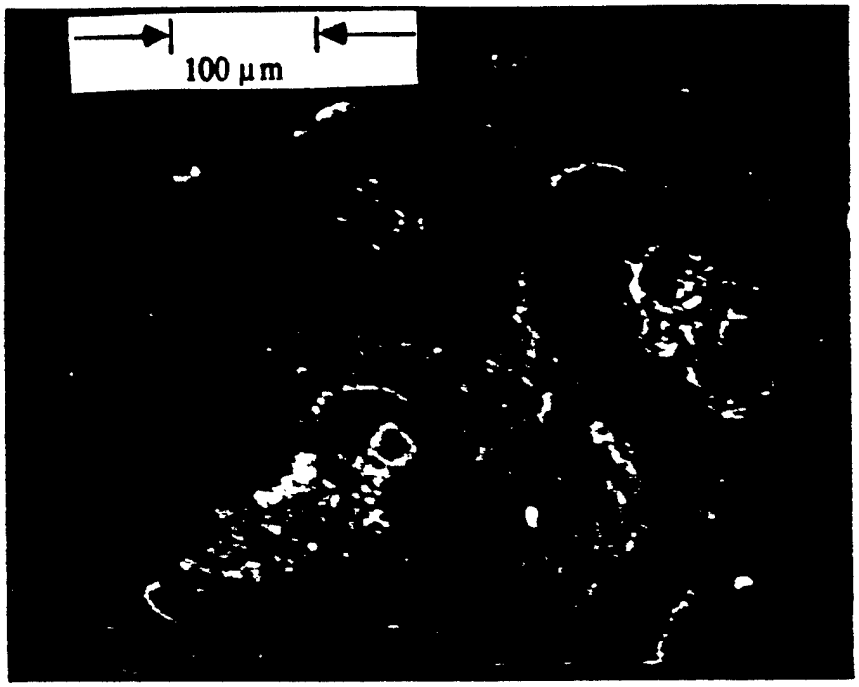

(c)

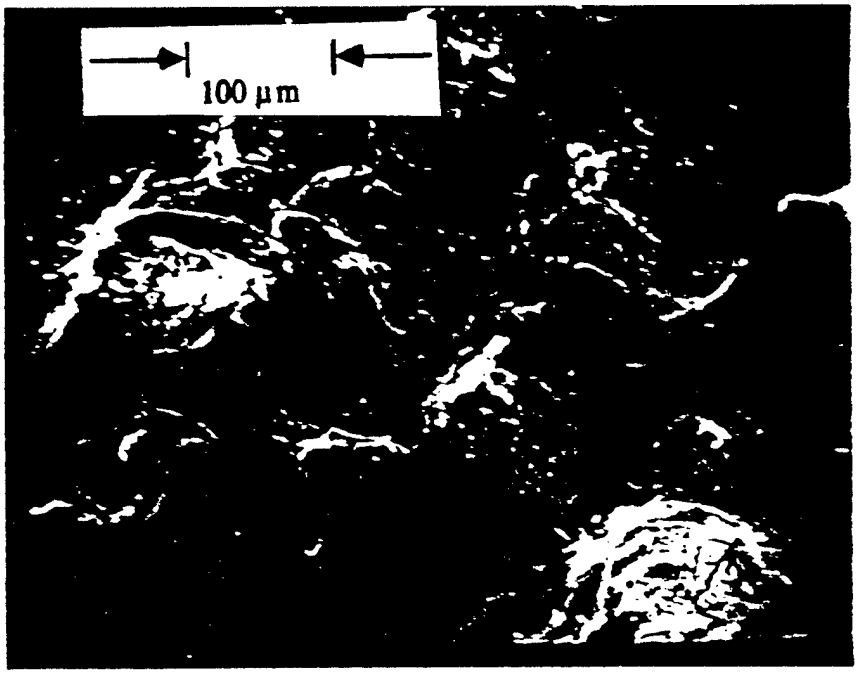

(d)

Figure 3--Surface features of Mix #4 (reference) propellant
(c) 1000 psi
(d) 1500 psi

(e)

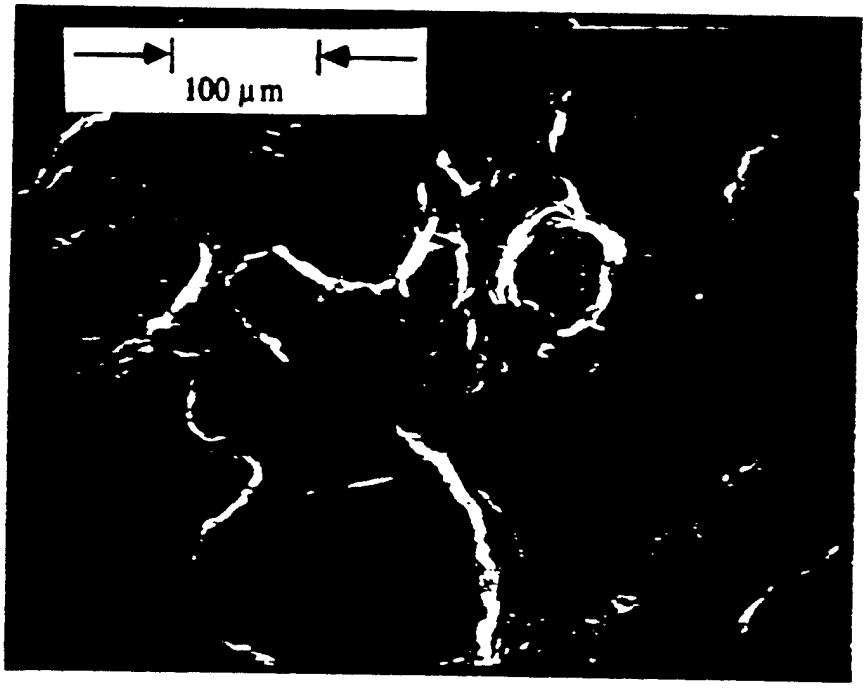

(f)

Figure 3--Surface features of Mix #4 (reference) propellant
(e) 1500 psi
(f) 1800 psi

(g)

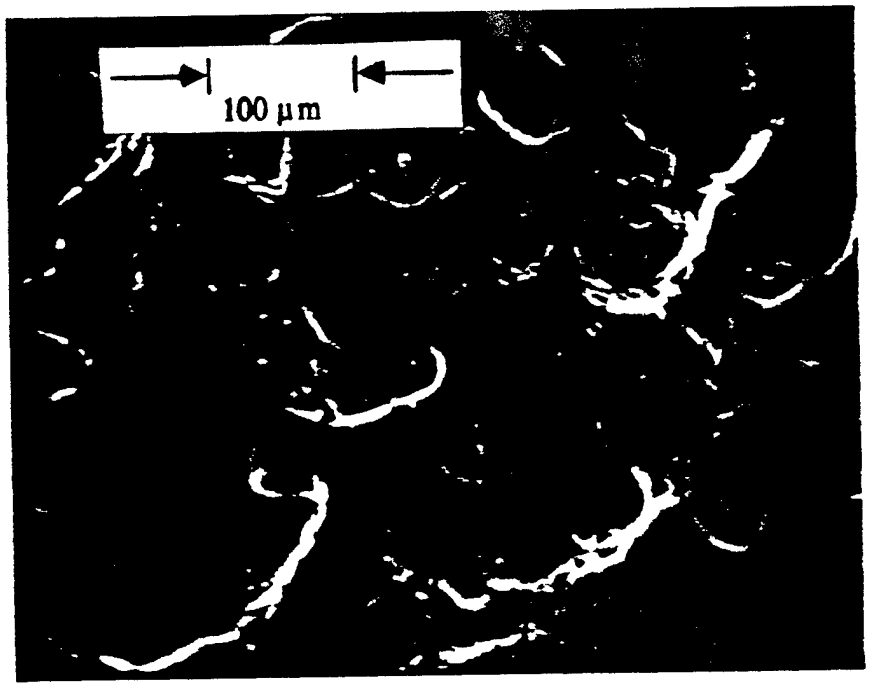

(h)

Figure 3--Surface features of Mix #4 (reference) propellant
(g) 2000 psi
(h) 2300 psi

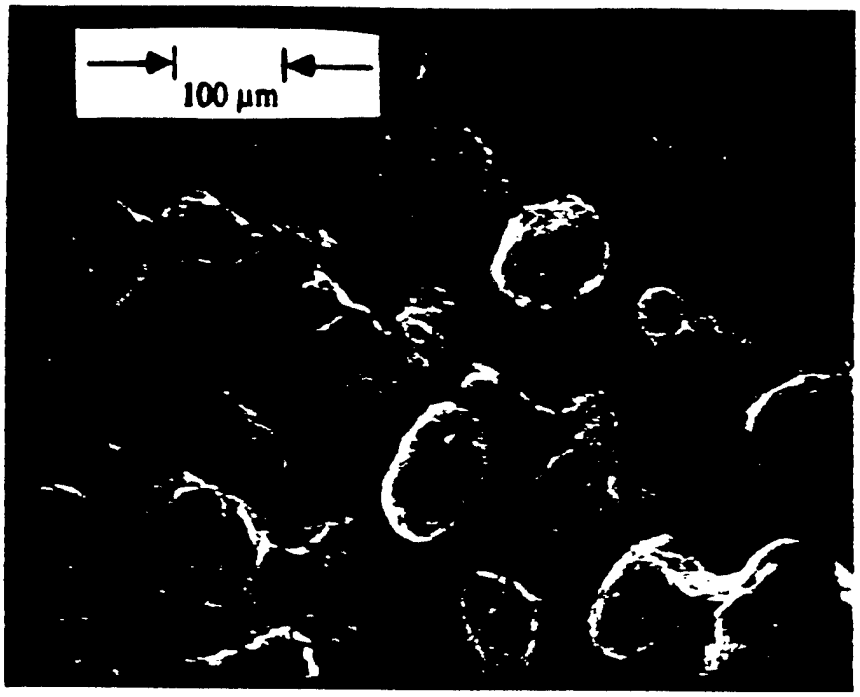

(a)

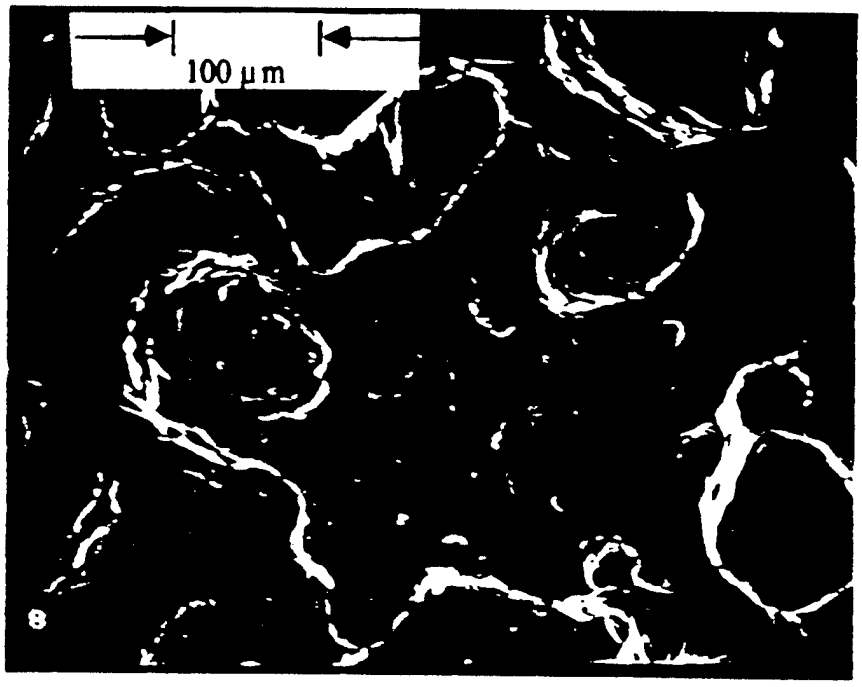

(b)

Figure 4–Surface Features of Mix #5 (IPDI cured HTPB: compare with Fig. 3, DDI cured HTPB)
(a) 1300 psi
(b) 1500 psi

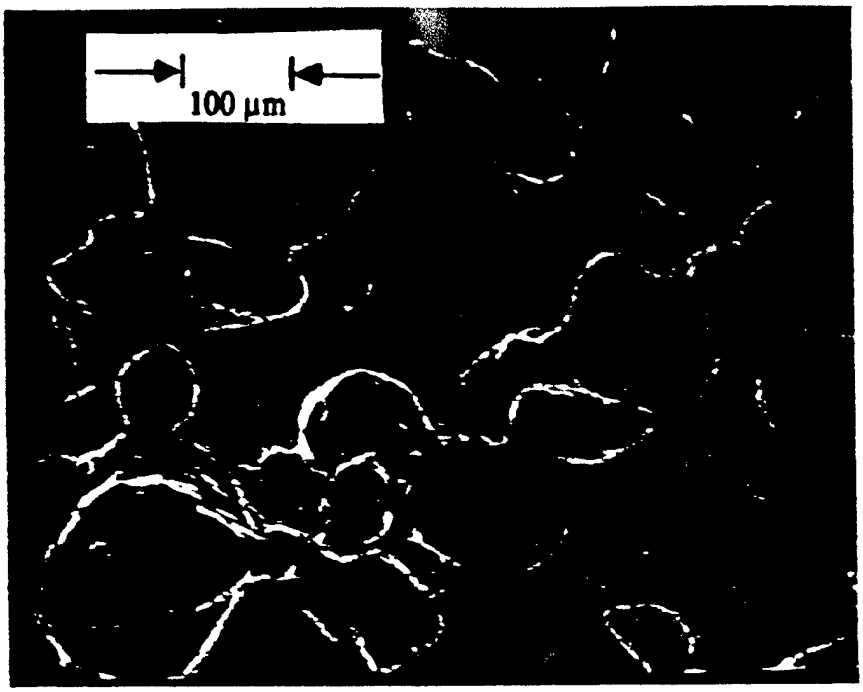

(c)

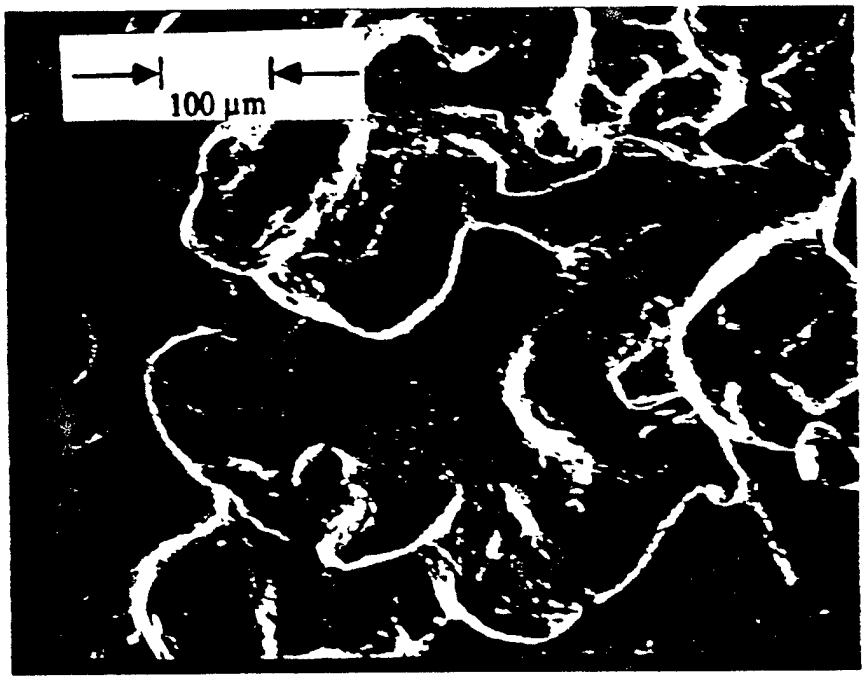

(d)

Figure 4--Surface Features of Mix #5 (IPDI cured HTPB: compare with Fig. 3, DDI cured HTPB)
(c) 2000 psi
(d) 2200 psi

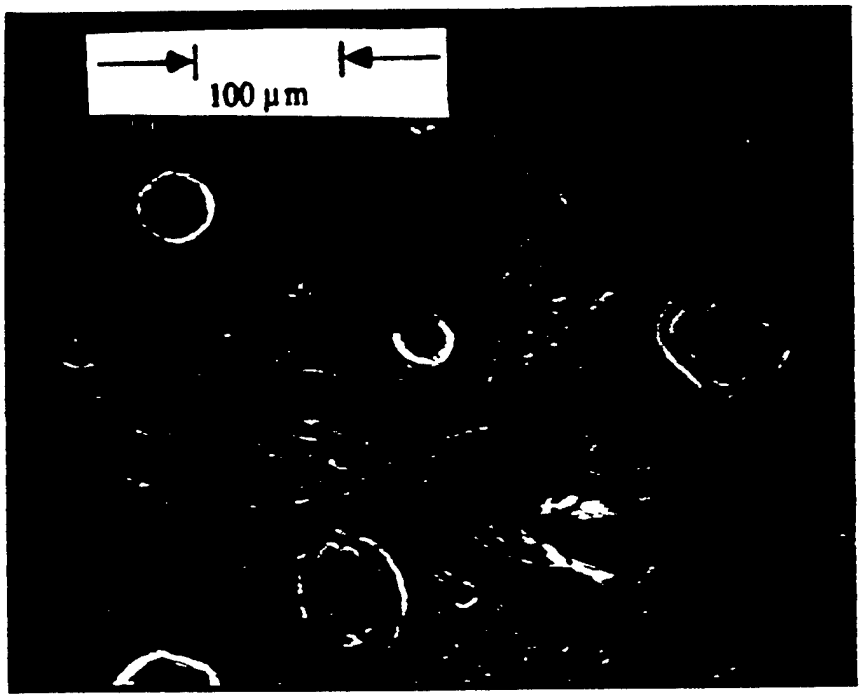

(a)

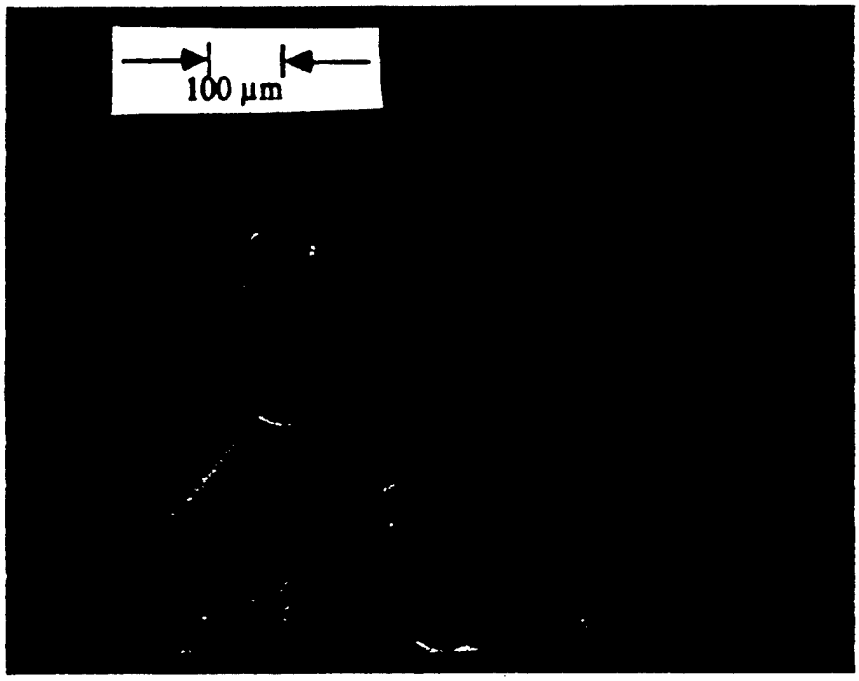

(b)

Figure 5–Surface Features of Mix #10 (0% TiO_2) compare with mix #4

(a) 200 psi

(b) 500 psi

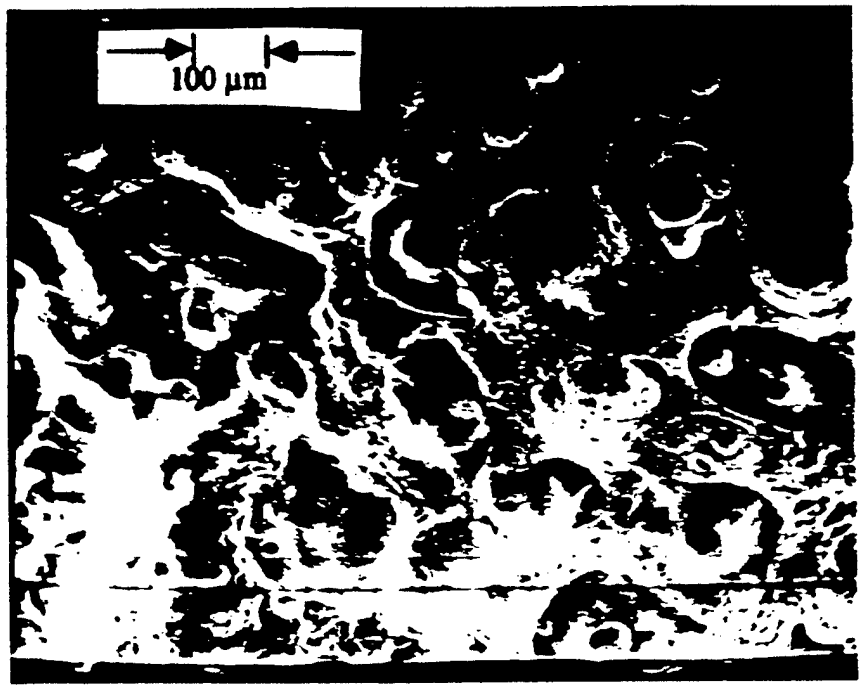

(c)

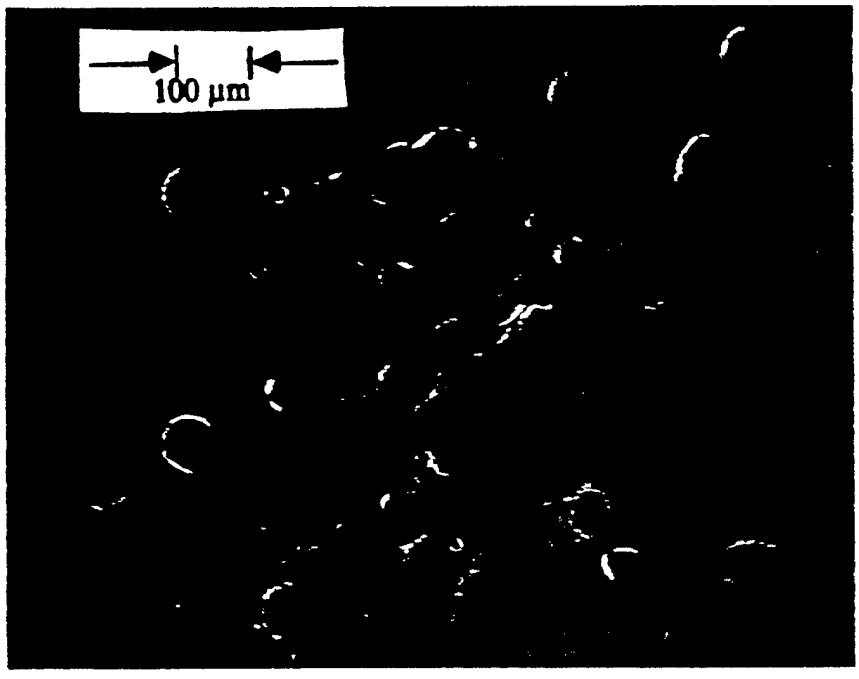

(d)

Figure 5--Surface Features of Mix #10 (0% TiO_2) compare with mix #4

(c) 1000 psi

(d) 1800 psi

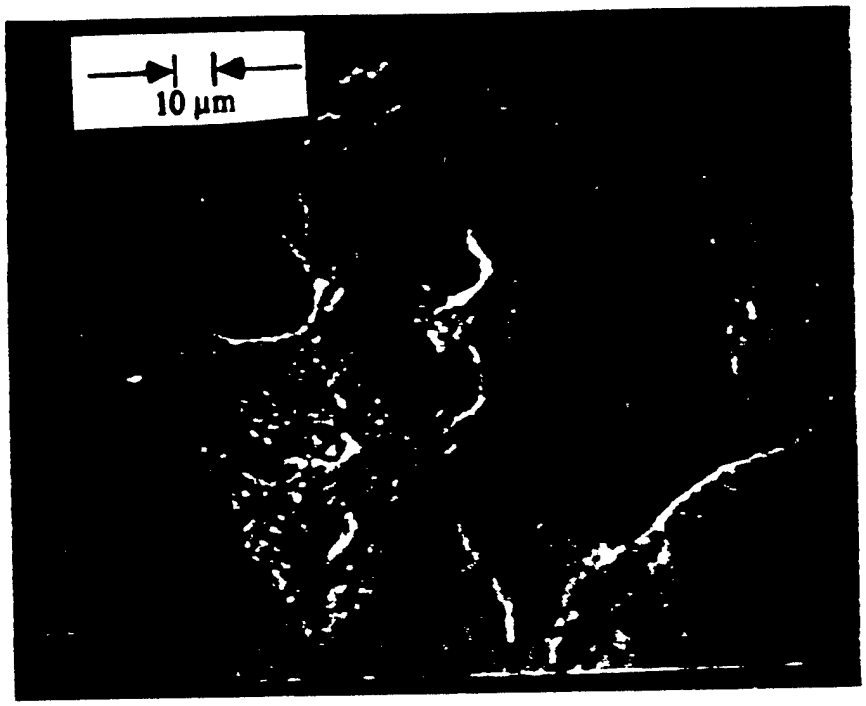

(e)

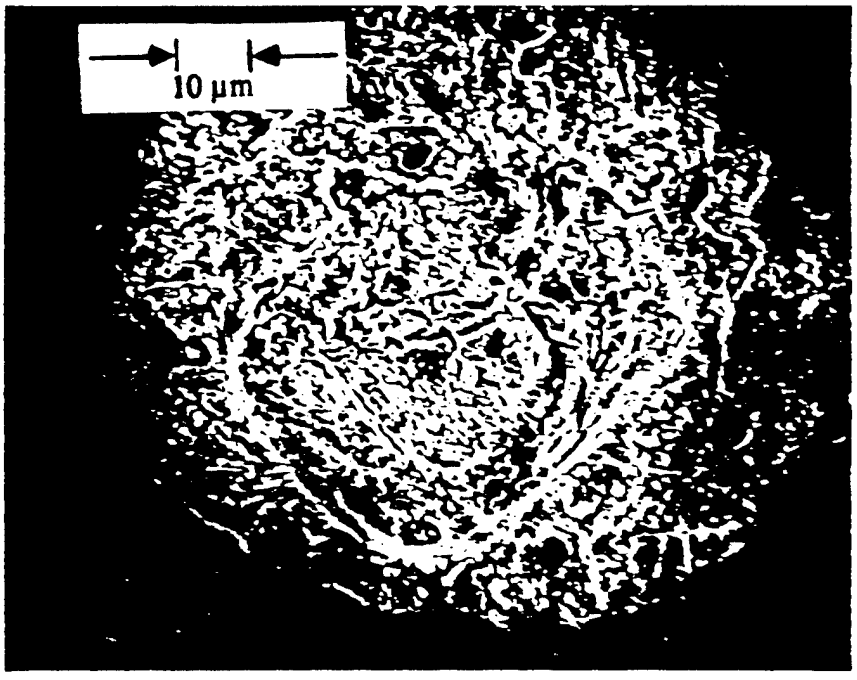

(f)

Figure 5--Surface Features of Mix #10 (0% TiO_2) compare with mix #4

(e) 2300 psi

(f) 2300 psi (porous AP surface)

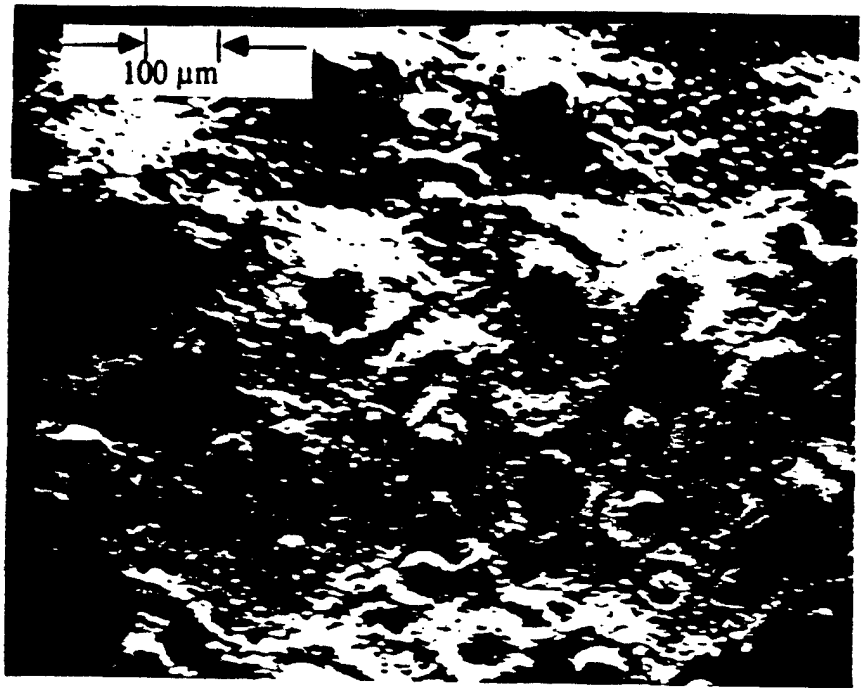

(a)

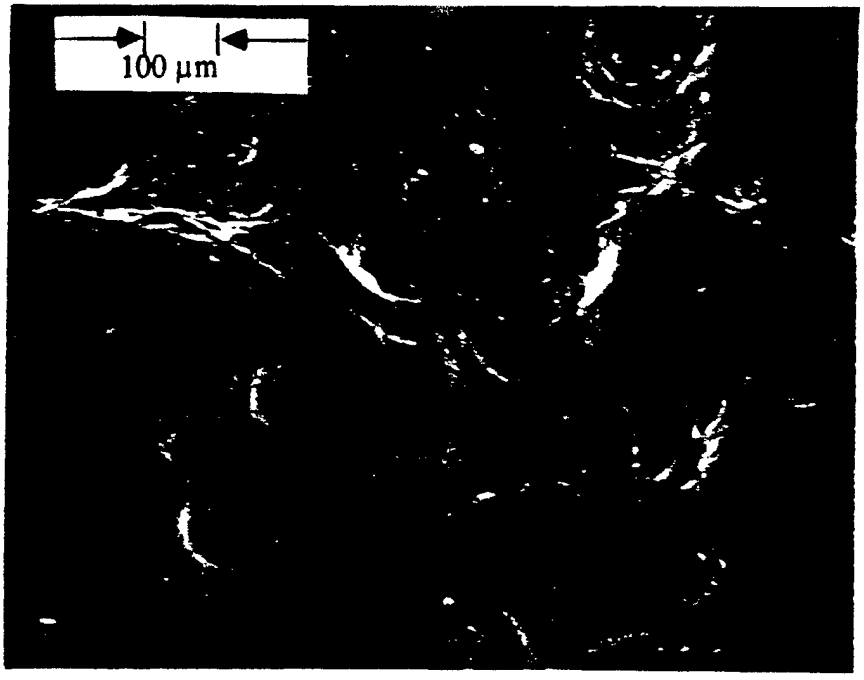

(b)

Figure 6--Effect of ratio of coarse to fine AP (Mix #8 C/F=55/45, compare to Mix #4 C/F=62/38, Fig. 3)
(a) 500 psi
(b) 800 psi

(c)

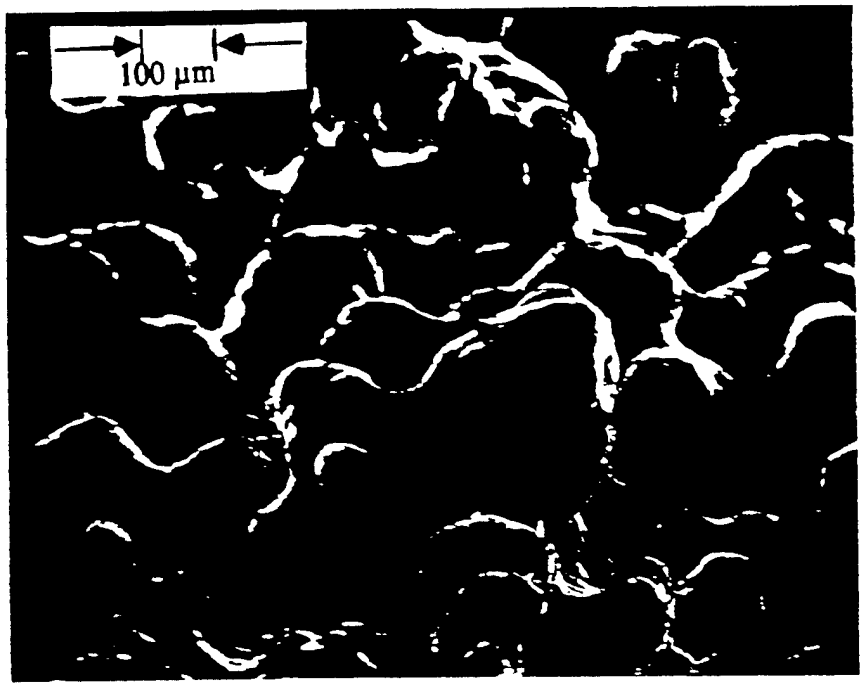

(d)

Figure 6--Effect of ratio of coarse to fine AP (Mix #8 C/F=55/45, compare to Mix #4 C/F=62/38, Fig. 3)
(c) 1000 psi
(d) 1800 psi

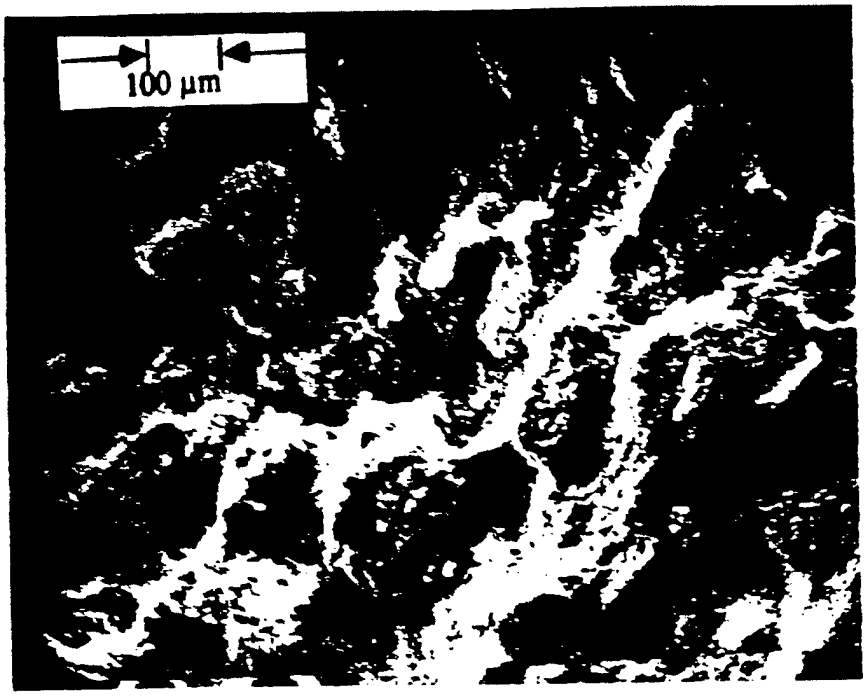

(e)

Figure 6--Effect of ratio of coarse to fine AP (Mix #8 C/F=55/45, compare to Mix #4 C/F=62/38, Fig. 3)
(e) 2300 psi

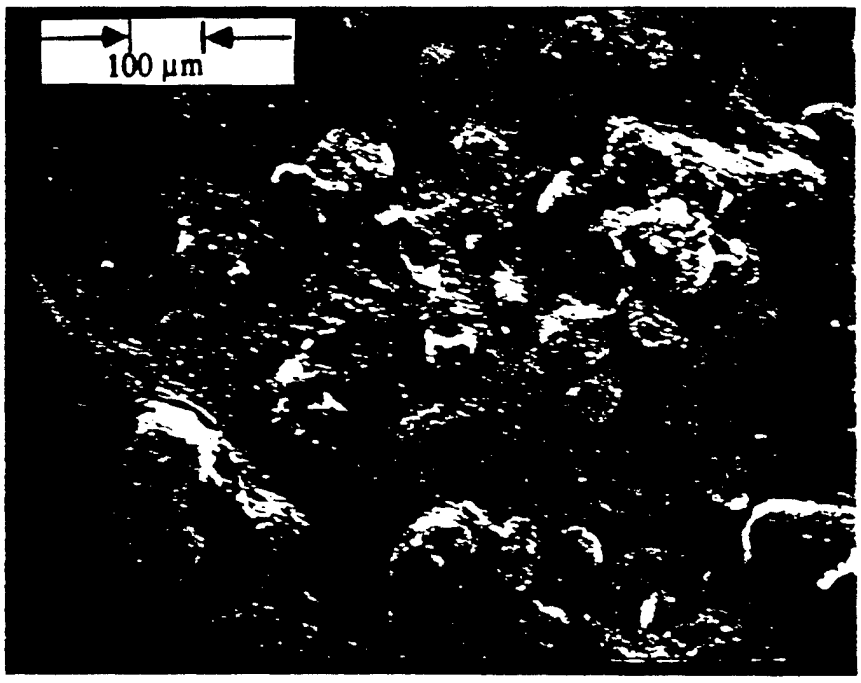

(a)

Figure 7--Effect of aluminum addition (at the expense of AP mix) (Mix #2 vs. Mix #5 in Fig. 4)
(a) 500 psi

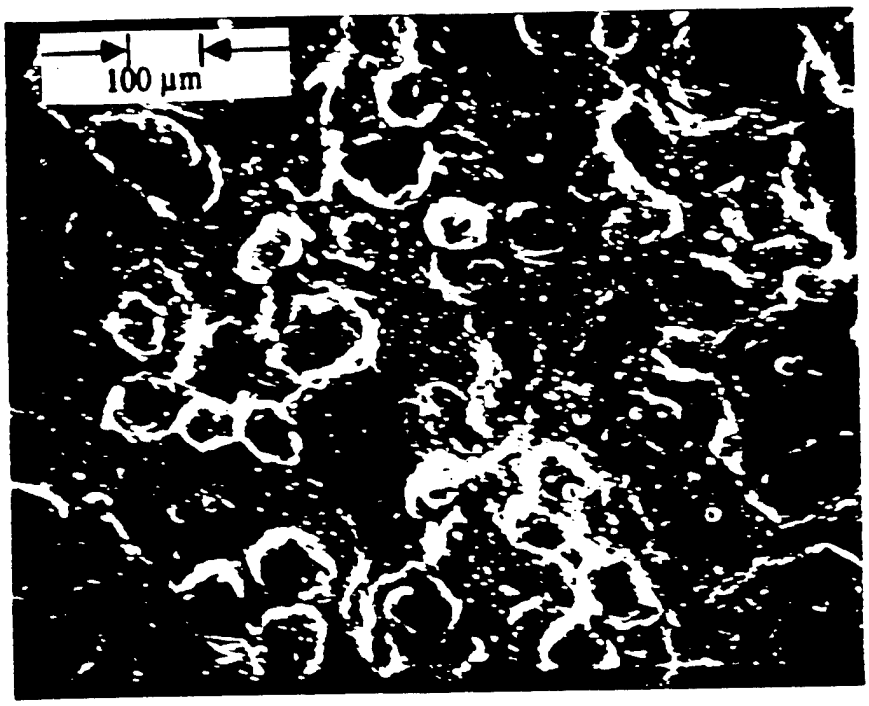

(b)

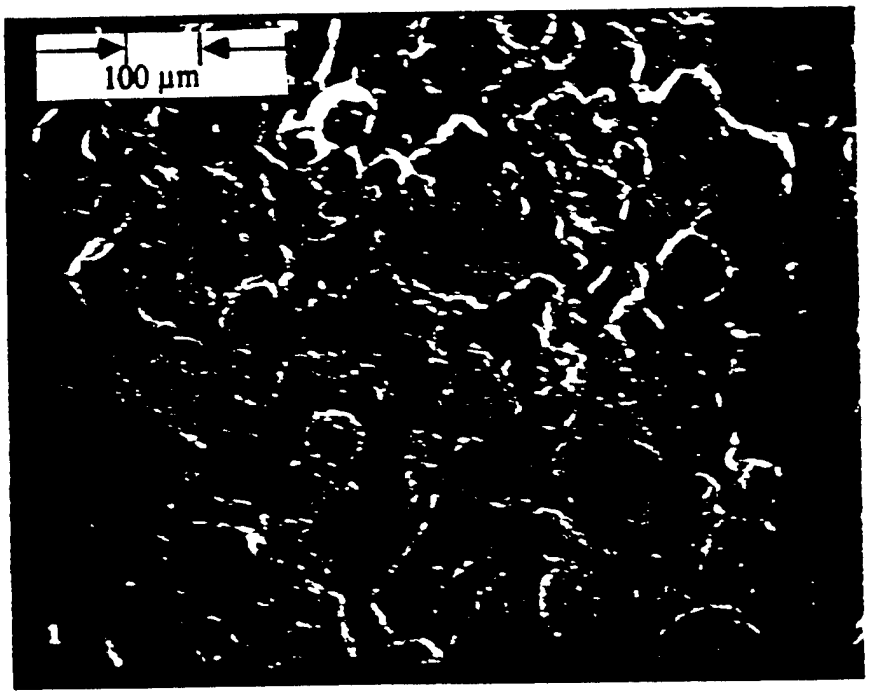

(c)

Figure 7--Effect of aluminum addition (at the expense of AP mix) (Mix #2 vs. Mix #5 in Fig. 4)
(b) 1000 psi
(c) 2000 psi

APPENDIX O

Price, E. W., Jeenu, R., Freeman, J. M., and Sigman, R. K.

"Burning Surface Features of Four Bimodal AP Plateau Propellants (as inferred from dp/dt quench samples for four pressures)"

presentation at ONR/MURI workshop

Reno, NV, Jan. 1998.

Burning Surface Features of Four Bimodal AP Plateau Propellants (as inferred from dp/dt quench samples for four pressures)

E. W. Price, R. Jeenu, J. M. Freeman
and R. K. Sigman

March 1998

Contents originally presented at an ONR/MURI Worlshop
in Reno, NV in January 1998.

This research was funded by ONR Contract
N000014-95-3-0559; Technical Monitor: Dr. R. S. Miller

Distribution Statement: Distribution Authorized to Department of Defense and U.S. DoD contractors only; Critical Technology, Specific Authority; Oct. 1997. Other requests shall be referred to The Phillips Lab (OLAC) PL/RK, Edwards AFB, CA 93524-7048.

Quenched Surfaces of Biplateau Propellants

Introduction

As part of the joint study of burning rate-controlling mechanisms, the burning quench method was used to study the features of the burning surfaces of four Thiokol propellants that were provided to the Multidisciplinary University Research Initiative (MURI) team. The propellants are referred to as "bimodal" propellants that use a blend of "coarse" AP and "fine" AP in which the "coarse diameter" is roughly 100 times the "fine diameter". These propellants **are described here as coarse particles contained in a fine AP/binder matrix**. This report presents scanning electron microscope (SEM) pictures of Thiokol Mixes 4, 5, 8, and 10, along with discussions of the significance of the results. The burning rates of the four formulations are shown in Fig. 1, based on data provided by Thiokol. A curve for the self deflagration rate of AP is also shown based on data of Boggs (Ref. 1)

Results are presented as one figure for each test pressures (200, 1000, 1800, and 2300 psi, Figs. 2-5). Each figure has four SEMs, one for each propellant, at one magnification and pressure. Subsequent figures are arranged in the same way, but using higher magnification to resolve specific aspects of the surface, eg. appearance of individual coarse AP particles and matrix areas around their periphery (Figs. 6-9), and details of the fine AP/binder matrix surfaces (Figs. 10-13).

The formulations of these propellants have been provided to members of the MURI team and are available from Dr. Carol Campbell at the Thiokol corporation at Brigham City, Utah. Mix 4 is used here as a baseline formulation and contains 87.5% of AP (mass ratio of coarse to fine AP is 62:38) and 12.5% DDI cured HTPB binder (of which 16.7% is DOA plastisizer) plus 2% of TiO_2 additive. The other mixes differ as follows: Mix 5 used an IPDI curative for binder; Mix 8 used a lower ratio of coarse AP to fine AP (a higher AP/binder ratio in the matrix); and Mix 10 contained no TiO_2.

Interpretation of SEMs

For convenience the quenched surfaces are described in terms of local areas that are quenched surfaces of the coarse AP particles, and surrounding areas that are quenched surfaces of the fine AP-binder "matrix". In some cases the demarcation between these areas is unambiguously defined (eg. Fig. 2). In some cases, demarcation can only be inferred on the basis of the expected size and spacing of the coarse particles (eg. Fig. 4c). In this later case the surface is visibly cluttered by TiO_2, and other debris, to such a degree that actual demarcation lines are obscured. Because a good deal of earlier information is available about how the AP and matrix burn alone and together (Refs. 2-5) the identification of the coarse AP areas and matrix areas will be inferred from whatever evidence of the SEM's reveal. Likewise evidence of binder melt concentrations and flow will be sought.

General Observations

At 200 psi (Fig. 2) the quenched surfaces are fairly flat and the coarse AP and matrix surfaces clearly distinguishable. The oxidizer-fuel flame is apparently near planar (premixed). The coarse AP surfaces appear to be concave upward except that they have protrusions at the center, sometimes porous in nature (Figs. 2a and 6a), with concentrations of TiO_2 on top when TiO_2 is present (Figs. 2b, c, d; 6b, c, d). The matrix areas are "lumpy" on a scale larger than the fine AP or TiO_2 particles. Same of the lumps looks like "blow holes" (eg. Fig. 6a). Other look like TiO_2 concentrations (Fig. 6c). There are no distinguishable glossy areas suggestive of binder melt concentration. At this pressure the burning rates of these mixes are not greatly different.

At 1000 psi (Fig. 3) the surfaces are more irregular, especially Mixes 8 and 5. The degree of irregularities is correlated with the mix burning rate, with major irregularities consisting of protrusions of the coarse AP (Figs. 4c and d). Mixes 8 and 5 have matrixes that might be expected to pyrolize relatively early (Mix 8 matrix has higher oxidizer-fuel ratio and Mix 5 has a low-melt binder). From the structure of the surface it appears that coupled burning of matrix and peripheral regions of the coarse AP are burning on ahead of the rest of the coarse AP particles (Mixes 5 and 8). At high magnification. (Figs. 7 and 11), the coarse AP-matrix interfaces are generally resolvable and concave upward with the edge height close to matrix height (but rising to domes with Mixes 5 and 8). The surfaces of the slow burning **mixes (4 and 10)** have very complex irregularity (Figs. 3a and b) **most notable for depressions in the central area of coarse AP particles** (Mix 10, no TiO_2, Figs. 3a and b; Mix 4 has TiO_2 aggregates in the depressions). The burning rates of these mixes (4 and 10) are about the same as the AP self deflagration rate at this pressure (Fig. 1) suggesting that **this central burning of this particles contributes appreciably to the overall rate**. On the outer portions of these AP particles, the surface shows substantial porosity (Figs. 7a and b), not conspicuous in most of the other test conditions. Figure 11a shows interspersed areas of smooth and porous AP on the coarse particles that may indicate a binder melt film over the otherwise porous AP (speculation). The **matrix areas at this pressure all look irregular and dry**, with irregularities of nominally 10μm width (Fig. 11). Finer structure (of size comparable to the fine AP) is visible in varying degree on the matrix areas of all mixes. There do not seem to be any areas of melt accumulations (no extensive areas with glossy surface or wrinkling).

At 1800 psi (Figs. 4 and 8) the situation is generally similar to 1000 psi. At this pressure the burning rate of Mix 8 is four times the AP self deflagration rate of pure AP, and the rate of Mix 5 is almost three times as high. The burning surfaces are dominated by boulder like AP protrusions, in such large numbers that there must be multiple protrusions on some particles (Fig. 4d). The leading areas of the burning "front" are the "canyons" around the "boulders", apparently controlled by the flame from the matrix and peripheral AP. In Figs. 8c, d and 12c, d, one gets the impression that a relevant mechanistic model of burning would have to embody a description of how burning progresses **around** the coarse AP particles, with **due regard for difference in matrix thickness** at different location around the periphery. Aside from serving as heat sinks, the fate of the central part of the coarse AP particles seems incidental to the burning

rate controlling "fires in the canyons". As at 1000 psi, the slower burning mixes, 4 and 10 have more level surfaces (Figs. 4a and b). The AP particles do not have any typical configuration. Mix 10 (no TiO_2, rate lower than AP rate) exhibits a variety of holes in the AP (perhaps various stages of particles burning ahead of the mean surface). Mix 4 (baseline, rate higher than AP, upon a plateau) shows some AP particle protruding, but there are depressions in the protruding particles (Figs. 4b and 8b). It is difficult to determine whether the rate is controlled by the peripheral AP/matrix area or the holes in the AP particles (presumably by both together?). This set of samples at 1800 psi is a good test of the idea of "melt depression" of rate (compare Mix 10, supposedly melt depressed, and Mix 4). There are no obvious areas of melt concentration (Figs. 4a, b; 8a, b; and 12a, b). The most suspicious sites are some smooth areas on protruding AP particles (Mix 4, Fig. 6; not severely melt depressed at this pressure).

At 2300 psi, the surfaces of **mix 4 and 10** samples (Figs. 5a and b) are not greatly different than at 1800 psi (the rates are also not much different). Fig. 9a (Mix10) shows a matrix area that looks like it has some surface binder melt which might extend onto some of the adjoining AP surface. The AP deflagration rate at this pressure is very low, but that is not manifested in the propellant surfaces (Mix 4, 10), which show many holes that appear to indicate rapid AP burning in their central areas. The surface of Mix 5 (Figs. 5d, 9d, and 13d) is qualitatively similar to the 1800 psi result, but the matrix/peripheral AP areas are less deeply recessed, consistent with the decreased burning rate. The surfaces are all dry looking and grainy on a 2μm scale (both matrix and AP surfaces). The **mix 8** burning rate is near the minimum of the mesa, and lower than mix 5. The surface is correspondingly less irregular (Figs.. 5c, 9c, and13c), but the matrix/peripheral AP surfaces still lead the burning front. The protruding AP has depressions in the protruding areas, depressions often surrounded by smooth areas that may be binder melt (strange place for binder melt).

Discussion

The goal of these quench burn studies is to get a look at the microscopic surface features of the burning propellant, with spatial resolution far beyond what can be attained in real time observations. Such observations would contribute to the limited supply of objective evidence regarding the combustion behavior responsible for the remarkable pressure dependence of the burning rate of these propellants. It is too much to expect that the outcome would constitute full understanding and mechanistic principles for burning rate tailoring. However, the results can be combined with those from matrix burning studies (e.g., Ref. 2) and sandwich burning studies(e.g., Refs. 4 and 5) to draw some important generalizations and pose some critical unresolved problems.

It was discovered long ago that propellants with only fine AP particles (plus binder) exhibited mesa burning in the mid pressure range, and that the extent of this anomalous behavior was dependent on the particle size, AP/binder ratio, and type of binder (Ref. 6). These effects have not been satisfactorily explained or fully investigated, but **seems to be basic to the plateau burning**, of more practical bimodal

AP propellants. In a comparison study to the one reported here, a more complete study of fine monomodal AP/binder matrix combustion is being conducted, specifically to understand and control the contribution of the fine AP/binder matrix combustion to plateau burning of bimodal AP propellants.

The collected results of all studies indicate that the burning characteristics of the fine AP matrix are crucial to the burning characteristics of the plateau propellant, **but that the cooperative burning with the coarse AP is also an essential factor in determining the burning rate**. This is not surprising since both the AP and the matrix burn somewhat marginally alone, far from stoichiometric conditions . Most practical AP/hydrocarbon binder propellants burn faster than either the AP or matrix alone (although all the mixes in the present study except Mix 10 tended toward the AP rate at 2000 psi). At 200 psi, all the mixes appear to **burn with a hot planar rate-controlling premixed flame**, with comparable burning rates and with relatively flat burning surfaces.

As pressure is increased, **the flame moves into the mixing flow**, especially at favored sites where the mixture from the matrix surface and adjoining (large AP) surfaces is closer to stoichiometric than in either the matrix or AP outflow, and closer to stoichiometric than in the fully mixed flow. In **response to this localization of hot near surface flamelets, the burning surface becomes more irregular** and the burning rates of the different mixes begin to show more effect of formulation variables. The **degree of surface irregularity increases with increase in the burning rate**, regardless of whether the rate increase is due to increase in pressure or due to formulation change. The detailed nature of the surface irregularities indicates that **the increase in rate is due to the increasing penetration of the hot flamelets upstream in the mixing fans of the matrix/AP outflows**. Only the peripheral areas of the (coarse) AP particles contribute to, or receive much heat from these hot near-surface O/F flamelets and the rest of the coarse AP particle lags behind, **producing grossly irregular surfaces** when the burning rate of the coupled matrix-peripheral AP region is very high (the burning rate of Mix 8 reaches values nearly four times the self deflagration rate of AP, at which point the surface is a "boulder field" of protruding AP).

From the present work it is not clear why this burning rate (Mixes 5 and 8) comes back down around 2000 psi. In accord with the above generalizations, the surface becomes less rough and the coarse AP particles cease to protrude so much. One may reasonable speculate that the hot AP/matrix flamelets "went away". Hinshaw and Cohen (Ref. 7) have attributed the decreased rate to suppression by binder melt flow. **No detailed mechanism of burning is proposed in which melt depression is explained**, but the onset at 2000 psi or so is attributed to increased melt flow due to decreased melt viscosity associated with higher melt temperature. **It is not explained why the melt temperature is increasing under conditions where the burning rate is decreasing**. In other words, melt depression of burning rate is not explained mechanistically, nor is it explained why it occurs when it is purported to occur. However, there is a great deal of evidence that melt is somehow involved (two scenarios were proposed in Ref. 8.).

The results of the present studies did not show convincing evidence of melt encroachment on the peripheral AP surfaces. They do reveal very complex surfaces on

matrix areas that remind us that we don't really know how these surface layers burn. Under no conditions was the surface "smooth" like one would expect of a melt layer. On the other hand, the **surface irregularities**, often showed a glossy appearance. These features were not clearly correlated with pressure. However, a current effort is examining the matrix surfaces at much higher magnification. An example is shown in Fig. 14, which shows the matrix surface to be made up of smooth melt areas interspersed with "open" areas containing irregularities comparable in size to the fine AP particles. We will be looking for the trend of such features with pressure and formulation variables.

In Ref. 8, a mechanism for melt suppression of burning rate was proposed under the name "disproportionation failure". In effect, it was proposed that, because of differences in the pyrolysis kinetics of the binder and oxidizer, a relative surface area accommodation between binder and oxidizer ingredients would be required in order to maintain an O/F ratio in the surface efflux matching the O/F ratio of the matrix. It may well be that there are conditions under which this accommodation is not possible, in which case burning would cease locally, giving the locally intermittent burning revealed in some photographic studies of matrix burning (Ref. 6). This would of course reduce the average burning rate of the propellant. This argument, like the melt viscosity one, depends on an implausible trend of increasing surface temperature in an increasing pressure range where the **burning rate is going down**. However, the rate may not be going down at the sites where disproportionation is incomplete (after all as the pressure is increased the flame should be moving in and the surface should be getting hotter **locally**). But the overall rate depends on the surface-time average rate and may go down if burning is locally intermittent. This may in fact be exactly how melt suppression of rate works.

An alternate explanation for the decline in rate as the pressure approaches 2000 psi (Ref. 1) is that the AP rate may be decreasing, just as the self deflagration rate of pure AP does in this pressure range. The present results suggest that the self deflagration rate of the AP is already very low compared to the propellant rate **before** the drop off in AP rate, as a result of which the AP protrudes (boulder field). On the other hand, at 2300 psi, where the AP rate has dropped conspicuously, the coarse AP protrudes **less**, not more. As at lower pressures, the burning rate is determined by the peripheral AP/matrix O/F flame, and the rest of the coarse AP particle lags behind. Even in Mix 10, where the burning rate is **below** the AP rate between 1000 and 2000 psi, the coarse AP does not control the rate (although the depressions in the center of the particles suggest that the coarse particles may contribute).

In spite of the obvious importance of the matrix burning to normal plateau behavior, it is not at all clear how the matrix burns. Are the fine AP particles that are in the binder melt layer decomposing and blowing vapors through the overlying melt? Is the AP decomposition simply endothermic dissociative sublimation to NH_3 and $HClO_4$, or does the $HClO_4$ decompose exothermally before clearing the melt layer? Is there any reaction with the binder? Such processes have been considered to be of minimal importance in the past (Refs.. 4 and 9) but are they possibly important when the surface consists of a melt layer and exceedingly high surface area of AP as in these propellants? From the figures in this report, it is evident that the concept of a pervasive

"melt layer" is overly simplistic, and that its rate suppression properties may have to do with the **extent** or persistence of surface average melt coverage.

We continue to be handicapped in our studies of matrix burning by the difficulty in obtaining matrix samples with 2 μm AP in the high AP/binder ratios achieved in matrixes of the propellants (up to 76 to 24). Thiokol has provided prepolymer with the highest loading they could achieve (AP/binder ratio 70 to 30); higher ratios are achieved in these propellants when coarse AP is present too. Matrix studies are continuing with attainable mixes, and high magnification studies of matrix surfaces of the quenched propellants (like Fig. 14) should shed further light on matrix burning and melt "layers".

References

1. Boggs, T.L., "Deflagration Rate, Surface Structure, and Subsurface Profile of Self-Deflagrating Single Crystals of Ammonium Perchlorate," *AIAA Journal*, Vol. 8, No. 5, May 1970, pp. 867-873.

2. Freedman. J. M., Price, E.W., Chakravarthy, S.R. and Sigman, R.K., "Burning Characteristics of Monomodal Ammonium Perchlorate/ Hydrocarbon Binder Propellants," 34th JANNAF Combustion Subcommittee Meeting, CPIA Publication 662, Vol. II, October 1997, pp 1-12.

3. Chakravathy, S.R., Price, E.W., and Sigman, R.K., "Binder Melt Flow Effects in the Combustion of AP-HC Composite Solid Propellants," AIAA Paper 95-2710, 31st AIAA/ASME/SAE/ASEE Joint Propulsion Conference and Exhibit, June 10-12, 1995.

4. Lee, S.T., Price, E.W., and Sigman, R.K., "Effect of Multidimensional Flamelets in Composite Propellant Combustion," *Journal of Propulsion and Power*, Vol. 10, No. 6, Nov.-Dec. 1994, pp. 761-768.

5. Chakravarthy, S.R., "The Role of Surface Layer Processes in Solid Propellant Combustion," Ph. D. Thesis, Georgia Institute of Technology, Atlanta, GA 1995.

6. Bastress, E. K., "Modification of the Burning Rates of Ammonium Propellants by Particle Size," Ph.D. Thesis, Princeton University, Princeton, NJ, January 1961.

7. Hinshaw, C. J. and Cohen, N. S., "Achievement of Plateau Ballistics in AP/HTPB Propellants," 34th JANNAF Combustion Subcommittee Meeting, CPIA Publication 662, Vol. IV, October 1997.

8. Price, E.W., Chakravarthy, S.R., Sigman, R.K., and Freeman, J. M., Pressure Dependence of Burning Rate of Ammonium Perchlorate-Hydrocarbon Binder Solid Propellants," AIAA Paper No. 97-3106, 33rd AIAA/ASME/SAE/ASEE Joint Propulsion Conference and Exhibit, July 6-9, 1997.

9. Price, E.W., "Effect of Multidimensional Flamelets in Comosite Propellant Combustion," *Journal of Propulsion and Power*, Vol. 11, No. 4, pp. 717-728.

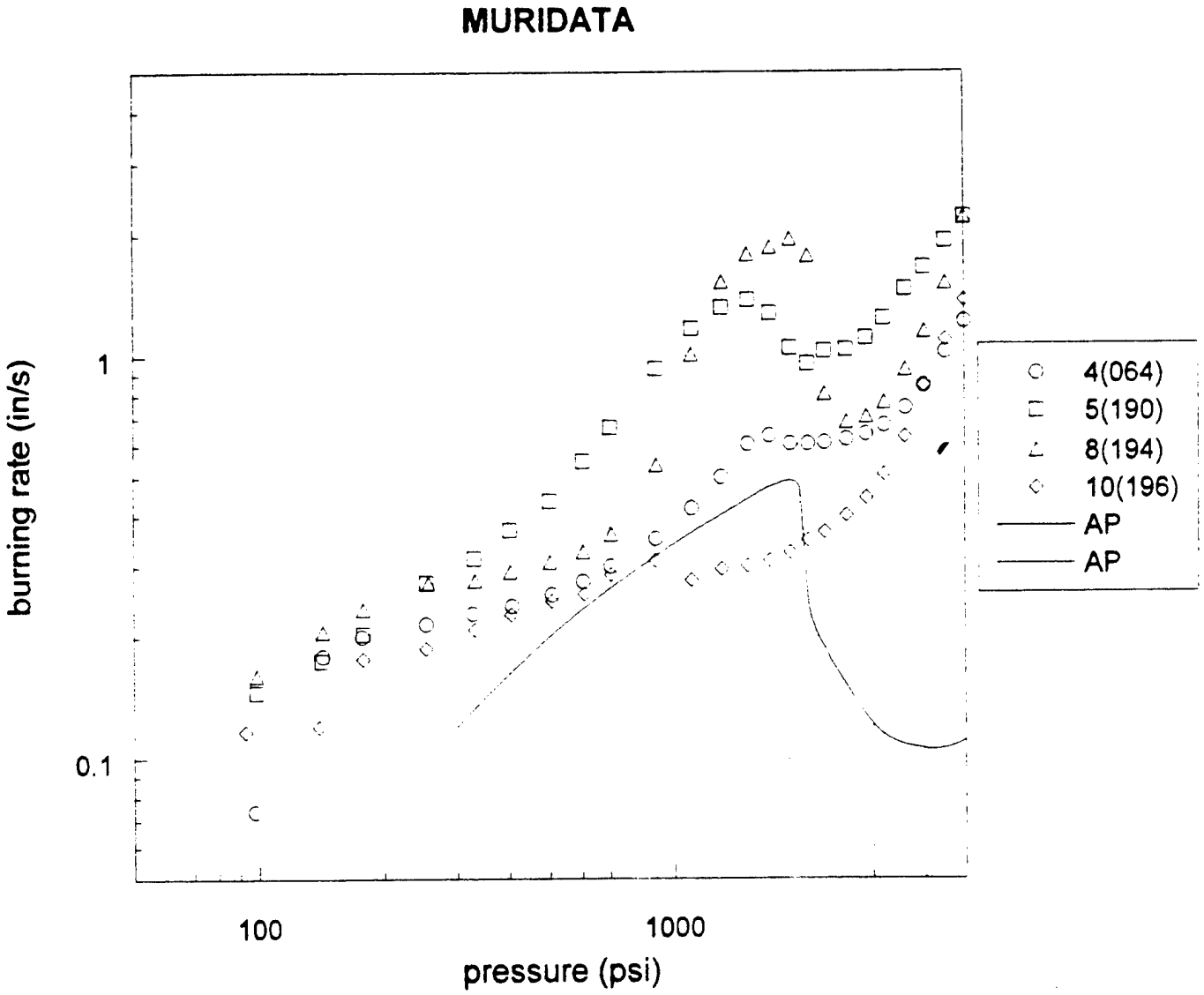

Fig. 1. Burning rate data provided by Thiokol (AP single crystal rate shown for reference).

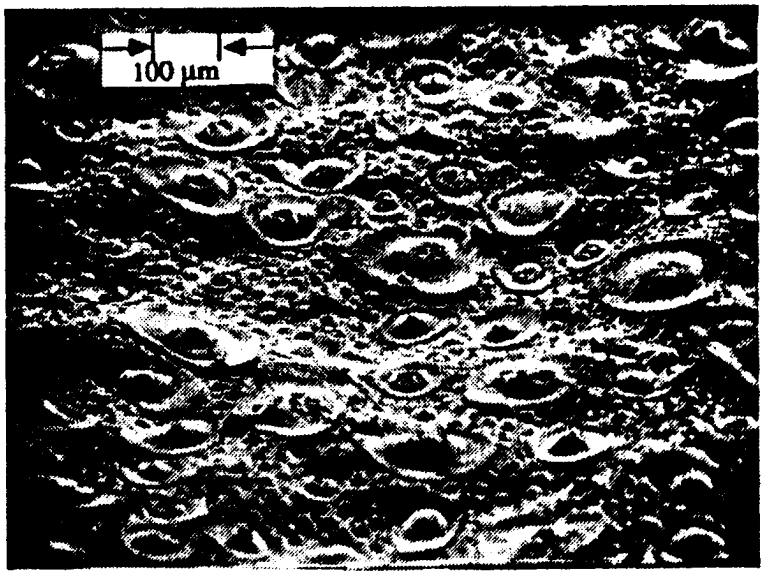

a) Mix-10

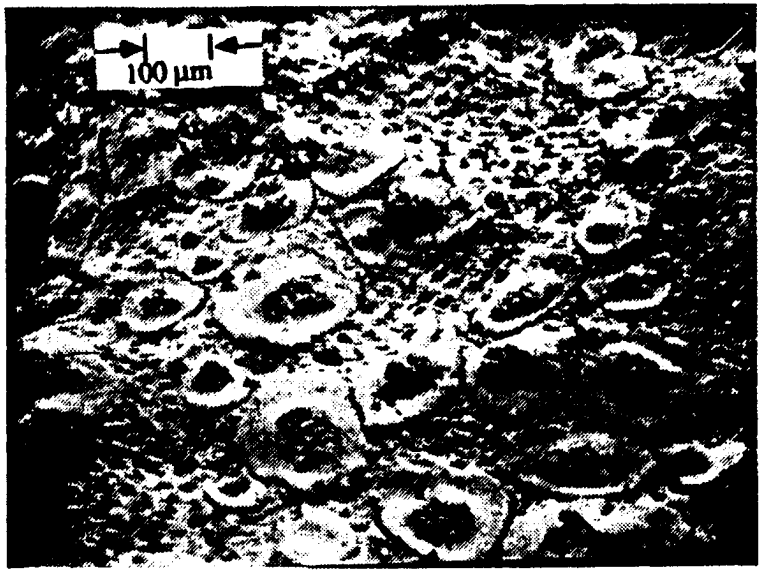

b) Mix-4

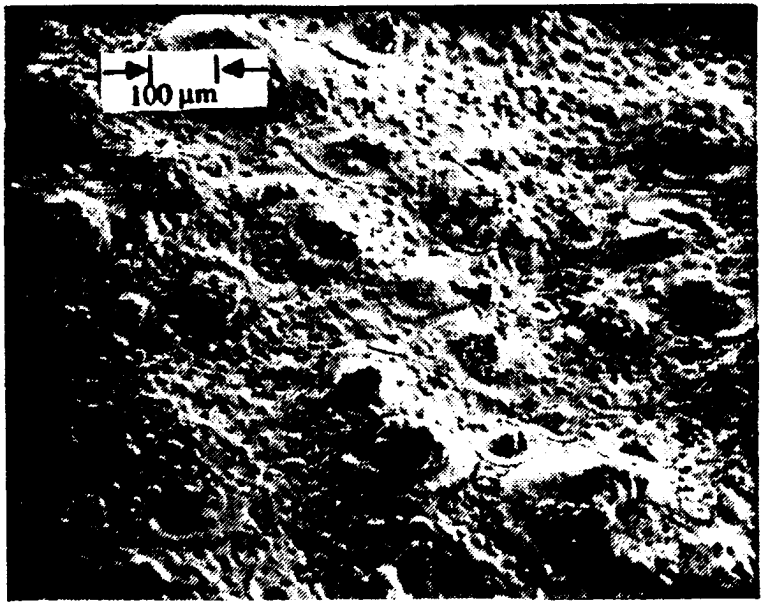

c) Mix-8

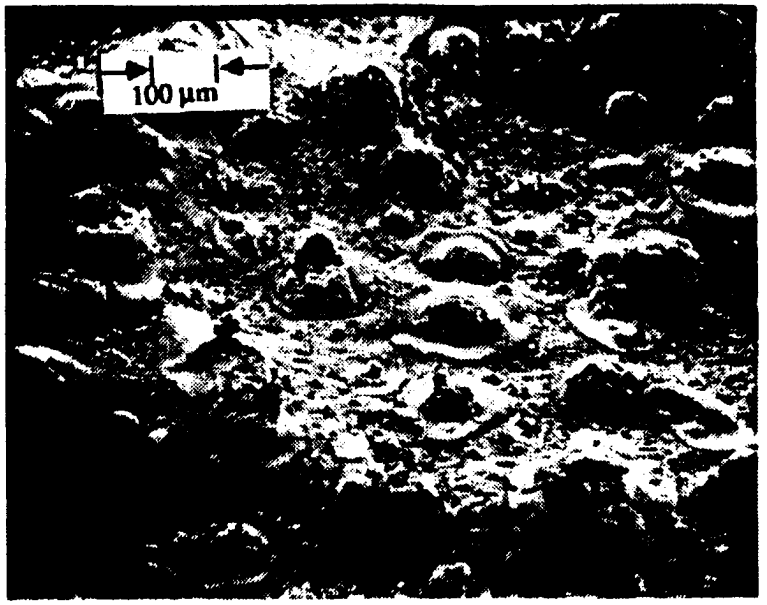

d) Mix-5

Fig. 2 SEM micrographs (100 times magnified) of MURI propellant surfaces; propellants are extinguished by using rapid depressurization at 1.4MPa (200 psi)

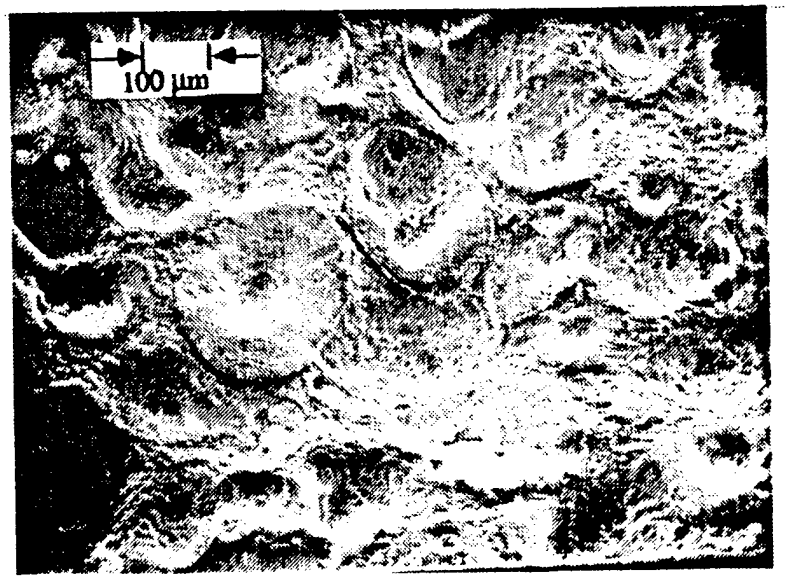

a) Mix-10

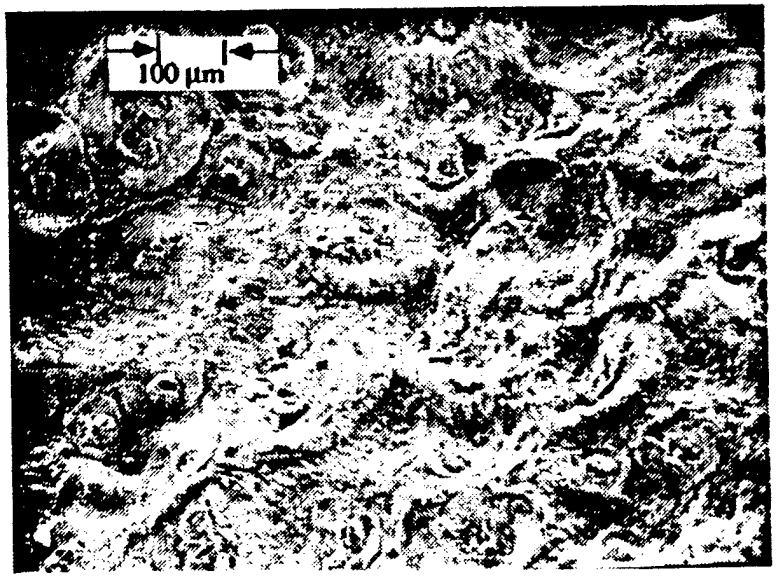

b) Mix-4

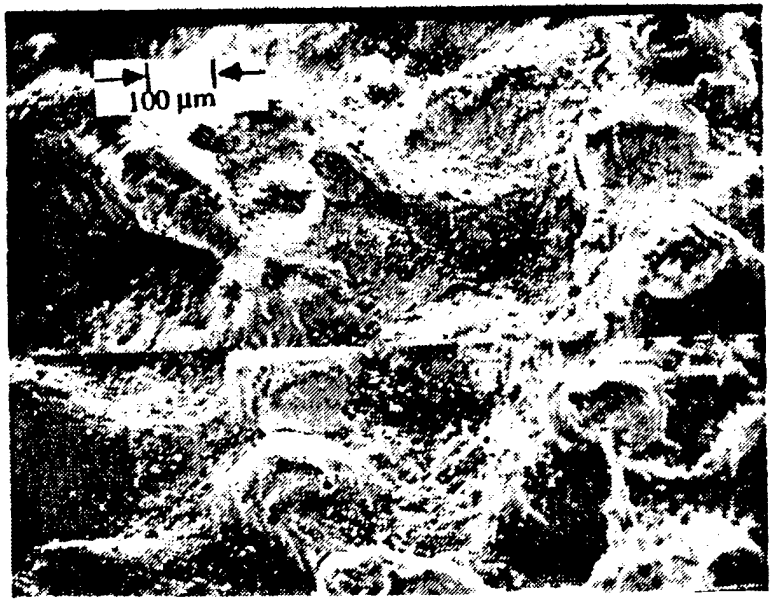

c) Mix-8

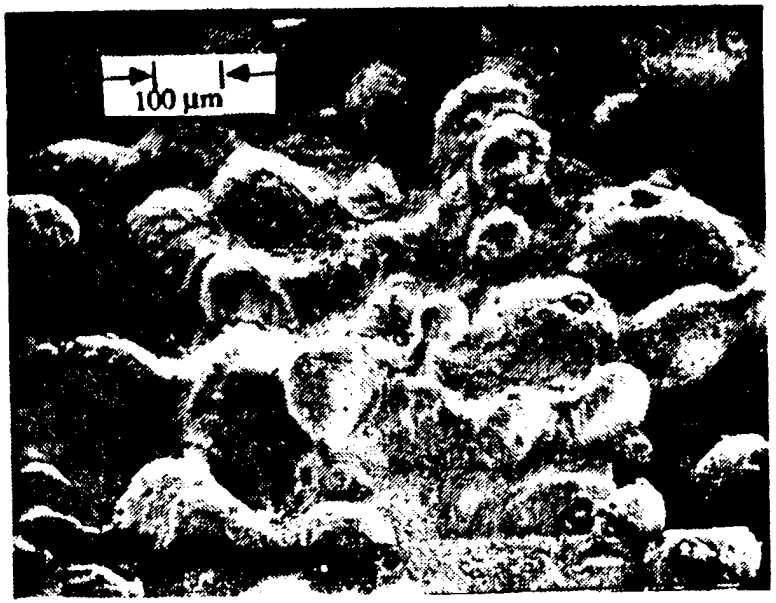

d) Mix-5

Fig. 3 SEM micrographs (100 times magnified) of MURI propellant surfaces; propellants are extinguished by using rapid depressurization at 8.9 MPa (1000 psi)

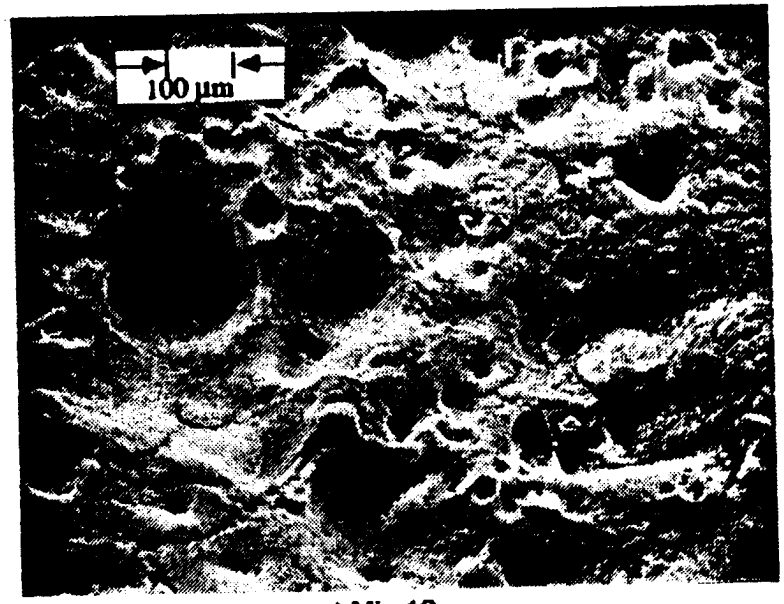

a) Mix-10

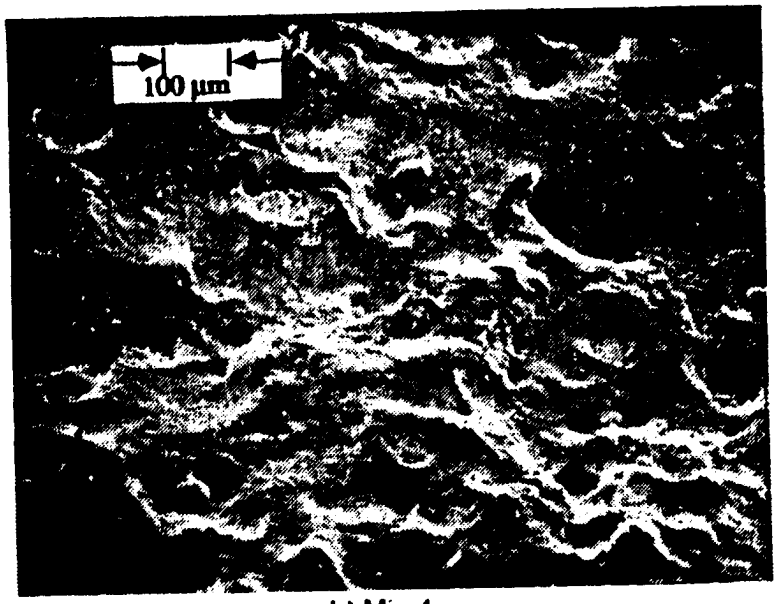

b) Mix-4

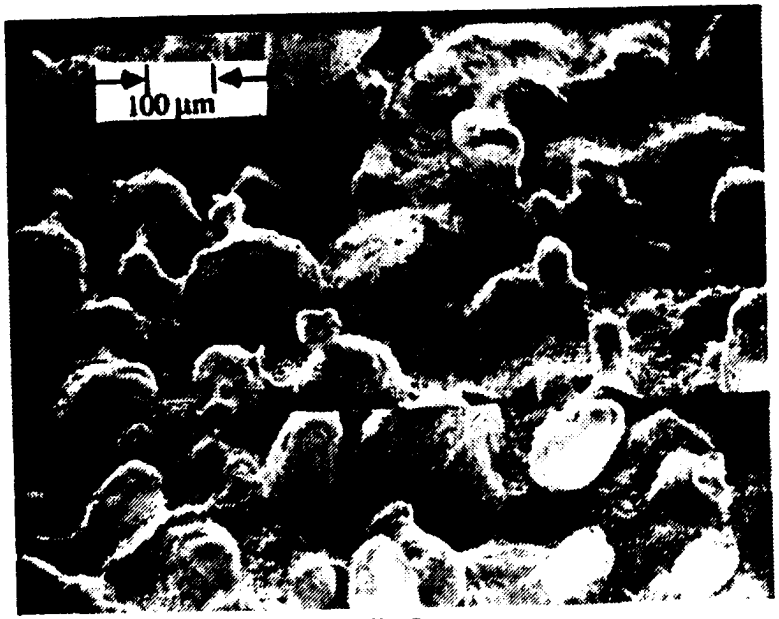

c) Mix-8

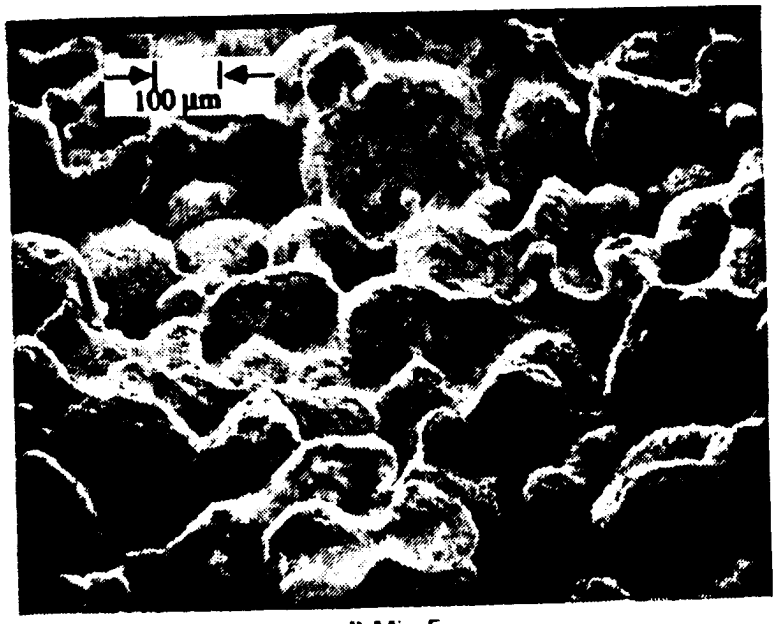

d) Mix-5

Fig. 4 SEM micrographs (100 times magnified) of MURI propellant surfaces; propellants are extinguished by using rapid depressurization at 12.4 MPa (1800 psi)

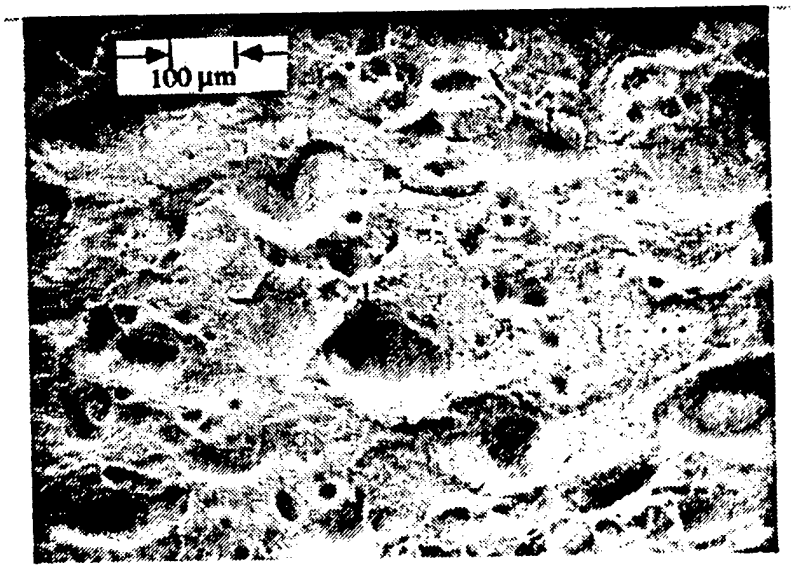

a) Mix-10

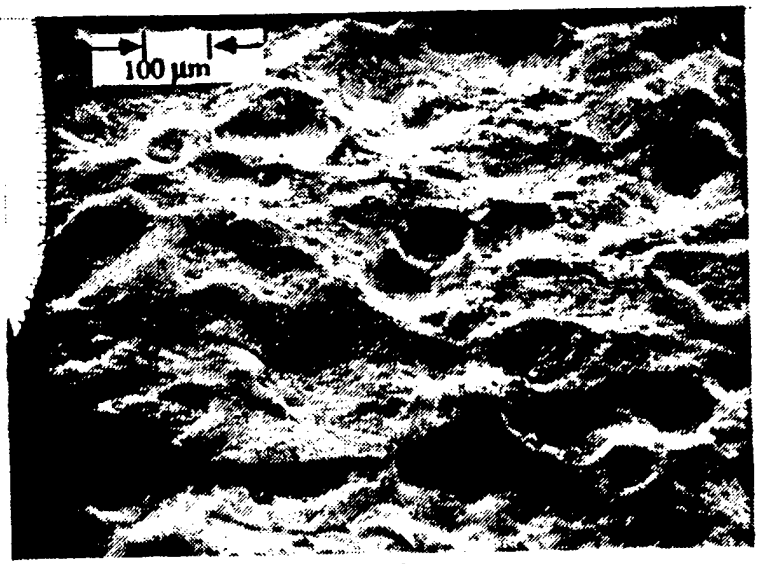

b) Mix-4

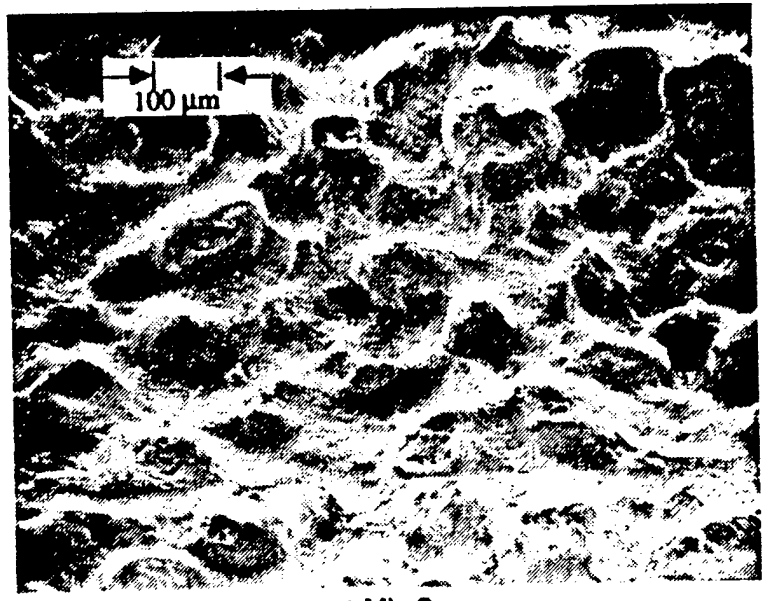

c) Mix-8

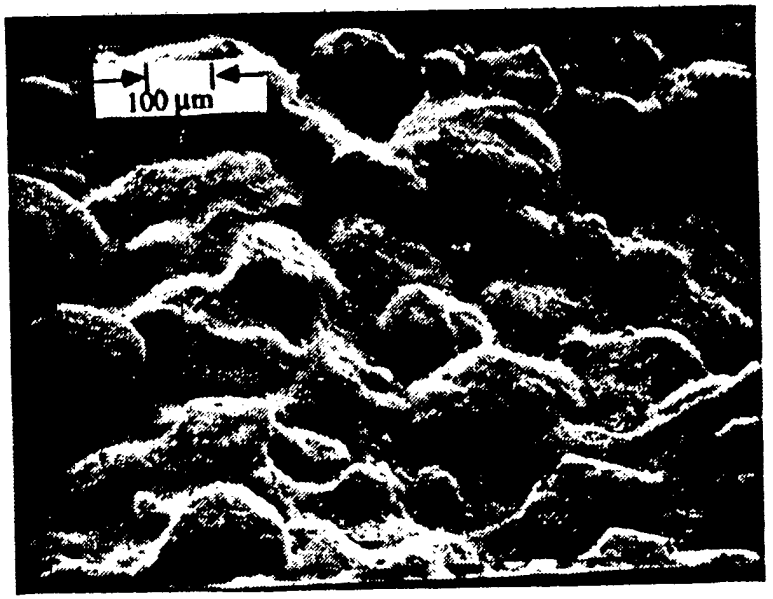

d) Mix-5

Fig. 5 SEM micrographs (500 times magnified) of MURI propellant surfaces; propellants are extinguished by using rapid depressurization at 15.9 MPa (2300 psi)

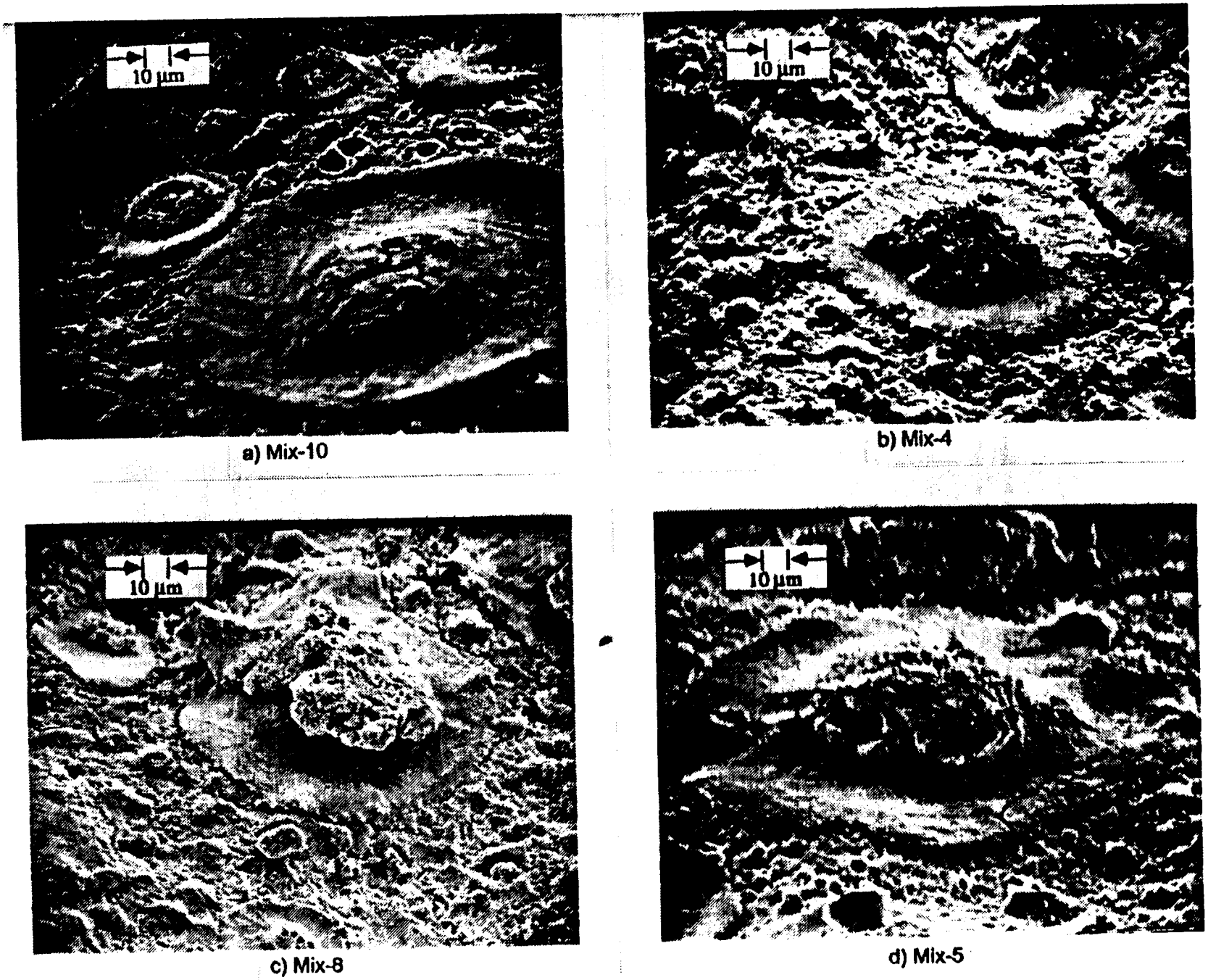

Fig. 6 SEM micrographs (500 times magnified) of MURI propellant surfaces; propellants are extinguished by using rapid depressurization at 1.4 MPa (200 psi)

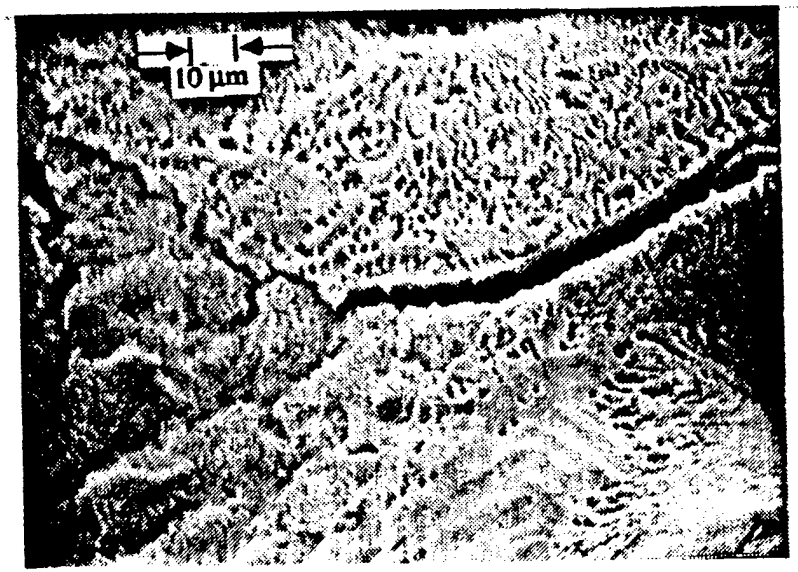

a) Mix-10

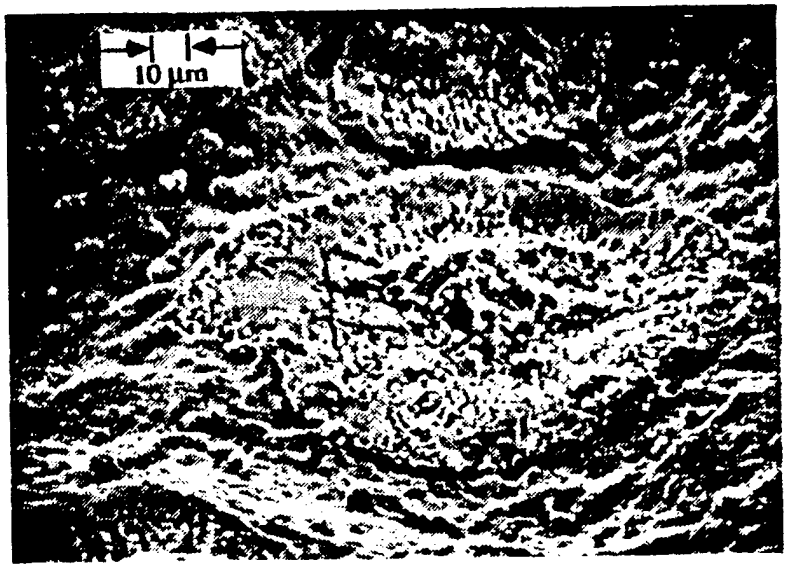

b) Mix-4

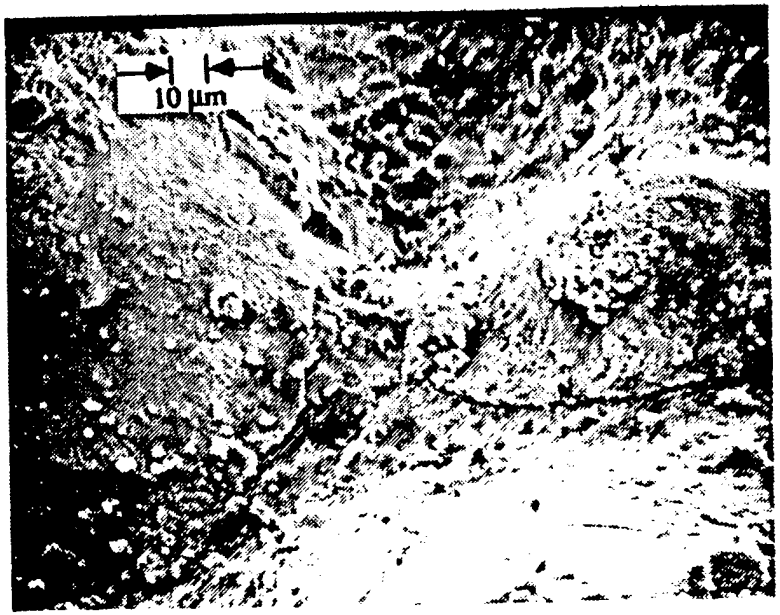

c) Mix-8

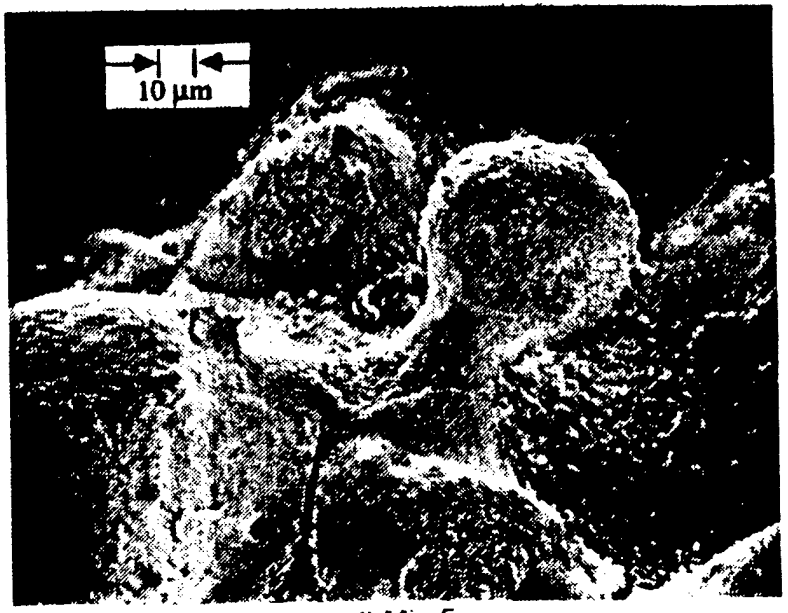

d) Mix-5

Fig. 7 SEM micrographs (500 times magnified) of MURI propellant surfaces; propellants are extinguished by using rapid depressurization at 6.9 MPa (1000 psi)

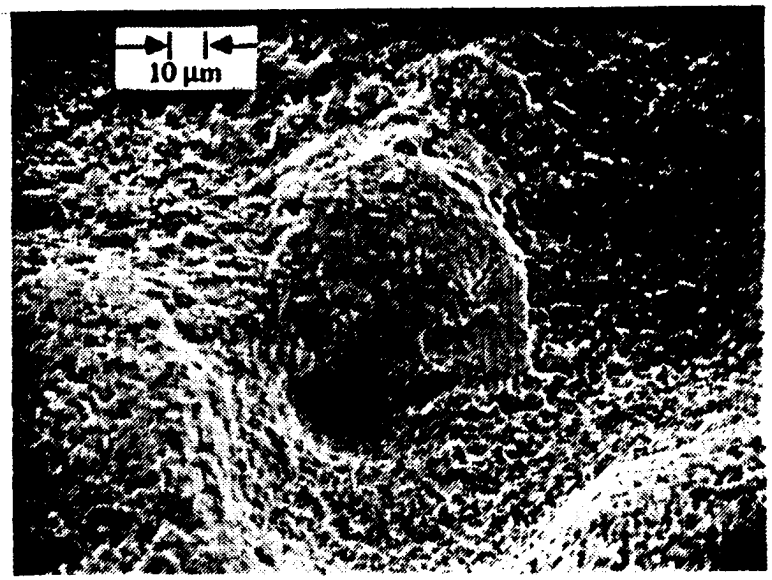

a) Mix-10

b) Mix-4

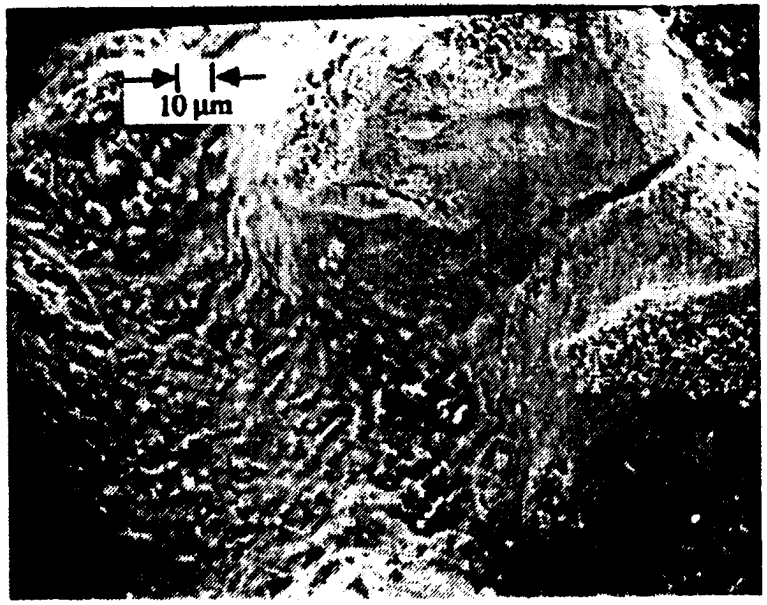

c) Mix-8

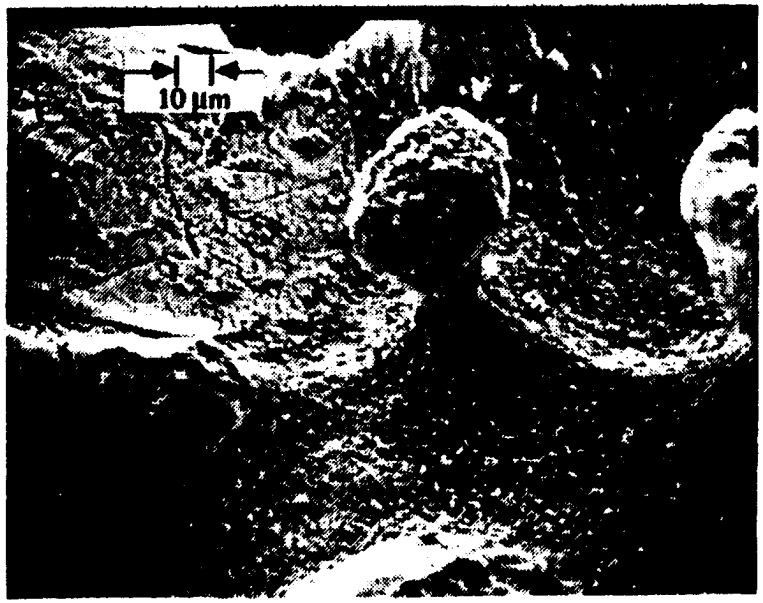

d) Mix-5

Fig. 8 SEM micrographs (500 times magnified) of MURI propellant surfaces; propellants are extinguished by using rapid depressurization at 12.4 MPa (1800 psi)

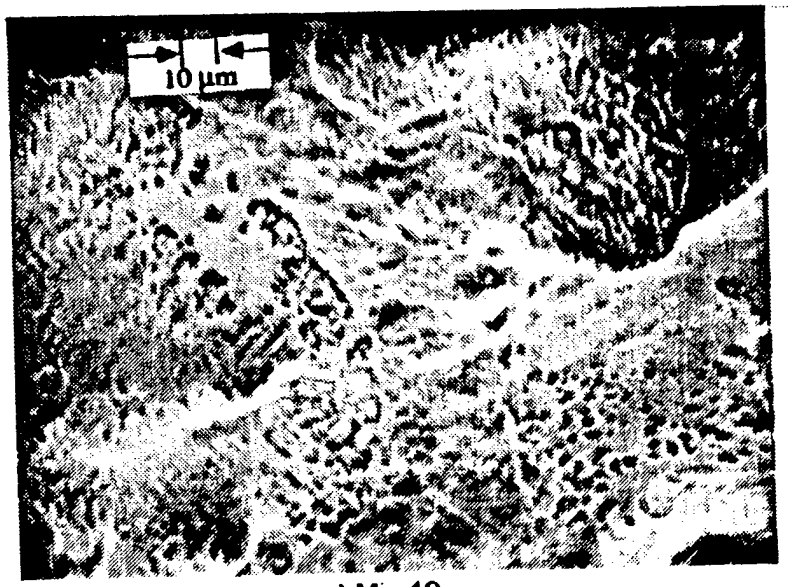

a) Mix-10

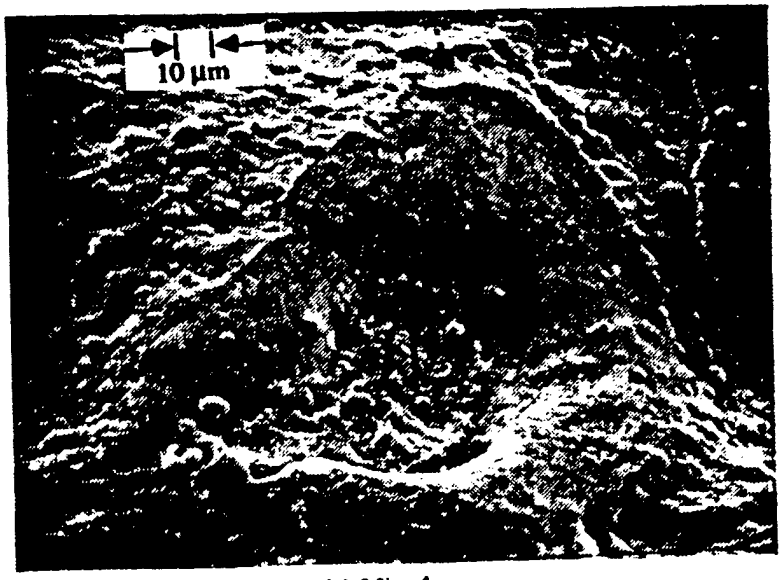

b) Mix-4

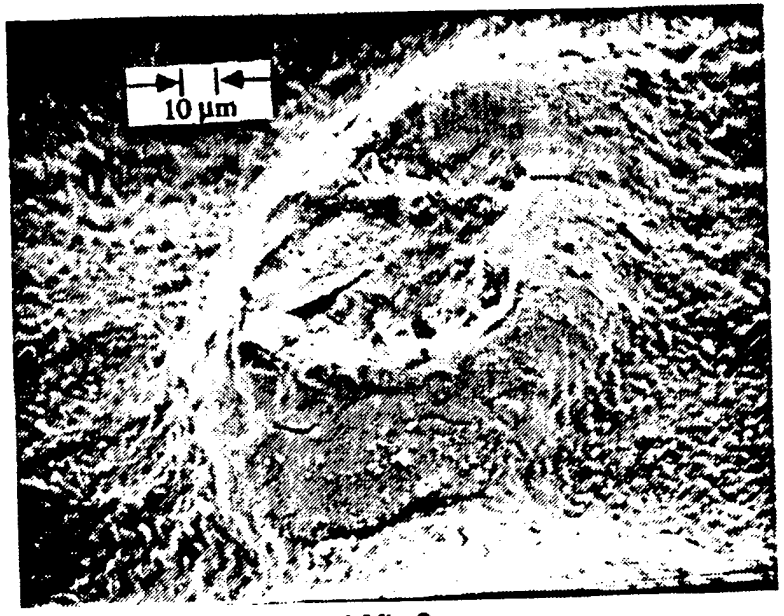

c) Mix-8

d) Mix-5

Fig. 9 SEM micrographs (500 times magnified) of MURI propellant surfaces; propellants are extinguished by using rapid depressurization at 15.9 MPa (2300 psi)

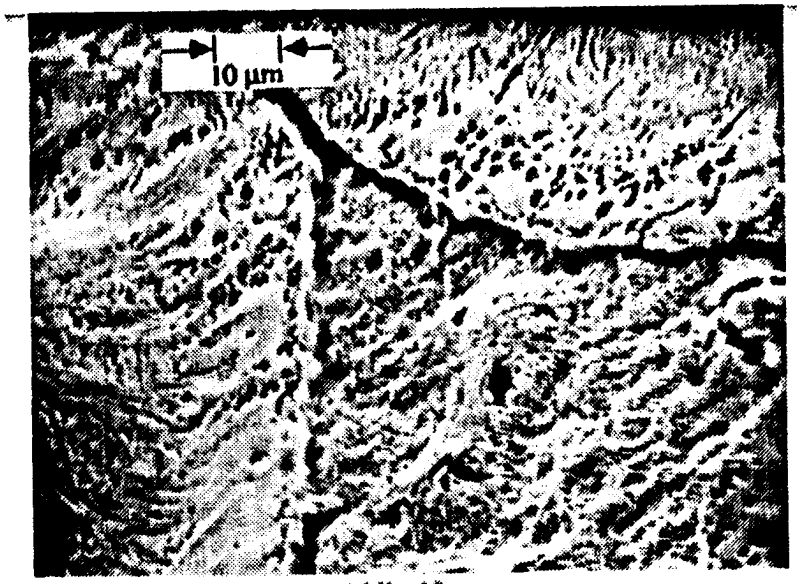

a) Mix-10

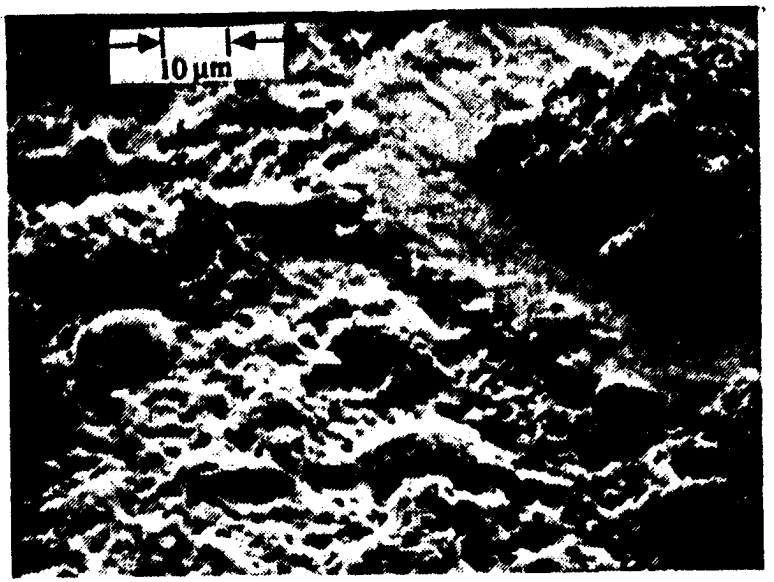

b) Mix-4

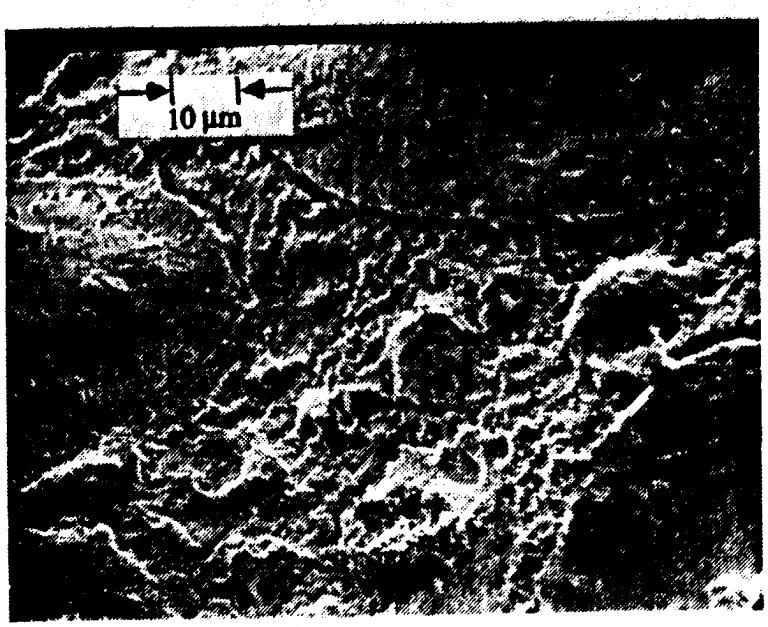

c) Mix-8

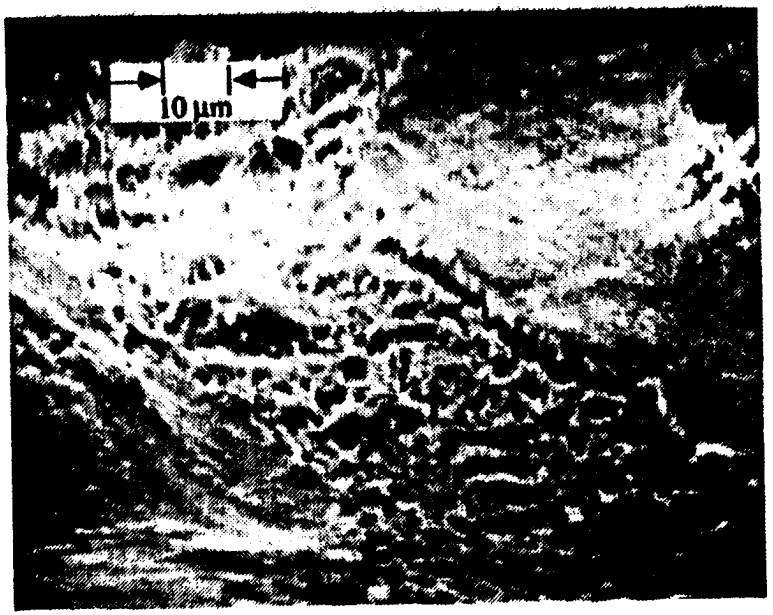

d) Mix-5

Fig. 10 SEM micrographs (~1000 times magnified) of MURI propellant surfaces; propellants are extinguished by using rapid depressurization at 1.4 MPa (200 psi)

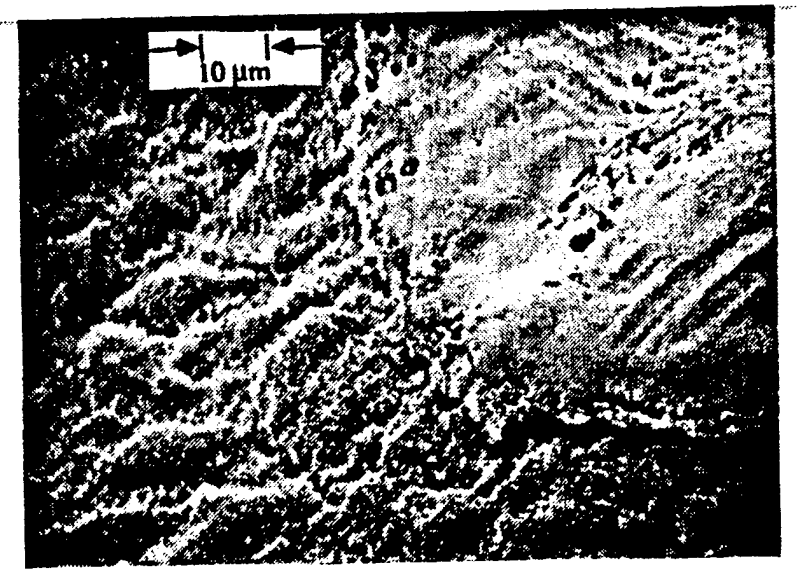

a) Mix-10

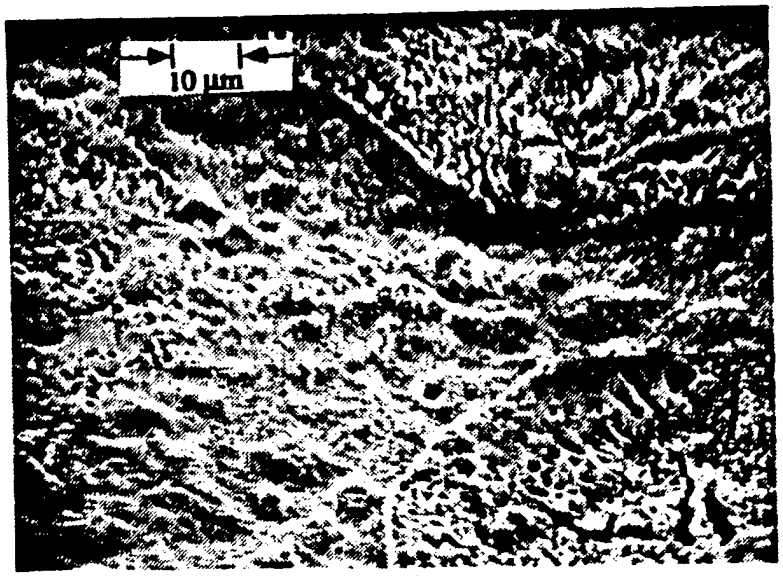

b) Mix-4

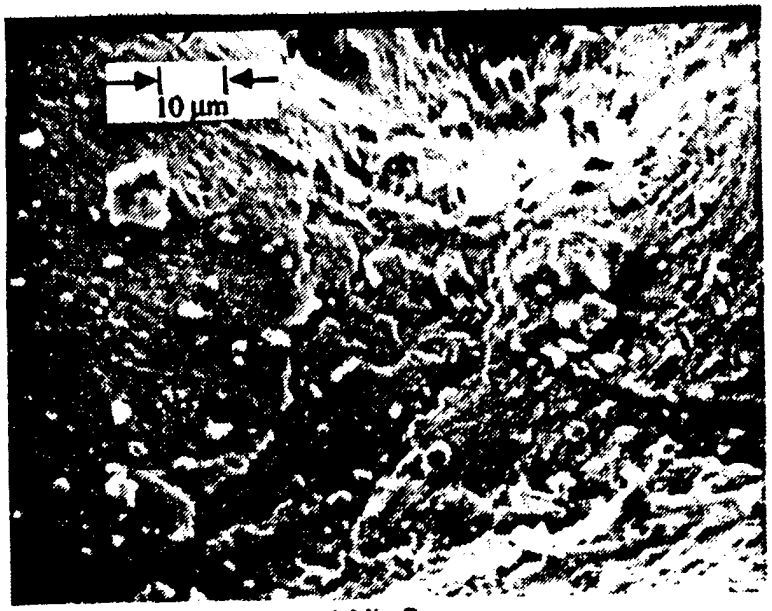

c) Mix-8

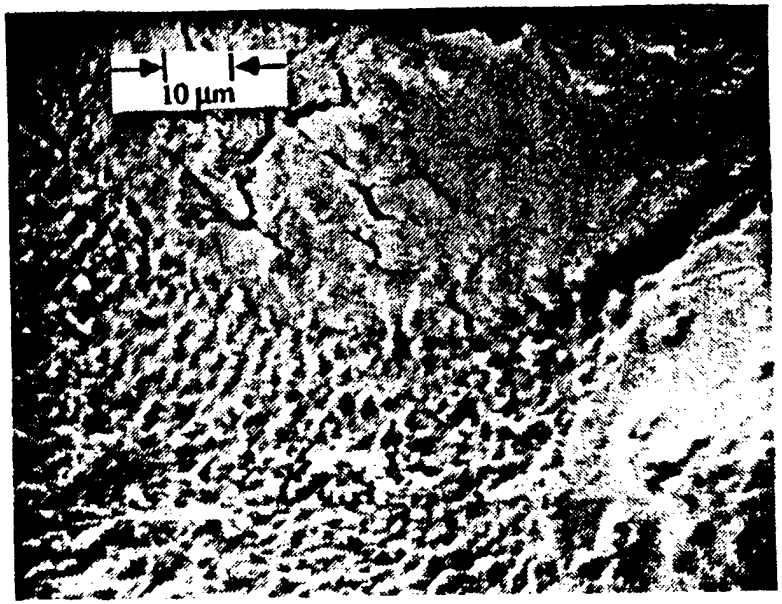

d) Mix-5

Fig. 11 SEM micrographs (~1000 times magnified) of MURI propellant surfaces; propellants are extinguished by using rapid depressurization at 6.9 MPa (1000 psi)

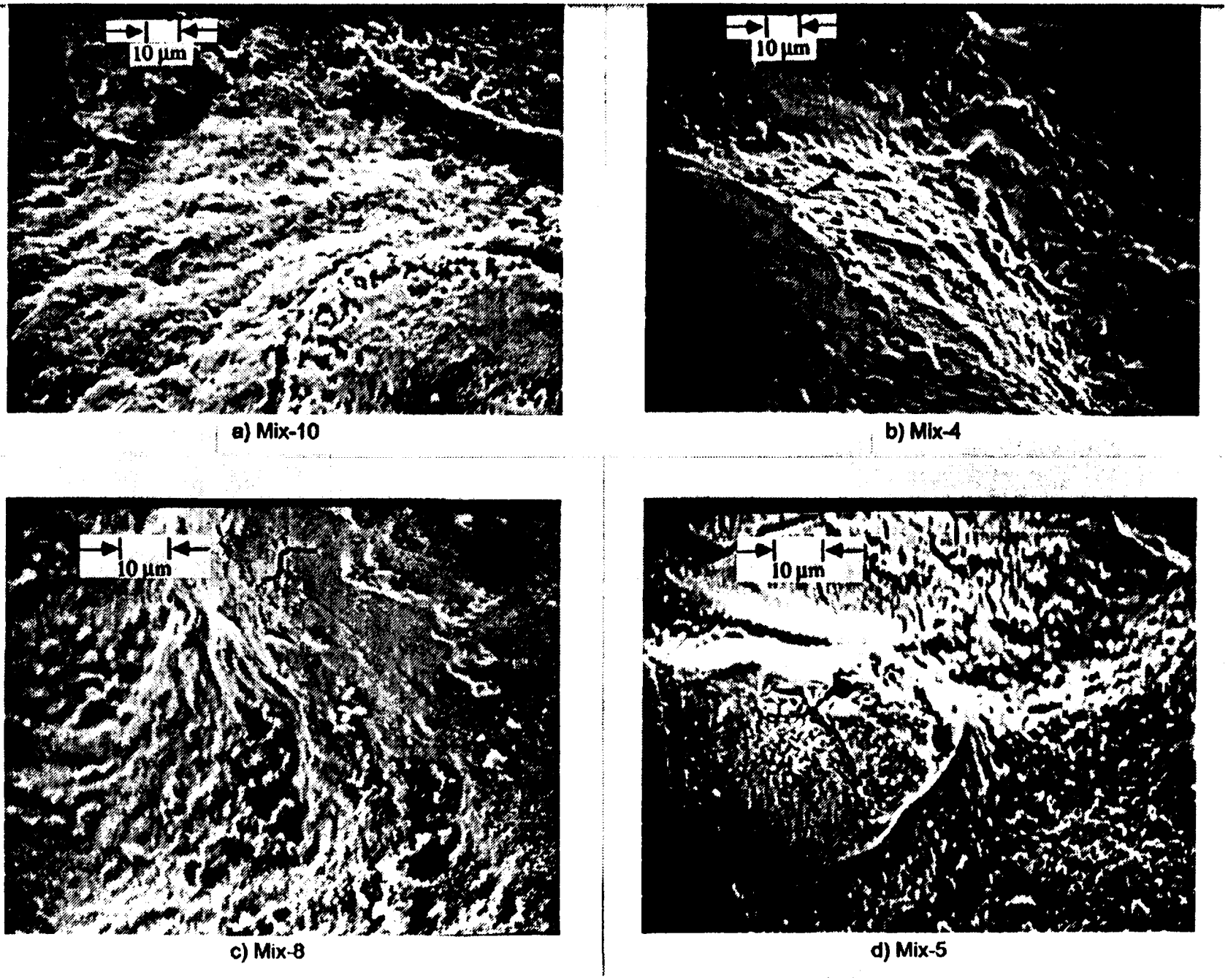

Fig. 12 SEM micrographs (~1000 times magnified) of MURI propellant surfaces; propellants are extinguished by using rapid depressurization at 12.4 MPa (1800 psi)

a) Mix-10

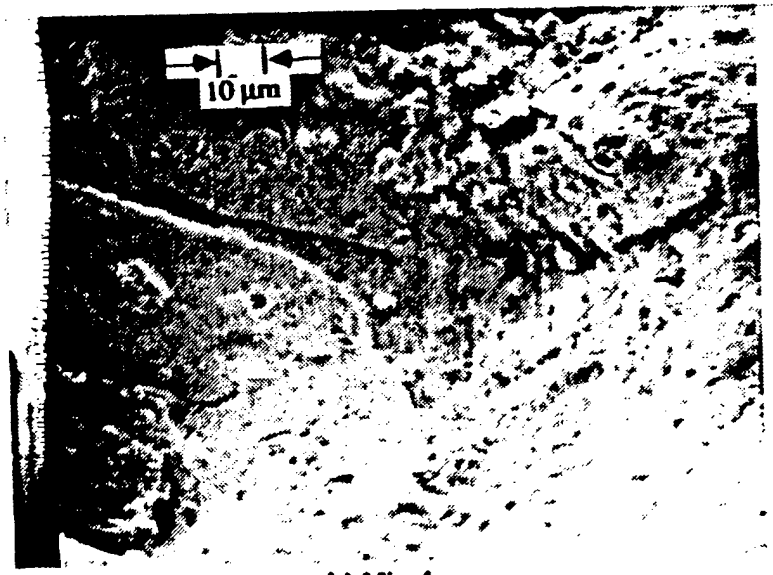

b) Mix-4

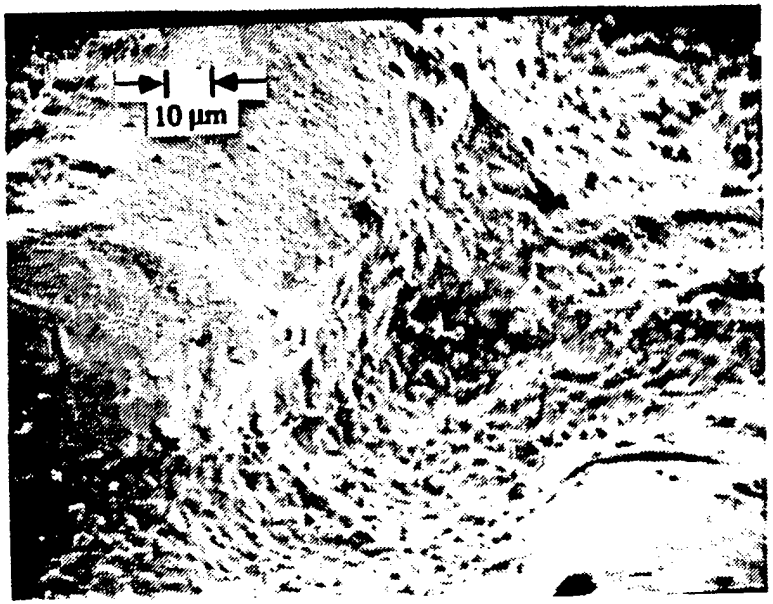

c) Mix-8

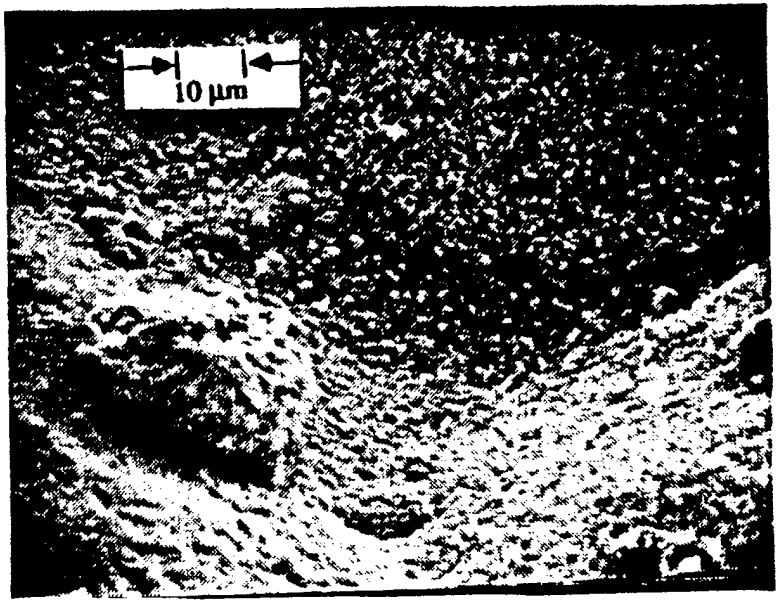

d) Mix-5

Fig. 13 SEM micrographs (~1000 times magnified) of MURI propellant surfaces; propellants are extinguished by using rapid depressurization at 15.9 MPa (2300 psi)

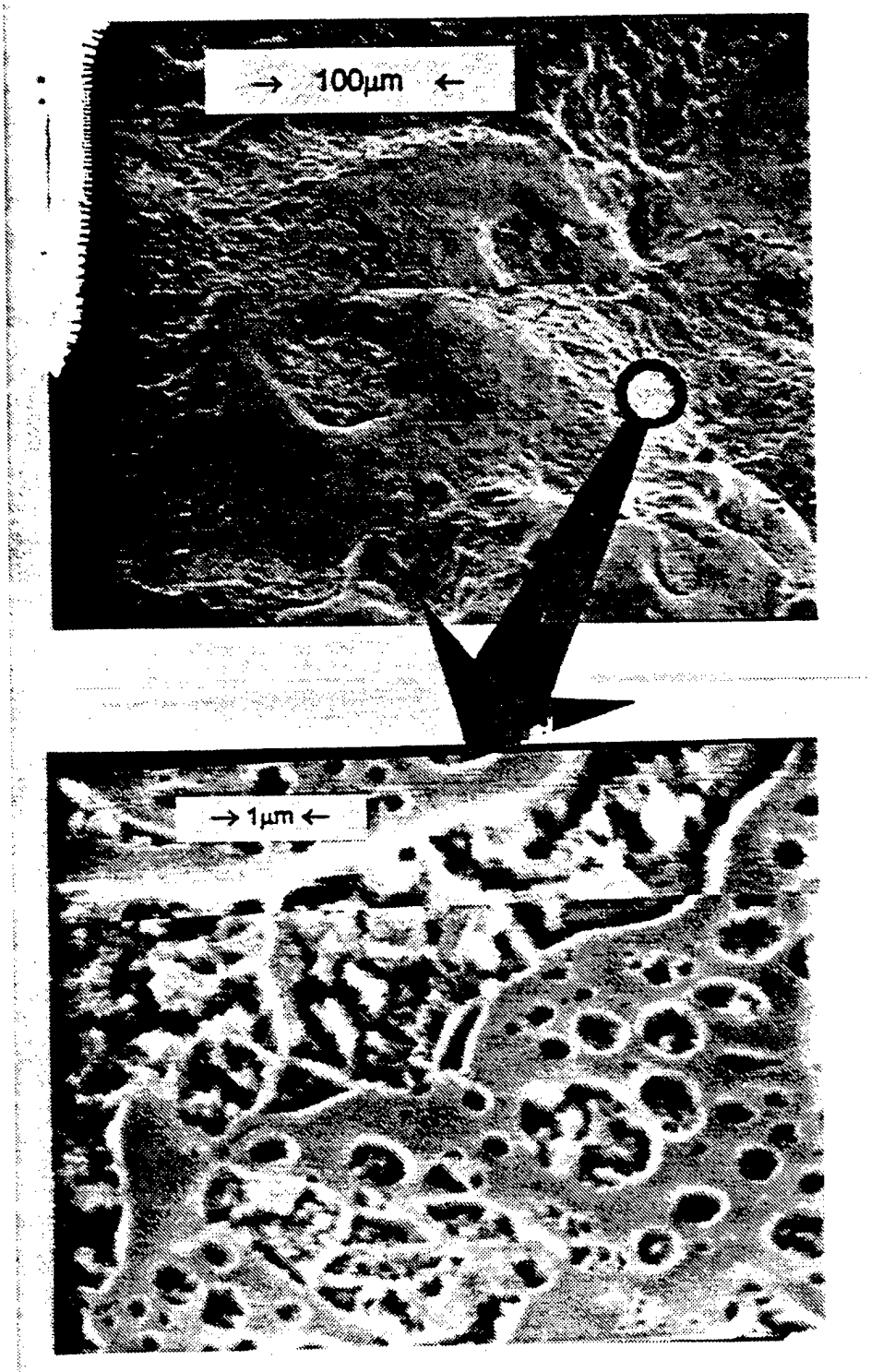

Fig. 14 The matrix surface (magnified 10000 times) of Mix4 extinguished at 12.4 MPa (1800 psi).

APPENDIX P

Price, E. W., Jeenu, R., Freeman, J. M., and Sigman, R. K.

"Quenched Surface Studies of Plateau Propellants"

Proceedings of the 35th JANNAF Combustion Meeting

Tucson, AZ, Dec. 1998

JANNAF 98

QUENCHED SURFACE STUDIES OF PLATEAU BURNING PROPELLANTS

E. W. Price, R. Jeenu, J. M. Freeman, and R. K. Sigman
School of Aerospace Engineering
Georgia Institute of Technology
Atlanta, Georgia 30332-0150

ABSTRACT

Microscopic studies of the quenched surfaces of four AP/HTPB propellants are reported. The propellants have bimodal AP particle distribution and exhibit a wide range of plateau-burning reflecting effects of binder curing agent, ballistic modifier, and ratio of coarse-to-fine AP. The quench sample studies show major differences as a function of formulation and pressure, indicative of burning rate control by a complex, pressure dependent interplay of AP self-deflagration (large particles), oxidizer-fuel diffusion flamelets (around large particles), premixed flames (low pressure, and at all pressures over fine AP-binder matrix areas), and exothermic reactions in the near surface region of the matrix that were enhanced by surface concentration of the ballistic modifier. Binder melt effects were not clarified in the study, but results suggest that they are operative in the very complex matrix surface layer, on a two micron scale where surface tension forces probably control the "melt flow". A Discussion section seeks to describe the coupled combustion zone processes responsible for the diversity of burning rate behavior.

INTRODUCTION

The burning rate of a solid propellant ordinarily increases with increased pressure. Motor designers prefer that this sensitivity of rate to pressure be as low as possible because motor operation is then less sensitive to other variables such as nozzle erosion, unintended variations in propellant properties and initial temperature. It has long been known that certain additives produce "plateau" and "mesa" burning-rate pressure dependence (Fig. 1) in double-base (nitroglycerin-nitrocellulose) propellants, but such properties have until recently not been achieved in practical ammonium perchlorate (AP)-Hydrocarbon (HC) binder propellants. However, investigators at the Thiokol Corporation (Refs. 1-3) have produced plateau, mesa, and biplateau burning (Fig. 2) with AP/HC binder propellants that have high solids loading. Samples of several formulations have been provided to several laboratories and universities where the burning rate controlling mechanisms are being studied under auspice of a BMDO-ONR multi university research initiative (MURI). This paper summarizes part of an associated ONR funded study of plateau burning. Specifically, this paper summarizes results of microscopic examination of surfaces of four Thiokol-MURI propellants, surfaces quenched from various pressures by abrupt depressurization. When interpreted in terms of an extensive background of theory and earlier sandwich burning studies (Refs. 4-8), a fairly complete theory of burning rate-controlling mechanisms is proposed.

THE PROPELLANTS

Of the Thiokol-MURI propellants, mixes 4, 5, 8, and 10 were chosen for study because they provided a baseline formulation (mix 4) and 3 variants involving variables that were viewed as important to burning rate behavior (a view drawn in part by comparison of the burning rate versus pressure curves (Fig.

Distribution authorized to U.S. Government Agencies and their contractors; Critical Technology; September 1995. Other requests for this document shall be referred to Office of Naval Research NSWCIH, Code 333, 800 N. Quincy Street, Arlington, VA 22217-5000.

This research was sponsored by the Office of Naval Research under contract no. N00014-95-1-0559. Since March 1998 the funding for that contract has been from BMDO. The authors would like to thank ONR technical monitors Dr. R. S. Miller and Dr. J. Goldwasser for their continued support in this challenging and enlightening investigation.

burning rate behavior (a view drawn in part by comparison of the burning rate versus pressure curves (Fig. 2) supplied by Thiokol. The basic formulation (mix 4) was 86% AP and 12% DDI cured HTPB with 2% of 0.5μm TiO_2 added. The AP consisted of 200 μm and 2μm in a 62/38 mass ratio. In mix 10, the TiO_2 was replaced with AP; in mix 5, IPDI cured HTPB binder was used; in mix 8 the ratio of coarse-to-fine AP was 55/45. Each propellant contained 2% DOA plasticizer. Formulation details are shown in Table I.

EXPERIMENTAL PROCEDURE

The quench experiment uses a nitrogen pressurized test chamber of 102.9 cm^3 volume. Sample ignition is accomplished by an electrically heated nichrome wire. Samples were rectangular, 4 mm by 4 mm by 10 mm, burned on the 4 by 4 mm face. Samples were uninhibited*. The end of the chamber cavity is closed by a multiple-layer of mylar disks, which were rutured on demand by heating with a nichrome wire. Quench was timed to occur at 1/3 to 2/3 of full burn out time, so as to assure attainment of steady burning before quench. Quench tests were run at combustion pressures from 100 to 2300 psi, mainly at 200, 1000, 1800, and 2300 psi. Details of the apparatus and procedure are given in Ref. 10.

SCANNING ELECTRON MICROGRAMS (SEMS)

Examination of quenched surfaces was made with an ISI Super 60 Scanning Electron Microscope. Samples were sputter coated with gold, and examined at magnifications of 100 to 10,000. Figure 3 illustrates features of a quenched surface, selected to illustrate various features to be found in the full set of SEMs. Figures 3a and 3b show low magnification pictures of mix 8 at 200 and 1800 psi respectively. At 200 psi the surface is relatively flat, a feature manifested in all four mixes, and is interpreted as a result of control of rate by a premixed flame. The coarse AP particles are clearly distinguishable. There is no indication of binder melt flow onto the AP surface. The AP surface has a raised central region which appears to consist of a concentration of TiO_2 particles. At 1800 psi the quenched surface looks like a boulder strewn landscape. The "boulders" are the central portions of AP particles, which simply did not keep up with the rest of the surface. The "valleys" in between the "boulders" are areas of fine AP-binder matrix and peripheral areas of the coarse AP particles. It will be argued later that the burning rate is controlled here by matrix burning, assisted by the leading edge of the stoichiometric flame (LEF) in the mixing fan of matrix and AP vapors formed above the contact lines of matrix and AP particles. The degree of this surface irregularity correlates closely with burning rate, and is seen also with mix 5, which like mix 8 has a high burning rate at 1800 psi. Figure 3c shows an intermediate magnification SEM of a surface area of mix 4 quenched at 200 psi. The coarse AP periphery, AP surface and concentration of TiO_2 are shown more clearly than in 3a. The matrix surface is seen to be very irregular on a 10 μm scale. Irregularity is also evident on the 2 μm scale of the fine AP particles, but the irregularities are not recognizable as particles. On the other hand, the matrix surface does not show any sign of flooding of the surface by binder melt. Figure 3d shows a high magnification SEM of a matrix area of a quenched sample of mix 4 burned at 1800 psi. The surface is about 50% covered by a film of binder melt, which appears to be about 0.1μm thick (at least at its edges). The rest of the surface consists of an irregular array of openings in the film, openings containing TiO_2 and other as yet unidentified fine structures. Since the openings are typically of dimensions similar to the fine AP particle size, they may be the sites of decomposing particles. As will be seen in the following, the above features of the quenched matrix surfaces do not differ quantitatively with test pressure or mix number (except for absence of TiO_2 in the case of mix 10).

SEMs for all test conditions

Selected results of the SEMs of quenched samples of mixes 4, 5, 8 and 10 are presented in Figs. 4-15. Each of these figures shows SEMs of each mix for one pressure and magnification. Figures 4–7 are low magnification SEMs for 200, 1000, 1800, and 2300 psi. Figures 8-11 are a similar set with intermediate magnification and Figs. 12-15 are a similar set with high magnification views of the matrix surfaces. In the case of these high magnification images there is some qualitative variation in the features of the matrix

* In earlier tests (Ref. 9), samples were inhibited on the sides with vacuum grease, which apparently produced a glossy film over the quenched surface.

surfaces as a function of surface site chosen for imaging; the examples shown were selected as "most typical". Figure 16 is a larger picture of the matrix of mix 4 at 200 psi to show the details better. In that picture some clearly identifiable TiO_2 particles are encircled. Computations based on volume fraction of TiO_2 in the matrix indicated that this "population density" of TiO_2 is close to that in the solid (i.e., the TiO_2 particles are "far apart" on the scale of the fine AP particle arrays. However, examination of all the high magnification SEMs led to the conclusion that concentrations of TiO_2 particles were present in some of the "open areas" (and possibly under the binder film areas?). In order to define the principle features of quenched surfaces and describe in words how they depend on sample and test conditions, the following description is provided.

Summary of SEM Results

At 200psi (Figs. 3a, 3c, 4, 8, and 12) the quenched surfaces are fairly flat. The coarse AP and matrix areas are clearly distinguishable. There is no evidence of binder melt flows on-to the coarse AP surfaces. The particle surfaces are concave upward except for raised areas at the center. With mix 10 (no TiO_2) it was found that the raised central area was a bubble-like structure with a concave-upward underlying surface. With the other mixes the raised area consisted of a concentration of TiO_2 particles. At higher magnification (Fig. 8) the AP surface varies from smooth to porous on a 0.5 μm scale, with the smooth areas tending to be nearer the particle periphery. A small crevice is usually evident between the matrix and coarse particles. The crevice has no features suggestive of interfacial burning, but is thought to be a separation during quench due to contraction of the cubic AP phase layer as it cools and returns to orthorhombic phase. These features are similar for all formulations. The matrix surfaces of all mixes are similar to those described for Fig. 4, but the irregularities on the 10 μm scale often appear to be bubbles. They appear to be more numerous in Fig. 8b and c, but this is partly due to choice of surface site and image contrast. At high magnification (10,000) the networks of binder film surrounding recessed areas are seen for all mixes with lateral dimensional scales mostly in the 1-3 μm range. For the examples shown, the degree of coverage by melt film appears to decrease with increasing burning rate for the 3 DDI cured formulations. However, as noted earlier, the trend with formulation is small on the average over multiple surface sites. Within the open areas of mixes 4 and 8 the population of TiO_2 particles is very high, suggestive of concentration on the surface. In the case of mix 5 (IPDI cured HTPB) the openings are deeper and their contents are not revealed. In all cases the openings have delicate filaments of lateral dimensions around 0.1 to 0.2 μm which seemingly consist of binder or binder decomposition residue.

At 1000 psi (Figs. 5, 9, and 13) the quenched surfaces are less flat, especially for mixes 5 and 8, for which the coarse AP particles protrude. The degree of protrusion is greater for mixes with higher burning rate. The burning front (mixes 5 and 8) seem to be led by the matrix and the outer periphery of the coarse AP particles. With mixes 10 and 4, the coarse AP particles are more concave than at 200 psi (at least in the centers), and the matrix areas are somewhat recessed relative to the outer periphery of the coarse AP particles. The matrix areas of mixes 4, 8, and 10 (DDI-cured binder) are still "lumpy" on a 10 μm scale (as at 200 psi). The matrix areas of mix 5 (IPDI-cured binder) are irregular on a scale close to the 2 μm AP particles. At high magnification (Fig. 13) the matrix surfaces of mixes 4, 8, and 10 are similar to those at 200 psi. There is a profusion of TiO_2 particles (mixes 4 and 8) visible particularly in the openings in the melt film. mix 5, (IPDI-cured binder) has a very "lumpy" character, with the lumps apparently consisting of 1–4 μm clusters of TiO_2 particles and binder. The clusters often have evidence of voids, suggesting that they may have had 2 μm AP particles inside (speculation). In the small spaces between clumps, the binder film is evident, with small openings (submicron) and individual TiO_2 particles. These features of mix 5 matrix surface are different than at 200 psi and different than the other mixes at this (1000 psi) pressure.

At 1800 psi (Figs. 3b, 3d, 6 ,10 and 14) the burning rates of mixes 5 and 8 are near the tops of mesas, with rates about 3 times the AP self deflagration rate (see Fig. 2). The AP particles on the surface protrude even more than at 1000 psi (Figs. 3b and 6). The valleys between the "boulders" are concave upwards and the sides of the boulders curve down and blend with the curve of the matrix surface, usually without undercutting the coarse AP boulders. The valley surfaces are cluttered with TiO_2 particles and small clusters (Fig. 10). At high magnification (Fig. 14) the matrix surface is similar to that at 1000 psi (Fig 13), with binder melt films with roughly 40% open areas consisting of holes in the 0.1 to 4 μm range and

with clusters of TiO_2 mostly in the 1-3 μm range. The openings in the film are smaller with mix 5 (IPDI-cured binder) than with mix 8 (high AP/binder ratio in the matrix). At this pressure the burning rate of mix 4 is somewhat higher than the AP self-deflagration (but low compared to mixes 5 and 8), while the rate for mix 10 (no TiO_2) is considerably lower than the AP rate. The surfaces are similar to those at 1000 psi, somewhat more irregular (but nothing like mixes 5 and 8 described above). The coarse AP particles are more recessed (especially in the center). With mix 10 the entire AP surface is concave upward, while in the case of mix 4 the outer periphery of the coarse particles is usually convex upward. The surrounding matrix areas are relatively flat for mix 10, concave upward (valleys) for mix 4 (a feature apparently related to higher rate). The bottoms of the recessed centers of the AP particles of mix 4 are filled by clustered TiO_2. At high magnification (Figs. 3d and 14a) the matrix surfaces of mixes 4 and 10 are similar, also similar to those at 1000 psi. Not noted before, the openings in the melt film seem to be "porous" areas roughly 5μm across that are raised areas, separated by valleys of complete melt coverage, shallow valleys nominally 1-2 μm wide. In the case of mix 5 (Fig. 14) the porous open areas reveal a profusion of "particles" about the size of the TiO_2 particles (but some could be partially burned AP particles). Such particles are not evident with mix 10 (no TiO_2).

At 2300 psi (Figs. 7, 11 and 15), the burning rates of mixes 5 and 8 are down (negative slope of the mesas) but still high compared to mix 10. Mix 4 is on a plateau, with rates only moderately below mix 8. The degree of surface irregularity (Fig. 7) increases in order of burning rate, and is less for mixes 5 and 8 than was the case at 1800 psi (where the rates were higher). The coarse particles of mixes 5 and 8 are still "domes", but mix 8 particles usually have moderate TiO_2-containing depressions not evident at 1800 psi. At intermediate magnification (Fig. 11), the valleys between the protruding AP particles curve upwards toward the AP particles; the demarcation between matrix and coarse AP is not clearly evident with mixes 5 and 8, but seems to be with mix 5 because the AP surface rises too steeply (like at 1800 psi). However some AP particles were removed from the surface (mix 8 at 1800 psi) and examined by SEM. It was found (Fig. 17) that the "valleys" include an outer periphery of the coarse AP particles, with the domed surfaces representing only the inner parts of the particles. This indicates that the fast burning valleys involve coupled burning of the matrix and peripheral AP. Another feature of domed surfaces ("boulders") occurs with mix 5, which exhibits a grainy surface, apparently, TiO_2 particles (1000, 1800, 2300 psi).

DISCUSSION

The object of the interurupted burning tests is to learn about details of the combustion zone that can't be resolved by real time observation. It is too much to expect that surface details will tell the whole story, but they provide clues and a critical test of any mechanistic arguments. In the case of the MURI propellants, they provide rather dramatic, pressure dependent surface features. These results, in combination with the remarkable burning rate curves and a background of earlier knowledge of composite propellant combustion, allow some useful conclusions about rate controlling processes, many of which are unique to these propellants. The approach here is to: a) note some singular features of the burning rate data (Fig. 2); b) examine what is known (or can be inferred) about the behavior and role of the coarse AP, matrix, and TiO_2; and then c) examine the interactive aspects of coarse AP, matrix and TiO_2 behavior. While it is beyond the scope of this study to produce a complete mechanistic explanation of the novel burning of these propellants, useful generalizations will be made, some earlier ones will be challenged, and some remaining questions will be posed.

Questions Posed by the Burning Rate Data (Fig. 2).

a) Why are rates with IPDI-cured binder (mix 5) always higher than with DDI-cured binder (mix 4)? (i.e., detailed mechanism)

b) Why does TiO_2 increase the burning rate at all pressures (mix 4 vs. mix 10)?

c) Why does mix 8 (higher O/F ratio in the matrix) give such a precipitous rate increase in the 900 to 1300 psi range, and precipitous decrease between 2100 and 2500 psi?

d) What causes the behavior similar to mix 8 when the change from DDI to IPDI curative is made (mix 4 → mix 5)?

e) Are plausible explanations of a)-d) consistent with the quenched surface results?

Coarse AP Particle Burning

Under all conditions the coarse AP particles were clearly visible, and free of binder melt encroachment. Noting that the AP self-deflagration rate (Fig. 2) was substantially lower than the propellant rate under most conditions, one might expect that the AP particles would protrude from the surface, especially at pressures below the AP low pressure self-deflagration limit of 280 psi. In general that was not the case at low pressure, indicating that the AP rate was enhanced by presence of the gas phase oxidizer/fuel (O/F) flame. At 200 psi the surfaces of the AP particles were concave upward, but with raised centers that were hollow (mix 10), or mounds of clustered TiO_2. The TiO_2 appears to have been deposited by the overlying matrix as the top of the particle emerged. It was present on coarse particles at low pressure at all stages of burning. TGA and self-deflagration tests on pressed samples of AP and TiO_2. Showed no effect of TiO_2, and the coarse AP particles seemed to be the same for mix 10 (no TiO_2) and the other mixes with TiO_2, indicating that it had little or no effect on the coarse AP particle combustion at low pressure.

As pressure was increased, the central areas of the coarse AP particles became more deeply recessed with mixes 4 and 10 (e.g. 1000 psi). At this point the AP self-deflagration rate is close to the propellant rates for these two mixes, and the particles leave depressions in the surface that are the leading part of the burning front (mix 10 at 1800 psi, Fig. 18). However, this feature changes to protruding AP particles for the fast burning formulations (mixes 8 and 5). At 1000 psi the matrix burning of these two formulations seems to run ahead, leaving the coarse AP behind. By 1800 psi the propellant burning rate is 3 to 4 times the AP self-deflagration rate and the coarse AP particles look like fields of boulders. The hot O/F flame is by now a set of diffusion limited flamelets, which don't heat the coarse AP enough to keep up. However, as noted relative to Fig. 17, the LEF portion of the hot O/F flamelets are increasingly localized at the periphery of the coarse AP particles and an outer peripheral region of the particles burns down with the matrix. In effect the O/F flamelet support of the AP deflagration has become increasingly localized, and the flamelets in turn owe their existence to the oxidizer vapor from that peripheral ledge of AP. It should be remembered that these O/F flamelets occur along stoichiometric surfaces in the mixing flows, and are hotter than either the matrix flame or the final equilibrium flame. This coupled matrix flame-AP flame-LEF[1] complex apparently burns its way around the AP periphery, leaving a more slowly deflagrating central portion of the particle protruding from the burning rate controlling part of the surface. A key question is: why does this rate controlling complex not develop for mixes 4 and 10 and why is its effect so critically dependent on pressure?

Above 1800 psi the burning rates of mixes 5 and 8 decrease, "dramatically" for mix 8. The protrusion of the AP decreases and at 2300 psi it is comparable to that at 1000 psi (the burning rates are about the same at 1000 and 2300 psi). The coarse AP surfaces of mixes 4 and 10 are similar to those at 1000 and 1800 psi, with recessed central regions that may be ahead of the mean propellant surface. The recesses of mix 4 contain clusters of TiO_2. The general surface roughness and AP recesses are less for mix 10 than for mix 4, consistent with the lower burning rate. The surfaces of the mix 10 AP particles have a unique dry porous appearance. The features of the surfaces of mix 10 and 4 do not give much information about the flame complex. The recesses in the AP particles of mix 10 are easy to explain in the 1500-2000 psi range, where the AP self-deflagration rate is higher than the propellant rate. However the recesses are harder to explain for mix 4, whose rate is higher than the AP rate. The similarity of the surfaces at 2300 psi suggests that the cause of the steep decline in AP self-deflagration rate above 2000 psi is not operative in the propellant combustion zone. Indeed, the mix 10 and 4 surfaces (especially mix 10) look like they are burning with a substantially premixed flame over the whole pressure range, a postulate that is implausible in the context of the low pressure sensitivity of burning rate unless the flame kinetic rate constants were slowing with increasing pressure.

[1] Leading edge portion of the diffusion flamelet

Matrix Burning

In discussing this subject it is appropriate to consider first some independent results on the nature of matrix burning. It has long been known that they often demonstrate "anomalous" burning, including plateau and mesa burning in the mid-pressure range, with locally intermittent burning, and often a mid-pressure range in which burning will not self sustain. Such behavior has been seen to be more pronounced with fine AP size and DDI-cured HTPB, features of the MURI propellants. No such data has been developed for the matrix formulations of the MURI propellants because it was found difficult to achieve such high 2 μm AP content (some results with lower AP content are reported in Refs. 12 and 13, using material supplied by Thiokol Corp.). These collected results suggest that mesa burning is associated with local intermittency of burning, especially in the "trough" of the mesa. In the case of the MURI matrixes, the fineness of the AP and the use of DDI-cured HTPB binder could result in failure to sustain burning in a wide pressure range (e.g., for the mix 10 matrix). Presence of TiO_2 tends to suppress anomalous burning (mixes 4, 5, 8), and use of higher O/F ratio or IPDI-cured HTPB (mixes 8 and 5) are also conducive to more "normal" burning. The relevance of such results to matrix burning in bimodal propellants is not well established, but it seems likely that these matrixes burn "reluctantly" without the oxidizer supply and heat supply provided by the coarse AP and its O/F flame. However focus here will be on the subject of matrix burning mechanisms and the evidence from the quenched surface studies.

Because of the very fine AP size in the MURI matrixes, it seems likely that the gas phase O/F flame is premixed. It is also plausible to consider the possibility of significant heat release very close to or on the surface due to reactions that are of minimal importance with coarser AP and/or no catalyst. Such reactions may be more extensive because of the high proximity of AP and binder with 2 μm AP (short diffusion distance for mixing).

If one views the burning of the matrix in terms of a micro-scale heterogeneous structure heated by a planar flame, the exposed ingredients will decompose each according to its own kinetics, with the more easily decomposed ingredients becoming recessed in the surface, and the other ingredient protruding. This adjustment, referred to as "surface disproportionation" (Ref. 14), is necessary in order for the two ingredients to pyrolize in the proportions present in the mixture. If the "slower" ingredient is a meltable binder, it may improve its share of the incident heat flux by covering over some of the oxidizer. If instead the "slower" ingredient is a particulate non-melting oxidizer, the binder will become recessed between the oxidizer particles. Over the pressure range pertinent to this study the nature of the disproportionation may change because of differing dependence of pyrolysis rate of the ingredients on pressure and temperature. In principle, if the matrix is not too fuel rich to burn, the disproportionation process is self limiting, i.e., it stabilizes automatically when conditions on the surface reach a point where the ratio of effluxes of ingredient vapors matches the ratio in the propellant bulk. If the pyrolysis kinetics were known, one might be able to forecast the appearance of the surface and then compare it with the high resolution SEMs of quenched surfaces. Unfortunately, there is no definitive source for the kinetic data for pyrolysis of the ingredients at these high rates and pressures.

In the MURI mixes, the areas of binder and AP in the matrix are roughly 40 and 60% respectively in a cut surface. On the quenched surfaces the binder covers 50-60% and the oxidizer correspondingly 50-40%, not particularly sensitive to pressure or formulation. The fine AP particles are always recessed, increasingly so with pressure (but not quantified because no particle surfaces can be resolved and measured: the observable structures associated with the openings may be partially decomposed surfaces of AP particles). This indicates a moderate degree of binder melt concentration, in a film that appears to be very thin at the edges of the openings (but may overlay more substantive binder structures). The surface has the look of an overlay of binder film that is blown or burned open by AP vapors.

Up to this point the recesses in the open areas of the matrix film are characterized only superficially. The TiO_2 clusters are identified by the consistent size of the particles. Other dry-looking structures are presumed to be AP. Tendrils bridging the openings are presumably binder. While one might expect open areas and recesses at varying stages of AP particle decomposition (including burn out), the

details in the recesses have not been revealed well enough to interpret in that way[2]. Because of the absence of conspicuous differences in matrix surfaces over the range of test variables, it seems likely that the so far unresolved details in the matrix surface may be important to explanation of the diversity of burning rate behavior that is shown in Fig. 2.

TiO_2

According to Thiokol personnel, the TiO_2 additive is effective in controlling the burning rate in the pressure intervals at which plateaus occur, and its effect depends on TiO_2 particle size. The detailed mechanism by which it acts is not made clear, except that it seems to intervene in the binder melt effects. In considering the possible TiO_2 effects in the present study, a computation was made of the expected distribution of the particles in the matrix. The result is depicted in Fig. 19, and shows that the particles are sparsely distributed in the array of fine AP particles in the matrix. In that array it is difficult to imagine that the particles would significantly affect either the melt mobility or the chemical reactions. However, the SEMs indicate that the TiO_2 concentrates on the burning surface, a condition that has been noted in the past with other nonvolatile particles, and found to be important for catalysis of burning rate when Fe_2O_3 is used (Ref. 7,15). To check the possibility that TiO_2 was acting as a chemical catalyst, TGA tests (Ref. 13) were run on binder with and without TiO_2, AP with and without TiO_2, and on samples of mix 10 and mix 4 propellants (with and without TiO_2). The results indicated that TiO_2 did not affect decomposition of either binder or AP, but did enhance decomposition of binder the combination of binder and AP. It was proposed that TiO_2 was a catalyst for $HClO_4$ decomposition, which in turn would lead to oxidizer-binder reactions, enhanced gas emissions in the matrix surface layer and to heat release near the surface. In the presence of concentrated TiO_2, the rate of such reactions on the surface of the matrix may well contribute to burning rate. This would require that the surface of the TiO_2 concentrations be free of binder melt (to permit contact with $HClO_4$). Both the concentration and "drying" of TiO_2 may be pressure dependent. Results in Ref. 13 show that TiO_2 enhances the burning rate of matrixes with other binders, minimizes the tendency to intermittent burning and to "no-burn" domains. Collectively, these results suggest that TiO_2 in MURI propellants enhances the burning rate, but the effect may be binder and pressure dependent because of the dependence of the concentration process and the surface "dryness" on binder and pressure. The SEM results establish the presence of concentration of TiO_2, but the degree and dryness or dependence on formulation and pressure can't be assessed from present results. Reference 13 describes a TGA test run on a thin surface slice of a quenched sample that indicated that the surface had 10-30 times the amount of TiO_2 that would be there if there were no concentration. This method may be useful to establish the dependence of concentration on relevant variables, but it has not been possible to do this within available project resources.

To the casual reader, the large concentrations of TiO_2 on the surfaces of coarse AP particles may attract more notice. However, the SEMs do not indicate that these TiO_2 concentrations (e.g., Fig. 4, 20) have any effect on burning rate. Further, tests were run (Ref. 13) comparing self-deflagration of pure AP and AP + TiO_2, which showed that TiO_2 did not affect rate. The TiO_2 on the coarse AP particles seems to be a residue from the burnout of an overlying matrix layer, that remained throughout the AP particle burning (and may even sometimes be handed down to successive particles).

In summary, it appears that the TiO_2 acts by chemical catalysis of $HClO_4$ and resulting matrix surface layer heat release. The fine AP size is particularly conducive to such reactions because of the short diffusion distances between sources of reactants. In addition to the pressure dependence of rate of such reactions, the burning rate dependence on pressure would depend on pressure dependence of TiO_2 concentration and surface exposure, still to be determined.

Burning Rate and Mechanism

Returning to the questions posed at the start of the "Discussion" concerning the burning rate curves in Fig. 2, some attempt at answers are offered here.

---

[2] Some caution should be exercised in interpretation of these details of the quenched surface because of possible artifacts of the quench event.

1. At low pressures the gas phase O/F flame is substantially premixed, possibly a little hotter over the central area of the coarse AP particles. That flame helps the coarse AP deflagration, and sustains matrix burning. It is concluded that TiO_2 acts as a mild chemical catalyst for $HClO_4$ decomposition in the matrix surface layer, with some heat release there that enhances burning rate. A higher O/F ratio in the matrix (mix 8) enhances such surface layer heat release, as does use of IPDI cured HTPB (mix 5).

2. It has been postulated (Ref. 1) that there is a "binder-melt suppression" of burning rate that is more conspicuous with DDI-cured HTPB, but the detailed mechanism has not been clarified. The SEM study does not reveal a mechanism, but does rule out some, and gives new insights regarding matrix burning that suggest a mechanism. It is observed that the 2 μm AP particles burn out ahead of the binder. Based on thermal wave calculations, the binder melt layer appears to be thicker than the 2 μm particles, and it seems likely that the binder-melt surface tension would draw the melt into the void left by the AP particle burnout, thereby locally obstructing the progression of burning through the matrix. In the case of mix 10 it appears that this effect is so extensive that the matrix won't burn on its' own, and even the burning of the propellant is seen to be locally intermittent, with many samples quenching spontaneously. In this context, the presence of a higher O/F ratio, a more viscous binder melt, or of catalyzed exothermic reactions in the surface layer would all tend to counter the "melt suppression" mechanism proposed here. The results to date seem to preclude explanations of melt suppression operating on any larger scale, but more detailed studies would be required to establish the real processes on the 2μm scale in the surface layer. Such an effort would be aided by availability of matrix samples matching those in the propellant, and counterparts for the mixes 5 and 8 without TiO_2 (both propellant and matrix).

3. The continued low burning rate of mix 10 to higher pressures is apparently due to intermittent burning which is so severe that the rate is well below the AP rate in the mid-pressure range.

4. As pressure is increased, the overall O/F flame becomes increasingly structured (not premixed), with correspondingly structured quenched surfaces (on the large scale). Hot stoichiometric diffusion flamelets form over the coarse AP particles, with leading edges penetrating closer to the surface and becoming increasingly coupled (1000-1800 psi) to areas on the periphery of the AP particles (Fig. 21). In the process, the LEFs also heat the adjoining matrix and act as near-surface flame holders for the matrix. The effect is evident in mixes 5 and 8, where the coupled O/F-matrix flamelets outpace the more distant central parts of the coarse AP particles, giving rise to the "boulder field" look at 1800 psi. However, it is notable that similar behavior does not develop for mixes 10 and 4, indicating that the reluctant matrix burning is not overcome by the penetration of the O/F flame at higher pressure (and especially without the catalyst-aided heat release in the surface layer (mix 10)).

5. The details of the burning rate-pressure curves may depend further on the degree of effectiveness of the catalyst, which may vary with pressure via three mechanisms, a) degree of concentration on the matrix surface, b) degree to which dry surface becomes available for catalysis (free of binder melt), and c) reaction progress of catalyst initiated reaction sequences. These effects would be expected to differ also with matrix formulation. The quench SEMs studies and subsidiary tests don't provide much information on these points, but do establish that TiO_2 concentrates on the surface and catalyses reaction rate.

6. The most challenging aspect of the burning rate data is the abrupt decline in burning rate with increasing pressure for mixes 5 and 8 in the 2000 to 2300 psi range. The coupled LEF-matrix flame apparently flame diminishes in importance and the protrusion of the coarse AP particles is correspondingly reduced. It has been suggested (Ref. 1) that this is due to decreasing melt-viscosity with increasing pressure, but this argument is based on a presumption that viscosity is decreasing due to rising surface temperature. But increasing temperature is not consistent with the observed decreasing burning rate. It is suggested here that the "collapse" in burning rate may be

due to a) failure of the TiO_2 to concentrate, b) loss of dry catalytic TiO_2 surfaces, or c) thermal quenching (retraction) of the leading edge portion of the diffusion flamelets (Fig. 21). The latter idea is posed because at 1800 psi the diffusion flamelet is essentially "wrapped around" the protruding AP "boulders" and subject to considerable heat loss to the AP particle. A further potential factor is the pressure dependence of fuel pyrolysis rate, which is thought to decrease with increasing pressure and decreasing temperature, and may cause increased binder melt on the surface. One further idea about the burning rate "collapse" is the collapse of the AP self-deflagration rate (Fig. 2) that occurs in the same pressure range. However, this does not seem plausible because of the protrusion of the coarse AP particles is decreasing rather than increasing with pressure in the range where self-deflagration rate is dropping. It seems likely that the anomalous AP deflagration does not occur in the presence of an O/F flame heat source.

CONCLUSIONS

The results and discussion probably identify all contributing combustion processes that, collectively, explain the "amazing" burning rate behavior of the four "MURI" propellants. The relative importance of the various coupled combustion steps as a function of pressure is proposed, but in some instances these proposals amount only to speculation because of incomplete supporting data. In particular, there continues to be a shortage of data on ingredient pyrolysis rate at the pressures and temperatures present in the combustion zone. In addition, there is evidence of important interactive behavior of the ballistic modifier, AP vapor ($HClO_4$) and binder that occurs in the geometrically complex surface region, on a less-than-3μm scale, that is only partially resolved by present studies. Some observations that do not seem to be speculative are:

a) The overall O/F flame is pre-mixed and yields a flat burning surface at low pressure (< 300 psi).

a) When burning rate is high the rate is dominated by a coupled premixed matrix flame and a localized part of the O/F diffusion flamelet (LEF) that burns down the outer periphery of the coarse AP particles.

b) The ballistic modifier concentrates on the matrix surface and catalyses exothermic reactions on or near the matrix surfaces, contributing to burning rate of all mixes (4, 5, and 8) at all pressures. The degree of the effect may be pressure-dependent, but was established only by inference. The influence is far less than with Fe_2O_3 catalyst.

c) No role for binder melt flows was revealed, but the results indicate that the role exists and is localized in the 2-3 μm-scale of the irregular surface region of the matrix surface, where melt mobility would be dominated by surface melt tension.

d) There is a good deal of evidence that the matrixes burn only marginally (not at all for mix 10), and propellant burning rate differs with formulation in a way that correlates with expected effects on matrix burning, i.e., increasing with presence of catalyst, use of "lower-melt" binder and increased O/F ratio of the matrix.

e) In contrast to some previously reported studies, the coarse AP particles do not exhibit "ignition delay" followed by rapid burning, but instead burn relatively slowly when the propellant rate is high, but burn faster than the AP self-deflagration rate under all conditions except for ambiguity of mix 10 in the mid-pressure range where burning was intermittent. (However, under low burning rate conditions, in the absence of the local diffusion flame after AP particle burn-out, burn-through to the underlying coarse AP particles may be slow because of lack of close-by O/F flame support.)

f) The deflagration of the coarse AP particles is assisted by the O/F flame under all conditions, most conspicuously at low pressure (below the AP self-deflagration limit) and in the "anomalous deflagration" range above 2000 psi. Under other conditions the flame support is reflected in recesses in the central areas of the surface (low rate conditions) and burning down the outer peripheries (high rate conditions).

Proposed future studies will be aimed at evaluation of the several speculations that were parts of the overall explanation in the Discussion of the novel burning rate behavior of mixes 4, 5, 8, and 10.

REFERENCES

1.Campbell, C. J. and Cohen, N. S., "Achievement of Plateau Ballistics in AP/HTPB Propellants," CPIA Pub. No. 662, pp. 1-16, 34th JANNAF Combustion Meeting, Oct. 97.

2. Cohen, N, S. and Hightower, J. O., "An Explanation for Anomalous Combustion Behavior in Composite Propellants," CPIA Pub. No. 593, pp. 253-273, *29h JANNAF Combustion Meeting*, Oct. 1992.

3.Cohen, N. S., Franklin, P. M., and Booth, D. W., "Literature Review of Plateau Ballistics in Nonaluminized Solid Propellants," CPIA Pub. 550, pp. 387-410, *27th JANNAF Combustion Meeting*, Oct. 1990.

4. Hightower, J. D. and Price, E. W., "Experimental Studies Relating to the Combustion Mechanism of Composite Propellants," Astronautica Acta, Vol. 14, No. 1, 1968, pp. 11-21.

5. Price, E. W., Sambamurthi, J. K., Sigman, R. K. and Panyam, R. R., "Combustion of Ammonium Perchlorate-Polymer Sandwiches," Combustion and Flame, Vol. 63, 1986, pp. 381-413.

6. Lee, S-T., Price, E. W., and Sigman, R. K., "Effect of Multidimensional Flamelets in Composite Propellant Combustion," *Journal of Propulsion and Power*, Vol. 10, No. 6, Nov.-Dec. 1994, pp. 761-768.

7. Chakravarthy, S. R., Price, E. W. and Sigman, R. K., "Mechanism of Burning Rate Enhancement of Composite Solid Propellants by Ferric Oxide," *Journal of Propulsion and Power*, Vol. 13, No. 4, July-Aug. 1997, pp. 471-480.

8. Price, E. W., "Effect of Multidimensional Flamelets in Composite Propellant Combustion," *Journal of Propulsion and Power*, Vol. 11, No. 4, pp. 717-728.

9. Price, E. W., Chakravarthy, S. R., Freeman, J. M., and Sigman, R. K., "Surface Features of Biplateau AP Composite Propellants," CPIA Pub. 662, Vol. IV, pp..45-71, *34th JANNAF Combustion Meeting*, October 1997.

10. Varney, A. M., "An Experimental Investigation of the Burning Mechanism of Ammonium Perchlorate Composite Solid Propellants," Ph. D. Thesis, Georgia Institute of Technology, Atlanta, GA, May 1970.

11. Chakravarthy, S. R., Price, E. W., and Sigman, R. K., "Binder Melt Flow Effects in the Combustion of AP-HC Propellants," AIAA Paper 95-2710, 31st AIAA/ASME/SAE/ASEE Joint Propulsion Conference and Exhibit, June 10-12, 1995.

12. Freeman, J. M., Price, E. W., Chakravarthy, S. R. and Sigman, R. K., "Contribution of Monomodal AP/HC Propellants to Bimodal Plateau-Burning Propellants," AIAA Paper # 98-3388, 34th AIAA/ASME/SAE/ASEE Joint Propulsion Conference and Exhibit, July 13-15, 1998.

13. Freeman, J. M., Price, E. W., Jeenu, R. and Sigman, R. K., "Effect of Matrix Variables on Bimodal Propellant Combustion," 35th JANNAF Combustion Meeting, (to be presented), Dec. 1998.

14. Price, E. W., Chakravarthy, S. R., and Sigman, R. K., "Pressure Dependence of Burning Rate of Ammonium Perchlorate-Hydrocarbon Binder Solid Propellants," AIAA Paper # 97-3106, 33rd AIAA/ASME/SAE/ASEE Joint Propulsion Conference and Exhibit, July 6-9, 1997.

15. Price, E. W., Sambamurthi, J. K., and Sigman, R. K., "Further Results on the Combustion of AP/Polymer Sandwiches with Additives," Proceedings of the 22nd JANNAF Combustion Meeting, CPIA Pub. 422, Vol. 1, 1985.

Table I Composition of the MURI propellants

Propellant	Curative	Percentage of			Ratio of AP(c) to AP(f)	
		Binder	AP	Catalyst	coarse	Fine
mix 4	DDI	12	86	2	62	38
mix 8	DDI	12	86	2	55	45
mix 5	IPDI	12	86	2	62	38
mix 10	DDI	12	88	0	62	38

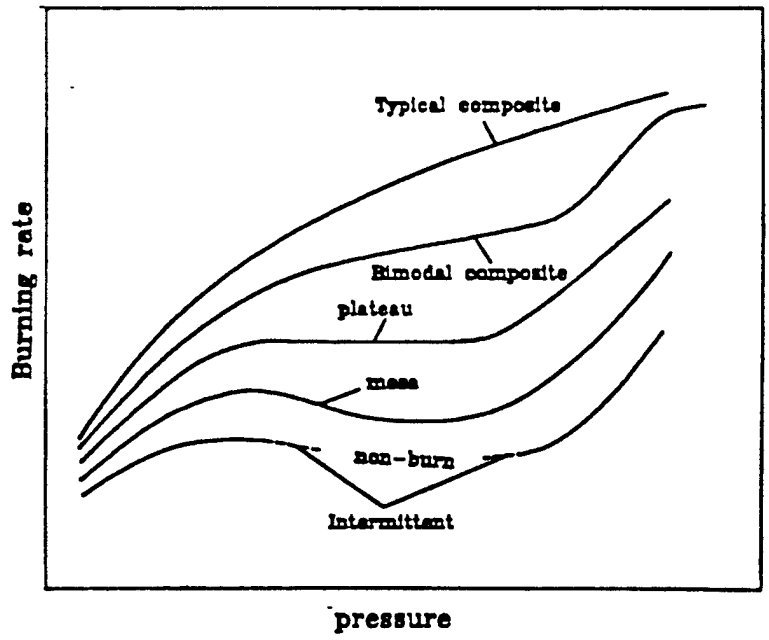

Fig. 1 Pressure dependence on burning rates of propellants

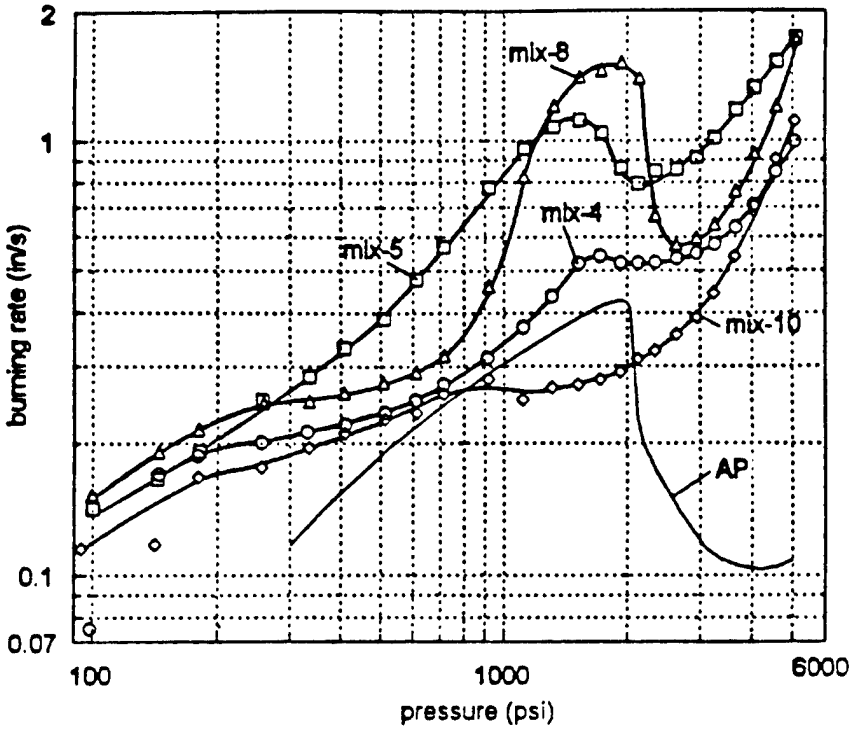

Fig. 2 Burning rates of MURI propellants and AP

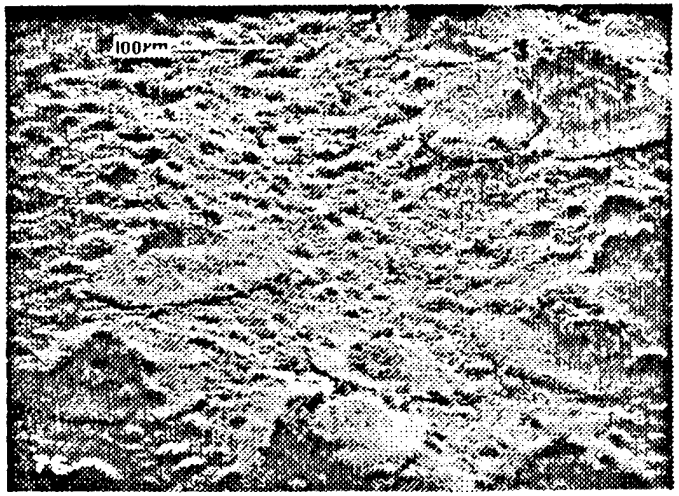

(a) Mix 8 at 200 psi (200x)

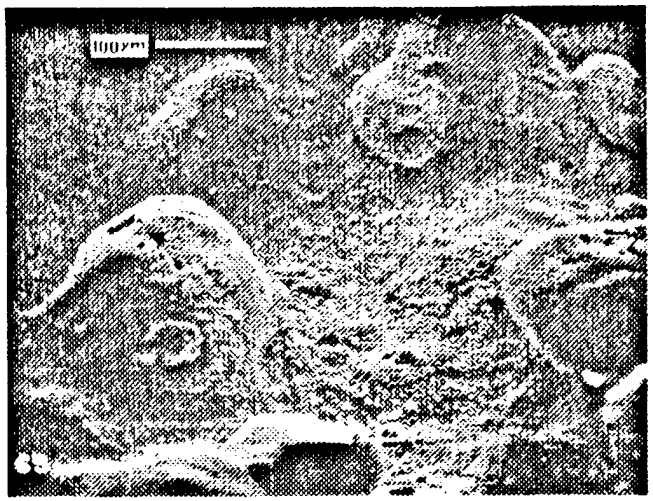

(b) Mix 8 at 1800 psi (200x)

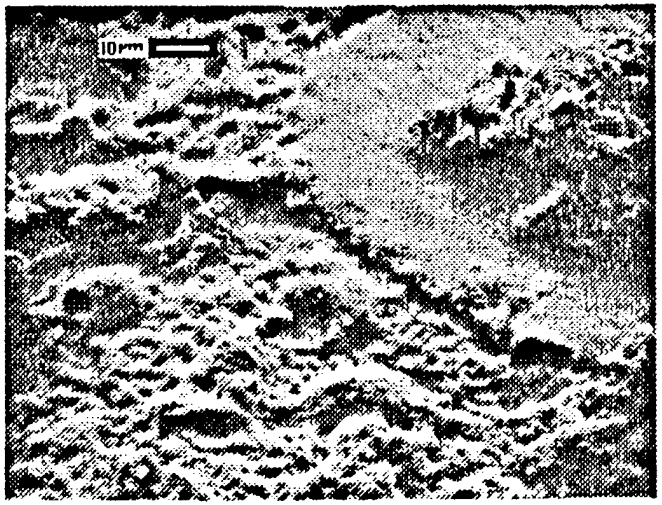

(c) Mix 4 at 200 psi (1000x)

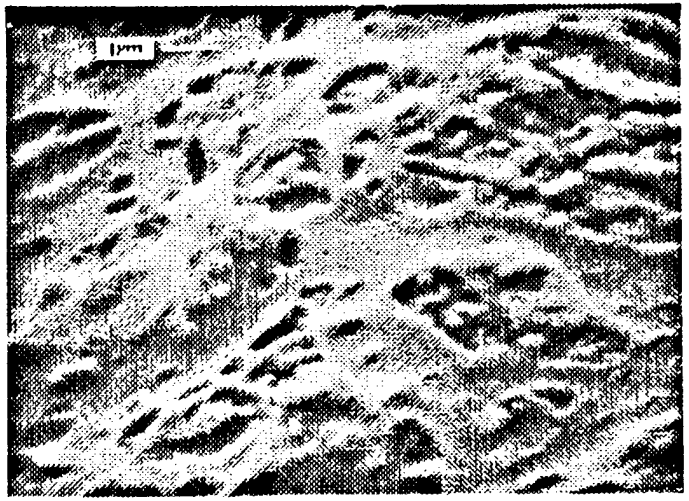

(d) Mix -4 at 1800 psi (10000x)

Fig. 3 General features of quenched surface of MURI propellants

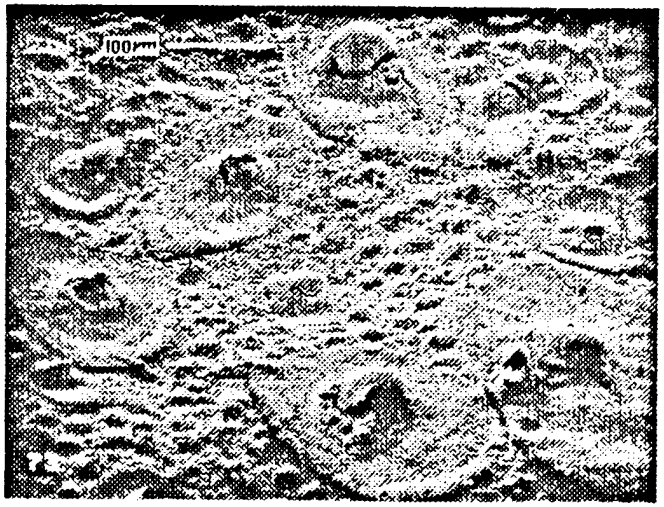

(a) Mix 10

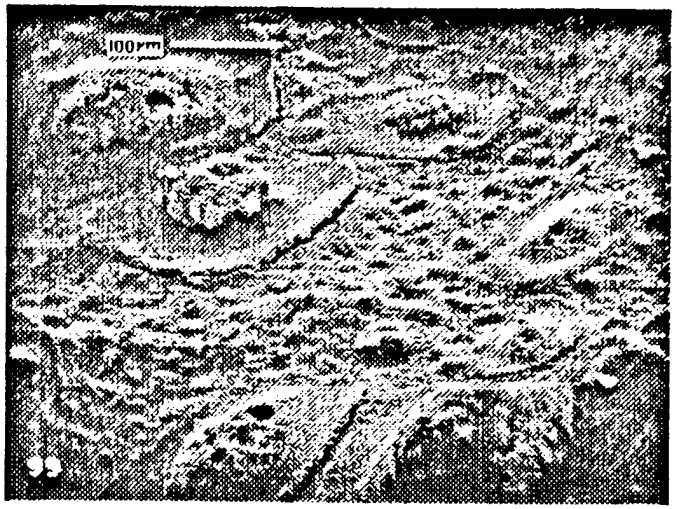

(b) Mix 4

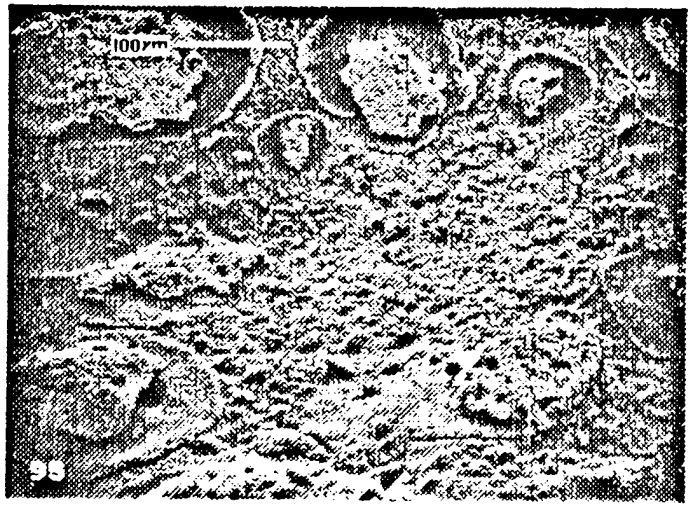

(c) Mix -5

Fig. 4 Features of quenched surface of MURI propellants at 200 psi (magnification - 200x)

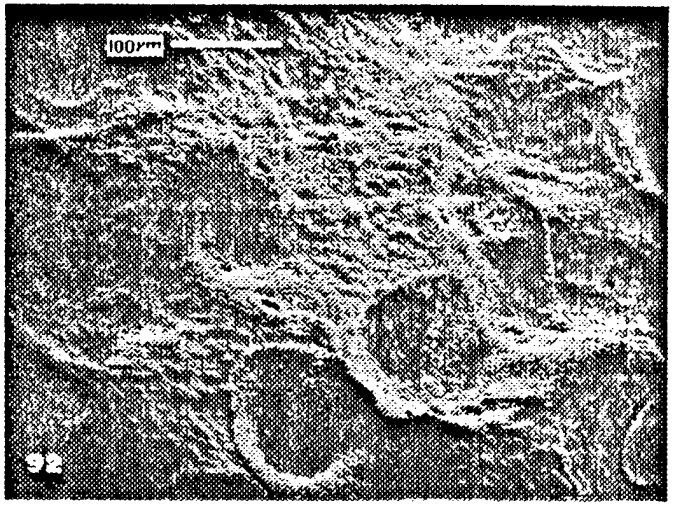

(a) Mix 10

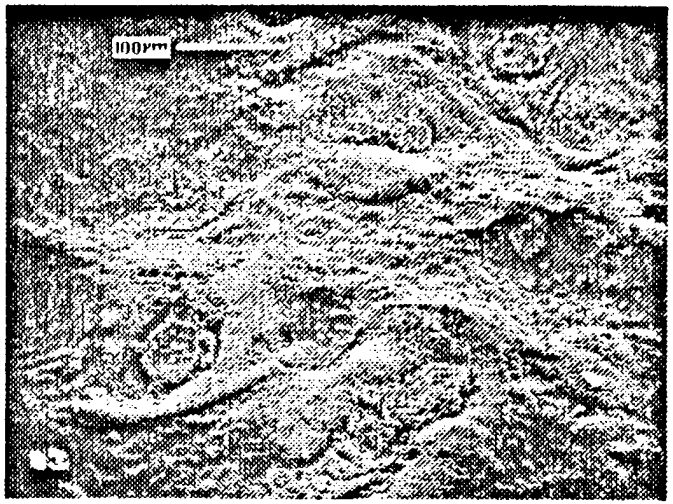

(b) Mix 4

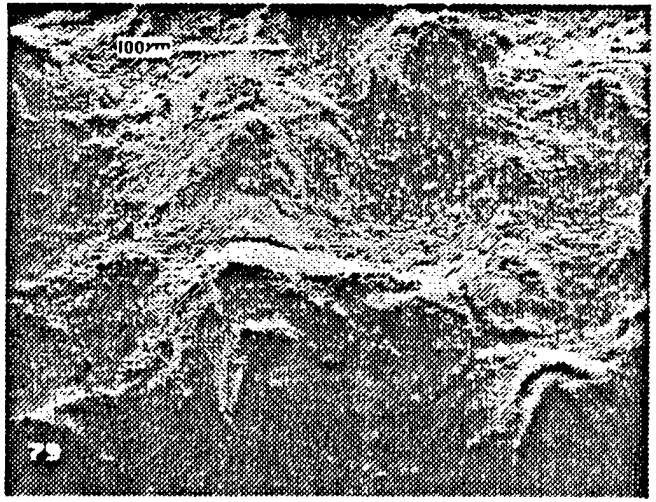

(c) Mix 8

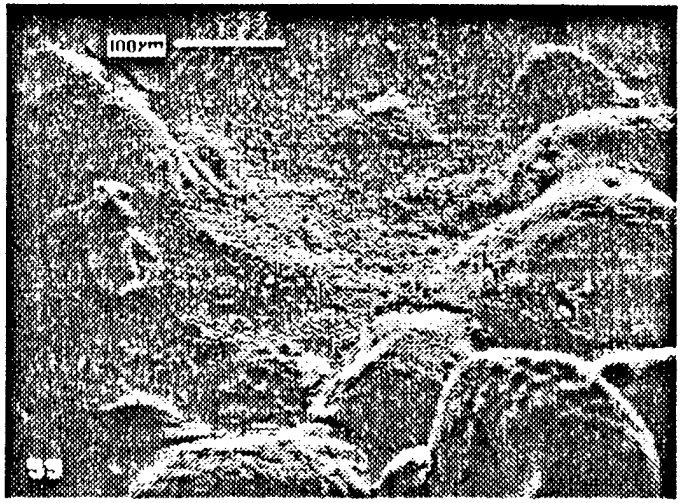

(d) Mix 5

Fig. 5 Features of quenched surface of MURI propellants at 1000 psi (magnification - 200x)

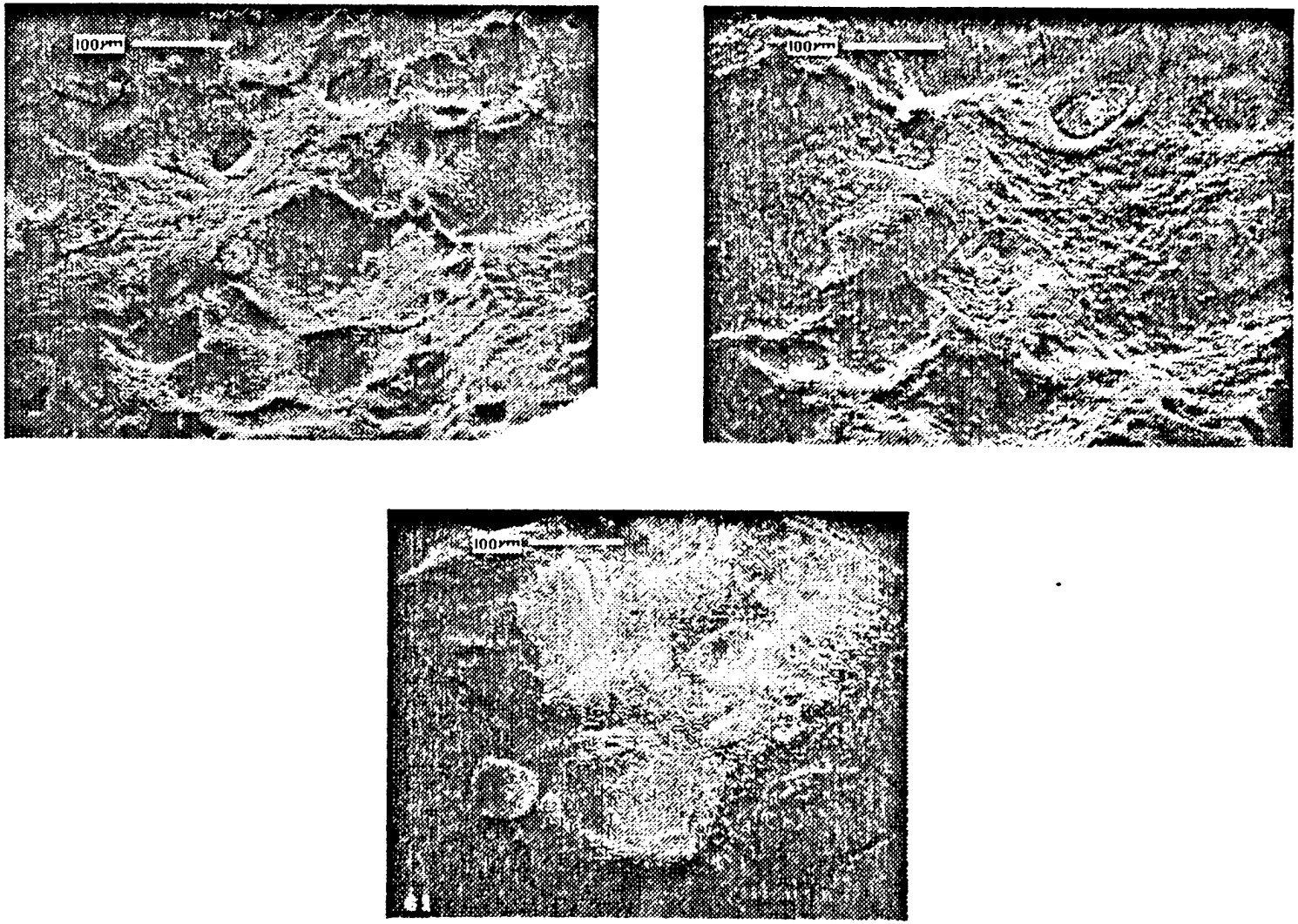

Fig. 6 Features of quenched surface of MURI propellants at 1800 psi (magnification - 200x)

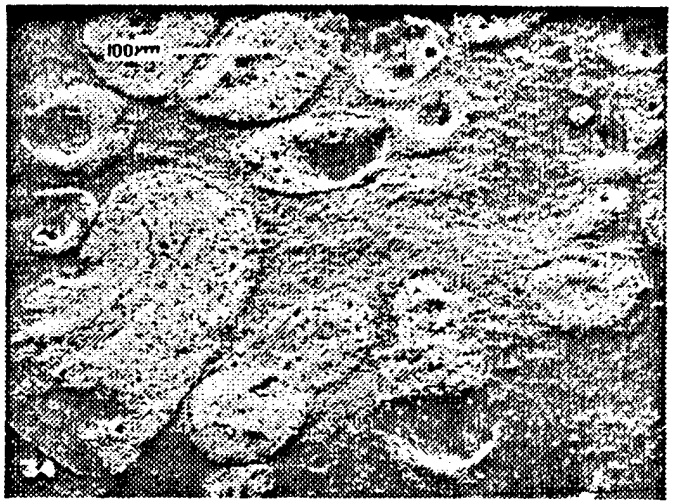

(a) Mix 10

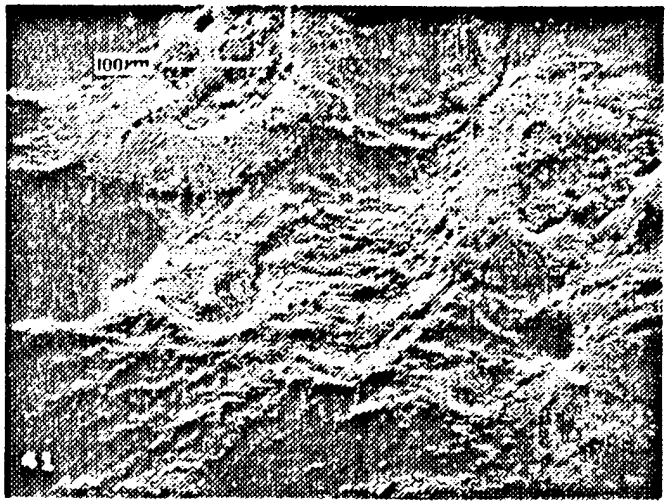

(b) Mix 4

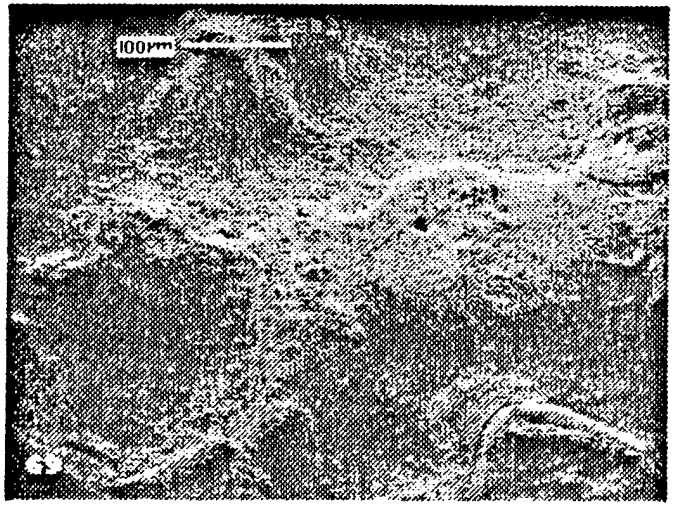

(c) Mix 8

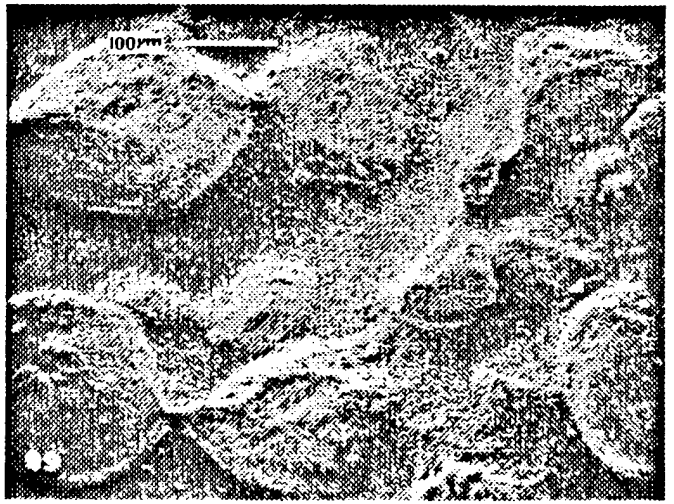

(d) Mix 5

Fig. 7 Features of quenched surface of MURI propellants at 2300 psi (magnification - 200x)

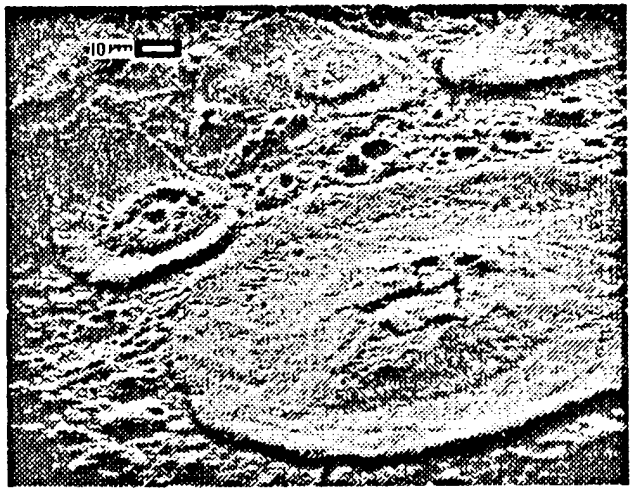

(a) Mix 10

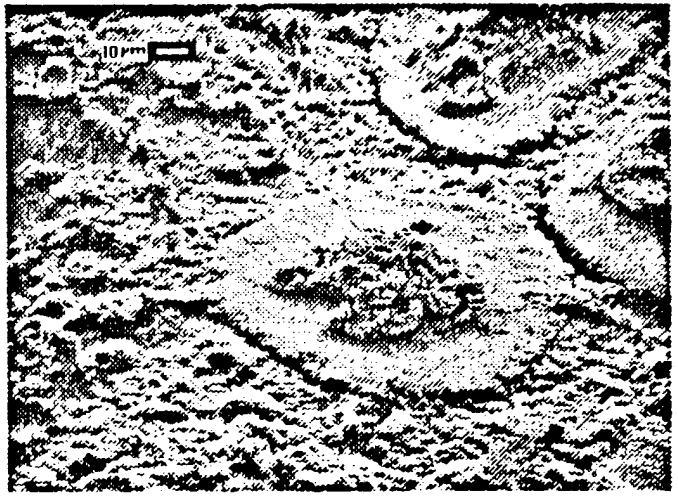

(b) Mix 4

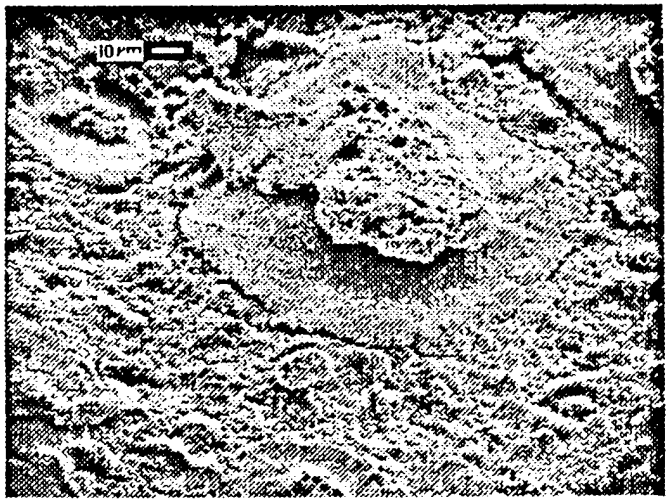

(b) Mix 8

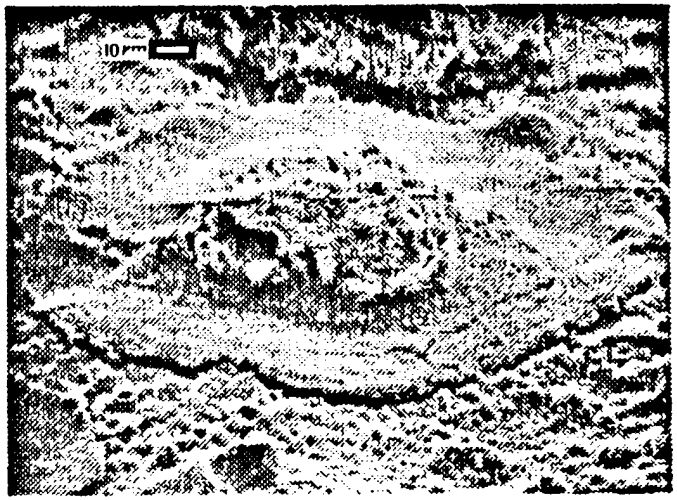

(c) Mix 5

Fig. 8 Features of quenched surface of MURI propellants at 200 psi (magnification - 500x)

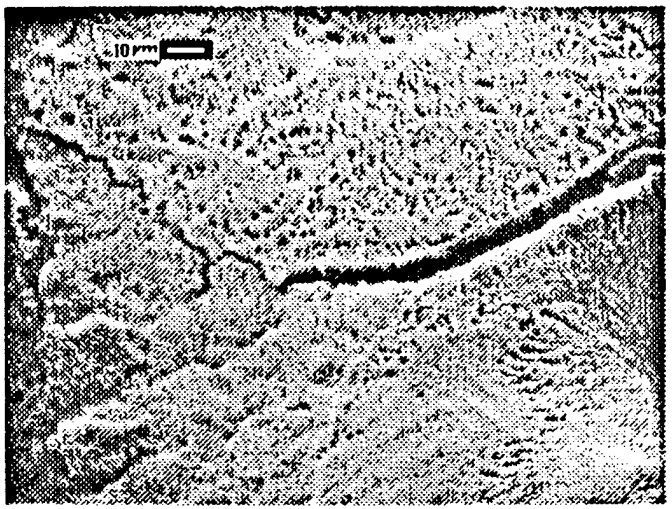

(a) Mix 10

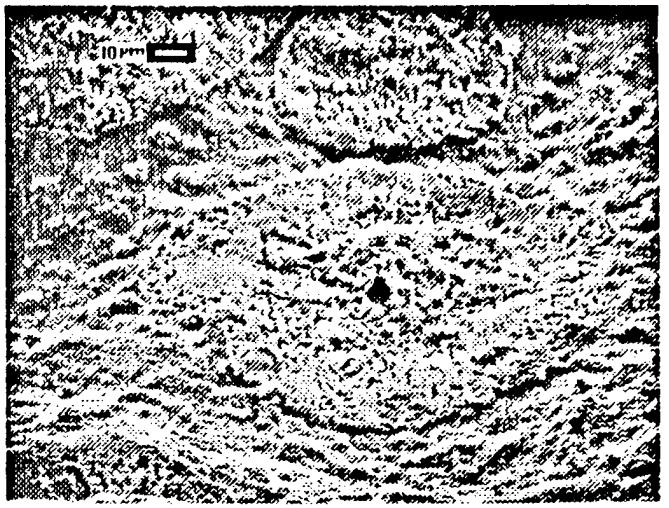

(b) Mix 4

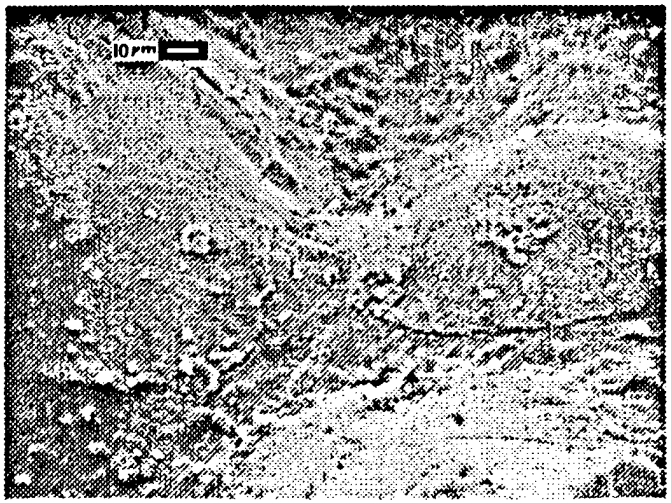

(c) Mix 8

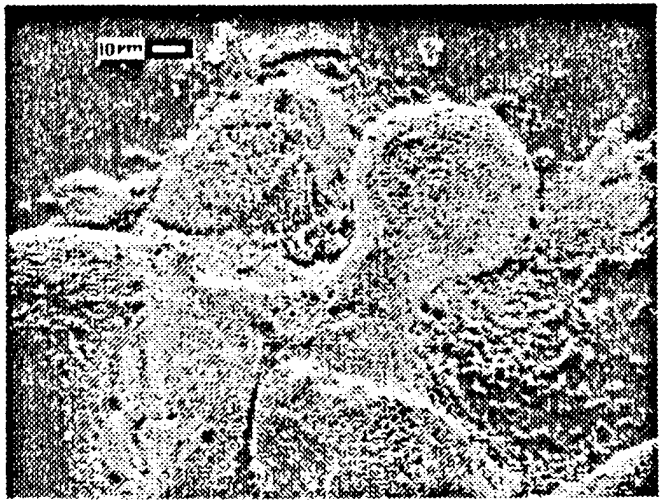

(d) Mix 5

Fig. 9 Features of quenched surface of MURI propellants at 1000 psi (magnification - 500x)

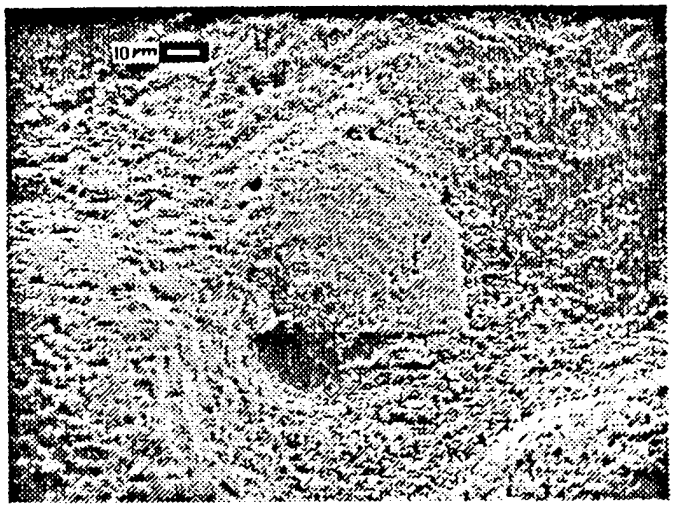

(a) Mix 10

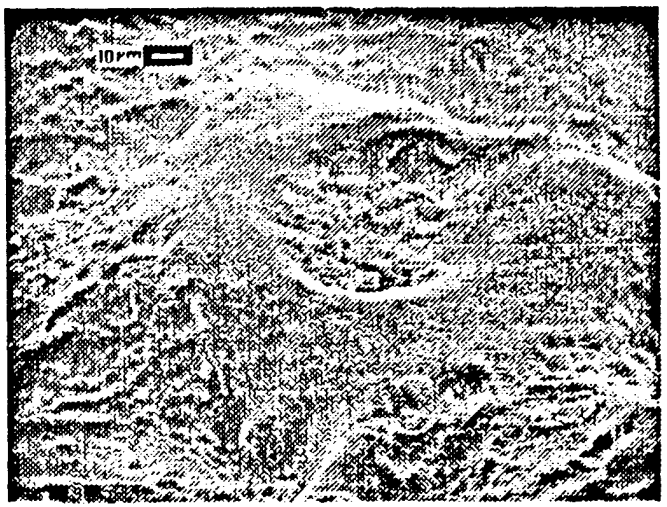

(b) Mix 4

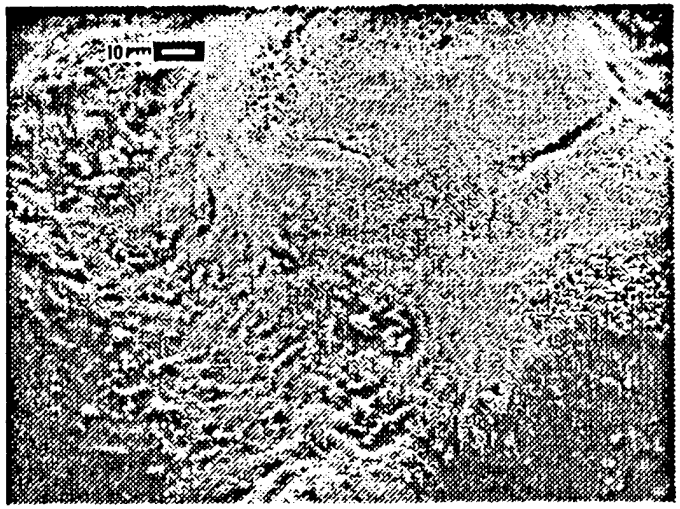

(c) Mix 8

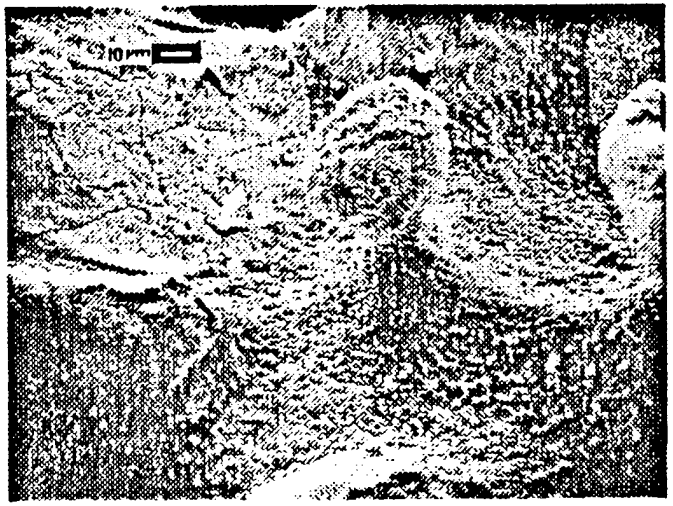

(d) Mix 5

Fig. 10 Features of quenched surface of MURI propellants at 1800 psi (magnification - 500x)

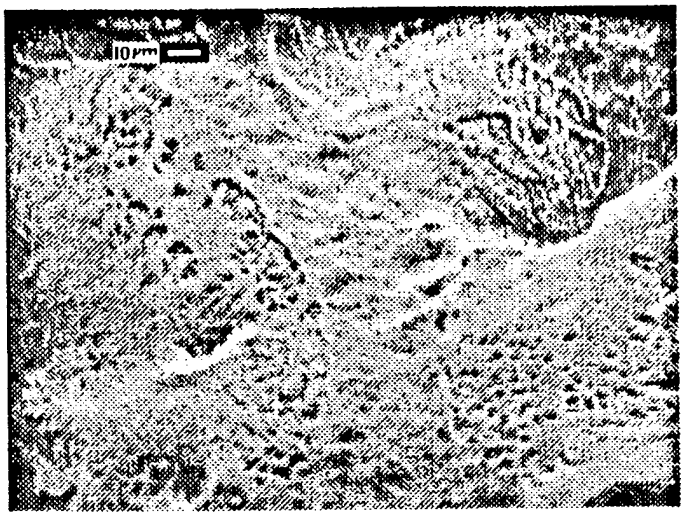

(a) Mix 10

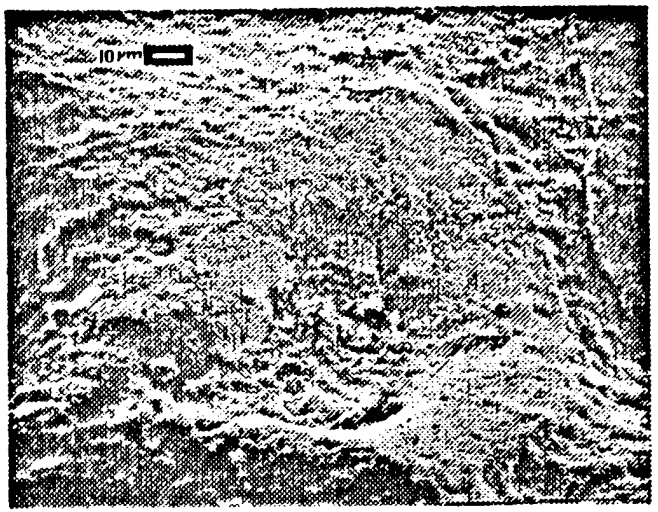

(b) Mix 4

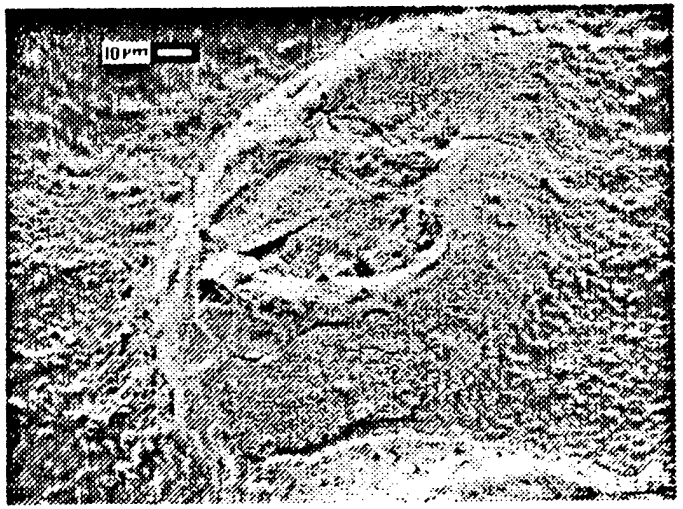

(c) Mix 8

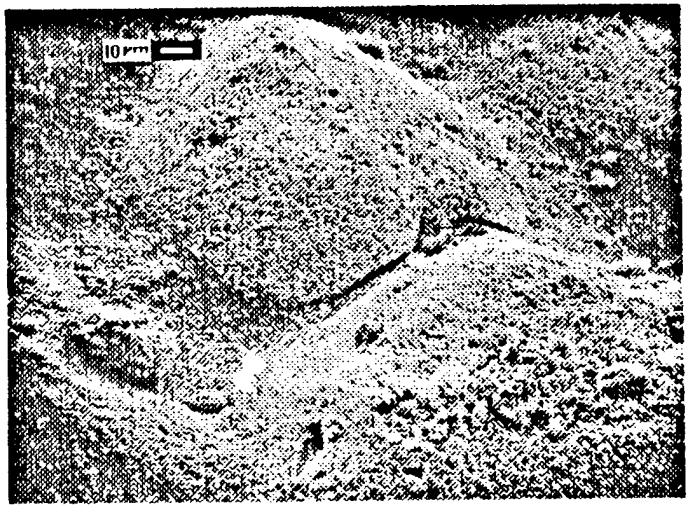

(d) Mix 5

Fig. 11 Features of quenched surface of MURI propellants at 2300 psi (magnification - 500x)

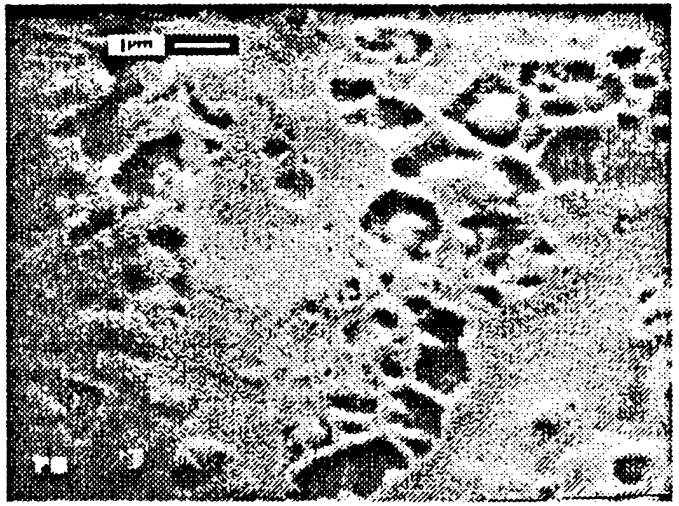

(a) Mix 10

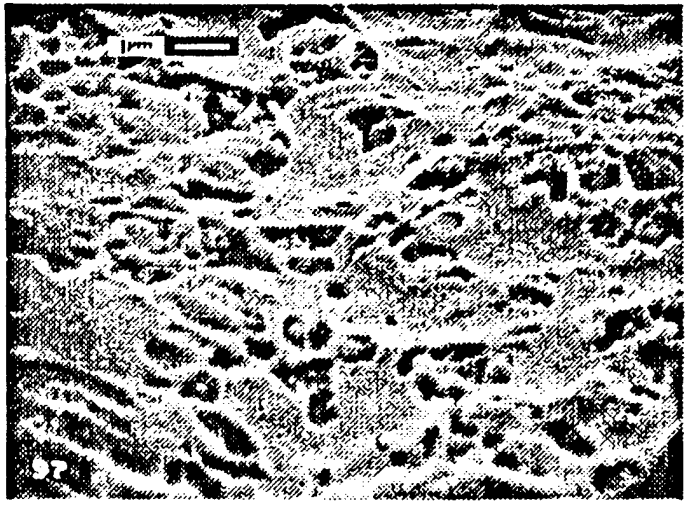

(b) Mix 4

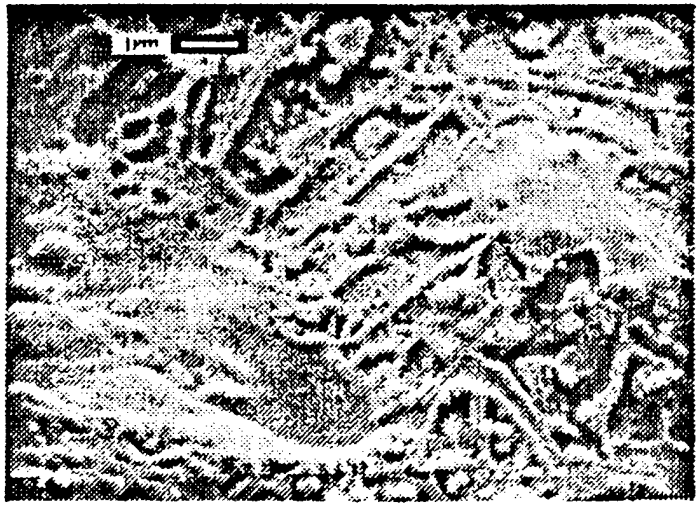

(c) Mix 8

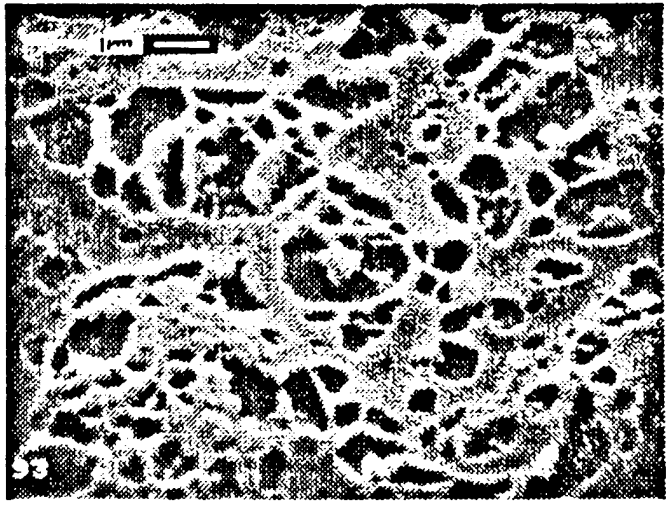

(d) Mix 5

Fig. 12 Features of the matrix surface of MURI propellants quenched at 200 psi (magnification - 10000x)

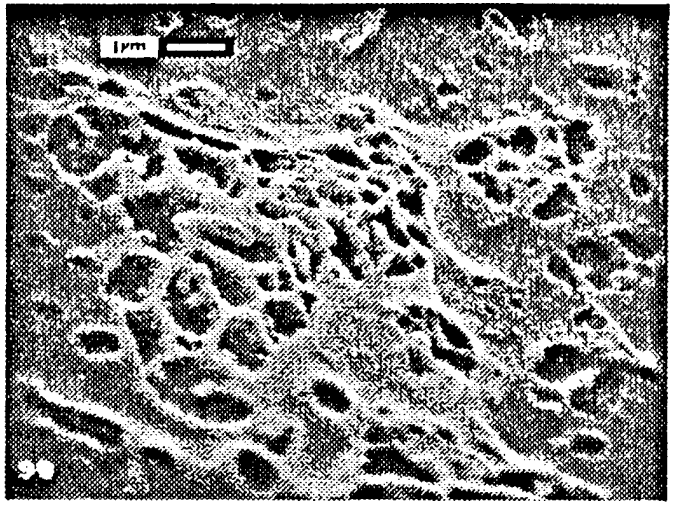

(a) Mix 10

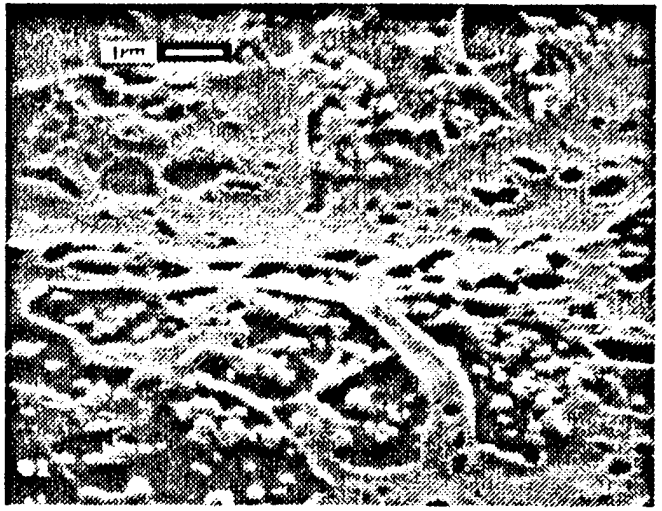

(b) Mix 4

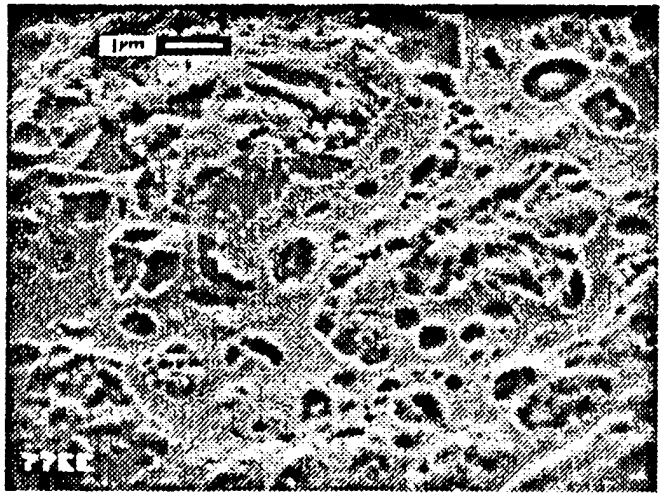

(c) Mix 8

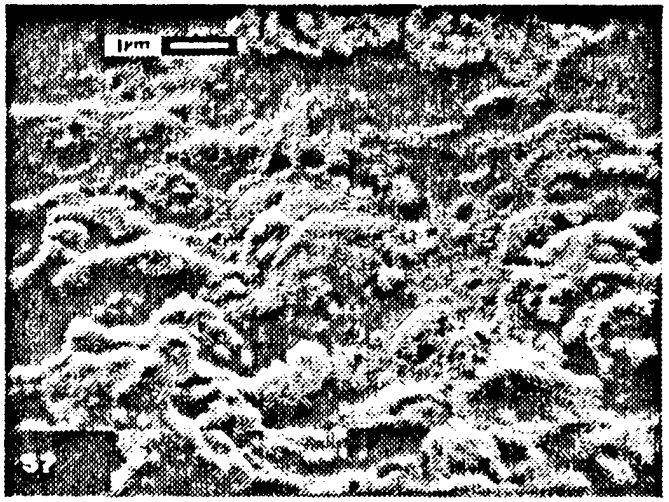

(d) Mix 5

Fig. 13 Features of the matrix surface of MURI propellants quenched at 1000 psi (magnification - 10000x)

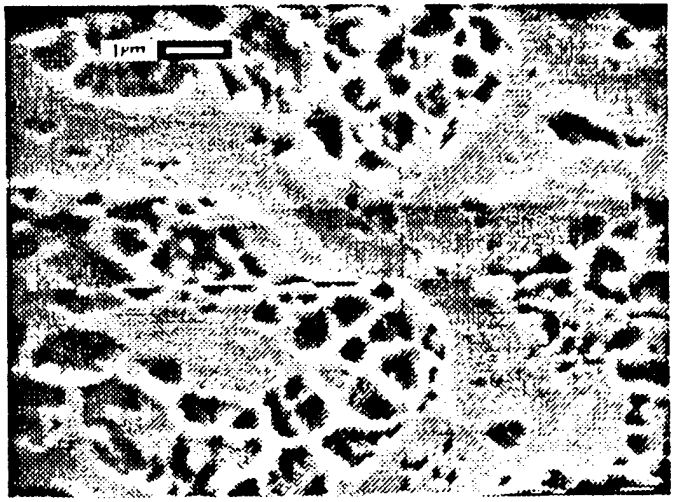

(a) Mix 10

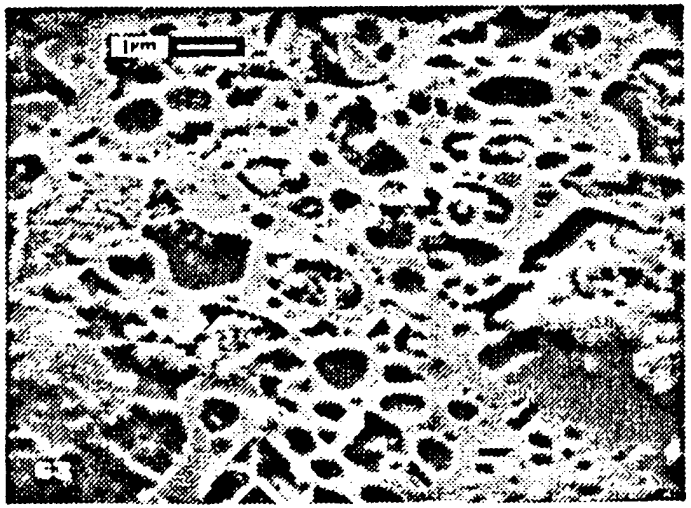

(b) Mix 8

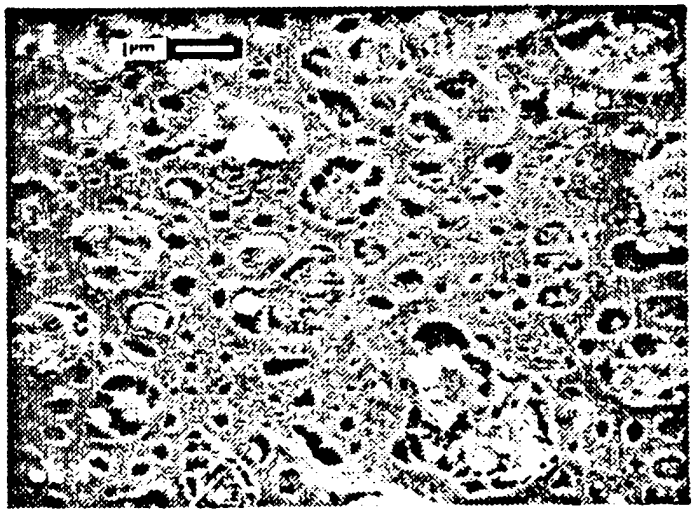

(c) Mix 5

Fig. 14 Features of the matrix surface of MURI propellants quenched at 1800 psi (magnification - 10000x)

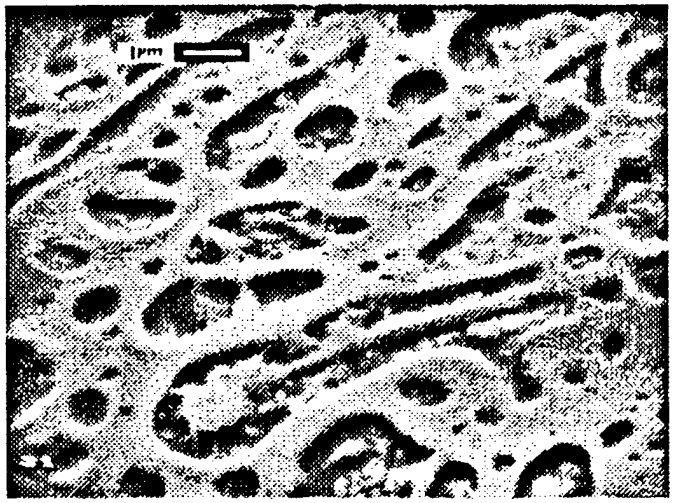

(a) Mix 10

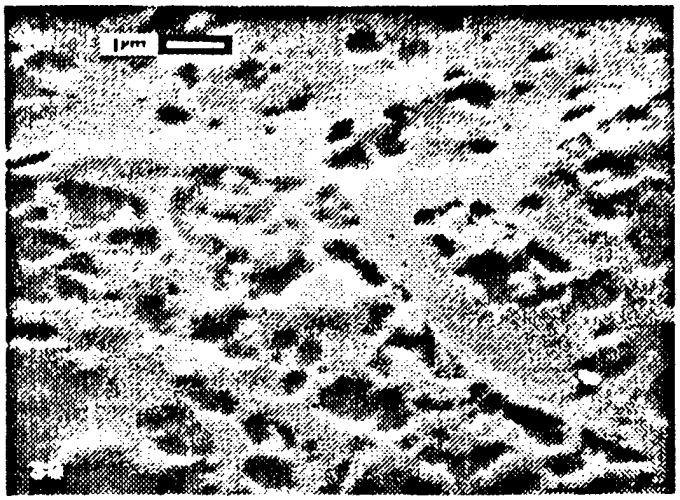

(b) Mix 4

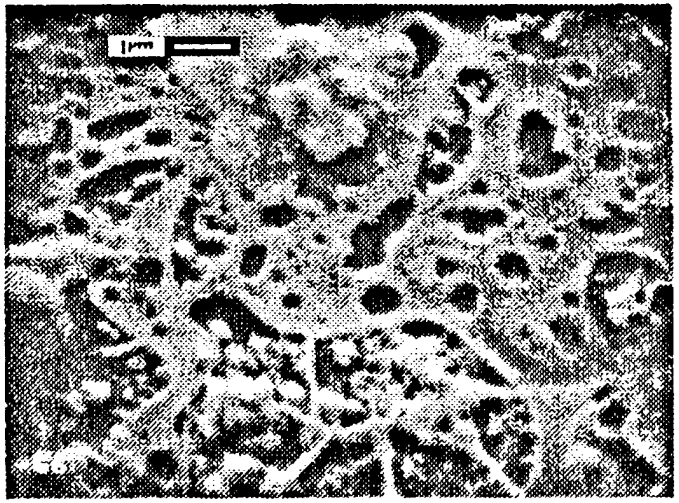

(c) Mix 8

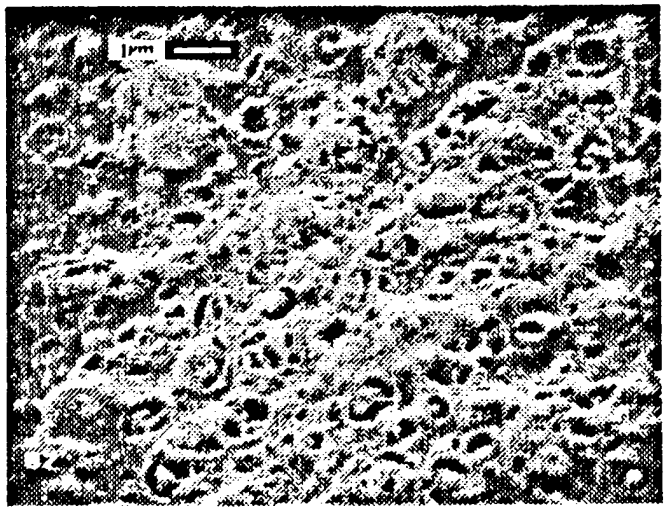

(d) Mix 5

Fig. 15 Features of the matrix surface of MURI propellants quenched at 2300 psi (magnification - 10000x)

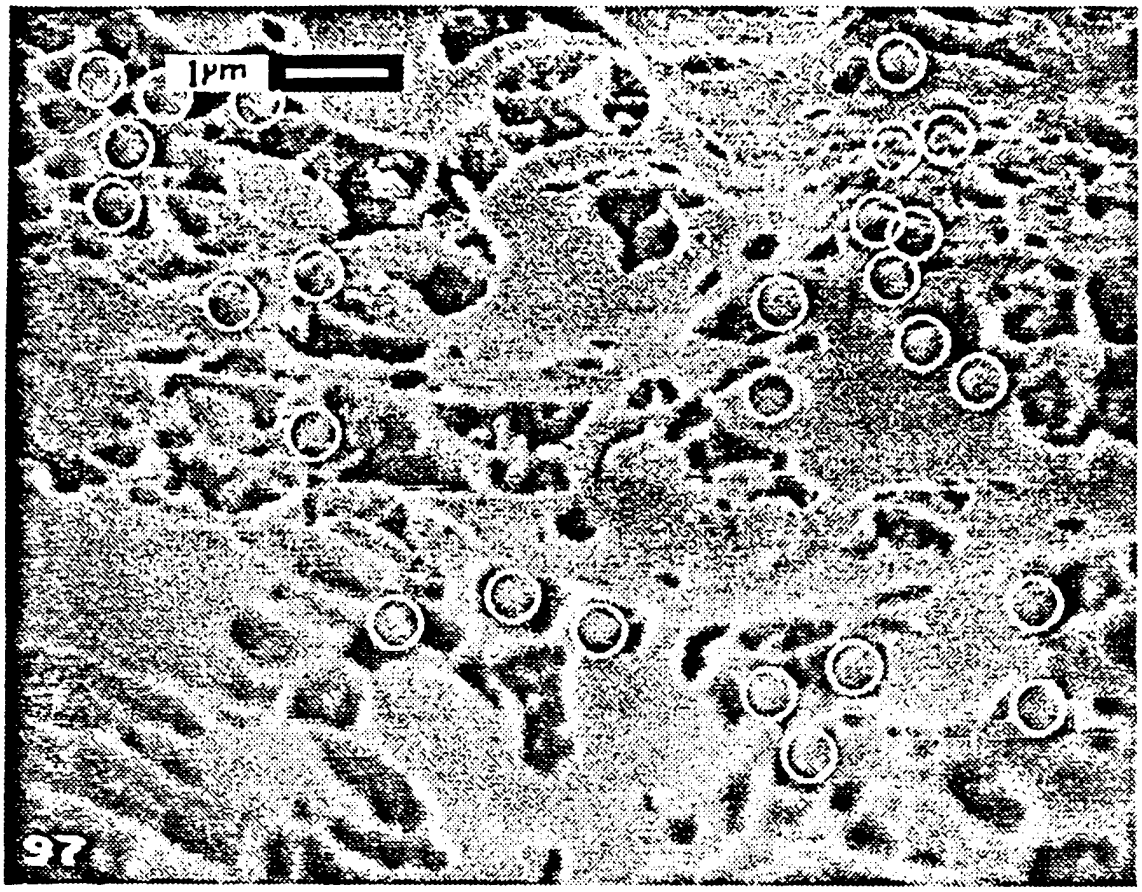

Fig. 16 TiO_2 particles (encircled) on the matrix surface (10000x) of mix 4 propellant quenched at 200 psi (see Fig. 12 b)

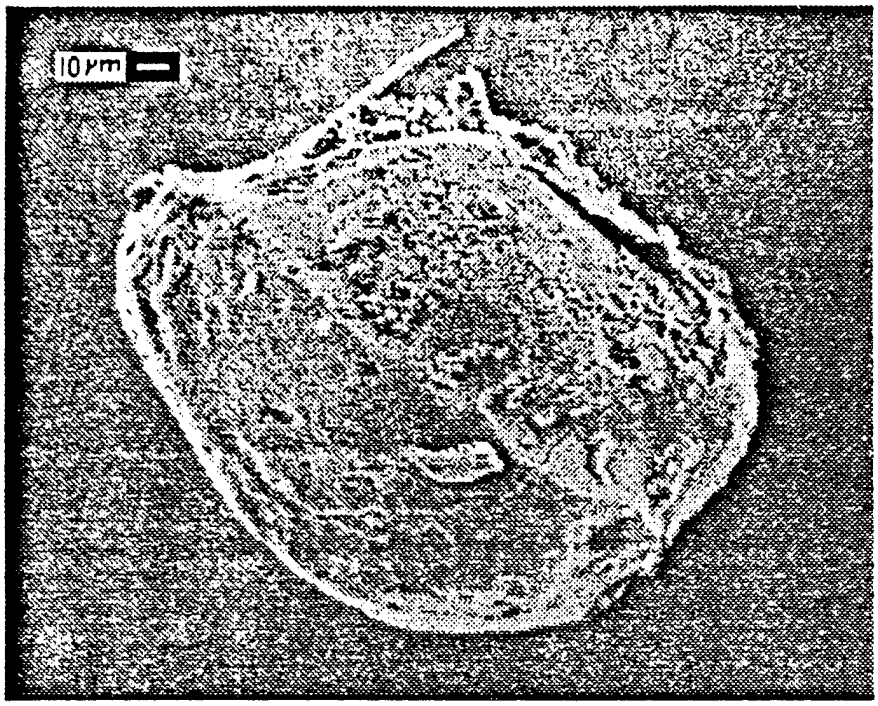

Fig. 17 A partially burned coarse AP particle removed from the surface of mix 8 propellant quenched at 1800 psi.

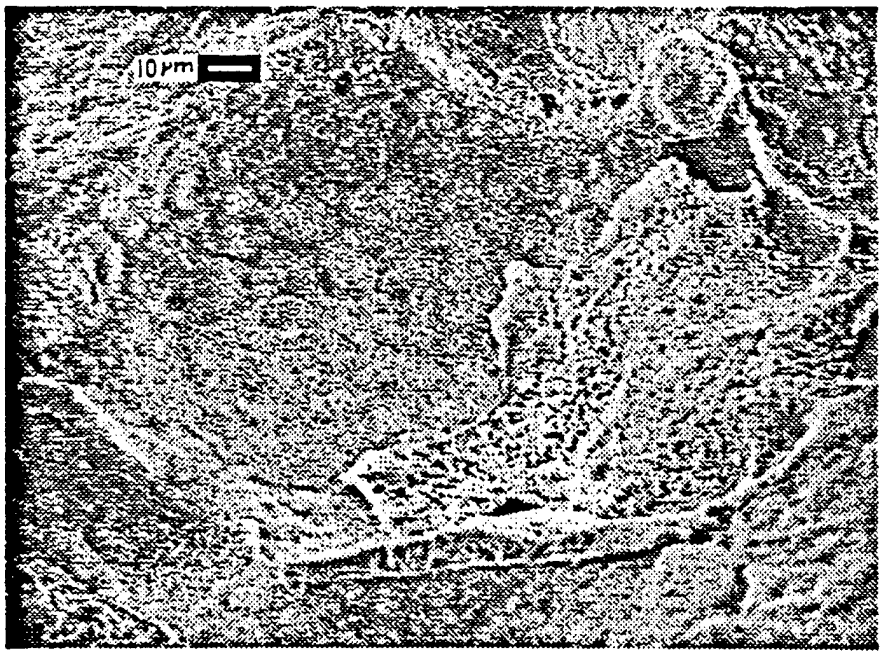

Fig. 18 A depression on the matrix surface (500x) due to the fast burning of a coarse AP particle of mix 10 propellant quenched at 1800 psi (see Fig. 6a).

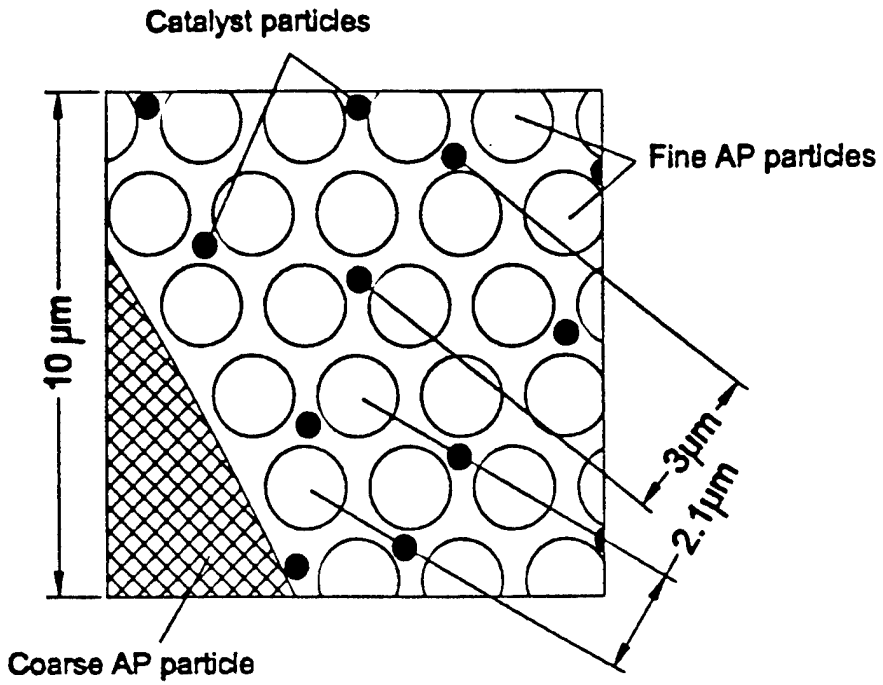

Fig. 19 Distribution of TiO_2 particles on the cut surface of mix 4 propellant

Fig. 20 TiO_2 particles concentrated at the center of a coarse AP particle of mix 4 propellant (quenched at 1000 psi)

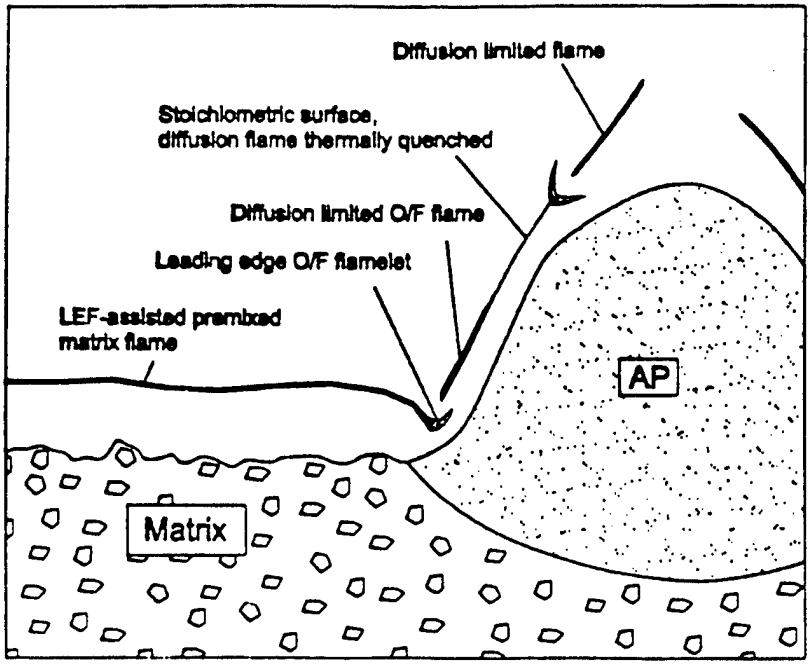

Fig. 21 Configuration of the O/F flame complex at 1800 psi (i.e. typical of mix 8).

APPENDIX Q

Price, E. W., Chakravarthy, S. R., Zachary, E. K., and Sigman, R. K.

"Ingredient Response and Interaction during Heating in a Hot State Microscope"

Proceedings of the 31st JANNAF Combustion Subcommittee Meeting

San Jose, CA, Oct. 1994

INGREDIENT RESPONSE AND INTERACTION DURING HEATING ON A HOT STAGE MICROSCOPE

E. W. Price, S.R Chakravarthy, E.K. Zachary and R. K. Sigman
Georgia Institute of Technology
Atlanta, Georgia

ABSTRACT

This paper consists of a video tape of observations of behavior of propellant ingredients during heating in an optical hot stage microscope.

INTRODUCTION

In our efforts to understand and exploit the controlling processes in the combustion of composite propellants, we have come to realize that very complex processes occur in a very thin layer at the burning surface, involving ingredient melting, flow, interaction and vaporization, possibly with bubbling and froth reactions. In this regard, the melting and decomposition of different ingredients often occur at widely different temperatures, giving rise to very different surface conditions (on the microscale of the propellant heterogeneity). As contrasting examples, a propellant consisting of ADN in a PBAN binder would exhibit subsurface decomposition of oxidizer in the still-solid binder, with the possibility of physical disruption of the binder and jetting of the oxidizer vapor from below the surface. On the other hand, a propellant with very fine AP in a DDI-cured HTPB binder would experience binder melting at 250° C with little or no decomposition of either ingredient until around 480° C. This would give rise to a molten layer filled with AP particles. Since the AP is believed to have a substantially higher surface temperature than the binder under propellant burning conditions, the concentration of fine AP particles in the surface layer of binder melt would have to be higher than in the propellant itself, giving a rather different surface than otherwise expected. This concentration process would be even greater for particulate ingredients that are even more thermally stable, such as aluminum, or Fe_2O_3.

While we don't really know much about the physical state of the surface layer under the high heat flux conditions present in combustion, the possibilities posed by combinations of the many old and new ingredients deserve serious consideration in combustion modeling.

The present study used a hot stage optical microscope to observe the conditions for crystal phase change, melting and decomposition of several binders, oxidizers, and combinations. The results are presented in a 25-minute video tape showing these processes. An audio description is included. Some of the observations are summarized in the table below. Also included are qualitative features of the energetics of decomposition and of oxidizer combustion with a typical hydrocarbon binder (obtained from other sources).

Approved for public release; distribution is unlimited.

* This work was performed under (Contract No. N00014-89-J-1293) with the Office of Naval Research; Dr. R. S. Miller, technical monitor.

[Presented at the 31st JANNAF Combustion Meeting, San Jose, CA, October 1994]

Table 1.

Approximate Comparison of Ingredient Thermal Response and Energetics of Oxidizer/Fuel Flames

Ingredient	Melting Temp. [°C]	Vaporization (Decomposition) Temp. [°C]	Energetics of Decomposition	Energetics of O/F Flame
1. PBAN binder	480	500	Endothermic	--
2. HTPB binder (DDI -cured)	260	500	Endothermic	--
3. NMMO binder	85	200	Mildly exothermic	--
4. AP oxidizer	~ 580*	rapidly above 400	Exothermic	--
5. AN oxidizer	145	245	Endothermic	--
6. KP oxidizer	--	400	Endothermic	--
7. HMX oxidizer	255	290	Exothermic	--
8. ADN oxidizer	90	165	Exothermic	--
9. CL-20 oxidizer	--	270	Exothermic	--
10. Aluminum	673	2493	Very endothermic	--
11. AP/PBAN	--	--	--	Very exothermic
12. AN/PBAN	--	--	--	Exothermic
13. HMX/PBAN	--	--	--	Nearly neutral
14. ADN/PBAN	--	--	--	Very exothermic

* Decomposes before melting except at heating rates > 10^5 °C/s

APPENDIX R

Chakravarthy, S. R., Price, E. W., and Sigman, R. K.

"Mechanism of Burning Rate Enhancement of Composite Soled Propellants by Ferric Oxide"

AIAA Journal of Propulsion and Power

Vol. 13, No. 4, July-Aug 1997, pp. 471-480.

JOURNAL OF PROPULSION AND POWER
Vol. 13, No. 4, July–August 1997

Mechanism of Burning Rate Enhancement of Composite Solid Propellants by Ferric Oxide

Satyanarayanan R. Chakravarthy,* Edward W. Price,† and Robert K. Sigman‡
Georgia Institute of Technology, Atlanta, Georgia 30332-0150

This paper reports a series of experimental studies performed on sandwich propellants, wherein a matrix lamina of particulate oxidizer and polymeric binder is sandwiched between two ammonium perchlorate (AP) laminae. The catalyst (ferric oxide) is incorporated in the matrix lamina. The variables are pressure (0.345–6.9 MPa), matrix lamina thickness, catalyst concentration, matrix mixture ratio, types of oxidizer and binder, and the dispersion ability of the catalyst. The combined results indicate that, under the conditions tested, near-surface reactions associated with the particulate AP/binder contact lines on the burning surface assume significance in the presence of the catalyst. These reactions are further augmented by the presence of the leading-edge portion of the diffusion flame above the interface of the matrix and AP laminae.

I. Introduction

THE burning rates of ammonium perchlorate (AP) composite solid rocket propellants are routinely adjusted by the addition of small amounts of ballistic modifiers to the propellant formulation. For increasing the burning rate, the most common catalyst is iron oxide (IO, Fe_2O_3). The rate-controlling steps in the combustion of composite propellants have been debated for 40 years, and the mode of action of ballistic modifiers remains uncertain because of the remaining debate about the rate controlling steps.

Kishore and Sunitha[1] have made a nearly comprehensive survey of the literature on burning rate catalysis spanning roughly two decades up to the late 1970s. They observe that a wide variety of sites and mechanisms of action of the catalysts are proposed by the numerous studies. Subsequent studies, steadily decreasing in number, have done little to alleviate this situation.

The diverse and fragmentary nature of the literature pertaining to the problem makes it difficult to summarize the different viewpoints presented therein. Reported studies include effects of catalysts on the combustion and thermal decomposition of AP, condensed mixtures, model propellants, and regular propellants. Although this study is concerned mainly with the effect of iron oxide (IO), it seems natural to consider it as part of a broader class of transition metal oxides from a chemical point of view, and, hence, studies with other such additives cannot be ignored.

Proposed mechanisms include 1) physical effect of IO accumulated on the surface getting heated up from the flame and aiding binder regression by direct contact[2]; 2) effect on binder melt flow behavior, physically or chemically[3]; 3) catalysis of binder thermal degradation at the urethane linkages in the condensed phase at low pressures (2–7 MPa)[4,5]; 4) enhanced near-surface breakdown of heavy fuel molecules,[6–10] better with finer AP particles,[9] supplying more reactive fuel species to the O/F flame,[6,7] thereby bringing it closer to the surface and increasing the burning rate[6,7,11]; 5) action in the gas phase by a) modification of gas phase reactions by chloride derivatives of the catalyst,[9] b) exothermic breakdown of the catalyst by reactions with other species,[11] c) catalysis of the O/F flame,[12,13] and/ or d) catalysis of $HClO_4$ decomposition[14] (heterogeneous surface reactions not excluded[10]); 6) heterogeneous gas phase exothermic reactions between catalyst particles and $HClO_4$ (Ref. 15); 7) gas phase and/or heterogeneous reactions in crevices between fuel and AP[12]; 8) catalysis of some process in the vicinity of the AP/binder interface[16]; 9) catalysis of AP deflagration,[12,17] or decomposition[13] (by proton transfer[10] or electron transfer[18]); 10) action in the condensed phase: a) at the AP/binder interfacial surfaces,[8,9,19] b) by altering the decomposition products of AP and binder,[10,11] or c) by catalyzing $HClO_4$ decomposition, the products of which eventually enhance binder degradation,[20] or by catalyzing the oxidative polymer degradation by $HClO_4$ (Ref. 21); and 11) formation of thermally unstable metal perchlorates[10,18] or metal perchlorate amines.[22]

In spite of the diverse views on the problem, some general impressions are gained and are noteworthy. It appears that copper chromite (CC) and IO are most effective among the class of transition metal oxide additives.[1,6,7] CC acts better on AP,[17] whereas IO acts better when both AP and binder are involved.[12,16,21] CC is a better catalyst at high pressure, and IO at low pressure.[19]

Many investigators have proposed multiple mechanisms. In some cases, the results do not allow resolution among these mechanisms, and in some others, the investigators believe that a single mechanism cannot exclusively account for the net catalytic effect.[1] Many of these investigations have been carried out under various conditions that are not directly related to rocket operating conditions, and as such, their inferences are restricted in applicability to specific domains of propellant burning. It would be desirable to delineate domains of test conditions (pressure, particle size, etc.), in which the different mechanisms predominate over the others in controlling the burning rate of the propellant.

The present study is part of a larger investigation on the combustion mechanisms of solid propellants using the sandwich-burning method. This method provides relative ease of preparation and variation of test samples, and observation and characterization of the combustion behavior. This method also provides a rich background of previous studies for comparison with new results. Earlier results are available for sandwiches of AP-binder–AP laminae, in which the binder lamina consisted of 1) pure binder,[23] 2) catalyzed binder,[6,7,24] and 3) particulate AP-filled binder.[25,26] The present study concerns combustion with various iron catalysts and oxidizers (primarily Fe_2O_3 and AP) in the binder lamina.

Received Feb. 20, 1996; revision received Feb. 19, 1997; accepted for publication April 8, 1997. Copyright © 1997 by the American Institute of Aeronautics and Astronautics, Inc. All rights reserved.

*Post Doctoral Fellow, School of Aerospace Engineering.
†Regents' Professor Emeritus, School of Aerospace Engineering. Fellow AIAA.
‡Senior Research Engineer, School of Aerospace Engineering.

Considering the complex nature of the problem, the goal of this study would be accomplished if evidence were obtained that indicated the possible sites of predominant action of the Fe_2O_3 for the given initial geometry of ingredients. Attempts at resolving the exact chemistry are beyond the scope of this work, although plausible mechanisms may be proposed.

II. Background

Sandwiches with AP-filled binder laminae can be thought of as a two-dimensionalized simulation of the microscopic region included by adjacent coarse AP particles in a typical propellant with bimodal AP size distribution.

In the case of pure binder sandwiches, the leading edges of the oxidizer/fuel (O/F) diffusion flames (LEFs) are the sites of major near-surface heat release[12,16,27,28] and, hence, behave as rate controlling.[13,23,29] For thin nonmelting binder lamina, e.g., polybutadiene acrylonitrile acrylic acid (PBAN), the LEFs are multidimensionally coupled (in terms of heat feedback to the surface), and this is reflected in a maximum in the burning rate at a binder lamina thickness ~50–75 μm (Fig. 1). When ferric oxide is present in the binder lamina,[6,7,24] it accumulates on the binder surface, facilitating breakdown of heavy fuel molecules into lighter, more reactive species. This enables the LEFs to be located closer to the surface, resulting in an increase in the burning rate.

The mechanics of AP-filled sandwiches have been elucidated in detail recently.[25–27] It is briefly revisited here to establish some terminology used in this study, and also to serve as a comparison with the situation when the catalyst is present. With AP-filled binder laminae, the previous LEFs are designated as lamina leading-edge flames (LLEFs), to distinguish them from smaller LEFs that could exist above the fine AP particles, particle leading-edge flames (PLEFs), in the AP/binder matrix lamina. The mutual interaction of the LLEFs again results in a peak in the burning rate vs lamina thickness curve, but at a matrix lamina thickness ~225–275 μm (Fig. 1). The larger thickness is because of the diluting effect of the AP particles; but they do not act as just a diluent:

1) The matrix is less fuel rich than the pure binder, and, hence, the stoichiometric surface above the lamina interface shifts inward.

2) The lateral extent of the fuel side of the LLEFs is increased.

3) The total heat release in the LLEFs is increased, enabling the flame to stand closer to the surface.

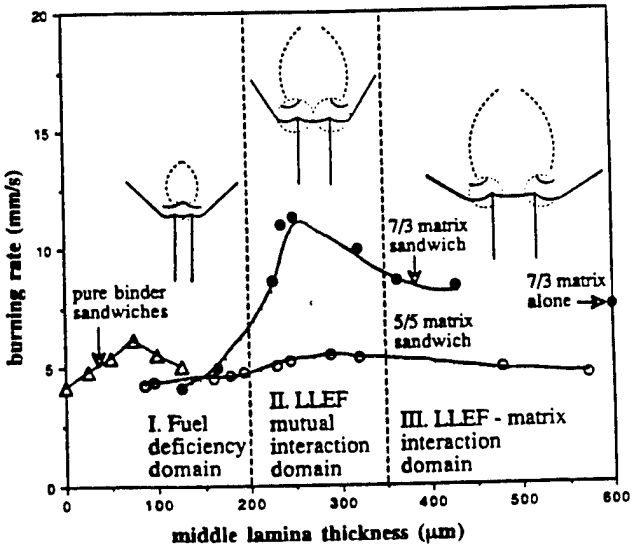

Fig. 1 Typical dependence of uncatalyzed sandwich burning behavior on matrix lamina thickness for pure PBAN binder, and AP/PBAN matrix.

These effects are favorable for direct heating of the matrix lamina, and so condensed phase lateral heat transfer from the AP lamina across the lamina interface plane is reduced. This is reflected in 1) reduced width of the smooth band[23] on the AP surface adjoining the lamina interface and 2) reduced extent of AP retardation in that region. When the matrix mixture is adequately less fuel rich, so that the premixing matrix gases can sustain combustion (as in AP/PBAN = 7/3), and when the thermal wave thickness >> fine AP particle size (small particles, low pressure), a premixed canopy flame exists above the matrix lamina, connecting the fuel-rich sides of the LLEFs; when the thermal wave thickness ~ fine AP particle size (large particles, high pressure), LEFs are attached to the individual fine particles, resulting in PLEFs.

The matrix flame does not control the rate, but augments the mutual interaction of the LLEFs (Fig. 1).[27] For large matrix thickness, the LLEFs are uncoupled, but the rate is still slightly higher than that of the matrix alone. This indicates a domain of LLEF-matrix interaction, where the interaction between a single LLEF and processes associated with the matrix (either in the gas phase, condensed phase, or heterogeneous) are rate controlling. It will be seen in this paper that this domain assumes importance in the presence of the catalyst.

III. Experimental

A. Experimental Techniques

Three principal techniques were employed in this study: 1) combustion videography, 2) examination of quenched samples in the scanning electron microscope (SEM), and 3) hot-stage (optical) microscopy (HSM) of ingredients. These techniques are rather routine and are detailed elsewhere.[24,25] Besides serving as a tool for macroscopic flame structure and surface profile studies, the video pictures were also used for burning rate measurements. Flame front positions in successive frames (typically 10–40 points, more for lower rates) were fitted with a straight line in the least-square sense, with a correlation $\geq$99.9%. The slope of this line gave the burning rate. Approximately 50% of the data points, selected at random, were checked by repeated tests for reproducibility within 5% variation. In the combustion experiments, the samples were coated with a very thin layer of high vacuum grease to inhibit burning down the sides, and were burned in a nitrogen atmosphere. The heating rate in the hot-stage experiments was ~3°C/s, and they were performed at atmospheric pressure in an argon atmosphere.

B. Samples

Fabrication of sandwiches is also detailed elsewhere.[25] The catalyst was thoroughly mixed in the binder first, before adding the oxidizer particles. All of the ingredients for the matrix were weighed within an error of 0.5%. The position of the samples in the oven was inverted periodically during the curing period to prevent the oxidizer particles in the matrix from settling on to one side of the sandwich as a result of gravity. Different size levels of AP particles were used, with appropriate designations: the 2-μm AP was a mixture of AP particles of that size and hydroxyl-terminated polybutadiene (HTPB) prepolymer; the 10-μm AP is from the same batch as used in previous studies[26]; the 33-μm AP and 75-μm AP are those that remained between sieves of mesh sizes 37 and 30 μm, and 90 and 75 μm, respectively. The particle sizes of ammonium dinitramide (ADN), hexanitro hexaazaisowurtzitane (HNIW), and cyclotetramethylene tetranitramine (HMX) were nominally 40, 10, and 10 μm, respectively. The potassium perchlorate (KP) nominal size was about 30 μm. No attempt was made to quantitatively characterize the size distributions of these oxidizer particles beyond ascertaining on the optical and/or SEM that samples of these ingredients did not contain particles of significantly different sizes than just specified. It is considered that such a qualitative approach is sufficient for the purposes of this study. The form of availability of the 2-μm AP restricted it to be used with HTPB-based binders only, and

Table 1 Binder compositions

No.	Binder	Prepolymer, %	Plasticizer, % (DOA)	Curing agent Type	Curing agent Amount, %
1	PBAN	64.14	15.00	ECA	20.86
2	HTPB-DDI	69.07	16.77	DDI	14.16
3	HTPB-IPDI	75.73	18.39	IPDI	5.88

up to a common maximum ratio of AP/binder = 65/35 with the different curing agents. Three different binder types were employed, and their compositions are given in Table 1. Throughout the text, the designations HTPB–IPDI and HTPB–DDI are used to denote HTPB cured by isophorone diisocyanate (IPDI) and dimeryl diisocyanate (DDI), respectively. 1–2 μl of a cure catalyst, dibutyl tin dilaurate (T-12) was usually added to 5 g of a HTPB-based matrix mixture. This enabled curing of HTPB samples in a day, instead of a week. [T-12 acts on diisocyanate curing agents and could not be used with PBAN/ECA (epoxy curing agent) binder.] The addition of T-12 does not seem to significantly alter the physical behavior of HTPB binder, as observed on the hot stage. The Fe_2O_3 used in this study, unless stated otherwise, is called Pyrocat (manufacturer's specifications: Nanocat™ SFIO catalyst, lot 3–1-125, α-type, particle size 0.003 μm, specific surface area 270 m^2/g, density 0.05 g/cc).

IV. Results

This section is a listing of results with detailed specifications of the test conditions. The implications of the results are discussed in Sec. V.

A. Effects of Matrix Lamina Thickness, Catalyst Concentration, and Matrix Mixture Ratio

Figure 2 shows the dependence of the sandwich burning rate on matrix lamina thickness for 0.2 and 1% Pyrocat in a matrix of AP/PBAN = 7/3 (Fig. 2a) and AP/PBAN = 5/5 (Fig. 2b) at 2.1, 3.5, and 6.9 MPa. The 10-μm AP was used in these tests. The burning rate vs matrix thickness trend for the corresponding uncatalyzed sandwiches (taken from Ref. 25) are presented for comparison. In general, the scatter in the data is slightly-to-considerably more when the catalyst is present; more at the 1% level than at the 0.2% level, and more for a mixture ratio of 5/5 than for 7/3. The AP/PBAN = 5/5, 1% Pyrocat sandwich data are highly scattered, but do not indicate any conspicuous dependence of the burning rate on the matrix lamina thickness. The scatter is not unexpected because the 5/5 mixture is in the region of flammability limits; the uncatalyzed 5/5 matrix alone does not sustain combustion, whereas the catalyzed ones barely burn, at very low rates. However, the following broad features are noted:

1) The 0.2 and 1% catalyzed AP-filled sandwich burning rates are several times higher (≥100%) than corresponding uncatalyzed sandwich rates, compared to a relatively marginal (~30%) increase in the burning rate of pure PBAN binder sandwiches with 10% catalyst.[24] (The corresponding curves are not shown for comparison in Fig. 2 in the interest of clarity.)

2) The 5/5 matrix alone begins to sustain combustion in the presence of as low a catalyst level as 0.2%, and the 7/3 matrix displays a major increase in the burning rate when catalyzed.

3) The catalyzed 5/5 matrix rates are very low, and the samples burn in a smoldering fashion, without a conspicuous visible flame; the pressure dependence of their burning rates is very weak.

4) The burning rates of the catalyzed 5/5 sandwiches are several times higher than their corresponding matrix rates. On the other hand, the 7/3 sandwiches burn only slightly faster than their corresponding matrices.

5) It must be remembered that no matter how high the catalyzed sandwich rates are, they should logically tend to the

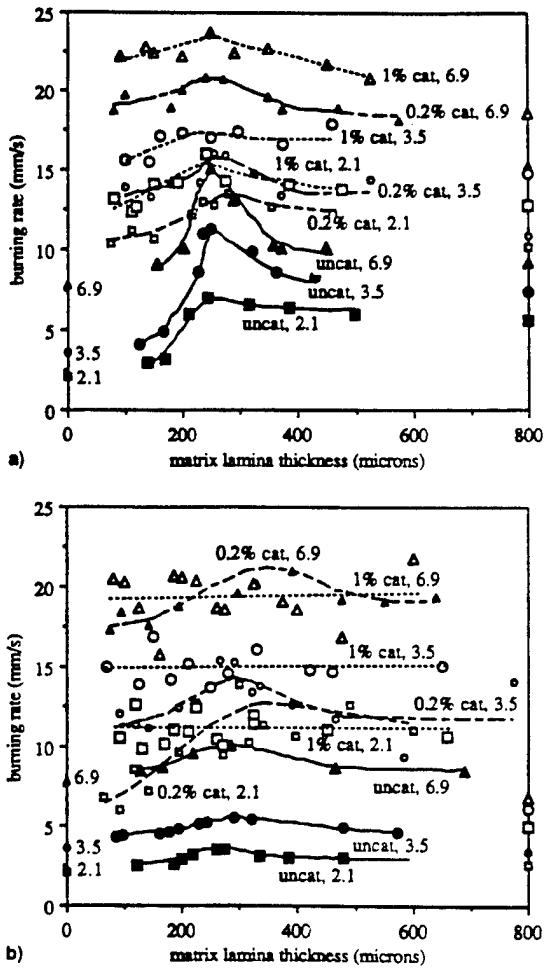

Fig. 2 Dependence of burning rate on matrix lamina thickness for uncatalyzed and catalyzed AP-filled sandwiches at different pressure levels (noted in MPa). Burning rates of pressed AP are shown on the left ordinate, and those of matrix burning alone on the right ordinate lines. AP/PBAN = a) 7/3 matrix and b) 5/5 matrix.

AP rate shown on the left ordinate line in Figs. 2a and 2b, in the limit of zero matrix lamina thickness. (This cannot be effectively tested because AP-filled sandwiches with very thin matrix laminae cannot be fabricated practically.) The curves show that even a thin lamina of matrix is sufficient for major catalytic action; it is greater for higher AP loading and catalyst concentration in the matrix.

6) The effect of catalyst concentration (0.2 vs 1%) is slight in the case of the 7/3 samples and the 5/5 matrix; it is nearly negligible for the 5/5 sandwiches, except perhaps in the thin matrix lamina limit. Weak dependence of catalytic effect on the catalyst concentration is also reported in the literature.[4,9,15]

7) Except for the case of the 5/5, 0.2% catalyst sandwiches in the thin matrix lamina limit again, and the dependence of sandwich burning rates on the matrix lamina thickness is weakened in the presence of the catalyst.

B. Surface Profile and Features

Sandwiches of the type in item Sec. IV.A in the previous text were quenched by rapid depressurization while burning, and their quenched surfaces were examined in the SEM. The matrix and the lamina AP in the immediate vicinity of the lamina interface burn down so fast, compared to the outer region of the AP laminae, that the surface profile assumes an almost V shape. This makes SEM observations difficult. No remarkable differences are seen between the various quenched samples in an overall sense. A typical quenched surface is

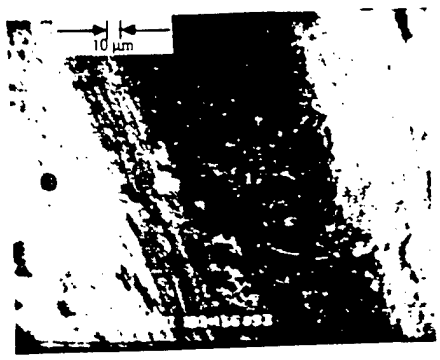

Fig. 3 Quenched surface of a typical catalyzed AP-filled sandwich: ❶ matrix surface, ❷ dry band in the AP lamina, ❸ frothy surface of the AP lamina (not in focus).

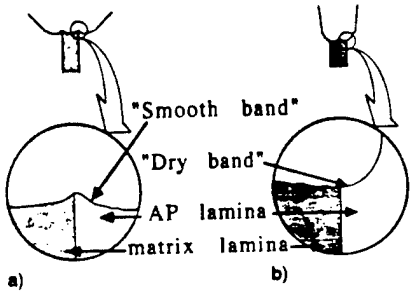

Fig. 4 Typical burning surface profile for AP-filled PBAN sandwiches: a) uncatalyzed and b) catalyzed by Pyrocat.

presented in Fig. 3. Figure 4 shows a typical sketch of the surface profile of these sandwiches in comparison to that of the uncatalyzed case. The following features are noted:

1) There is no retardation in the regression of the AP lamina in the immediate vicinity of the lamina interface in the case of catalyzed sandwiches, as against such a protrusion in uncatalyzed sandwiches.[26] The AP lamina surface in that region has a curvature that is concave upward.

2) The AP surface in the immediate vicinity of the interface has a dry and parched appearance (dry band), as against a smooth and soft surface region (smooth band) in the uncatalyzed sandwiches. The dry bandwidth is much smaller than the corresponding smooth bandwidth.

3) Accumulation of catalyst particles can be observed as sporadic thin white filigrees (size $\gg$ catalyst particle size), randomly distributed on the surface of the matrix lamina. The extent of accumulation is lower at the 0.2% catalyst level when compared to the 1% level. Considering the high oxidizer loading, low catalyst content, very fine size of the catalyst, and the fact that the catalyst is in the binder, accumulation of the catalyst cannot be expected to be as high as in earlier work, with sandwiches having 10% IO in pure binder lamina.[6,7,24] Catalyst accumulation in propellants is also reported in the literature.[2,6]

C. Combustion Videography of Very Thick Sandwiches

Video pictures of burning of sandwiches with 10-μm AP/PBAN = 7/3 and 5/5, 1% Pyrocat matrices of lamina thickness > 1000 μm (much larger than typical values) were taken. Figure 5 shows frames from such video pictures for the two mixture ratios. The pictures show some protrusion of the matrix lamina for the 5/5 matrix (Fig. 5a), whereas no such protrusion is found in the case of the 7/3 matrix (Fig. 5b). The burning rates of these sandwiches agree very well with the burning rates of sandwiches in the thick limit of matrix lamina shown in Fig. 2.

D. Effect of Oxidizer Type

Five different oxidizers, AP, KP, ADN, HNIW, and HMX, were tested in conjunction with PBAN (oxidizer/PBAN = 7/3), with and without 1% Pyrocat. Attempts to study ammonium nitrate (AN) did not succeed because of the lack of

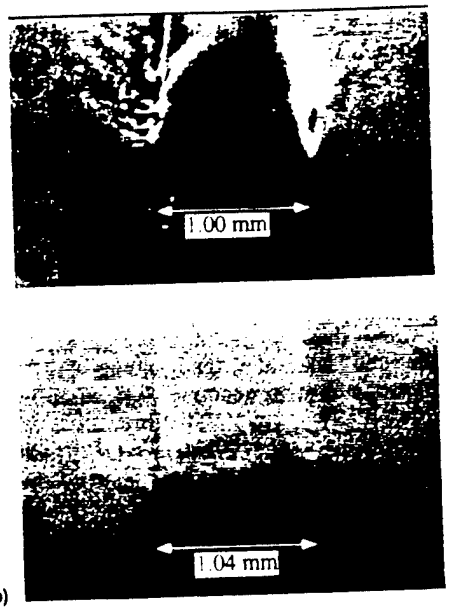

Fig. 5 Video pictures of the combustion of sandwiches with a very thick lamina of 10-μm AP/PBAN, 1% Pyrocat matrix at 3.5 MPa. AP/PBAN = a) 5/5 and b) 7/3.

proper wetting properties between that oxidizer and PBAN. In all cases, the oxidizer/PBAN matrix was sandwiched between two AP laminae.

The rationale behind sandwiching these matrices by AP laminae is to see how the matrix burning responds to the presence of a pair of LLEFs. Ideally, it would be desirable to test sandwiches with the same oxidizer in the matrix and oxidizer laminae, but this could not be done because 1) some of the materials (notably ADN and HNIW) were available only in very small quantities, and 2) safety concerns about pressing pellets of these materials persist. However, the matrix lamina thickness in all of these sandwiches was designed to be ~375–400 μm, to be out in the LLEF–matrix interaction domain rather than the LLEF mutual interaction domain (see Fig. 1).

It was difficult to obtain these different oxidizer particles in the same size range. Also, the particle size effects of these oxidizers are either unknown or mostly different from each other. In any case, the available supplies seem to fall into two size ranges: 10–20 μm for HMX and HNIW, and 30–40 μm for KP and ADN. For effective comparison, the 10-μm AP was used in connection with the first range, and the 33-μm AP was used for the second range.

The ratios of the burning rates of catalyzed and uncatalyzed samples (both sandwiches and matrices) are shown in Fig. 6. This parameter helps reduce the number of curves by half, but inevitably conceals the actual burning rate information. However, it would suffice for the present purpose to note that the burning rates of all samples at a given pressure are comparable on an order of magnitude basis (1.5–8 mm/s at 0.69 MPa; 9–25 mm/s at 6.9 MPa), except HMX matrices, which are lower by one order at every pressure level (0.6 mm/s at 0.69 MPa; 2 mm/s at 6.9 MPa). It is seen clearly from Fig. 6 that the burning rate increase is markedly the highest for AP ($\geq$100%), with the curves corresponding to the other oxidizers lying around a burning rate ratio of unity or slightly more (marginal catalytic effect). Tests on propellants with different oxidizers found in the literature also support the choice of AP for maximum catalysis.[14,15]

E. Effect of Susceptibility of the Binder to Melt Flow

The susceptibility of HTPB binders to melt before vaporization is significantly altered by the choice of different diisocyanate curing agents, which in turn is different from that of PBAN cured by ECA. Aspects related to binder melt flow,

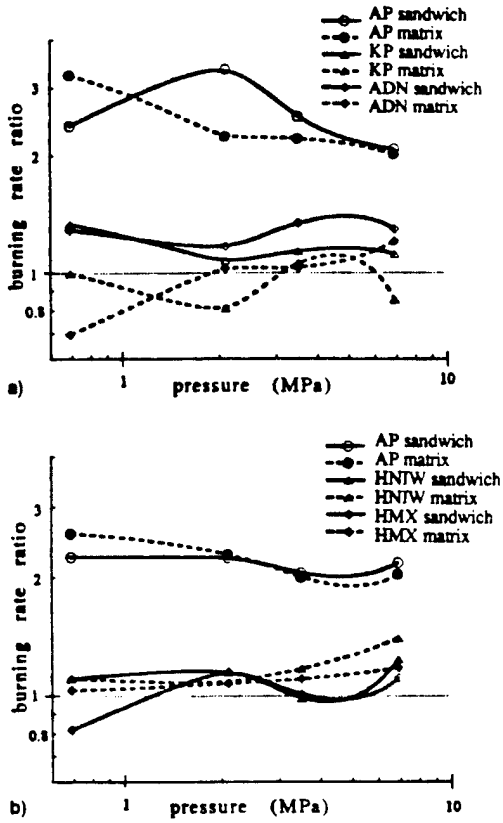

Fig. 6 Ratio of burning rate of catalyzed to uncatalyzed samples with oxidizer-filled PBAN matrices (oxidizer/PBAN = 7/3) in two oxidizer particle size categories: a) 30–40 and b) 10–15 μm.

such as plateau burning behavior of propellants, are addressed in detail in a separate paper.[30] It would suffice here to point out that, as observed in the hot-stage microscope, PBAN melts above 450°C, HTPB–IPDI melts slowly between 300–360°C, whereas HTPB–DDI melts rather abruptly at 230°C. All of these binders vaporize vigorously at 500°C, a value not too different from the decomposition temperature of AP. The hot-stage microscope experiments,[31] and various other combustion tests with pure binder as well as AP-filled sandwiches, have indicated that a qualitative order of increasing susceptibility for melt flow of the binders considered in this work is PBAN < HTPB–IPDI < HTPB–DDI. It should be recorded here that the addition of Pyrocat to the HTPB samples seems to retard the curing process, and advances the onset of melting (conspicuously noticeable in HTPB–DDI) to a lower temperature. The implications of this has been reported in the literature.[4,5,32]

Tests on sandwiches and matrices with and without 1% Pyrocat in a mixture of these binders and the 10-μm AP in the ratio AP/binder = 7/3 resulted in Fig. 7. The sandwiches have a matrix lamina thickness of ~250–275 μm, corresponding to maximum burning rates in Fig. 2. Figure 7a shows burning rates vs pressure for the uncatalyzed samples. In the case of PBAN, the sandwich and matrix curves are more or less parallel to each other. The HTPB–IPDI matrix curve exhibits a plateau in the pressure range 0.7–2 MPa, an effect suspected to be caused by the binder melt flow. The corresponding sandwich burning rate increases steadily with pressure in the entire pressure range tested. The HTPB–DDI matrix does not sustain combustion in the entire pressure range tested; however, it tends to burn, but self-quenches soon after ignition in the low-pressure range 0.35–0.7 MPa. The corresponding sandwich burning rate increases in that pressure range, but subsequently falls back to the AP rate at higher pressures. Above 2.1 MPa, when the AP begins to self-deflagrate, the AP laminae lead the sandwich burning surface (as can also be seen in the video pictures).

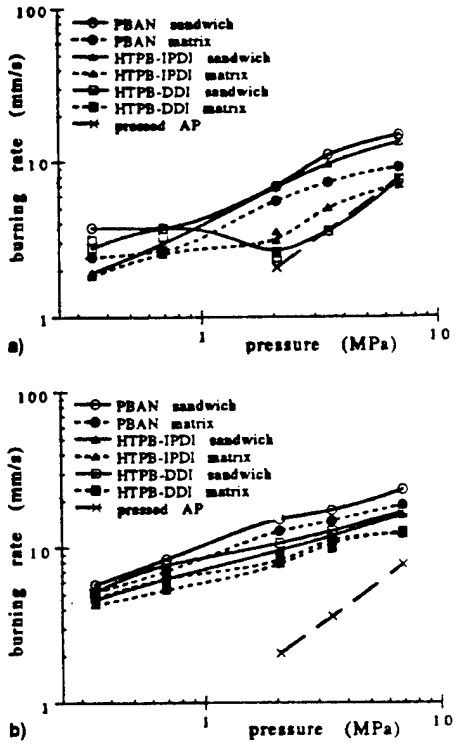

Fig. 7 Effect of binder melt flow characteristics on the burning rate of sandwiches and matrices of 10-μm AP/binder = 7/3: a) uncatalyzed and b) catalyzed by 1% Pyrocat.

Figure 7b shows the burning-rate curves for the catalyzed samples. The overall rates for all of the binders are substantially higher than for their corresponding uncatalyzed samples. Also, in all of the cases, the corresponding matrix and sandwich curves are almost parallel to each other. In fact, the differences in the curves for HTPB–IPDI and HTPB–DDI are slight. The PBAN rates are slightly higher than those of the HTPB-based samples. The effects caused by binder melt flow witnessed in the uncatalyzed situation are considerably washed out when the catalyst is present.

F. Effect of AP Particle Size

This subsection reports a systematic variation of the size of fine AP particles in a wide range of sizes (approaching different orders of magnitude). Three ranges of AP size were employed: the 2, 10, and the 75-μm AP. Since the 2-μm AP was available only with HTPB, and in a mixture ratio of AP/binder = 65/35, for reasons explained earlier, all of the other test samples in this subsection also conform to these stipulations. The HTPB is cured with IPDI, which has reduced melt flow effects compared to DDI, the other diisocyanate curing agent studied in this work. 1% Pyrocat was used in the catalyzed samples. The matrix lamina thickness in the sandwiches is again ~250–275 μm, as in Sec. IV.E. The burning rates for matrix and sandwich are shown separately in Figs. 8a and 8b for the sake of clarity.

The uncatalyzed 2-μm AP matrix does not burn in the entire pressure range tested. Other uncatalyzed matrices burn only in the pressure ranges indicated in Fig. 8a. Note that the particle size effect on the uncatalyzed matrix is the reverse of the conventional trend of increasing burning rate with decreasing particle size. The 2- and 10-μm AP uncatalyzed sandwiches exhibit a mesa in the 1.04–3.5 MPa range, and a plateau in the 3.5–6.9 MPa range, and higher (not shown here), respectively (Fig. 8b). The uncatalyzed 75-μm AP sandwich curve also exhibits a relatively low exponent in the midpressure range (0.69–2.1 MPa). Such effects, explained as related to the relative length scales of lateral binder melt flow and fine AP particle size in the matrix,[30] are smeared by the presence of

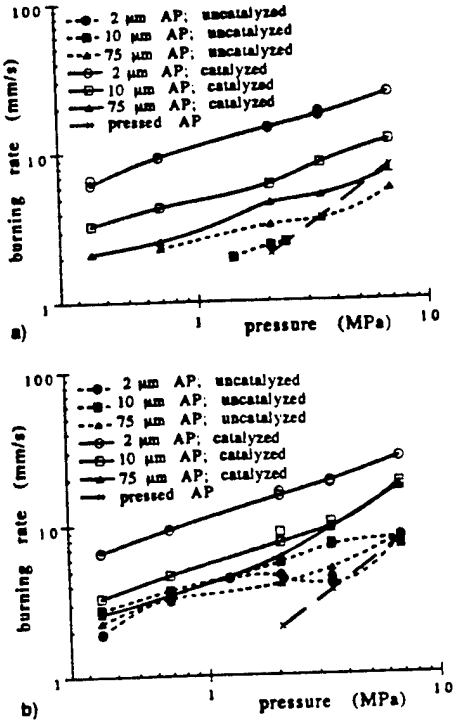

Fig. 8 Effect of fine AP particle size on the catalytic effect of 1% Pyrocat on samples with a matrix of AP/HTPB-IPDI = 65/35: a) matrix and b) sandwich burning rates.

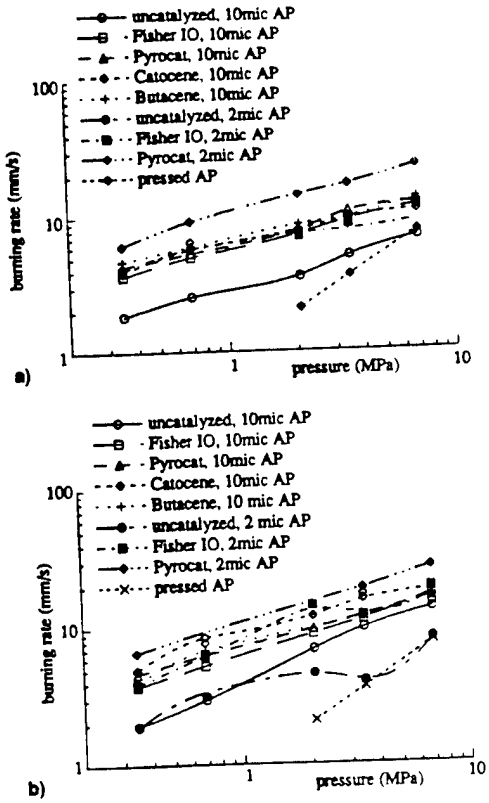

Fig. 9 Effect of dispersion ability of iron catalysts on the burning rate catalysis of AP/HTPB-IPDI samples: a) matrix and b) sandwich.

the catalyst. As for the effect of AP particle size on the catalysis, the 2-μm AP samples clearly register the highest catalytic effect, followed by the 10- and 75-μm AP samples. The effect is clearer in matrices than in sandwiches; the differences in the particle-size dependence of the catalytic effect in the sandwiches is diminished, particularly between that of the 10- and 75-μm AP sandwiches and at higher pressures. Similar AP particle size effects on catalysis are also reported in the literature.[9] Also, the conventional trend of increasing burning rate with decreasing particle size is restored in the presence of the catalyst.[7]

G. Effect of Dispersibility of the Catalyst

Four different iron-containing catalysts were chosen to investigate the effect of the degree and scale of dispersion of the catalyst in the binder: 1) Fisher Fe_2O_3, particle size ~1 μm (larger than Pyrocat); 2) Pyrocat; 3) Catocene, a liquid catalyst; and 4) Butacene®, a specialty resin, produced by SNPE, France, in which a ferrocenic silane group is grafted to the backbone of the HTPB molecule.[32]

1. *HSM Observations*

Both Fisher and Pyrocat IO are rust colored and turn black at ~200°C; no further changes are observed up to ~900°C. Catocene vaporizes at ~360°C, leaving a fine bed of black particulate residue. Butacene (uncured) vaporizes between 470–500°C, just as HTPB prepolymer would, leaving a residue similar to that left by Catocene. A blend of HTPB:Butacene = 62:38 cured by IPDI behaves similarly to HTPB binder without Butacene; it slowly melts at ~300–360°C, and boils at 480–500°C, but leaves a residue characteristic of uncured Butacene, as opposed to no significant residue for HTPB with no catalyst.[31]

2. *Burning Rate Measurements*

Two sets of tests were performed. In the first set, all the four iron catalysts were used in combination with 10-μm AP in the matrix. The IO particulate catalysts were added at the 1% level, and 2% Catocene was used as in typical rocket propellants, twice as much Catocene is generally used as the amount of IO to roughly equalize the iron content[24] (the exact equivalent amount is slightly more than 2% in an AP/binder = 7/3 mixture). Butacene has an average iron content of approximately 7.8% by weight. A blend of HTPB:Butacene = 62:38 was used to obtain an iron content that is equivalent to the other catalyzed mixtures. For the sake of compatibility with the Butacene tests, HTPB was chosen as binder in the other tests where the catalyst was externally added. Again, IPDI was chosen as the curative to have reduced binder melt flow effects. The matrix is a mixture of 10-μm AP and HTPB–IPDI in the ratio of 7/3. Matrix lamina thickness in all sandwiches is ~250–275 μm, corresponding to maximum burning rates in Fig. 2, as in Secs. IV.E and IV.F.

The results are presented as part of Figs. 9a and 9b, as matrix and sandwich burning rates vs pressure, respectively. The sandwich rates are always slightly higher than the corresponding matrix rates, except for the Butacene samples at 0.345 MPa. Curves for the different catalysts are clustered in the case of matrix (similar results are reported in the literature[2,11]), and slightly spread out in the case of sandwich rates. In either case, the arrangement of the curves does not directly correlate to the extent of dispersion of the catalyst in the binder.

The second set of tests is on a smaller scale. Here, the Fisher IO was used at the 1% level in combination with the 2-μm AP in a matrix of AP/HTPB–IPDI = 65/35. The remaining parameters are the same as in the first case. This situation corresponds to comparable orders of magnitude for the particle sizes of the catalyst and the oxidizer. These results are also shown in Fig. 9. The Fisher IO matrix burns in the entire pressure range 0.345–6.9 MPa, in contrast to no deflagration by the uncatalyzed 2-μm AP matrix. The Fisher IO sandwich rates have a greater overall burning rate, but preserve the mesa exhibited by the corresponding uncatalyzed sandwich burning rate curve; this is in contrast with washout of plateau and mesa behavior with the addition of Pyrocat. In both the matrix and

sandwich, the burning rates of the Fisher IO samples are significantly lower than those of Pyrocat samples at all of the pressures tested, registering a definite effect of the dispersibility of the catalyst when in combination with the 2-μm AP.

3. SEM Observations

Sandwiches, in Sec. IV.G.2, were quenched while burning by rapid depressurization, and the quenched surfaces were examined in the SEM. The relevant pictures are not presented here in the interests of economy of space, and because they are not too different from Fig. 3. In all of the cases, accumulation of the catalyst on the surface is evident. Qualitatively, the extent of accumulation varies from dense but sporadic clusters in the case of Fisher IO, to a more uniform web of thin filigrees in the case of Butacene. The overall matrix surface does not indicate any undulations at the locations of these clusters. Even in the case of the Fisher IO, the dense clusters are smaller than the fine AP particle size, so that any such undulations in the surface caused by them are smaller in length scale than those caused by the AP particles and, therefore, may go unnoticed.

V. Discussion

A. Perspective Based on Previous Studies

Earlier studies in the present project involved tests on sandwiches with outer AP laminae and either pure binder,[23] catalyzed binder,[6,7,24] or AP-filled binder[25,26] as the middle laminae. In these studies it was concluded that the exothermic reactions that controlled the sandwich burning rate were in the gas phase flames (LEFs), and that high burning rate resulted from close proximity of those flames to the burning surface. In the case of sandwiches with catalyzed binder, it was concluded that the catalyst acted at the binder surface by the breakdown of heavy fuel molecules into more reactive species, but that the dominant rate enhancement resulted from greater proximity of the O/F flames to the surface because of the more reactive fuel species. In the case of sandwiches with fine AP added to the binder, it was recognized that the contact area of AP and binder in the solid was enormously increased, posing the possibility of a significant increase in heat release in condensed phase, interfacial, and heterogeneous surface reactions, if any. However, the results suggested that gas phase flames (LLEFs and PLEFs/canopy premixed flames) still controlled the burning rate. In the present study, a catalyst was added to the AP-filled binder, providing greater opportunities for exothermic reactions associated with the greater proximity of the catalyst to O/F interfaces, oxidizer, and all vapors at the surface.

B. Opportunity for Catalytic Action at Different Sites in the Combustion Zone and Its Implications

When discussing the mechanism of catalytic enhancement of the burning rate in the present case, it is important to remember several physical aspects of the test samples and propellants in general, aspects often overlooked in past studies on burning rate catalysis. Items 1–5, shown next, roughly pertain to the condensed phase, items 6–10 pertain to the surface layer, and items 11 and 12 pertain to the gas phase of the propellant combustion zone (Fig. 10).

1) The catalyst is present in test samples only in the binder, poorly situated to directly catalyze the oxidizer in the condensed phase.

2) The catalyst has the opportunity to affect the oxidizer in the condensed phase only at the oxidizer/binder interfacial surfaces.

3) The catalyst may be able to directly act on the binder in the condensed phase within the thermal wave.

4) Catalytic action in the condensed phase, on the binder, and/or at the interfacial surfaces, might a) be exothermic, b) accelerate the condensed phase decomposition of the ingredients, and/or c) alter the decomposition vapors, probably into a more reactive species. As for item a, catalytic action on conventional hydrocarbon binders is expected not to be exothermic, but catalyzed interfacial surface reactions might be. Exothermicity in the condensed phase is effective in terms of heat feedback and rate enhancement. An additional implication of such a mechanism is a relatively higher catalytic effectiveness at low pressures, and vice versa.[33] Item b would merely allow the surface of the ingredient that pyrolyzes faster to be recessed more,[34] without considerably affecting the burning rate. Item c is a potential mechanism because it would facilitate the gas phase flames being held closer to the burning surface, and thereby increase the burning rate.

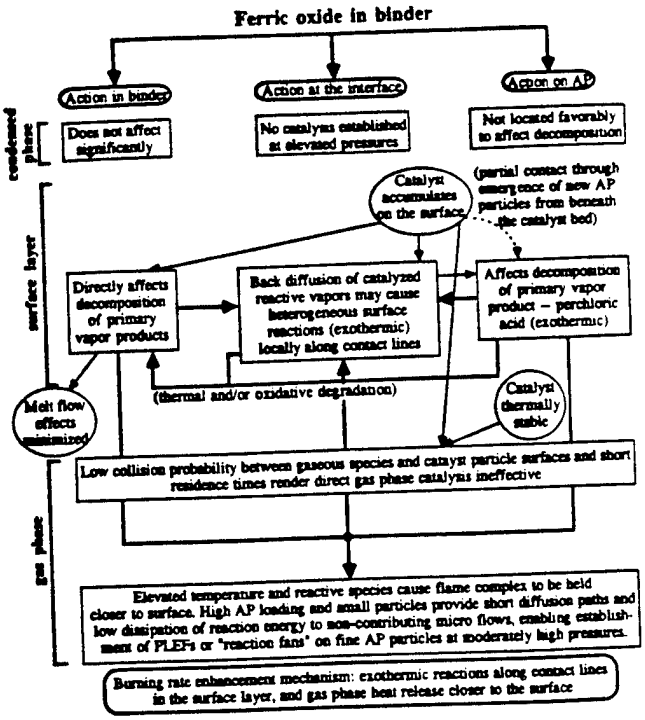

Fig. 10 Overview schematic of the mechanistic arguments for the action of ferric oxide in the combustion of AP composite propellants.

5) In considering factors that influence the burning rate, it is important not only to note sites of exothermic heat release, but also regions (usually) adjacent to those sites that are receptors of heat, but not contributors to local heat release. With fine oxidizer particles, the increase in the interfacial area facilitates enhanced thermal diffusion between oxidizer particles and adjacent binder layers, so that the heat generated at interfacial surfaces can be readily distributed uniformly into parts of the solid that do not directly participate in the local exothermic reactions.

6) The catalyst has been observed in the past,[2,6] and the present studies to concentrate on the binder surface, providing an enhanced opportunity for the breakdown of primary fuel decomposition products into more reactive vapor species.

7) With very small oxidizer particle size, the catalyst concentration may be encountered by some of the primary oxidizer vapors, raising the possibility of a catalyzed near-surface breakdown of some of those primary oxidizer product vapors. With AP oxidizer, it is quite likely that the catalyzed decomposition of $HClO_4$ is accompanied by exothermic heat release,[10] and more reactive oxidizer species.

8) With a very fine oxidizer, the diffusion distances for heterogeneous surface reactions are short, i.e., all oxidizer vapor is near fuel surfaces, and all fuel vapor is near oxidizer surfaces, increasing the possible role of vapor–surface O/F reactions. The presence of the catalyst can further enhance such reactions.

9) Besides the possibility noted in item 8, the opportunity exists for catalytic decomposition vapors of fuel and oxidizer to undergo gas phase (exothermic) reactions in the mixing region along the oxidizer/binder contact lines while diffusing to each other's surfaces.

10) Remarks about thermal diffusion in the solid made in item 5 are also pertinent to near-surface and heterogeneous reactions noted in items 6–9.

11) Fe_2O_3 is thermally stable up to ~1000°C (Ref. 9). Therefore, it would remain in condensed form in most of the combustion zone, except possibly as it enters the gas phase flame. Considering the low initial concentration of the catalyst in the propellant, and the fact that it accumulates on the surface, catalyst particles may, at best, be sporadically distributed in the gas phase at any instant of time. Thus, the catalyst does not have much opportunity to catalyze the LEF reactions directly because such flames are thin, and the opportunity for catalysis is small because of low collision probability with catalyst particles in the thin O/F flamelets. To the extent that direct flame catalysis might be present, one would expect the effect to be proportional to concentration used in the propellant, a corollary contrary to the test results (Fig. 2).[15] Thus, it seems that catalysis in the gas phase has a minimal role in influencing burning rate.

12) On the other hand, if the inclusion of the catalyst can result in exothermic heat release at or below the surface, and/or release more reactive fuel and oxidizer species into the gas phase, it can cause the gas phase flame complex to stand closer to the surface, and increase the burning rate correspondingly. It appears that this could potentially change the gas phase flame structure, the implications of which will be addressed later.

C. Present Results

The new results described in the last section indicate that the use of iron catalysts in the fine AP/binder matrix lamina produced a much larger enhancement in sandwich rates than did the addition of either catalyst[6,7,24] or AP alone[25,26] to the binder lamina. The catalyst also enhanced the rate of the matrix burning alone (Fig. 2a), and led to matrix burning under conditions for which the uncatalyzed matrix would not burn alone [binder melt + fine AP (Figs. 7 and 8), and more fuel-rich mixtures (Fig. 2b)]. The burning rates of sandwiches with catalyzed matrices were relatively insensitive to matrix lamina thickness (Fig. 2). All of these effects are indicative of an enhanced role for the matrix in determining the burning rate when the iron catalyst is present. The extent of the enhanced role for the catalyzed matrix appears to be dependent on the AP/binder mixture fraction and the size of the AP particles, but not on the dispersibility of the catalyst in the binder or the susceptibility of the binder to melt. The implications of these dependencies will be discussed next.

1. *Effect of Dispersibility of the Catalyst*

The different iron catalysts (dispersed differently in the binder) retain differences in their structural identity only beneath the surface, but all emerge as a fine bed of black particles accumulated on the surface (see Secs. IV.G.1 and IV.G.2). However, the dependence of the burning rate on the difference in the way the iron catalysts are dispersed beneath the surface is negligible (Fig. 9).[2,11] Iron atoms are contained in Fe_2O_3 when particulate catalysts are used, and in ferrocenic structures in Catocene and Butacene, with the latter being attached to binder molecules. Considering that catalytic effectiveness depends upon contact with AP oxidizer (discussed next), and assuming that the chemical mechanism of action of all these catalysts is fundamentally the same, it is unlikely that the different catalysts would have the same opportunity for action in the condensed phase. Furthermore, the pressure dependence of the matrix burning rate is preserved, even with the inclusion of the catalyst (e.g., Fig. 9a); in other words, there is an overall increase in burning rate with the catalyst present, without particular preference to any pressure level in the 0.69–6.9 MPa pressure range. To the contrary, any exothermicity in the condensed phase caused by the catalyst would result in a lower pressure exponent of the catalyzed matrix rate than the uncatalyzed matrix rate, i.e., more catalytic effectiveness at low pressure. These considerations indicate that the condensed phase is not the location of prominent action of the catalyst in the 0.69–6.9 MPa range. The catalytic effectiveness of the sandwich burning rates (Fig. 9b) weakens with an increase in pressure because of the increased predominance of the LLEFs in the uncatalyzed sandwiches at higher pressures. This indicates that catalysis of the LLEFs (by way of more reactive species) is probably not the primary mechanism controlling the burning rate of the catalyzed AP-filled binder sandwiches.

2. *Effect of Oxidizer Type*

The relatively weak (or negative) effect of the iron catalysts on burning rate with non-AP oxidizers (Fig. 6) indicates that either 1) the oxidizer–fuel reactions are not important contributors to heat flow to the surface, or 2) the non-AP oxidizer reactions are not catalyzed by iron catalysts. For instance, HMX/PBAN reactions are not considered as important, but KP/PBAN reactions are considered adequately exothermic to influence burning rate. The noneffect of Fe_2O_3 on KP-based samples (Fig. 6)[14,15] lends support to the view in 2. Among the oxidizers that were tested, AP was unique in that one of its two primary decomposition products is $HClO_4$. This gives rise to the possibility of a variety of heterogeneous and vapor phase reactions involving Fe_2O_3, some exothermic, such as 1) catalyzed decomposition of $HClO_4$ (Refs. 10, 13–15) (products of which may, in turn, accelerate binder destruction),[20] 2) catalysis of $HClO_4$ + binder → products,[21] and/or 3) the formation of thermally unstable intermediates such as iron perchlorate amines (with associated heat release).[10,18,22] With item 1, indeed, lighter fuel fragments are reported with finer AP particles.[9]

But recall that the catalyst is primarily in the binder. With fine AP particles, the opportunity for the catalyst concentration on the surface to come in contact with AP primary decomposition vapors along the AP/binder contact lines is enormous. Furthermore, the finer the dispersion of the catalyst in the binder, the more uniform the web of concentrated catalyst on the surface, allowing for the possibility of direct contact between the catalyst and new AP particles emerging on the surface from beneath the web. An immediate implication of such a scenario is that the catalyst may not be very effective if it is of comparable particle size to the oxidizer particles. This is indeed attested to by the results of this study (see Sec. IV.G.2, third paragraph).

3. *Effect of Fine AP Size*

Figure 8 clearly shows that the effect of Fe_2O_3 increases with a decrease in fine AP particle size. Since direct action of the catalyst in the condensed phase or gas phase is unlikely, as discussed previously, the remaining plausible scenarios that can explain this effect are: 1) increased catalytic action, gas phase and heterogeneous, along the contact lines between AP particles and the binder in the surface layer that are increased by decreasing particle size; and 2) attachment of gas phase PLEFs in the mixing fans arising from the contact lines of the AP particles, which may increase in number as a result of a decrease in particle size. Considering that Pyrocat is much finer than the smallest AP size tested (the 2-μm AP), the results in Fig. 8 strongly support the possibility in 1, as also suggested in the last paragraph. The possibility suggested in 2 is not mutually exclusive to that in 1; in other words, they can happen simultaneously. This will be addressed in some detail later. However, since the mixing distances in the gas phase would be very short for the 2-μm AP particles, it is unlikely that PLEFs can be attached before complete mixing takes

place. But the catalytic effect is maximum with the 2-μm AP particles (Fig. 8). The possibility in 2 is speculative in view of this aspect.

4. Effect of Binder Melt Flow

The presence of binder melt flows 1) significantly affects the flammability of fuel-rich mixtures such as the matrices tested in this study, 2) reverses the trend of AP particle size effect on burning rate, and 3) is also strongly associated with the plateau and mesa burning behavior of sandwiches.[30] It is notable that the presence of iron catalysts tends to support combustion of fuel-rich mixtures, independent of the degree of susceptibility of the binder to melt (Fig. 7), re-establishes the particle size effect trend (Fig. 8), and eliminates the plateau-burning features attributed to melt flow (Figs. 7 and 8). The effect of binder melt flows can be better explained when the importance of the microscopic regions along fine AP/binder contact lines in the matrix is considered because this is the region where the melt flow is most intrusive on the adjacent AP particles. The present results suggest that the catalyst may initiate or catalyze exothermic reactions at sites aligned with the contact lines that accelerate the decomposition of binder melts that would otherwise flow onto AP surfaces and cause the anomalous effects listed earlier. Unfortunately, these three-dimensional microscopic details (e.g., of the 1-μm scale) are not resolvable in photography, and surface details appear to be obscured in quench tests by binder melt flow during or after flame quench (even for binders that are less susceptible to melt, e.g., PBAN).

The amount of heat release from these reactions may not be large because of the limitation on the availability of reactants at the reaction sites, but such reactions may be important because of the abundance of such reaction sites with the inclusion of fine AP particles, and their strategic location along contact lines close to or at the surface.

5. Interpretation of Surface Features

The catalytic exothermic reactions at the O/F contact lines would furnish hotter and more reactive vapor species for reaction at the gas phase flame (premixed or LEF). This is conducive to greater proximity of the flame complex to the surface than in the absence of the catalyst. The quenched surface features of catalyzed sandwiches (Figs. 3 and 4) may be explained based on the previous scenario. The enormity of interfacial contact in the fine AP/binder matrix lamina affords a net heat release sufficient to pyrolyze the matrix without having to cause lateral heat drain from the adjoining AP laminae, preventing retarded regression of the lamina AP immediately adjacent to the interface. The external heating of the lamina AP self-deflagration in the immediate vicinity of the interface edge by the LLEFs is speculated to cause the thin liquid layer on the deflagrating AP surface to dry up, resulting in a parched appearance of the surface in that region. (The smooth quality of the AP lamina in the corresponding region of an uncatalyzed sandwich is speculated to be caused by the dissociative sublimation of AP, owing to lateral heat loss to the binder/matrix lamina.[23]) The greater proximity of the LLEFs to the lamina interface edges (compared to the case of uncatalyzed sandwich) explains the smaller width of the dry band (when compared to the smooth band of the uncatalyzed sandwich).

D. Implications on the Gas Phase Flame Structure

The closer location of the overall flame complex would increase the temperature gradient in the gas phase and provide increased heat feedback to the surface, thereby causing the burning rate to increase. However, the details of how the gas phase flame above the fine AP/binder matrix lamina responds to exothermic reactions along the contact lines in the presence of the catalyst is not clear (because of the lack of direct observation). It appears that the catalyzed breakdown of both the binder and oxidizer primary decomposition products (the latter accompanied by heat release), would produce hotter and more reactive species (than without the catalyst) in the micro O/F mixing fans above the AP/binder contact lines, as mentioned earlier. It is not hard to visualize, then, the possibility of a buildup of subsequent exothermic O/F reactions along these mixing fans in a diffusion limited fashion. The limitations on such reactions are 1) the diffusion length scales dictated by AP particle size, the thickness of adjacent binder layers (governed by matrix mixture fraction), and the extent of peripheral contact between the oxidizer particles and the catalyst; and 2) upstream–lateral thermal diffusion from the mixing fans to adjacent nonparticipating species both in the gas phase and particularly in the condensed phase that needs to be pyrolyzed, again dictated by the same geometric factors as in 1. Such a three-dimensional mass and energy balance applied locally to these microscopic sites would, in reality, yield fairly low temperatures for reactions in the mixing fans in the immediate vicinity of the AP/binder contact lines on the surface. For this reason, such reaction fans attached to AP particles (if present) would not behave like conventional diffusion (Burke–Schumann) flames, but with an axially increasing temperature and reactivity (greatest along the stoichiometric contours in the mixing fans) in the immediate vicinity of the surface. If the catalytic action is less, or the upstream heat loss is greater, then reactivity near the surface would be less, and the reaction fans may be replaced by PLEFs. Under favorable conditions of high AP fraction and optimum (explained shortly) particle size in the matrix, it is quite possible that such reaction fans or PLEFs are established in the presence of the catalyst, whereas the corresponding uncatalyzed matrix may burn with a premixed canopy flame considerably far away from the surface. The reason for the optimum size stipulation is as follows: the finer the AP size, the greater the contact line density, the greater the total catalytic heat release at the contact lines, and the lesser the thermal burden on the reaction fans. Finer AP size also implies shorter diffusion distances, which means the reactants may mix completely before appreciable heat release above the contact lines, and burn in a premixed flame slightly farther away (still much closer than in the uncatalyzed case). Note that the optimum size stipulation is for the existence of reaction fans or PLEFs and is not to imply higher burning rates as being associated with reaction fans or PLEFs as opposed to a premixed flame. The following subsection is aimed at further clarifying the gas phase details.

In the case of an AP (10-μm)/PBAN = 5/5 matrix, the uncatalyzed matrix does not burn, whereas the catalyzed matrix sustains combustion in a smoldering fashion with low burning rates that exhibit negligible pressure dependence. In such a case, it is very likely that the heat loss to the excess binder precludes establishment of reaction fans or PLEFs, and the pyrolysis is barely sustained by the catalytic reactions along the AP/binder contact lines. When such a matrix is sandwiched between AP laminae, significant assistance is obtained by these surface-layer reactions from the LLEFs in the vicinity of the lamina interface edge, probably by way of an increased temperature at which to react. The result is a tremendous jump in the burning rate for the sandwiches when compared to the matrix burning alone (Fig. 2b). The sandwich surface profile also exhibits a conspicuous protrusion of the central portion of a very thick matrix lamina (Fig. 5a), commensurate with such a hypothesis.

In the case of the sandwiches with catalyzed 10-μm AP/PBAN = 7/3 matrix, there is no protrusion of the matrix lamina (Fig. 5b). In such a situation, it is not clear whether the matrix burning proceeds with a premixed flame or with PLEFs/reaction fans; the AP loading and particle sizes are not unfavorable for the establishment of PLEFs or reaction fans. Recall that the uncatalyzed 7/3 matrix is expected to burn with a premixed flame at the pressures tested.[26] However, since the PLEFs or reaction fans in the catalyzed matrix would be closer to the surface than the LLEFs above the lamina interface edges (owing to the catalytic action), it is likely that a matrix (alone) with PLEFs or reaction

fans burns just as fast as, or faster than, its corresponding sandwich. The results of this study are contrary to such an expectation, i.e., the sandwich rates are almost always greater than the corresponding matrix rates for the present test variables. Therefore, the matrix lamina in these tests most probably burns with a premixed flame, held closer to the surface (along with the LLEFs) than in the uncatalyzed case. The LLEFs do not directly control the burning rate as in the uncatalyzed case, but do so in interaction with the catalytic reactions and the matrix gas phase flame (premixed or PLEF/reaction fan array). For this reason, the interaction between adjacent LLEFs is weakened relative to the matrix processes, and this is borne out by the weaker peaks in the burning rate vs matrix lamina thickness curves of the catalyzed sandwiches when compared to the corresponding uncatalyzed sandwich curves (Fig. 2).

VI. Conclusions

The results of the present study indicate that the Fe_2O_3 catalyst in AP/hydrocarbon binder propellants can act by multiple paths to increase the burning rate. As reported earlier,[6,7,24] the catalyst is located in the binder and concentrates on the surface, and is best suited to alter the fuel decomposition products. However, the present results with fine particulate oxidizer-filled matrices indicate that the catalyst enhances exothermic reactions at, and/or very close to the surface along the oxidizer-binder contact lines on the surface. These reactions become an increasingly important source of heat release and reactive fuel and oxidizer species as the density of contact lines increases with decreasing AP particle size and increasing proportion of AP in the AP/binder matrix.

Acknowledgments

This work was performed under Contract N00014-89-J-1293 with the U.S. Office of Naval Research, with Richard S. Miller as the Technical Monitor. Useful guidance was offered by Russell Reed, U.S. Naval Air Warfare Center, China Lake, California. Some ingredients used in this study were supplied by Woodward Waesche, Science Applications International Corp.; Carol Hinshaw and Robert Wardle, Thiokol Corporation; John Murphy, Elf Atochem North America, Inc.; and Elizabeth Katres, Hüls America, Inc.

References

[1]Kishore, K., and Sunitha, M. R., "Effect of Transition Metal Oxides on Decomposition and Deflagration of Composite Solid Propellant Systems: A Survey," *AIAA Journal*, Vol. 17, No. 10, 1979, pp. 1118–1125.

[2]Lengellé, G., Brulard, J., and Moutet, H., "Combustion Mechanisms of Composite Solid Propellants," *Proceedings of the 16th Symposium (International) on Combustion*, The Combustion Inst., Pittsburgh, PA, 1976, pp. 1257–1269.

[3]Handley, J. C., and Strahle, W. C., "Behavior of Several Catalysts in the Combustion of Solid Propellant Sandwiches," *AIAA Journal*, Vol. 13, No. 1, 1975, pp. 5, 6.

[4]Fong, C. W., and Hamshere, B. L., "The Mechanism of Burning Rate Catalysis in Composite HTPB—AP Propellant Combustion," *Combustion and Flame*, Vol. 65, 1986, pp. 61–69.

[5]Fong, C. W., and Hamshere, B. L., "The Mechanism of Burning Rate Catalysis in Composite Propellants by Transition Metal Complexes," *Combustion and Flame*, Vol. 65, 1986, pp. 71–78.

[6]Price, E. W., and Sambamurthi, J. K., "Mechanism of Burning Rate Enhancement by Ferric Oxide," *Proceedings of the 21st JANNAF Combustion Meeting*, Chemical Propulsion Information Agency, Publ. 412, Vol. 1, 1984.

[7]Price, E. W., Sambamurthi, J. K., and Sigman, R. K., "Further Results on the Combustion of AP/Polymer Sandwiches with Additives," *Proceedings of the 22nd JANNAF Combustion Meeting*, Chemical Propulsion Information Agency, Publ. 432, Vol. 1, 1985.

[8]Krishnan, S., and Jeenu, R., "Subatmospheric Burning Characteristics of AP/CTPB Composite Propellants with Burning Rate Modifiers," *Combustion and Flame*, Vol. 80, 1990, pp. 1–6.

[9]Krishnan, S., and Jeenu, R., "Combustion Characteristics of AP/HTPB Propellants with Burning Rate Modifiers," *Journal of Propulsion and Power*, Vol. 8, No. 4, 1992, pp. 748–755.

[10]Pearson, G. S., "The Role of Catalysts in the Ignition and Combustion of Solid Propellants," *Combustion Science and Technology*, Vol. 3, 1971, pp. 155–163.

[11]Bobolev, V. K., Gen, M. Y., Mal'tsev, V. M., Melesov, G. P., Pokhil, P. F., Seleznev, V. A., Stasenko, A. N., and Chuiko, S. V., "Mechanism of Action of Iron Catalysts on the Combustion of Composite Systems," *Fizika Goreniya i Vzryva*, Vol. 7, No. 3, 1971, pp. 366–375.

[12]Jones, H. E., and Strahle, W. C., "Effects of Copper Chromite and Iron Oxide Catalysts on AP/CTPB Sandwiches," *Proceedings of the 14th Symposium (International) on Combustion*, The Combustion Inst., Pittsburgh, PA, 1973, pp. 1287–1295.

[13]Ermolaev, B. S., Korotkov, A. I., and Frolov, Y. V., "Study of the Action of Catalysts Using Layered Systems," *Fizika Goreniya i Vzryva*, Vol. 5, No. 2, 1969, pp. 286–289.

[14]Pittman, C. U., Jr., "Location of Action of Burning-Rate Catalysts in Composite Propellant Combustion," *AIAA Journal*, Vol. 7, No. 2, 1969, pp. 328–334.

[15]Bakhman, N. N., Nikiforov, V. S., Avdyunin, V. I., Fogelzang, A. E., and Kichin, Y. S., "Catalytic Effect of Ferrous Oxide on Burning Rate of Condensed Mixtures," *Combustion and Flame*, Vol. 22, 1974, pp. 77–87.

[16]Strahle, W. C., Handley, J. C., and Milkie, T. T., "Catalytic Effects in the Combustion of AP-HTPB Sandwiches to 3200 PSIA," *Combustion Science and Technology*, Vol. 8, 1974, pp. 297–304.

[17]Boggs, T. L., Zurn, D. E., Cordes, H. F., and Covino, J., "Combustion of Ammonium Perchlorate with Various Inorganic Additives," *Journal of Propulsion and Power*, Vol. 4, No. 1, 1988, pp. 27–40.

[18]Kishore, K., and Sunitha, M. R., "Mechanism of Catalytic Activity of Transition Metal Oxides on Solid Propellant Burning Rate," *Combustion and Flame*, Vol. 33, 1978, pp. 311–314.

[19]Krishnan, S., and Periasamy, C., "Low-Pressure Burning of Catalyzed Composite Propellants," *AIAA Journal*, Vol. 24, No. 10, 1986, pp. 1670–1675.

[20]Korobeinichev, O. P., Anisiforov, G. I., and Tereschenko, A. G., "High-Temperature Decomposition of Ammonium Perchlorate-Polystyrene-Catalyst Mixtures," *AIAA Journal*, Vol. 13, No. 5, 1975, pp. 628–633.

[21]Korobeinichev, O. P., Kovalenko, K. K., and Lesnikovich, A. I., "Investigation of Effect of Oxide and Organometallic Catalysts on Thermal Decomposition and Combustion of a Model Ammonium Perchlorate-Polymer System," Plenum, New York, 1978.

[22]Kishore, K., Pai Verneker, V. R., and Sunitha, M. R., "Action of Transition Metal Oxides on Composite Solid Propellants," *AIAA Journal*, Vol. 18, No. 11, 1980, pp. 1404, 1405.

[23]Price, E. W., Sambamurthi, J. K., Sigman, R. K., and Panyam, R. R., "Combustion of Ammonium Perchlorate-Polymer Sandwiches," *Combustion and Flame*, Vol. 63, 1986, pp. 381–413.

[24]Markou, C. P., "Effect of Different Binders and Additives on Sandwich Burning," Ph.D. Dissertation, Georgia Inst. of Technology, Atlanta, GA, May 1988.

[25]Lee, S.-T., "Multidimensional Effects in Composite Propellant Combustion," Ph.D. Dissertation, Georgia Inst. of Technology, Atlanta, GA, May 1991.

[26]Lee, S.-T., Price, E. W., and Sigman, R. K., "Effect of Multidimensional Flamelets in Composite Propellant Combustion," *Journal of Propulsion and Power*, Vol. 10, No. 6, 1994, pp. 761–768.

[27]Price, E. W., "Effect of Multidimensional Flamelets in Composite Propellant Combustion," *Journal of Propulsion and Power*, Vol. 11, No. 4, 1995, pp. 717–728.

[28]Prasad, K., and Price, E. W., "A Numerical Study of the Leading Edge of Laminar Diffusion Flames," *Combustion and Flame*, Vol. 90, 1992, pp. 155–173.

[29]Fenn, J. B., "A Phalanx Flame Model for the Combustion of Composite Solid Propellants," *Combustion and Flame*, Vol. 12, June 1968, pp. 201–216.

[30]Chakravarthy, S. R., Price, E. W., and Sigman, R. K., "Binder Melt Flow Effects in the Combustion of AP-HC Composite Solid Propellants," AIAA Paper 95-2710, July 1995.

[31]Price, E. W., Chakravarthy, S. R., Zachary, E. K., and Sigman, R. K., "Ingredient Response and Interaction During Heating on a Hot Stage Microscope," *Proceedings of the 31st JANNAF Combustion Meeting*, Chemical Propulsion Information Agency, Publ. 620, Oct. 1994.

[32]Chen, J. K., Cheng, S. S., and Chou, S. C., "DSC, TG and Infrared Spectroscopic Studies of HTPB and Butacene Propellant Polymers," AIAA Paper 94-3176, June 1994.

[33]Krishnan, S., and Jeenu, R., "A Surface Reaction Model for Catalyzed Composite Propellants," *AIAA Journal*, Vol. 30, No. 11, 1992, pp. 2788–2791.

[34]Deur, J. M., and Price, E. W., "Steady State One-Dimensional Pyrolysis of Oxidizer-Binder Laminates," AIAA Paper 86-1446, June 1986.